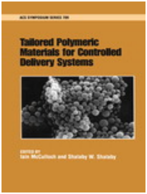

ACS SYMPOSIUM SERIES 709

Tailored Polymeric Materials for Controlled Delivery Systems

EDITED BY
Iain McCulloch and Shalaby W. Shalaby

Downloaded by 89.163.35.42 on October 31, 2012 | http://pubs.acs.org
Publication Date: September 24, 1998 | doi: 10.1021/bk-1998-0709.fw001

Tailored Polymeric Materials for Controlled Delivery Systems

In Tailored Polymeric Materials for Controlled Delivery Systems; McCulloch, I., et al.;
ACS Symposium Series; American Chemical Society: Washington, DC, 1998.

Downloaded by 89.163.35.42 on October 31, 2012 | http://pubs.acs.org
Publication Date: September 24, 1998 | doi: 10.1021/bk-1998-0709.fw001

ACS SYMPOSIUM SERIES **709**

Tailored Polymeric Materials for Controlled Delivery Systems

Iain McCulloch, EDITOR
Hoechst-Celanese Corporation

Shalaby W. Shalaby, EDITOR
Poly-Med Inc.

Downloaded by 89.163.35.42 on October 31, 2012 | http://pubs.acs.org
Publication Date: September 24, 1998 | doi: 10.1021/bk-1998-0709.fw001

Developed from a symposium sponsored by the
Division of Polymer Chemistry
at the 214th National Meeting
of the American Chemical Society,
Las Vegas, Nevada,
September 7–11, 1997

American Chemical Society, Washington, DC

RS 201 .C64T35 1998 c.1

Tailored polymeric materials
for controlled delivery

Downloaded by 89.163.35.42 on October 31, 2012 | http://pubs.acs.org
Publication Date: September 24, 1998 | doi: 10.1021/bk-1998-0709.fw001

Library of Congress Cataloging-in-Publication Data

Tailored polymeric materials for controlled delivery systems / Iain McCulloch, editor, Shalaby W. Shalaby, editor.

p. cm.—(ACS symposium series ; 709)

"Developed from a symposium sponsored by the Division of Polymer Chemistry at the 214th National Meeting of the American Chemical Society, Las Vegas, Nevada, September 7–11, 1997."

ISBN 0–8412–3585–6

1. Drugs—Controlled release—Congresses. 2. Controlled release preparations—Congresses. 3. Polymeric drug delivery systems—Congresses.

I. McCulloch, Iain, 1964- II. Shalaby, Shalaby W. III. American Chemical Society. Division of Polymer Chemistry. IV. American Chemical Society. Meeting (214th : 1997 : Las Vegas, Nev.) V. Series.

RS201.C64T35 1998
615′.6—dc21 98–25962
CIP

The paper used in this publication meets the minimum requirements of American National Standard for Information Sciences—Permanence of Paper for Printed Library Materials, ANSI Z39.48–1984.

Copyright © 1998 American Chemical Society

Distributed by Oxford University Press

All Rights Reserved. Reprographic copying beyond that permitted by Sections 107 or 108 of the U.S. Copyright Act is allowed for internal use only, provided that a per-chapter fee of $20.00 plus $0.25 per page is paid to the Copyright Clearance Center, Inc., 222 Rosewood Drive, Danvers, MA 01923, USA. Republication or reproduction for sale of pages in this book is permitted only under license from ACS. Direct these and other permissions requests to ACS Copyright Office, Publications Division, 1155 16th Street, N.W., Washington, DC 20036.

The citation of trade names and/or names of manufacturers in this publication is not to be construed as an endorsement or as approval by ACS of the commercial products or services referenced herein; nor should the mere reference herein to any drawing, specification, chemical process, or other data be regarded as a license or as a conveyance of any right or permission to the holder, reader, or any other person or corporation, to manufacture, reproduce, use, or sell any patented invention or copyrighted work that may in any way be related thereto. Registered names, trademarks, etc., used in this publication, even without specific indication thereof, are not to be considered unprotected by law.

PRINTED IN THE UNITED STATES OF AMERICA

American Chemical Society
Library
1155 16th St., N.W.
Washington, D.C. 20036

Downloaded by 89.163.35.42 on October 31, 2012 | http://pubs.acs.org
Publication Date: September 24, 1998 | doi: 10.1021/bk-1998-0709.fw001

Advisory Board

ACS Symposium Series

Mary E. Castellion
ChemEdit Company

Arthur B. Ellis
University of Wisconsin at Madison

Jeffrey S. Gaffney
Argonne National Laboratory

Gunda I. Georg
University of Kansas

Lawrence P. Klemann
Nabisco Foods Group

Richard N. Loeppky
University of Missouri

Cynthia A. Maryanoff
R. W. Johnson Pharmaceutical
Research Institute

Roger A. Minear
University of Illinois
at Urbana–Champaign

Omkaram Nalamasu
AT&T Bell Laboratories

Kinam Park
Purdue University

Katherine R. Porter
Duke University

Douglas A. Smith
The DAS Group, Inc.

Martin R. Tant
Eastman Chemical Co.

Michael D. Taylor
Parke-Davis Pharmaceutical
Research

Leroy B. Townsend
University of Michigan

William C. Walker
DuPont Company

Downloaded by 89.163.35.42 on October 31, 2012 | http://pubs.acs.org
Publication Date: September 24, 1998 | doi: 10.1021/bk-1998-0709.fw001

Foreword

THE ACS SYMPOSIUM SERIES was first published in 1974 to provide a mechanism for publishing symposia quickly in book form. The purpose of the series is to publish timely, comprehensive books developed from ACS sponsored symposia based on current scientific research. Occasionally, books are developed from symposia sponsored by other organizations when the topic is of keen interest to the chemistry audience.

Before agreeing to publish a book, the proposed table of contents is reviewed for appropriate and comprehensive coverage and for interest to the audience. Some papers may be excluded in order to better focus the book; others may be added to provide comprehensiveness. When appropriate, overview or introductory chapters are added. Drafts of chapters are peer-reviewed prior to final acceptance or rejection, and manuscripts are prepared in camera-ready format.

As a rule, only original research papers and original review papers are included in the volumes. Verbatim reproductions of previously published papers are not accepted.

ACS BOOKS DEPARTMENT

In Tailored Polymeric Materials for Controlled Delivery Systems; McCulloch, I., et al.;
ACS Symposium Series; American Chemical Society: Washington, DC, 1998.

Preface

The molecular engineering design and application of polymeric materials for use in delivery systems has evolved into one of the most promising advanced technology areas of polymers as well as contemporary medical, agricultural, and pharmaceutical sciences. This book examines a range of polymer materials that facilitate the controlled delivery of active moieties for medical, dental, agricultural, and industrial applications. The symposium was designed to address a broad spectrum of topics, covering both fundamental and applied research. This was to stimulate cross-discipline interactions, while maintaining a strong polymer science and engineering focus. To compliment the chapters derived from the symposium, selected authors were invited to contribute critical reviews and contemporary updates of fast growing areas. We feel that this has offered a unique and exciting perspective.

Although the book covers a wide range of applications, those pertinent to pharmaceuticals are clearly dominant. Collectively the book offers chapters with a review perspective, as well as new, innovative research, with a very high quality of contributing articles. It emphasizes the role of molecular architecture and associated design and synthesis of new chain molecules, as well as assembling strategies for modulation of release profiles. This entailed discussions of nanospheres, micelles, microspheres, solid implants, and injectable liquid gelformers. Concise accounts of key administration routes and clinical applications are provided.

This book will be particularly valuable for those in the pharmaceutical and allied industries who seek specific chemistry, polymer science, and engineering information pertinent to the development of advanced delivery systems.

IAIN MCCULLOCH
Hoechst-Celanese Corporation
86 Morris Avenue
Summit, NJ 07901

SHALABY W. SHALABY
Poly-Med Inc.
6309 Highway 187
Anderson, SC 29625

Downloaded by 89.163.35.42 on October 31, 2012 | http://pubs.acs.org
Publication Date: September 24, 1998 | doi: 10.1021/bk-1998-0709.pr001

Chapter 1

Intravitreal Treatment of Cytomegalovirus Retinitis and the Need for Controlled Release Systems

Marc Shalaby[1] **and Shalaby W. Shalaby**[2]

[1]**University of North Carolina School of Medicine, Chapel Hill, NC 27599**
[2]**R&D Laboratories, Poly-Med, Inc., Pendleton, SC 29670**

Downloaded by 89.163.35.42 on October 31, 2012 | http://pubs.acs.org
Publication Date: September 24, 1998 | doi: 10.1021/bk-1998-0709.ch001

As a topic of considerable contemporary interest, cytomegalovirus (CMV) retinitis is briefly reviewed and its relevance to the acquired immunodeficiency syndrome (AIDS) has been highlighted. Traditional therapies for halting the progression of CMV retinitis, which culminates in loss of eyesight, are outlined, and limitations to these therapies are analyzed. The local route for controlled drug delivery through intravitreal application is advocated as the choice strategy. Among the intravitreal controlled release systems that show some promise are (a) non-absorbable implants for administering ganciclovir; and (b) intravitreal liposomal formulations of antiviral agents. The latter approach was cited among the emerging trends along with the use of minimally invasive injectable gel-forming liquids for the controlled release of highly potent, but considerably toxic drugs such as cidofovir.

Cytomegalovirus (CMV), a member of the herpes virus family, is known to infect anywhere from 40-80% of the population, depending on geographics, age, socioeconomic class, and sexual orientation. The virus remains latent after the primary infection and becomes reactivated in immunocompromised hosts. Reactivation of CMV disease in such patients can lead to end-organ damage such as retinitis, esophagitis, pneumonitis, adrenalitis, colitis, encephalitis, and radiculopathy (*1*). Retinitis, however, is the most common clinical consequence of CMV disease (*2*). Before the acquired immunodeficiency syndrome (AIDS) epidemic, the greatest number of cases of CMV retinitis were reported to have occurred in renal transplant patients receiving a host of immunosuppressive medications (*3,4*). Currently, however, CMV retinitis occurs almost exclusively in AIDS patients whose CD4+ cell (helper T-cell) count has fallen to less than 100 per mm^3 (approximately 75 % of these cases occur when the CD4+ count falls below 50 per mm^3) (*2*).

In Tailored Polymeric Materials for Controlled Delivery Systems; McCulloch, I., et al.;
ACS Symposium Series; American Chemical Society: Washington, DC, 1998.

CMV disease represents the most common serious viral opportunistic infection in patients with AIDS (*2*). It is estimated that approximately 90% of all AIDS patients will develop an active CMV infection sometime during the course of their disease (*4*). The prevalence of CMV retinitis in AIDS patients has been estimated to be between 15% to 40%, but a more accurate estimate is probably closer to 25% (*5*, *6*). Patients with CMV retinitis typically suffer from blurred vision, loss of central or peripheral vision, and multiple "floaters." The rate of progression of CMV retinitis is highly variable, but left untreated, CMV retinitis may lead to blindness within 6 months (*6-9*).

Intravenous Therapy: Scope and Limitations

For many years, intravenous antiviral therapy was the only means to combat CMV retinitis. Currently, there are three intravenous agents in use—ganciclovir, foscarnet and most recently, cidofovir. Each of these agents decreases viral replication by the same mechanism, namely through inhibiting CMV DNA polymerase (*10*), and has been shown to be efficacious in delaying the progression of CMV retinitis. The significant toxicities associated with the drugs limits their use.

Downloaded by 89.163.35.42 on October 31, 2012 | http://pubs.acs.org
Publication Date: September 24, 1998 | doi: 10.1021/bk-1998-0709.ch001

Intravenous Ganciclovir. Ganciclovir is a nucleoside analog of acyclovir, with the only difference being the addition of a 3'-carbon and hydroxyl group to the acyclic side chain. Early studies of ganciclovir revealed that not only did CMV retinitis cease to progress with intravenous therapy, the retinitis actually went through a process of involution in which the retinal opacification and hemorrhage resolved (*4*). In a study by Spector et al. (*11*), patients with active CMV retinitis were randomized to receive either deferred or immediate treatment with intravenous ganciclovir, 5 mg/kg twice a day for two weeks followed by 5 mg/kg/day. Using Kaplan-Meier estimates, it was determined that the mean time to progression was 19.3 days in the deferred-treatment group compared to 49.5 days in the immediate treatment group (*10*, *11*). Intravenous ganciclovir soon became the standard of care for treatment of CMV retinitis. Recently, Elliot and associates found that adding an intravenous infusion of the bradykinin agonist RMP-7 to the intravenous ganciclovir increased the ocular uptake of intravenous ganciclovir in guinea-pigs (*12*). Applicability to human subjects has not yet been determined.

Ganciclovir is designed to preferentially inhibit CMV DNA polymerase activity. Unfortunately, uninfected cells in the bone marrow phosphorylate small amounts of ganciclovir resulting in the inhibition of their native DNA polymerase. The result is a dose-limiting neutropenia and thrombocytopenia. Such toxicity, coupled with the hematological toxicity of zidovudine (ZDV, AZT)—the first and most frequently used antiviral agent for the human immunodeficiency virus (HIV)—results in a cumulative toxicity (*4*). In a study by Hochster, it was determined that AZT at 600 mg per day plus intravenous ganciclovir led to a severe, life-threatening hematological toxicity in as many as 82% of patients (*13*). Granulocyte colony stimulating factor (G-CSF) and granulocyte-macrophage colony stimulating factor (GM-CSF), previously used only in chemotherapy-related myelosuppression, are now being employed to limit the extent of hematological toxicity incurred with concomitant AZT and ganciclovir. No adverse interactions have been reported with concomitant use of G-CSF or GM-CSF and ganciclovir therapy (*14*).

At present, ganciclovir is the only anti-CMV agent that is available in an oral preparation. A study by Drew and co-workers (*15*) has shown that after proper intravenous induction therapy with ganciclovir, maintenance therapy with oral ganciclovir is equally as effective as intravenous ganciclovir in delaying retinitis progression in a given eye. One drawback was that the rates of new bilateral disease was significantly higher in the oral therapy group compared to the intravenous therapy group (*15*). These results indicate that while oral ganciclovir is a promising endeavor, currently it is not as effective as intravenous therapy.

Intravenous Foscarnet. Foscarnet is a pyrophosphate analog which acts as a noncompetitive inhibitor of many viral RNA and DNA polymerases, including CMV DNA polymerase. In a study of its clinical efficacy in the treatment of CMV retinitis, Palestine et al. (*16*), reported a median time to retinitis progression of 22 days in the treatment-deferred group compared to 93 days in patients who underwent immediate treatment with foscarnet, 60 mg/kg three times per day for three weeks followed by 90 mg/kg/day thereafter (*16*). This encouraging data, however, was overshadowed by foscarnet's severe side effect and pharmacokinetic profile. Nephrotoxicity, decreased renal function, electrolyte abnormalities, and anemia are among the most serious toxicities of foscarnet (*1,4*). In addition, since foscarnet is hydrophilic and negatively charged, it has poor penetration into cells and is rapidly cleared by the kidney, resulting in a short plasma half-life (*17,18*). All of these factors significantly limit the clinical usefulness of foscarnet.

Intravenous Combination Therapy. Studies have shown that combination therapy with intravenous ganciclovir and foscarnet have been more effective in delaying retinitis progression compared to monotherapy with either agent. In one study, median time to progression with combination therapy was 4.3 months versus 1.3 months with foscarnet and 2.0 months with ganciclovir. Unfortunately, there was an increase in the frequency of neutropenia and a greater rate of discontinuation of therapy with the combination regimen. In addition, despite the delay in progression that was noted, combination therapy did not improve visual acuity, rate of retinal detachment or involvement of the fellow eye. Furthermore, the combination conferred no survival benefit (*19*).

Intravenous Cidofovir. Cidofovir ([S]-1-[3-hydroxy-2-phosphonylmethoxypropyl] cytosine), also known as HPMPC, is an acyclic nucleoside phosphonate analog that has been shown to have excellent anti-CMV activity (*20*). In a study by Lalezari and co-workers on cidofovir efficacy, it was reported that the median time to retinitis progression was 22 days in the treatment-deferred group compared with 120 days in the group who immediately received cidofovir, 5 mg/kg once a week for two weeks followed by a maintenance dose of 5 mg/kg every other week (*21*). Further work by Lalezari and Kupperman (*22*) included a study in which, after induction therapy with

Downloaded by 89.163.35.42 on October 31, 2012 | http://pubs.acs.org
Publication Date: September 24, 1998 | doi: 10.1021/bk-1998-0709.ch001

Downloaded by 89.163.35.42 on October 31, 2012 | http://pubs.acs.org
Publication Date: September 24, 1998 | doi: 10.1021/bk-1998-0709.ch001

cidofovir 5 mg/kg once weekly for two weeks, patients were randomized to receive either cidofovir 5 mg/kg or 3 mg/kg every other week as maintenance therapy. They found that the 5 mg/kg maintenance group had a median time to retinitis progression of 115 days as compared to 49 days in the 3 mg/kg maintenance group (*22*).

And while the higher dose appears to be significantly more efficacious, it is important to note that dose-limiting nephrotoxicity with cidofovir monotherapy begins at doses of 3 mg/kg and higher (*23*). Fortunately, concomitant saline hydration and oral probenecid offer some degree of protection from the nephrotoxic effects of cidofovir. It is suggested that a dose of 5 mg/kg every other week should not be exceeded and that a full 4 g of oral probenecid should be administered with each cidofovir dose. In addition, careful renal function monitoring is essential (*22*).

One benefit of cidofovir over the previously discussed antivirals is that it is far easier to administer. Every other week dosing is a clear advantage over daily dosing. Such infrequent dosing negates the need for an indwelling central line which precludes the development of a host of catheter-related complications and gives patients greater freedom and mobility.

Drawbacks to Intravenous Therapy. While it is clear that each of these intravenous therapies delay the progression of CMV retinitis, it must be reemphasized that there are several drawbacks to their use. Reactivation of disease occurs at some time during each of the intravenous therapies. In fact, almost all patients experience disease progression while actively receiving treatment (*10*). In addition, each of the antiviral preparations has its own dose-limiting toxicity and requires careful monitoring during administration. Furthermore, the need for an indwelling catheter for intravenous therapy with foscarnet and ganciclovir increases the risk of catheter-related infection and complications.

Another serious drawback to systemic therapy is that patients with advanced HIV disease are often taking a host medications that can potentially interact with anti-CMV therapy. For example, pharmacokinetics studies have shown that ganciclovir interacts with the antiretroviral didanosine (ddI) in such a way that increases plasma concentrations of ddI. In addition, since neutropenia is the dose-limiting toxicity of both AZT and ganciclovir, severe hematological toxicity may result without the concomitant use of G-CSF or GM-CSF. Foscarnet, with its ability to cause renal impairment should not be used with other nephrotoxic drugs such as aminoglycosides, amphotericin B or intravenous pentamidine. Such medications are all commonly used in patients with advanced HIV disease. In addition, drugs that alter serum levels of calcium, potassium, phosphates and magnesium may also be problematic with concomitant foscarnet use (*2*).

Local Therapy

The aforementioned complications and drawbacks of systemic antiviral therapy have led efforts to develop effective local therapy to combat CMV retinitis. In theory, local therapy should reduce systemic toxicity and reduce the risk of local viral resistance by providing higher intraocular drug levels with minimal systemic levels.

Local treatment modalities may entail intravitreal injections of antiviral agents, absorbable sustained release preparations, and implantable, nonabsorbable systems for drug delivery. Such advances have permanently changed the way patients with CMV retinitis are treated and are expected to become the standard of care.

In order for a drug to be efficacious against CMV retinitis, it needs to be present within the vitreous. Therapeutic intravitreal drug levels are attainable with systemic antiviral therapy, but often at the expense of systemic toxicity. It seems logical that one could inject the drug of choice directly into the vitreous and attain high intravitreal drug levels without having any significant systemic toxicity. Such a technique has been employed by numerous researchers with very encouraging results (*20,24-35*).

Downloaded by 89.163.35.42 on October 31, 2012 | http://pubs.acs.org
Publication Date: September 24, 1998 | doi: 10.1021/bk-1998-0709.ch001

Intravitreal Ganciclovir Injections. One of the first reported cases in which intravitreal injections of ganciclovir were used as therapy for CMV retinitis appeared in 1987 (*24*). Henry and associates (*24*) described an AIDS patient who developed rapidly progressive CMV retinitis, whose marked bone marrow suppression precluded him from receiving intravenous ganciclovir therapy. He was subsequently treated with intravitreal injections of 200 μg/0.1 ml ganciclovir. The elimination half-life was determined to be 13.3 hours, and the intravitreal concentration was found to remain above the ID_{50} for 62 hours after a single injection. Over the course of three months, the patient received a total of 28 injections (2 injections per week), tolerated the injections without difficulty, and had useful vision and temporary resolution of his retinitis. This period may have been prolonged, but the patient left town against medical advice for two weeks and received no therapy. When he returned, he had a worsening of his clinical course. This study was one of the first to demonstrate that repeated invasion of the vitreous with twice-a-week intravitreal injections of ganciclovir was not only clinically efficacious, but safe and well tolerated (*24*).

Numerous studies then emerged during the subsequent years that all supported the effectiveness and the tolerability of repeated intravitreal injections of ganciclovir (*25-28*). Most studies used 0.1 ml injections of 200 μg of ganciclovir. The studies found favorable initial response rates with 78 to 100% of patients attaining resolution of their active retinitis (*25,27,28*) . Upon relapse, Ussery and associates (*28*) increased the dose of ganciclovir to 300 μg and found that one of two eyes responded well (*28*). Cochereau-Massin and co-workers chose to employ doses of 400 μg per injection with excellent results (*26*).

The study by Cochereau-Massin and co-workers is one of the comprehensive investigations that warrants a detailed discussion (*26*). In this prospective open study, sixty-four eyes of 44 AIDS patients who refused or were intolerant of intravenous therapy received a total of 710 intravitreal injections of ganciclovir at doses of 400 μg per injection. This represents twice the dose employed in previous studies. The researchers expected that by using a higher dose of ganciclovir, they could increase the peak drug concentration within the vitreous as well as prolong the duration of the therapeutic dose. All injections were performed in a sterile operating room. Induction therapy consisted of injections twice per week until resolution and healing of the retinitis occurred. This was followed by maintenance therapy consisting of weekly injections which were continued until relapse. Cicatrization occurred in 53 of 54 induction courses after a mean of 6.6 injections. In 54 maintenance courses 53% of eyes had relapsed by eight weeks. In addition, during therapy, active CMV disease developed in the previously uninvolved fellow eye in 11% of the patients and in a nonocular site in 16% of the patients. A total of five retinal detachments, but no cases of endophthalmitis or cataract were noted. The authors attributed the detachments to microbreaks in the porous junction between the atrophic and normal retina, but they conceded that the intravitreal pH elevation caused by the ganciclovir may have been a contributing factor. Two intravitreal hemorrhages were noted in two thrombocytopenic patients during the course of 710 injections. Both hemorrhages spontaneously resolved within 2 weeks and intravitreal injections were resumed. Cochereau-Massin and co-workers (*26*) concluded that intravitreal ganciclovir injections were safe and effective in the treatment of CMV retinitis. The 400 μg dose employed in this study did not appear to cause any clinical toxicity but failed to show a clear advantage over the previously described 200 μg dose (*26*).

The major complications encountered in most intravitreal administration studies were post-injection endophthalmitis and retinal detachment. The rates of intraocular infection with repeated injections have been reported to be 0.4% and 0.6% (*25,27*). All researchers employed sterile technique during the injections, but only Ussery's group and Cochereau-Massin's group performed their injections in sterile operating rooms instead of the outpatient clinic (*26,28*). This is a possible explanation for the fact that neither group reported any cases of post-injection endophthalmitis. Heinemann (*27*) concedes that injections done under operating room conditions may indeed reduce the infection rate, but such technique is not practical in clinical settings in which large numbers of patients are treated.

Retinal detachment rates are reported to be between 7% and 11% (*26-28*). However, it is difficult to determine if these reported cases of retinal detachment were due to the trauma of repeated injections into the friable and necrotic retina or the result of the natural course of the resolving CMV retinitis. With this in mind, Cochereau-Massin and co-workers (*26*) contend that the 5 retinal detachments (8%) noted in their study is similar to the observed rates of detachment noted in several studies of intravenous ganciclovir.

In the above noted studies, intravitreal therapy was employed in patients who were either intolerant of (secondary to thrombocytopenia or neutropenia) or refused systemic ganciclovir therapy (*25-28*). Daikos and coworkers (*29*), however, set out to study the clinical efficacy and toxicity of the concomitant administration of intravitreal ganciclovir injections and intravenous ganciclovir. The study consisted of nine patients with active CMV retinitis. Five of the patients had retinitis with macular involvement in six of their sighted eyes and six patients had only peripheral involvement in seven eyes. Of those with macular involvement, the two patients who received both intravitreal and intravenous ganciclovir maintained sight while the remaining three patients who received only intravenous ganciclovir became blind. In those patients with peripheral retinitis only, vision was preserved regardless of

Downloaded by 89.163.35.42 on October 31, 2012 | http://pubs.acs.org
Publication Date: September 24, 1998 | doi: 10.1021/bk-1998-0709.ch001

whether or not intravitreal ganciclovir was administered. The researchers concluded that patients with CMV retinitis of the macula may benefit from concomitant intravitreous and intravenous ganciclovir therapy, while those patients with only peripheral involvement may not require such bimodal therapy (*29*).

Intravitreal Foscarnet Injections. Intravitreal foscarnet has two major advantages over intravitreal ganciclovir. For one, foscarnet has a relatively long elimination half-life from the vitreous which perhaps prolongs its antiviral effect. In addition, the pH of foscarnet is more physiologic, which conceivably avoids potential acid/base disturbances. There have been three major studies of intravitreal foscarnet injections for the treatment of CMV retinitis (*30-32*). Diaz-Llopis and coworkers (*30*) first described a patient who had advanced renal disease (thus precluding him from receiving intravenous foscarnet) and intolerance to acyclovir (which is similar in structure to ganciclovir). The patient received intravitreal injections of 1200 μg of foscarnet—two injections per week for three weeks as induction therapy followed by weekly injections thereafter for maintenance therapy. The injections were well tolerated, and the patient experienced no reactivation of his retinitis during the four month follow-up.

The authors then studied the clinical efficacy of increasing the dose of intravitreal foscarnet from 1200 μg to 2400 μg (*32*). Patients with active retinitis received, at the elevated dose, induction therapy (twice-a-week injections) followed by maintenance therapy (weekly injections). After receiving six injections over the course of three weeks, five of eight eyes experienced complete resolution of active CMV retinitis. The remaining three eyes experienced partial resolution. The researchers concluded that the elevated dose of foscarnet was not only efficacious, but well tolerated (*32*).

Liebermann et al. (*30*), described a patient with CMV retinitis surrounding the optic nerve. This patient received foscarnet injections every other day for eight days while receiving no systemic therapy. The patient experienced an improvement of his vision by his second visit and had no further progression of his retinitis at the end of the induction therapy.

Intravitreal Cidofovir Injections. In a phase I/II clinical trial, Kirsch and associates studied the safety and efficacy of intravitreal injections of cidofovir (*20*). The first phase of the study was a preliminary safety study in which ten eyes of nine patients received 14 injections of cidofovir while receiving concomitant intravenous ganciclovir therapy. The researchers were primarily looking for incidences of ocular complications such as hypotonia, retinal detachment, choroidal detachment, or endophthalmitis. The second phase of the study was a dose escalating efficacy study in which eight eyes of seven patients received a total of eleven intravitreal injections while not receiving any concurrent systemic antiviral therapy. The primary outcome for this group of patients was the time to retinitis progression after the first cidofovir injection. Other data recorded included the development of active CMV retinitis in the fellow eye that had either been previously uninvolved or that had harbored a previously inactive retinitis.

Downloaded by 89.163.35.42 on October 31, 2012 | http://pubs.acs.org
Publication Date: September 24, 1998 | doi: 10.1021/bk-1998-0709.ch001

Downloaded by 89.163.35.42 on October 31, 2012 | http://pubs.acs.org
Publication Date: September 24, 1998 | doi: 10.1021/bk-1998-0709.ch001

Looking at the phase I results, it is important to note that the first two patients who received injections developed post-injection vitreitis and hypotony after receiving a 100 μg dose of cidofovir without concomitant oral probenecid. Subsequently, the remainder of the patients were pretreated with 2 g of oral probenecid three hours before injection and 1 g at two and eight hours after injection. After this regimen was instituted, only one further episode of hypotony occurred. No other complications were noted. Those patients who received intravenous ganciclovir therapy plus 20 μg of cidofovir all responded to therapy and experienced a halting of their retinitis. The mean time to retinitis progression was determined to be 78 days. Eight of the nine patients in this phase had unilateral cidofovir treatment, and by the end of the study, seven of the eight fellow, untreated eyes demonstrated active CMV retinitis despite continuation of intravenous ganciclovir. In all seven of these eyes, however, active retinitis had been documented at the outset of the study.

In the second phase of the study, in patients who received intravitreal cidofovir without concomitant intravenous ganciclovir, the mean time to progression of retinitis after the first 20 μg injection was 63 days. Kirsch and coworkers (*20*) contend that since no systemic therapy was employed, their results more conclusively illustrate the clinical efficacy of intravitreal cidofovir in the treatment CMV retinitis.

Subsequent work by Kirsch and associates entailed an unmasked consecutive case series trial in which AIDS patients received 20 μg cidofovir intravitreal injections (plus concomitant oral probenecid) as the sole treatment for their CMV retinitis (*33*). In this study, retreatments were employed in patients who demonstrated progression of retinitis. The primary outcomes of interest were 1) the time to retinitis progression after the initial intravitreal injection of cidofovir and 2) the time to retinitis progression after retreatment with a second injection of cidofovir. There was a total of 37 injections of 24 eyes in 17 patients. All patients responded to the initial cidofovir injection by exhibiting an arrest to the progression of their CMV retinitis. The median time to progression after the initial 24 injections was 55 days. After 8 repeat cidofovir injections, the mean time to progression was determined to be 63 days. Kirsch and coworkers contend that there is no significant difference in the time to retinitis progression after the first injection compared with the second, but concede that further work is necessary (*33*).

In the Kirsch study, five eyes (20.8%) developed a mild iritis that responded well to topical therapy. Two of the 24 eyes experienced retinal detachments at 21 and 33 days after injection, respectively. The authors, however, did not attribute these detachments to the injection procedure since the detachments were too temporally distant from the injection procedure and typical atrophic retinal holes were observed in both cases. Also noted was a significant decrease in intraocular pressures from baseline at both the 2 and 4 week post-injection follow-up visits. The researchers believe that this effect of lowered intraocular pressure appeared to stabilize as there was no significant difference between the intraocular pressures at 2 and 4 weeks (*33*). The significance of this decrease in pressure requires further study.

Given the incidence of iritis and hypotony that occurred with the 20 μg injections of cidofovir, the researchers next evaluated the safety and efficacy of 10 μg intravitreal injections (*34*). Twenty-seven eyes of 18 patients were injected with the lower dose and had complete follow-up. The researchers found that the median time to retinitis progression after a single 10 μg dose of cidofovir was 45 days, compared to 55 days with the 20 μg dose (20,34). This difference was statistically significant ($p=0.033$). The authors attributed this difference to the 26% incidence of primary failure in the patient group that received the 10 μg dose. Progression of retinitis after a second injection of 10 μg of cidofovir was 32 days, which is a significantly shorter than 63-day period that was obtained with the 20 μg dose ($p=0.037$) (*20,34*). And while the 10 μg dose of cidofovir was determined to be less effective than the 20 μg dose, it did have fewer and less pronounced episodes of decreased intraocular pressures and iritis. Taskintuna and coworkers (*34*) concluded that intravitreal cidofovir "appears to have a narrow therapeutic index, and other attempts at reducing the side effects while preserving the long-acting effect, such as liposome delivery, may be warranted."

Downloaded by 89.163.35.42 on October 31, 2012 | http://pubs.acs.org
Publication Date: September 24, 1998 | doi: 10.1021/bk-1998-0709.ch001

Intravitreal Fomivirsen Injections. Fomivirsen (formerly ISIS 2922) is a synthetic phosphorothioate antisense oligonucleotide specifically designed to combat CMV. In a phase I trial, patients with AIDS and CMV retinitis who had repeatedly failed ganciclovir and foscarnet therapy received 75, 150, or 300 μg of intravitreal fomivirsen once a week for a month and then every other week thereafter. Initially, the drug appeared to be well tolerated with only mild, reversible ocular complications, but as the study progressed, irreversible stippling of the retinal pigmented epithelium occurred with subsequent visual field loss (35). Obviously, the initial studies of fomivirsen are not as encouraging as those of other antivirals, but multicenter trials of fomivirsen are currently underway.

Controlled Drug Delivery Systems

Because of the rapid drug clearance of many antiviral medications, single intravitreal injections often do not maintain intravitreal drug levels long enough in order to have a substantial therapeutic effect. Simply increasing the dose of medication may maintain higher drug levels in target tissues, but often at the expense of toxicity. As a result, multiple and frequent injections are employed. It follows that as the number of injections increases, there is an increased chance that a complication such as retinal detachment, hypotonia, or endophthalmitis can occur. In efforts to balance efficacy with toxicity, there has been a search for novel drug delivery systems that are capable of providing a controlled release. Such systems would serve to maintain therapeutic drug levels for longer periods of time and eliminate potentially toxic peaks in drug concentration. Examples of such drug delivery systems include liposomally-encapsulated preparations, polymeric nanoparticle preparations, polymeric microsphere preparations, nondegradable intraocular implants, and most recently, absorbable gel-forming injectable liquids.

Liposomally-Encapsulated Ganciclovir. Liposomes are small, nontoxic, biodegradable vesicles composed of a lipid bilayer. They were first described by

Bangham in 1968 (*36*). He demonstrated that phospholipids, when placed in an aqueous environment, form multilamelar vesicles. The vesicle can be thought of as three functional layers. The outer layer is made up of polar head groups that are in contact with the aqueous environment. Next, there is a hydrophobic region made up of two layers of acyl chains. The inner space of the vesicle is an aqueous environment lined with polar head groups from the inner phospholipid layer. This inner space allows polar compounds, such as ganciclovir and cidofovir, to be encapsulated within the liposome. With time, the lipid wall of the liposomes burst, thereby allowing the drug to be slowly released into the outside environment (*37*). Such a drug delivery system avoids maximum peak concentrations of a drug and increases a drug's efficiency by maintaining prolonged therapeutic drug levels (*38*).

Much of the early work on liposomally-encapsulated ganciclovir was done by Peyman and coworkers (*37,39*). In one study, the authors set out to determine the intravitreal clearance of liposomally-encapsulated ganciclovir in order to determine whether such preparations could improve the intravitreal concentration time profile without producing local toxicity (*39*). Initially, 16 eyes of 8 rabbits were intravitreally injected with 84.1 μg/0.1 ml of the liposomally-encapsulated drug. Next, these animals were sacrificed at 1, 7, 14, and 28 days after injection. The authors found that total intravitreal ganciclovir levels, up to 28 days, remained higher than the ID_{50} of many strains of viruses belonging to the herpes-virus family. The authors contend that these data suggest that liposomally-encapsulated ganciclovir may be valuable for the treatment of, or prophylaxis for, CMV retinitis (*39*).

The first report of liposomally-encapsulated ganciclovir being administered to humans was by Peyman and co-workers in 1988 (*37*). In their case report, they treated a 36-year-old male with AIDS and bilateral retinitis (presumed to be CMV retinitis based on positive serologies and a classic retinal picture). Into his right eye was injected a combination of free ganciclovir (200 μg) and gentamicin (50 μg). Into his left eye, he received injections of liposomally-encapsulated ganciclovir (200 μg) and gentamicin (50 μg). The injection of free drugs into the right eye was repeated every four days for three weeks while the liposomal injection in the left eye was repeated only once, after two weeks. In both eyes, the areas of retinal necrosis became atrophic and pigmented and no new areas of necrosis appeared. Unfortunately, despite these encouraging signs and a subjective improvement in his eye pain, the patient experienced a worsening of his eyesight and was lost to follow-up. The researchers felt that the patient's visual acuity did not improve since he had macular involvement of the retinitis (*37*).

In a study by Diaz-Llopis and co-workers (*38*), one control group of rabbits were injected with varying doses of free ganciclovir (0.2-20 mg), and another group received 1 mg of liposomally-encapsulated ganciclovir. Intraocular ganciclovir concentrations were then measured at 2, 3, 7, and 14 days after injection. After 72 hours, only the vitreous of rabbits injected with 5 mg or more of free ganciclovir demonstrated therapeutic levels of the drug, and no detectable drug appeared with any of the doses of free ganciclovir one week following injection. Microscopic study of the rabbit eyes revealed that there was ganciclovir-induced retinal damage in rabbits that had been injected with 15 mg or more of free ganciclovir. Those rabbits

Downloaded by 89.163.35.42 on October 31, 2012 | http://pubs.acs.org
Publication Date: September 24, 1998 | doi: 10.1021/bk-1998-0709.ch001

injected with the liposomal preparations had no such retinal damage identified, and had therapeutic drug levels that were maintained for up to 14 days following injection. After the encouraging results, Diaz-Llopis and co-workers completed a small clinical trial in which five AIDS patients with CMV retinitis were injected with weekly doses 0.5 mg of liposomally-encapsulated ganciclovir. Complete remission was observed in all patients after three injections and relapse did not occur in the 2-4 month follow-up (*38*).

In a study by Le Bourlais and associates (*40*), the intravitreal clearance of a free ganciclovir solution (200 µg/0.1 ml) and a liposomally-encapsulated ganciclovir preparation (with 41% load; 82 µg drug load and 118 µg free) was determined after a single injection. Intravitreal concentrations were measured at various time intervals up to a total of 43 days. The results of the study demonstrated that prolonged intravitreal drug levels above the mean inhibitory concentration of CMV (1 µg/ml) could be obtained after a single injection of the liposomally encapsulated ganciclovir preparation. Such levels were estimated to continue beyond 30-43 days while an injection of 200 µg/0.1 ml of free drug solution could only be expected to attain such levels for 55 hours. In addition, the researchers found that there was no evidence of retinal toxicity by clinical or light microscopy examination (*40*).

Liposomally-Encapsulated Cidofovir. Early work has been done with regards to assessing the efficacy and toxicity of liposomal preparations of cidofovir. In a study by Besen and co-workers (*41*), cidofovir was encapsulated into a liposome delivery system at concentrations of 100, 500, and 1000 µg. These preparations were subsequently injected into the vitreous of rabbits. Clinical, light microscopic, and electron microscopic examinations of the rabbit eyes after injection revealed no evidence of drug-induced damage at any of the administered doses.

Besen et al., (*41*) chose to use a herpes retinitis animal model in which herpes simplex virus type I (HSV-1) was inoculated onto the retinal surfaces. A focal, non-lethal expanding retinitis then developed in 100% of the eyes that were inoculated. The rabbits then received 1000 µg of liposomally-encapsulated cidofovir and were evaluated at 60, 90,120, 170, and 240 days after injection. The researchers determined that the efficacy range of the liposomal preparation was between 170 days (when excellent protection was observed) and 240 days (when retinitis was prevented in half of the cases). The authors contend that since the ratio of viral inhibitory concentration for cidofovir to CMV is 50 times higher than for HSV-1, their data may be extrapolated to such an extent that one injection of liposomally-encapsulated cidofovir may prevent reactivation of CMV retinitis for longer than 8 months (*41*). It should be noted, however, that such an extrapolation may not be appropriate.

One criticism of Besen's study was that 1000 µg of liposomally-encapsulated cidofovir may lead to toxic drug levels even if a small percentage of the liposomes prove unstable since toxic complications were reported to occur at 100 µg of cidofovir (*20*). With this in mind, Kuppermann and coworkers studied the effects of a more appropriate, nontoxic dose of liposomally-encapsulated cidofovir (*42*). In this study, the effect of a liposome preparation of cidofovir was evaluated as

Downloaded by 89.163.35.42 on October 31, 2012 | http://pubs.acs.org
Publication Date: September 24, 1998 | doi: 10.1021/bk-1998-0709.ch001

prophylaxis for retinitis in the same rabbit model previously described. Liposome-encapsulated cidofovir (100 μg) was injected intravitreally 10-120 days before retinal inoculation with HSV-1. In the end, 22 of 26 eyes pretreated with the 100 μg dose of liposomally-encapsulated cidofovir 10-60 days before HSV-1 inoculation were protected from the experimentally-induced retinitis. In addition, 2 of 5 eyes pretreated 120 days before inoculation were protected. Intravitreal levels of cidofovir were assayed in 3 eyes that received their injection 120 days before inoculation. The average drug concentration was 0.73 μg/ml, which is about 15 times the IC_{50} for cytomegalovirus (*42*). One could possibly extrapolate this data and infer that with such intravitreal concentrations of cidofovir, there may be fewer treatment failures in human studies of CMV retinitis.

Downloaded by 89.163.35.42 on October 31, 2012 | http://pubs.acs.org
Publication Date: September 24, 1998 | doi: 10.1021/bk-1998-0709.ch001

Ganciclovir-Loaded Polymer Microspheres. Even though liposomal drug delivery systems have been shown to be effective, some argue that liposomes characteristically have an unstable shelf life that may limit their widespread use and increase the cost of treatment (*43*). As a result, studies have been done with biodegradable polymers to evaluate their potential as a vehicle for intraocular drug delivery. One such polymer is Poly(DL-lactide-co-glycolide) (PLGA), a biocompatible polymer that degrades to metabolic by-products that may be eliminated from the body (*44,45*). Recently, PLGA microspheres have been successfully loaded with ganciclovir in order to develop a sustained release drug delivery system (*46*).

Veloso and coworkers (*47*) tested the antiviral effect of ganciclovir-loaded microspheres on rabbit eyes that had been inoculated with human CMV. The ganciclovir-loaded microspheres were prepared using a relatively new oil in oil emulsion technique (*46*). In Veloso's study, 62 of 92 pigmented rabbit eyes were inoculated intravitreally with 0.1 ml of a CMV supernatant, and the remaining 30 were injected with a balanced salt solution. In those eyes that were inoculated with CMV, all exhibited grade 2 to 3 vitreitis, grade 1 to 2 retinitis and grade 1 to 2 optic neuritis. In those eyes that received the balanced salt solution "inoculum," no vitreitis, retinitis, or neuritis was observed. In those eyes that received intravitreal injections of the ganciclovir-loaded microspheres (10 mg dose), vitreitis decreased from days 3 to 14 after injection, and retinitis and optic neuritis decreased from days 3 to 9. In those eyes that received blank microspheres, vitreitis increased from days 3 to 7, retinitis increased form days 3 to 9, and optic neuritis increased form days 3 to 14. Immunoflourescence studies of CMV antigens revealed CMV antigens only in retinas of eyes injected with the blank microspheres. Histopathologic studies revealed minimal focal disruption of the retinal architecture in those eyes injected with the ganciclovir-loaded microspheres. No adverse tissue reaction was observed clinically or histopathologically after 8 weeks. Veloso and coworkers concluded that 10 mg of 300 to 500 μm ganciclovir-loaded PLGA microspheres controls the progression of ocular CMV disease without being toxic to ocular structures. They contend that the biodegradable nature of the system is an added advantage over other intraocular drug delivery systems and suggest that ganciclovir-loaded microspheres may be shown to be effective in clinical trials (*47*).

Downloaded by 89.163.35.42 on October 31, 2012 | http://pubs.acs.org
Publication Date: September 24, 1998 | doi: 10.1021/bk-1998-0709.ch001

Ganciclovir Nanoparticles. Additional studies have been done with other biodegradable polymers to evaluate them as potential systems for intraocular drug delivery. In a recent study by El-Samaligy and co-workers, bovine serum albumin (BSA), polyethylcyanoacrylate (PEC), and chitosan were employed as drug delivery systems for ganciclovir (*43*). These three types of ganciclovir-loaded nanoparticle dispersions were prepared and evaluated with regard to drug loading capacity, particle size, and drug release. The study was intended to determine which of the three systems is most suitable for *in vivo* studies. Spherical or nearly spherical nanoparticles were obtained; particle size analysis revealed a diameter range of 0.3 to 1.2 μm. Mean particle size increased in the following order: PEC (0.58 μm) < chitosan (0.82 μm) < BSA (1.20 μm). Mean drug loading efficiency was very similar among polymers and ranged between 62.5 and 66.9%. Ganciclovir was released from the nanoparticles by first order kinetics for up to 4 days. Release rates decreased in the following order: BSA > PEC ≥ chitosan. PEC was selected as the polymer of choice for the *in vivo* studies. It demonstrated the most efficient drug loading and the smallest particle size. Intravitreal ganciclovir levels remained higher than its MIC (0.25-1.22 μg/ml) (*38*) for up to ten days following intravitreal administration of 0.1 ml of the ganciclovir loaded PEC nanoparticle dispersion (equivalent to 1 mg of ganciclovir). The vitreous level on the tenth day was 5.1 +/- 0.43 μg/ml. In addition, plasma ganciclovir levels were considerably lower compared to intravitreal injections of free drug. The only significant complication that was noted with the PEC nanoparticle preparation was that on day 6 after injection some lens opacification and vitreous turbidity occurred in several eyes. Despite this complication, the authors concluded that ganciclovir loaded PEC nanoparticles, with their selective drug deposition in the vitreous and retina, should be effective treatment for CMV retinitis. They added that its decreased systemic absorption may mean fewer side effects and less toxicity (*43*). It should be noted that the authors studied the kinetics of ganciclovir loaded PEC nanoparticle and not the clinical efficacy of such a preparation. Such studies are currently underway.

Sustained-Release Intraocular Ganciclovir Implants. As the search for local therapy for CMV retinitis continued, there were efforts made to increase the length of time between intervention and reintervention. Repeated ganciclovir injections, while effective therapy, require frequent (twice per week) administration which increases the potential for complications including retinal detachment, endophthalmitis, and intravitreal hemorrhage (*25-27*). Recently, an implantable, nondegradable sustained-release ganciclovir delivery device has been approved for the treatment of CMV retinitis with the expectation that such a device would deliver intravitreal ganciclovir for months at a time before requiring replacement.

Two types of delivery devices were first developed. The first (series 1) delivered ganciclovir at 5 μg/h and the second (series 2) delivered ganciclovir at 2 μg/h (*48*). In the preparation of both devices, a 6 mg pellet of ganciclovir is coated with polyvinyl alcohol (PVA) which is permeable to ganciclovir. To prepare series 1 devices, two 3 mm disks made of poly(ethylene-co-vinyl acetate) (an impermeable polymer to ganciclovir), are coated with PVA and fixed to the top and bottom of the ganciclovir pellets with PVA. To prepare the series 2 device, the ganciclovir pellets are instead coated on three sides with a film of prepressed poly(ethylene-co-vinyl acetate) (EVA) and later capped with a 3 mm EVA disk coated with PVA. After the addition of EVA, both devices are completely coated with PVA. The devices are then surgically implanted into the intravitreal space and anchored to the sclera with a suture (*48*). After developing these two devices, Smith and co-workers (*48*) studied the pharmacokinetics of the series 1 and 2 implants in rabbit eyes. Analysis revealed that the two devices released ganciclovir at rates of 5.2 +/- 0.5 μg/h and 1.9 +/- 0.3 μg/h until more than 90% of the ganciclovir had been released. In series 1 (5 μg/h) implanted eyes, the mean intravitreal ganciclovir levels were maintained at 16 mg/L for up to 42 days. In series 2 (2 μg/h) implanted eyes, the drug levels of 9 mg/L were maintained for up to 80 days (*48*).

The devices first appeared to be well tolerated, but there were some complications noted in the eyes that received series 1 implant . Five of the 9 series 1 eyes developed lens opacification after injection, and 2 experienced retinal detachments. No series 2 eyes or series 1 control eyes (those implanted with drug-free implants) developed any observable abnormalities. The authors attributed the lens opacification to the trauma resulting from the frequent taking of vitreous samples and not to the elevated ganciclovir dose. They admit that it might seem that the elevated drug levels may have played a role, but argue that the implantation of 6 mg ganciclovir pellet (representing the worst possible scenario of device failure) did not cause such abnormalities (*48*). The authors attributed the retinal detachments to the difficulty in working with the small rabbit eyes and to the trauma from repeated vitreous sampling. They do, however, concede that in human eyes, the potential for retinal detachment and vitreous hemorrhage does exist. They concluded that intravitreal ganciclovir implants are generally well tolerated in rabbit eyes and may be an effective therapy in humans with CMV retinitis (*48*).

In a phase I clinical trial, Sanborn and co-workers (*7*) studied the clinical efficacy of the 2 μg/h ganciclovir implant in a series of 8 patients with active CMV retinitis. In this study, thirteen eyes underwent surgical implantation of the device. All eyes showed a halting of the progression of the retinitis within two weeks of implantation, and complete resolution within 8 to 10 weeks. In terms of visual acuity, vision improved in 6 of the 13 eyes, 4 eyes had a decrease in vision, and the remaining three had no demonstrable change.

Complications included mild vitreous hemorrhage that spontaneously resolved (3 of 13), suprachoroidal placement of the device (2 of 13), and one case of a bacterial corneal ulcer that responded to systemic antibiotics. Another complication noted in two eyes was astigmatism after surgery. This astigmatism resolved gradually over 5 weeks, and was not identified in subsequent patients after the suturing technique was modified. Retinal detachment occurred in three eyes of two patients after the retinitis was known to have completely resolved. The authors attributed these occurrences to the natural course of the disease process and not to the trauma of surgery nor the presence of the device. The authors also evaluated the *in vivo* drug delivery rate by removing the implants from five eyes after the death of the patients. The rates ranged from 1.69 to 2.42 μg/h with an average rate of 1.89

Downloaded by 89.163.35.42 on October 31, 2012 | http://pubs.acs.org
Publication Date: September 24, 1998 | doi: 10.1021/bk-1998-0709.ch001

μg/h. Assuming a constant rate of release, the authors estimated the total release time of the implantable device was between 103 and 191 days (*7*).

In another study by the same group, 30 eyes of 22 AIDS patients with CMV retinitis received the ganciclovir implant as the sole therapy for CMV retinitis and were followed prospectively for up to 419 days (*49*). In the study, 27 of the 30 eyes showed initial stabilization of the retinitis with replacement of the opacified area of retina with atrophic pigmented retina. However, reactivation of the retinitis occurred in 9 of the eyes; reactivation time ranged from 106 to 362 days (mean, 188 days). In seven of these 9 eyes, the intraocular device was replaced with a fresh device and the retinitis progression was once again halted. Analysis of the intravitreal drug levels of these seven patients at the time of reimplantation revealed very low or nondetectable drug levels of ganciclovir. The authors contend that these progressions of retinitis were the result of the devices becoming depleted of ganciclovir. This notion is supported by the excellent responses obtained upon reimplantation of a fresh device. In their previous study, the authors stated that the devices should release drug for an average of 137 days (*7*). The authors attributed the discrepancy between these study patients and this prediction to variation in the release rates of the implants (*49*).

After such encouraging results with the 2 μg/h ganciclovir implant (renamed the Mark I device) as the sole therapy for CMV retinitis, work was done to evaluate the safety and efficacy of a lower dose ganciclovir implant that released drug at a rate of 1 μg/h (Mark II device) (*50,51*). The hope was that this lower dose device may be as effective as the higher dose device with fewer side effects. Martin et al., (*50*) performed a randomized control trial involving 30 eyes of 26 AIDS patients who had recently been diagnosed with CMV retinitis and had not received any prior systemic therapy (*50*). Patients were randomly assigned to receive either immediate treatment with the ganciclovir implant or to defer treatment. The authors found that the estimated median time to retinitis progression in the deferred group was 15 days versus 226 days in the immediate treatment group.

One unique aspect of this trial was that the initial implants were replaced with fresh implants at 32 weeks, or earlier if CMV retinitis progression was noted. Previous studies did not have scheduled reimplantations but instead had used retinitis progression as an endpoint to dictate when the implant should be replaced (*49*). Scheduled replacement of the implants at 32 weeks was done to minimize the patients' chances of having progression given that the expected lifetime for the device was between 32.5 and 39.7 weeks. Only five of the fourteen eyes in the immediate treatment group developed retinitis progression. Four of these five underwent reimplantation. Three of these four implants were noted to be devoid of ganciclovir. In addition, the intravitreal drug levels were noted to be zero in these patients. All three of these eyes responded well to reimplantation of a fresh device (*50*). This series of events has been previously reported (*49*). In those eyes in which an *in vivo* drug release rate could be determined, the mean rate was 1.4 μg/h (range 0.5 to 2.88 μg/h) and the mean drug level was 4.1 μg/ml. Given the wide range of release rates, it is not surprising that some of the implants were devoid of ganciclovir prior to the 32-week scheduled reimplantation.

Downloaded by 89.163.35.42 on October 31, 2012 | http://pubs.acs.org
Publication Date: September 24, 1998 | doi: 10.1021/bk-1998-0709.ch001

In total, 39 primary implants and 12 exchange implants were placed in immediate-treatment eyes, deferred-treatment eyes that progressed, and contralateral eyes that developed new CMV disease. The authors reported 7 retinal detachments and one retinal tear. No cases of endophthalmitis were noted. It is noteworthy that the authors estimated the risk of developing CMV retinitis in a previously uninvolved fellow eye was 50% at six months. In addition, 8 (31%) of the 26 patients developed biopsy proven visceral CMV disease. The authors concluded that the Mark II ganciclovir implant is effective in halting progression of CMV retinitis but does not prevent CMV disease systemically or in the fellow eye (*50*).

Further work studying the efficacy of the Mark II device (1 μg/h rate) was done by Duker and co-workers with similar success (*51*). In their study, 29 eyes of 29 patients received implantation of the Mark II device. The authors found that 28 of 29 patients (97%) had no progression of retinitis at the 4-week post-operative evaluation and the median time to progression was 205 days. This group reported similar rates of complications, systemic CMV disease, and fellow eye involvement compared to the study by Martin and co-workers (*50,51*).

In a case study by Gentile and coworkers (*52*), it was reported that the placement of an intravitreal ganciclovir implant was complicated by the formation of cyclodialysis. This necessitated the repositioning of the implant to a different quadrant. Despite gonioscopic evidence of the cyclodialysis cleft, the eye remained normotensive post-operatively.

One of the major criticisms of the ganciclovir implant as the sole therapy for CMV retinitis is that it does not protect a previously uninvolved fellow eye or other organ systems from CMV disease. In patients who initially have unilateral disease, 40-50% develop CMV retinitis in their previously disease-free fellow eye (*50,51*). In addition, 17-30% of patients have been shown to develop systemic CMV disease while receiving only local therapy for their CMV retinitis (*50,51*). In response to these limitations of therapy, Marx and co-workers (*52*) evaluated the utility of using the ganciclovir implant as an adjunct to systemic ganciclovir therapy. In this study, AIDS patients with recurrent CMV retinitis, who had been treated previously with intravenous ganciclovir and/or foscarnet, were implanted with the Mark II device. Of the 57 patients who had follow-up longer than one month, 48 (84%) of them received systemic therapy in addition to the intraocular implant. By the conclusion of the study, 76% of eyes had inactive CMV retinitis at the one month post-operative visit (positive initial response). In addition, only 36% of eyes developed recurrence of retinitis after a positive initial response (median time to progression of 7 months). The authors did not comment on the incidence of systemic CMV during therapy since patients with known systemic disease were included at the outset of the trial. Interestingly, however, of the 18 patients who initially suffered from unilateral retinitis, only 5 (28%) developed disease in the contralateral eye (*53*). This is a mild improvement over what has been reported in previous studies (*50,51*). Therefore, there appears to be some benefit in continued intravenous therapy. The authors concluded that it is necessary to continue systemic therapy to control intraocular and visceral CMV. They do concede, however, that in 30% of these patients, CMV retinitis will eventually recur despite double therapy (*53*).

Downloaded by 89.163.35.42 on October 31, 2012 | http://pubs.acs.org
Publication Date: September 24, 1998 | doi: 10.1021/bk-1998-0709.ch001

Not only was work being undertaken to study the efficacy of the intraocular implants, clinicopathologic studies were also being done to study the histologic changes that occur secondary to CMV retinitis and/or the implant (*54,55*). One of the earliest studies was conducted by Anand and coworkers (*54*), who obtained 7 eyes from 5 patients 2 to 10 hours post-mortum and examined them histologically. In all 7 eyes, varying degrees of retinal atrophy and gliosis were noted, but the investigators concluded that there was no evidence of retinal toxic effects or inflammation at the site of the implant (*54*). Later studies by Charles and co-workers also concluded that histologically, they could find no toxic or adverse effects attributable to the implant (*55*).

Emerging Trends

Liposomally-Encapsulated Foscarnet. As discussed earlier, severe nephrotoxicity, decreased renal function, electrolyte abnormalities, and anemia are among the most serious toxicities of foscarnet that severely limit its use as an antiviral (*1,4*). In addition, its poor penetration into cells and its rapid clearance by the kidney cause it to have a short plasma half-life (*17,18*). Given that the drug is a hydrophilic, negatively charged molecule, it is perfectly suited for liposomal encapsulation.

In a study done by Bergers and coworkers, foscarnet was encapsulated in one of two liposomal preparations (*56*). The first preparation consisted of a mixture of partially hydrogenated egg-phosphatidylcholine (PHEPC), phosphatidylserine (PS), and cholesterol in a molar ratio of 185:15:100, respectively. The second preparation consisted of PHEPC, distearoyl phosphotidylethanolamine with a covalently attached polyethyleneglycol 1900 headgroup (PEG-DSPE), and cholesterol in a molar ratio of 185:15:100, respectively. Both liposomal preparations were evaluated with respect to their *in vitro* efficacy against CMV in differentiated monocytic cells and embryonic lung fibroblasts. The authors found that both liposomal preparations of foscarnet inhibited CMV late antigen expression in monocytic cells and, to a lesser extent, in fibroblasts. They attributed the antiviral effects to the direct uptake of the preparations by the cells. And while the *in vitro* activity of free foscarnet is superior to that of the liposomal preparation, the authors feel that the ability of the latter to stay the in circulation for extended periods of time (half-life 20 hours in a rodent model) may allow it to be more effective *in vivo*—potentially making it an effective intravenous drug delivery system for the treatment of the manifestations of CMV, including retinitis (*56*).

Absorbable Gel-forming Injectable Liquids. In a recent disclosure, Shalaby (*57*) described a novel family of drug carriers for the controlled release of several bioactive agents, including antibiotics, antiviral agents, and vaccines. These carriers are liquid copolymers of polyethylene glycol and absorbable polyester segments that can be injected into biological tissues and transform into flexible or hard gels. Most pertinent to this review is Shalaby's most recent report (*58*) which describes the use of these gel-formers for administration into rabbit vitreous space. Preliminary indications are that neither the examined drug-free gel-formers nor their active

Downloaded by 89.163.35.42 on October 31, 2012 | http://pubs.acs.org
Publication Date: September 24, 1998 | doi: 10.1021/bk-1998-0709.ch001

formulations, which contain up to 10% ganciclovir, cause discernable adverse effects upon intravitreal administration during the 4-week study period. *In vitro* and *in vivo* release studies indicate that these carriers can be used for controlled drug release for at least two weeks. Ongoing activity is focusing on optimizing the composition of the gel-former to prolong the release profile beyond two months.

Conclusion

CMV retinitis continues to be a detrimental sequela of advanced HIV disease despite advances in systemic and local therapy. Early on, studies of systemic antivirals were encouraging, but the toxicities associated with the medications and the eventual recurrence of the retinitis caused efforts to be directed toward developing local therapies to treat the ocular complications of CMV infection. Intravitreal injections of free antivirals proved to have efficacy but were hindered by toxic peak drug levels and unfavorable pharmacokinetic profiles. One active area of research has been the development of sustained-release preparations of antivirals. These include injectable, minimally invasive bioabsorbable systems and nonabsorbable intraocular implants that require one or more surgical procedures. And while these therapies provide effective local therapy for a relatively longer period of time, there is often progression of retinitis despite adequate therapy. One area of research that deserves more exploration is prophylactic therapy for CMV retinitis. Some animal studies of CMV prophylaxis have been undertaken with moderate success (*42*), but human trials are lacking at this time.

Downloaded by 89.163.35.42 on October 31, 2012 | http://pubs.acs.org
Publication Date: September 24, 1998 | doi: 10.1021/bk-1998-0709.ch001

Literature Cited

1. Friedberg, D.N., *Journal of the Acquired Immune Deficiency Syndromes and Human Retrovirology,* **1997**, *14*(*Suppl. 1*), pp. S1-S6.
2. Hardy, W.D., *Journal of the Acquired Immune Deficiency Syndromes and Human Retrovirology,* **1997**, *14*(*Suppl. 1*), pp. S7-S12.
3. McAuliffe, P.F., Hall, M.J., Castro-Malaspina, H., Heinemann, M.H., *American Journal of Ophthalmology,* **1997**, *123*, pp. 702-703.
4. Bright, D.C., *Journal of the American Optometric Association,* **1997**, *68*, pp. 11-30.
5. Jabs, D.A., Enger, C., Bartlett, J.G., *Archives of Ophthalmology,* **1989,** *107*, pp. 75-80.
6. Hennis, H.L., Scott, A.A., Apple, D.J., *Survey of Ophthalmology,* **1989**, *34*, pp. 193-203.
7. Sanborn, G.E., Anand, R., Torti, R.E., Nightingale, S.D., Cal, S.X., Yates, B., Ashton, P., Smith, T., *Archives of Ophthalmology,* **1992**, *110*, pp, 188-195.
8. Kupperman, B.D., *Journal of the Acquired Immune Deficiency Syndromes and Human Retrovirology,* **1997**, *14*(*Suppl. 1*), pp S13-S21.
9. Polis, M.A., Masur, H., *JAMA*, **1995**, *273*, pp. 1457-1459.
10. Spector, S.A., *Journal of the Acquired Immune Deficiency Syndromes and Human Retrovirology,* **1997**, *14*(*Suppl. 1*), pp. S32-S35.

11. Spector, S.A., Weingeist, T., Pollard, R.B., Dieterich, D.T., Samo, T., Benson, C.A., Busch, D.F., Freeman, W.R., Montague, P., Kaplan, H.J., Kellerman, L., Crager, M., De Armond, B., Buhles, W., Feinberg, J., *Journal of Infectious Diseases,* **1993,** *168,* pp. 557-563.
12. Elliot, P.J., Bartus, R.T., Mackic, J.B., Zlokovic, B.V., *Pharmaceutical Research,* **1997**, *14*, pp. 80-85.
13. Hochster, H., Dieterich, D., Bozzette, S., Reichman, R.C., Connor, J.D., Liebes, L., Sonke, R.L., Spector, S.A., Valentine, F., Pettinelli, C., Richman, D.D., *Annals of Internal Medicine,* **1990**, *113*, pp. 111-117.
14. Hardy, W.D., *Journal of the Acquired Immunodeficiency Syndromes and Human Retrovirology*, **1991**, *4(Suppl 1*), pp. S22-S28.
15. Drew, W.L., Ives, D., Lalezari, J.P., Crumpacker, C., Follansbee, S.E., Spector, S.A., Benson, C.A., Friedberg, D.N., Hubbard, L., Stempien, M.J., Shadman, A., Buhles, W., *The New England Journal of Medicine,* **1995**, *333*, pp. 615-620.
16. Palestine, A.G., Polis, M.A., De Smet, M.D., Baird, B.F., Falloon, J., Kovacs, J.A., Davey, R.T., Zurlo, J.J., Zunich, K.M., Davis, M., Hubbard, L., Brothers, R., Ferris, F.L., Chew, E., Davis, J.L., Rubin, B.I., Mellow, S.D., Metcalf, J.A., Manischewitz, J., Minor, J.R., Nussenblatt, R.B., Massur, H., Lane, H.C., *Annals of Internal Medicine.* **1991**, *115*, pp. 665-673.
17. Sjovall, J., Bergdahl, S., Movin, G., Ogenstad, S., Saarimaki, M., *Antimicrobial Agents and Chemotherapy,* **1989**, *33*, pp. 1023-1031.
18. Hengge, U.R., Brockmeyer, N.H., Malessa, R., Ravens, U., Goos, M., *Antimicrobial Agents and Chemotherapy,* **1993**, *37*, pp. 1010-1014.
19. Studies of Ocular Complications of AIDS Research Group in Collaboration with the AIDS Clinical Trials Group. Combination Foscarnet and Ganciclovir therapy vs Monotherapy for the Treatment of Relapsed Cytomegalovirus Retinitis in Patients with AIDS: the Cytomegalovirus Retreatment Trial. *Archives of Ophthalmology,* **1996**, *114*, pp. 23-33.
20. Kirsch, L.S., Arevalo, J.F., DeClercq, E., Chavez, D. E., Munguia, D., Garcia, R., Freeman, W.R., *American Journal of Ophthalmology,* **1995**, *119*, pp. 466-476.
21. Lalezari, J.P., Stagg, R.J., Kupperman, B.D., Holland, G.N., Kramer, F., Ives, D.V., Youle, M., Robinson, M.R., Drew, W.L., Jaffe, H.S., *Annals of Internal Medicine,* **1997**, *126*, pp. 257-263.
22. Lalezari, J.P., Kupperman, B.D., *Journal of the Acquired Immune Deficiency Syndromes and Human Retrovirology,* **1997**, *14*(*Suppl. 1*), pp. S27-S31.
23. Lalezari, J.P., *Journal of the Acquired Immune Deficiency Syndromes and Human Retrovirology,* **1997**, *14*(*Suppl. 1*), pp. S22-S26.
24. Henry, K., Cantrill, H., Fletcher, C., Chinnock, B.J., Balfour, H.H., *American Journal of Ophthalmology,* **1987**, *103*, pp. 17-23.
25. Cantrill, H.L., Henry, K., Melroe, N.H., Knobloch, W.H., Ramsay, R.C., Balfour, H.H., *Ophthalmology,* **1989**, *96*, pp. 376-374.

Downloaded by 89.163.35.42 on October 31, 2012 | http://pubs.acs.org
Publication Date: September 24, 1998 | doi: 10.1021/bk-1998-0709.ch001

26. Cochereau-Massin, I., Lehoang, P., Lautier-Frau, M., Zazoun, L., Marcel, P., Robinet, M., Matheron, S., Katlama, C., Gharakhanian, S., Rozenbaum, W., Ingrand, D., Gentilini, M., *Ophthalmology,* **1991**, *98*, pp. 1348-1355.
27. Heinemann, M.H., *Archives of Ophthalmology,* **1989**, *107*, pp. 1767-1772.
28. Ussery, F.M., Gibson, S.R., Conklin, R.H., Piot, D.F., Stool, E.W., Conklin, A.J., *Ophthalmology,* **1988**, *95*, pp. 640-648.
29. Daikos, G.L., Pulido, J., Kathpalia, S.B., Jackson, G.G., *British Journal of Ophthalmology,* **1988**, *72*, pp. 521-524.
30. Diaz-Llopis, M., Chipont, E., Sanchez, S., Espana, E., Navea, A., Menezo, J.L., *American Journal of Ophthalmology,* **1992**, *114*, pp. 742-747.
31. Lieberman, R.M., Orellana, J., Melton, R.C., *The New England Journal of Medicine,* **1994**, *330*, pp. 868-869.
32. Diaz-Llopis, M., Espana, E., Munoz, G., Navea, A., Chipont, E., Cano, J., Menezo, J.L., Romero, F.J., *British Journal of Ophthalmology,* **1994**, *78*, pp. 120-124.
33. Kirsch, L.S., Arevalo, J.F., Chavez, D.E., Munguia, D., DeClercq, E., Freeman, W.R., *Ophthalmology,* **1995**, *102*, pp. 533-543.
34. Taskintuna, I., Rahhal, F.M., Arevalo, J.F., Munguia, D., Banker, A.S., De Clercq, E., Freeman, W.R., *Ophthalmology,* **1997**, *104*, pp. 1049-1057.
35. Palestine, A.G., Cantrill, H.L., Luckie, A.P., Ai, E., ISIS 2922 [Abstract]. *Abstracts of the Xth International Conference on AIDS,* **1994**, pp. 332B.
36. Bangham, A.D., *Progressive Biophysics and Molecular Biology,* **1968**, *18*, pp. 31-37.
37. Peyman ,G.A., Charles, H.C., Liu, K.R., Khoobehi, B., Niesman, M., *International Ophthalmology,* **1988**, *12*, pp. 175-182.
38. Diaz-Llopis, M., Martos, M.J., Espana, E., Cervera, M., Vila, A.O., Navea, A., Molina, F.J., Romero, F.J., *Documenta Ophthalmologica,* **1992**, *82*, pp. 297-305.
39. Peyman, G.A., Khoobehi, B., Tawakol, M., Schulman, J.A., Mortada, H.A., Alkan, H., Fiscella, R., *Retina,* **1987**, *7*, pp. 227-229.
40. Le Bourlais, C., Chevanne, F., Ropert, P., Bretagne, G., Acar, L., Zia, H., Sado, P.A., Needham, T., Leverge, R., *Journal of Microencapsulation,* **1996**, *13*, pp. 473-480.
41. Besen, G., Flores-Aguilar, M., Assil, K.K., Kuppermann, B.D., Gangan, P., Pursley, M., Munguia, D., Vuong, C., De Clerq, E., Bergeron-Lynn, G., Azen, S.P., Freeman, W.R., *Archives of Ophthalmology,* **1995**, *113*, pp. 661-668.
42. Kuppermann, B.D., Assil, K.K., Vuong, C., Besen, G., Wiley, C.A., DeClercq, E., Bergeron-Lynn, G., Connor, J.D., Pursley, M., Munguia, D., Freeman, W.R., *The Journal of Infectious Diseases,* **1996**, *173*, pp. 18-23.
43. El-Samaligy, M.S., Rojanasakul, Y., Charlton, J.F., Weinstein, G.W., Lim, J.K., *Drug Delivery,* **1996**, *3*, pp. 93-97.
44. Gilding, D.K., in *Biocompatibility in Clinical Implant Materials,* Williams, D.F., Ed., Vol. 2, CRC Press, Boca Raton, **1981**, pp. 209-232.
45. Cohen, S., Yoshioka, T., Lucarelli, M., Hwang, L.H., Langer, R., *Pharmaceutical Research,* **1991**, *8*, pp. 713-720.

Downloaded by 89.163.35.42 on October 31, 2012 | http://pubs.acs.org
Publication Date: September 24, 1998 | doi: 10.1021/bk-1998-0709.ch001

46. Refojo, M.F., Herrero-Vanrell, R., ARVO Abstracts, *Investigative Ophthalmology and Visual Science*, **1996**, *37*, pp. S41.
47. Veloso, A.A.S., Zhu, Q., Herrero-Vanrell, R., Refojo, M.F., *Investigative Ophthalmology and Visual Science*, **1997**, *38*, pp. 665-675.
48. Smith, T.J., Pearson, P.A., Blandford, D.L., Brown, J.D., Goins, K.A., Hollins, J.L., Schmeisser, E.T., Glavinos, P., Baldwin, L.B., Ashton, P., *Archives of Ophthalmology*, **1992**, *110*, pp. 255-258.
49. Anand, R., Nightingale, S.D., Fish, R.H., Smith, T.J., Ashton, P., *Archives of Ophthalmology*, **1993**, *111*, pp. 223-227.
50. Martin, D.F., Parks, D.J., Mellow, S.D., Ferris, F.L., Walton, R.C., Remaley, N.A., Chew, E.Y., Ashton, P., Davis, M.D., Nussenblatt, R.B., *Archives of Ophthalmology*, **1994**, *112*, pp. 1531-1539.
51. Duker, J.S., Robinson, M., Anand, R., Ashton, P., *Ophthalmic Surgery and Lasers*, **1995**, *26*, pp. 442-448.
52. Gentile, C.G., Lewis, J.M., Puklin, J.E., *Archives of Ophthalmology*, **1997**, 15, pp. 1204
53. Marx, J.L., Kapusta, M.A., Patel, S.S., LaBree, L.D., Walonker, F., Rao, N.A., Chong, L.P., *Archives of Ophthalmology*, **1996**, *114*, pp. 815-820.
54. Anand, R., Font, R.L., Fish, R.H., Nightingale, S.D., *Ophthalmology*, **1993**, *100*, pp. 1032-1039.
55. Charles, N.C., Steiner, G.C., *Ophthalmology*, **1996**, *103*, pp. 416-421.
56. Bergers, J.J., Hengge, U.R., Snijders, S.V., Bakker-Woudenberg, I.A., *Journal of Controlled Release*, **1997**, *47*, pp. 163-171.
57. Shalaby, S.W., U.S. Patent (to Poly-Med, Inc.), 5,612,058, **1997**.
58. Shalaby, S.W., Final Report on Phase I SBIR entitled, Injectable Absorbable Ocular Inserts for Controlled Drug Delivery, **July 1997**.

Downloaded by 89.163.35.42 on October 31, 2012 | http://pubs.acs.org
Publication Date: September 24, 1998 | doi: 10.1021/bk-1998-0709.ch001

Downloaded by YORK UNIV on October 31, 2012 | http://pubs.acs.org
Publication Date: September 24, 1998 | doi: 10.1021/bk-1998-0709.ch002

Chapter 2

Key Features and Future Perspectives in the Development of Intravaginal Drug Delivery Systems

Waleed S. W. Shalaby[1] and Shalaby W. Shalaby[2]

[1]Department of Obstetrics and Gynecology, University of Pennsylvania Medical Center, Philadelphia, PA 19104
[2]R&D Laboratories, Poly-Med, Inc., Pendleton, SC 29670

Intravaginal drug delivery is an area of growing interest for topical, local, and systemic therapy. As women's health issues come to the forefront of medical research, intravaginal drug delivery may play a significant role. The successful development of intravaginal drug delivery systems will require a basic appreciation for an array of topics ranging from vaginal anatomy and physiology to the design of novel biomaterials. It is clear, however, that a multidisciplinary approach will not only facilitate our understanding of this field, but identify key barriers that will need to be overcome to optimize drug efficacy, patient compliance, and safety. This review attempts to address the variety of areas pertinent to the development of intravaginal drug delivery systems. The topics discussed include the anatomy and physiology of the vagina, mechanisms of drug absorption and drug disposition, mechanisms of drug delivery, and the design of drug delivery systems for the vagina. In addition, current examples of intravaginal drug delivery in obstetrics, reproductive medicine, hormone replacement therapy, infectious diseases, and gynecologic oncology will be reviewed. Finally, new trends in the development of new polymeric drug carriers and future perspectives are noted.

In recent years, a number of women's health issues have generated considerable interest. Areas of particular importance to women of reproductive age include obstetrics, medical terminations, contraception, infertility, sexually transmitted diseases, and cancers of the reproductive tract. In the postmenopausal women, the lack of endogenous estrogen profoundly influences bone remodeling, the cardiovascular system, and the lower urogenital tract. Thus, the benefits of hormone replacement therapy are without debate in terms of osteoporosis, vaginal atrophy, urinary incontinence, and reducing the risk of myocardial infarction.

Many therapeutic strategies have been developed to improve women's health. While oral, intravenous, and transdermal routes of drug administration have been widely utilized, intravaginal drug delivery has been studied to a far lesser extent. Interestingly, there are many instances where intravaginal drug delivery may be ideal. Drug specificity intended for the reproductive tract may be more effectively achieved through intravaginal administration. As a result, high local drug levels may be achieved at a fraction of the oral or IV doses, respectively. A secondary benefit would be to improve patient compliance in terms of dosing frequency and/or systemic side effects. The rich vascular supply of the vagina also represents a rapid portal of entry when systemic drug levels are desired. Because of the anatomy, first-pass hepatic metabolism is bypassed which may serve to improve the bioavailability of certain agents. While the possibility of treating many disease states is attractive, a number of important questions need to be addressed before the true potential of this drug administration route can be realized. As in many areas of applied science, a multi-disciplinary approach often yields the most efficient, yet practical results. Therefore, this review attempts to examine a number of areas pertinent to the design and application of intravaginal drug delivery systems. In this regard, topics ranging from basic anatomy and physiology of the vagina to the design of sustained released drug delivery systems are discussed. Current examples of intravaginal drug delivery will also be reviewed in an effort to highlight areas for future investigation.

Downloaded by YORK UNIV on October 31, 2012 | http://pubs.acs.org
Publication Date: September 24, 1998 | doi: 10.1021/bk-1998-0709.ch002

Anatomy and Physiology of the Vagina

The concept of intravaginal drug delivery encompasses a number of considerations beginning with a basic appreciation for the anatomic, physiologic, and microbiologic aspects of the vagina. Understanding the vagina under normal and disease states will aid in identifying critical physiological barriers that will facilitate the rational design and characterization of intravaginal drug delivery systems.

Key Histological Features. The vagina is a fibromuscular tube that exists in a relaxed state. The walls are suspended by their attachment to the paravaginal lateral connective tissue and the arcus tendineus (*1*). Grossly, the vagina possesses many rugal folds. While the pattern varies dramatically, the folds provide a certain degree of distensibility to minimize laceration. The vagina is lined by stratified squamous epithelium that are rich in glycogen during the reproductive years. The surface of the vaginal cell is made up of numerous microridges that run longitudinally or in circles (*2*). It is believed that the morphology and pattern of the microridges affect the firmness of the epithelium (*3*). The epithelium is comprised of 5 layers (*4,5*). The first three layers are the superficial, transitional, and intermediate layers. Deep to these layers reside the parabasal and basal layers. Traversing along the vaginal epithelium is a system of intercellular channels. It is believed that this network provides a route for transport of macromolecules, fluids, and cells from the basal lamina to the vaginal lumen. Furthermore, transport may also proceed in the opposite direction, which would have unique implications for high molecular weight agents including peptide drugs. The basal lamina contains macrophages, lymphocytes, plasma cells, Langerhan's cells, eosinophils, and mast cells. Lymphocytes reside predominantly in the intermediate, parabasal, and basal layers. During infection, these cells can migrate into the intercellular channels toward the surface epithelium. Post-menopausally, the vagina undergoes an alteration in the pattern of the rugae with an associated decrease of epithelial thickness, glycogen deposition, and cell size. Furthermore, the microridges become irregular with increased cell fragmentation (*6*). Beneath the epithelium resides a thin layer of elastic fibers followed by a well-developed fibromuscular layer. The latter is described as a muscular meshwork of smooth muscle oriented longitudinally in the innermost aspect while becoming more circularly arranged peripherally (*7*). External to the muscular layer is a fibrous capsule that contains large venous plexuses as well as elastic fibers.

Downloaded by YORK UNIV on October 31, 2012 | http://pubs.acs.org
Publication Date: September 24, 1998 | doi: 10.1021/bk-1998-0709.ch002

Vaginal Anatomy. The vagina is a potential space with walls that are easily distensible. The overall shape of the vaginal canal and its distensibility is limited by the elasticity of the vaginal wall and its proximity to other pelvic organs. The introitus of the vagina is located between the urethra and symphysis superiorly and the rectum posteriorly. In the upright position, the vagina is directed obliquely upward and backward at approximately a 45 degree angle to the horizontal axis. The vagina has a convex curve, resulting in an almost horizontal axis of the upper two-thirds of the vagina. The anterior and posterior walls of the vagina are slack and remain in contact with each other. The lateral walls of the vagina are fairly rigid and defined by the anatomical pelvic support. The lower third of the vagina is supported by connection with fibers of the pelvic and urogenital diaphragms. The middle third receives its main support from the lateral and inferior segments of the cardinal ligament. The upper third, however, rests mainly on the rectum which overlies the pubococcygei of the levator plate (*1*). It maintains its position over the levator plate through lateral attachments to the upper cardinal ligaments (*8*). Because the lateral walls remain separated, cross sections of the vagina take on a classic H-shaped appearance (*1*). The dimensions of the vagina vary considerably depending on both sexual arousal and reproductive stage. In a normal reproductive aged woman the anterior wall of the vagina measures 6 to 8 centimeters in length while the posterior wall is up to 14 centimeters in length (*9-11*). Since the cervix is incorporated in the anterior vaginal wall, the length of the anterior vagina plus cervix approximates the length of the posterior wall. The shape of the vagina also varies considerably among women. Common features of the vagina include a posterior widening around and behind the cervix with posterior fornices being quite deep in some subjects. Anterior to the cervix, the caliper of the vagina is constricted especially near the introitus.

Vascular and Lymphatic Systems of the Pelvis. In general, the arteries of the pelvis are bilateral with multiple collateral vessels (*12*). They enter their respective organ laterally and unite at the midline through multiple anastomoses. The arteries interpenetrate a large venous meshwork to terminate via branching arcades. The venous system of the reproductive organs lie within a meshwork of large veins that form numerous interconnecting venous plexuses. The arterial supply is intimately related as it interpenetrates the venous plexus on route to respective organs (*12*). Venous drainage of the pelvis begins in small sinusoids which lead to adjacent venous plexuses. These venous plexuses, interestingly, communicate with plexuses in the paravaginal tissue, perineum, rectum, and bladder (*1*). The veins of the pelvis and perineum are generally thin walled and contain few valves. They drain the pelvic plexuses along the course of their corresponding arterial supply.

A minor contribution to drug absorption and disposition may reside with the lymphatic architecture of the pelvis (*13*). In the vagina, the lymphatic system is divided into three anatomical groups. At the mucosal surface, lymphatics originate from numerous mucosal plexuses that anastomose with deeper muscular plexuses. The superior group of lymphatics join those of the cervix where they follow the uterine artery to terminate in either the external iliac nodes or anastomose with the uterine plexus. The middle group of lymphatics drain the greater part of the vagina. They follow the vaginal arteries to the hypogastric channels. The inferior group forms anastomoses with the opposite side and travel either upward to connect with the middle group of lymphatics or toward the vulva to drain into the inguinal nodes. Lymphatic drainage of the uterus includes several chains of lymph nodes--the external iliac chain or lateral sacral nodes.

Downloaded by YORK UNIV on October 31, 2012 | http://pubs.acs.org
Publication Date: September 24, 1998 | doi: 10.1021/bk-1998-0709.ch002

Vaginal Microbiology. Infectious diseases involving the vagina have received considerable interest in recent years. With the rise in incidence of pelvic inflammatory disease and HIV transmission, research efforts have focussed both on treatment and prophylactic strategies. While our understanding of the vaginal microbiology has largely resulted from research in bacterial vaginitis, vaginal immunology is comparatively in its infancy. These areas will be briefly discussed since it is likely that future therapeutic interventions will be in the form of delivery systems containing various microbicidal and virucidal agents as well as vaccines.

Microbial colonization involves multiple species of organisms that are neither uniform in growth requirements nor metabolic end products (*14*). The vagina contains 109 bacterial colony forming units/gram of secretions (*15*). Isolates include a variety of aerobic and anaerobic bacteria, yeast, viruses, and parasites. An extensive review of these organisms is discussed by Sweet and Gibbs (*15*). The microecology of the vagina is characterized by a dynamic equilibrium of host-microbe and endogenous-exogenous microbe interactions (*14*). Thus, synergistic or antagonistic effects arise depending on the nature of the physiological stress on the microecology. Metabolic end products have long been considered to be significant flora-controlling substances. They may serve as a growth substrate for one species of bacteria or inhibit the growth of others. For example, lactic acid produced by lactobacilli is well recognized for its ability to control bacterial growth in the adult vagina through pH regulation between 4.0 and 5.0 (*16*). For this reason, only acid tolerant species are permitted to grow. Hydrogen peroxide has also been postulated as an alternative explanation for the growth-controlling success of certain lactobacilli strains (*16*). Other agents may also serve to control bacterial

Downloaded by YORK UNIV on October 31, 2012 | http://pubs.acs.org
Publication Date: September 24, 1998 | doi: 10.1021/bk-1998-0709.ch002

colonization. It is believed that antibacterial toxins, such as gliotoxin and hemolysin from G. vaginalis, as well as bacteriotoxins exert antagonistic effects (*14,17*). Another aspect of the vaginal microenvironment that controls bacterial colonization is the low oxidation-reduction potential. Studies have shown that anaerobic bacteria outnumber facultative species by a factor of 10 (*18*). Investigators believe that the low redox potential is related to the presence of obligate anaerobes and facultative organisms in addition to oxygen-consuming organisms such as staphylococci, streptococci, and E. coli.

The microbial environment of the vagina is also be influenced by other factors, such as age, sexual activity, contraceptive and antibiotic use, and childbirth. At birth, maternal estrogen facilitates vaginal colonization by Lactobacilli. However, Lactobacilli disappear over the course of several weeks as the estrogen effect diminishes. Lactobacilli later dominate the vaginal flora with the onset of puberty and thereafter during the reproductive years (*14*). Lactobacillus colonization declines during menopause. From these observations, it appears that Lactobacillus colonization is largely influenced by estrogenic effects. It should be noted, however, that control of vaginal colonization is still not well understood. Much of the debate is focussed on whether the production of metabolic substrates that are used by Lactobacilli are solely influenced by estrogen. Estrogen is believed to promote glycogen deposition in the vaginal epithelium. Most Lactobacilli utilize glycogen through fermentation to yield lactic acid. However, studies have shown that some Lactobacilli are not capable of utilizing glycogen. Furthermore, glycogen deposition does not change between pre- and post-menopausal women (*14*). Despite the specific mechanisms involved, it is generally agreed that estrogen stimulation plays an important role in the normal colonization of the vagina. Sexual intercourse also leads to changes in the vagina. This occurs through the introduction of the sexually transmitted pathogens such as N. gonorrhoeae, C. trachomatis, and herpes virus. The use of intrauterine devices for contraception has been found to increase the number of anaerobic bacteria in the cervix. It is believed that this increases the risk for bacterial vaginitis (*19,20*). The use of diaphragms in conjunction with spermicide have been associated with recurrent urinary tract infections through vaginal colonization by E. coli (*21*). Interestingly, oral contraceptives have a minimal effect on the vaginal environment (*19*). The effects of parenteral antibiotics on vaginal flora has been studied (*22-24*). Short-term prophylactic use with antibiotics, such as penicillin or cefazolin has been shown to have little effect while longer courses increase the presence of Pseudomonas or enterococci. During pregnancy, there is a progressive increase in Lactobacillus colonization as well as the prevalence of yeast (*25*). Whether a synergism exists between yeast and Lactobacillus or other vaginal flora has yet to be determined (*14*). After delivery, the vaginal flora undergo a dramatic change with the prevalence of anaerobic species. It is postulated that anaerobic colonization is related to birth trauma, the presence of lochia and suture materials, and hormonal changes (*15*). The vaginal flora, however, is restored to a normal distribution by the sixth week postpartum. In summary, it should be stressed that the vaginal ecosystem represents an array of organisms that are in a dynamic equilibrium undergoing shifts in population density in response to exogenous and endogenous influences. The net response either benefits the host by minimizing colonization of exogenous microorganisms or produces undesirable lower and upper genital tract infections.

Intravaginal Drug Delivery

Intravaginal drug delivery can be utilized for topical, local, or systemic effects. Topical administration has been used to treat various bacterial or fungal infections, atrophic vaginitis, and vaginal intraepithelial neoplasia. In terms of local pelvic therapeutics, intravaginal drug delivery has been used in the treatment of stress urinary incontinence, labor induction, and medical abortions. However, some of the most dramatic advances in the future may be seen in the areas of hormone replacement therapy, contraception, and infertility. This is largely due to the relative ease of vaginal drug absorption and avoidance of first pass hepatic metabolism. The benefits of biomaterials to provide sustained drug release and increase vaginal residence times may serve to improve therapeutic efficacy. To date, there has been limited attempts to study the mechanisms that control both vaginal drug absorption and drug distribution. Models for drug absorption have stemmed from early studies in mice and rabbits which have not been validated in human studies. Furthermore, recent observations in the areas of infertility and oncology raise many questions regarding the mechanisms of drug disposition from the vagina. In the next sections, the data from both animal and human studies are reviewed in an effort to develop kinetic models for both drug absorption and drug distribution.

Downloaded by YORK UNIV on October 31, 2012 | http://pubs.acs.org
Publication Date: September 24, 1998 | doi: 10.1021/bk-1998-0709.ch002

Drug Absorption. The large surface area of the vaginal epithelium combined with the rich vascular supply make it an ideal route for drug administration. Contributions by Benzinger et al. and Aref et al. have extensively reviewed the various classes of drugs and chemical agents that undergo vaginal absorption (*26,27*). The mechanisms involved in vaginal drug absorption obey many of the basic concepts developed from gastrointestinal drug absorption (*28-33*). Drug absorption depends on the physicochemical properties of the drug in terms molecular weight, dissolution characteristics, and ionic character. Absorption may proceed either by simple diffusion and/or by active transport. Many drugs, however, are weakly acidic or basic. Therefore, the equilibrium dissociation constant of the drug, the microenvironment pH of the delivery vehicle, and the vaginal pH will have an important effect on the extent of drug absorption. The pH-partition hypothesis was developed and based on the observation that biologic membranes were predominately lipophilic and that drug penetration occurs mainly in the undissociated form (*34*). It was believed that drug transport by passive diffusion favored the fraction of undissociated drug at a given pH. In biological systems, however, this was found to be partly applicable given the observations that appreciable amounts of ionized drug partitioned across lipophilic membranes. This was explained, in part, when ionic and nonionic species were found to be transported across the aqueous channels of biologic membranes (*35-37*). These observations led to a diffusion model for drug absorption. The model incorporated a simple aqueous boundary layer in series with the biologic membrane. The membrane was composed of lipophilic regions in parallel with aqueous pores. This model was later applied to vaginal drug absorption and tested in rabbits. Under steady state conditions, drug diffusion across the vaginal mucosa may be described by Fick's Law:

$$-dM/dt = DmSK/h\,(Cv - Cp) \qquad (1)$$

where M is the amount of drug in the vagina at time t, Dm is the diffusivity in the vaginal membrane, S is the surface area, K is the partition coefficient between the aqueous medium of the vagina and the vaginal epithelium, h is the thickness of the vaginal epithelium, and Cv and Cp are the drug concentrations in the vagina and plasma, respectively. If the vaginal drug concentration is kept high relative to the plasma compartment, then sink conditions are meet and Cp is omitted from Equation 1.

$$-dM/dt = DmSKCv/h \qquad (2)$$

Equation 2 can be rearranged to describe the permeability of drug across the vaginal epithelium. By converting the left side of Equation 2 to concentration units, the permeability coefficient can be described as follows:

$$Pv = -V/Cv\,(dCv/dt) \qquad (3)$$

where V is the volume of the vaginal compartment, and Pv is the permeability coefficient (cm/sec) for drug passage from vagina to plasma. It should be noted that certain stimulating hormones such as estrogen will increase the thickness of the vaginal epithelium, and thus, alter drug permeability (*28*). Drug flux across mucosal membranes is described by Equation 4:

$$J = PappCv \qquad (4)$$

where J is the flux and Cv represents total drug concentration in the vagina (Dolusio et al.). The apparent permeability coefficient (Papp) is expressed by Equation 5

$$Papp = (1/Paq + 1/Pm)-1 \qquad (5)$$

in which Paq is the permeability coefficient of drug in the aqueous boundary layer and Pm is the effective permeability coefficient for drug in the lipophilic and aqueous regions of the membrane. The flux may be expressed in terms of concentration Cv in the vagina by combining with it a term for vaginal volume (V) and surface area (S) as shown in Equation 6:

$$J = -V/S(dCv/dt) \qquad (6)$$

Downloaded by YORK UNIV on October 31, 2012 | http://pubs.acs.org
Publication Date: September 24, 1998 | doi: 10.1021/bk-1998-0709.ch002

Downloaded by YORK UNIV on October 31, 2012 | http://pubs.acs.org
Publication Date: September 24, 1998 | doi: 10.1021/bk-1998-0709.ch002

Since rate of drug loss from the vagina can be written as

$$dCv/dt = - K_aCv \qquad (7)$$

then Equation 7 may be substituted into Equation 6 yielding

$$J = V/S(K_aCv) \qquad (8)$$

where K_a is the absorption rate constant (sec^{-1}). The absorption rate constant may then be expressed as follows by combining Equations 4 and 5 with Equation 8.

$$K_a = (S/V)(Paq)/(1 + Paq/Pm) \qquad (9)$$

In effect, the above derivation shows that vaginal drug absorption will be influenced by the interplay of pH, drug dissociation and lipophilicity, membrane permeability via lipid and aqueous pore pathways, and permeability across the aqueous diffusion layer (Figure 1).

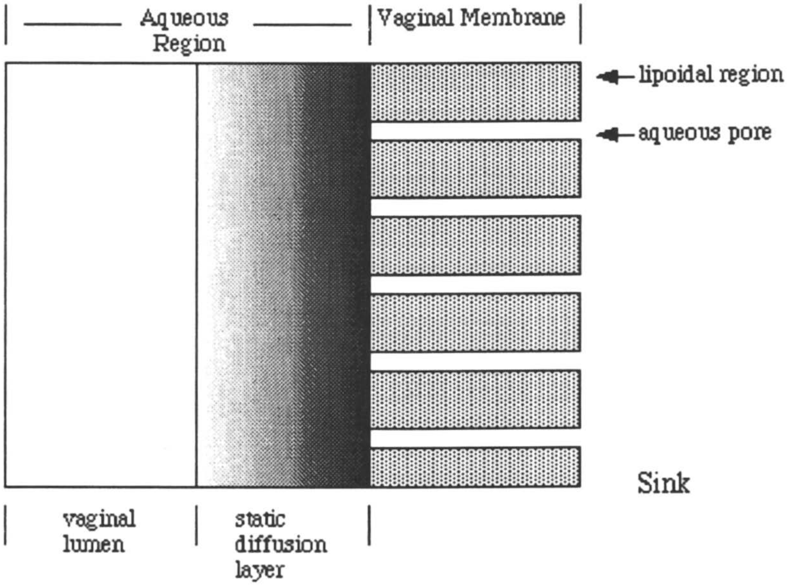

Figure 1. Model of drug absorption from the vagina. (adapted from Reference *32*)

Drug Disposition After Vaginal Administration. As mentioned earlier, vaginal administration of drugs provide unique advantages in terms of high local drug levels and decreased systemic side effects (*38,39*). For drugs with low bioavailability, the vaginal route is ideal for achieving therapeutic levels since it bypasses hepatic first-pass metabolism. The administration of estradiol and micronized progesterone are excellent examples of how bioavailability can be optimized through the intravaginal route (*40-42*). Rigg et al. studied systemic levels of 17b-estradiol and conjugated estrogens using vaginal creams (*43*). A 2 mg dose produced detectable levels of estradiol within 15 minutes with peak concentrations reached at 4 hours. Circulating levels of estradiol were also found to be dose-dependent. Peak concentrations after a 0.2 mg dose and 2 mg dose were 7 and 45 times the mean basal level, respectively. Administration of conjugated estrogens, in contrast, resulted in a slower rise in serum levels with lower peak concentrations. Drug levels were first detected 3 hours after administration with peak concentrations that were 2.5 times the basal level. Similar data have been reported elsewhere (*44,45*). Heimer et al., compared the systemic levels of estriol after oral and vaginal administration (*46*). They showed that the 24 hour levels as measured by the area under the curve (AUC) were nearly equivalent when 1 mg of estriol was given vaginally as compared with a 10 mg oral dose. Furthermore, estriol levels after 21 days of intravaginal dosing were still equivalent to the 10 mg oral dose despite a mature vaginal epithelium.

Chakmakjian et al., studied the bioavailability of micronized progesterone as a function of administration route (*47*). Micronized progesterone levels were measured after 50 mg to 200 mg doses were given sublingually, orally (capsule and tablet), vaginally, and rectally. Peak levels were observed within one hour via the sublingual route and between 2 and 3 hours for the other routes. The 24 hour serum levels after vaginal and rectal dosing were found to be nearly 2 - 2.5 times that of the oral route. The AUC calculations for the first 8 hours showed that the rectal route displays the highest bioavailability (169.9 cm2) , followed by the vaginal (96 cm2), sublingual (95 cm2), and oral (76.9 cm2) routes, respectively. The authors postulated that the bioavailability difference between the vaginal and rectal routes was due to drug loss from the vagina. Similar studies using different delivery vehicles have indicated improved bioavailability presumably by minimizing vaginal drug loss (*38, 48*).

It is evident from the above-noted studies that vaginal drug administration can be utilized to achieve systemic levels for certain agents. However, a poorly understood phenomenon are the high local levels observed throughout the reproductive system that are not attainable through intravenous or oral routes of administration. Recent studies by Miles et al. compared endometrial tissue levels of progesterone after vaginal and intramuscular administration (*49*). Twenty functionally agonadal women, aged 25 to 54 years, were enrolled in the study. All subjects underwent estrogen and progesterone simulated replacement cycle. On day 16 of the estrogen replacement cycle, patients either received vaginally administered micronized progesterone capsules (200 mg) every 6 hours or intramuscular progesterone (50 mg) twice daily. Endometrial sampling with a pipelle endocurette was performed on day 21 of the simulated cycle. Samples were then assayed for progesterone concentration as well as estrogen and progesterone receptor content. Serum progesterone levels by cycle day 21 were 221.89 + 18.78 nmol/L after IM

Downloaded by YORK UNIV on October 31, 2012 | http://pubs.acs.org
Publication Date: September 24, 1998 | doi: 10.1021/bk-1998-0709.ch002

injection and 37.83 + 3.82 nmol/L after intravaginal administration. However, endometrial concentrations were 4.45 + 1.27 after IM versus 36.56 + 8.27 nmol/L vaginally. Thus, an 8-fold increase in endometrial levels was achieved despite serum concentrations that were nearly 6-fold less. These studies clearly identified the significance local drug distribution following vaginal administration. Mizutani et al. determined danazol concentrations in the ovary, uterus, and serum after daily vaginal administration (*50*). Patients making up the study were women with regular menstrual cycles, ages 23 to 43 years, who were to undergo hysterectomy and unilateral oophorectomy. A single vaginal administration of danazol resulted in rapid uptake in the ovary and uterus within 4 hours. The highest levels were achieved in the ovary. The authors postulated that vaginally and orally administered danazol reach the ovary and uterus by different routes. They proposed that a venous plexus or lymphatic system was the probable route from the vagina to the reproductive organs. Similar findings were observed using a human ex-vivo uterine perfusion model (*51*). In this study, uterine specimens were obtained immediately after abdominal hysterectomy for early stage cervical cancer or uterine prolapse. A mixture of tritiated and unlabelled progesterone was applied to the cuff of vaginal tissue removed with the uterus (*51*). The 3H and 14C radioactivity were measured in the uterine tissue following a 12 hour perfusion period. Progesterone concentrations were 185 + 155 ng/100 mg and 254 + 305 ng/100 mg of endometrial and myometrial tissue, respectively. Autoradiography performed 4 hours after perfusion showed a uniform capture of radioactivity by the endometrium. In the myometrium, however, radioactive tracer accumulated within or proximal to the vascular casts. The authors suggested that this may reflect counter arterial-to-venous perfusion. It should be noted that this study sample was small and the model, although rigorously tested, may not accurately reflect perfusion physiology (*52,53*). Nonetheless, the findings provide additional support for local drug distribution following vaginal absorption. Fujii et al. studied the distribution and effects of intravaginal cisplatin for the treatment of cervical cancer (*54*). Four patients ranging in stage from Ib to IIa were pre-operatively treated with 20 mg cisplatin suppositories. Post-operative tissue samples showed significant drug levels in the cervix, vagina, endometrium, uterine wall, and ovary. Lymph nodes sampled showed significant levels in the parametrial, obturator, inguinal, external iliac, internal iliac and common iliac groups. Post-treatment colposcopy showed a disappearance of bleeding and reduction of tumor outgrowth. Microscopically, the authors observed degeneration and necrosis of cancer nests from the surface to approximately 2 mm. The results provide additional support for local drug distribution after vaginal absorption.

Mechanisms of Pelvic Drug Distribution. Pelvic drug distribution after intravaginal administration may be dependent on a number of mechanisms. It is possible that drug may distribute topically in an antegrade or retrograde manner within the vaginal canal. This could account for drug loss through the introitus as well as distribution to the upper reproductive structures. Following vaginal absorption, simple diffusion across parenchymal and interstitial structures may contribute to

Downloaded by YORK UNIV on October 31, 2012 | http://pubs.acs.org
Publication Date: September 24, 1998 | doi: 10.1021/bk-1998-0709.ch002

Downloaded by YORK UNIV on October 31, 2012 | http://pubs.acs.org
Publication Date: September 24, 1998 | doi: 10.1021/bk-1998-0709.ch002

local distribution as well. However, growing evidence suggests that the predominant route of drug distribution occurs after vaginal absorption through drug exchange between the rich venous plexuses that surround the reproductive organs. Studies by Chakmakjian et al. (*47*), Miles et al. (*49*), Mizutani et al. (*50*) show that vaginal drug absorption leads to elevated levels of drug in all the reproductive structures within 4 to 6 hours. Conventionally, venous transport is a unidirectional process favoring systemic transport rather than redistribution to proximal pelvic structures. The data presented raises the possibility that another mechanism may be involved with distributing drug to the upper reproductive structures. Retrograde transport through the endocervical canal, uterine cavity, and fallopian tubes may be partially responsible. However, it may not adequately describe the relatively rapid kinetics of drug uptake observed by tissues such as those of the ovaries. A mechanism that may explain these findings involves the exchange of drug between venous and arterial segments of capillaries known as countercurrent exchange. The countercurrent exchange model has been described in the uterine addenda, kidney, and small intestine (*55-57*). The model is dependent on the close association between venous and arterial limbs in a vascular loop. It was originally proposed as an autocrine function in the ovary (*58-62*). In short, a certain area of ovarian tissue was responsible for secreting factors into efferent venules which could be directly transferred to an arterial branch supplying another region of the ovary. The authors speculated that this may account for the influence of prostaglandins on the corpus luteum. After vaginal absorption, it is conceivable that drug initially distributes along the reproductive tract via exchange between venous plexuses. Countercurrent exchange may then occur between adjacent arterial vessels leading to drug transport to respective reproductive organs. The cited studies supporting countercurrent exchange are small in patient number and limited to the utero-ovarian vasculature. However, it is one of the few models that may account for the rapid kinetics of drug distribution to pelvic organs after vaginal absorption.

Drug Delivery Systems

Drug delivery systems can be manipulated in a number ways to achieve the desired therapeutic levels in the body. The design of the delivery system takes into account the route of administration, the duration of drug action, and the need for removal after drug is released. During the last two decades, significant advances have been made in the area of controlled release technology (*63-70*). Early efforts were focused on the development of zero-order release devices. The premise of zero-order release was to maintain steady state drug concentrations through a constant rate of drug release. Initial studies, however, had shown that zero-order release does not necessarily correlate with constant drug levels in the blood. Recent advances in controlled drug delivery have resulted from the design of novel polymers in terms of charge density, side chain functionality, phase transformation, crystallinity, and degradability. This has resulted in the ability to achieve sustained drug levels in the body while minimizing side effect profiles and improving patient compliance. The development of controlled release devices for vaginal drug delivery has received considerably less interest as compared to other routes of administration. Interestingly, many of the technological advances seen with more conventional routes of drug administration have unique applicability to intravaginal drug delivery. In this next section, the wide range of materials used to construct delivery systems and the mechanisms controlling drug release are reviewed to illustrate their potential use for intravaginal drug delivery.

Diffusion-Controlled Systems. Diffusion-controlled systems can be divided into reservoir and monolithic devices (*71,72*). In reservoir systems, the drug is encapsulated by a polymeric membrane through which it is released by diffusion. Reservoir systems have the advantage of providing constant release rates over a substantial portion of their release profile. Polymer films used in diffusion-controlled reservoir systems are given in Table I (*73*). The polymer can either be porous or nonporous. Drug release through the nonporous regions is controlled by diffusion, whereas the release through the porous region is dependent on drug solubility and size. Microporous membranes are useful in the delivery of high molecular weight protein drugs. One of the most recognized diffusion-controlled reservoir systems is the Norplant® system which delivers levonorgestrel for more than 5 years. Monolithic devices have drug uniformly dispersed or dissolved in an inert polymer matrix. Various geometries, such as slabs and cylinders, have been developed to control drug release rates. The kinetics of diffusion-controlled release has been correlated with theoretical models (*74-77*). Thus, the release rates may be controlled by the choice of polymer as well as the diffusion and partition coefficient in the polymer. (*71,78*). Drug release from a monolithic device where drug is dissolved in polymer follows Fick's Law. And, the drug release from a slab geometry is described by the following equation:

$$M_t/M_o = 4(Dt/ph2)^{1/2} \qquad (10)$$

where M_t is the amount of drug released at time t, Mo is the total amount of drug incorporated in the device, D is the diffusion coefficient of a drug, p is 3.14 and h is the thickness of the device (*78-80*). This equation is an early time approximation which describes the first 60% of total drug release. The late time approximation, as defined by Equation 11, holds for the final portion of drug release from 40% to 100% release.

Table I. Polymers Used in Diffusion-Controlled Drug Release Formulations
(Adapted from Reference 73)

Collagen	Chitin
Poly(alkyl cyanoacrylate)	Nylon
Poly(ethylene-co-vinylacetate)	Polyethylene
Poly(hydroxypropylethyl methacrylate)	Poly(hydroxyethyl methacrylate)
Poly(vinyl alcohol-co-methacrylate)	Poly(methyl methacrylate)
Polyisobutene	Poly(vinyl chloride)
Silicon rubber	Polyurethane

Downloaded by YORK UNIV on October 31, 2012 | http://pubs.acs.org
Publication Date: September 24, 1998 | doi: 10.1021/bk-1998-0709.ch002

$$M_t/M_o = 1 - (8/\pi^2)e^{-[\pi^2 Dt/h^2]} \qquad (11)$$

Mathematical solutions for the release of a drug from devices with other geometries can be found in the literature (*74-79*). Drug release from monolithic dispersions depends on the geometry of the device and the loading dose (*74,75,79,81,82*). Drug release from a slab where the drug concentration is less than 5% by volume is described by the Higuchi model:

$$M_t = A[DC_s(2C_o - C_s)t]^{1/2} \qquad (12)$$

where M_t is the amount of drug released at time t, A is the total surface area of the slab, D is the diffusion coefficient of the drug in the polymer, Cs is the drug solubility in the polymer matrix, and Co is the initial drug concentration which includes dissolved and dispersed drug (*76,81,82*). On the other hand, higher drug loading levels in the range of 5 - 15 % by volume changes the equation to account for the formation of fluid-filled cavities resulting from dissolution. The presence of cavities at the surface increases the apparent permeability of the drug and its release can be expressed by the following equation:

$$M_t = A[2DC_sC_ot(1+ 2C_o/\rho)/1 - C_o/\rho)]^{1/2} \qquad (13)$$

where ρ is the density of the permeant (*78*). At much higher drug loading levels (15 - 20 % by volume), particles dispersed are in contact with one another. Thus, drug is released through pores formed by the dissolution of the drug. The partition coefficient is replaced by porosity (e) which is the volume fraction of the pores. The diffusion coefficient (Dw) is modified to represent drug diffusing through the formed pores left by drug dissolution. A tortuosity term (t) is added to account for drug diffusion through the tortuous pores which is a longer distance than the thickness of the membrane:

$$M_t = A[2(\epsilon/\tau)D_wC_wC_ot]^{1/2} \qquad (14)$$

where C_w is the concentration of drug in water (*74,78,83*).

Dissolution-Controlled Systems. Polymers used in the design of dissolution-controlled dosage forms are usually water-soluble. Water-insoluble materials may also be used provided they absorb significant amounts of water to disintegrate the delivery system. Dissolution generally refers to the physical disentanglement of polymer chains in the presence of excess water without involving any chemical changes. Dissolution-controlled systems can have either a reservoir or matrix design. In the reservoir system, the drug core is coated with a water-soluble polymeric membrane. Drug release rates will be controlled by the solubility of the

Downloaded by YORK UNIV on October 31, 2012 | http://pubs.acs.org
Publication Date: September 24, 1998 | doi: 10.1021/bk-1998-0709.ch002

polymeric membrane which is dependent on the thickness of the membrane and type of polymer used. During the early phase of dissolution, the polymer undergoes swelling due to water penetration. The outer portion forms a mucinous-like barrier that limits further water penetration. Drug diffusion through this barrier may also contribute to drug release in addition to dissolution kinetics of the polymer. Table II lists the various polymers used in dissolution-controlled drug release. The most widely used polymers are the cellulose ethers, particularly hydroxypropylmethylcellulose (HPMC) (*73*).

Table II. Polymers Used in Dissolution-Controlled Release Formulations
(Adapted from Reference 73)

Albumin	Carboxymethycellulose, sodium salt
Dextran derivatives	Gelatin
Hydroxypropylmethylcellulose	Poly(ethylene glycol)
Poly(malic acid)	Poly(vinyl alcohol)
Polyvinyl pyrrolidone	Starch, thermally modified
Xanthum gum	

Cleavage of polymer chains into smaller segments by either chemical or enzymatic processes in biological systems is referred to as biodegradation. With respect to drug delivery, the rate of drug release will be dependent on the rate of biodegradation. Biodegradable systems may be considered a special type of dissolution-controlled system since they share similar physical properties. Commonly used biodegradable polymers are listed in Table III. Biodegradable systems can be divided into surface-degrading and bulk-degrading systems. True surface degrading systems include the polyorthoester (*84-86*) and polyanhydrides (*87-89*). In many cases, however, drug release is controlled by a combination of bulk and surface degradation mechanisms. Biodegradable and dissolution-controlled delivery systems are highly desirable since they are eliminated from the body after their intended use.

Table III. Examples of Biodegradable Polymers
(Adapted from Reference 73)

Chitosan	Poly(lactic acid)
Poly(glycolic acid)	Poly(lactide-co-glycolide)
Poly(ϵ-caprolactone-co-glycolide)	Poly(β-hydroxybutyrate)
Poly(β-hydroxyvalerate)	Poly(dioxanone)
Poly(orthoesters)	Poly(phosphazenes)
Polyanhydrides	

Swelling-Controlled Systems. Certain materials, when placed in water, are able to swell rapidly to retain excess water within their swollen structures. These materials do not dissolve, but rather maintain a three-dimensional structure. Such aqueous gel networks are referred to as hydrogels. Hydrogels are generally made up of

Downloaded by YORK UNIV on October 31, 2012 | http://pubs.acs.org
Publication Date: September 24, 1998 | doi: 10.1021/bk-1998-0709.ch002

hydrophilic polymer molecules which are crosslinked either by chemical bonds, ionic interactions, hydrogen bonding, or hydrophobic interactions. Hydrogels are elastic solids in that there exists a remembered reference configuration to which the system may return even after being deformed for an extended period of time (*90*). Hydrogels have been the topic of extensive investigation because of there unique bulk and surface properties (*68,69*). Cumulative evidence has shown that hydrogels are highly biocompatible. This is largely due to the low interfacial tensions produced with surrounding tissues and fluids that minimizes protein adsorption and cell adhesion (*91,92*). Their biocompatibility is also related to comparable hydrodynamic properties with natural biological gels (*93-95*). One of the key attributes of hydrogels is their high compliance, which is associated with being soft; this minimizes mechanical and frictional irritations with surrounding tissue (*96*). Hydrogels can be prepared from either natural polymers, synthetic polymers, or combinations thereof. Common polymers used in hydrogel preparation are listed in Table IV. It should be noted that biomechanical properties of hydrogels can be altered depending on the molecular weight and hydrophilicity of the polymer, the crosslinking density of network (physical or chemical crosslinks), and the presence of degradable moieties either within the backbone of the polymer chain or in the crosslinks. Reviews on the preparation, mechanical properties, and application of hydrogels in drug delivery have recently been published by Park et al. (*69*) and Peppas (*68*).

Downloaded by YORK UNIV on October 31, 2012 | http://pubs.acs.org
Publication Date: September 24, 1998 | doi: 10.1021/bk-1998-0709.ch002

Table IV. Polymers Used for Hydrogel Preparation
(Adapted from Reference 73)

Synthetic Polymers	
Poly(acrylic acid)	Poly(acrylamide)
Poly(methacrylic acid)	Poly(hydroxyethyl methacrylate)
Poly(vinyl pyrrolidone)	Poly(N-isopropylacrylamide)
Poly(vinyl alcohol)	Poly(ethylene glycol)
Poly(amino acids)	
Natural Polymers	
Dextran	Gelatin
Algenic acid	Albumin
Hyaluronic acid	Fibrin
Agar	Actin
Starch	Chitosan
Pectin	Hydroxypropylmethylcellulose
Hydroxymethylcellulose	Sodium carboxymethylcellulose
Hydroxyethylcellulose	Carageenan
Guar gum	

Drug release from hydrogels is unique in that the absorption of water from the environment changes the dimensions and physical properties of the system, and thus the release kinetics. Hydrogel swelling is a dynamic phenomena leading to the formation of physically distinct zones (*97*). At the outer surface, adjacent to bulk water, is a layer of completely swollen gel. Below the swollen gel is a thin layer in which the polymer chains are slowly hydrating and relaxing. The innermost zone is a matrix of unswollen, completely dried, rigid polymer. The diffusion of water or permeant can be classified into three types based on the relative rates of diffusion and polymer relaxation (*97*). They are:

(1) Case I or Fickian diffusion which occurs when the rate of diffusion is much less than that of relaxation.
(2) Case II diffusion (relaxation-controlled transport) occurs when the diffusion is very rapid compared with the relaxation process.
(3) Non-Fickian or anomalous diffusion occurs when the diffusion and relaxation rates are comparable.

Downloaded by YORK UNIV on October 31, 2012 | http://pubs.acs.org
Publication Date: September 24, 1998 | doi: 10.1021/bk-1998-0709.ch002

The above classifications for permeant diffusion may also be used to classify drug release profiles from swelling polymers (*98*). Fick's law will be followed when drug release occurs from a gel that is in its equilibrium swollen state (See Equation 16). In Case II transport drug release will be controlled by the rate polymer chain relaxation (*99*).

Bioadhesive Delivery Systems. Adhesion is defined as a state in which two condensed phases are held together by interfacial forces (*100,101*). The types of forces may be related to combination of chemical and physical interactions. A bioadhesion defines adhesion between a biological substrate and some natural or synthetic adherent. Bioadhesion in the presence of water (wet adhesion) is distinguished from adhesion to dry surfaces in that adhesion maintains a dynamic state. It is believed that wet adhesion occurs through the interdiffusion of the adhesive and adherend across an interface. This theory has been applied to polymeric materials whereby hydrated polymer chains become entangled when brought in close contact with the mucus layer of the GI tract (*102*). Once entangled, active adhesion sites interact with the substrate to form adhesive bonds. This may be in the form of hydrogen bonding, van der Waals forces, or electrostatic interactions. The theoretical advantage of bioadhesives in drug delivery is their ability to achieve sustained drug release at specific sites of drug absorption. For this reason, considerable interest has focused on the oral, buccal, nasal, and ocular routes of administration (*102*). The most widely studied bioadhesive is polycarbophil which is polyacrylic acid crosslinked with divinylglycols. Other polymers which appear to show promise are some of the cellulose derivatives (*103*). Once localized to an adsorption site, drug release may occur through one or a combination of the mechanisms described above. It is also conceivable that drug delivery systems may be dispersed in a bioadhesive hydrogel where it acts as a platform for drug delivery at a specific site. The study of bioadhesive hydrogels for intravaginal drug delivery is an area of growing interest. The obvious advantage of prolonged residence in the vagina while maintaining some degree of mechanical integrity make this an attractive application of these polymers. It is expected that many future intravaginal drug delivery systems will have some component of

Downloaded by YORK UNIV on October 31, 2012 | http://pubs.acs.org
Publication Date: September 24, 1998 | doi: 10.1021/bk-1998-0709.ch002

bioadhesion. Interestingly, the study of bioadhesive polymers for intravaginal drug delivery is relatively unexplored. Thus, a unique opportunity exists for the development of new bioadhesive polymers to meet specific therapeutic needs.

Microspheres. Microspheres are another type of drug delivery system that have been studied for sustained parenteral, intranasal, transdermal, and oral drug administration (*104-109*). The types of drugs studied range from chemotherapeutic agents to peptide drugs. Microspheres are unique in that rate of drug release can be modulated as a function of size distribution in a formulation, mode of drug incorporation, degree of swelling or crosslinking, and rate of degradation. Microspheres can be prepared from both natural and synthetic polymers or combinations thereof. The most common methods of preparation include emulsion polymerization, solvent extraction, or air atomization. Microsphere size distribution can be as narrow as 5 μm to 15 μm or as high as 100 μm depending on the processing parameters. The drug can be dispersed or microencapsulated in the polymeric carrier. Table V lists the different types of polymers used to prepare microspheres. In the case of many natural polymers, side chain modification is necessary to provide functionality for crosslinking. The chemical modification of proteins and polysaccharides has recently been reviewed by Shalaby et al. (*110*). While the study of microspheres for sustained drug delivery is well established, its application to intravaginal drug delivery has never been studied. It is conceivable that microsphere formulations ranging from 5 μm to 15 μm could be used for intravaginal drug delivery providing that prolonged residence times could be achieved. The advantage of microspheres is that drug release could be manipulated to provide either a bolus and/or sustained level of drug followed by microsphere degradation for removal.

Table V. Natural and Synthetic Polymers Used to Prepare Microspheres
(Adapted from Reference 73)

Natural Polymers	Synthetic Polymers
Albumin	Ethylvinyl Acetate
Dextran	Poly(D, L-lactic acid)
Gelatin	Poly(D,L/Lactide-co-glycolide)
Ethylcellulose	Poly(hydroxybutyrate)
Starch	Poly(cyanoacrylate)
Chitosan	
Algenic Acid	

Ion-Exchange Delivery Systems. Controlled release of ionizable drugs may be achieved through ion-exchange systems. Ion-exchange resins may be formed through the crosslinking of polyelectrolyte polymers. They may be designed as swellable gel slabs or as microspheres ranging in size from 5 μm to 100 μm. These types of hydrogels contain bound drug through salt linkages that are formed during drug absorption. Drug is subsequently released by replacement with appropriately charged ions from the surrounding media. Therefore, cationic drugs may form complexes with carboxyl or sulfonic groups of an ion-exchange resin while anionic drugs complex with basic amino or quaternary ammonium groups. Polyelectrolytes that have been used in ion-exchange systems include poly(styrene sulfonic acid), poly(acrylic acid), and poly(dimethylaminoethyl methacrylate) (*73*).

Osmotic Delivery Systems. Osmotic drug delivery systems may also conceivably be utilized for intravaginal drug delivery. The osmotic delivery system is composed of a core reservoir of drug, in the absence or presence of an osmotic agent, coated with a semipermeable polymeric membrane. The membrane has a single delivery orifice usually with the diameter of 0.1 - 0.4 mm. The presence of an osmotic agent creates an osmotic pressure gradient across the membrane which causes diffusion of water into the device. As water diffuses into the reservoir, the drug is gradually forced through the delivery orifice. The mechanical strength of the semi-permeable membrane determines the mechanical integrity of the device which should be maintained throughout the functional lifetime of the system. The rate of drug release is determined by the rate of water penetration into the device. Penetration rates can be controlled as a function of type, thickness, and area of the semi-permeable polymeric membrane. Table VI lists some of the polymers used to form semipermeable membranes. Osmotic devices such as the OROS system and the Alzet osmotic pump have been developed by Alza Corporation for oral and implantable drug delivery (*73,111*).

Table VI. Polymers Used to Prepare Semipermeable Membranes
(Adapted from Reference 73)

Poly(vinyl alcohol)	Polyurethane
Cellulose acetate	Ethylcellulose
Cellulose acetate butyrate	Poly(vinyl chloride), cast, extruded, and rigid
Polycarbonate	Poly(vinyl fluoride)
Poly(vinylidene fluoride)	Ethylene vinyl acetate
Polyesters	Ethylene propylene copolymer
Polypropylene	

Current Trends in Intravaginal Drug Delivery

Labor Induction. Spontaneous labor and delivery involve a sequence of events that include softening, or ripening, and effacement of the cervix. Labor induction is indicated when there is evidence of preeclampsia, diabetes, heart disease, or fetal-placental insufficiency. Prolonged labor in the context of an unfavorable cervix can increase the likelihood of numerous maternal and fetal complications such as infection, fetal distress/demise, the need for operative delivery, and postpartum hemorrhage. Pharmacological intervention is often implemented in an effort to 'ripen' the cervix to facilitate vaginal delivery. Numerous studies dating back to the 1970s have documented the successful use of prostaglandins for labor induction through intracervical or intravaginal routes of administration. In recent years, dinoprostone (a synthetic prostaglandin E2) has been used for cervical ripening via

Downloaded by YORK UNIV on October 31, 2012 | http://pubs.acs.org
Publication Date: September 24, 1998 | doi: 10.1021/bk-1998-0709.ch002

vaginal administration. Early efforts utilized glycerol ester based formulations to deliver dinoprostone (*112-114*). Currently methylcellulose based materials (*115,116*) and polyethylene oxide based hydrogels (*117-122*) have been formulated for cervical ripening. Early concerns for these devices were related to dose dumping and ease of removal. While a burst release of drug in the early phase is difficult to avoid, signs and symptoms of toxicity have been less significant with current devices. This has largely been due to incorporating drug into hydrogel delivery systems where the release is swelling-controlled and more predictable. In terms of retrieval, Cervidil® (a polyethylene oxide/urethane based hydrogel) is incorporated within a polyester net that can be used to remove the device should signs or symptoms of hyperstimulation result. It is expected that future delivery systems will utilize some of the new agents being studied as cervical ripening agents. Although considerable interest has been placed on labor induction, it bears mention that other areas in obstetrics may benefit from intravaginal therapeutics. This includes the management of preterm labor with intravaginal tocolytic agents or through administration of antibiotics in the context of preterm rupture of membranes to prolong intrauterine gestational time. Labor augmentation in latent phase may be another aspect that may benefit from intravaginal drug delivery.

Downloaded by YORK UNIV on October 31, 2012 | http://pubs.acs.org
Publication Date: September 24, 1998 | doi: 10.1021/bk-1998-0709.ch002

Hormone Replacement Therapy. Postmenopausal estrogen replacement has received considerable attention in recent years. It is well accepted that estrogen is beneficial in terms of its cardioprotective effects (*123,124*) and in the treatment of osteoporosis (*125-127*). Estrogen therapy has also been widely used for the treatment of vaginal and urogenital atrophy. Hormone replacement therapy can be achieved by many routes of administration. The most common of which are oral, transdermal, and vaginal. Vaginal estrogen creams have been in existence for many years. While systemic levels are achieved, daily administrations combined with patient compliance issues make this a less desirable approach to estrogen replacement. In response, vaginal estrogen-releasing rings have been developed to provide sustained drug release in a manner similar to transdermal delivery. Stumpf et al., were among the early investigators to homogeneously disperse estradiol into polysiloxane vaginal rings for this purpose (*128*). These delivery systems were capable of maintaining estradiol levels ranging from 109 pg/ml to 159 pg/ml for 3 months in postmenopausal volunteers. Serum levels could also be adjusted based on the loading dose of estradiol and surface area of the device (*129*). Estring® and other similar devices were later designed with an inner core or reservoir of estradiol and an outer polysiloxane sheath for diffusion-controlled release. Stable serum levels have been achieved for up to 3 months for the treatment of vaginal and urogenital atrophy (*130-133*).

Contraception. The development of new hormonal contraceptive modalities has been an ongoing effort for over forty years. Oral, injectable, and implantable contraceptives have all been widely used with exceptional efficacy. Intravaginal hormonal contraception was initially investigated by Mishell et al. using medroxyprogesterone (*134*). Medroxyprogesterone was homogeneously dispersed in cylindrical rings prepared from polysiloxane. Over a 28 day cycle, an absence of the midcycle LH surge was observed. Endometrial biopsies taken were found to be consistent with progestational effects. Furthermore, removal of the device resulted in prompt withdrawal bleeding. Similar designs have also been developed for 90 day clinical trials (*135*). Ballagh et al., tested core designed vaginal ring containing norethindrone acetate and ethinyl estradiol (*136*). Ovulation and breakthrough bleeding were better controlled with average daily ethinyl estradiol release rates ranging from 30 to 65 mcg. However, unacceptably high levels of nausea resulted with the 65 mcg daily released rates. Similar rings containing levonorgestrel have also been studied (*137,138*). Unlike the preceding ethinyl estradiol vaginal rings, there was greater individual variation in levonorgestrel levels, incomplete suppression of ovulation, and breakthrough bleeding.

The medical management of abortions and ectopic pregnancies are two areas of converging study. Recent randomized trials by Creinin et al. utilize oral or intramuscular methotrexate with intravaginal administration of misoprostol to provide safe and efficacious medical abortions (*139,140*). These studies suggest that oral administration of methotrexate may have improved efficacy while minimizing systemic side effects. It is conceivable that intravaginal methotrexate administration offers additional advantages in terms of higher local drug concentrations at lower doses. This could conceivably improve efficacy while further minimizing systemic side effects. Similarly, the medical management of ectopic pregnancies requires the intramuscular administration of methotrexate over 1 to 4 doses followed by leucovorin rescue. In this regard, an intravaginal methotrexate delivery system may be capable of releasing lower doses of drug over a predictable time course to improve efficacy and compliance while decreasing systemic side effects.

Infertility. Progesterone supplementation or replacement is widely implemented for assisted reproductive technology in the treatment of infertility. Oral administration of progesterone leads to extensive intestinal and hepatic metabolism. The standard of treatment for progesterone deficiency is through intramuscular administration which can be painful. Recently, an intravaginal progesterone gel (Crinone®) has been developed. The delivery system is a bioadhesive gel formulation prepared from polycarbophil. The gel is administered once or twice daily delivering 90 mg of micronized progesterone with each dose. Treatment may be continued for up to 12 weeks until placental autonomy is achieved. The manufacturers (Wyeth-Ayerst Laboratories) purport less drowsiness as compared to the oral form. This delivery system is also being studied in conjunction with oral estrogen for hormone replacement therapy.

Infectious Diseases. Interest in the administration of intravaginal agents for the treatment and prophylaxis of sexually-transmitted diseases and other infections has been considerable. Early efforts in this field had focussed on treatment modalities for bacterial vaginosis. The latter is a syndrome in women of reproductive age where the normal Lactobacillus-dominated vaginal microflora is replaced by high

Downloaded by YORK UNIV on October 31, 2012 | http://pubs.acs.org
Publication Date: September 24, 1998 | doi: 10.1021/bk-1998-0709.ch002

concentrations of mixed anaerobic and facultative flora. Typically, this includes Peptostreptococcus sp., Gardnerella vaginalis, Mycoplasma hominis, and Ureaplasma urealyticum (*141,142*). It is considered to be the most common vaginal infection and has been associated with an increased risk of preterm labor and delivery (nos. 4,5,6 in Livengood et al., 1990--*155*), premature rupture of membranes (*144*), chorioamnionitis (*144-146*), and pelvic inflammatory disease (*147*). Topical administration of clindamycin or metronidazole has been most successful in the treatment of bacterial vaginosis. Hillier et al. studied the efficacy of 0.1% to 2.0% clindamycin creams administered daily for seven days in nonpregnant women (*148*). They found that the 2% cream had the greatest effect on bacterial vaginosis-associated flora with a 94% resolution of bacterial vaginosis both one week and one month after treatment. Similar findings have been reported elsewhere (*149,150*). The efficacy of intravaginal clindamycin has also been shown to be similar to oral metronidazole (*151*). The bioavailability of clindamycin has been shown to be minimal ranging from 2.7% to 4.7% (*152*). Intravaginal metronidazole has also been studied to improve patient compliance and decrease side systemic side effects. Edelmen et al. administered intravaginal sponges containing either 250 mg (twice daily for two days) or one gram (once daily for three days) of metronidazole (*153*). While the study was carried out in a small group of women, cure rates of 85% and 92% were noted after one week, respectively. Failure rates after one month were 42% in the low dose and 12% in the high dose group. Systemic side effects such as nausea, headache and metallic taste were slightly more frequent in patients using the higher dose sponge. Hillier et al. studied the efficacy of 5 gram metronidazole gels (0.75%) administered twice daily for 5 days (*154*). A clinical cure rate of 87% was observed after 9 to 21 days with a recurrence rate of 15% after one month. Furthermore, there were no significant side effects noted in the treatment group. Similar results have been reported in a larger study by Livengood et al. (*155*). Systemic levels of metronidazole after vaginal administration are significant (*156*). The relative bioavailability compared to the oral form is 56%.

Current standards in the treatment of sexually transmitted diseases have focussed on oral and intravenous administration of antibiotics and antiviral agents. While little has been done in terms of intravaginal treatment strategies, a growing interest in prophylaxis has emerged using vaginal microbiocides and antiviral agents. The ultimate goal is to develop a vaginal delivery system that has activity against a broad spectrum of pathogens, including HIV. A number of compounds have been considered such as benzalkonium chloride, chlorhexidine, nonoxynol-9, and polymyxin B (*157,158*). In terms of HIV transmission, both virucidal agents and biomaterials that prevent HIV adsorption/fusion are being studied (*158*). Although this area is still in its infancy, the growing urgency for prevention strategies will quickly attract many investigators from multidisciplinary backgrounds to study this problem. It is clear, however, that the active agent as well as the delivery system will play an equal role in optimizing efficacy.

Downloaded by YORK UNIV on October 31, 2012 | http://pubs.acs.org
Publication Date: September 24, 1998 | doi: 10.1021/bk-1998-0709.ch002

Downloaded by YORK UNIV on October 31, 2012 | http://pubs.acs.org
Publication Date: September 24, 1998 | doi: 10.1021/bk-1998-0709.ch002

Gynecologic Oncology. Intravaginal administration of chemotherapy has been evaluated for the treatment of vaginal and cervical dysplasias. The rational is based on the assumption that higher localized levels can be achieved at a fraction of the intravenous dose with minimal systemic side effects. A case report by Bowens-Simpkins et al. were one of the first groups to describe topical administration of 5-flurouracil (5-FU) for treatment of multifocal vaginal intraepithelial neoplasia (*159*). Twice daily administration of 5% 5-FU cream for two weeks resulted in benign cytological findings for up to a 15 month follow-up period. However, evidence of excoriation and thinning of the vaginal wall was noted one month after treatment. This resulted in some dyspareunia for up to 7 months. Similar efficacy and side effects were noted using different 5-FU concentrations (*160*) and dosing regimens (161,162). Piver et al. studied the administration of 20% 5-FU over monthly 5 day courses in patients with postirradiation vaginal carcinoma *in situ* (*163*). Seven of the eight women studied had an initial complete response with three of the patients developing a recurrence after treatment was stopped. Retreatment, however, resulted in a complete response in two of the three recurrences. The authors noted that most of the patients developed vulvovaginitis which they claim was well controlled by sitz baths and analgesics. Human Papillomavirus (HPV)-associated lesions of the vulva and vagina have been treated with topical 5-FU. Krebs studied prophylactic topical 5-FU following ablative treatment (*164*). Patients administering biweekly doses of 5% 5-FU creams for six months developed recurrence in 13% of the cases as compared to 35% in the control group. The authors noted that maintenance therapy was most effective in women with multiple lesions, multiple organ involvement (vulva, vagina, cervix, anus, distal urethra), or a depressed immune system. Similar findings were noted using a once-a-week dosing regimen (*165*). Long-term use of topical 5-FU, however, can lead to chronic ulcerative changes in the vagina. Krebs et al. found that the incidence of ulcers was higher in women who used 5-FU for longer than 10 weeks (*166*). Associated symptoms included serosanguinous or water discharge, postcoital spotting or bleeding, irregular bleeding, and pain. Conservative treatment with estrogens and/or cauterizing agents did not facilitate healing. However, excision of the ulcer with primary closure was found to be curative.

The treatment of cervical intraepithelial neoplasias (CIN) has been recently studied. Meyskens et al. studied the regression CIN II with topically administered all-trans-retinoic acid (RA) (*167,168*). The device used to deliver RA was collagen sponge which was inserted into a cervical cap comprised of bioadhesive hydrogel (*169*). The results showed that locally applied RA (daily for 4 days) led to complete histologic regression of CIN II in 43% of the patients. Patients returned at 3 and 6 months for follow-up as well as maintenance treatment consisting of daily RA for 2 days. In contrast, no treatment effect was observed for patients with severe dysplasia. Side effects included cervical inflammation by colposcopic evaluation, mild vaginal inflammation, and vulvar burning and irritation during the initial treatment. It should also be mentioned that intravaginal administration of interferon gamma has also been studied for the treatment of CIN (*170,171*). In terms of cervical cancer, standard treatments for it include radiation therapy with or without combination neoadjuvant chemotherapy. In this context, some investigators have proposed intravaginal administration of cisplatin (*172*). However, very few case reports exist. Thus, any perceived benefit is purely speculative at this time. The above discussion illustrates the possible benefit of intravaginal chemotherapy in the treatment of vaginal and even cervical dysplasias. Again, the choice of the chemotherapeutic agent and mode of delivery will be equally as important if efficacy is to be appreciated.

New Trends in the Development of Drug Carriers

Of the many new polymeric carriers that have been described in the recent patent and technical literature, a few are most pertinent to intravaginal drug delivery. Most interesting among these are (1) members of the family of absorbable polymers with chemical structures which are tailored to provide specific attributes as discussed by Shalaby and coworkers (*173-176*); (2) thermoreversible gels (*177*); (3) novel hydroxyethyl-cellulose formulations (*178*); and (4) certain new chitosan derivatives (*179*). Brief accounts of these systems are given below.

Injectable, liquid copolymers of the water-soluble polyethylene glycol (PEG) and hydrophobic polyester segments were tailor-made to undergo phase transformation into adhering, flexible gels upon contacting aqueous surfaces such as wet tissues (*174*). The gel-formation was postulated to take place through the hydrophobic-hydrophobic interaction of the polyester or polycarbonate segment and its association to form a 3-dimensional gel stabilized by the resulting quasi-crosslinks. Depending on the molecular weight of the PEG and the type of polyester segments, the gel-formers can display a wide range of absorption, adhesivity to wet tissues, and barrier properties for the controlled release of drugs. Typical examples of these gel-formers were made by grafting a lactone or cyclic carbonate on the two hydroxylic terminals of a liquid PEG such as PEG-400. Examples of the cyclic monomers used for grafting include glycolide, dl-lactide, ϵ-caprolactone, and trimethylene carbonate. Representative gel-formers were studied as carriers for the controlled delivery of vaccines by subcutaneous and intranasal injection (*175*) and intravitreal administration of antiviral agents (*176*). The gel-formers were described as potentially useful matrices for the development of intravaginal controlled delivery systems for their noticeable tendency to adhere to mucosal membranes. This will allow for a prolonged residence time at the application site as compared with commercial water-soluble carriers.

Aqueous solutions of certain polymers, such as block copolymers of PEG and polypropylene glycol (PPG) and certain N-alkyl polyacrylamides undergo reversible gelation by minor changes in temperature and are usually described as aqueous reversible gels (*177*). Most interesting among those gels are the PEG-PPG block copolymers which are moderately viscous injectable aqueous solutions at room temperature but undergo gelation at body temperature. Although the PEG-PPG systems have a tendency to adhere to mucosal surfaces such as that of the vagina, this desirable feature is compromised considerably by their water-solubility and brief residence time at the administration site. Concerns about the solubility of

Downloaded by YORK UNIV on October 31, 2012 | http://pubs.acs.org
Publication Date: September 24, 1998 | doi: 10.1021/bk-1998-0709.ch002

PEG and PEG-PPP block polymers and the desire to exploit their adhesive properties led contemporary investigators to develop a few novel formulations with upgraded carrier properties. These include the preparation of (1) mucoadhesive formulations containing hydroxyethyl cellulose (HEC) or carbopol and polycarbophil (*178*) and (2) chitosan/ethylene oxide-propylene oxide block copolymers, CS/PEO-PPO (*179*). Mucoadhesive formulations containing metronidazole were evaluated as syringable delivery systems for controlled release to the periodontal pockets. On the other hand, the CS/PEO-PPO system was converted to nanoparticles of CS core and hydrophilic PEO-PPO surfaces (*178*). The nanoparticles were suggested to provide suitable substrates for the development of oral controlled release systems (179). Although the use of these nanoparticles in intravaginal delivery systems was not suggested, they may very well make suitable candidate carriers for such applications.

Downloaded by YORK UNIV on October 31, 2012 | http://pubs.acs.org
Publication Date: September 24, 1998 | doi: 10.1021/bk-1998-0709.ch002

Future Perspectives

The field of intravaginal drug delivery is largely in its infancy compared to other routes of drug administration. We have seen in the preceding discussions that a great deal is yet to be understood. The successful development of intravaginal drug delivery systems will require identifying critical physiological barriers that will control efficacy. Key areas that will require further study include (1) vaginal immunology; (2) perfusion physiology of the upper and lower reproductive system; (3) mechanisms of drug absorption and drug disposition; (4) controlling drug release and duration of action; and (5) development of new biomaterials that will optimize drug efficacy, patient compliance, and safety. While some of these areas may be studied in the lab, many require investigation in suitable animal models and human studies. Delineating these areas will be paramount in the successful design of novel intravaginal delivery systems. While this review was not meant to be all encompassing, its intent was to help define intravaginal drug delivery as a viable route for therapeutics and to elucidate critical areas in this field that are poorly understood. Clearly, the development of this field could have a profound influence on many women's health issues ranging from obstetrics to gynecologic oncology.

Literature Cited

1. Nichols, D.H., Randall, C.L. in *Vaginal Surgery*, Fourth Edn.,William & Wilkins, London, **1996**, pp.1-42.
2. Hafez, E.S.E. in *Scanning Electron Microscopy Atlas of Mammalian Reproduction*, Springer-Verlag, New York, **1975**.
3. Schuchner, E.B.; Foix, A.; Borenstein, C.A.; Marchese,C.J. *Reprod. Fertil.*, **1974**, 36, 231-238.
4. Witkin, S.S. *Clin. Obstet. and Gynec.*, **1993**, 36, 1, pp. 122-128.
5. Burgos, M.H.; Roig de Vargas-Linares, C.E. In *The Human Vagina*, Hafez,E.S.E.; Evans, E.T., Eds., Elsevier, Amsterdan, **1978**.

6. Steger, R.W.; Hafez, E.S.E. In *The Human Vagina*; Eds., Hafez,E.S.E.; Evans, E.T., Elsevier, Amsterdan, **1978**.
7. Smout, D.F.V.; Jacoby, F.; Lillie, E.W.; *In Gynecological and Obstetrical Anatomy*, Williams & Wilkins, Baltimore, **1969**.
8. Peham, H. vonAmerich, *J. Operative Gynecology*, JB Lippincott, Philadelphia, **1934**.
9. Pendergrass, P.;Reeves, C; Belovicz, M.; Molter, D; White, *J. Gyn. Obstet. Invest.*, **1996**, 42, pp. 178-182.
10. Forsberg, J. *Acta. Obstet Gynecol. Scand.*, **1996**, Suppl., 163, 75, pp. 3-10.
11. Weber, A.; Walter, M.; Schover,L; Mitchinson, A. *Obstet. Gynecol.*, **1995**, 86, pp. 946-949.
12. *Comprehensive Gynecology*, Herbst, A.L.; Daniel, R.M.; Stenchever, M.A.; Droegemueller,W., Eds., Second Edn., Mosby, St. Louis, **1992**, pp. 43-77.
13. Murphy, J.F.; Krantz, K. In *Obstetric and Gynecologic Infectious Disease*, Pastorek, J.G., Ed., Raven Press, New York, **1994**; pp. 27-36.
14. Larsen, B. *Clin. Obstet. and Gynec.*, **1993**, 36, 1, pp. 107-122.
15. *Infectious Diseases of the Female Genital Tract*, Sweet, R.L.; Gibbs, R.S., Eds., Third Edn., Williams & Wilkins, Baltimore, **1995**, pp. 3-15.
16. Eschenback, D.A.; Davick, P.R.; Williams,B.L. *J. Clin., Microbiol.*, **1989**, 27, pp. 251-259.
17. Cohen, M.S.; Black, J.R.; Proctor, R.A.; Sparling, P.F. *Scand. J. Urol. Nephrol. Suppl.*,**1985**, 86, pp. 13-24.
18. Bartlett, J.G.; Ondernonk, A.B., Drude, E. *J. Infect. Dis.*, **1977**, 136, pp. 271-277.
19. Mardh, P.A. *Am. J. Obstet. Gynecol.*, **1991**, 165,1, pp. 1163-1168.
20. Houkkamaa, M.; Stranden, P.; Jousimies-Somer, H.; Siitonen, *Am. J. Obstet. Gynecol.*, **1986**, 154, pp. 520-524.
21. Fihn, S.D.; Lathan, R.H.; Roberts, P. *JAMA* , **1985**, 253, pp. 240-245.
22. Spence, M.R.; Hollander, D.H.; Smith, J. *Sex. Transm. Dis.*, **1980**, 7, pp. 168-171.
23. Krieger, J.N.; Tam, M.R.; Stevens, C.R. *JAMA*, **1988**, 259, pp. 1223-1227.
24. Lossick, J.G.; Muller, M.; Gorrell, T.E. *J. Infect. Dis.*, **1986**, 153, pp. 948-955.
25. Larsen, B.; Galask, R.P. *Obstet. Gynecol. Suppl.*, **1980**, 55, pp. 100s-113s.
26. Benziger, D.P.; Edelson, *J. Drug Metabolism Reviews*, **1983**, 14,2, pp. 37-168.
27. Aref, I.; El-Sheikha, Z.; Hafez, E.S.E. In *The Human Vagina*, Hafez,E.S.E.; Evans, E.T. Eds., Elsevier, Amsterdan, **1978**, pp. 179-181.
28. Hsu, C.C.; Park, J.Y.; Ho,N.F.; Higucho, W.I.; Fox, J.L. *J. Pharm. Sci.*, **1983**, 72,6, pp. 674-680.
29. Yotsuyanagi, T.; Molokhia, A.; Hwang, S.; Ho, N.F.; Flynn, G.L.; Higuchi, W.I.J. *J. Pharm. Sci.*, **1975**, 64, 1, pp. 71-76.
30. Hwang, S.; Owada, E.; Yotsuyanagi, T; Suhardja, L.; Ho, N.F.; Flynn, G.L.; Higuchi, W.I. *J. Pharm. Sci.*, **1976**, 65, 11, pp. 1574-1578.
31. Ho, N.F.; Suhardja, L; Hwang, S.; Owada, E.;'Molokhia, A.; Flynn, G.L.; Higuchi, W.I.; Park, J.Y. J. *Pharm. Sci.*, **1976**, 65, 11, pp. 1578-1585.

Downloaded by YORK UNIV on October 31, 2012 | http://pubs.acs.org
Publication Date: September 24, 1998 | doi: 10.1021/bk-1998-0709.ch002

American Chemical Society
Library
1155 16th St., N.W.
Washington, D.C. 20036

32. Hwang, S.; Owada, E.; Suhardja, L.; Ho, N.F.; Flynn, G.L.; Higuchi, W.L. *J. Pharm. Sci.*, **1977**, 66, 6, pp. 781-784.
33. Hwang, S.; Owada,E.; Suhardja, L.; Ho N.F.; Flynn, G.L.; Higuchi, W.I. *J. Pharm. Sci.*, **1977**, 66, 6, pp. 778-781.
34. Jollow, D.J.; Brodie, B.B. *Pharmacology*, **1972**, 8, 1, pp. 21-32.
35. Stehle, R.G.; Higuchi, W.I. *J. Pharm. Sci.*, 1967, 56, 10, pp.1367-1368.
36. Suzuki, A.; Higuchi, W.I.; Ho, N.F. *J. Pharm. Sci.*, **1970**, 59, 5, pp. 644-651.
37. Ho, N.F.; Higuchi, W.I.; Turi, J. *J. Pharm. Sci.*, **1972**, 61, 2, pp. 192-197.
38. Nahoul, K.; Dehennin,L.; Jondet, M.; Roger, M. *Maturitas*, **1993**, 16, pp. 185-202.
39. Casson, P.R.; Straughn, A.B.; Umstot, E.S.; Abraham, G.E.; Carson,S.A.; Buster, J.E. *Am. J. Obstet. Gynecol.*, **1996**, 174, pp. 649-653.
40. Simon, J.A. *Clin. Obstet. Gynecol.*, **1995**, 38, 4, pp. 902-914.
41. Johnston, A. *Acta. Obstet. Gynecol. Scand.*, **1996**, Suppl. 163, 75, pp.16-25.
42. Heimer, G.U. *Acta. Obstet. Gynecol. Scand.*, **1987**, Suppl. 139, pp. 5-23.
43. Rigg. L.A.; Hermann, H.; Yen, S.S.C. *New England Journal of Medicine*, **1978**, 298, 4, pp. 195-197.
44. Martin, P.L.; Yen, S.S.C.; Burnier, A.M.; Hermann, H. *JAMA*, **1979**, 242, 24, pp. 2699-2700.
45. Deutsch,S.; Ossowski, R.; Benjamin, I. *Am. J. Obstet. Gynecol.*, **1981**, 139, 8, pp.967-970.
46. Heimer, G.M.; Englund, D.E. *Acta. Obstet. Gynecol. Scand.*, **1984**, 63, pp. 563-567.
47. Chakmakjian, Z.H.; Zachariah, N.Y. *J. Reprod. Med.*, **1987**, 32, 6, pp.443-448.
48. Devroey, P.; Palermo, G.; Bourgain, C. *J. Fertil.*, **1990**, 34, pp. 188-193.
49. Miles, R.A.; Paulson, R.J.; Lobo, R.A.; Press, M.F.; Dahmoush, L.; Sauer, M.V. *Fertil. Steril.*, **1994**, 62, 3, pp. 485-490.
50. Mizutani, T.; Nishiyama, S.; Amakawa, I.; Watanabe, A.; Nakamuro, K.; Terada, N. *Fertil. Steril.*, **1995**, 63, 6, pp. 1184-1189.
51. Bulletti, Ziegler, D.; Flamigni, C.; Giacomucci, E.; Polli, V.; Bolelli, G.; Franceschetti, F. *Human Reproduction*, **1997**, 12, 5, pp. 1073-1079.
52. Bulleti,C.; Jasonni, V.M.; Tabanelli, S.; Gianaroli, L.; Ciotti, P.M.; Ferraretti, A.P.; Flamigni, C. *Fertil. Steril.*, **1988**, 49, 6, pp. 991-996.
53. Bulleti, C.; Jasonni, V.M.; Lubicz, S.; Flamigni, C.; Gurpide,E. *Am. J. Obstet. Gynecol.*, **1986**, 154, pp. 683-688.
54. Fujii,T.; Naito, H.; Kioka, H.; Tanioka, Y.; Murakami,J.; Sanada, M.; Tanimoto,H.; Nakagawa,H.; Tanak, T.; Furui, J. *Japanese Journal of Cancer & Chemotherapy*, **1995**, 22, 1, pp. 99-103.
55. Lundgren, O.; Haglund, U. *Life Sciences*, **1978**, 23, pp. 1411-1422.
56. Dan-Axel Hallback,B.M.; Hulten, L.; Jodal, M.; Lindhagen, J.; Lundgren, O. *Gastroenterology*, **1978**, 74, pp. 683-690.
57. Bendz, A.; Lundgren, O.; Hamberger, L. *Acta Physiol. Scand.*, **1982**, 114, pp. 611-616.
58. Bendz, A. *Prostaglandins*, **1977**, 13, 2, pp. 355-362.

Downloaded by YORK UNIV on October 31, 2012 | http://pubs.acs.org
Publication Date: September 24, 1998 | doi: 10.1021/bk-1998-0709.ch002

Downloaded by YORK UNIV on October 31, 2012 | http://pubs.acs.org
Publication Date: September 24, 1998 | doi: 10.1021/bk-1998-0709.ch002

59. Bendz, A.; Hansson, H.A.; Svendsen, P.; Wiqvist, N. *Acta Physiol. Scand.*, **1982**, 115, pp. 179-182.
60. Bendz, A.; Einer-Jensen, N.; Lundgren, O.; Janson, P.O. *J. Reprod. Fert.*, **1979**, 57, pp. 137-142.
61. Halket, J.M.; Leidenberger, F.; Einer-Jensen, N.; Bendz, A. *Biomedical Mass Spectrometry*, **1985**, 12, 8, pp. 429-431.
62. Einer-Jensen, N.; McCracken, J.A.; Schram, W.; Bendz, A. *Acta Physiologica Polonica*, **1989**, 40, 1, pp. 3-11.
63. *Controlled Release Polymeric Formulations*, Paul, D.R.; Harris, F.W., Eds; American Chemical Society, Washington DC, **1976**.
64. *Sustained and Controlled Release Drug Delivery Systems*, Robinson, J.R. Ed., Marcell Dekker, Inc., New York, **1978**.
65. *Biomedical Polymers. Polymeric Materials and Pharmaceutical for Biomedical Use*, Goldberg, E.P.; Nakajima, A.; Eds. Academic Press, New York, **1980**.
66. *Medical Applications of Controlled Release*, Langer, R.S.; Wise, D.L., Eds., CRC Press, Boca Raton, FL, **1984**, Vol. I, II.
67. *Controlled Drug Delivery. Fundamentals and Applications*, Robinson, J.R.; Lee, V.H.L., Eds., Marcell Dekker, New York, **1987**.
68. *Hydrogels in Medicine and Pharmacy*, Peppas, N.A., Ed., CRC Press, Boca Raton, FL, **1987**, Vol. I - III.
69. Park, K.; Shalaby, W.S.W.; Park, H. *Biodegradable Hydrogels for Drug Delivery*, Technomic Publishing Co., Inc., Lancaster, PA, **1993**.
70. *Biomedical Polymers, Designed to Degrade Systems*, Shalaby, S.W. , Ed., Hanser Publishers, New York, **1994**.
71. Zeoli, L.T.; Kydonieus, A.F. *In Controlled Release Technology, Bioengineering Aspects*, Das, K.G., Ed., John Wiley & Son, New York, **1983**, pp. 61-120.
72. Kost, J.; Langer, R. In *Hydrogels in Medicine and Pharmacy*, Peppas, N.A., Ed., CRC Press, Boca Raton, FL, **1987**, Vol.III, pp. 95-108.
73. Park, H.; Park, K. In *Polymers of Biological and Biomedical Significance*, Shalaby, S.W.; Ikada, Y.; Langer, R.; Williams, J.,Eds., American Chemical Society, Washington, DC, **1994**, No. 540, pp. 2-15.
74. Higuchi, T. *J. Pharm. Sci.*, **1963**, 52, 12, pp. 1145-1149.
75. Roseman, T.J. *J. Pharms. Sci.*, **1972**, 61, 1, pp. 46-50.
76. Roseman, T.J.; Higuchi, W.I. *J. Pharm. Sci.*, **1970**, 59, 3, pp. 353-357.
77. Luzzi, L.A.; Zoglio, M.A.; Maulding, H.V. *J. Pharm. Sci.*, **1970**, 59, pp. 338-341.
78. Baker, R.W. In *Controlled Release of Biologically Active Agents*, John Wiley & Son, New York, **1987**, pp. 1-83.
79. Crank, J. In *The Mathematics of Diffusion*, Oxford University Press, London, **1975**, Second Edition, pp. 44-68.
80. Ritger, R.L.; Peppas, N.A. *J. Controlled Release*, **1987**, 5, 23, pp. 23-36.
81. Higuchi, T. *J. Pharm. Sci.*, **1961**, 50, 10, pp. 874-875.
82. Higuchi, W. *J. Pharm. Sci.*, **1962**, 51, 8, pp. 802-804.

Downloaded by YORK UNIV on October 31, 2012 | http://pubs.acs.org
Publication Date: September 24, 1998 | doi: 10.1021/bk-1998-0709.ch002

83. Schwartz, J.B.; Simonelli, A.P.; Higuchi, W.I. *J. Pharm. Sci.*, **1968**, 57, 2, pp. 274-277.
84. Heller, J.; Baker, R.W.; Gale, M.; Rodin, J.O. *J. Appl. Polym. Sci.*, **1978**, 22, pp. 1191-2009.
85. Windle, A.H. In *Polymer Permeability*, Comyn, J., Ed., Elsevier Applied Science Publishers, New York, **1985**, pp. 75-118.
86. Heller, J. *J. Controlled Release*, **1987**, 6, pp. 217-224.
87. Linhardt, R.J.; Rosen, H.B.; Langer, R. *Polymer Preprints*, **1983**, 24, pp. 47-48.
88. Leong, K.W.; Brott, B.C.; Langer, R. *J. Biomed. Mat. Res.*, **1985**, 19, pp. 941-955.
89. Mathiowitz, E.; Langer, R. *J. Controlled Release*, **1987**, 5, pp. 13-22.
90. Silberberg, A. In *Molecular Basis of Polymer Networks*, Baumgartner, A; Picot, C.E., Eds., Spring-Verlag, Berlin, **1989**, pp. 147-151.
91. Wichterle, O.; Lim, D. *Nature*, **1960**, 185, pp. 117-118.
92. Jhon, M.S.; Andrada, J.D. *J. Biomed. Mater. Res.*, **1973**, 7, pp. 509-516.
93. Piirma, I. In *Polymer Surfactants*, Marcel Dekker, Inc., New York, **1992**, Chapter 10.
94. Brook, S.D. In *Properties of Biomaterials in Physiological Environment*, CRC Press, Boca Raton, FL, **1980**, Chapter 4.
95. *Hydrogels for Medical and Related Applications*, Andrade, J.D., Ed., American Chemical Society, Washington, DC, **1976**, pp. xi-xiii.
96. Ratner, B.D. In *Biocompatibility of Clinical Implant Materials*, Williams, D.F., Ed., CRC Press, Boca Raton, FL, **1981**, Vol. II, Chapter 7.
97. Alfrey, T.; Gurnee, E.F.; Lloyd, W.G. *J. Polym. Sci.*, **1966**, Part C, 12, pp. 249-261.
98. Peppas, N.A.; Korsmeyer, R.W. In *Hydrogels in Medicine and Pharmacy*, Peppas, N.A., Ed. CRC Press, Boca Raton, FL, **1987**, Vol. III, pp. 118-121.
99. Hopfenberg, H.B.; Hsu, K.C. *Polym. Eng. Sci.*, **1978**, 18, 15, pp. 1186-1191.
100. Skeist, I. In *Handbook of Adhesives*, Von Nostrand Reinhold, New York, **1977**, p. xi.
101. Good, R.J. *J. Adhes.*, **1976**, 8, pp. 1-9.
102. Park, K.; Cooper, S.L.; Robinson, J.R. In *Hydrogels in Medicine and Pharmacy*, Peppas, N.A., Ed. CRC Press, Boca Raton, FL, **1987**, Vol.III, pp. 151-175.
103. Jones, D.S.; Woolfson, A.D.; Brown, A.F. *Int. J. Pharm.*, **1997**, 151, 2, pp. 223-233.
104. Lee, T.K.; Sokoloski, T.D.; Royer, G.P. *Science*, **1981**, 213, 10, pp. 233-235.
105. Morimoto, Y.; Fujimoto, S. *Critical Reviews in Therapeutic Drug Carrier Systems*, **1985**, 2,1, pp.19-63.
106. Bodmeier, R.; Chen, H.; Paeratkul, O. *Pharm. Res.*, **1989**, 6,5, pp. 413-417.
107. Ratcliffe, J.H.; Hynneyball, I.M.; Smith, A.; Wilson, C.G.; Davis, S.S. *J. Pharm. Pharmacol.*, **1984**, 36, pp. 431-436.

108. Davis, S.S.; Illum, L.; Burgess, D.; Ratcliffe, J.; Mills, S.N. *In Controlled Release Technology, Pharmaceutical Applications*, American Chemical Society, Washington, DC, **1986**, No. 348, pp. 201-213.
109. Shalaby, W.S.W. *Clin. Immunol. Immunopath.*, **1995**, 2, pp. 127-134.
110. Shalaby, W.S.W.; Park, K. In *Biomedical Polymers, Designed to Degrade Systems*, Shalaby, S.W. , Ed., Hanser Publishers, New York, **1994**, pp. 213-258.
111. Theeuwes, F. *Pharm. Ther.*, **1981**, 13, pp. 149-191.
112. Liggins, G.C. *Prostaglandins*, **1979**, 18, 1, pp. 167-172.
113. Shepherd, J.; Pearce, J.M.; Sims, C.D. *British Medical Journal*, **1979**, 2, pp. 108-110.
114. Mackenzie, I.Z., Bradley, S. Embrey, M.P. *Am. J. Obstet. Gynecol.*, **1981**, 141, 2, pp. 158-162.
115. Norchi, S.; Zanini, A.; Ragusa, A.; Maccario, L.; Valle, A. *Int. J. Gynecol. Obstet.*, **1993**, 42, pp. 103-107.
116. Smith, C.V.; Miller, A.; Livezey, G. *J. Reprod. Med.*, **1996**, 41, pp. 745-748.
117. Taylor, A.V.G.; Boland, J.; Mackenzie, I.Z. *Prostaglandins*, **1990**, 40, 1, pp. 89-98.
118. Macneill, M.E.; Graham, N.B. *J. Controlled Release*, **1984**, 2, pp. 99-117.
119. Embrey, M.P.; Graham, N.B.; Macneill, M.E., Hillier,K. *J. Controlled Release*, **1986**, 3, pp. 39-45.
120. Graham, N.B.; McNeill, M.E. *Biomaterials*, **1984**, 5, 1, pp. 27-36.
121. Embrey, M.P.; Graham, N.B.; McNeill, M.E. *British Medical Journal*, **1980**, 6245, pp. 901-902.
122. Smith, C.V.; Ryaburn, W.F.; Miller, A.M. *J. Reprod. Med.*, **1994**, 39, pp. 381-386.
123. Grodstein, F; Stampfer,M.; Colditz, G.; Willet, W.; Manson, J.; Joffe, M.; Rosner, B.; Fuchs, C.; Hankinson, S.; Hunter, D.; Hennekens, C; Speizer, F., *N. Engl. J. Med.*, **1996**, 335, pp. 453-461.
124. Grodstein, F; Stampfer,M.; Colditz, G.; Willet, W.; Manson, J.; Joffe, M.; Rosner, B.; Fuchs, C.; Hankinson, S.; Hunter, D.; Hennekens, C; Speizer, F., *N. Engl. J. Med.*, **1997**, 336, 1769-1775.
125. Nanada,F.; Eckman, M.; Karas, R.; Pauker, S.; Goldberg, R.; Ross, E.; Orr, R.; Wong, J. *JAMA*, **1997**, 277, 14, pp. 1140-1147.
126. Postmenopausal Estrogen/Progestin Interventions (PEPI) Trial, *JAMA*, **1996**, 76, 17, pp. 1389-1396.
127. Wimalawansa, S.J. *Am. J. Med.*, **1995**, 99, pp. 36-42.
128. Stumpf, P.G.; Maruca, J.; Santen, R.J.; Demers, L.M. *J. Clin. Endocrinol. Met.* **1982**, 54, 1, pp. 208-210.
129. Stumpf, P.G. *Obstet. Gynecol.*, **1986**, 67, 1, pp. 91-94.
130. Schmidt, G.; Anderson, S.B.; Nordle, O.; Johansson, C.; Gunnarsson, P.O. *Gynecol. Obstet. Invest.*, **1994**, 38, pp. 253-260.
131. Nachtigall, L.E. *Maturitas*, **1995**, 22, Suppl., pp. S43-S47.
132. Smith, P.; Heimer, G.; Lindskog, M.; Ulmsten, U. *Maturitas*, **1993**, 16, pp. 145-154.

Downloaded by YORK UNIV on October 31, 2012 | http://pubs.acs.org
Publication Date: September 24, 1998 | doi: 10.1021/bk-1998-0709.ch002

133. Bachmann, G. *Maturitas*, **1995**, 22, Suppl., pp. S21-S29.
134. Mishell, D.; Talas, M.; Parlow, A. *Am. J. Obstet. Gynecol.*, **1970**, 107, 1, pp. 100-107.
135. Burton, F.G.; Skiens, W.E.; Gordon, N.R.; Veal, J.T.; Kalkwarf, D.; Duncan, G.W. *Contraception*, **1978**, 17, 3, pp. 221-231.
136. Ballagh, S.; Mishell, D.; Lacarra,M.; Shoupe, D.; Jackanicz, T.; Eggena, P. *Contraception*, **1994**, 50, pp. 517-533.
137. Landgren, B.; Aedo, A.R.; Johannisson, E.; Cekan, S.Z. *Contraception*, **1994**, 49, pp. 139-150.
138. Landgren, B.; Aedo, A.R.; Johannisson, E.; Cekan, S.Z. *Contraception*, **1994**, 50, pp. 87-100.
139. Creinin, M.D.; Vittinghoff, E.; Keder, L.; Darney, P.D.; Tiller, *Contraception*, **1996**, 53, pp. 321-327.
140. Creinin, M.D.; Vittinghoff, E.; Galbraith, S.; Klaisle, C. *Am. J. Obstet. Gynecol.*, **1995**, 173, pp. 1578-1584.
141. Hill, G.B. *Am. J. Obstet. Gynecol.*, **1993**, 169, pp. 450-454.
142. Hill, G.B.; Eschenbach, D.A.; Holmes, K.K. *J. Urol. Nephrol. Suppl.*, **1985**, 86, pp. 23-39.
143. Gravett, M.G.; Hummel, D.; Eschenbach, Holmes, K.K. *Obstet. Gynecol.*, **1986**, 67, pp. 229-237.
144. Gravett, M.G.; Nelson, H.; DeRouen, T.; Critchlow, L.; Eschenbach, D.A.; Holmes, K.K. *JAMA*, **1986**, 256, pp. 1899-1903.
145. Lamont, R.F.; Taylor-Robinson, D.; Newman, M.; Wigglesworth, J.; Elder, M.G. *Br. J. Obstet. Gynecol.*, **1986**, 93, 804-810.
146. Hillier, S.L.; Martius, J.; Krohn, M.; Kiviat, N.; Holmes, K.K.; Eschenbach, D.A. *N. Engl. J. Med.*, **1988**, 319, pp. 972-978.
147. Eschenbach, D.A.; Hillier, S.L.; Critchlow, C.; Stevens, C.; DeRouen, T.; Holmes, K.K. *Am. J. Obstet. Gynecol.*, **1988**, 158, pp. 819-828.
148. Hillier, S.; Krohn, M.; Watts, H.; Wolner-Hanssen, P.; Eschenbach, D. *Obstet. Gynecol.*, **1990**, 76, pp. 407-413.
149. Livengood, C.H.; Thomason, J.; Hill, G. *Obstet. Gynecol.*, **1990**, 76, pp. 118-123.
150. Hill, G.; Livengood, C.H. *Am. J. Obstet. Gynecol.*, **1994**, 171, pp. 1198-1204.
151. Schmitt, C.; C, Pa; Sobel, J.; Curtiz, M. *Obstet. Gynecol.*, **1992**, 79, pp. 1020-1023.
152. Borin, M.T.; Powley, G.; Tackwell, K.; Batts, D.H. *Journal of Antimicrobial Chemotherapy*, **1995**, 35, pp. 833-841.
153. Edelman, D.; North, B. *J. Reprod. Med.*, **1989**, 34,5, pp.341-344.
154. Hillier, S.L.; Lipinski, C.; Briselden, A.; Eschenbach, D.A. *Obstet. Gynecol.*, **1993**, 81, pp. 963-967.
155. Livengood, C.; McCregor, J.; Soper, D.; Newton, E.; Thomason, J. *Am. J. Obstet. Gynecol.*, **1994**, 170, pp. 759-764.
156. Cunningham, F.; Kraus, D.; Brubaker, L.; Fischer, J. *J. Clin. Pharmacol.*, **1994**, 34, pp. 1060-1065.
157. Lyons, J.; Ito, J. *Clinical Infectious Diseases*, **1995**, 21, Suppl, pp. s174-s177.

Downloaded by YORK UNIV on October 31, 2012 | http://pubs.acs.org
Publication Date: September 24, 1998 | doi: 10.1021/bk-1998-0709.ch002

158. Pauwels, R.; De Clercq, E. *Journal of Acquired Immune Deficiency Syndromes and Human Retrovirology,* **1996**, 11, 3, pp. 211-221.
159. Bowen-Simpkins, P.; Hull, M.G.R. *Obstet. Gynecol.*, **1975**, 46,3, pp.360-362.
160. Woodruff, J.D.; Parmley, T.H.; Julian, C.G. *Gynecologic Oncology*, **1975**, 3, pp. 124-132.
161. Caglar, H; Hertzog, R.W.; Hreshchyshyn, M.M. *Obstet. Gynecol.*, **1981**, 58, pp. 580-583.
162. Kirwan, P. *Br. J. Obstet. Gynecol.*, **1985**, 92, pp. 287-291.
163. Piver, M.S.; Barlow, J.J.; Tsukada, S.; Gamarra, M.; Sandecki, A. *Am. J. Obstet. Gynecol.*, **1979**, 135, pp. 377-380.
164. Krebs, H.B. *Obstet. Gynecol.*, **1986**, 68, pp. 837-841.
165. Krebs, H.B. *Obstet. Gynecol.*, **1987**, 70, pp. 68-208.
166. Krebs, H.B.; Helmkamp, B.F. *Obstet. Gynecol.*, **1991**, 78, pp. 205-208.
167. Meyskens, F.L.; Surwit, T.; Moon, T.; Childers, J.; Davis, J.; Dorr, R.; Johnson, C.; Alberts, D. *J. Natl. Cancer Inst.*, **1994**, 86, 7, pp. 539-543.
168. Meyskens, F.L.; Graham, V.; Chvapil,M. *J. Natl. Cancer Inst.*, **1983**, 71, pp. 921-925.
169. Dorr, R.; Surwit, E.; Meyskins, F.L. *J. Biomed. Mater. Res.*, **1982**, 16, pp. 839-850.
170. Singer, Z.; Beck, M.; Jusic, D.; Soos, E.; *Jugoslavenska Ginekologijai Perinatologija*, **1990**, 30, 1-2, pp. 27-29.
171. Schneider, A.; Grubert, T.; Kirchmayr, R.; Wagner, D.; Papendick, U.; Schlunck, G. *Arch. Gynecol. Obstet.*, **1995**, 256, 2, pp. 75-83.
172. Nakayama, K.; Shimizu, Y.; Hasumi, K.; Masubuchi,K. *J. Jap. Soc. Cancer Ther.*, **1990**, 25, 4, pp. 826-829.
173. Shalaby, S.W., ed. *Biomedical Polymers: Designed to Degrade Materials*, Hanser, NY, **1994**.
174. Shalaby, S.W., U.S. Patent (to Poly-Med, Inc.) 5,612,052, **1997**.
175. Corbett, J.T., Trans. Soc. Biomater., **1997, XX**, p 362.
176. Corbett, J.T., Trans Soc. Biomater. **1998**, in press.
177. Shalaby, S.W., in *Water Soluble Polymers*, Shalaby, S. W., et al., eds., ACS Symp. Series, Vol. 467, American Chemical Society, Washington, DC, 1991.
178. Jones, D.S.; Woolfson, A.D.; Brown, A.G.; O'Neill, M.J., *J. Controlled Rel.*, 1997, 49, p. 71.
179. Calvo, P.; Remunan-Lopez, C.; Vila-Jato, J.; and Alonso, M., *J., Pharm. Res.*, **1997**, 14, p. 1431.

Downloaded by YORK UNIV on October 31, 2012 | http://pubs.acs.org
Publication Date: September 24, 1998 | doi: 10.1021/bk-1998-0709.ch002

Downloaded by NORTH CAROLINA STATE UNIV on October 31, 2012 | http://pubs.acs.org
Publication Date: September 24, 1998 | doi: 10.1021/bk-1998-0709.ch003

Chapter 3

Cationic Hydrogels for Controlled Release of Proteins and Other Macromolecules

Lisa M. Schwarte, Kairali Podual, and Nicholas A. Peppas[1]

Biomaterials and Drug Delivery Laboratories, School of Chemical Engineering, Purdue University, West Lafayette, IN 47906

The use of hydrogels in biomedical and pharmaceutical applications is growing every day. The nontoxicity and biocompatibility of these materials make them very attractive as biomaterials and carriers of drug in the body (1). As a result, they have been used quite frequently as scaffolds in tissue culture (2), for artificial organs (3), drug targeting (4), and transdermal delivery systems (5). As drug delivery devices, these swellable matrices help to modulate release rates and to maintain desirable levels of drug in the body (6). Application of hydrogels is not limited to the biological area only, but is extended to agricultural and environmental areas. Hydrogels have been used for the delivery of certain pesticides and herbicides over long periods of time (7). In the chemical and environmental area, hydrogels are used as flocculants for treatment of sludge (8).

One important property of these hydrogels is their environment-sensitivity. These materials can be designed to respond to changes in pH, ionic strength (9), temperature (10) and other external stimuli. The stimulus-sensitive behavior of these hydrogels can be used for biosensing (11) and environment-responsive drug release (12). Ionic hydrogels have been used extensively as ion-exchange membranes for the monitoring of environmental pollution, for chemical separation systems (13), and for molecular imprinting (14,15).

The environment-sensitive behavior of hydrogels is due to the electrolytic nature of the polymer chains. These polyelectrolytic chains contain ionizable moieties which protonate and deprotonate depending on the surrounding conditions. These gels exhibit a transition in swelling when they change from a collapsed state to a highly swollen state. For a pH-sensitive hydrogel, changes in the hydrogen concentration in the surrounding fluid can bring about an abrupt change in the swelling. These pH-responsive gels can be grouped as anionic and cationic gels based on the type of ions that are present in the charged state.

---

[1] Contributing author.

In Tailored Polymeric Materials for Controlled Delivery Systems; McCulloch, I., et al.;
ACS Symposium Series; American Chemical Society: Washington, DC, 1998.

Anionic hydrogels are polymers containing carboxylic or sulphonic acid groups which ionize above their pK_b values. These hydrogels swell in high pH regimes due to the electrostatic repulsion between the anions formed along the chains (16,17). Cationic hydrogels, on the other hand, contain tertiary amine groups. These groups are known to protonate at low pH (9,18). Thus, they exhibit a swelling behavior which is quite complementary to that of the anionic hydrogels as shown in Figure 1. Under the influence of a high pH solution, the non-ionized pendant amine groups are very hydrophobic. As a result, they form clusters and exclude water from the system. When the pH is decreased below the pK_a of the ionizable group, protonation occurs resulting in the formation of positive charges along the backbone chain. Ionization of the pendant groups gives rise to two phenomena, each of which contributes to the swelling behavior of the hydrogel. Due to the electrostatic repulsion, the positively charged pendant groups repel each other causing the polymer chains to move apart spatially. In addition, ionization alters the hydrophobic nature of the matrix and the latter becomes more hydrophilic. Both these phenomena lead to the increased sorption of water into the hydrogel, causing it to swell.

The size exclusion which occurs in these polymers can be characterized using the effective mesh size of the matrix. In the collapsed state, the mesh size is small. Solute diffusion under these conditions is slow, often regulated to be zero. On the other hand, in the swollen state, the diffusion of solute out of the matrix is enhanced due to increased mesh size. Thus, we can observe that the release rates can be modulated to obtain a pulsatile delivery depending on the external stimulus. Cationic hydrogels have been tested for release of different solutes. The diffusion of caffeine (19), vitamin B_{12} and other model drugs (12, 18-20) have been studied under different pH conditions. The release properties of these molecules were seen to be strongly dependent on the pH of the release media. As expected, larger molecules showed slower rates of release compared to smaller molecules indicating that size exclusion occurs in the hydrogel matrix.

The incorporation of poly(ethylene glycol) (PEG) in a hydrogel increases the biocompatibility of the matrix. This is because PEG is known to have ‘stealth’ properties, that is, it can prevent the immunoreaction of the body to the biomaterial. The presence of PEG can also increase the stability of certain proteins and enzymes immobilized or physically entrapped into the matrix. In certain cases, there is evidence that the PEG forms hydrogen bonds with the ionic polyelectrolyte. In such cases, hydrogel collapse is more drastic resulting in a more pronounced size-exclusion effect in the hydrogel (17).

One application of the stimulus-driven release properties of ionic hydrogels is as carriers for the glucose-sensitive release of insulin. The pH-sensitivity of these ionic hydrogels can be coupled with glucose-responsive properties by the use of the enzyme, glucose oxidase (GOD) (21-23). Usually, the enzyme is immobilized into the matrix using covalent bonds. Glucose is converted to gluconic acid under the effect of glucose oxidase. Due to the formation of an acid, the pH in the microenvironment of the hydrogel decreases. In the case of anionic hydrogels, the reduction in pH results in a decrease in the mesh size and the squeezing out of insulin from the matrix (23). On the other hand, in cationic hydrogels, the decrease in pH brings about a sudden increase in the mesh. Thus,

Downloaded by NORTH CAROLINA STATE UNIV on October 31, 2012 | http://pubs.acs.org
Publication Date: September 24, 1998 | doi: 10.1021/bk-1998-0709.ch003

insulin is released from the network by diffusion. The physical interpretation of the release process is shown in Figure 2.

ASPECTS OF HYDROGEL DESIGN

Cationic hydrogels are synthesized from multifunctional monomers containing tertiary amine or quaternary ammonium groups. These hydrogels swell in low pH regimes absorbing large amounts of water into the matrix. There are a number of parameters that influence the swelling behavior of a cationic gel. One factor that influences its behavior is the type and concentration of ionizable groups. These groups not only control the degree to which a polymer swells but also determine the transition pH where the gel converts from a collapsed state to a highly swollen state. The hydrophobicity of the monomers also affects the transition pH. A monomer which is more hydrophobic has a lower transition pH value than a monomer which is less hydrophobic. Another structural parameter often used to characterize hydrogel matrices is the mesh size. It describes the distance between two consecutive crosslinks or junctions. The mesh size depends primarily on the degree of crosslinking in the hydrogel and the swelling. With variations in pH, significant changes in mesh size are observed in these ionic hydrogels. Increase in the mesh size involves increases in the diffusion coefficients of solute molecules through the network at low pH values. Thus, there is an enhancement in the diffusion of solutes from the hydrogel when the surrounding medium has a lower pH than the transition value.

The diffusion rate is also a function of the nature of the solute which is being released from the network. Due to presence of charges along the backbone chain, it is common to observe interactions between the solute and polymer. Therefore, the release dynamics of the molecules of positive and negative charges can be entirely different from one another. Also, the presence of PEG grafts and enzymes immobilized in the matrix affects the swelling and the release properties of the hydrogels considerably.

EXPERIMENTAL

Diethylaminoethyl methacrylate (DEAEM, Aldrich, Milwaukee, WI) is a typical monomer, often used for the preparation of cationic hydrogels. The disubstituted amine group in this monomer is responsible for the strong hydrophobic nature of the resulting hydrogel in high pH. In low pH, $-N(C_2H_5)_2$ ionizes to form $-NH^+(C_2H_5)_2$. This is responsible for the transition behavior of the material. PEG was attached to the cationic backbone as grafts by using the functionalized monomer, poly(ethylene glycol) monomethacrylate (PEGMA, Polysciences, Warrington, PA). The crosslinking agent used was tetra(ethylene glycol) dimethacrylate (TEGDMA, Aldrich, Milwaukee, WI). The structure of the terpolymer formed is shown in Figure 3. The termonomer mixture containing the crosslinking agent was diluted using a 50% ethanol solution to give 60:40 monomer to solvent ratio. For redox initiation, 0.01 g each of ammonium persulfate (Baker, Phillipsburg, NJ) and sodium metabisulfite (Fisher, Fairlawn NJ) were added to the monomers. Nitrogen was bubbled into the reaction mixture to remove oxygen which acts as a free radical scavenger. Polymerization was carried out at 37°C in a nitrogen atmosphere for 24 hrs. Films of poly(diethylaminoethyl methacrylate-g-ethylene glycol), henceforth designated as

Downloaded by NORTH CAROLINA STATE UNIV on October 31, 2012 | http://pubs.acs.org
Publication Date: September 24, 1998 | doi: 10.1021/bk-1998-0709.ch003

Downloaded by NORTH CAROLINA STATE UNIV on October 31, 2012 | http://pubs.acs.org
Publication Date: September 24, 1998 | doi: 10.1021/bk-1998-0709.ch003

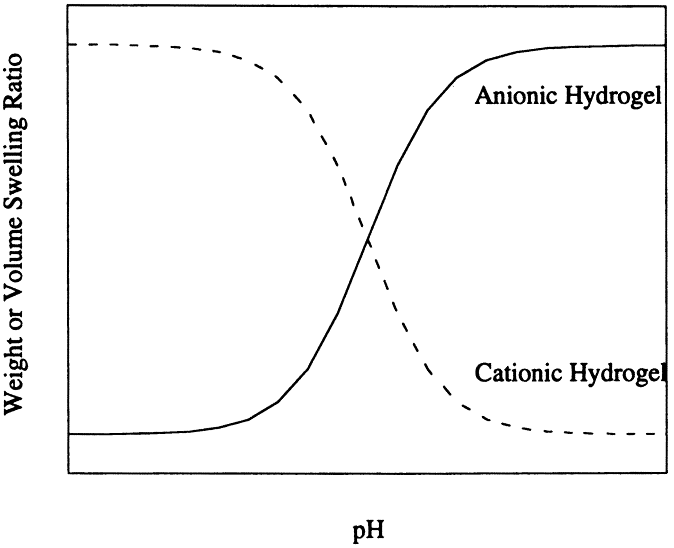

Figure 1 : Dependence of equilibrium degree of swelling on pH for anionic and cationic gels. The transition pH value are located at the inflection points of the curves.

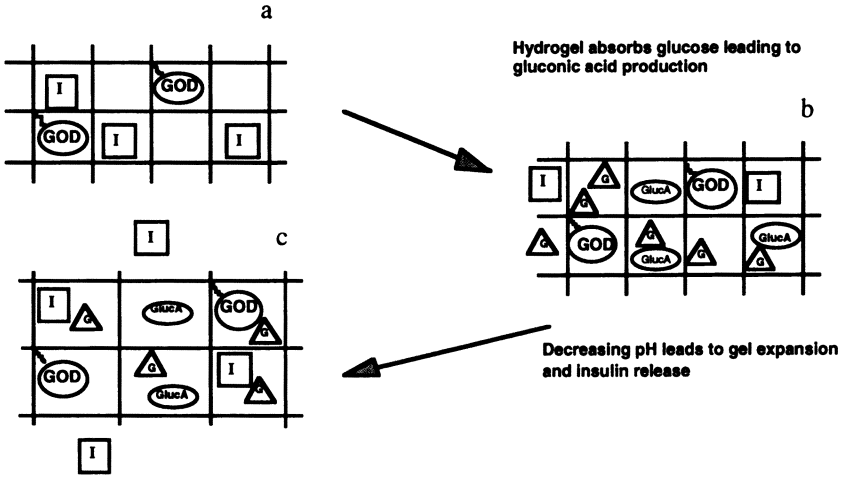
a
I
GOD
GOD
I
I
Hydrogel absorbs glucose leading to gluconic acid production
b
I
G
G
GlucA
GOD
I
G
GOD
G
GlucA
G
GlucA
G
I
c
I
G
GlucA
GOD
G
GOD
G
GlucA
I
G
I
Decreasing pH leads to gel expansion and insulin release

Figure 2. Release mechanism from cationic hydrogels: (a) the gel is a crosslinked network with glucose oxidase (GOD) immobilized in it and insulin (I) is physically entrapped into the system; (b) in the presence of glucose (G), gluconic acid is produced (GluA); (c) increase in mesh size results in release of insulin

P(DEAEM-g-EG)), were cast in between glass slides separated by teflon spacers. Samples of hydrogel were prepared using different ratios of methacrylate repeats to PEG grafts. The investigated ratios were 10:1, 50:1, 75:1, and 99:1. Samples were also prepared having different crosslinking ratios, ranging between 0.005 and 0.04 moles crosslinking agent per mole of all monomers.

For the immobilization of glucose oxidase (GOD, Sigma, St. Louis, MO), the enzyme was first functionalized with acryloyl chloride (Aldrich, Milwaukee, WI). The ensuing acid chloride group was used to attach the enzyme covalently to the methacrylate chains. A 1% enzyme solution in a phosphate buffer of pH 7.4 was initially reacted with the binding agent at 4°C for one hour. The enzyme solution was added to the monomer mixture to obtain a 60 wt% monomer solution. The final mixture was polymerized by redox-initiated or photo-initiated (0.01 g of hydroxymethyl phenyl ketone, Ciba-Geigy, Hawthorn, NY, as initiator) reactions to prepare polymers with different crosslinking ratios and enzyme loadings.

The different hydrogel samples were tested for their equilibrium and dynamic swelling properties. The buffered solutions used in this study were phosphate buffers and dimethylglutaric acid (DMGA, Sigma, St. Louis, MO) with sodium hydroxide buffers. For equilibrium swelling, the dry hydrogel samples were weighed and immersed in buffers of different pH at 37°C. The final weights of the samples were recorded and the swelling ratios were calculated using Eqs. (1) and (2).

$$\text{Weight Swelling Ratio } q = \frac{\text{Weight of swollen hydrogel}}{\text{Weight of dry hydrogel}} \tag{1}$$

$$\text{Volume Swelling Ratio } Q = \frac{\text{Volume of swollen hydrogel}}{\text{Volume of dry hydrogel}} \tag{2}$$

The volumes were calculated by weighing the samples in air and in heptane. The dynamic swelling characteristics of these hydrogels were investigated by studying the variation of the swelling ratio with time at various values of pH. It is important that these variations be reproducible over cycles of pH changes. Therefore, the pulsatile swelling behavior of these hydrogels were studied by changing the pH between two values at definite intervals of time.

The absorbance of ultraviolet light at 220 nm of the wash solutions from these hydrogels were measured to estimate the amount of glucose oxidase immobilized in the network. It was found that, on the average, 72% of the enzyme had attached to the network. To measure the activity of the immobilized enzyme, a hydrogel sample was immersed in a saline solution containing 200 mg/dl of glucose. The formation of gluconic acid was monitored using a pH-meter. The initial rate of the reaction was compared to the activity of the native enzyme. It was found that the immobilized enzyme was 29%±7 as active as the free enzyme.

Insulin was loaded into the hydrogel matrix by imbibition. A hydrogel disc was allowed to swell in a 1% insulin solution at pH 5.2. The amount of insulin

Downloaded by NORTH CAROLINA STATE UNIV on October 31, 2012 | http://pubs.acs.org
Publication Date: September 24, 1998 | doi: 10.1021/bk-1998-0709.ch003

incorporated was calculated as the difference in the dry weights of the hydrogels before and after loading of insulin. In a typical loading process, the discs contained upto 18 wt% insulin.

RESULTS AND DISCUSSIONS

The equilibrium weight ratios have been plotted as a function of pH as shown in Figure 4. It is seen that at high pH values, all of the gels were collapsed and had equilibrium weight ratios between 2 and 3. As they reached the transition region, the gels began to swell. There was a general trend toward increasing equilibrium weight ratio with increasing content of the pH-sensitive material, DEAEM, until the polymer with a 99:1 methacrylate to PEG molar ratio. This polymer had a relatively lower equilibrium swelling ratio than the other compositions used. This was due to the fact that there was so much of the pH-sensitive material included in the network, it could not fully overcome its hydrophobic tendencies and did not swell to as great an extent as expected. From the equilibrium swelling curves, the pH at which the gels experienced a transition from their collapsed to their swollen states was determined. The transition pH for these hydrogels was estimated to be 6.42±0.13.

The equilibrium swelling characteristics of glucose-sensitive cationic hydrogels are shown in Figure 5. Each graph in this figure represents a different crosslinking ratio. The maximum swelling ratio obtained for each of the graphs is a strong function of the crosslinking ratio. As expected, the hydrogel having the smallest crosslinking ratio has the largest maximum swelling ratio. Using Eqs. (3) and (4) (24), the diffusion coefficient of insulin in the fully swollen state relative to the collapsed state was calculated for each crosslinking ratio.

$$\xi = C_n Q^{1/3} N^{1/2} l \qquad (3)$$

$$D \cong \left[1 - r/\xi\right] e^{-Y/(Q-1)} \qquad (4)$$

Here D defines the diffusion coefficient, r is the molecular radius of insulin which is equal to 16 Å, ξ is the mesh size of the network, Q is the swelling ratio, Y is a constant often equal to 1, C_n is the characteristic constant of the polymer, taken to be 14.4 for the methacrylate chains, N is the number of links in a single chain and l is the –C–C– bond length. It is seen that the ratio between the largest and the smallest mesh size at equilibrium is equal to 4.5. The rate of diffusion of insulin can thus be varied to a large extent by changing the crosslinking ratio of the material. Theoretical prediction and experimental verifications of the diffusion data have been reported by Schwarte and Peppas (25). The equilibrium swelling characteristics of the hydrogels containing different amounts of enzymes have been shown in Figure 6. It is seen that by varying the enzyme content we can change the equilibrium concentration by a small percentage. Larger amount of enzyme results in phase separation and poor mechanical stability of the hydrogels.

Figure 7 shows the dynamic swelling behavior of the hydrogel having 10:1 and 50:1 methacrylate to graft ratios. The samples were pre-equilibrated at a pH 9.3 The initial weight swelling ratio was about 2.7, and the polymer swelled to

Downloaded by NORTH CAROLINA STATE UNIV on October 31, 2012 | http://pubs.acs.org
Publication Date: September 24, 1998 | doi: 10.1021/bk-1998-0709.ch003

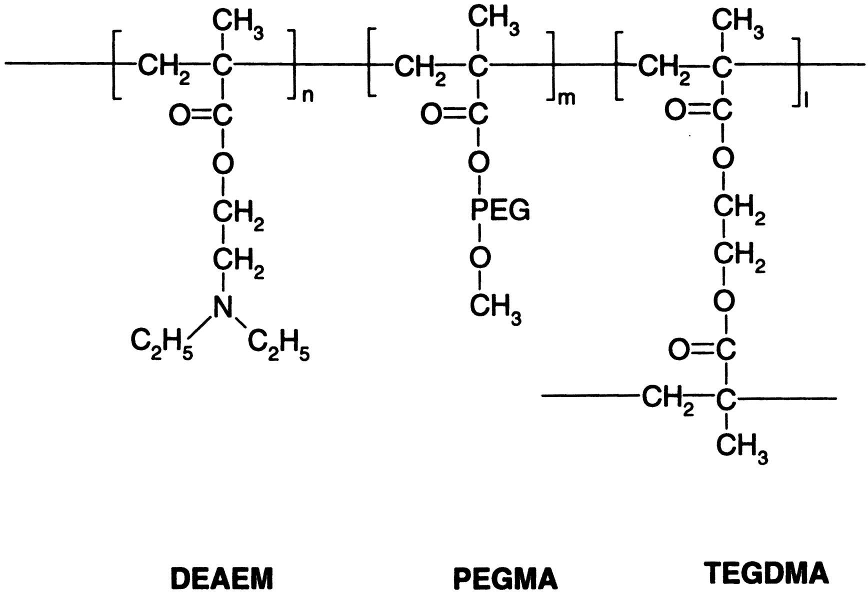

Figure 3: The structure of P(DEAEM-g-EG) hydrogels prepared from diethylaminoethyl methacrylate (DEAEM), poly(ethylene glycol) 1000 monomethacrylate (PEGDMA) and crosslinking agent, tetra(ethylene glycol) dimethacrylate (TEGDMA).

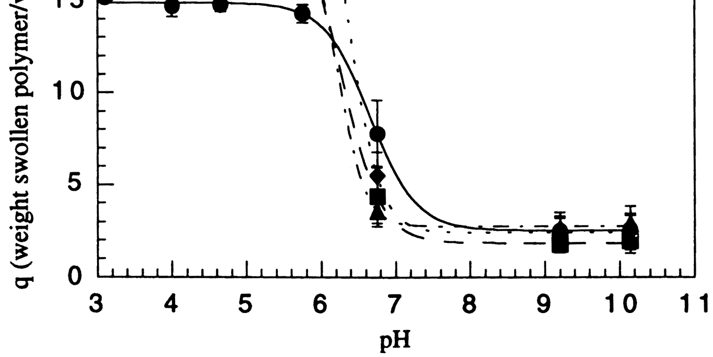

Figure 4: Equilibrium swelling behavior of P(DEAEM-g-EG) gels containing molar ratios of 10:1 (●), 50:1 (■), 75:1 (◆), and 99:1 (▲) and crosslinking ratio X=0.02, as a function of pH at 37°C.

Downloaded by NORTH CAROLINA STATE UNIV on October 31, 2012 | http://pubs.acs.org
Publication Date: September 24, 1998 | doi: 10.1021/bk-1998-0709.ch003

Downloaded by NORTH CAROLINA STATE UNIV on October 31, 2012 | http://pubs.acs.org
Publication Date: September 24, 1998 | doi: 10.1021/bk-1998-0709.ch003

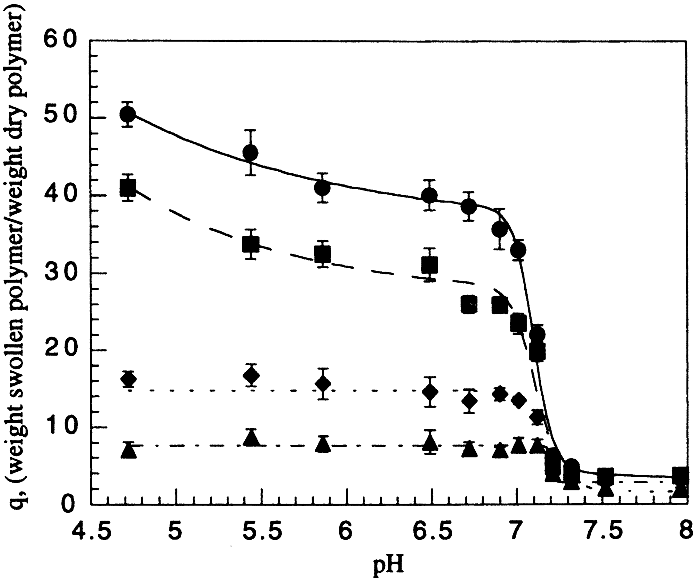

Figure 5: Equilibrium swelling behavior as a function of pH for glucose-sensitive P(DEAEM-g-EG) hydrogels with molar ratio 10:1 and enzyme concentration $1x10^{-3}$ mg/cm^3 containing different crosslinking ratios: X=0.005 (●), X=0.01 (■), X=0.02 (◆), and X=0.04 (▲) at 37°C in phosphate buffer solutions.

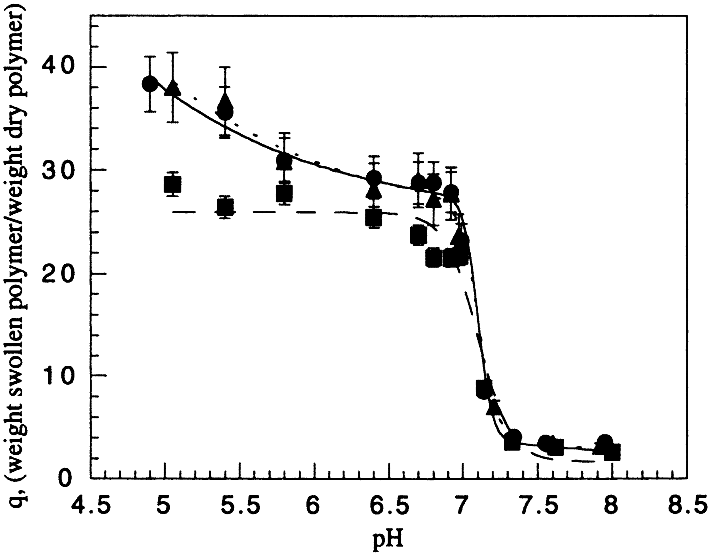

Figure 6: Equilibrium swelling behavior of P(DEAEM-g-EG) hydrogels with molar ratio 10:1 and X=0.01 loaded with different amounts of glucose oxidase. Enzyme concentration is measured as milligrams of enymes per unit volume of polymer: $8.333x10^4$mg/cm^3 (●), $4.1671x0^{-4}$mg/cm^3 (■), and $2.083x10^{-4}$mg/cm^3 (▲) at 37°C in phosphate buffer solutions.

Downloaded by NORTH CAROLINA STATE UNIV on October 31, 2012 | http://pubs.acs.org
Publication Date: September 24, 1998 | doi: 10.1021/bk-1998-0709.ch003

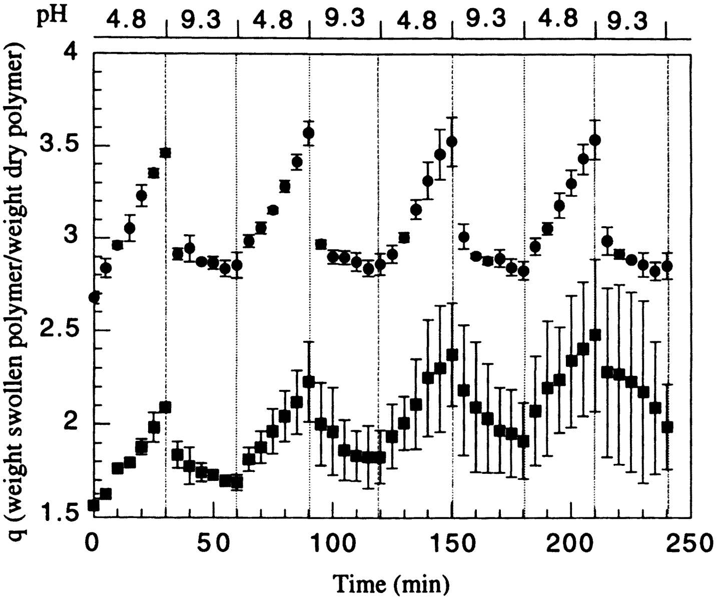

Figure 7: Oscillatory response of P(DEAEM-g-EG) gels with molar ratios 10:1(●) and 50:1(■) and X=0.01 to cyclic changes in pH between 4.8 and 9.3 at 37°C.

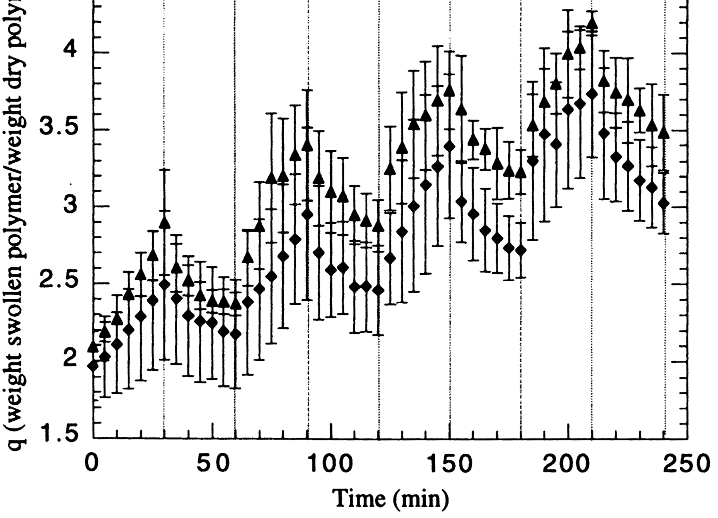

Figure 8: Oscillatory response of P(DEAEM-g-EG) gels with molar ratios 75:1(◆) and 99:1(▲) and X=0.01 to cyclic changes in pH between 4.6 and 9.4 at 37°C.

a weight ratio of about 3.5 after 30 minutes in a solution of pH 4.8. When the polymer was transferred to a pH 9.3 buffer, it began to collapse, and after 30 minutes had reached a weight ratio of about 2.9. The gel with a 10:1 methacrylate to PEG molar ratio was able to return to its original equilibrium value after each of its swelling/collapse cycles. The gel containing 50:1 methacrylate to PEG molar ratio started at a lower swelling ratio of 1.6. This sample appeared to have a higher response time as it retained more of its weight after each cycle of pH change. Oscillatory swelling experiments were also performed on samples containing 75:1 and 99:1 methacrylate repeat to PEG graft ratios. The pH of the medium was changed between 4.6 and 9.3 at 30 in intervals. The results are shown in Figure 8. Both these samples showed oscillatory swelling behavior in response to the changes in the pH field.

Downloaded by NORTH CAROLINA STATE UNIV on October 31, 2012 | http://pubs.acs.org
Publication Date: September 24, 1998 | doi: 10.1021/bk-1998-0709.ch003

CONCLUSIONS

pH-Sensitive hydrogels of poly(diethylaminoethyl methacrylate-g-ethylene glycol) were prepared. Samples having different commoner ratios, crosslinking ratios and characteristic sizes were studied to establish the dependence of swelling on each of these parameters. Equilibrium swelling studies showed a transition pH where the polymer converts from a collapsed state to a swollen state. Oscillatory swelling of the samples shows the dynamic nature of response of the hydrogel to pH and the reversibility of the transition. Glucose-sensitive hydrogels of the same materials were also studied for applications in insulin release. The parameter stated earlier can be tuned to establish the desired release profiles of insulin in the body.

ACKNOWLEDGMENTS

This work was supported by grant No. GM43337 from the National Institutes of Health (LS) and the Showalter Foundation (KP).

REFERENCES

1. Hoffman, A. S. *Polym. Preprints*, **1990**, 31(1), 220.
2. Lu, L. and Mikos, A. G. *MRS Bull.*, **1996**, 21, 28.
3. Ratner, B. in Biocompatibility of Clinical Implant Materials, D. F. Williams, editor, CRC Press Boca Raton, 1981, p. 145.
4. Kopecek, J and Kopeckova, P. *Polym. Preprints*, **1990**, 31(1), 196.
5. Brannon-Peppas, L. *Adv. Drug Del. Rev.*, **1993**, 11, 169.
6. Peppas, N. A. and Korsmeyer, R. W. in *Hydrogels in Medicine and Pharmacy*, N. A. Peppas, editor, CRC Press, Boca Raton, 1986, p. 109.
7. Langer, R. S. and Peppas, N. A. *J. Macromol. Sci., Rev. Macromol. Chem. Phys.*, **1983**, C23, 61.
8. Liaw, D-J., Shiau, S-J., and Lee, K-R. *J. Appl. Polym. Sci.*, **1992**, 45, 61.
9. Siegel, R. A., Firestone, B. A., Johannes, I., and Cornejo, J. *Polym. Preprints*, **1993**, 34(1), 231.
10. Hoffman, A. S. in *Polymers in Medicine III*, C. Migliaresi, E. Cheillini, P. Guisti, and N. Luigi, eds., Elsevier, Amsterdam, 1988, p. 161.
11. Vaidya, R. and Wilkins, E. *Med. Eng. Phys.*, **1994**, 16, 416.
12. Bell, C. L. and Peppas, N. A. *Biomaterials*, **1996**, 17, 1203.
13. Grodinsky, A. J. and Weiss, A. M. *Sep. Purif. Methods*, **1985**, 14, 1.

14. Piletsky, S. A., Parhometz, Y. P., Lavryk, N. V., Panasyuk, T. L., and El'skaya, A. V. *Sensors and Actuators B*, **1994**, 18-19, 629..
15. Peppas, N. A. and Foster, L. K. *J. Appl. Polym. Sci.*, **1992**, 52, 763.
16. Khare, A. R. and Peppas, N. A. *Biomaterials*, **1995**, 16, 559.
17. Bell, C. L. and Peppas, N. A. *Adv. Polym. Sci.*, **1994**, 122, 125.
18. Hariharan, D. and Peppas, N. A. *Polymer*, **1996**, 37, 149.
19. Cornejo-Bravo, J. M., Arias-Sanchez, V., Alvarez-Anguiano, A., and Siegel, R. A. *J. Controlled Release*, **1995**, 33, 223.
20. Khare, A. R. and Peppas, N. A. *J. Biomater. Sci. Polymer Edn.*, **1993**, 4, 275.
21. Goldraich, M. and Kost, J. *Clin. Mater.*, **1993**, 13, 135.
22. Albin, G., Horbett, T. A. and Ratner, B. D. *J. Controlled Rel*ease, **1985**, 2, .
23. Dorski, C. M., Doyle III, F. J. and Peppas, N. A. *Polym. Preprints*, **1996**, 37(1), 475.
24. Lustig, S. R. and Peppas, N. A. *J. Appl. Polym. Sci.*, **1986**, 43, 533.
25. Schwarte, L. S. and Peppas, N. A. *Polymer*, in press.

Downloaded by NORTH CAROLINA STATE UNIV on October 31, 2012 | http://pubs.acs.org
Publication Date: September 24, 1998 | doi: 10.1021/bk-1998-0709.ch003

In Tailored Polymeric Materials for Controlled Delivery Systems; McCulloch, I., et al.;
ACS Symposium Series; American Chemical Society: Washington, DC, 1998.

Downloaded by YORK UNIV on October 31, 2012 | http://pubs.acs.org
Publication Date: September 24, 1998 | doi: 10.1021/bk-1998-0709.ch004

Chapter 4

Water-Soluble Polyanions as Oral Drug Carriers: Poly(sulfopropyl methacrylate potassium-*co*-alkyl methacrylate)

Yvonne N. Nujoma[1], Cherng-ju Kim[1,3], and Rey T. Chern[2]

[1]School of Pharmacy, Temple University, Philadelphia, PA 19140
[2]Merck & Co., Merial, P.O. Box 4, West Point, PA 19486

New synthetic polymeric materials have been investigated as oral controlled release systems based on the theory of ion exchange. The polymeric carriers are water-soluble copolymers consisting of an ionic monomer, sulfopropyl methacrylate potassium salt (SPMK), and hydrophobic monomers of alkyl methacrylate (AMA), methyl methacrylate (MMA) and ethyl methacrylate (EMA). Drug-copolymer complexes were obtained by adding aqueous solutions of model drugs, propranolol HCl, verapamil HCl, diltiazem HCl, and labetalol HCl to aqueous solutions of the copolymers enabling the basic amine drugs to complex to the sulfonate groups of the copolymers. Compact tablets were fabricated from the resultant drug-copolymer complexes and dextrose USP. The drug-copolymer complexes are characterized by differential scanning calorimetry and UV spectroscopic methods. The release kinetics from the drug-copolymer tablets are zero-order and are well described by a mathematical model which is based on a heterogeneous dissociation/erosion controlled mechanism. Varying the copolymer composition by increasing the alkyl side chain length of the AMA comonomer or decreasing the ratio of SPMK to AMA prolong the release kinetics. Other aspects such as the type and solubility of the drug complexed with the copolymers and the ionic strength and pH of the artificial gastric/intestinal fluid buffers were also investigated.

In Tailored Polymeric Materials for Controlled Delivery Systems; McCulloch, I., et al.;
ACS Symposium Series; American Chemical Society: Washington, DC, 1998.

Ion exchange is a reversible, equilibrium process by which a solid material furnishes ions to its surrounding liquid medium in return for an equivalent amount of ions of equal charge (*1*). The solid materials which facilitate ion exchange are known as ion exchange resins (*2*). The synthetic organic resins are the most recognized and widely used due to their stability, high exchange capacity, and commercial availability (*3*). They are spherical, high molecular weight, water-insoluble polymers possessing acidic or basic functional groups which are covalently bound to a hydrophobic matrix and associated with oppositely charged mobile counterions which enable the resin to undergo ion exchange(*4*).

Although ion exchange resins were mainly used as separation materials, they quickly gained popularity as agents for oral drug delivery (*4*). Drugs which possess ionic sites in their molecular structure are chemically bound to the ion-active groups of the resin and are only released by exchanging with ions present in the gastric/intestinal fluids (*4*). These dosage forms provide numerous advantages. They are easy and inexpensive to prepare, accommodate more than half the drug population, prolong drug action and availability compared to free base or common salt dosage forms, permit high drug loading without rapidly releasing the drug and causing deleterious side effects, protect drugs which are inactivated by enzymatic degradation in the GI tract, aid in tastemasking bitter and unpleasant tasting drugs, and can be manufactured as various types of dosage forms, solutions, suspensions, gums, tablets, and capsules (*5-8*).

Despite the numerous benefits, resin dosage forms furnish square-root-of-time kinetics characterized by incomplete exhaustion of the drug and significant tailing in the later stages of release due to the highly crosslinked resin structure which causes drug release to be controlled by diffusion (*9-11*). Resin dosage forms have these shortcomings because ion exchange resins were adapted rather than designed for drug delivery.

To design oral drug delivery systems based on the theory of ion exchange without the limitations of their precursors, ion exchange resins, polyelectrolyte gels (synthesized by polymerizing ionic monomers with neutral hydrophilic or hydrophobic monomers) were investigated (*12*). Cross-linked, hydrophobic, ionic polymer gels possessing tertiary amine or carboxylic acid pendant groups deliver drugs with non-Fickian kinetics. However, the pH-dependent swelling characteristics of the weakly acidic and basic functional groups do not make them candidates for oral drug delivery (*13-14*). Erodible polyelectrolyte gels possessing carboxylic acid groups render zero-order release kinetics with drug loadings greater than 40% (*15*). However, like their cross-linked counterparts, they also are prone to pH-dependent release kinetics. Buffer strength and pH-independent release kinetics have been reported for swellable polyelectrolyte gels consisting of sulfopropyl methacrylate potassium and 2-hydroxyethyl methacrylate (PSPMK/HEMA) due to the pH insensitivity of the strongly acidic sulfonate groups (*16*). However, drug release followed Fickian kinetics due to the low degree of swelling in phosphate buffers (0.05 - 0.1 M). To design polymeric drug carriers which will provide pH-independent, zero-order release kinetics, one should prepare a sulfonate polyelectrolyte gel which is water-soluble so that the release kinetics are governed by polymer erosion. In this report we present

Downloaded by YORK UNIV on October 31, 2012 | http://pubs.acs.org
Publication Date: September 24, 1998 | doi: 10.1021/bk-1998-0709.ch004

the zero-order, pH independent drug release kinetics for water-insoluble (soluble in ionic environment) drug-PSPMK/AMA (poly-(sulfopropyl methacrylate potassium-co-alkyl methacrylate) tablets (Scheme 1).

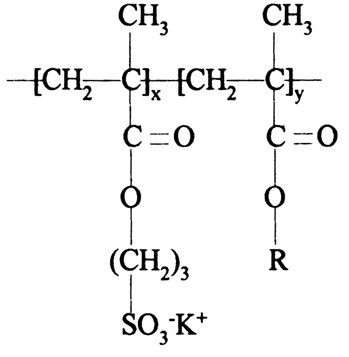

$R = CH_3$ or C_2H_5

Scheme 1. Chemical structure of copolymers

Experimental Methods and Procedures

Polymer Synthesis. Copolymers (PSPMK/MMA and PSPMK/EMA) were synthesized at 45°C by the free radical solution polymerization of 3-sulfopropyl methacrylate potassium salt (SPMK) (Aldrich Chemical, WI) and the alkyl methacrylate esters, methyl methacrylate (MMA) (Aldrich Chemical, WI) or ethyl methacrylate (EMA) (Aldrich Chemical, WI), in the ratios of 40/60 and 60/40 mole% using 2,2' azobis(2,4-dimethylvaleronitrile) (V65B) (Wako, Japan) as the thermal initiator (*17*).

Dosage Form Preparation. Dosage forms were prepared by dissolving the copolymer in deionized water and adding aqueous solutions of model drugs, propranolol HCl (Sigma Chemical, MO), labetalol HCl (Sigma Chemical, MO), verapamil HCl (Sigma Chemical, MO), and diltiazem HCl (Sigma Chemical, MO). The addition of basic amine drugs to the strongly acidic copolymers yield water-insoluble precipitates which indicates that the drug is bound to the sulfonate groups of the copolymers producing drug-copolymer complexes. The drug-copolymer complexes were recovered and washed several times with deionized water before being dried and crushed to a powder with a mortar and pestle. Tablets (200mg) containing drug-copolymer complexes and dextrose USP (20 wt%) (Amend Co, NJ) were fabricated in a 9.0 mm diameter die with a flat punch and Carver press (Wasaka, IN) under a pressure of 4400 lbs. The tablets had an average thickness of 2.5 mm.

Downloaded by YORK UNIV on October 31, 2012 | http://pubs.acs.org
Publication Date: September 24, 1998 | doi: 10.1021/bk-1998-0709.ch004

Drug Release Kinetic Studies. The release kinetics from dry, drug-copolymer complex tablets were carried out at 37°C in simulated gastric/intestinal fluid buffers by the USP basket method at 100 rpm. Simulated gastric fluid buffers (pH 1.2) were prepared by adding concentrated HCl (Fisher Scientific, NJ) to NaCl (Fisher Scientific, NJ) solutions of different concentrations to vary the ionic strength. The intestinal fluid buffers (pH 7) were prepared by adding different amounts of NaCl to 0.01 M phosphate buffer prepared from potassium phosphate dibasic (JT Baker, NJ) and sodium phosphate monobasic (Fisher Scientific, NJ). Drug release was monitored on a HP 8452A diode-array spectrophotometer at 270 nm, 252 nm, 266 nm, and 278 nm for propranolol HCl, labetalol HCl, diltiazem HCl, and verapamil HCl, respectively. Drug release data up to 60% release were treated with the following phenomenological equation (*18*) to investigate the linearity of the release kinetics:

$$\frac{M_t}{M_\infty} = kt^n \qquad (1)$$

where M_t and M_∞ are the amount of drug released at time t and the total amount of drug in the tablet, respectively, and k and n are a constant and a release exponent, respectively. When $n > 0.89$ for cylindrical geometry (tablet), the release is referred to as zero-order. The standard error of the release exponent (n) and the 95% confidence level were calculated.

Characterization of Copolymers and their Complexes. The composition of the copolymers were determined by the elemental analysis of nitrogen and sulfur in the propranolol-copolymer complexes (Quantitative Technology Inc., Whitehouse NJ). Complexes were analyzed for nitrogen using a 2400 Perkin-Elmer CHN Elemental Analyzer to combust and convert each complex to its simple gases in a pure oxygen environment. Complexes were analyzed for sulfur by combustion in an oxygen combustion flask containing hydrogen peroxide. The resultant mixture which contained DMSA III indicator was titrated with barium perchlorate until a purple to blue to aqua end point was achieved.

The thermal properties of 60/40 mole% PSPMK/MMA, the pure drugs, propranolol hydrochloride, labetalol hydrochloride, diltiazem hydrochloride, and verapmil hydrochloride, and the drug-copolymer complexes were analyzed using a Perkin Elmer DSC7 at a heating rate of 20°C/min.

Results and Discussion

The thermograms of 60/40 mole% PSPMK/MMA, the hydrochloride drugs, and the complexes formed between the copolymer and these drugs are shown in Figures 1 and 2. The DSC curves of propranolol hydrochloride, verapmil hydrochloride, labetalol hydrochloride, and diltiazem hydrochloride show characteristic melting peaks of 167.37°C, 152.24°C, 195.63°C, and 214.55°C respectively. The copolymer shows a glass transition temperature (T_g) of 229.50°C. The DSC curves of the drug-copolymer

Downloaded by YORK UNIV on October 31, 2012 | http://pubs.acs.org
Publication Date: September 24, 1998 | doi: 10.1021/bk-1998-0709.ch004

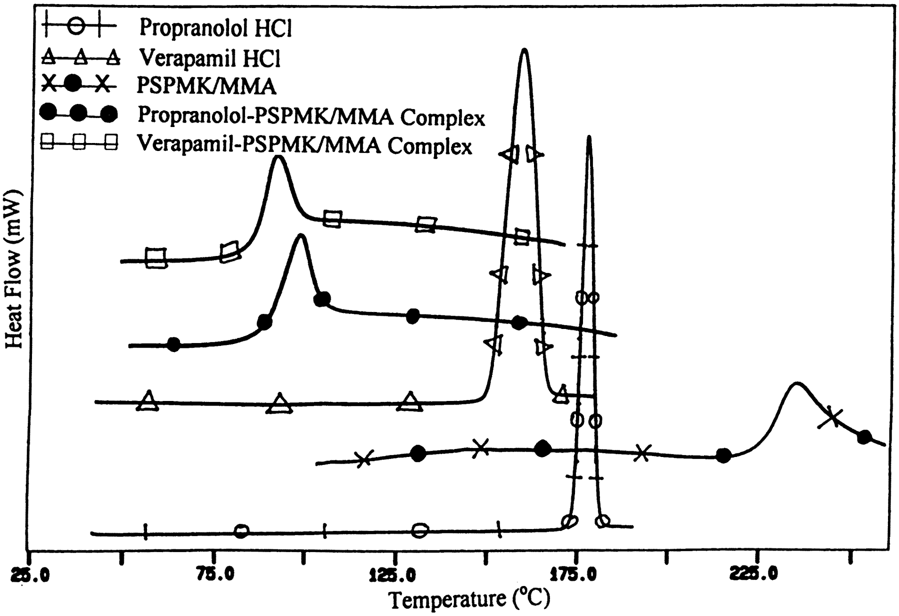

Figure 1. DSC spectra of 60/40 mole% PSPMK/MMA 45°C, Propranolol HCl, Verapamil HCl, and drug-PSPMK/MMA complexes.

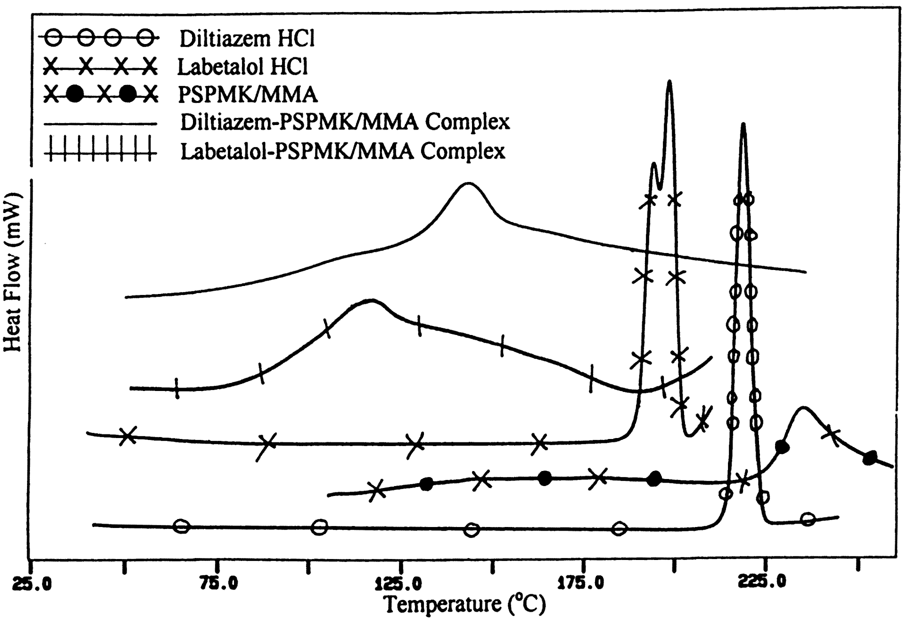

Figure 2. DSC Spectra of 60/40 mole% PSPMK/MMA 45°C, Diltiazem HCl, Labetalol HCl, and drug-PSPMK/MMA complexes.

Downloaded by YORK UNIV on October 31, 2012 | http://pubs.acs.org
Publication Date: September 24, 1998 | doi: 10.1021/bk-1998-0709.ch004

complexes also showed T_gs. Drug-copolymer complexes prepared with propranolol hydrochloride, verapamil hydrochloride, labetalol hydrochloride, and diltiazem hydrochloride showed T_gs of 86.49°C, 78.41°C, 96.29°C, and 130.62°C, respectively. The characateristic melting temperature (T_m) of each drug is absent from the thermal profiles of their respective drug-copolymer complexes, indicating that the drugs are bound to the functional groups of the copolymer creating new materials with different thermal properties from either the copolymer or drugs. Notably, the higher the drug's T_m, the higher the glass transition (T_g) of the resulting drug-copolymer complexes.

The copolymer composition was determined by elemental analysis of the nitrogen and sulfur content of the propranolol complexes of PSPMK/MMA and PSPMK/EMA. The composition can be easily determined because the sources of nitrogen and sulfur are furnished by propranolol and SPMK, respectively. The %S values were converted to grams of SPMK and then into moles of SPMK. Grams of AMA were determined by assuming 100 g sample of the complex. Moles of AMA were determined from grams of AMA. The values of mole% SPMK are determined for each copolymer using the values for moles of SPMK and moles of AMA and are summarized in Table 1. The copolymer compositions are close to the feed monomer values, except for 60/40 mole% SPMK/EMA. In addition, propranolol HCl binds with the copolymers in a 1:1 mole ratio represented by near 100% binding values (determined from moles of N divided by moles of S), except for 60/40 mole% SPMK/EMA.

Downloaded by YORK UNIV on October 31, 2012 | http://pubs.acs.org
Publication Date: September 24, 1998 | doi: 10.1021/bk-1998-0709.ch004

Table I. Composition of Copolymers of PSPMK/MMA and PSPMK/EMA

	SPMK (mole%)		% Binding
	feed	copolymer*	
1. SPMK/MMA	40	36.8	96.8
2. SPMK/MMA	60	52.6	95.6
3. SPMK/EMA	60	41.5	81.9

* Based on elemental analysis of propranolol-copolymer complexes

The drug loading levels of propranolol in the drug-copolymer complexes are 41.4 wt%, 48.4 wt%, and 47.1 wt% for 40/60 mole% PSPMK/MMA, 60/40 mole% PSPMK/MMA, and 60/40 mole% PSPMK/EMA, respectively. These values were determined by dissolving approximately 100 mg of the propranolol complex in a 100 ml volumetric flask containing 0.01 M phosphate buffer and 0.05 M NaCl. After the complex was fully dissolved, the solution was assayed spectrophotometrically at 270 nm to determine how much drug dissociated from the polymer. Each of the values reported are the average of 5 measurements.

The release profiles of propranolol HCl from drug-PSPMK/MMA (40/60 mole%) tablets in simulated intestinal and gastric fluid buffers of varying ionic strength are shown in Figures 3 and 4, respectively. The release time of propranolol HCl from

Downloaded by YORK UNIV on October 31, 2012 | http://pubs.acs.org
Publication Date: September 24, 1998 | doi: 10.1021/bk-1998-0709.ch004

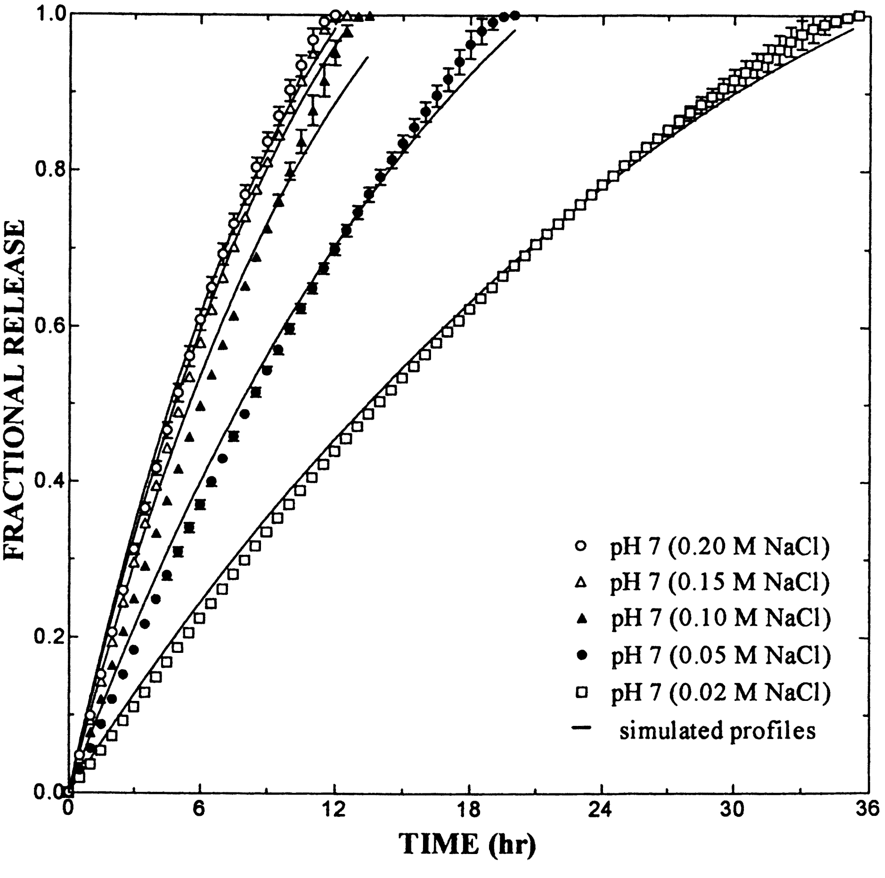

Figure 3. Effect of buffer strength (pH 7) on the release of propranolol HCl from drug-PSPMK/MMA (40/60 mole%) tablets.

Downloaded by YORK UNIV on October 31, 2012 | http://pubs.acs.org
Publication Date: September 24, 1998 | doi: 10.1021/bk-1998-0709.ch004

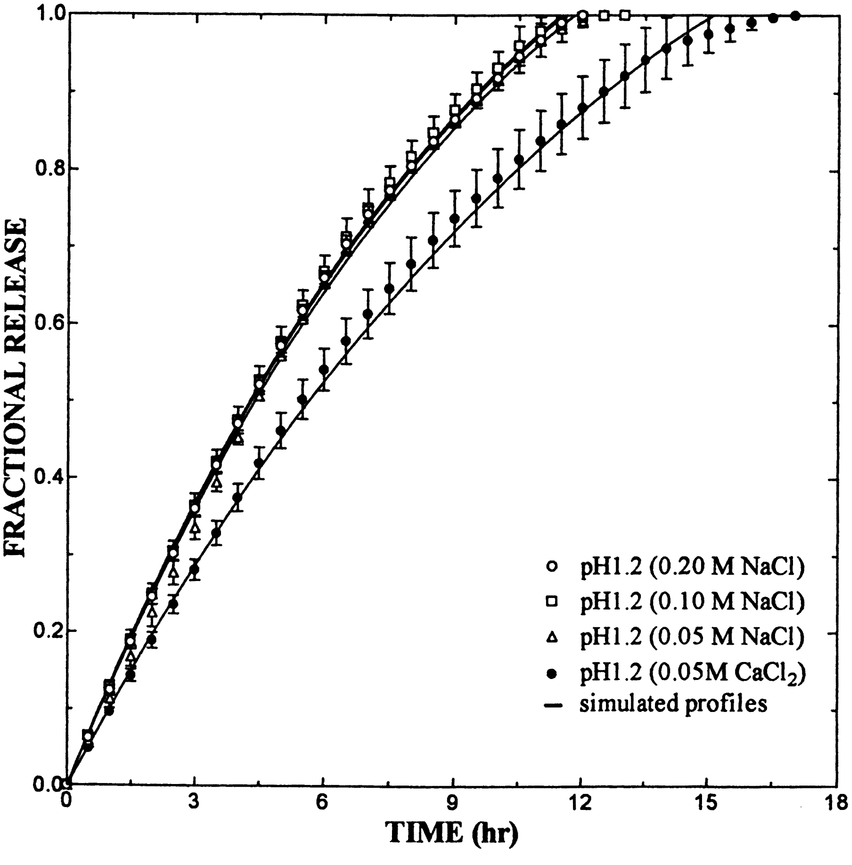

Figure 4. Effect of buffer strength on the release of propranolol HCl from drug-PSPMK/MMA (40/60 mole%) tablets.

Downloaded by YORK UNIV on October 31, 2012 | http://pubs.acs.org
Publication Date: September 24, 1998 | doi: 10.1021/bk-1998-0709.ch004

drug-copolymer tablets decreases as the ionic strength of the intestinal fluid buffer increases up to a concentration of 0.15 M NaCl after which it reaches a plateau. The total release time of propranolol HCl is 36, 18, and 12 hours in intestinal fluid containing 0.02 M, 0.05 M, and 0.10 M - 0.20 M NaCl, respectively. Above an ionic strength of 0.10 M, the release profiles do not differ much, indicating that the dissociation of propranolol from the complex reaches a threshold above which an increase in the concentration does not significantly affect the release kinetics. Similar results were found for the release kinetics of the dosage form in gastric fluid buffers. Release profiles are superimposable for drug-copolymer tablets studied in gastric fluid buffers containing sodium chloride concentrations ranging from 0.05 M - 0.20 M. The ionic strength of the gastric fluid buffer containing 0.05 M NaCl is equivalent to that of the intestinal fluid buffer containing a sodium chloride concentration of 0.15 M. In fact, the release profiles in gastric and intestinal fluid buffers which have ionic strengths of 0.15 M and greater are superimposable regardless of pH. The release of propranolol from the drug-copolymer tablets is approximately 1.3 times faster in the gastric fluid buffer containing univalent electrolytes (0.05 M Na^+) compared to divalent electrolytes (0.05 M Ca^{2+}) because calcium sulfonate erodes at a slower rate than sodium sulfonate. As shown in the release profiles, the drug-PSPMK/MMA tablets do not exhibit a significant burst effect nor tailing in the later stages of release as other erodible (or swelling/erosion-controlled) polymer materials such as low molecular weight PEO and HPMC do.

The release kinetics may be characterized by a dissociation/erosion mechanism as described by:

$$\frac{M_t}{M_\infty} = 1 - \left(1 - \frac{k_o t}{C_o r_o}\right)^2 \left(1 - \frac{2k_o t}{C_o l}\right) \tag{2}$$

where k_o, C_o, r_o, and l are the drug-copolymer dissociation/erosion rate constant, the drug concentration in the tablet, the radius of the tablet, and the thickness of the tablet, respectively. Equation 2 is the identical form derived by Zhang et al (*19*) except their erosion rate constant (k_{er}) is k_o/C_o in our expression.

The results of the release profiles are reflected in the dissociation/erosion characteristics of the dosage form as shown in Figure 5 and Table 2. Figure 5 shows that the dissociation/erosion rate of the tablets in the intestinal fluid buffer increases until a concentration of 0.10 M NaCl is reached. The dissociation/erosion rate of the tablets in gastric fluid buffer remains constant for sodium chloride concentrations ranging from 0.05 M to 0.10 M because the ionic strengths are greater than 0.15 M. The drug-PSPMK/MMA complex does not follow a simple zero order reaction at low ionic strengths. It has been reported that Michaelis-Menten type (or Langmuir type) equations can be used to describe the ion exchange reaction (*20*). Therefore, at high ionic strengths the rate of dissociation/erosion is independent of the ionic strength (zero order with respect to the counterion concentration).

In Table 2 it can be seen that the erosion rate constant increases as the ratio of SPMK to AMA is increased. For example, the erosion rate of propranolol-copolymer

Downloaded by YORK UNIV on October 31, 2012 | http://pubs.acs.org
Publication Date: September 24, 1998 | doi: 10.1021/bk-1998-0709.ch004

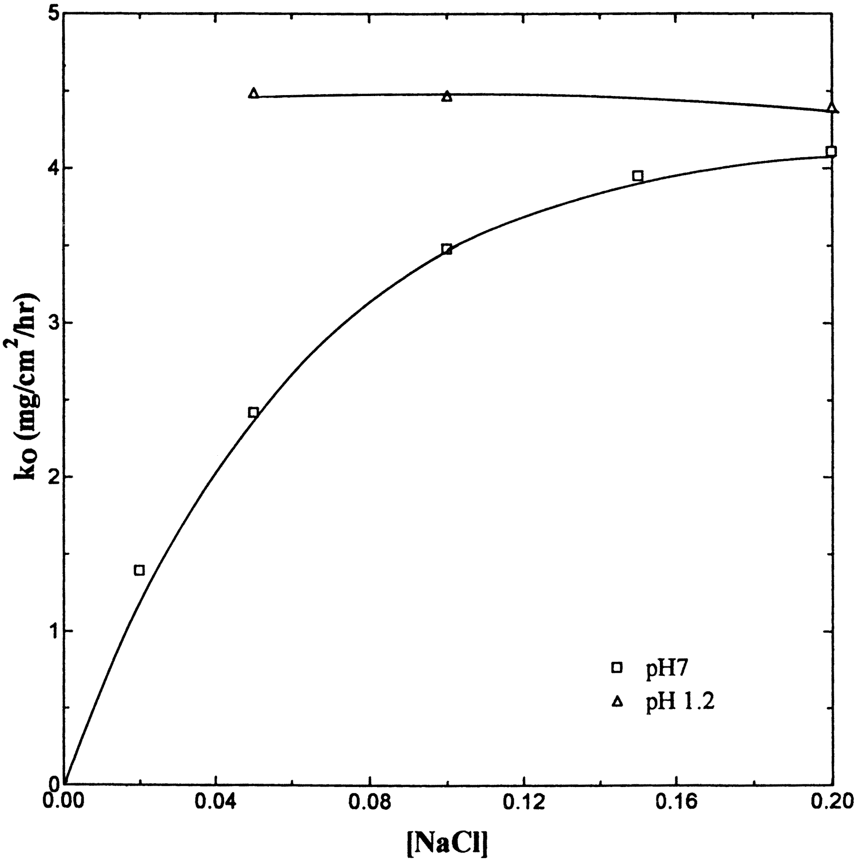

Figure 5. Effect of buffer strength and pH on the erosion rate of propranolol-PSPMK/MMA (40/60 mole%) tablets.

Downloaded by YORK UNIV on October 31, 2012 | http://pubs.acs.org
Publication Date: September 24, 1998 | doi: 10.1021/bk-1998-0709.ch004

Table II. Dissociation/Erosion Rate Constant (k_o) and Release Exponent (n) for the Release Kinetics of Drug-PSPMK/AMA Tablets (20% dextrose, 4400 lbs pressure, and 100 rpm)

			(mm x mm)				(wt%)
Tablet	Copolymer (mole%)	Drug (HCl)	Tablet Size	Buffer	k_o	n	drug loading
1.	40/60 PSPMK/MMA	Propranolol	2.57 x 9.0	pH7.0, 0.20M NaCl	4.11±0.062	0.999±0.032	40.6
2.	40/60 PSPMK/MMA	Propranolol	2.54 x 9.0	pH7.0, 0.15M NaCl	3.95±0.063	0.997±0.019	41.7
3.	40/60 PSPMK/MMA	Propranolol	2.67 x 9.0	pH7.0, 0.10M NaCl	3.48±0.089	1.004±0.011	40.7
4.	40/60 PSPMK/MMA	Propranolol	2.51 x 9.0	pH7.0, 0.05M NaCl	2.42±0.030	0.979±0.017	41.2
5.	40/60 PSPMK/MMA	Propranolol	2.69 x 9.0	pH7.0, 0.02M NaCl	1.39±0.009	0.948±0.009	40.3
6.	40/60 PSPMK/MMA	Propranolol	2.58 x 9.0	pH1.2, 0.20M NaCl	4.40±0.030	0.934±0.033	40.7
7.	40/60 PSPMK/MMA	Propranolol	2.60 x 9.0	pH1.2, 0.10M NaCl	4.47±0.067	0.927±0.053	41.3
8.	40/60 PSPMK/MMA	Propranolol	2.61 x 9.0	pH1.2, 0.05M NaCl	4.49±0.053	0.998±0.051	42.4
9.	40/60 PSPMK/MMA	Propranolol	2.57 x 9.0	pH1.2, 0.05M $CaCl_2$	3.33±0.060	0.947±0.060	40.9
10.	60/40 PSPMK/MMA	Propranolol	2.68 x 9.0	pH7.0, 0.20M NaCl	15.20±0.64	0.906±0.040	52.3
11.	60/40 PSPMK/MMA	Propranolol	2.68 x 9.0	pH1.2, 0.20M NaCl	14.19±0.16	0.965±0.026	49.7
12.	60/40 PSPMK/EMA	Propranolol	2.62 x 9.0	pH7.0, 0.20M NaCl	3.01±0.048	0.742±0.022	47.4
13.	60/40 PSPMK/EMA	Propranolol	2.54 x 9.0	pH1.2, 0.20M NaCl	2.69±0.053	0.728±0.037	47.3
14.	60/40 PSPMK/MMA	Verapamil	2.56 x 9.0	pH7.0, 0.20M NaCl	4.64±0.016	0.921±0.013	50.0
15.	60/40 PSPMK/MMA	Diltiazem	2.50 x 9.0	pH7.0, 0.20M NaCl	27.13±0.54	0.990±0.062	61.1
16.	60/40 PSPMK/MMA	Labetalol	2.54 x 9.0	pH7.0, 0.20M NaCl	5.03±0.076	0.924±0.026	53.1

In Tailored Polymeric Materials for Controlled Delivery Systems; McCulloch, I., et al.;
ACS Symposium Series; American Chemical Society: Washington, DC, 1998.

Downloaded by YORK UNIV on October 31, 2012 | http://pubs.acs.org
Publication Date: September 24, 1998 | doi: 10.1021/bk-1998-0709.ch004

tablets is approximately 3.7 times faster for tablets prepared from the 60/40 mole% PSPMK/MMA than from 40/60 mole% PSPMK/MMA. Also, the type of drug complexed with 60/40 mole% PSPMK/MMA affect the release kinetics quantitated by the dissociation/erosion rate constants. The differences are due to the solubility and type of drug and is discussed later. In addition, the release kinetics are zero-order for all tablets, except for the 60/40 mole% PSPMK/EMA copolymer from which drug diffusion contributes in the drug release.

The effect of the copolymer composition of SPMK and MMA on the release kinetics in simulated intestinal fluid containing 0.20 M NaCl is shown in Figure 6. As the ratio of SPMK to MMA in the copolymer is reduced, the total release time is significantly prolonged. It takes almost twice as long for propranolol to dissociate from 40/60 mole% PSPMK/MMA than from 60/40 mole% PSPMK/MMA. This is because the hydrophilicity of the copolymer decreases as the amount of the ionic monomer, SPMK, is reduced, resulting in a decreased influx of water and counterions into the drug-copolymer matrix. However, drug loading increases as the content of SPMK is increased because it furnishes more ion exchange sites along the copolymer chain. The hydrophilicity of the polymeric carrier may also be altered by changing the hydrophobic comonomer from MMA to EMA. The longer alkyl group of EMA is responsible for reducing the hydrophilicity of the copolymer, causing it to erode at a slower rate, thereby extending the release time of the bound drug. This effect may be seen in Figure 7 where the release of propranolol from the drug-PSPMK/AMA (60/40 mole%) tablets increased from 4 hrs to 22 hrs when MMA was replaced by EMA as a comonomer. However, both drug-copolymer complexes are not affected by the pH of the buffer (0.2 M NaCl).

The type (secondary (2°) and tertiary (3°) amine) and solubility of the drug complexed with the copolymer affects the release kinetics as shown in Figure 8. Complexation of 60/40 mole% PSPMK/MMA with drugs which have low water-solubility, labetalol HCl (1.25% w/w) and verapamil HCl (8.19% w/w), furnished release kinetics which lasted for 15 hours compared to 3 and 4.5 hours for complexes prepared with diltiazem HCl (61.6% w/w) and propranolol HCl (7.37% w/w), respectively. (The water solubilities of the drugs were determined at 37°C). Although the solubilities of verapamil HCl and propranolol HCl are comparable, drug release from drug-PSPMK/MMA complexes prepared with verapamil HCl is almost 4 times longer in terms of release time because it complexes more strongly with sulfonate groups of the copolymer than its secondary amine drug counterpart (*4*).

Conclusions

New biomaterials based on PSPMK/AMA are promising oral controlled release drug carriers. They furnish high, drug loadings and pH-independent release kinetics. The release kinetics of the drug-copolymer tablets are well described by a dissociation/erosion mechanism.

Acknowledgements

The authors (Y.N. Nujoma and C.J. Kim) would like to express their deepest gratitude to the United Negro College Fund and Merck for supporting this research with a

Downloaded by YORK UNIV on October 31, 2012 | http://pubs.acs.org
Publication Date: September 24, 1998 | doi: 10.1021/bk-1998-0709.ch004

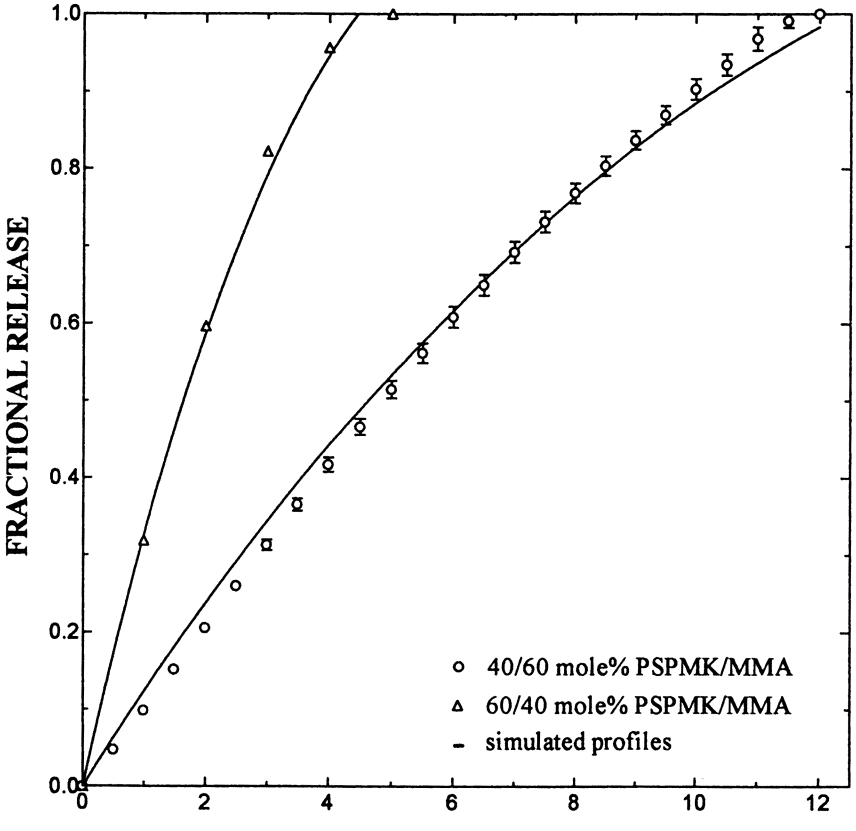

Figure 6. Effect of copolymer composition on the release of propranolol HCl from drug-PSPMK/MMA tablets in simulated intestinal fluid (pH 7.0, 0.20 M NaCl).

Downloaded by YORK UNIV on October 31, 2012 | http://pubs.acs.org
Publication Date: September 24, 1998 | doi: 10.1021/bk-1998-0709.ch004

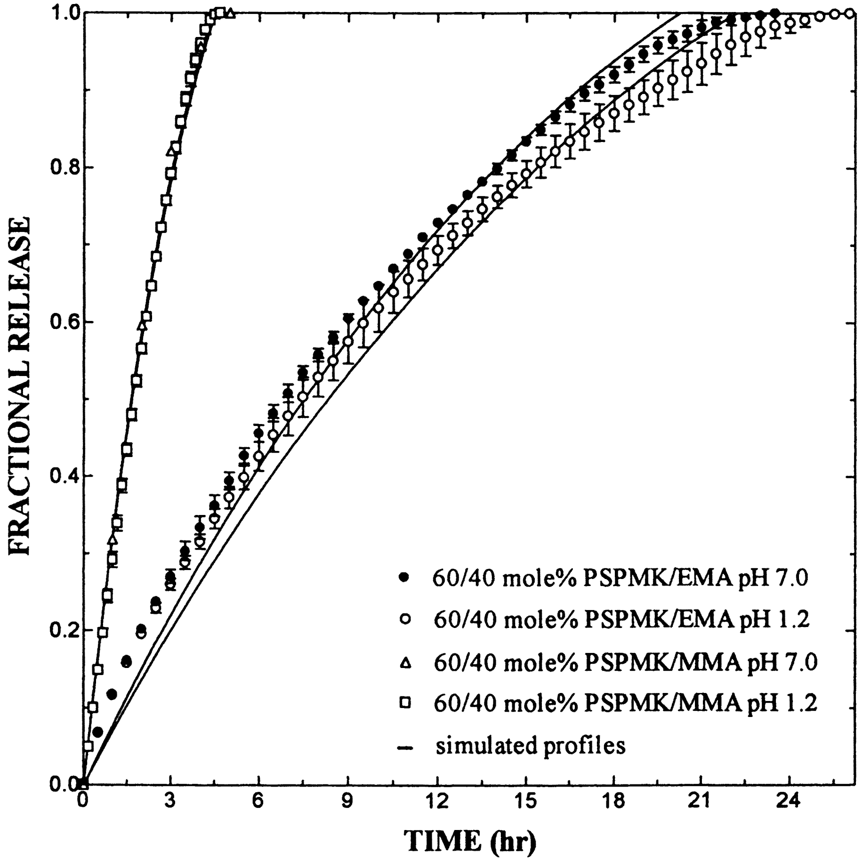

Figure 7. Effect of pH and the AMA comonomer on the release of propranolol HCl from drug-PSPMK/AMA tablets in simulated intestinal (pH 7.0, 0.20 M NaCl) and gastric (pH 1.2, 0.20 M NaCl) fluids.

Downloaded by YORK UNIV on October 31, 2012 | http://pubs.acs.org
Publication Date: September 24, 1998 | doi: 10.1021/bk-1998-0709.ch004

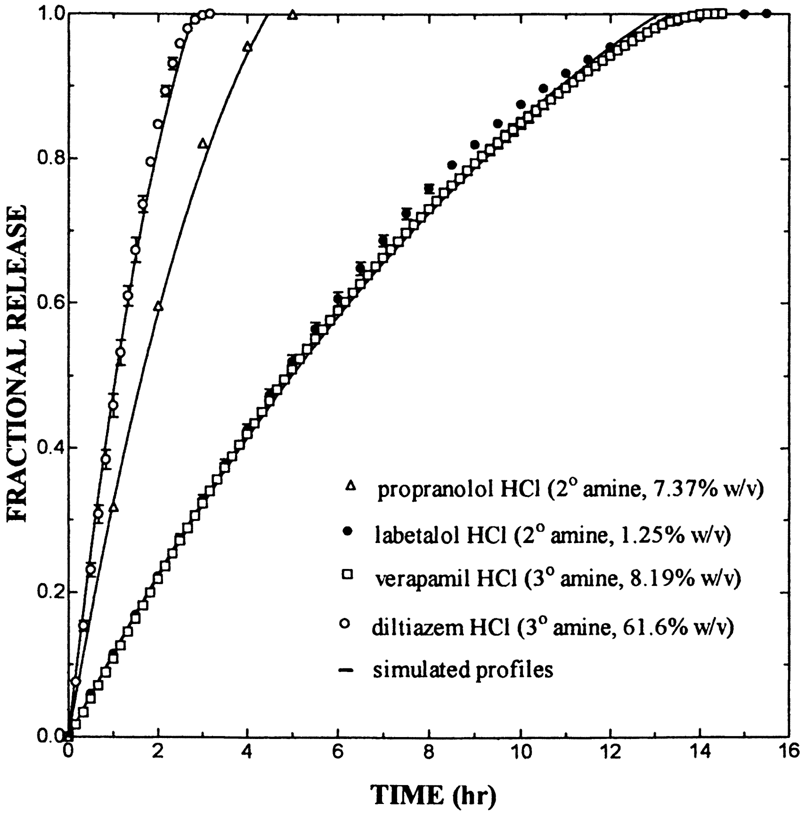

Figure 8. Effect of drug type and solubility on the release of drugs from drug-PSPMK/MMA (60/40 mole%) tablets in simulated intestinal (pH 7.0, 0.20 M NaCl) fluid.

UNCF/Merck science initiative fellowship (Y.N.N.) and UNCF/Merck equipment grant (C.J.K).

Literature Cited

1. The Dow Chemical Company. *Dowex: Ion Exchange*; Lakeside Press: Chicago, IL, 1958.
2. Kunin, R. *Elements of Ion Exchange*; Reinhold Publishing Corporation: New York, NY, 1960.
3. Bender, G. T. In *Principles of Chemical Instrumentation*; Benson, H., Ed.; W.B. Saunders Company: Philadelphia, PA, 1987, pp. 195-207.
4. Schacht, E. H. In *Controlled Drug Delivery*; Bruck, S. D., Ed.; CRC Press: Boca Raton, FL, 1983, Vol. I; pp. 150-173.
5. Brudney, N.; US Patent 2,987,441, **1961**.
6. Borodkin, S. In *Polymers for Controlled Drug Delivery*; Tarcha, P. J., Ed.; CRC Press: Boca Raton, FL, 1991, pp 216-230.
7. Keating, J. W.; US Patent 2,990,332, **1961**.
8. Hui, H.; Lee, V. H. L.; and Robinson, J. R. In *Controlled Drug Delivery: Fundamentals and Applications*; Robinson, J. R. and Lee, V. H. L., Eds.; Marcel Dekker: New York, NY, 1987, pp. 412-415.
9. Gyselinck, P.; Van Severen, R.; Braeckman, P.; and Schacht, E. *Pharmazie*. **1981**, 36, pp. 769.
10. Burke, G. M.; Mendes, R. W.; and Jambhekar, S. S. *Drug Dev. and Ind. Pharm.* **1986**, 12, pp. 713.
11. Jayaswal, S. B.; and Bedi, G. S. *Ind. Drugs.* **1980**, 17, pp. 102.
12. *Hydrogels in Medicine and Pharmacy*; Peppas, N. A., Ed.; CRC Press: Boca Raton, FL, 1986; Vol. 1.
13. Falamarzian, M.; Moxley, B. B.; Firestone, B.; and Siegel, R. A. *Proceed. Intern. Symp. Control. Rel. Bioact. Mater.* **1988**, 15, pp. 23.
14. Brannon-Peppas, L.; and Peppas, N. A. *J. Control. Rel.* **1989**, 8, pp. 267.
15. Kim, C. J. *J. Appl. Polym. Sci.*, **1994**, 54, pp. 1179.
16. Kim, C. J. *J. Macrom. Sci. Pure Appl. Chem.* **1993**, A31, pp. 701.
17. Nujoma Y. N.; and Kim, C. J. *J. Pharm. Sci.* **1996**, 85, pp. 1091.
18. Ritger, P .L.; and Peppas, N. A. *J. Control. Rel.* 1987, 5, pp. 37.
19. Zhang, G. H.; Vadino, W. A.; and Chaudry, I. *Proc. Int. Symp. Control. Rel. Bioact. Mater.* **1990**, 17, pp. 333.
20. Holl, W.; and Sontheimer, H. *Chem. Eng. Sci.* **1977**, 32, pp. 755.

Downloaded by YORK UNIV on October 31, 2012 | http://pubs.acs.org
Publication Date: September 24, 1998 | doi: 10.1021/bk-1998-0709.ch004

Downloaded by NORTH CAROLINA STATE UNIV on October 31, 2012 | http://pubs.acs.org
Publication Date: September 24, 1998 | doi: 10.1021/bk-1998-0709.ch005

Chapter 5

Polymeric Prodrugs: Novel Polymers with Bioactive Components

Laura Erdmann, Cheryl Campo, Christi Bedell, and Kathryn Uhrich[1]

Department of Chemistry, Rutgers University, Piscataway, NJ 08855–0939

Our goal is to synthesize a polymer that will act as a controlled delivery device in targeting specific areas, such as the colon, over an extended period of time. The polymers we are synthesizing, poly(anhydride-esters), are composed of alkyl chains linked by ester bonds to aromatic moieties, specifically salicylic acid -- the active component of aspirin. With the medicinal properties attributed to salicylic acid and the ease of metabolism, the incorporation of this compound into a polymer backbone yields a polymeric prodrug that may have potential in a variety of applications, in particular, inflammatory bowel disease. For these reasons, we designed a synthetic scheme that yields the desired poly(anhydride-esters). Interest in these polymers arises from the fact that the polymer degradation products may reduce symptoms associated with inflammatory bowel disease.

Aromatic polyanhydrides are biocompatible, biodegradable polymers that are clinically used as drug delivery systems for the treatment of brain cancer (*1*). However, the slow degradation rate of the polymer and the relative insolubility of the degradation products (*2*) are major drawbacks for use in other biomedical applications.

In consideration of these limitations, we are synthesizing polyanhydrides with suitable degradation and solubility characteristics. In our approach, longer alkyl chains ($n \geq 4$) and alternate aromatic ring substitution patterns (from *para* to *ortho*) are used to increase the degradability and solubility of aromatic polyanhydrides. Both changes have been found to enhance the processing characteristics of the resulting polymer. One of the most promising polymers is 1,6-bis(*o*-carboxyphenoxy)hexane (*o*-CPH) (**1**), a poly(anhydride-ether), which is significantly more soluble in water and organic solvents than the corresponding *para*-substituted polymer (*p*-CPH). This polymer has also excellent tensile and solubility properties.

---

[1] Corresponding author.

In Tailored Polymeric Materials for Controlled Delivery Systems; McCulloch, I., et al.;
ACS Symposium Series; American Chemical Society: Washington, DC, 1998.

Downloaded by NORTH CAROLINA STATE UNIV on October 31, 2012 | http://pubs.acs.org
Publication Date: September 24, 1998 | doi: 10.1021/bk-1998-0709.ch005

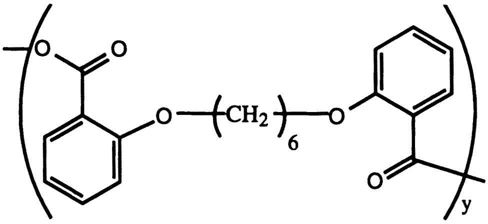

1

Consideration of the degradation products obtained from these poly(anhydride-ethers) led to the design of a new polymer structure, poly(anhydride-ester), with a seemingly small backbone modification but with potentially significant applications. Replacing the ether bond in polymer **1** with an ester bond yields a polymer (**2**) that hydrolytically degrades into salicylic acid (**3**). The hydrolytic degradation of polymer **2** yielding salicylic acid (**3**) and a nontoxic aliphatic acid is outlined in **Scheme 1**.

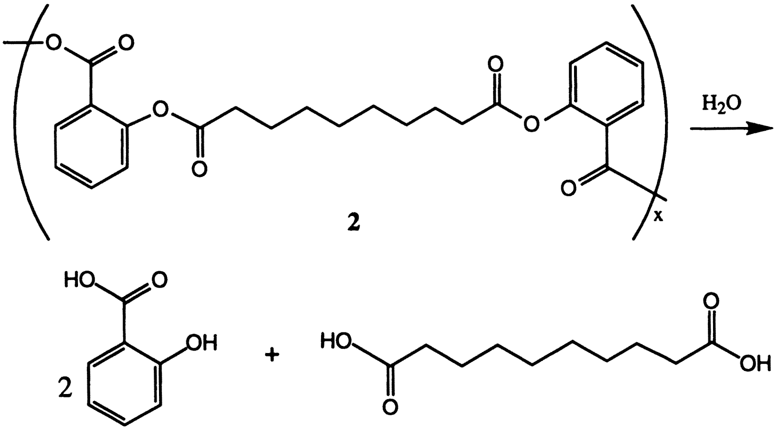

Scheme 1

There are many examples in the literature whereby a drug is attached to a polymer via a degradable linkage (*3*). These polymeric prodrugs have a minimum amount of drug attached to the polymer (circa 55 wt%) (*4*) relative to the polymer itself. Therefore, due to the percentage of drug actually present within these systems, along with the complicated syntheses involved, the development of a polymeric prodrug with the capability of delivering a larger amount of drug is extremely desirable. We may achieve this result by incorporation of a drug into the polymer backbone to increase the amount of drug released. For example, with the poly(anhydride-esters) a maximum of 62 wt% of salicylic acid will be released upon total polymer degradation. This polymer structure is the first example where the polymer backbone degradation yields the drug moieties.

In this paper, we describe the synthesis of *ortho*-substituted poly(anhydride-ethers) and poly(anhydride-esters).

Poly(anhydride-ethers). Conix synthesized the first aromatic polyanhydrides in 1958 with the general structure shown below (*5*).

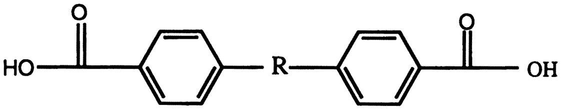

R = -O-$(CH_2)_n$-O-

-$(CH_2)_n$-

n=3

Currently, aromatic polyanhydrides are clinically used in drug delivery devices in the treatment of brain cancer and demonstrate near zero-order drug release (*1*). The desirable properties of these polymers also include long term degradation and high mechanical strength yet insolubility of the aromatic polyanhydrides is a limitation for the widespread applications of polyanhydrides.

Our preparation of *ortho*-substituted polyanhydrides has addressed the issue of processibility; these polymers have high solubility in organic solvents. Thus, our next goal was to design polymer systems with a greater array of characteristics. Our goal was to synthesize a polymer that will act as a controlled delivery device in targeting specific areas (i.e. colon) over an extended period of time. The polymer itself should be hydrolytically degradable, noncytotoxic and biocompatible. The degradation products arising from the metabolism of the polymer should give pharmaceutically active components. "Polymeric prodrugs" are pharmacologically active compounds bound covalently to a biocompatible and soluble macromolecular support that may target specific areas within the body and therefore are investigated for use as a controlled drug delivery method (*3*). It has been noted that other prodrugs, such as salicylic acid-L-alanine conjugate (*10*), yield prolonged blood concentrations of the drug when administered. This indicates that the prodrugs, whether polymeric or conjugated, have the ability to release the active metabolite in a controlled manner, possibly allowing for site-specific drug targeting and reduced side effects which may normally be incurred if the drug is released immediately.

The polymer we synthesized is a poly(anhydride-ester) which are composed of alkyl chains linked by ester bonds to aromatic moieties, specifically salicylic acid -- the active component of Aspirin. Aspirin is hydrolyzed to salicylic acid during and after absorption with a half life of approximately 15 minutes. Salicylic acid is an antipyretic, antiinflammatory analgesic with a half life of 2-3 hours in low doses and 20 hours in higher doses (*11*). Salicylates, such as Sulfasalazine (Azulfidine Pharmacia, SASP) have been used for over 30 years to treat individuals afflicted with inflammatory bowel disease, in particular, mild ulcerative colitis and Crohn's disease. This biologically active compound consists of sulfapyridine (SP) linked by an azo bond to 5-aminosalicylic acid (5-ASA).

About one third of SASP is absorbed in the upper gastrointestinal tract with the remaining portion of the drug reaching the colon intact. Upon entering the colon, the azo bond is split by a bacterial azo reductase enzyme into its metabolites yielding SP and 5-ASA (*6*). The metabolite responsible for the anti-inflammatory and medicinal properties of SASP is 5-ASA (*6*). Side effects, however, are seen in 10 to 45% of the individuals treated with SASP and these are due to acetylator phenotype and dose dependency or hypersensitive reactions of the patient (*7,8*). 5-ASA has been found to be nephrotoxic in animals (*9*) and thus, long term exposure to this metabolite may be harmful in humans. It has also been noted that SASP is not as effective in the treatment of Crohn's disease as in ulcerative colitis, as it does

Downloaded by NORTH CAROLINA STATE UNIV on October 31, 2012 | http://pubs.acs.org
Publication Date: September 24, 1998 | doi: 10.1021/bk-1998-0709.ch005

not maintain remission or prevent recurrence. The limitations of the present drug have necessitated the development of a new synthetic material with enhanced capability.

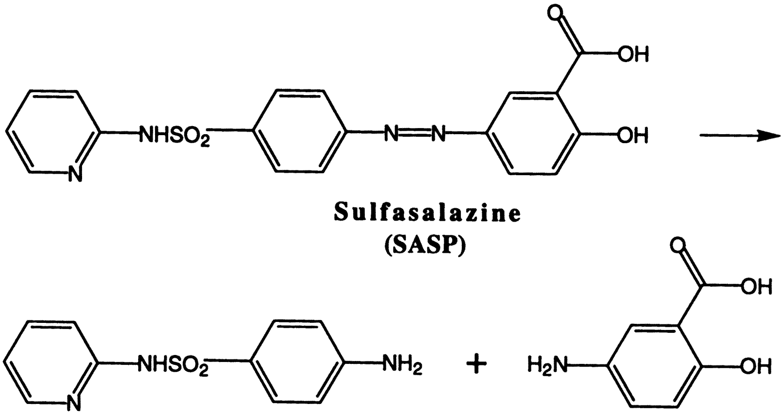

Sulfasalazine (SASP)

sulfapyridine (SP)

5-aminosalicylic acid (5-ASA)

With the medicinal properties attributed to salicylic acid and the ease of metabolism, the incorporation of this compound into a polymer backbone would yield a drug that may have potential in a variety of applications. The alkyl component, sebacic acid, of these poly(anhydride-esters) is also known to be biocompatible and biodegradable in vivo.

Poly(anhydride-esters). Kricheldorf synthesized numerous poly(anhydride-esters) using aromatic moieties (*12*). However, these polymers were of low molecular weight and insoluble in most organic solvents. Our poly(anhydride-ester) synthesis is an adaptation of the poly(anhydride-ether) synthetic procedure previously developed by Uhrich (Uhrich, K.E., Rutgers - The State University of New Jersey, unpublished data.). Replacement of the ether bond with an ester bond yields a new set of polymers with properties that may have applications in the treatment of patients with inflammatory bowel disease due to the release of salicylic acid, the primary degradation product.

Experimental Section

Methods. Infrared spectroscopy is performed on an ATI Mattson Genesis (M100) FTIR spectrophotometer. Samples are prepared by solvent casting on NaCl plates. ^1H and ^{13}C nuclear magnetic resonance spectroscopy is obtained on a Varian 200MHz or Varian 400MHz spectrometer in solutions of $CDCl_3$ or DMSO-d_6 with solvent as the internal reference.

Gel permeation chromatography is performed on a Perkin-Elmer Advanced LC Sample Processor (ISS 200) with a PE Series 200 LC Pump and PE Series LC refractive index detector to determine molecular weight and polydispersity. Turbochrom 4 software on a Digital Celebris 466 computer will carry out the data

Downloaded by NORTH CAROLINA STATE UNIV on October 31, 2012 | http://pubs.acs.org
Publication Date: September 24, 1998 | doi: 10.1021/bk-1998-0709.ch005

analysis. Samples are dissolved in tetrahydrofuran and eluted through a mixed bed column (PE PL gel, 5µm, mixed bed). Molecular weights are determined relative to narrow molecular weight polystyrene standards (Polysciences, Inc.).

Thermal analysis is performed on a Perkin-Elmer system consisting of a TGA7 thermal gravimetric analyzer equipped with PE AD-4 autobalance, and Pyris 1 DSC analyzer. Pyris software is used to carry out data analysis on a Digital Venturis 5100 computer. For DSC, an average sample weight of 5-10 mg is heated at 10°C/min under a flow of N_2(30 psi). For TGA, an average sample weight of 10 mg is heated at 20°C/min under a flow of N_2 (8 psi).

Degradation studies. Polymer (**2**) was compressed in 13 mm circular molds to a thickness of 0.1mm. Molding was performed at 50°C for 30 min with a Carver press. Polymer disks were placed in 10 ml of phosphate buffer solution at pH 3.5, 7, and 10 over 3 weeks.

Synthesis. The poly(anhydride-ethers) were synthesized according to methods established by Conix (*5*). An example of the synthesis of 1,6-bis (*o*-carboxyphenoxy)hexane (*o*-CPH) is shown in **Scheme 2.**

1,6-bis(*o*-carboxyphenoxy)hexane diacid (**4**). To a mixture of salicylic acid (**3**) (77.12 g, 0.5580 mol) and distilled water (84.00 ml), sodium hydroxide (44.71 g 1.120 mol) was added. The reaction mixture was brought to reflux temperature before 1,6-dibromohexane (44.21 g, 0.2790 mol) was added dropwise. After 23 h, additional sodium hydroxide (11.17 g, 0.2790 mol) was added to the reaction mixture. The mixture was heated to reflux temperature for another 16 h, cooled, and the product isolated by filtration. Purification involved recrystallization from water followed by a methanol wash. Yield: 48.8% (white solid). ^{1}H NMR (δ): 7.85 (d, 2H, Ar-H), 7.65 (t, 2H, Ar-H), 7.25 (d, 2H, Ar-H), 7.10 (t, 2H, Ar-H), 4.05 (t, 4H, CH_2), 1.75 (m, 4H, CH_2), 1.45 (t, 4H, CH_2).

1,6-bis(*o*-carboxyphenoxy)hexane monomer (**5**). The diacid (**4**) (74.02 g, .1362 mol) was acetylated in an excess amount of acetic anhydride (150.00 ml) under nitrogen at reflux temperature. After 2.5 hr, the reaction mixture was filtered and the filtrate evaporated to dryness. The monomer was triturated with ethyl ether and precipitated upon cooling. Yield: 66.8% (white solid). ^{1}H NMR (δ): 7.85 (d, 2H, Ar-H), 7.65 (t, 2H, Ar-H), 7.25 (d, 2H, Ar-H), 7.10 (t, 2H, Ar-H), 4.10 (t, 4H, CH_2), 2.25 (s, 6H, CH_3), 1.80 (m, 4H, CH_2), 1.50 (t, 4H, CH_2).

1,6-bis(*o*-carboxyphenoxy)hexane polymer (**1**). Melt condensation polymerizations were performed at 260°C for 3.5 hr under vacuum (2 mm Hg) in a side-armed test tube. The reaction mixture was flushed with dry nitrogen every 15 minutes. The polymers were isolated by precipitation into diethyl ether from methylene chloride. Brown solid. Yield: quantitative (brown solid). ^{1}H NMR (δ): 7.85 (br, 2H, Ar-H), 7.55 (br, 2H, Ar-H), 7.05 (br, 4H, Ar-H), 3.85 (br, 4H, CH_2),), 1.40 (br, 4H, CH_2), 1.10 (m, 4H, CH_2). T_g: 34°C; T_d: 410°C

Downloaded by NORTH CAROLINA STATE UNIV on October 31, 2012 | http://pubs.acs.org
Publication Date: September 24, 1998 | doi: 10.1021/bk-1998-0709.ch005

Downloaded by NORTH CAROLINA STATE UNIV on October 31, 2012 | http://pubs.acs.org
Publication Date: September 24, 1998 | doi: 10.1021/bk-1998-0709.ch005

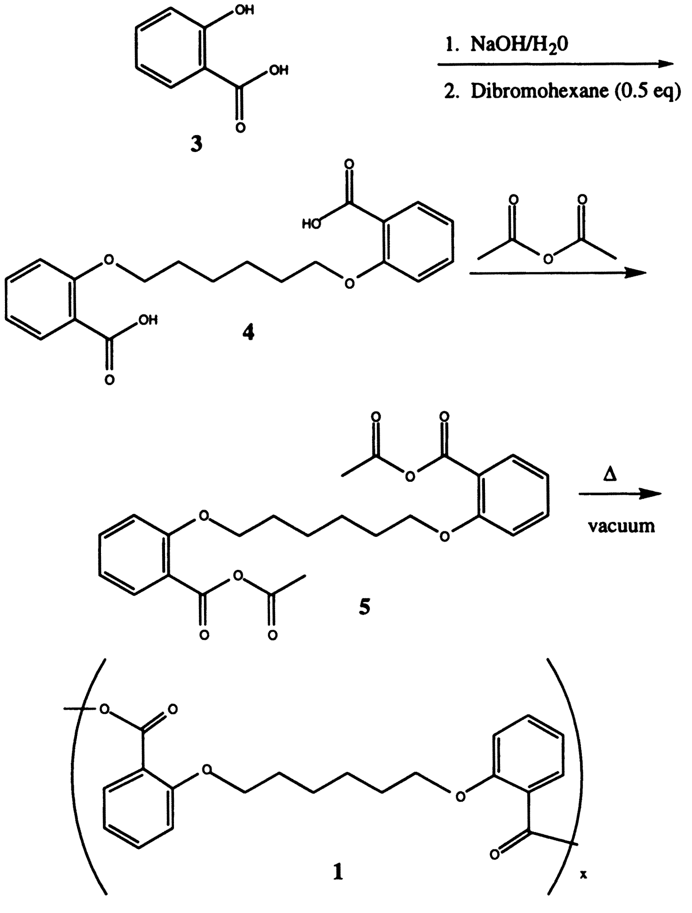

Scheme 2

Compound 7. Benzyl salicylate (1.530 g, 6.720 mmol) (**6**) and distilled tetrahydrofuran were combined under an inert atmosphere. An ice/salt bath was placed under the reaction flask and addition of 60% sodium hydride (0.4840 g, 12.10 mmol) followed. After 1 h, sebacoyl chloride (0.7850 g, 3.280 mmol) was added dropwise. After 30 min, the reaction mixture was vacuum filtered, the filtrate collected, and the solvent removed to yield a white solid residue. Purification was performed using a chromatotron with ethyl acetate/methylene chloride (20/80) as the solvent system. Yield: 43% (white solid). ^{1}H NMR (δ): 8.05 (d, 2H, Ar-H), 7.55 (t, 2H, Ar-H), 7.40 (s, 10H, Ar-H), 7.40 (t, 2H, Ar-H), 7.10 (d, 2H, Ar-H), 5.30 (s, 4H, CH_2), 2.40 (t, 4H, CH_2), 1.65 (s, 4H, CH_2), 1.40 (s, 8H, CH_2).

Downloaded by NORTH CAROLINA STATE UNIV on October 31, 2012 | http://pubs.acs.org
Publication Date: September 24, 1998 | doi: 10.1021/bk-1998-0709.ch005

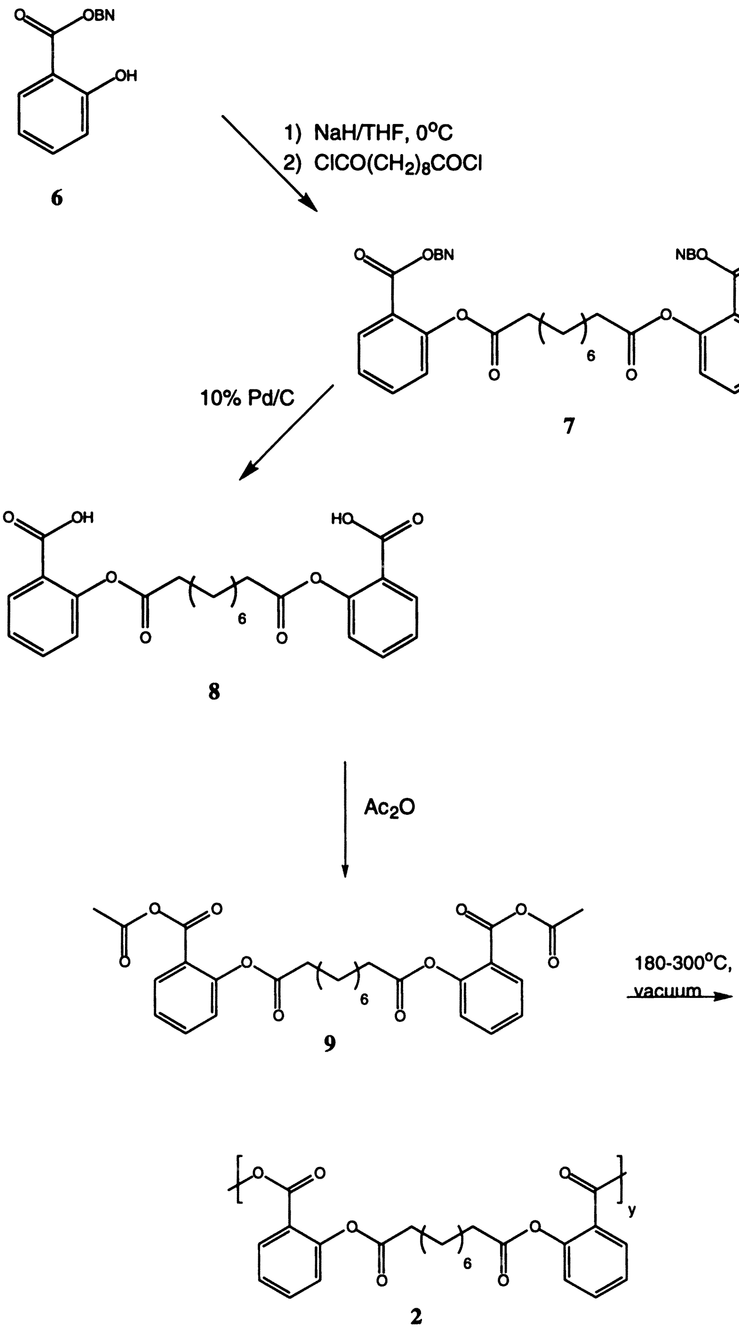
OBN
OH
6
1) NaH/THF, 0°C
2) ClCO(CH2)8COCl
NBO
7
10% Pd/C
HO
8
Ac2O
9
180-300°C, vacuum
y
2

Scheme 3

Compound 8. Compound **7** (0.6000 g, 0.9620 mmol) was dissolved in methylene chloride (60.00 ml). The catalyst, Pd-C (10%, 1.200 g), was added to the reaction flask. After 30 min, the reaction was complete. The reaction mixture was filtered and the solvent removed to yield a white solid residue which was recrystallized using petroleum ether and methylene chloride. Yield: 45% (white solid). ^{1}H NMR (δ): 8.15 (d, 2H, Ar-H), 7.65 (t, 2H, Ar-H), 7.40 (t, 2H, Ar-H), 7.15 (d, 2H, Ar-H), 2.60 (t, 4H, CH_2), 1.80 (t, 4H, CH_2), 1.45 (m, 8H, CH_2).

Monomer 9. Acetylation of the diacid monomer (**8**) (0.1470 g, 0.3363 mmol) was performed using excess acetic anhydride (3.00 ml) heated to reflux temperatures (145°C) for 2 h. Removal of the excess acetic anhydride yielded the acetylated monomer.

Polymer 2. Monomer **9** was polymerized using methods previously described for polymer **1**. M_w 3000, PDI 1.40

Results and Discussion

Poly(anhydride-ethers). Dibromohexane was added dropwise to a reaction mixture containing salicylic acid and sodium hydroxide in water at reflux temperatures to yield the diacid (**4**). Activation of the carboxylic acid end groups of **4** using excess acetic anhydride at reflux temperatures gave the monomer (**5**). Under vacuum at 260°C, a self condensation of **5** occurred giving the desired polymer (**1**). The molecular weights (M_w) of the polymers ranged from 15,000 to 25,000.

Poly(anhydride-esters). Initial syntheses of the poly(anhydrides-esters) was attempted using the same methodology as for the poly(anhydride-ethers). We found however, that the reactivity of the phenol was enhanced by benzylation of the carboxylic acid group. In addition, the solubility of benzyl salicylate in organic media increased the ability of the reaction to move forward.

Benzyl salicylate (**6**) in tetrahydrofuran was combined with sodium hydride at 0°C to give the free carboxylate. Addition of sebacoyl chloride dropwise allowed for coupling to proceed and the reaction was observed to have reached within 30 min. Filtration of the reaction mixture followed by rotoevaporation gave a pure white solid residue (**7**). The use of triethylamine as base was also explored. However, low yields and more complex purification methods were necessary to isolate the product.

The next step of the reaction involved removal of the benzyl protecting groups from **7** to yield the free diacid (**8**). The reaction was performed at room temperature using 10% Pd/C and the reaction was complete after 30 min. The reaction mixture was filtered through Celite to remove the 10% Pd/C and the filtrate rotoevaporated to yield a white solid residue (**8**). Recrystallization afforded pure product. As performed on the poly(anhydride-ethers), acetylation of **8**, followed by polymerization of **9**, afforded the polymer (**2**). Molecular weights (M_w) have ranged from 2000 to 5000 with corresponding polydispersities of approximately 1.4.

Downloaded by NORTH CAROLINA STATE UNIV on October 31, 2012 | http://pubs.acs.org
Publication Date: September 24, 1998 | doi: 10.1021/bk-1998-0709.ch005

Downloaded by NORTH CAROLINA STATE UNIV on October 31, 2012 | http://pubs.acs.org
Publication Date: September 24, 1998 | doi: 10.1021/bk-1998-0709.ch005

Degradation studies. The poly(anhydride-esters) were compression molded into circular discs and placed in phosphate buffered saline solution under acidic, neutral, and basic conditions. Over the course of the three week degradation study, the polymers in the acidic and neutral solution showed no observable changes whereas the polymer in the basic media showed significant morphological changes over time. Chemical quantitation of the degradation process are currently underway.

Conclusion

Replacement of the ether bond in the poly(anhydride-ethers) with an ester bond creates a new series of polymers with medically relevant degradation products (i.e. salicylic acid). The use of salicylic acid within the polymer backbone will allow this polymer prodrug to be used in a variety of applications including the treatment of inflammatory bowel disease, (*7,8*) possible blood thinning related to heart disease, prevention of adherence of bacteria to catheters, (*13*) and many other areas.

Acknowledgments

The authors wish to thank the New Jersey Commission of Science and Technology for financial support.

Literature Cited

(1) Brem, H., et al.*The Lancet* . **1995**, *345*, , 1008-1012
(2) Wu, M.P.; Tamada, J.A.; Brem, H.; Langer, R. *J. Biomed. Mater. Res.* **1994**, *28*, 387-395
(3) Liso, P.A.; Rebuelta, M.; Roman, J.S.; Gallardo, A.; Villar, A.M. *J. Biomed. Mater. Res.* **1996**, *32*, 553-560
(4) Gallardo, A., et al. *Polymer* **1993**, *34*, 394-400
(5) Conix, A. *Macromol. Synth.* **1966**, *2*, 95-99
(6) Klotz, U.; Maier, K; Fischer, C.; Heinkel, K. *The New Eng. J. Med.* **1980**, *303*, , 1499-1502
(7) Das, K.M.; Eastwood, M.A. *Clin Pharm. & Ther.* **1975**, *18*, , 514-520
(8) Das, K.M. *Gastroent. Clin. N. Amer.* **1989**, *18*, , 1-20
(9) Calder, I.C.; Funder, C.C.; Green, C.R.; Ham, K.N.; Tange, J.D. *Brit. Med. J.* **1972**, *1*, 152-154
(10) Nakamura, J.; Tagami, C.; Nishida, K.; Sasaki, H. *J. Pharma. Pharmacol.* **1992**, *44*, 295-299
(11) Levy, G. *Arch Intern Med.* **1981**, *141*, 279-281
(12) Kricheldorf, H.R.; Lubbers, D. *Makromol. Chem., Rapid Commun.* **1990**, *11*, 303-307
(13) Farber, B.; Wolff, A. *J. Biomed. Mater. Res.* **1993**, *27*, pp. 599-602

Downloaded by MONASH UNIV on October 31, 2012 | http://pubs.acs.org
Publication Date: September 24, 1998 | doi: 10.1021/bk-1998-0709.ch006

Chapter 6

Synthesis of Thioester End-Functionalized Poly(ε-caprolactone) and Its Application in Chemoselective Ligation

Qiang Ni and Luping Yu[1]

Department of Chemistry and The James Franck Institute, The University of Chicago, 5735 South Ellis Avenue, Chicago, IL 60637

In order to synthesize novel poly(ε-caprolactone) (PCL) conjugates, thioester functionalized PCL has been synthesized by using dimethylaluminum benzylthiolate as an initiator. The living character and quantitative introduction of thioester end in this ring opening polymerization (ROP) process have been confirmed by GPC and ^{1}H NMR characterization. Furthermore, the applicability of chemoselective ligation to the thioester end has been demonstrated with compounds containing a cysteine terminal.

Increasing attention is being directed to the design and synthesis of polymeric drug delivery systems since they show a great potential to achieve controlled release as well as site-specific targeting (*1-3*). In this regard, synthetic polymers have been studied extensively along with their natural counterparts (e.g., sugars, proteins). Aliphatic polyesters, such as poly(lactic acid) (PLA), poly(glycolic acid) (PGA), poly(ε-caprolactone) (PCL), and their copolymers, rank among the most promising candidates in the synthetic polymer category due to their unique property of combining biocompatibility, biodegradability, and permeability (in the case of PCL and its copolymers) (*3, 4*). Their incorporation into other biocompatible polymeric materials or bioactive species (e.g., peptides, enzymes) may lead to novel polymer conjugates. In fact, novel drug delivery systems (*5*) and potential prodrugs (*6*) have been developed based on these biodegradable polyesters. To this end, their heterobifunctional analogs are truly valuable intermediates, as elucidated in the model for pharmacologically active polymers by Ringsdorf (*7*).

Ring opening polymerization (ROP) of lactones and related compounds has been the major polymerization approach to the sythesis of aliphatic polyesters (*8*). Numerous initiator systems based on organo aluminum, tin, and rare earth metal compounds have been developed (*8-10*). It is well recognized that the mechanism of the ROP using these initiators is a so called coordination-insertion mechanism (Scheme 1) and the polymer chain thus formed should carry the alkoxide (OR') group from the initiator (dialkylaluminum alkoxide, **1**) while the other chain end is a hydroxyl group after hydrolysis. Accordingly, a functionalized initiator approach (e.g., using initiators like **1**, where R = $-CH_2CH_3$; R' = $-(CH_2)_2Br$; $-(CH_2)_3CH{=}CH_2$; $-(CH_2)_3NEt_2$) has been developed to achieve the synthesis of

In Tailored Polymeric Materials for Controlled Delivery Systems; McCulloch, I., et al.;
ACS Symposium Series; American Chemical Society: Washington, DC, 1998.

heterobifunctional aliphatic polyesters (*11*). However, this approach is limited by the available functionalities which can survive the reaction conditions. For example, attempts to synthesize primary amine-terminated PCL using an initiator like **1**, where R' = $-(CH_2)_3NH_2$, failed to yield the expected polyester due to amide linkage formation.

Our interest in introducing thioester functionality into the PCL chain ends is motivated by the following considerations. First, known to be a kind of moderately activated carboxy derivative, thioester has many synthetic applications (*12-16*), especially in peptide synthesis. In particalar, chemoselective ligation (CSL) between two peptide segments, which possess a thioester end and N-Cys terminal, respectively, has provided direct synthetic access to polypeptide chains with the size of typical protein domains (*16-18*). The desirable features of this CSL lead us to reason that this approach should make a complement to the coupling methods currently employed for the synthesis of polymer conjugates (*2*). Secondly, living polymerization of lactones using dialkylaluminum alkanethiolate is likely since its analog, dialkylaluminum alkoxide (**1**), is an excellent initiator in such cases (*8*). Therefore, well-defined polyesters and their copolymers with thioester end functionality can be synthesized. Furthermore, chemical modifications of these heterobifunctional polyesters (i.e., one thioester and one hydroxyl end) may provide useful materials for a variety of applications.

In this paper we report a facile method for the introduction of thioester end group to PCL, and results on the reactivity of this functional group in CSL processes.

Experimental Section

Materials. ε-Caprolactone (Aldrich) was dried over CaH_2 and distilled under reduced pressure. L-Lactide (Aldrich) was recrystallized twice from ethyl acetate. Benzyl mercaptan (Aldrich) was purified by distillation. Trimethylaluminum (2.0 M) in methylene chloride (Aldrich) was used as received without further purification. Poly(ethylene glycol) methyl ether (mPEG, Mn ca. 550) was purchased from Aldrich. Toluene and methylene chloride (Fisher) were dried by refluxing over CaH_2 and distilled just before use. THF (Fisher) was purified by distillation over sodium chips and benzophenol. All other chemicals were purchased from Aldrich and used as received.

Characterization. The ^1H and ^{13}C NMR spectra were collected on a Bruker 400 MHz and a QE-300 75 MHz NMR spectrometer, respectively. The GPC measurements were performed on a Waters 410 RI system equipped with a differential refractometer detector using THF (HPLC grade) as an eluent. Molecular weight and molecular weight distributions were calculated according to a modified universal calibration curve derived from polystyrene standards and the Mark-Houwink equations for both polystyrene and PCL (*19*).

Initiator preparation (Scheme 2). Dimethylaluminum benzylthiolate (**2**) was prepared by reaction of benzyl mercaptan with trimethylaluminum as described by Corey *et al* (*12*). To a previously flamed and argon purged 25 mL round-bottomed flask , CH_2Cl_2 (4.0 mL) and benzyl mercaptan (0.14 mL, 1.2 mmol) were introduced through a rubber septum. To this solution was added slowly a 2.0 M solution of $Al(CH_3)_3$ in toluene (0.60 mL, 1.2 mmol) with stirring at -5 °C. This solution was then warmed up to room temperature and kept for 2 to 4 hrs before use.

Downloaded by MONASH UNIV on October 31, 2012 | http://pubs.acs.org
Publication Date: September 24, 1998 | doi: 10.1021/bk-1998-0709.ch006

Downloaded by MONASH UNIV on October 31, 2012 | http://pubs.acs.org
Publication Date: September 24, 1998 | doi: 10.1021/bk-1998-0709.ch006

Scheme 1. Coordination-Insertion Mechanism of ROP of Lactones Using Initiator R_2AlOR'(1)

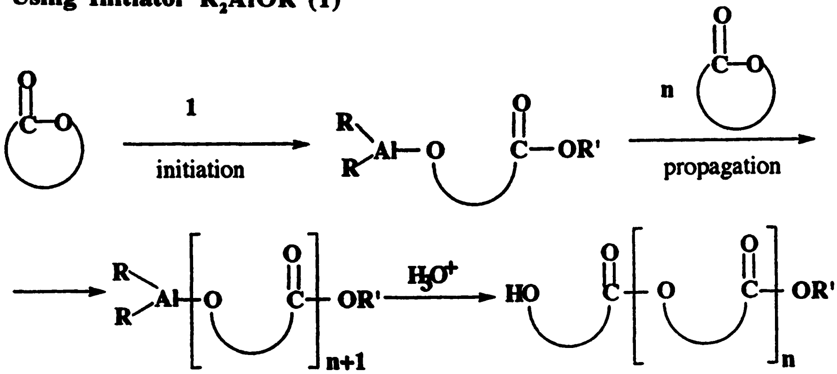
1
initiation
R
Al
O
C
OR'
n
propagation
n+1
H_3O^+
HO
n

Scheme 2. Tailored Synthesis of Thioester End-Funtionalized PCL

$$(CH_3)_3Al + HSCH_2C_6H_5 \xrightarrow[Tol/CH_2Cl_2]{-5^\circ C} \underset{2}{(CH_3)_2AlSCH_2C_6H_5} + CH_4 \quad (1)$$

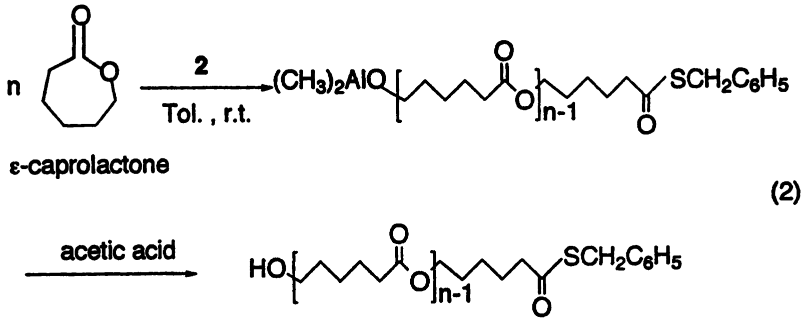
n
2
Tol., r.t.
ε-caprolactone
$(CH_3)_2AlO$
n-1
$SCH_2C_6H_5$
acetic acid
HO
n-1
$SCH_2C_6H_5$

(2)

Downloaded by MONASH UNIV on October 31, 2012 | http://pubs.acs.org
Publication Date: September 24, 1998 | doi: 10.1021/bk-1998-0709.ch006

Synthesis of thioester end-functionalized PCLs (Scheme 2). A typical polymerization was exemplified by the synthesis of PCL-40 (the number 40 indicates the designed monomer to initiator ratio). To a previously flamed and argon purged 25 mL Schlenk tube, toluene (8.0 mL) and ε-CL (0.93 mL, 8.4 mmol) monomer were introduced through a rubber septum. To this solution was added quickly the initiator (**1**) solution (0.8 mL, 0.21 mmol) with vigorous stirring. The Schlenk tube was then sealed with valve and kept at room temperature for 16 hrs. An increase in viscosity was noted. After quenching the reaction by adding excess acetic acid, the polymer was precipitated into n-heptane, dissolved in THF, reprecipitated into n-heptane and then dried under vacuum for 2 days. There was no ε-CL monomer detectable by ^{1}H NMR in the residue collected from the n-heptane part. The yield was quantitative.

Synthesis of diblock copolymer PCL-b-PLA (Scheme 3). The living prepolymer PCL-120 was synthesized by a similar approach as described above. After 24 hrs, certain portion of the living PCL solution was transfered to another Schlenk tube containing L-lactide in toluene at 80 °C. After another 24 hrs, the reaction was quenched by adding excess acetic acid. The polymer was precipitated into n-heptane, dissolved in THF, then precipitated into methanol. The conversions of ε-CL and L-lactide monomer were 100% and 80% respectively.

Synthesis of N-Cys-terminated mPEG (3d). The general synthetic approach is outlined in Scheme 4.

Synthesis of nitrophenyl-terminated mPEG (3a). To a solution of mPEG (6.18 g, 11.2 mmol), Ph_3P (3.07 g, 11.7 mmol) and 4-nitrophenol (1.63 g, 11.7 mmol) in THF (25 mL) was added slowly diethyl azodicarboxylate (DEAD) (1.9 mL, 12.1 mmol) at 0 °C. The reaction mixture was stirred overnight at room temperature. After removal of the solvent, the residue was dissolved in distilled water and then filtered. The filtrate was extracted with CH_2Cl_2 several times. The combined organic layer was washed with distilled water, dried over Na_2SO_4, concentrated by rotary evaporation and dried under vacuum to yield a light orange oil (5.93 g, 79%). This crude product was purified by gel chromatography using hexane:ethyl acetate:methanol (5:5:1) as an eluent.

Synthesis of aminophenyl-terminated mPEG (3b). A Parr hydrogenation bottle was charged with **3a** (2.8 g, 4.2 mmol), 95% ethanol (30 mL) and 10% Pd/C (0.45 g). The bottle was pressurized with hydrogen (50 psi) and allowed to shake overnight. The filtrate was concentrated by rotary evaporation and dried under vacuum to yield a pale yellow oil (2.6 g, 97%).

Synthesis of 3c. To a solution of **3b** (2.6 g, 4.0 mmol), N,N'-bis(t-Boc)-L-cystine (1.9 g, 4.3 mmol) and DMAP (0.08 g, 0.6 mmol) in CH_2Cl_2 (40 mL) was added dropwise 1.0 M DCC in CH_2Cl_2 (4.5 mL, 4.5 mmol) at 0 °C with stirring. The reaction mixture turned to be cloudy after several minutes and it was stirred overnight at room temperature. The precipitate formed was filtered off and the solution was washed with dilute hydrochloric acid and then distilled water. After the organic layer was dried over Na_2SO_4, the CH_2Cl_2 was evaporated under vacuum to yield a viscous oil (3.5 g, 80%). The crude product was purified by gel chromatography using hexane:ethyl acetate:acetone (1:3:2) and then acetone as eluents.

Downloaded by MONASH UNIV on October 31, 2012 | http://pubs.acs.org
Publication Date: September 24, 1998 | doi: 10.1021/bk-1998-0709.ch006

Synthesis of 3d. Compound **3c** (1.9 g, 1.7 mmol) was dissolved in CH_2Cl_2 (15 mL) and treated with trifluoroacetic acid (4 mL) under N_2. After 1 hr stirring at room temperature, the solvent was removed. The residue was taken up in CH_2Cl_2 (15 mL), concentrated by rotary evaporation (this procedure was repeated four times), and finally dried under vacuum for 2 hr. The resulting deprotection product was dissolved in distilled water (10 mL) under N_2, and pH of the solution was adjusted to be ca. 8 by adding 1 M NaOH. The solution was then treated with dithiothreitol (DTT) (0.95 g, 6.2 mmol) and stirred overnight at room temperature. The resulting reaction mixture was acidified by adding 2 M hydrochloric acid and extracted with CH_2Cl_2 several times. The combined organic layer was washed with saturated aqueous NaCl, dried over Na_2SO_4 and then under vacuum to yield a viscous oil (1.4 g, quantitative). This crude product was dissolved in THF for chemoselective ligation without further purification.

Chemoselective ligation. Under various reaction conditions, chemoselective ligation using the thioester end functionalized PCLs with L-cysteine ethyl ester hydrochloride and **3d** has been investigated. Two representative examples are given below.

Chemoselective ligation using PCL-15 with L-cysteine ethyl ester hydrochloride. To a solution of PCL-15 (50 mg, 0.03 mmol) and 18-C-6 (4 mg) in THF (5 mL) was added another solution of N-cysteine ethyl ester hydrochloride (8 mg, 0.05 mmol) and K_2CO_3 (20 mg) in distilled water (1 mL) with stirring under N_2 at room temperature. The reaction mixture was acidified and precipitated into n-heptane after 12 hr. The precipitate formed was washed with dilute hydrochloric acid then distilled water, and finally dried under vacuum to give the ligation product.

Chemoselective ligation using PCL-15 with 3d (Scheme 5). To a solution of PCL-15 (54 mg, 0.03 mmol) in THF (8 mL), acetonitrile (6 mL), K_2CO_3 (0.6 g), $KHCO_3$ (0.4 g) and 18-C-6 (6 mg) were introduced under N_2 in that order. After stirring for about 10 miniutes, to this inhomogeneous solution was added a solution of **3d** (60 mg, 0.08 mmol) in THF (1 mL). The reaction mixture was acidified and the solvent was removed under vacuum after stirring at room temperature for 18 hr. The residue was dissolved in THF and precipitated into n-heptane. The precipitate was washed with dilute hydrochloric acid then distilled water, and finally dried under vacuum to give the ligation product.

Results and Discussion

For the synthesis of thioester end-functionalized PCL, dialkylaluminum benzylthiolate (**2**) was chosen as the initiator because it is easily prepared and very effective in the synthesis of thioesters from lactones and esters. The general synthetic approach is outlined in Scheme 2. Polymerizations under different reaction conditions have been systematically conducted. Selected data on the molecular weight and molecular weight distributions (MWDs) of PCLs synthesized are collected in Table 1. While the quite narrow molecular weight distributions (1.09 - 1.34) and the linear relationship between the number-average molecular weight (Mn) at total monomer conversion and the monomer to initiator ratio (M/I) (Figure 1) imply the living character of the polymerization process, more conclusive evidence was from the polymerization resumption experiment. In this experiment, more ε-CL monomer was added after the polymerization of the first addition of ε-CL had gone to completion. Figure 2 shows that the molecular weight increased

Downloaded by MONASH UNIV on October 31, 2012 | http://pubs.acs.org
Publication Date: September 24, 1998 | doi: 10.1021/bk-1998-0709.ch006

Scheme 3. Synthesis of Diblock Copolymer PCL-b-PLA

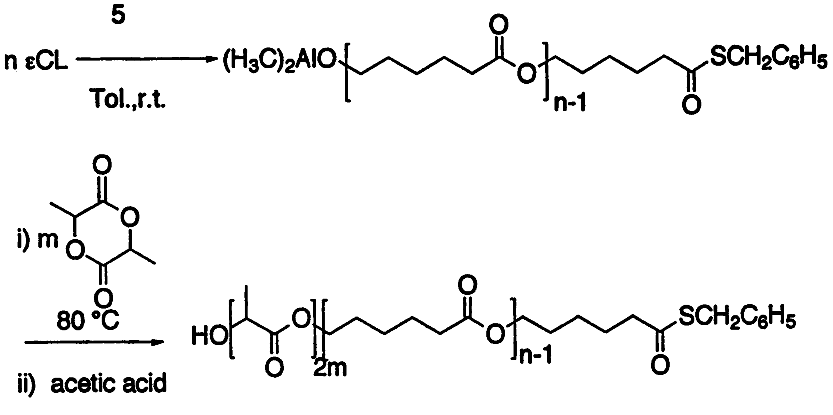
5
n εCL
Tol.,r.t.
(H3C)2AlO
SCH2C6H5
n-1
i) m
80 °C
ii) acetic acid
HO
2m
n-1
SCH2C6H5

PCL-b-PLA

Scheme 4. Synthesis of N-Cys-Terminated mPEG(3d)

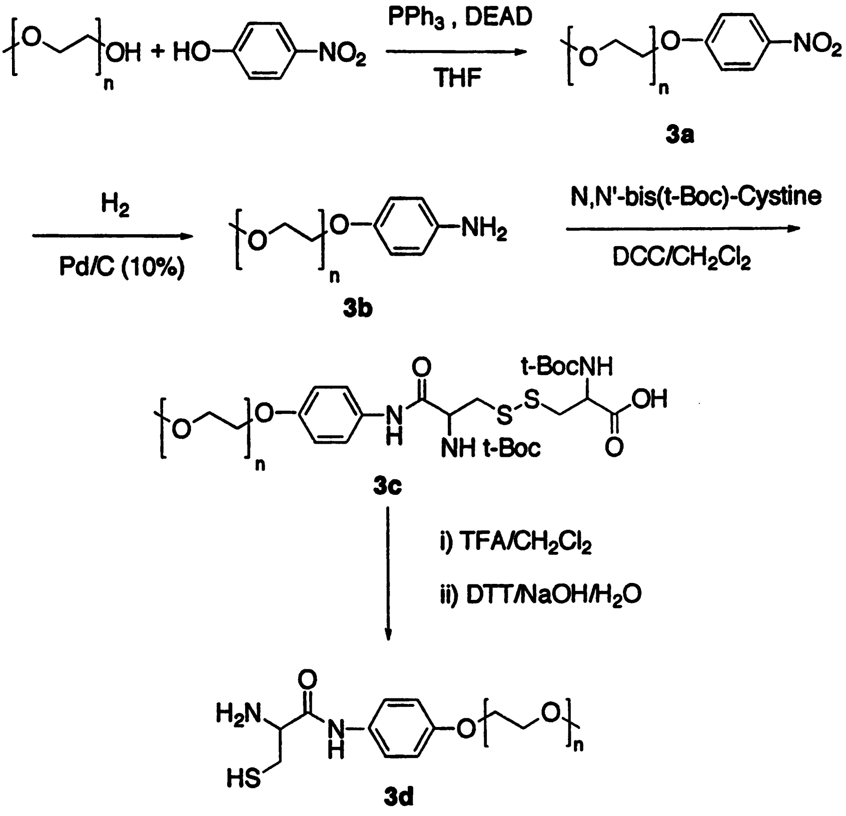
OH + HO
NO2
PPh3, DEAD
THF
NO2
3a
H2
Pd/C (10%)
NH2
3b
N,N'-bis(t-Boc)-Cystine
DCC/CH2Cl2
t-BocNH
OH
NH t-Boc
3c
i) TFA/CH2Cl2
ii) DTT/NaOH/H2O
H2N
HS
3d

Downloaded by MONASH UNIV on October 31, 2012 | http://pubs.acs.org
Publication Date: September 24, 1998 | doi: 10.1021/bk-1998-0709.ch006

Scheme 5. Chemoselective Ligation between Thioester End-Functionalized PCL and N-Cys-Terminated mPEG(3d)

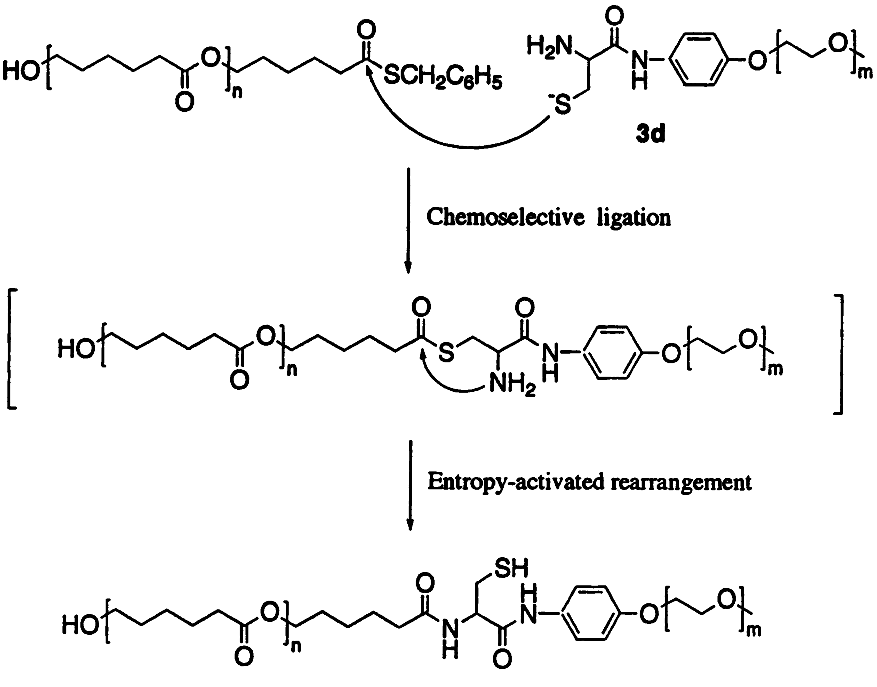
HO
O
O
n
O
SCH₂C₆H₅
H₂N
O
N
H
⁻S
O
m
3d
Chemoselective ligation
HO
O
O
n
O
S
O
NH₂
N
H
O
m
Entropy-activated rearrangement
HO
O
O
n
O
N
H
SH
H
N
O
O
m

Downloaded by MONASH UNIV on October 31, 2012 | http://pubs.acs.org
Publication Date: September 24, 1998 | doi: 10.1021/bk-1998-0709.ch006

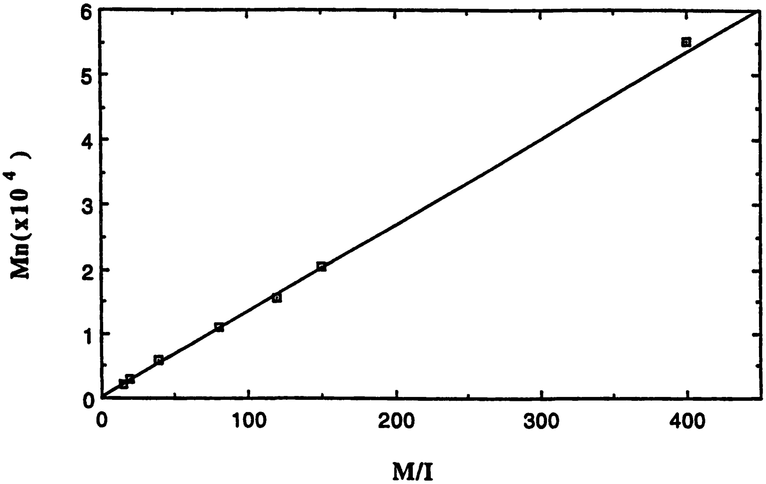

Figure 1. Plot of number-average molecular weight (Mn) versus monomer to initiator ratio(M/I).

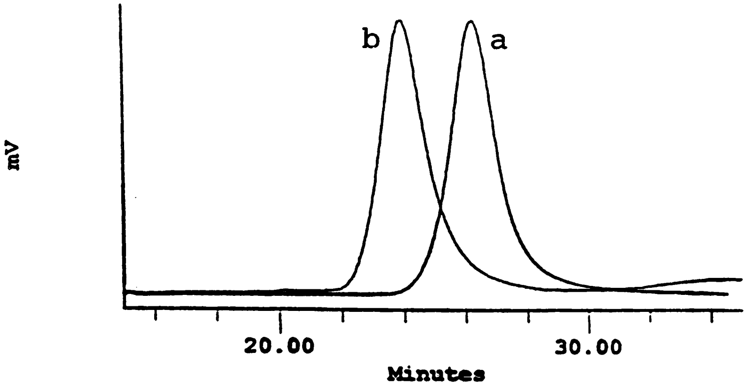

Figure 2. GPC profiles of polymerization resumption experiment:
peak a: PCL after addition of ε-CL. M/I = 60;
peak b: PCL after second addition of ε-CL, M/I = 150.

for the final polymer (peak b, Mn = 20400, MWD = 1.21), relative to the first peak (peak a, Mn = 7810, MWD = 1.13), and there was no detectable residual peak. This result indicates that the polymerization proceeds in the absence of chain termination and intramolecular chain transfer since either mechanism will produce inactive polymers or cyclic structures. Since we are more concerned with the polymer chain ends, ^1H NMR study on this system was carried out in detail. As a typical example, shown in Figure 3, the ^1H NMR spectrum of PCL-20 gave an intensity ratio (1.00/1.02) between Hc (2.58ppm, methylene group from ε-CL at the thioester chain end) and Hh (3.64ppm, methylene group from ε-CL at the hydroxy end) very close to unity, which was in agreement with our expectation that the polymer chain should be capped with one thioester end and one hydroxy end. Moreover, further study on the initiator in $CDCl_3$ (data not shown here) has shown that during the initiation step, all the initiators were reactive, and only the acyl-oxygen cleavage was involved. All these results allow us to conclude that this initiator is effective not only for the ROP of ε-CL but also for the quantitative introduction of the thioester end group as well. On the other hand, these results also suggest that this initiator might be suitable for the synthesis of pure block copolymers such as PCL-b-PLA. Consequently,the synthesis of PCL-b-PLA with 2 was carried out (Scheme 3). Both results from GPC (Figure 4) (peak a, Mw = 17600, MWD = 1.21; peak b, Mw = 29100, MWD = 1.20) and ^{13}C NMR (Figure 5) characterization are consistent with our prediction (*20*).

Table 1. Polymerization of ε-CL Initiated with 2 in Toluene at Room Temperature.

Entry (PCL-n)[a]	[CL]	t(h)	conv.(%)	M_n[b]	M_w/M_n[b]
PCL-15	1.0	12	>99	2190	1.11
PCL-20	1.0	12	>99	3090	1.10
PCL-40	1.1	16	>99	5890	1.09
PCL-80	1.0	18	>99	11000	1.21
PCL-120	1.8	18	>99	15600	1.20
PCL-150	1.2	20	>99	20500	1.21
PCL-400	1.8	18	90	49600	1.34

a. The number n indicates the designed degree of polymerization.
b. GPC results: THF as an eluent and calculated by a modified universal calibration curve.

Application of the thioester end-functionalized PCL in CSL. Since the goal of our efforts toward the introduction of thioester group into PCL is to further utilize this functionality to achieve the synthesis of novel PCL conjugates, it is vital to understand the reactivity of the thioester end. As mentioned above, the CSL using thioester functionality has been very successful in peptide synthesis. However, application of such a method to polymer synthesis is unprecedented. To test the applicability of the CSL approach, we first chose L-cysteine ethyl ester hydrochloride as a small model compound to react with the thioester end-functionalized PCL. Under appropriate conditions (see experimental section), the reaction went smoothly. The ^1H NMR spectrum of the resulting product shows a complete disappearance of the 2.58 ppm signal (methylene group from ε-CL at the

Downloaded by MONASH UNIV on October 31, 2012 | http://pubs.acs.org
Publication Date: September 24, 1998 | doi: 10.1021/bk-1998-0709.ch006

Downloaded by MONASH UNIV on October 31, 2012 | http://pubs.acs.org
Publication Date: September 24, 1998 | doi: 10.1021/bk-1998-0709.ch006

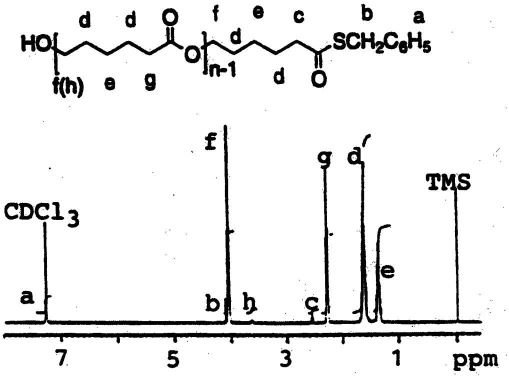

Figure 3. ^{1}H NMR spectrum of PCL-20 in $CDCl_3$.

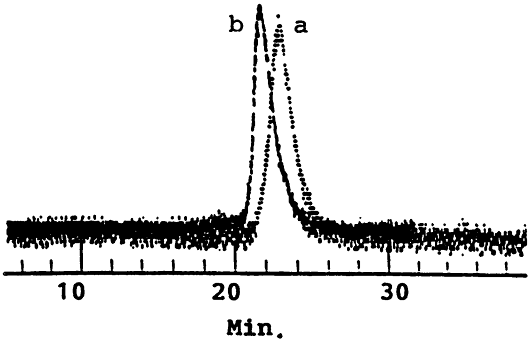

Figure 4. GPC profiles of PCL-b-PLA (b) and its PCL prepolymer (a).

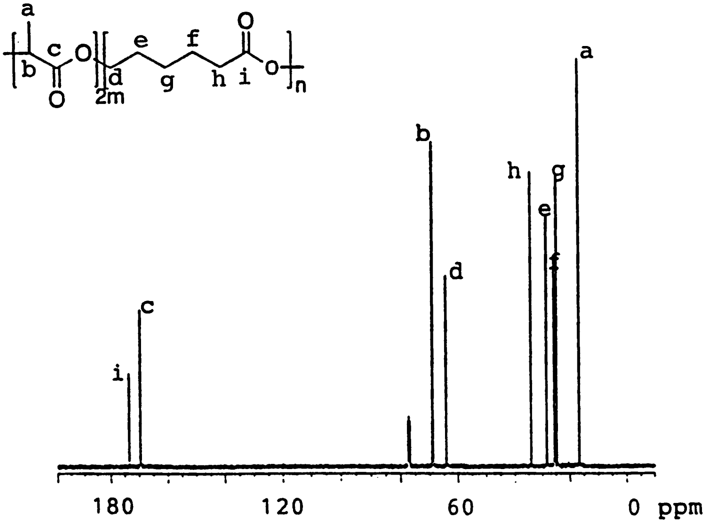

Figure 5. ^{13}C NMR spectrum of PCL-b-PLA.

PCL thioester end), instead, a new peak characteristic of the formation of an amide bond appeared at 6.47 ppm. To exclude the interference caused by hydrolysis of the thioester end or the vulnerable ester backbone of PCL, the thioester end-functionalized PCL was also treated under the same conditions without adding L-cysteine ethyl ester hydrochloride as a control. According to the ^1H NMR and GPC results, there were no detectable changes of Mn and MWDs from the PCL samples before and after the treatment. Therefore, the thioester at PCL chain end is indeed a reactive functional group. Furthermore, N-Cys-terminated mPEG (**3d**) has been synthesized (Scheme 4) to reacact with thioester end-functionalized PCL. Not only because its coupling product may be interesting for drug delivery systems, but more importantly, the results from these reactions can be readily generalized since PEG is soluble in both aqueous medium and common organic solvents. Detailed study on the CSL between thioester end-functionalized PCL and N-Cys mPEG (**3d**) has been carried out by systematically changing solvents, reagents and temperature as well. The results from our experiments are very encouraging. High coupling efficiencies (>80%) with regard to the benzyl thioester were observed under several different reaction conditions. For example, under room temperature, using CH_3CN/THF as mixing solvent and $KHCO_3/K_2CO_3$/18-C-6 as reagents, the coupling reaction went to completion within 18 hr. The ^1H NMR spectrum and GPC profile of the coupling product are shown in Figure 6 and 7. The doublet at 6.63 ppm unambiguously indicates the formation of a new amide linkage. Although the complete disappearance of the 2.58 ppm triplet, which is due to the thioester end, does not ensure a quantitative coupling, the results from its GPC profile (i.e., no residual peak and no MWD broadening) excluded the presence of any detectable side reactions under these conditions. Combined with the observation that there was virtually no reaction using ethanolamine instead of N-Cys-mPEG under the same reaction conditions, the coupling reaction is believed to proceed in a similar fashion as that in peptide synthesis (Scheme 5).

Conclusions

A facile method for the introduction of thioester end group in the ROP of ε-CL using dimethylaluminum benzylthiolate (**2**) as an initiator has been developed. The living character shown in the polymerization process has enabled us to synthesize novel thioester end-functionalized PCL as well as diblock copolymer PCL-b-PLA in a controlled way. More importantly, the chemoselective ligation method has also been demonstrated to be applicable to the thioester end-functionalized PCL. This may provide a new approach to the design and synthesis of novel PCL conjugates such as PCL-peptide conjugate. Moreover, it is worth pointing out that recent extension work (*18*) on the CSL using thioester functionality will certainly make this approach more promising in polymer synthesis along with the development of novel synthetic methods that allow convenient incorporation of thioester functionality into either polymer chain ends or side chains.

Acknowledgments

This work was supported by the National Science Foundation. Support from the National Science Foundation Young Investigator program is gratefully acknowledged.

Literature Cited

1. Ouchi, T.; Ohya, Y. *Prog. Polym. Sci.* **1995**, *20*, 211.

Downloaded by MONASH UNIV on October 31, 2012 | http://pubs.acs.org
Publication Date: September 24, 1998 | doi: 10.1021/bk-1998-0709.ch006

Downloaded by MONASH UNIV on October 31, 2012 | http://pubs.acs.org
Publication Date: September 24, 1998 | doi: 10.1021/bk-1998-0709.ch006

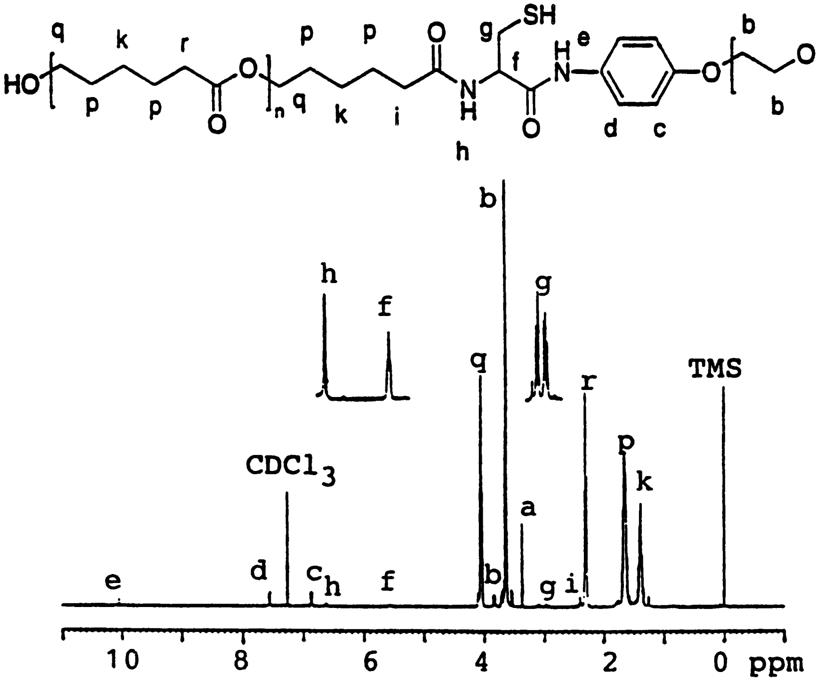

Figure 6. ^{1}H NMR spectrum of PCL-mPEG.

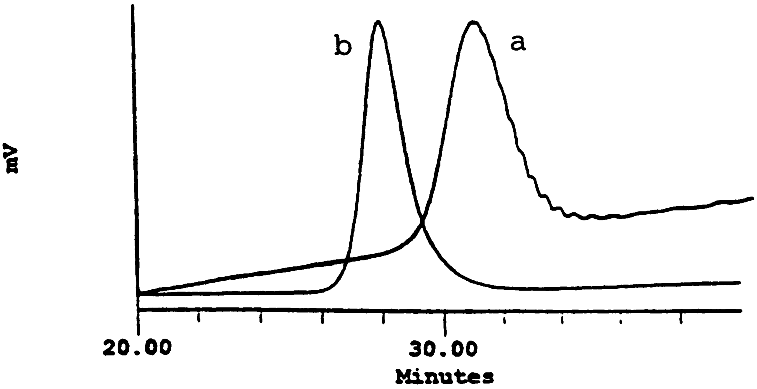

Figure 7. GPC profiles of PCL-15 (a) and PCL-mPEG(b).

2. Putnam, D.; Kopecek, *J. Adv. in Polym. Sci.* **1995**, *122*, 55.
3. Hayashi, T. Prog. *Polym. Sci.* **1994**, *19*, 663.
4. Chiellini, E.; Solaro, R. *Adv. Mater.* **1996**, *8*, 305.
5. Gref, R.; Minamitake, Y.; Peracchia, M. T.; Trubetskoy, V.; Torchilin, V.; Langer, R. *Science*, **1994**, *263*, 1600.
6. Kricheldorf, H. R.; Kreiser-Saunders, I. *Polymer* **1994**, *35*, 4175.
7. Ringsdorf, H. *J. Polym. Sci. Symp.* **1975**, *51*, 135.
8. Lofgren, A.; Albertsson, A. C.; Dubois, Ph.; Jerome, R. *J.M.S. - Rev. Macromol. Chem. Phys.* **1995**, *C35(3)*, 379.
9. Abdel-Fattah, T. M.; Pinnavaia, T. J. *J. Chem. Soc., Chem. Commun.* **1996**, 665.
10. Yamashita, M.; Takemoto, Y.; Ihara, E.; Yasuda, H. *Macromolecules* **1996**, *29*, 1798.
11. Dubois, Ph.; Jerome, R.; Teyssie, Ph. *Makromol. Chem., Macromol. Symp.* **1991**, *42/43*, 103.
12. Corey, E. J.; Beames, D. J. *J. Am. Chem. Soc.* **1973**, *95*, 5829.
13. Masamune, S.; Kamata, S.; Schilling, W. *J. Am. Chem. Soc.* **1975**, *97*, 3515.
14. Mihara, H.; Maeda, S.; Kurosaki, R.; Ueno, S.; Sakamoto, S.; Niidome, T.; Hojo, S.; Aimoto, S.; Aoyagi, H. *Chem. Lett.* **1995**, 397.
15. Zhang, L.; Tam, J. P. *J. Am. Chem. Soc.* **1997**, *119*, 2363.
16. Dawson, P. E.; Muir, T. W.; Clark-Lewis, I.; Kent, S. B. H. *Science* **1994**, *266*, 776.
17. Lu, W.; Qasim, M. A.; Kent, S. B. H. *J. Am. Chem. Soc.* **1996**, *118*, 8518.
18. Canne, L. E.; Bark, S. J.; Kent, S. B. H. *J. Am. Chem. Soc.* **1996**, *118*, 5891.
19. Chindler, A.; Hibionada, Y. M.; Pitt, C. G. *J. Polym. Sci., Polym. Chem. Ed.* **1982**, *20*, 319.
20. Jacobs, C.; Dubois, Ph.; Jerome, R.; Teyssie, Ph. *Macromolecules* **1991**, *24*, 3027.

Downloaded by MONASH UNIV on October 31, 2012 | http://pubs.acs.org
Publication Date: September 24, 1998 | doi: 10.1021/bk-1998-0709.ch006

Downloaded by NORTH CAROLINA STATE UNIV on October 31, 2012 | http://pubs.acs.org
Publication Date: September 24, 1998 | doi: 10.1021/bk-1998-0709.ch007

Chapter 7

The Reactive Polymeric Micelle, Convenient Tool for Targeting Drug Delivery System

Yukio Nagasaki and Kazunori Kataoka

Materials Science Department, Science University of Tokyo, Noda 278, Japan

Formation of amphiphilic poly(ethylene glycol)-b-polylactide (PEG/PLA) block copolymers was accomplished using potassium alkoxides to initiate the anionic polymerization of ethylene oxide, with the living chain end initiating the polymerization of lactide. Using potassium 3,3-diethoxypropoxide as an initiator, block copolymers with an acetal moiety at the PEG chain end, which was later converted into an aldehyde group, were obtained. Block copolymers were analyzed by ^{1}H-NMR spectroscopy and GPC. The amphiphilic block copolymers formed micelles in aqueous milieu. The conversion of acetal end groups to aldehyde group was carried out by an acid treatment using 0.01 mol L^{-1} hydrochloric acid. The extent of the conversion attained more than 90 % without any side reaction such as aldol condensation. The micellar structure may play an important role in preventing a possible aldol-condensation between two neighboring aldehyde groups at the PEG chain end. From a dynamic light scattering measurement, the micelle size and shape were estimated. No angular dependency of the scaled characteristic line width was observed in the case of acetal-PEG/PLA(52/56) micelle, suggesting a spherical structure. The diameter and polydispersity factor of the polymeric micelle were influenced by the molecular weights and the composition of the two components of the block copolymer. The block copolymer having a molecular weight of 5,200 for PEG and 5,600 for PLA was the most suitable balance for micelle formation with narrow distribution. Actually, the diameter and polydispersity factor (μ/Γ^2) of the micelles from acetal-PEG/PLA(52/56) determined by the cumulant method were 33 nm and 0.03, respectively. No change in the micelle size and shape was observed before or after the conversion of the acetal end groups to aldehyde groups on the

Downloaded by NORTH CAROLINA STATE UNIV on October 31, 2012 | http://pubs.acs.org
Publication Date: September 24, 1998 | doi: 10.1021/bk-1998-0709.ch007

micelle. Critical association concentrations (cac) of polymeric micelles were characterized by fluorescence spectroscopy using pyrene as fluorescence probe. The cac was determined to be 2 - 4 mg L^{-1}. This functionalized micelle, in particular the one carrying terminal aldehyde groups, is expected to provide a new entity of supramolecular architechture as well as to have wide biomedical application in the fields of drug delivery, diagnosis and surface modification through the coupling of bioactive.

Recently, polymer chemistry was challenged to design novel polymeric systems for various biomedical applications. Drug delivery required the development of polymeric carrier systems which are capable of compartmentalizing drugs as well as meeting all requirements in terms of biocompatibility. Polymeric micelles based on biocompatible amphiphilic block copolymers were found to comply with the expectations.(*1*) For a target-site specific drug delivery, a creation of a new functionalized polymeric micelle is required. The idea of a drug acting only at a target site dates back to 1906 when Ehrlich introduced his prospect known as the "magic bullet".(2) Ringsdorf described in 1975 the concept of a polymeric drug which included all features necessary to connect a drug to a carrier system and to deliver the drug to a specific target site, where it is to be released at a certain rate from the carrier.(*3*) Such matrices as well as fragments thereof are requested to be non-toxic, biodegradable and bioresorbable. To avoid a rapid uptake by the reticuloendothelial system, such drug carrier should be small enough(*4*) (virus mimicking) or should be given a stealth character by modifying the surface, for instance, of the liposomal drug delivery system.(*5*)

In the present work, functionalized amphiphilic block copolymers consisting of poly(ethylene glycol) (PEG) and polylactide (PLA), both FDA-approved polymers, were studied and their formation of micellar systems in selective solvents, i.e., a good solvent for one segment and a precipitant for the other

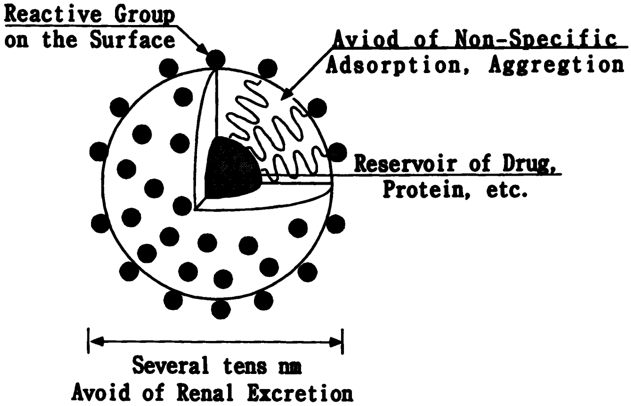

Figure 1. Schematic Illustration of Reactive Polymeric Micelle

segment, was investigated. These nanospheric particles combine the advantages provided by the hydrophobic core which can act as a container for drugs and the unique properties of a hydrophilic shell.(*6*) The small size, apparent thermodynamic stability and exceptional biological features of polymeric micelles favor their application in the biomedical field.(*7*) PEG chains attached to a surface or forming the corona of a nanospheric particle exhibit rapid chain motions in an aqueous medium and have a large excluded volume. The steric repulsion resulting from the loss of configurational entropy of the bound PEG-chains upon approach of a foreign particle and the low interfacial free energy of PEG in water contribute to the extraordinary physiological properties of nanospheres and surfaces covered with PEG.(*8*) Moreover, PEG grafted to surfaces of biomedical devices has been shown to increase their biocompatibility and to reduce thrombogenicity.(*9*) To improve the active targeting properties of the polymeric micelle, we designed the "Reactive Polymeric Micelle" (Figure 1).

Experimental

Materials and Methods: Commercial tetrahydrofuran (THF), 3,3-diethoxypropanol, ethylene oxide (EO) and lactide (LA) were purified conventionally.(*10*) Potassium naphthalene was used as a THF-solution,(*11*) the concentration of which was determined by titration. GPC measurements were carried out using a Shimadzu 6A Liquid Chromatograph equipped with a TSK gel column ($G4000_{HXL}$ + $G3000_{HXL}$ + $G2500_{HXL}$) and an internal RI detector (RID-6A). THF containing 2 wt.% triethylamine was used as eluent at a flow rate of 1 mL min^{-1}. ^{1}H-NMR spectra were obtained using chloroform-d solutions with a JEOL EX400 spectrometer at 400 MHz. Fluorescence measurements were carried out using a 770F JASCO Fluorometer at an excitation wavelength of 333 nm and emission wavelengths of 339 and 390 nm, respectively. A light scattering spectrophotometer (DLS-7,000 Photal, Otsuka Electronics) equipped with a 75 mW Ar-laser that produces vertically polarized incident beams at λ_0 = 488 nm was used in the present study for dynamic and static light scattering measurements. The vertically scattered beam was collected over an angular range of 30_ to 150_ for photon correlation spectroscopy measurements. The concentration varied from $5 \bullet 10^{-4}$ to 2 g L^{-1}.

Polymer synthesis: One of the representative procedures for preparation of α-acetal-PEG/PLA block copolymers is described. α-Acetal-PEG/PLA block copolymers have been synthesized by an one-pot anionic ring opening polymerization of EO followed by LA initiated with potassium 3,3-diethoxypropanolate (PDP) as an initiator at room temperature under argon. One mmol (0.16 mL) of 3,3-diethoxypropanol and 1 mmol (3.5 mL) of potassium naphthalene were added to 30 mL of dry THF to form PDP. After stirring for 10 min 120 mmol (6 mL) of condensed EO was added via a cooled syringe to the formed PDP solution. The polymerization of the EO proceeded for two days resulting in a light brown, highly viscous solution. Supplementary THF was added to decrease the viscosity of the reaction mixture and potassium naphthalene (about 1.5 mL) was added until the solution turned green to stabilize the living chain end. Twenty mmol (10.1 mL) of an LA solution in THF (c=1.98 mol L^{-1}) was introduced, and the polymerization proceeded for 90 min. The polymer was

Downloaded by NORTH CAROLINA STATE UNIV on October 31, 2012 | http://pubs.acs.org
Publication Date: September 24, 1998 | doi: 10.1021/bk-1998-0709.ch007

Downloaded by NORTH CAROLINA STATE UNIV on October 31, 2012 | http://pubs.acs.org
Publication Date: September 24, 1998 | doi: 10.1021/bk-1998-0709.ch007

recovered by precipitation into a 20 fold excess of cold isopropyl alcohol (-15 °C), stored for 2 hours in the freezer and centrifuged for 30 min at 6,000 rpm. The polymer was then freeze-dried in benzene and the yield of the obtained polymer was ca. 90%.

Polymer characterization: The molecular weight of the PEG segment was determined by GPC at the end of the EO polymerization. The molecular weight of the PLA segment was determined using an ^{1}H NMR spectrum by the ratio of methine protons in the PLA segment and methylene protons in PEG segment based on the Mn of PEG determined from the GPC result. The extent of conversion of the acetal to aldehyde groups at the end of the polymer chain was estimated by the ^{1}H NMR spectroscopy after the acid treatment and purification (see below).

Micelle preparation: The procedure has been detailed previously.(*5c, 6*) Briefly, 100 mg of the copolymer was dissolved in 20 mL of dimethyl acetamide, and the polymer solution was transferred into a pre-swollen membrane (Spectra/Por® molecular weight cutoff size 12,000 - 14,000), dialyzed against water for 24 hours and subsequently lyophilized. The yield of the micelle formation was about 90 %.

To convert the α-diethoxy-terminated micelle into a micelle with aldehyde groups at the end of the PEG chain, the polymeric micelle solution was adjusted to pH 2 without the lyophilization, kept for 1 h and readjusted to pH=7 with NaOH. The solution was again dialyzed against water for 24 hours using a pre-swollen membrane to remove the salt. The aldehyde micelle thus obtained was analyzed directly by the DLS or frozen in liquid nitrogen and lyophilized, resulting in a yield of 85 to 90%.

The polymerizations of the end methacryloyl groups in the micelle core were carried out as follows: After the preparation of the polymeric micelle by the dialysis method, methylene chloride solution (0.5 mL) of AIBN (0.5 mg) was added to the solution (1 mg mL^{-1}, 50 mL). After argon bubbling was carried out for 10 min to exclude oxygen, the solution was reacted for 24h at 60 °C. The reaction extent was analyzed by ^{1}H NMR spectra in CDCl$_3$ after the polymer was isolated by freeze dry with water.

Scheme 1

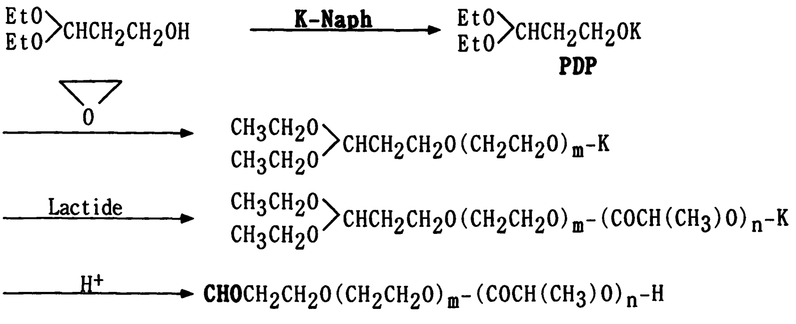
EtO
EtO
CHCH$_2$CH$_2$OH
K-Naph
EtO
EtO
CHCH$_2$CH$_2$OK
PDP
O
CH$_3$CH$_2$O
CH$_3$CH$_2$O
CHCH$_2$CH$_2$O(CH$_2$CH$_2$O)$_m$-K
Lactide
CH$_3$CH$_2$O
CH$_3$CH$_2$O
CHCH$_2$CH$_2$O(CH$_2$CH$_2$O)$_m$-(COCH(CH$_3$)O)$_n$-K
H+
CHOCH$_2$CH$_2$O(CH$_2$CH$_2$O)$_m$-(COCH(CH$_3$)O)$_n$-H

Downloaded by NORTH CAROLINA STATE UNIV on October 31, 2012 | http://pubs.acs.org
Publication Date: September 24, 1998 | doi: 10.1021/bk-1998-0709.ch007

Results and discussion

Synthesis of Acetal-PEG/PLA Block Copolymer: As reported previously (*12*) a potassium alkoxide initiator, which possesses a functional group, can initiate the polymerization of EO without any side reaction to form heterotelechelic PEO having a functional group at one end and a potassium alkoxide at the other end. This polymerization technique is also applicable to a block copolymerization of EO with lactide, forming a block copolymer, with a functional group at the α-terminal in a one-pot synthesis. For an introduction of an acetal group at the PEG end, we have employed an initiation method, *viz*, potassium alkoxide having an acetal moiety (PDP) was used for the polymerization of ethylene oxide (EO) to obtain the α-acetal-PEG.

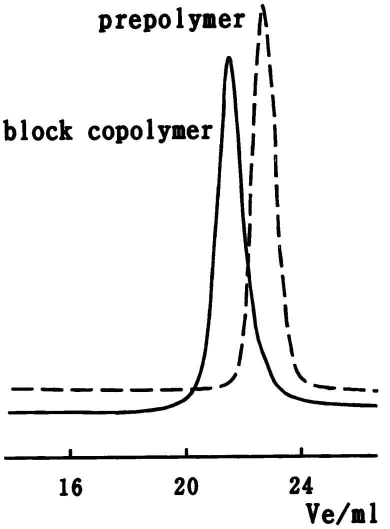

Figure 2. GPC Chromatograms of Acetal-PEG and Acetal-PEG/PLA

When PDP is used as an initiator for EO polymerization, PEG with an acetal moiety at the α-terminus is obtained quantitatively. Because potassium alkoxide has the ability to initiate lactide (LA) polymerization, a PEG-PLA block copolymer having a functional group at the PEG chain end can be prepared. The molecular weight of each segment can be controlled by the initial monomer/initiator ratio. Figure 2 shows the stepwise block copolymerization profile monitored by GPC.

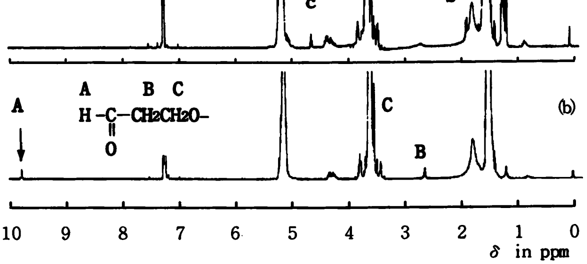

Figure 3. ^{1}H NMR spectra of Acetal-ended PEG-PLA (a) and Aldehyde-ended PEG-PLA (b)

After the EO polymerization initiated with PDP, the Mn and the molecular weight distribution (MWD) were 5,200 and 1.04, respectively. The MW of the obtained PEG was in good accordance with the initial monomer/initiator ratio ($[EO]_0/[(PDP]_0 = 120 / 1$).

After the block copolymerization of LA, the segment length of the PLA was determined by a ^1H NMR analysis. Using PLA and acetal-ended PEG as reference compounds, the assignments of the spectrum were carried out and described in Figure 3a. By the ratio of methine in LA unit appearing in 5.2 ppm vs. methylene in EO unit appearing in 3.6 ppm, the ratio of LA vs. EO units in the block copolymer can be determined. Assuming the MW of PEG determined by the GPC result, the MW of PLA unit can be calculated by the ratio as 5,600.

^1H NMR spectrum of the acetal-PEG/PLA block copolymer provides another information on the end group of the polymer. As can be seen in Figure 3a, triad signal appearing in 4.6 ppm can be attributable to the acetal methine protons at the PEG end. By comparison of the acetal protons with methylene protons in PEG segment and with methine protons in PLA segment, each block copolymer possess an acetal end group almost quantitatively.

Scheme 2

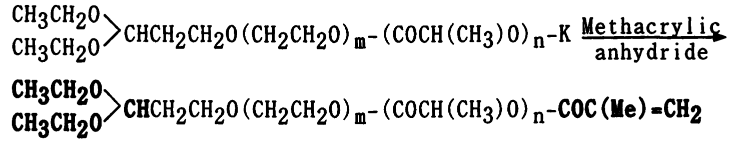

$$\begin{array}{l}CH_3CH_2O\\ CH_3CH_2O\end{array}\!\!>CHCH_2CH_2O(CH_2CH_2O)_m\text{-}(COCH(CH_3)O)_n\text{-}K \xrightarrow[\text{anhydride}]{\text{Methacrylic}}$$

$$\begin{array}{l}CH_3CH_2O\\ CH_3CH_2O\end{array}\!\!>CHCH_2CH_2O(CH_2CH_2O)_m\text{-}(COCH(CH_3)O)_n\text{-}COC(Me){=}CH_2$$

Synthesis of Acetal-PEG/PLA-methacryloyl Block Copolymer: To introduce a polymerizable group at the end of Acetal-PEG/PLA block copolymers, methacryloyl anhydride was added after the block copolymerization of PEG/PLA

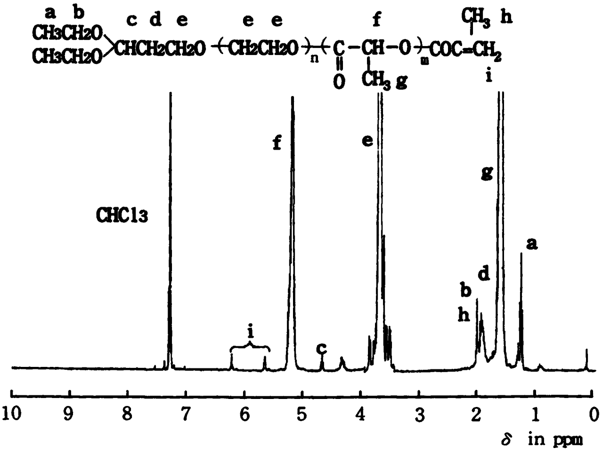

Figure 4. ^1H NMR Spectrum of Ald-PEG/PEG-methacryloyl

Downloaded by NORTH CAROLINA STATE UNIV on October 31, 2012 | http://pubs.acs.org
Publication Date: September 24, 1998 | doi: 10.1021/bk-1998-0709.ch007

Downloaded by NORTH CAROLINA STATE UNIV on October 31, 2012 | http://pubs.acs.org
Publication Date: September 24, 1998 | doi: 10.1021/bk-1998-0709.ch007

initiated with PDP (Scheme 2). From the ^{1}H NMR spectrum after the ω-end modification reaction shown in Figure 4, it was clearly confirmed the quantitative introduction of end methacryloyl group, *viz.*, vinyl protons appear around 6 ppm, retaining acetal methine proton at 4.8 ppm. By the comparison of these signal areas, it is concluded that both α-acetal and ω-methacryloyl groups were introduced quantitatively.

Preparation of Reactive Polymeric Micelles

Preparation of Acetal-PEG/PLA Micelle: It is known that amphiphilic block copolymers with a suitable hydrophilic/hydrophobic balance form micelle structures when exposed to a selective solvent. When PEG/PLA block copolymers were exposed into water, polymeric micelles with nanometer dimension were prepared.

It is very important, however, to choose preparation conditions for the polymeric micelle having desirable size and shape. Very large aggregates with a wide polydispersity factor are often observed. For example, it is reported that 80 - 110 nm size micelles were prepared by the direct dissolution of PEG/PLA(40/80) and PEG/PLA(40/26) block copolymers into water (where the numbers in parenthesis denote the MW of the PEG segment and PLA segment of 4,000 and 8,000, respectively).*(13)* When the block copolymers having a rather longer hydrophilic segment [PEG/PLA(20/9) - PEG/PLA(50/11)] were exposed to water, however, micelles of 15 - 25 nm in diameter could be prepared though the polydispersity factors were fairly large.*(14)* Bazile et al. reported the preparation of PEG/PLA nanoparticles by a solvent diffusion method, *viz.*, an acetone solution of the block copolymer was exposed to water. In this case, micelles of 50 - 110 nm in diameter were prepared from PEG/PLA having fairly large hydrophobic segments [PEG/PLA(20/100) - PEG/PLA (50/350)]. *(15)*

In the present study, a dialysis method was employed to prepare the polymeric micelle, *viz.*, after the block polymer was dissolved in a good solvent for both segments such as dimethylacetamide (DMAc), the solution was dialyzed against water.*(16)* The size and the shape of the obtained polymeric micelle were estimated by a dynamic light scattering measurements.

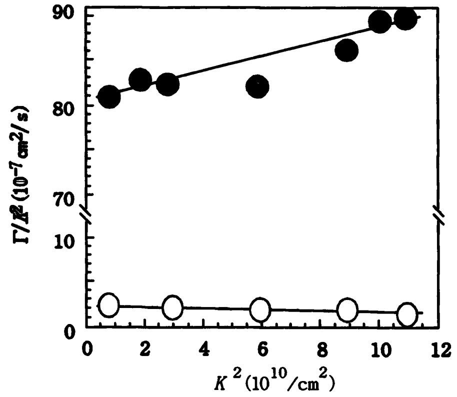

Figure 5. Plots of the K^2-scaled Average Characteristic Line Width Γ, Γ / K^2, vs. K^2 for acetal-PEG/PLA(52/56) (open circle) and acetal-PEG-PLA(91/51) (closed circle)

Downloaded by NORTH CAROLINA STATE UNIV on October 31, 2012 | http://pubs.acs.org
Publication Date: September 24, 1998 | doi: 10.1021/bk-1998-0709.ch007

Before the estimation of size of the prepared micelles, the angular dependency of the sample solutions was analyzed by the DLS as shown in Figure 5. When the micelle was prepared from acetal-PEG/PLA(52/56), it was observed a negligible angular dependence of the scaled characteristic line width on the scattering vector, indicating the almost spherical shape of the obtained micelle. Contrary to this, a fairly large angular dependency of acetal-PEG/PLA(91/51) was observed (slope = 0.088), which is probably due to the secondary aggregations of the micelles for acetal-PEG/PLA(91/51).

Figure 6 shows the size distribution pattern of PEG/PLA(52/56). As can be seen in the figure, the PEG/PLA(52/56) micelle diameter was 31.2 nm, keeping extremely low dispersion factor.

The critical micelle concentration (cmc) is a measure describing the physical properties of the micelle and refers to the micelle stability.(*17*) The term is actually derived from low molecular weight micelles, known for instances as detergents, but it is also an appropriate measure characterizing the stability of polymeric micelles. To avoid a possible misunderstanding, the term critical association concentration (cac) was employed for the polymeric micelle. Pyrene was used as a fluorescence probe, which partitioned preferably into the hydrophobic microdomain, i.e., the PLA-core of the micelle and caused changes in the photophysical properties. (*18*)

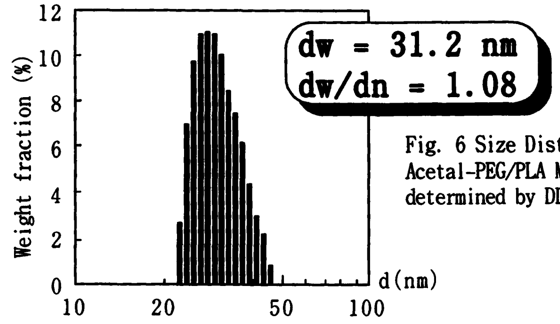

Fig. 6 Size Distribution of Acetal-PEG/PLA Micelle determined by DLS

The mean value of the cac based on the changes in the total fluorescence, the red shift of the pyrene excitation spectrum and the change in the I/III band intensity ratio of pyrene was determined to be 2 mg L^{-1} for acetal-PEG/PLA(52/56). On the other hand, the mean value of acetal-PEG/PLA(91/51) was 12 mg L^{-1}, indicating the difference in stability of acetal-PEG/PLA by the PEG segment length. These phenomena agreed well with the previously reported data. [i.e., 350 mg L^{-1} for PEG/PLA(18/9) (*19*); 35 mg L^{-1} for PEG/PLA(20/9) (*13*)] Thus, the very low cac indicates that the polymeric micelle composed of acetal-PEG/PLA(52/56) is very stable in aqueous media as well as PEG/polystyrene polymeric micelles in water(cf. the cac of PEG/polystyrene was 1 - 4 mg L^{-1}. (*20*))

Conversion of the Acetal to Aldehyde: The conversion of the diethoxy end group into the aldehyde end group was conducted after the micelle formation. After the acetal-PEG/PLA micelle was prepared in aqueous media, the media was adjusted to pH = 2 with hydrochloric acid. From the ^{1}H NMR analysis, the extent of the conversion to the aldehyde was estimated to be 90% (Figure 3b).

It should be noted that no cleavage reaction of the PLA unit took place, indicating the exclusion of aqueous media from the core of the micelle. After the transformation of the end groups, it was confirmed that no change in the micelle diameter took place.

To verify that the surface aldehyde groups can be utilized for modification reactions, conjugation reactions with model compounds were employed and monitored by means of HPLC. As shown in Figure 7, the UV absorption of the micelles after the reaction with benzoic hydrazide significantly increased, retaining the elution at void volume. It should be noted that no remarkable increase in UV absorption observed in the HPLC pattern when the acetal-PEG/PLA micelle was treated with benzoic hydrazide under the same condition as the aldehyde-micelle. The facts indicated the effective conjugation of the aldehyde-micelle with the hydrazide, thus maintaining the micelle structure.

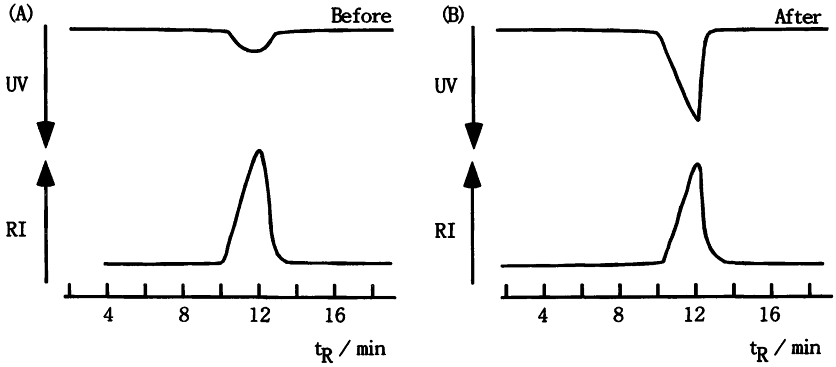

Figure 7. GPC Profiles of Ald-Micelle Before (A) and After (B) the Reaction with Benzoic Hydrazide

Stabilization of Polymeric Micelle: As stated above, a fairly stable and almost complete spherical polymeric micelle with ca. a 30 nm diameter was obtained by using the PEG/PLA copolymer. The physical coagulation force is one of the important factors to keep the core-shell structure. For utilization of polymeric micelle as a vehicle for drug delivery system, the association through physical force may not be enough for the stabilization of drugs in polymeric micelles, because such polymeric micelle drug must be exposed to a blood stream, where the micelle must be diluted to the concentration lower than the cac. Thus, chemical stabilization of the hydrophobic core in the polymeric micelle was examined.

For the core stabilization, the polymerization of the methacryloyl group at the PLA chain end was carried out. After AIBN was incorporated into the micelle core, the micelle solution was heated to 60 °C.

Figure 8 shows size distribution patterns of the methacryloyl-ended block copolymer before and after the polymerization. Before the polymerization, the size and polydispersity factor were almost the same as the MeO-PEG/PLA-OH and

Downloaded by NORTH CAROLINA STATE UNIV on October 31, 2012 | http://pubs.acs.org
Publication Date: September 24, 1998 | doi: 10.1021/bk-1998-0709.ch007

Downloaded by NORTH CAROLINA STATE UNIV on October 31, 2012 | http://pubs.acs.org
Publication Date: September 24, 1998 | doi: 10.1021/bk-1998-0709.ch007

Acetal-block polymers. After the polymerization reaction, the size and shape of the micelle were unchanged, though small amounts of large particles around 100 nm were observed, which was considered to be secondary aggregates of the spherical micelles.

To evaluate the stability of the micelle before and after the reaction, SDS treatments of the micelle solution were carried out, *viz.*, the polymeric micelle thus obtained was treated with the same volume of sodium dodecylsulfonate (SDS) solution (20 g L^{-1}) and stirred for 1 d at rt. After the treatment, the DLS measurements were carried out. As can be seen in the same figure, the polymeric micelle before the polymerization reaction completely disappeared after the SDS treatment, while one after the polymerization reaction maintained its spherical shape even after the SDS treatment though the size of the micelle increased ca. 40 % in diameter. It should be noted that the total intensity of the particles after the SDS treatment was almost the same as the initial value, indicating almost all particles remained without shape change. The increase in the polymerized micelle after the SDS treatment was probably due to the solubilization of SDS in the micelle. These results showed that an extremely stable polymeric micelle with a 30 nm diameter can be prepared by the polymerization of the end methacrylate group in the micelle core using a hydrophobic radical initiator. This core stabilizations were also carried out using CHO-PEG/PLA-methacryloyl micelle using chemical polymerizations in the presence of AIBN as well as photopolymerization in the presence of BME in the core.

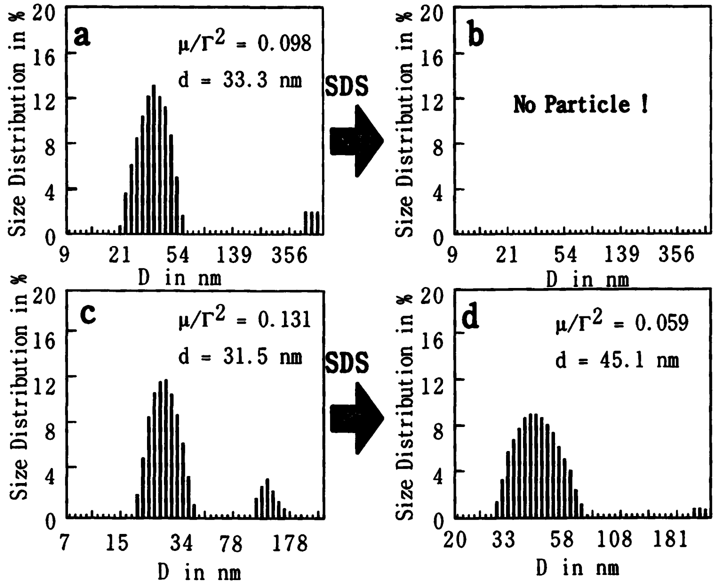

Figure 8. Size Distribution of MeO-PEG/PLA-COC(CH_3)=CH_2 Micelles (a) before Polymerization; (b) SDS Treatment before Polymerization; (c) after Polymerization; (d) SDS Treatment after Polymerization

On the basis of these results, it is concluded the Acetal-PEG/PLA shows completely spherical core-shell type polymeric micelle with acetal groups on the surface which can be converted to aldehyde groups by the acid treatment. Size of the micelle thus prepared was 20 - 40 nm in diameter, which is suitable to exclude RES when used as drug carrier. Core of the reactive polymeric micelle can be stabilized by polymerization of the end group of PLA segment. The core-polymerized micelle was extremely stable in aqueous media. Therefore, reactive polymeric micelle thus prepared can be promising as materials for controlled drug release.

Acknowledgments: The authors would like to express their sincere appreciation to *Professor M. Kato, Dr. C. Scholz, Messrs. M. Iijima and T. Okada,* for carrying out a part of this study. A part of this study was supported by a Grant-in-Aid for Scientific Research on Priority Areas of "New Polymers and Their Nano-Organized Systems", (No. 08246249), The Ministry of Education, Science, Sports and Culture, Japan.

References

1. a)Kataoka, K. *"Targetable Polymeric Drugs"*, Chapter 4 in *"Controlled Drug Delivery: The Next Generation"*, (Ed. K. Park) American Chemical Society, Washington, D.C. **1996**; b)Kataoka, K *J. Macromol. Sci.-Pure Appl. Chem.* **1994**, A31, 1759; c) Yokoyama, M.; Okano, T.; Sakurai, Y.; Kataoka, K. *J. Controlled Rel.* **1994**, 32, 269
2. Ehrlich, P. *"Collected Studies on Immunity"* John Wiley: New York, N.Y. **1906**, 2
3. Ringsdorf, H. *J. Polym. Sci. Symp.* **1975**, 51, 135
4. a)Kwon G. S.; Kataoka, K. *Adv. Drug Delivery Reviews* **1995**, 16, 295; b) Yokoyama, M.; Okano, T.; Sakurai, Y.; Ekimoto, H.; Shibazaki, C.; Kataoka, K. *Cancer Res.* **1991**, 51, 3229
5. a)Zalipsky, S. Bioconjugate Chem. **1993**, 4, 296; b) Lee, R. J.; Low, P. S. *J. Biol. Chem.* **1994**, 269 (5), 3198
6. Kataoka, K.; Kwon, G. S.; Yokoyama, M.; Okano, T.; Sakurai. Y. *J. Controlled Release* **1993**, 24, 119
7. a)Yokoyama, M.; Miyauchi, M.; Yamada, N.; Okano, T.; Sakurai, Y.; Kataoka, K.; Inoue, S. *J. Controlled Rel.* **1990**, 11, 269; b) Yokoyama, M.; Miyauchi, M.; Yamada, N.; Okano, T.; Sakurai, Y.; Kataoka, K.; Inoue, S. *Cancer Res.* **1990**, 50, 1693
8. a) Tuzar, Z.; Kratochvil, P. Adv. *Colloid. Interface Sci.* **1976**, 6, 201; b) Jeon, S. J.; Lee, J. H.; Andrade, J. D.; De Genneus, P. G. *J. Coll. Interface Sci.* **1991**, 142, 149; c) Kjellander, R.; Florin, E. *J. Chem. Soc. Faraday Trans. I.* **1981**, 77, 2053; d) Grainger, D. W.; Nojiri, C.; Okano, T.; Kim, S. W. *J. Biomed. Mater. Res.* **1989**, 23, 979; e) Bergström, K.; Österberg, E.; Holmberg, K.; Hoffman, A. S.; Schuman, T. P.; Kozlowski, A.; Harris, J. M. *J. Biomater. Sci. Polym. Edn.* **1994,** 6, 122; f) Lee, J. H.; Kopecekova, P.; Kopecek, J.; Andrade, J. D. *Biomaterials* **1990**, 11, 455; g) Desai, N. P.; Hubbel, J. A. *J. Biomed. Mater. Res.* **1991**, 25, 829

Downloaded by NORTH CAROLINA STATE UNIV on October 31, 2012 | http://pubs.acs.org
Publication Date: September 24, 1998 | doi: 10.1021/bk-1998-0709.ch007

9.a) Brinkman, E.; Poot, A.; van der Does, L.; Bantjes, A. *Biomaterials* **1990**, 11, 200; b)Desai, N. P.; Hubbel, J. A. *Biomaterials* **1990**, 12, 144; c) Akizawa, T.; Kino, K.; Koshikawa, S.; Ikada, Y.; Kishida, A.; Yamashita, M.; Imamura, K. *Trans. Am. Soc. Artific. Internal Organs* **1989**, 35, 333; d) Kopecekova, P.; Kopecek, J.; Andrade, J. D. *New Polymeric Mater.* **1990**, 1, 2891

10. Perrin, D. D.; Armarego, W. L. F.; Perrin, D. R. *"Purification of Laboratory Chemicals"*, Pergamon Press, Oxford, **1980**

11. Scott, N. D.; Walker, J. F.; Hansley, V. L. *J. Am. Chem. Soc.* **1936**, 58. 2442

12. a) Kim, Y. J.; Nagasaki, Y.; Kataoka, K.; Kato, M.; Yokoyama, M.; Okano, T.; Sakurai, Y. *Polym. Bull.* **1994**, 33, 1. b) Nagasaki, Y.; Iijima, M.; Kato, M.; Kataoka, K. *Bioconjugate Chem., Tech. Note.* **1995**, 6, 702. c) Cammas, S.; Nagasaki, Y.; Kataoka, K.; *Bioconjugate Chem., Tech. Note.* **1995**, 6, 224. d) Nagasaki, Y.; Kutsuna, T.; Iijima, M.; Kato, M.; Kataoka, K.; Kitano, S.; Kadoma, Y. *Bioconjugate Chem., Tech. Note.* **1995**, 6, 231.

13. Zareie, H. M.; Kaitian, X.; Piskin, E. *Coll. Sur.*, A, **1996**, 112, 19.

14. Hagan, S. A.; Coombes, A. G. A.; Garnett, M. C.; Dunn, S. E.; Davies, M. C.; Illum, L.; Davis, S. S.; Harding, S. E.; Purkiss, S.; Gellert, P. R. *Langmuir*, **1996**, 12, 2153

15. Bazile, D.; Prud'homme, C.; Bassoullet, M.-T.; Marlard, M.; Spenlehauer, G.; Veillard, M. J. Pharmaceu. Sci., **1995**, 84, 493

16. Kwon, G. S.; Naito, M.; Kataoka, K.; Yokoyama, M.; Sakurai, Y.; Okano, T. Coll. Surf. B: *Biointerfaces* **1994**, 2, 429

17. Kwon, G. S.; Naito, M.; Yokoyama, M.; Okano, T.; Sakurai, Y.; Kataoka, K. *Langmuir* **1993**, 9, 945

18. a) Dowling, K. C.; Thomas, J. K. Macromolecules **1990**, 23, 1059: b) Zhao, C.; Winnik, M. A.; Riess, G.; Croucher, M. D. *Langmuir* **1990**, 6, 514

19. Tanodekaew, S.; Pannu, R.; Heartley, F.; Attwood, D.; Booth, C. *Macromol. Chem. Phys.*, **1997**, 198, 927.

20. Zao, C.; Winnik, M. A. *Langmuir*, **1990**, 6, 514

Downloaded by NORTH CAROLINA STATE UNIV on October 31, 2012 | http://pubs.acs.org
Publication Date: September 24, 1998 | doi: 10.1021/bk-1998-0709.ch007

Downloaded by MONASH UNIV on October 31, 2012 | http://pubs.acs.org
Publication Date: September 24, 1998 | doi: 10.1021/bk-1998-0709.ch008

Chapter 8

Branched Polymeric Micelles: Synthesis and Encapsulation

S. Anna Jiang, Hongbo Liu, and Kathryn E. Uhrich[1]

Department of Chemistry, Rutgers University, Piscataway, NJ 08855–0939

Highly branched polymers with hydrophobic interiors and hydrophilic exteriors have been synthesized. These polymers that mimic micellar structures are hence referred to as unipolymeric micelles. Photospectroscopic methods have been employed to investigate the microenvironment of these polymers. The fluorescence quenching of the chemical probe, naphthalene, in the presence of these polymers, as well as encapsulation of the model drug, lidocaine, showed that the polymeric micelles encapsulate small hydrophobic organic molecules. By changing the hydrophobicity of the interior relative to exterior region, several property-structure relationships (e.g., water-solubility) have been established.

The efficacy of pharmaceuticals is strongly affected by the way they are administered. There are many problems associated with the introduction of free drugs into the bloodstream. First, many drugs are deactivated when delivered in the free form. Although deactivation mechanisms can be quite complicated, interactions between drugs and components in the bloodstream (e.g., proteins and enzymes as well as water) are the most common factors (1). Second, free drugs frequently have short circulation times (i.e., minutes) and are quickly excreted from the body (2). Third, free drugs are often distributed randomly among organs and tissues. The inability of most drugs to discriminate between normal and diseased cells contributes to drug toxicity, especially for anti-tumor drugs. Another problem associated with drug delivery is water solubility; most drugs are too hydrophobic to be water-soluble (2). This water-insolubility limits both the applicable administration methods as well as dosage levels. Over the years, drug delivery systems have been devised to overcome all or some of the problems described above such as enhancing solubility and efficacy, prolonging circulation time, achieving controlled release and site-specific delivery. Delivery systems range from the use of starch as an additive to form tablets, to the use of capsules to achieve slow release, to more complex devices consisting of hydrogels, polymers, liposomes and various surfactants.

---

[1] Corresponding author.

In Tailored Polymeric Materials for Controlled Delivery Systems; McCulloch, I., et al.;
ACS Symposium Series; American Chemical Society: Washington, DC, 1998.

The use of surfactants is one of the promising answers for drug delivery (3). The possibilities and advantages of polymeric surfactants to be used as drug delivery devices have been reviewed extensively (4) and several successful examples demonstrated (5-14). For example, micelles have a hydrophobic core that can solubilize hydrophobic materials, such as drugs, as well as a hydrophilic outer shell that makes the assembly water-soluble. Polymeric surfactants have been favored over smaller organic surfactants because they usually have much lower critical micelle concentration, or cmc, (~ 10^{-5} M) compared to smaller organic surfactants (~ 10^{-2} M). Site-specific drug delivery has been shown possible by controlling the size and/or the surface properties of the polymeric surfactants (11-14). However, the thermodynamic instability that is both concentration and temperature dependent of these conventional micelles limits their use in drug delivery. In drug delivery, the reversal of micelle to surfactant causes a flux of drug concentration which can cause serious toxicity problems.

One way to overcome the thermodynamic instability of conventional micelles is to construct an assembly that topologically resembles the micelle architecture but with all components covalenly bound together. Structures with the above topology and properties have been termed unimolecular micelles (15-18). These compounds are polymers consisting of both hydrophobic (usually aliphatic) and hydrophilic (ionic or non-ionic) components (16-19). Most examples of such materials are dendrimers with hydrophilic end functional groups based on amine or carboxylate groups (16-18). In a few systems, guest molecules have been entrapped within the structures (19-22). Meijer et al. demonstrated that different entrapped guest molecules could be liberated by selective chemical removal of the outer shell components (23). In general, unimolecular micelles showed either dynamic encapsulation (Newkome's work) or physical entrapment (Meijer's work) of guest molecules depending on the steric compactness of the structures (23). The guest molecules either escape from the unimolecular micelles too soon (in the case of dynamic encapsulation) or do not diffuse at all (in the case of physical entrapment) unless the micellar structures are chemically disrupted.

We have synthesized a series of polymers with topological and functional features similar to unimolecular micelles. The synthetic scheme is shown in Scheme 1. In contrast to the previously described unimolecular micelles, our systems are designed to be biodegradable and biocompatible for use in medical applications. Our polymeric micelles consist of biocompatible elements, such as mucic acid (a sugar), alkyl chains (fatty acids like) and polyethylene glycols (PEG), such that the resulting polymers will also be biocompatible.

Downloaded by MONASH UNIV on October 31, 2012 | http://pubs.acs.org
Publication Date: September 24, 1998 | doi: 10.1021/bk-1998-0709.ch008

Experimental

Materials. Polyethylene glycols were obtained from Shearwater Polymers, dipalmitoyl-phosphatidylcholine was obtained from Avanti Polar Lipids, all other chemicals were obtained from Aldrich and used as received. Methylene chloride, tetrahydrofuran, chloroform and diethyl ether were obtained from Aldrich (spectroscopic grade) and used without further purification.

Methods. ^{1}H NMR and ^{13}C NMR spectra were recorded on a Varian 200 MHz spectrometer. Samples (5 ~ 10 mg/ml) were dissolved in either $CDCl_3$ or DMSO-d_6 with the solvent used as an internal reference. IR spectroscopy was performed on a Mattson Series spectrophotometer by solvent-casting samples onto a KBr pellet. Mass spectrometry analyses were performed by Washington University, St. Louis. Elemental analyses were provided by QTI, Inc.

Downloaded by MONASH UNIV on October 31, 2012 | http://pubs.acs.org
Publication Date: September 24, 1998 | doi: 10.1021/bk-1998-0709.ch008

Scheme 1.

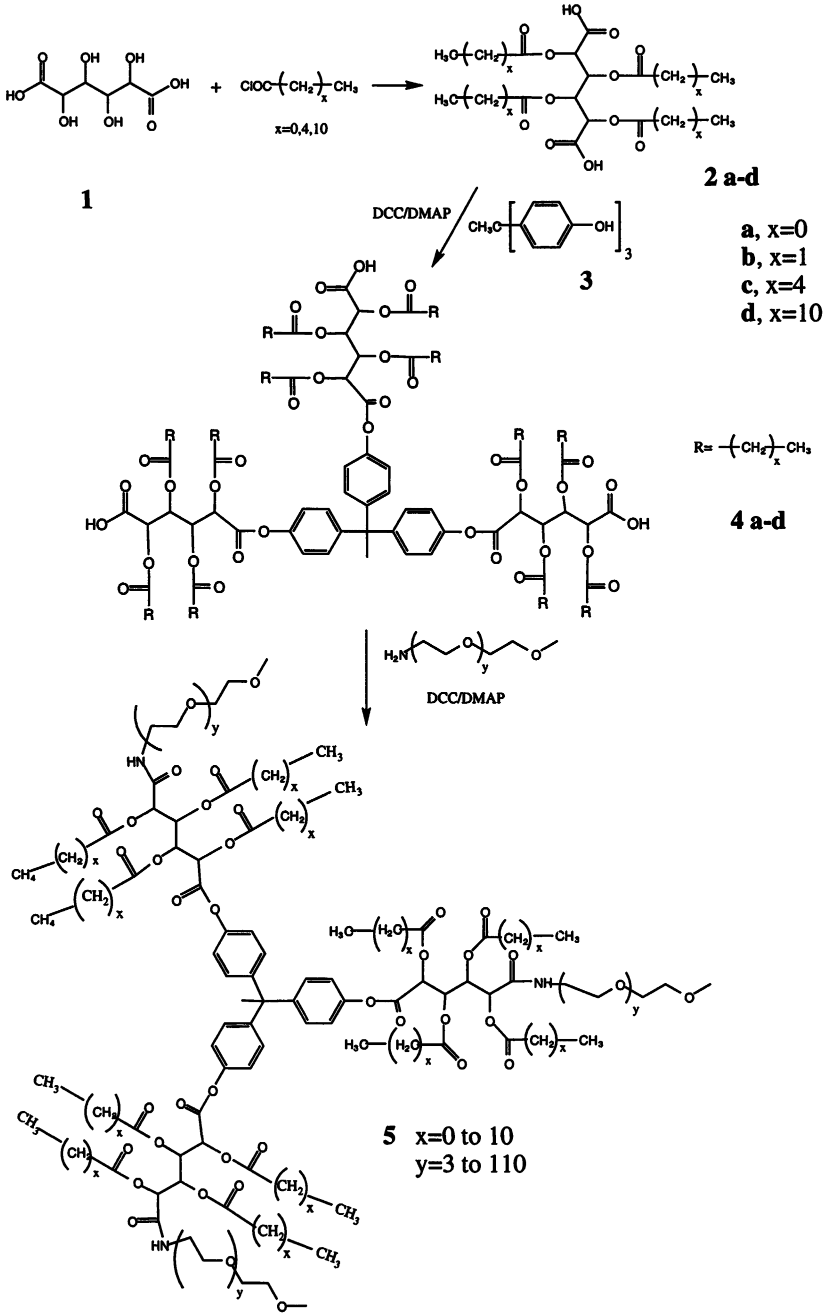
1
x=0,4,10
2 a-d
DCC/DMAP
3
a, x=0
b, x=1
c, x=4
d, x=10
R= $-(CH_2)_x-CH_3$
4 a-d
DCC/DMAP
5 x=0 to 10
y=3 to 110

Molecular weights were determined on a Perkin Elmer Series 200 LC system equipped with PL-Gel column (5 µm, mixed bed), Series 200 refractive index detector, Series 200 LC pump and ISS 200 autosampler. A digital Celebris 466 computer was used to automate the analysis via PE Nelson 900 interface and PE Nelson 600 Link box. PE Turbochrom 4 software was used for data collection and processing. Tetrahydrofuran (THF) was used as eluent for analysis at a flow rate of 0.5 ml/min. Sample (~ 5 mg/ml) was dissolved into THF and filtered using 0.45 µm syringe filter prior to column injection. Molecular weights were calibrated relative to narrow molecular weight polystyrene standards (Polysciences, Inc.).

Thermal analysis was determined on a Perkin Elmer system consisting of Pyris 1 DSC and TGA7 analyzers with TAC 7/7 instrument controllers. PE Pyris 1 and TGA7 software was used for data collection and processing on a digital Venturis 5100 computer. For DSC, ~ 5 mg samples were heated under dry nitrogen gas. Data was collected at a heating and cooling rate of 10°C/min after a two cycle minimum. For TGA, ~ 10 mg of sample was heated under dry nitrogen gas. Data was collected at a heating rate of 20 °C/min. Decomposition temperatures were defined as the onset of decomposition.

Downloaded by MONASH UNIV on October 31, 2012 | http://pubs.acs.org
Publication Date: September 24, 1998 | doi: 10.1021/bk-1998-0709.ch008

Preparation of mucic acid derivatives. For all mucic acid derivatives, similar synthetic procedures were used. The synthesis of MA(hex) (**2c**) is used as a typical example. To a neat mixture of MA (4.2 g, 20 mmol) and hexanonyl chloride (18 ml, 200 mmol) was added $ZnCl_2$ (0.28 g, 2.0 mmol). The reaction mixture was heated to reflux temperature for 3 h. After cooling, diethyl ether (20 ml) was added to the reaction mixture and the solution poured onto ice chips (~ 100 g) with stirring. Additional diethyl ether (80 ml) was added to the mixture and stirred for another 30 min. The ether portion was washed with water to neutral pH, dried over anhydrous Na_2SO_4 and evaporated to dryness. The crude product was purified by recrystallization from diethyl ether:CH_2Cl_2 (1:1), collected by vacuum filtration, washed with ice cold CH_2Cl_2 and dried at 105°C (12 H) to constant weight.

MA(hex), 2c. Yield: 68% (white solid). ^1H NMR (DMSO): δ 5.57 (s, 2H, CH), 4.96 (s, 2H, CH), 2.37 (t, 4H, CH_2), 2.27 (t, 4H, CH_2), 1.50 (m, 8H, CH_2), 1.26 (m, 16H, CH_2), 0.86 (t, 12H, CH_3). ^{13}C NMR ($CDCl_3$): δ 172.7, 172.0 (C=O), 68.7, 67.7 (CH), 33.5, 31.0, 24.2, 22.2 (CH_2), 13.8 (CH_3). IR (KBr, cm^{-1}): 1751, 1731 (C=O), 1251 (C-O). Anal. Calc: C, 59.78; H, 8.36. Found: C, 59.33; H, 8.17.

Preparation of core molecules. The procedure for core(hex) (**4 a-d**) is described as a typical example. MA(hex) (**2 a-d**) (3.7 g, 6.0 mmol) and 1,1,1-trishydroxyphenyl ethane (0.51 g, 1.7 mmol) were dissolved in anhydrous ethyl ether (150 ml). To the reaction mixture, a solution of dicyclohexylcarbodiimide (DCC) (1.2 g, 6.0 mmol) and 4-dimethylaminopyridine (DMAP) (0.74 g, 6.0 mmol) in 25 ml CH_2Cl_2 was added dropwise. After 15 min, the DCC side-product (dicyclohexylurea) was removed by suction filtration. The filtrate was washed with 20 ml portions of 0.1 N HCl solution (2 x), brine (4 x), dried over anhydrous Na_2SO_4 and evaporated to dryness. The crude product was purified by flash chromatography using ethyl ether:methanol:acetic acid (90:5:5) as eluent. 1.1 g (33% yield) of white solid was obtained.

Core(hex), 4c. Yield: 36% (white solid). ^{1}H NMR ($CDCl_3$): δ 7.00 (m, 12H, ArH), 5.68 (t, 6H, CH), 5.20 (q, 6H, CH), 2.44 (t, 12H, CH_2), 2.30 (t, 12H, CH_2), 2.10 (s, 3H, CH_3), 1.61 (m, 24H, CH_2), 1.31 (br, 48H, CH_2), 0.87 (br, 36H, CH_3). ^{13}C NMR ($CDCl_3$): δ 172.9, 171.9, 165.5 (C=O), 148.3, 146.4, 129.6, 120.6 (Ar-C), 69.5, 68.7, 67.8, 67.6 (CH), 51.6 (CH_3), 33.6, 31.0, 24.2, 22.2 (CH_2), 13.8 (CH_3). IR (KBr, cm^{-1}): 2931, 2873 (C-H), 1734 (C=O) Anal. Calc: C, 64.12; H, 7.93. Found: C, 64.73; H, 8.21. MS (LRFAB): 2060 (theor. 2060).

Core(hex)-NH-PEG5000, 5c. Yield: 17% (white solid). ^{1}H NMR ($CDCl_3$): δ 7.00 (ArH), 3.62 (CH_2), 1.28 (CH_2), 0.859 (CH_3). IR (KBr, cm^{-1}): 1734 (C=O), 1666(N-C=O), 1554(C-N), 1118(C-O) T_m = 61.0°C, T_d = 410°C. M_n: 17,800; PDI, 1.04.

Downloaded by MONASH UNIV on October 31, 2012 | http://pubs.acs.org
Publication Date: September 24, 1998 | doi: 10.1021/bk-1998-0709.ch008

Results and Discussion

Synthesis. The four hydroxyl groups of mucic acid are acylated by acyl chlorides of various alkyl chains (i.e. propanoyl, hexanoyl and lauroyl). The products, MA derivatives were purified by crystallization in 70% yield. THPE was chosen as the central point because it's trifunctional, allows for easy measurement of spectroscopic identification and may also enhance encapsulation. The MA derivatives (**2**) were coupled to THPE using DCC and DMAP in excess. The addition sequence of the reagents and the ratio of starting materials were crucial to minimize the formation of unreactive anhydride and/or oligomers, i.e., the mixture of DCC and DMAP was added dropwise separations were achieved by flash chromatography.

The complexity in the ^{1}H NMR spectra, multiplets in the region of 5.7 to 5.9 and 5.2 to 5.4 (in $CDCl_3$) for the methine protons of the mucic acid component of these core molecules indicated the complex microenvironment of the structure (Figure 1). This could be explained by the unsymmetrical interactions between various components in the core molecules. The multiplets were strongly solvent dependent (between $CDCl_3$ and DMSO-d_6) suggesting that they were caused by several conformations.

The final polymer structures were generated by attachment of the H_2N-PEG-m to the core derivatives using DCC/DMAP. The polymers were purified by repeated precipitations to remove the unreacted PEG and other impurities. PEG chains not only give rise to the water-solubility of the final polymers, but have also been reported to afford the long circulation time of many other polymer systems *in vivo* (24-27). Additionally, PEG has proven to make devices coated with PEG undetectable by biological systems.

By varying the length of alkyl and ethylene oxide chains, a series of polymers with different hydrophobic/hydrophilic ratios have been synthesized. The polymers with long PEG chains on the surface (or shell), like core(hex)(PEG2000) and core(hex)(PEG5000) (**5**) (where, x=4, y=110) were very soluble in water and organic solvents such as CH_2Cl_2, DMF, DMSO, MeOH and aromatic hydrocarbons, but insoluble in diethyl ether or hexane. In contrast, polymers with shorter PEG chains, such as Core(hex)(TEG) where TEG is triethylene glycol, were sparingly soluble in water but soluble in organic solvents such as CH_2Cl_2, DMF and aromatic hydrocarbons. Predictably, the water-solubility of the polymeric micelles are strongly dependent on the length of the terminal PEG chains. Because the core(hex)-PEG2000 has similar solubility characteristics to core(hex)(PEG5000), the PEG2000 chain is long enough to form an encompassing and efficient hydrophilic shell to make the polymeric micelle highly water-soluble.

Downloaded by MONASH UNIV on October 31, 2012 | http://pubs.acs.org
Publication Date: September 24, 1998 | doi: 10.1021/bk-1998-0709.ch008

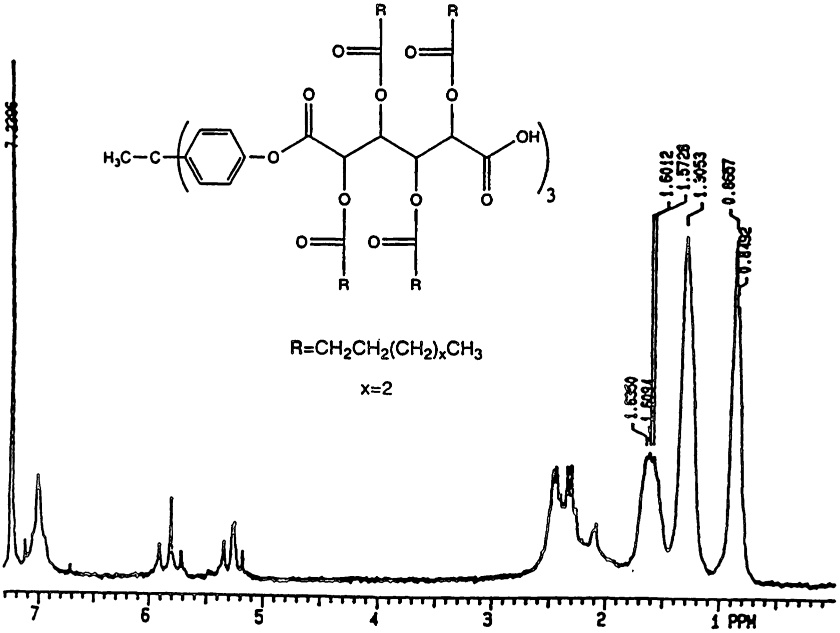

Figure 1. ^{1}H NMR spectrum of the core(hex) compound.

Downloaded by MONASH UNIV on October 31, 2012 | http://pubs.acs.org
Publication Date: September 24, 1998 | doi: 10.1021/bk-1998-0709.ch008

For the encapsulation studies, core(hex)PEG5000 was used. The encapsulation of small hydrophobic organic molecules such as naphthalene was evaluated using fluorescence spectroscopy. A decrease in the fluorescence intensity of naphthalene in the presence of **5** was proportional to increasing polymer concentrations. In contrast, PEG alone did not affect the fluorescence of naphthalene where a model compound, 1,1,1-tris(acetoxyphenyl)ethane, caused a decrease in the fluorescence intensity of naphthalene in a fashion similar to the polymeric micelle Therefore, we attribute our observations to the strong interaction between naphthalene and the aryl moieties within the polymeric interior.

From the reduction of naphthalene fluorescence intensity in the presence of polymer, the amount of naphthalene incorporated into the polymer can be calculated. The number of naphthalene molecules encapsulated by one polymer molecule (encapsulation number) was estimated as 0.7.

In a similar experiment, lidocaine, a hydrophobic drug exhibiting anesthetic properties, was evaluated using HPLC. The concentration of solutions of lidocaine and polymer **5** was quantitated by HPLC to give an encapsulation number of 0.8 (about 1% in weight), thus agreeing with the fluorescence studies.

A preliminary *in vitro* degradation study of polymer **5** in phosphate buffer solution at 37.5^{0}C was performed at neutral pH. No change in appearance (the solution remained clear) or chemical composition was detected by IR and NMR within four months.

Conclusions

Several polymers were prepared with molecular weights ranging from 2500 to 18 ,000. Fluorescence studies suggest that the polymers have micelle-like behavior as they can encapsulate hydrophobic guest molecules such as naphthalene and lidocaine. The excellent water-solubility of these polymers make intravenous injection and oral administration possible. Future studies will be focused on the effect of the core and surface functionality on the degradation, biocompatibility, and drug release rates of the polymeric micelles.

Acknowledgments

The authors are grateful to Johnson & Johnson and Hoechst Celanese for financial support.

Literature Cited

(1) Yokoyama, M.; Miyauchi, M.; Yamada, N.; Okano, T.; Sakurai, Y.; Kataoka, K.; Inoue, S. *Cancer Res.* **1990**, *50*, 1693-1700.

(2) Yokoyama, M. G.; Okano, T.; Sakurai, Y.; Kataoka, K. In *Polymeric Drugs and Administration*; Ottenbrite, R. M., Ed; ACS Symposium Series 545, 1992, pp126-134.

(3) Lawrence, M. J. *Chem. Soc. Rev.* **1994**, *23*, 417-424.

(4) Kataoka, K.; Yokoyama, M.; Okano, T.; Sakurai, Y. *J. Controlled Rel.* **1993**, *24*, 119-132.

(5) Gref, R.; Peracchia, M.T.; Trubetskov, V. Z.; Torchilin, V.; Langer, R. *Science* **1994**, *263*, 1600-1603.

(6) Kwon, G. S.; Naito, M.; Yokoyama, M.; Okano, T.; Sakurai, Y.; Kataoka, K. *Langmuir* **1993**, *9*, 945-949.

(7) Kwon, G. S.; Naito, M.; Kataoka, K.; Yokoyama, M.; Sakurai, Y.; Okano, T. *Colloids and Surfaces* **1994**, *2*, 429-434.

(8) Hagan, S.A.; Garnett, M.C.; Dunn, S.E.; Davies, M.C.; Illum, L.; Davis, S.S. *Langmuir* **1996**, *12*, 2153-2161.

(9) Yokoyama, M.; Miyauchi, M.; Yamada, N.; Okano, T.; Sakurai, Y.; Kataoka, K.; Inoue, S. *J. Controlled Rel.* **1990**, *11*, 269-278.

(10) Kwon, G. S.; Naito, M.; Yokoyama, M.; Okano, T.; Sakurai, Y.; Kataoka, K. *Pharm. Res.* **1995**, *12*, 192-195.

(11) Dunn, S.E.; Davis, S.S.; Davies, M.C.; Illum, L. *Pharm. Res.* **1994**, *11*, 1016-1021.

(12) Kabanov, A. V.; Batrakova, E. V.; Melik-Nubarov, N. S.; Fedoseev, N. A.; Dorodnich, T. Y.; Alakhov, V. Y.; Chekhonin, V. P.; Nazarova, I. R.; Kabanov, V. A. *J. Controlled Rel.* **1992**, *22*, 141-158.

(13) Kabanov, A. V.; Chekhonin, V. P.; Alakhov, V. Y.; Batrakova, E. V.; Lebedev, A. S.; Melik-Nubarov, N. S.; Arzhakov, S. A.; Levashov, A. V.; Morozov, G. V.; Severin, E. S.; V.A. Kabanov, V. A. *FEBS Lett.* **1989**, *258*, 343-345.

(14) Yokoyama, M.; Okano, T.; Sakurai, Y.; Kataoka, K.; Shimizu, K.; Okamoto, K.; Machida, M.; Fukushima, S. *Trans. Soc Biomaterials* **1997**, *20*, 142.

(15) Tomalia, D. A.; Berry, V.; Hall, M.; Hedstrand, D. M. *Macromolecules* **1987**, *20*, 1164-1167.

(16) Kim, Y. H.; Webster, O. W. *J. Am. Chem . Soc.* **1990**, *112*, 4592-4593.

(17) Newkome, G. R.; Moorefield, C. N.; Baker, G. R.; Johnson, A. L.; Behera, R. *Angew. Chem. Int. Ed. Engl.* **1991**, *30*, 1176-1178.

(18) Chichi, A.; Nose, T. *Polymer* **1996**, *37*, 5889-5896.

(19) Stevelmans, S.; van Hest, J. C. M.; Jansen, J. F. G. A.; van Boxtel, D. A. F. J.; de Brabander-van den Berg, E. M. M.; Meiyer, E. W. *J. Am. Chem. Soc.* **1996**, *118*, 7398-7399.

(20) Newkome, G. R.; Moorefield, C. N.; Baker, G. R.; Saunders, M. J.; Grossman, S. H. *Angew. Chem. Int. Ed. Engl.* **1991**, *30*, 1178-1180.

(21) Jansen, J. F. G. A.; de Brabander-van den Berg, E. M. M.; Meijer, E. W. *Science* **1994**, *266*, 1226-1229.

(22) Jansen, J. F. G. A.; Meijer, E. W. *Macromol. Symp.* **1996**, *102*, 27-33.

(23) Jansen, J. F. G. A.; Meijer, E. W. *J. Am. Chem. Soc.* **1995**, *117*, 4417-4418

(24) Nucci, M. L.; Shorr, R.; Abuchoswki, A. *Adv. Drug Delivery Rev.* **1991**, *6*, 133-151.

(25) Delgrado, C.; Francis, G. E.; Fisher, D. *Crit. Rev. Ther. Drug Carrier Syst.* **1992**, *9*, 249-304.

(26) Veronese, F. M.; Caliceti, P.; Schiavon, O.; Sartore, L. In *Poly(Ethylene Glycol) Chemistry: Biotechnical and Biomedical Applications*; Harris, J. M., Ed; Plenum, New York, 1992; pp127-137.

(27) Katre, N. V. *Adv. Drug Delivery Rev.* **1993**, *10* , 91-114.

Downloaded by MONASH UNIV on October 31, 2012 | http://pubs.acs.org
Publication Date: September 24, 1998 | doi: 10.1021/bk-1998-0709.ch008

Downloaded by UNIV OF GUELPH LIBRARY on October 31, 2012 | http://pubs.acs.org
Publication Date: September 24, 1998 | doi: 10.1021/bk-1998-0709.ch009

Chapter 9

Injectable Absorbable Gel-Formers for the Controlled Release of Bioactive Agents–Drugs

Shalaby W. Shalaby

R&D Laboratories, Poly-Med, Inc., Westinghouse Road, Pendleton, SC 29625

The concept of hydrogel-forming, self-solvating absorbable polyester copolymers and typical examples are noted. Application of representative gel formulations for the controlled release of a number of bioactive agents, including antibiotics, immunosuppressants, and a vaccine are presented. On-going studies and future perspectives on the broad-based applications of this new family of drug carriers are briefly discussed.

Growing interest in developing absorbable pharmaceutical and surgical products which degrade in the biological environment to safe by-products and leave no residual mass at the application site (*1-9*), justified the search for novel, absorbable gels. In a recent disclosure (*10*), novel gel formers were described to be based on absorbable copolymers which, upon hydration, result in hydrogels that are stabilized by pseudo-crosslinks provided by hydrophobic polyester components covalently linked to hydrophilic ones made of pharmaceutically acceptable polymer, such as polyoxyethylene. The polyester component is made of safe monomers, such as p-dioxanone, ϵ-caprolactone, glycolide, lactide, and mixtures thereof. Contrary to a related study (*11*), which describes *in-situ* formation of biodegradable, microporous, solid implants in a living body through coagulation of a solution of a polymer in an organic solvent such as N-methyl-2-pyrrolidine, the new hydrogel formers do not require the use of solvents. Such solvents did include low molecular organic ones that can migrate from the application site and cause damage to living tissue, such as cell dehydration and necrosis. Equally important is the fact that previously known systems are solid implants which can elicit mechanical incompatibility and, hence, patient discomfort as compared with the new compliant, swollen, mechanically compatible hydrogels (*10*). Meanwhile, potential applications of the *in-situ*-forming implants, and the more recent gel-formers, have been described to entail their use for tissue regeneration and release of growth factors (*12*). Depending on the composition of the

In Tailored Polymeric Materials for Controlled Delivery Systems; McCulloch, I., et al.;
ACS Symposium Series; American Chemical Society: Washington, DC, 1998.

gel-formers used in the present study, these absorbable matrices can be used for the controlled release of antibiotics over a period of 1 to 6 weeks (*10*).

The use of absorbable gel-formers may very well lead to some of the most important applications of absorbable polymers in the pharmaceutical and biomedical industries. These would include use of the gel-formers in (1) periodontal application of antibiotics; (2) antibiotics formulations for osteomyelitis; (3) intraocular drug delivery; (4) wound healing and hemostasis; (5) controlling the release of insulin; and (6) controlling the bioavailability of ricin A-chain. These uses are discussed in the following paragraphs.

Downloaded by UNIV OF GUELPH LIBRARY on October 31, 2012 | http://pubs.acs.org
Publication Date: September 24, 1998 | doi: 10.1021/bk-1998-0709.ch009

Explored Application of Gel-Formers in Controlled Release Systems

Periodontal Application. This entails the use of injectable gel-forming formulations for controlled delivery of antibiotics, such as tetracycline or doxycycline, for combating periodontal infections for periods of one to four weeks (*10*).

Antibiotic Formulations for Bone Infection. In a Phase I study of an NIH-SBIR program addressing osteomyelitis, available results indicate that (1) selected gel-formers are capable of controlling the *in vitro* release of gentamicin and vancomycin for at least two weeks; (2) two types of gel-formers can be formulated, with clinically relevant doses of vancomycin, into injectable forms; (3) injection of the vancomycin formulation about the periosteum of the goat tibia for localized drug delivery; and (4) controlled release of the vancomycin formulation is feasible without leading to toxic blood levels.

Injectable Intraocular Delivery Systems. In an SBIR (Phase I) supported by the DoD, the feasibility of using tailored gel-formers to develop an injectable, controlled release system for intraocular delivery of key drugs is being investigated. Available data indicate that (1) injectable gel-formers containing pilocarpine, naproxen, cyclosporin and ganciclovir in clinically relevant doses can be prepared; (2) a continued release in a buffered medium for at least one week can be achieved; and (3) active formulations of the four drugs and a placebo can be readily injected into the vitreous cavity of the rabbit eye without eliciting unacceptable, gross tissue reactions.

Wound Healing and Hemostatic Application. Preliminary results of a study supported by a DoD grant on wound healing and hemostatic agents (using hairless rats and rabbits) indicate that (1) certain gel-forming formulations can be used for the controlled delivery of antibiotics to incisional and burn wounds in hairless rats; (2) incisional wound strength regain in hairless rats can be improved when placebo gel-formers are used; and (3) selected gel-forming formulations can induce hemostasis in a rabbit animal model.

Insulin Controlled Release Systems. Preliminary study on the use of certain gel-formers for the controlled release of insulin demonstrate the feasibility of this concept.

Downloaded by UNIV OF GUELPH LIBRARY on October 31, 2012 | http://pubs.acs.org
Publication Date: September 24, 1998 | doi: 10.1021/bk-1998-0709.ch009

Controlled Release of Ricin A-chain. This has been the subject of a Phase I SBIR program supported by the DoD and available results (*13,14*) on subcutaneously (SC) administered active formulations do verify that (1) gel formulations can be easily prepared and appear suitable for scale-up; (2) one SC formulation is capable of releasing sufficient amounts of ricin A-chain (RAC) to elicit IgG formation at protective levels over a period of 4-6 weeks; (3) one formulation provides persistent protection at least 6 weeks post-immunization; and (4) a correlation can be established between IgG formation and the composition of the polymeric carriers. Available Phase I results suggest that (1) a single-dose, absorbable SC formulation, GF-II, exhibits potentially unique *in vivo* performance as it comprises a microparticulate cation-exchanger; (2) upon comparing commercial RAC solution (RAC-L) with GF-II, the latter elicits a more gradual antibody response that peaks at 10 weeks and it exceeds a fast-decaying, initially higher response to RAC-L; (3) in terms of antibody response, GF-II is associated with higher durability over the 10- to 20-week period; and (4) GF-II elicits a higher response of IgG-2A than RAC-L at 6 weeks.

On-Going Studies—Future Perspective

Preliminary results of on-going studies on the use of selected members of the gel-formers family of copolymers indicate their potential use for accelerating wound healing, in treating burn wounds, and in hemostatic formulations. In this context, it is reasonable to suggest that suitable bioactive agents/drugs can be used in conjunction with the aforementioned systems to modulate their performance through the controlled release of the desired agents required for the corresponding biological events, such as tissue regeneration and hemostasis. Success in treating burn wounds can very well be extrapolated to effective treatment of chronic skin ulcers. Demonstrated feasibility studies on the intraocular administration of gel-forming formulations can open a new area in eye therapy. The use of the gel-formers is likely to find use as sealants in vascular and soft-tissue repair as well as carriers of living cells and growth factors in tissue engineering.

Literature Cited

1. Shalaby, S.W., Chap. 3 in *High Technology Fibers* (Lewin & Preston, Eds.), Dekker, New York, 1985.
2. Shalaby, S.W., in *Encyclopedia of Pharmaceutical Technology* (J.C. Boylan & J. Swarbrick, eds.), Vol. 1, Dekker, New York, 1988, p. 465.
3. Shalaby, S.W., in *Water-Soluble Polymers*, (Shalaby et al., Eds.), Vol. 467, Chapt. 33, ACS Symp. Ser., Amer. Chem. Soc., Washington, DC, 1991a.
4. Shalaby, S.W., *Polym. News*, 16, 238 (1991b).
5. Shalaby, S.W., *J. Appl. Biomater.*, 3, 73 (1992).
6. Shalaby, S.W. (Ed.), *Biomedical Polymers: Designed to Degrade Systems*, Hanser Publ., New York 1994a.
7. Shalaby, S.W. et al, *Polymers of Biological & Biomedical Significance*, Vol. 540, ACS Symp. Ser., Amer. Chem. Soc., Washington 1994b.

8. Shalaby, S.W. et al, Irish Patent (to Kinerton, Ltd.) S-61251 (1994c).
9. Shalaby, S.W. and Shalaby, W.S.-W., *Indian J. Tech.*, 31,464 (1993).
10. Shalaby, S.W., U.S. Patent (to Poly-Med, Inc.) 5,610,052 (1997).
11. Dunn, R.L. et al, U.S. Pat. 4,938,763 (1990).
12. Dunn, R.L. et al, *Polym. Prepr.*, 35(2), 437 (1994).
13. Corbett, J.T. et al, Ninth International Conference on Antiviral Research, Fukusima, Japan, 1996.
14. Corbett, J.T. et al, Ninth International Conference on Antiviral Research, Fukusima, Japan, 1996b.

Downloaded by UNIV OF GUELPH LIBRARY on October 31, 2012 | http://pubs.acs.org
Publication Date: September 24, 1998 | doi: 10.1021/bk-1998-0709.ch009

Chapter 10

Novel Ionogenic Acrylate Copolymer Networks for Sustained Solute Delivery

Robert A. Scott and Nicholas A. Peppas

School of Chemical Engineering, Purdue University, West Lafayette, IN 47907

Downloaded by MONASH UNIV on October 31, 2012 | http://pubs.acs.org
Publication Date: September 24, 1998 | doi: 10.1021/bk-1998-0709.ch010

The present work is concerned with the formulation and evaluation of delivery devices based on highly crosslinked ionogenic acrylates. Loaded materials were prepared by an extremely rapid, solvent-free photopolymerization process. The polymeric delivery matrices examined were copolymers of oligo(ethylene glycol) multiacrylates and acrylic acid (AA). By manipulation of the structure of the crosslinking monomer and of the AA feed ratio in the comonomer-solute mixture, systems possessing a wide variety of delivery characteristics were attained. The novel materials were shown to facilitate sustained release over a period of many hours; the detailed release profiles depended very strongly on the copolymer composition. Polymers were loaded up to 15% solute content, and the delivery characteristics of glassy and of rubbery materials were considered. Additionally, the presence of the ionogenic AA moieties along the polymer backbone allowed for environmental sensitivity and complexation-mediated release under appropriate conditions.

Swollen crosslinked polymeric materials (hydrogels) have been used for more than 25 years as suitable carriers for drug delivery.[1,2] They are desirable for such applications because they are non-toxic and exhibit a three-dimensional structure that can control solute (drug, peptide, or protein) release.[3] The overall release behavior from such gels is a function of the swelling characteristics of the (typically loosely) crosslinked systems. Highly crosslinked systems would obviously provide slow drug release. Yet, such systems are very rarely reported because of their quite brittle behavior. Of particular interest to us are new types of slowly swelling, mechanically stable hydrogels that can be used as carriers in swelling controlled release devices[4] for the delivery of drugs. Such systems can be improved by incorporation of poly(ethylene glycol) (PEG) segments, and physiological sensitivity can be achieved by incorporation of ionizable monomers such as acrylic or methacrylic acid.[5]

The present work is concerned with the formulation and evaluation of delivery devices based on highly crosslinked ionogenic acrylates. These materials, prepared in loaded form by an extremely rapid, solvent-free photopolymerization process, are multiacrylate-acrylic acid copolymers having nominal crosslinking ratios ranging from 60% to 100%. Release rates are therefore substantially lower than those exhibited by typical hydrogel formulations. By manipulation of the structure of the PEG-containing crosslinking monomer and of the acrylic acid (AA) feed composition ratio in the comonomer-solute mixture, systems possessing a wide variety of delivery characteristics are attainable. Additionally, the presence of ionogenic AA moieties along the polymer backbone allows for environmental sensitivity and complexation-mediated release under appropriate conditions.

Experimental

The various monomers used are shown in Figure 1. The diacrylates were diethylene glycol diacrylate (DEGDA, n=2) and tetraethylene glycol diacrylate (PEG200DA, n≈4) (Polysciences, Warrington, PA), and the triacrylates were trimethylolpropane triacrylate (TrMPTrA, Polysciences) and a series of ethoxylated TrMPTrA analogs (Aldrich, Milwaukee, WI). The analogs contained 3 (PEG130TrA), 7 (PEG250TrA), and 14 (PEG450TrA) ethoxy groups per monomeric unit. Tables I and II describe the various compositions considered. The AA feed composition ratio in copolymerizations was varied from 0 - 40 mol%, based on double bonds.

Monomer-drug mixtures were prepared by mixing distilled AA (Aldrich), crosslinking monomer, and proxyphylline (Sigma, St. Louis, MO) in appropriate quantities. A typical formulation contained 40 mol% AA and 60 mol% TeEGDA, with proxyphylline added in an amount equal to 10 wt% of the total mixture. Photoinitiator 2,2-dimethoxy-2-phenylacetophenone (DMPA, Aldrich) was added at a concentration of 1 wt%, based on total monomer weight, and photopolymers were prepared as films of approximate thickness 0.8 mm by exposure to 1 mW/cm^2 of incident UV irradiation in a nitrogen atmosphere. The films were prepared in planar glass molds.

The release characteristics of the loaded polymer samples were determined in phosphate buffer (pH 7.4) and in HCl buffer (pH 2.2) at 37 °C. The ionic strength of all buffers was adjusted to 0.13 M by addition of KCl. Polymer slabs of known weight (~ 200 mg) were placed in dissolution cells each containing 400 ml of buffer. Liquid samples were withdrawn from the cells at regular intervals, and the proxyphylline concentration was determined spectrophotometrically from the UV absorbance at 279 nm.

Glass transition temperature (T_g) values for non-loaded polymer films were determined by dynamic mechanical analysis (DMA). DMA experiments were performed in the resonant frequency mode with oscillation amplitude 0.3 mm on a DMA 983 dynamic mechanical analyzer (TA Instruments, New Castle, DE). Sample lengths were adjusted to give an average resonant frequency of 5.5 ± 0.3 Hz, and T_g was measured as the maximum in the damping factor tan δ. The dynamic swelling behavior of non-loaded polymer films was examined by immersing dry polymer slabs of known weight in acetone, a solvent of high thermodynamic compatibility for the multiacrylate polymers, or in aqueous buffers having pH 2.2 (HCl) or pH 7.4 (phosphate). Samples were kept at 30 °C in a thermostatted water bath, and the slabs were periodically removed and weighed in order to determine the rate of penetrant uptake.

Results and Discussion

Polymer Design and Preparation. As illustrated in Figure 2, the morphology of networks prepared by copolymerization of AA with PEG-containing multifunctional acrylate macromers is such that two types of network chains exert an influence on the observed macroscopic polymer properties. The first type of network chain is the poly(acrylate-*co*-acrylic acid) chain (denoted by D in the figure) that is built up as the polymerization proceeds by radical propagation

Downloaded by MONASH UNIV on October 31, 2012 | http://pubs.acs.org
Publication Date: September 24, 1998 | doi: 10.1021/bk-1998-0709.ch010

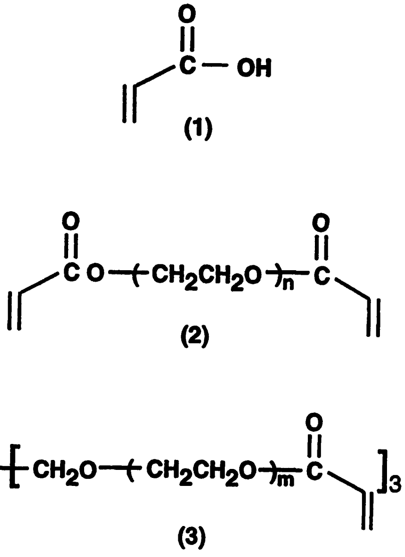

Figure 1. The various monomers used in network synthesis: acrylic acid (1); poly(ethylene glycol) diacrylate (2); and trimethylolpropane ethoxylate triacrylate (3).

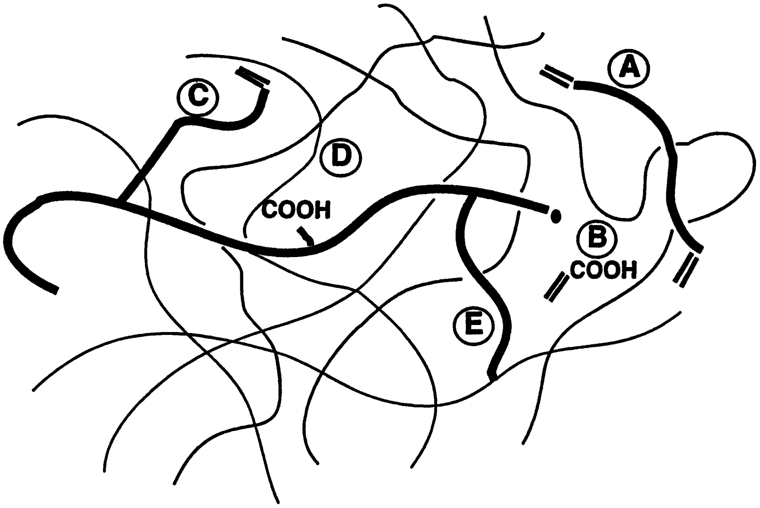

Figure 2. A schematic representation of structural issues in acrylic acid/multiacrylate copolymerization. (A) is the oligomeric multiacrylate monomer, (B) is the acrylic acid monomer, (C) is a tethered double bond, (D) is the poly(acrylate-*co*-AA) main chain, and (E) is a crosslink.

Downloaded by MONASH UNIV on October 31, 2012 | http://pubs.acs.org
Publication Date: September 24, 1998 | doi: 10.1021/bk-1998-0709.ch010

Downloaded by MONASH UNIV on October 31, 2012 | http://pubs.acs.org
Publication Date: September 24, 1998 | doi: 10.1021/bk-1998-0709.ch010

through acrylate and AA double bonds. The second type of network chain is the oligomeric PEG chain which connects acrylate functionalities within the same macromer unit (denoted by E in the figure). Each type of network chain represents an independently "tunable" parameter in the design of materials with precisely controlled solute release characteristics.

Our approach to the development and characterization of controlled release devices based on highly crosslinked acrylate copolymers has initially involved systematically and independently examining the effects of varying the crosslinking monomer structure *and* the AA feed ratio on the polymers' network structure and mechanical properties. To this end, a series of AA copolymers were prepared from tetra- and hexa- functional (two and three double bonds, respectively) PEG-containing acrylate macromers. The crosslinking monomers were chosen to provide oligomeric PEG segments of varying lengths. The various compositions examined are presented in Table I.

Subsequently, we have prepared drug-loaded polymer networks in order to study the dependence of the polymers' solute release characteristics on the network structure. The compositions of drug-loaded polymer samples are provided in Table II.

Structural Characterization. In order to determine the extent to which the copolymer network architecture could be controlled by varying the copolymerization feed parameters, each copolymer system described in Table I was characterized by DMA and by penetrant sorption studies.

Table III shows that the dynamic mechanical T_g for the multiacrylate homo- and co- polymers depended very strongly both upon the AA feed ratio and upon the structure of the crosslinking monomer. Both glassy and rubbery polymer matrices were obtained, depending on the comonomer feed characteristics. In general, T_g decreased as the PEG chain length of the multiacrylate monomer was increased. This result reflects the decrease in crosslinking density for systems composed of longer PEG chains. However, T_g increased as the AA content was increased, reflecting a compositional effect on the poly(acrylate-*co*-AA) main chain.

Additional information regarding the dependence of the crosslinked structure on monomer feed characteristics was obtained from a series of penetrant sorption experiments. Table IV shows the dependence of the equilibrium weight swelling ratio q_∞ on the molar comonomer feed ratio of AA for various poly(diacrylates) at pH 2.2 and at pH 7.4.

Table IV demonstrates clearly that increasing the AA comonomer feed ratio in multiacrylate copolymerizations led to an increase in the amount of swelling agent that could be accommodated by the copolymer network at equilibrium. The equilibrium penetrant uptake value also increased as the PEG chain length was increased (over the range 1 - 9 ethylene glycol units in the table). These results reflect the increasing network mesh size which accompanied copolymerization with AA or an increase in the PEG chain length.

Table IV also shows that the swelling behavior of AA-containing networks was substantially pH-dependent. Equilibrium swelling ratio values for 40% AA copolymers in pH 7.4 buffer were 2 - 4 times higher than swelling ratio values measured at pH 2.2. This pH sensitivity arises due to ionization of carboxylic acid sites along the network backbone above the poly(acrylic acid) pK_a of about 5. Hence, no pH sensitivity was observed for the multiacrylate homopolymers which contained no AA.

The swelling behavior of the multiacrylate copolymers was more carefully considered by a Fickian analysis of the short-time dynamic swelling data. For this analysis, the fractional penetrant uptake M_t/M_∞ was plotted as a function of $t^{1/2}/L$,

Table I. Compositions of the various multiacrylate systems examined. The parameters w_{AA} and f_{AA} are the weight fraction and mole fraction (based on double bonds), respectively, of AA in comonomer mixtures. $\overline{M}_c$ values are theoretical values based on the structure of the PEG-containing monomer.

PEG units	$\overline{M}_c$ (g/mol)	System	w_{AA}	f_{AA}
1	170	D1	0	0
EGDA		D1AA3	0.0255	0.0300
		D1AA10	0.0866	0.101
		D1AA40	0.360	0.399
2	214	D2	0	0
*DEGDA		D2AA3	0.0298	0.0436
		D2AA10	0.0741	0.106
		D2AA40	0.311	0.401
3	258	D3	0	0
TrEGDA		D3AA3	0.0170	0.0300
		D3AA10	0.0585	0.100
		D3AA40	0.271	0.400
~4	326	D4	0	0
*PEG200DA		D4AA3	0.0156	0.0322
		D4AA10	0.0512	0.102
		D4AA40	0.241	0.409
~9	526	D9	0	0
*PEG400DA		D9AA3	0.0126	0.0446
		D9AA10	0.0293	0.0992
		D9AA40	0.155	0.400
~3	299	T3	0	0
*PEG170TrA		T3AA3	0.0165	0.0321
		T3AA10	0.0500	0.0943
		T3AA40	0.259	0.409
~6	416	T6	0	0
*PEG290TrA		T6AA3	0.0111	0.0310
		T6AA10	0.0378	0.0990
		T6AA40	0.189	0.394
~10	622	T10	0	0
PEG500TrA		T10AA3	0.0111	0.0450
		T10AA10	0.0248	0.0968
		T10AA40	0.135	0.397

* indicates multiacrylate sytems chosen for release studies.

Table II. Compositions of the various drug-loaded multiacrylate monomer formulations. The parameters w_{AA} and f_{AA} are the weight fraction and mole fraction (based on double bonds), respectively, of AA in comonomer mixtures.

System	w_{AA}	f_{AA}	wt% proxyphylline
D2AA30-P	0.230	0.307	10.4
D4AA30-P	0.169	0.299	11.3
D4AA40-P	0.235	0.392	11.7
D4AA50-P	0.313	0.489	10.6
D9AA40-P	0.155	0.401	10.0
T3AA30-P	0.178	0.300	11.2
T6AA30-P	0.152	0.334	10.7

Downloaded by MONASH UNIV on October 31, 2012 | http://pubs.acs.org
Publication Date: September 24, 1998 | doi: 10.1021/bk-1998-0709.ch010

Downloaded by MONASH UNIV on October 31, 2012 | http://pubs.acs.org
Publication Date: September 24, 1998 | doi: 10.1021/bk-1998-0709.ch010

Table III. Measured glass transition temperatures T_g for poly(multiacrylate) homo- and co- polymers.

PEG units	$\overline{M}_c$ (g/mol)	System	T_g (± 5 °C)	PEG units	$\overline{M}_c$ (g/mol)	System	T_g (± 5 °C)
1	170	D1	61	~ 3	299	T3	108
		D1AA3	73			T3AA3	113
		D1AA10	90			T3AA10	111
		D1AA40	150			T3AA40	131
2	214	D2	118	~ 6	416	T6	39
		D2AA3	111			T6AA3	40
		D2AA10	115			T6AA10	42
		D2AA40	115			T6AA40	59
3	258	D3	65	~ 10	622	T10	-8
		D3AA3	73			T10AA3	-8
		D3AA10	76			T10AA10	-4
		D3AA40	79			T10AA40	18
~ 4	326	D4	47				
		D4AA3	50				
		D4AA10	53				
		D4AA40	68				
~ 9	526	D9	-12				
		D9AA3	-11				
		D9AA10	-7				
		D9AA40	12				

Downloaded by MONASH UNIV on October 31, 2012 | http://pubs.acs.org
Publication Date: September 24, 1998 | doi: 10.1021/bk-1998-0709.ch010

Table IV. Measured swelling parameters and calculated solubility parameters for diacrylate systems at pH 2.2 and at pH 7.4, having various AA contents. The parameter $\overline{M}_c$ is the theoretical value of the molecular weight between crosslinks, and q_∞ is the equilibrium value of the weight swelling ratio.

$\overline{M}_c$ (g/mol)	System	PEG/AA (mer/mer)	q_∞ (g/g) pH 2.2	q_∞ (g/g) pH 7.4
170	D1	0.50	1.023	1.024
	D1-40	0.30	1.136	1.184
214	D2	1.0	1.052	1.051
	D2-40	0.60	1.145	1.494
258	D3	1.5	1.071	1.071
	D3-40	0.9	1.171	1.471
326	D4	2.0	1.092	1.102
	D4-3	1.9	1.123	1.119
	D4-10	1.8	1.133	1.151
	D4-40	1.2	1.160	1.468
526	D9	4.5	1.320	1.315
	D9-40	2.7	1.347	1.643

where M_t is the total amount of absorbed penetrant at any given time, M_∞ is the equilibrium amount of absorbed penetrant, t is time, and L is the polymer slab thickness. The dynamic swelling data is provided in Figure 3 for TeEGDA homo- and co- polymers at pH 2.2 and in Figure 4 for the same polymer systems at pH 7.4. The data are plotted as a function of time in Figures 3a and 4a and as a function of $t^{1/2}/L$ in Figures 3b and 4b. The samples swelled quite slowly, due to their highly crosslinked nature, with measured equilibrium swelling times as long as 100 hours.

For a Fickian diffusion process, M_t/M_∞ depends linearly on $t^{1/2}/L$ at short times, with a slope directly proportional to the penetrant diffusion coefficient D. Hence, the first 60% of the fractional sorption data for each copolymer system was fitted to a line (Figures 3b and 4b), and D values were calculated for the various copolymer compositions. The correlation coefficient for each linear fit was > 0.99. Some samples exhibited two-stage sorption behavior due to chain relaxation effects on the diffusion process. To obtain meaningful diffusion coefficient data for these systems, the M_∞ values were adjusted to reflect intermediate plateau values of swelling. For example, the data for the D4AA40 system in Figure 4b reflect the fractional rate of approach of the system to a fractional sorption value of 0.65, as suggested by Figure 4a.

Calculated diffusion coefficient values are tabulated in Table V for penetrants acetone, pH 2.2 buffer, and pH 7.4 buffer. For most cases, the acetone diffusion coefficient D_{ac} was less than the aqueous diffusion coefficients $D_{aq,2.2}$ and $D_{aq,7.4}$ due to penetrant size effects. The diffusion coefficients increased as the network mesh size was increased by modification of the crosslinking monomer structure. Effects due to varying the AA content were substantially less.

Solute Release Behavior. The slow swelling behavior exhibited by the ionizable acrylate networks suggested that these materials might provide a basis for swelling controlled release formulations which exhibit sustained release over long periods of time. Additionally, the strong dependence of the copolymer mechanical properties and the penetrant diffusion coefficients on the comonomer feed characteristics suggested that manipulation of the crosslinking monomer structure and the AA feed ratio would offer a means of precisely tuning the release characteristics of such formulations. Hence, proxyphylline-loaded acrylate copolymer formulations were prepared as described in the experimental part, and the dependence of the solute release characteristics on the formulation parameters was investigated.

Figures 5 - 7 show the time dependence of the fractional proxyphylline release for various diacrylate formulations. Clearly the rate of solute release and the final fractional release achieved depended very strongly on the length of the PEG spacer on the diacrylate monomer and on the pH of the release medium. In order to quantify this dependence, proxyphylline diffusion coefficients were calculated in a manner analogous to that used to calculate penetrant diffusion coefficients from the dynamic swelling data. Figure 8 shows a typical plot of the dependence of the early time fractional proxyphylline release on $t^{1/2}/L$, and Table VI provides calculated values of the proxyphylline diffusion coefficient for the various systems considered.

Table VI shows clearly that manipulation of the crosslinking monomer structure in poly(acrylate-*co*-AA) formulations provides a means of coarsely tuning the solute release behavior. Measured D values varied over 2 -3 orders of magnitude, depending on the diacrylate structure. The data for the D4AA30,

Downloaded by MONASH UNIV on October 31, 2012 | http://pubs.acs.org
Publication Date: September 24, 1998 | doi: 10.1021/bk-1998-0709.ch010

Downloaded by MONASH UNIV on October 31, 2012 | http://pubs.acs.org
Publication Date: September 24, 1998 | doi: 10.1021/bk-1998-0709.ch010

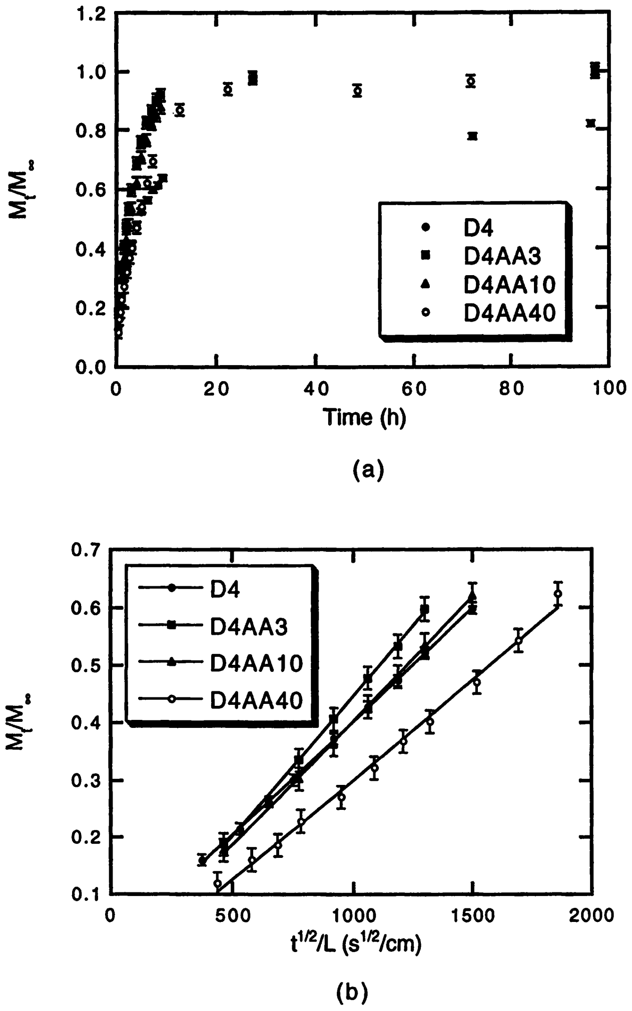

Figure 3. Dynamic swelling behavior of various PEG(200)diacrylate systems in pH 2.2 buffer. Part (a) shows the fractional penetrant sorption as a function of time; part (b) shows the early-time dependence on $t^{1/2}/L$, used for calculating diffusion coefficients.

Downloaded by MONASH UNIV on October 31, 2012 | http://pubs.acs.org
Publication Date: September 24, 1998 | doi: 10.1021/bk-1998-0709.ch010

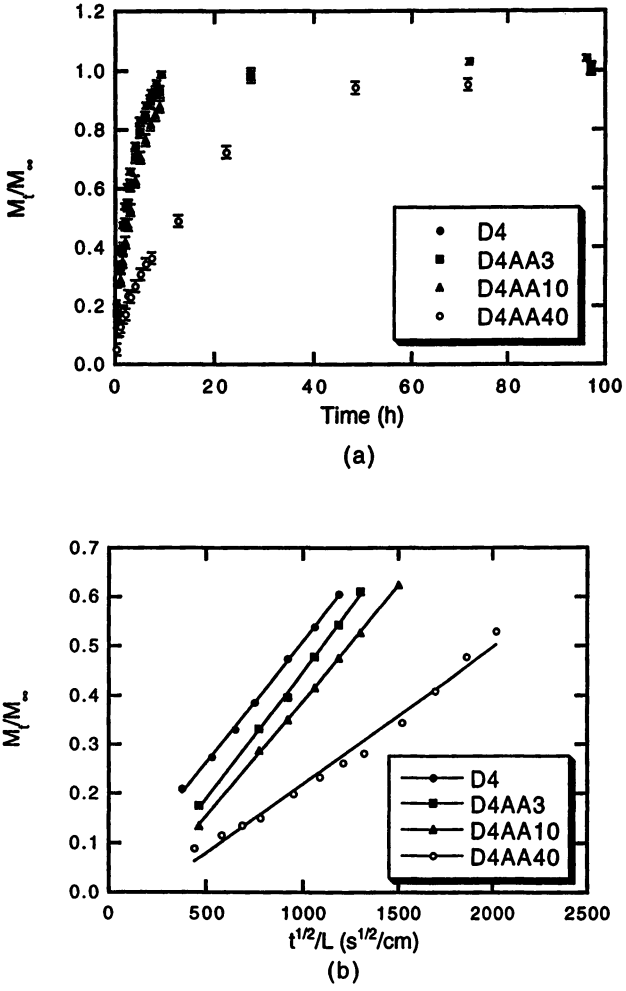

Figure 4. Dynamic swelling behavior of various PEG(200)diacrylate systems in pH 7.4 buffer. Part (a) shows the fractional penetrant sorption as a function of time; part (b) shows the early time dependence on $t^{1/2}/L$, used for calculating diffusion coefficients.

Table V. Penetrant diffusion coefficients describing the dynamic swelling of various multiacrylate polymer systems. D_{ac} describes the diffusion of acetone, $D_{aq,2.2}$ describes the diffusion of pH 2.2 buffer, and $D_{aq,7.4}$ describes the diffusion of pH 7.4 buffer.

System	Penetrant Diffusion Coefficients $D_{ac} \times 10^9$ (Acetone, cm^2/s)	$D_{aq,2.2} \times 10^9$ (pH 2.2, cm^2/s)	$D_{aq,7.4} \times 10^9$ (pH 7.4, cm^2/s)
D2	1.1	11	11
D2AA40	2.0	20	19
D3	1.5	18	17
D3AA40	1.9	13	11
D4	20	39	42
D4AA40	3.5	19	13
T3	0.34	NA	NA
T3AA40	2.0		
T6	51	NA	NA
T6AA40	5.0		

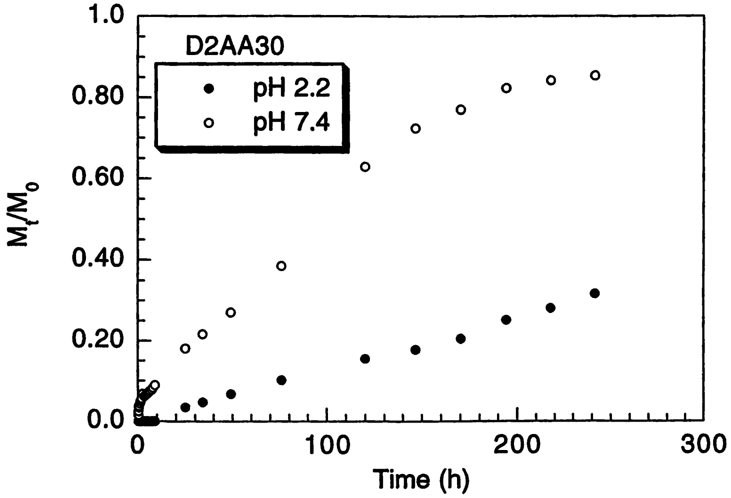

Figure 5. Fractional release of proxyphylline from loaded D2AA30 system at pH 2.2 (●) and pH 7.4 (○).

Downloaded by MONASH UNIV on October 31, 2012 | http://pubs.acs.org
Publication Date: September 24, 1998 | doi: 10.1021/bk-1998-0709.ch010

Downloaded by MONASH UNIV on October 31, 2012 | http://pubs.acs.org
Publication Date: September 24, 1998 | doi: 10.1021/bk-1998-0709.ch010

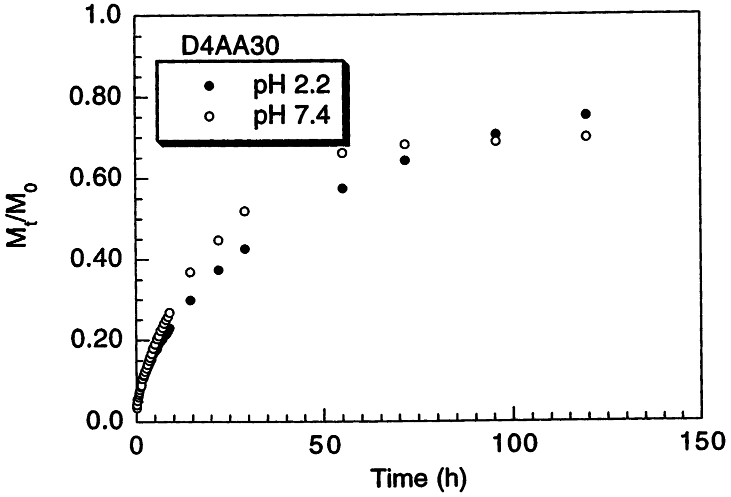

Figure 6. Fractional release of proxyphylline from loaded D4AA30 system at pH 2.2 (●) and pH 7.4 (○).

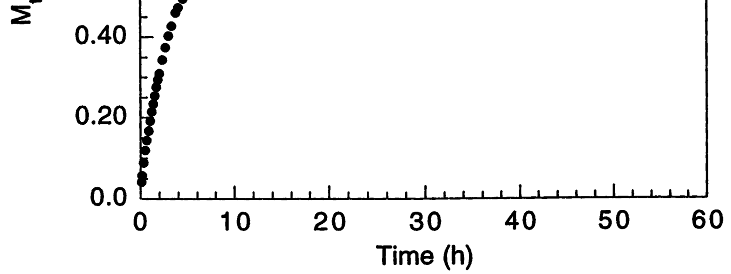

Figure 7. Fractional release of proxyphylline from loaded D9AA40 system at pH 7.4.

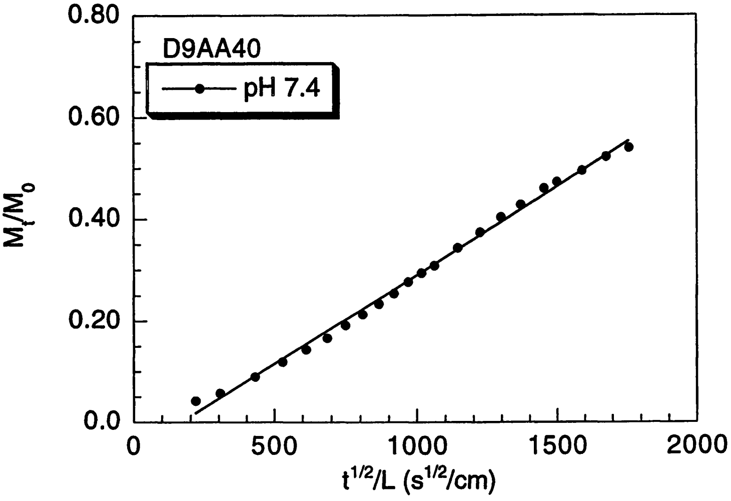

Figure 8. Early time dependence of fractional proxyphylline release on $t^{1/2}/L$ for D9AA40 system.

Table VI. Proxyphylline diffusion coefficients describing the rate of release of proxyphylline from multiacrylate polymer networks in a swelling medium. $D_{aq,2.2}$ describes the rate of release in pH 2.2 buffer, and $D_{aq,7.4}$ describes the rate of release in pH 7.4 buffer.

System	Proxyphylline Diffusion Coefficients $D_{aq,2.2} \times 10^9$ (pH 2.2, cm^2/s)	 $D_{aq,7.4} \times 10^9$ (pH 7.4, cm^2/s)
D2AA30	0.10	0.64
D4AA30	1.8	3.4
D4AA40	2.0	5.5
D4AA50	2.6	5.8
D9AA40	NA	23
T3AA30	0.0047	0.036
T6AA30	0.90	2.1

Downloaded by MONASH UNIV on October 31, 2012 | http://pubs.acs.org
Publication Date: September 24, 1998 | doi: 10.1021/bk-1998-0709.ch010

D4AA40, and D4AA50 systems show that varying the AA content in the formulations allows for a more subtle tuning of the release characteristics.

Conclusions

Novel polymer networks were synthesized by photopolymerization techniques. The properties of these materials were shown to vary over a wide range, depending on the copolymerization parameters. It was demonstrated that the strong relationship between the polymer network structure and the polymer properties could be exploited in the design of unique controlled release devices with precisely tuned release characteristics.

Literature Cited

1. Kost, J., and R. Langer, in *Hydrogels in Medicine and Pharmacy,* Vol. 3, N. A. Peppas, ed., CRC Press, Boca Raton, FL, pp. 95-108 (1987).
2. Peppas, N. A., in *Pulsatile Drug Delivery*, R. Gurny, H. Junginger, and N. A. Peppas, eds., Wissenschaftliche, Stuttgart, pp. 41-56 (1993).
3. Peppas, N. A., in *Trends and Future Perspectives in Peptide and Protein Drug Delivery*, V. Lee, M. Hashida, and Y. Mizushima, eds., Harwood, pp. 23-37 (1995).
4. Peppas, N. A., S. Vakkalanka, C. S. Brazel, A. S. Luttrell, and N. K. Mongia, in *Advanced Biomaterials in Biomedical Engineering and Drug Delivery Systems*, N. Opata, S. W. Kim, J. Feijeu, and T. Okano, eds., Springer, pp. 3-7 (1996).
5. Scranton, A. B., B. Rangarajan, and J. Klier, *Adv. Polym. Sci.*, **122**, 1-54 (1995).
6. Kurdikar, D. L., and N. A. Peppas, *Polymer*, **36**, 2249-2255 (1994).

Downloaded by MONASH UNIV on October 31, 2012 | http://pubs.acs.org
Publication Date: September 24, 1998 | doi: 10.1021/bk-1998-0709.ch010

Chapter 11

Direct Synthesis of Polyester Microspheres, Potential Carriers of Bioactive Compounds

S. Slomkowski[1], S. Sosnowski[1], M. Gadzinowski[1], C. Pichot[2], and A. Elaissari[2]

[1]Center of Molecular and Macromolecular Studies, Polish Academy of Science, Sienkiewicza 112, 90-363 Lodz, Poland
[2]Unité Mixte CNRS-BioMérieux, ENSL, 46 Allée d'Italie, Lyon 69364, Cédex 07, France

Downloaded by UNIV OF GUELPH LIBRARY on October 31, 2012 | http://pubs.acs.org
Publication Date: September 24, 1998 | doi: 10.1021/bk-1998-0709.ch011

Polyester microspheres, composed of poly(ϵ-caprolactone) and polylactides, were obtained directly by pseudoionic and/or ionic dispersion polymerizations of parent cyclic esters carried out in 1,4-dioxane/heptane mixed solvent. Particles with narrow diameter polydispersity ($\bar{D}_v/\bar{D}_n < 1.1$) were synthesized by using poly(dodecyl acrylate)-*g*-poly(ϵ-caprolactone) (poly(DA-CL)), with ratio of $\bar{M}_n$(poly(ϵ-caprolactone)/$\bar{M}_n$(poly(DA-CL)) ≈ 0.25, as a surfactant. Poly(L,L-lactide) microspheres were obtained as an amorphous or crystalline material, depending on particle treatment after synthesis. Described is an application of ^{13}C-NMR MAS spectroscopy for determination of the degree of crystallinity of these products. Pseudoanionic dispersion polymerization of L,L-lactide carried out in the presence of omeprasol (5-methoxy-2-{[(4-methoxy-3,5-dimethyl-2-pirydyl)-methyl]-sulfinyl}-1H-benzimidazole), inhibitor of gastric acid secretion, yielded microspheres with 11 wt% of drug. A method was developed which allows transfer of poly(ϵ-caprolactone) and polylactide microspheres from heptane to the water based media in which microspheres form suspensions of nonaggregated particles. This process consists of controlled basic hydrolysis of microspheres transferred from heptane to ethanol containing Triton X-405, followed by transferring them to buffered solutions with content of Triton X-405 as low as 0.2 wt%.

The best formulations of many drugs with required site specific activity are those which allow transportation of a bioactive compound to desired tissues and/or organs and then to assure the subsequent controlled release. During transportation the organism should be protected from drug activity in undesired locations and drugs should be screened from any action of an organism which would lead to drug decomposition before reaching the target. Polymeric carriers which are degradable to harmless products are often used for this purpose and, depending on the actual application, the polymer-drug composites can be formed into disks, capsules, and microspheres *(1-3)*. The latter have been found to be very

In Tailored Polymeric Materials for Controlled Delivery Systems; McCulloch, I., et al.;
ACS Symposium Series; American Chemical Society: Washington, DC, 1998.

convenient and were used for transportation of steroids and other hormones *(4-7,9)*, anticancer drugs *(4,5,8,10,11)*, antibiotics *(4,12)*, antiinflamatory drugs *(13,14)*, contraceptives *(15, 16)*, and vaccines *(17-20)*.

Microspheres are usually prepared from previously synthesized polymers by any of the oil-in-water emulsion or polymer-drug coprecipitation methods *(5,21)*. Recently a method was described for formation of amino acid oligomer microspheres by changing pH of the oligo(amino acid) solution *(22,23)*. However, these techniques provided particles with diameters usually exceeding 20 μm and broad particle diameter distribution *(5)*. Recently we have developed methods for obtaining poly(ε-caprolactone) (poly(CL)) and polylactide (racemic and optically active) (poly(Lc)) microspheres directly during polymerization *(24-28)*. Diameters of these microspheres were from 0.6 μm to 5 μm and their diameter polydispersity was narrow. Essential for these polymerizations was to use 1,4-dioxane/heptane mixtures as the reaction medium and poly(dodecyl acrylate)-*g*-poly(ε-caprolactone) (poly(DA-CL)) as a surface active agent. Before these microspheres can find any practical applications it is necessary to establish a relationsip between polymerization conditions and the parameters characterizing properties of microspheres. It is important also to find methods which allow incorporation of drugs into microspheres formed directly during polymerization. In this paper we discuss results of our studies on the above mentioned subjects. In particular, an attempt to incorporate 5-methoxy-2-{[(4-methoxy-3,5-dimethyl-2-pirydyl)-methyl]-sulfinyl}-1H-benzimidazole (omeprasol - inhibitor of $(H^+\text{-}K^+)$ATPase, an enzyme called the "pH pump" and responsible for HCl secretion in stomach) into microspheres during polymerization of L,L-lactide is described.

Experimental Part

Poly(DA-CL)s of various composition were synthesized according to descriptions given in our earlier papers *(24-26)*. Microspheres were synthesized and purified as it was described previously *(24,25,29)*. Diameters of microspheres were determined by scanning electron microscopy using a JEOL 35 C apparatus and by dynamic light scattering using a Coulter N4-MD Particle Analyzer. Molecular weight and molecular weight polydispersity ($\bar{D}_v/\bar{D}_n$) of poly(CL) and poly(Lc) was determined by GPC. Chromatograms were calibrated by using samples of poly(CL) synthesized earlier in our laboratory *(30-32)*. ^{13}C MAS NMR spectra were registered using a Bruker AC 200 spectrometer. DSC traces were registered using a Du Pont 2000 apparatus. Zeta-potentials for microspheres were measured using a Malvern Zeta Seizer 3 analyzer.

Results and Discussion

Relation between diameters, diameter distributions of poly(L,L-Lc) microspheres, molecular weight and molecular weight distribution of poly(L,L-Lc) in microspheres and concentration of poly(DA-CL) in reaction mixture. Poly(Lc) microspheres were synthesized by using tin(II)-2-ethylhexanoate (tin octoate) as an initiator. Polymerizations were carried out in 1,4-dioxane/heptane (1:4 v/v) mixture at 95 °C in the presence of poly(DA-CL). Particles with the lowest diameter polydispersity ($\bar{D}_v/\bar{D}_n = 1.03$) were obtained for poly(DA-CL) with $\bar{M}_n$ of poly(CL) grafts equal 0.23 of $\bar{M}_n$ of copolymer macromolecules *(11)*. It was important to establish how variations of the concentration of poly(DA-CL), with $\bar{M}_n$(poly(CL))/$\bar{M}_n$(poly(DA-CL)) close to

Downloaded by UNIV OF GUELPH LIBRARY on October 31, 2012 | http://pubs.acs.org
Publication Date: September 24, 1998 | doi: 10.1021/bk-1998-0709.ch011

Downloaded by UNIV OF GUELPH LIBRARY on October 31, 2012 | http://pubs.acs.org
Publication Date: September 24, 1998 | doi: 10.1021/bk-1998-0709.ch011

0.25, will influence diameters of microspheres and polymer partition between these particles and coagulum. Polymerizations of lactides are reversible and therefore some monomer remains at equilibrium unreacted *(33)*. At the conditions at which polymerizations were carried out the overall yield of poly(Lc) close to 50% corresponds to this equilibrium *(24)*. We established that microspheres did contain up to 4 wt% of poly(DA-CL), substantial part of which is composed of the biodegradable poly(CL) grafts. Dependencies of yield of polymer incorporated into microspheres (the remaining polymer constituted shapeless coagulum) and the number average diameter of microspheres, on the concentration of poly(DA-CL) is illustrated in Figure 1. Initially, the yield increases, because the higher concentrations of poly(DA-CL) ensure better stabilization of microspheres. However, when the yield of microspheres approaches 45% no further increase was observed. At these conditions all polymer is incorporated into microspheres. The remaining monomer crystals were separated by fractional sedimentation. The average diameter of microspheres decreases with increasing concentration of surfactant, similar to radical emulsion polymerizations, however, this dependence is rather weak. Molecular weight and molecular weight polydispersity were independent of concentration of poly(DA-CL) and, for polymers in microspheres characterized by plots in Figure 1, were equal $\overline{M}_n$ = 10 000 ± 1 000 and $\overline{M}_w/\overline{M}_n$ = 1.07 ± 0.01.

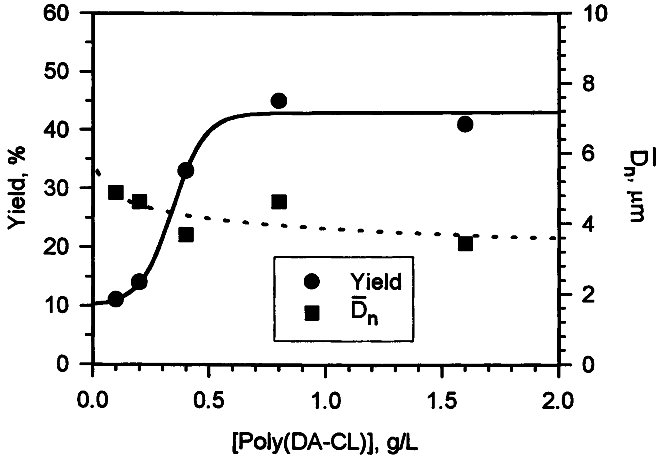

Figure 1 Dependence of yield and average diameter ($\overline{D}_n$) of poly(L,L-Lc) microspheres on concentration of poly(DA-CL) with $\overline{M}_n$ = 26 400 and poly(CL) grafts with $\overline{M}_n$ = 4 700. Initial monomer and initiator concentrations equal $2.77 \cdot 10^{-1}$ mol/l and $5 \cdot 10^{-3}$ mol/l, respectively.

Diameters, diameter distributions, molecular weights, and molecular weight distributions of poly(ε-caprolactone) microspheres obtained by pseudoanionic and anionic dispersion polymerizations of ε-caprolactone. Syntheses of poly(CL) microspheres by ring-opening pseudoanionic and anionic polymerizations of CL, carried out in 1,4-dioxane/heptane (1:9 v/v) mixture at room temperature, were described in our earlier papers *(24,27)*. Polymerizations were initiated with $CH_3CH_2OAl(CH_2CH_3)_2$ (initiator of pseudoanionic polymerization of CL *(34)*) and/or with $(CH_3)_3SiONa$ (initiator of anionic processes). Suspensions of microspheres were formed in the presence of poly(DA-CL) with $\bar{M}_n$ =49 000 ($\bar{M}_n$ of poly(CL) grafts equal 3 000) and with $\bar{M}_n$ =28 800 ($\bar{M}_n$ of poly(CL) grafts equal 3 600). In the former case we obtained particles with $\bar{D}_n$ = 0.628 µm and $\bar{D}_v/\bar{D}_n$ = 1.04 *(24)*, in the latter with $\bar{D}_n$ = 0.94 µm and $\bar{D}_v/\bar{D}_n$ = 1.26 *(27)*. The values of diameters of poly(CL) microspheres were determined by analysis of scanning electron micrographs. However, we encountered some difficulties during registration of SEM pictures of poly(CL) microspheres, especially in the case of magnifications higher than 7 000 times. At these conditions we noticed changes in shape of microspheres, apparently resulting from local decomposition of poly(CL) under action of electron beams, which made measurements of diameters of microspheres less accurate thus, independently we measured diameters of particles by dynamic light scattering. For microspheres with $\bar{D}_n$ = 0.94 µm, determined by SEM, the dynamic light scattering gave diameter value equal to 0.6 ± 0.1 µm. The difference is significant, but not very large.

Molecular weight of poly(CL) in microspheres was varied from 2 900 to 106 600 by proper adjustment of the initial monomer and initiator concentrations *(27,29)*. We found that, regardless whether $CH_3CH_2OAl(CH_2CH_3)_2$ or $(CH_3)_3SiONa$ were used, at the end of polymerization the number of polymer macromolecules was equal to the number of initiator molecules present at the beginning of the polymerization. Molecular weight distributions varied from $\bar{M}_w/\bar{M}_n$ =1.15 (for poly(CL) with $\bar{M}_n$ =106 600) to $\bar{M}_w/\bar{M}_n$ =1.37 (for poly(CL) with $\bar{M}_n$ =2 860).

Synthesis of poly(L,L-Lc) microspheres with omeprasol. Polymerization of L,L-Lc initiated with tin(II) 2-ethylhexanoate was carried out at 95 °C as previously described. Initial monomer and initiator concentrations were $[L,L\text{-}Lc]_0 = 2.5\cdot10^{-1}$ mol/l and $[\text{tin(II) 2-ethylhexanoate}]_0 = 4.6\cdot10^{-3}$ mol/l. Concentration of poly(DA-CL) was 1.6 g/l. At the moment when microspheres were nucleated (this was manifested by the onset of turbidity of the polymerizing mixture) omeprasol (in heptane) solution was added dropwise. Concentration of omeprasol in the reaction mixture reached eventually $5\cdot10^{-3}$ mol/l. After two hours this mixture was cooled down by addition of cold heptane and, after purification from the remaining monomer crystals by fractional sedimentation, the yellow microspheres were isolated. An example of SEM picture of these microspheres is shown in Figure 2. Final yield of purified microspheres was 10.5% (in relation to the amount of monomer which was used).

Number average diameter of poly(L,L-Lc/omeprasol) microspheres $\bar{D}_n$ = 1.73 µm (determined from SEM pictures) was smaller than diameter of particles obtained without drug (cf. Figure 1) but their diameter distribution was larger ($\bar{D}_v/\bar{D}_n$ = 1.17 for poly(L,L-Lc/omeprasol) and $\bar{D}_v/\bar{D}_n$ = 1.03 for poly(L,L-Lc) microspheres). It was important to find out whether omeprasol was incorporated into microspheres due to physical entrapment or as a result of chemical reaction with growing polymer macromolecules. To answer this question we analyzed poly(L,L-Lc/omeprasol) microspheres by GPC. The GPC trace of microspheres dissolved in THF is shown in Figure 3. There are two signals in this trace. The broad one with maximum at the elution volume equal to 26.9 ml corresponding to poly(L,L-Lc) and the second one at 36.1 ml which was assigned to the unbound omeprasol (maximum in GPC traces of low molecular weight compounds unbound to polymer occurs at this elution volume).

Downloaded by UNIV OF GUELPH LIBRARY on October 31, 2012 | http://pubs.acs.org
Publication Date: September 24, 1998 | doi: 10.1021/bk-1998-0709.ch011

Downloaded by UNIV OF GUELPH LIBRARY on October 31, 2012 | http://pubs.acs.org
Publication Date: September 24, 1998 | doi: 10.1021/bk-1998-0709.ch011

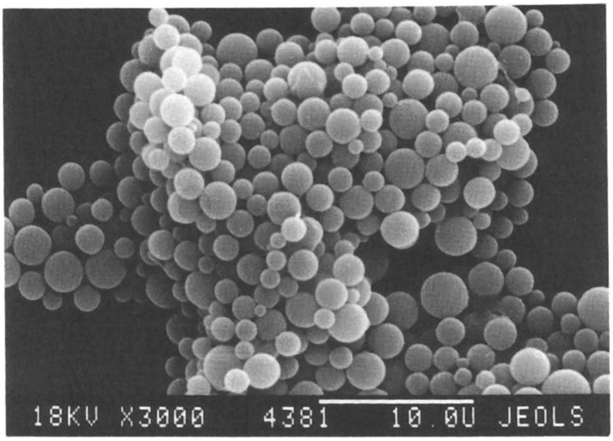

Figure 2 SEM microphotograph of poly(L,L-Lc/omeprasol) microspheres.

In the UV spectrum of poly(L,L-Lc/omeprasol) microspheres (cf. Figure 4) maximum at 297 nm corresponds to omeprasol whereas a shoulder, observed in the wavelengt region from 320 to 380 nm, was assigned to compound 1, which is known to be formed from omeprasol in acidic media *(35)*.

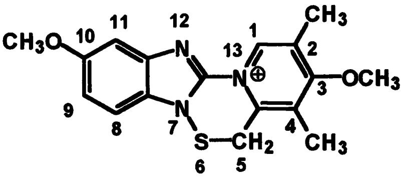

1

From this spectrum, by using extinction coefficient of omeprasol (ϵ_{297} = 14 000 mol/(l·cm)) and extinction coefficient of 1 (ϵ_{370} = 11 700 mol/(l·cm) *(35)*) we estimated that fraction of compound 1 equals ca. 10%. It is worth noting that compound 1 is considered to be an active metabolite of omeprasol, responsible for inhibition of the gastric (H^+-K^+)-ATPase *(35)*.

^{1}H NMR spectrum of poly(L,L-Lc/omeprasol) in $CDCl_3$ is shown in Figure 5. In this spectrum, in addition to signals of poly(L,L-Lc) (at δ = 1.56 (d) of CH_3 and at δ = 5.14 (q) of -CH< main chain groups and at δ = 1.46 of CH_3 end groups) also signals of omeprasol are present.

Downloaded by UNIV OF GUELPH LIBRARY on October 31, 2012 | http://pubs.acs.org
Publication Date: September 24, 1998 | doi: 10.1021/bk-1998-0709.ch011

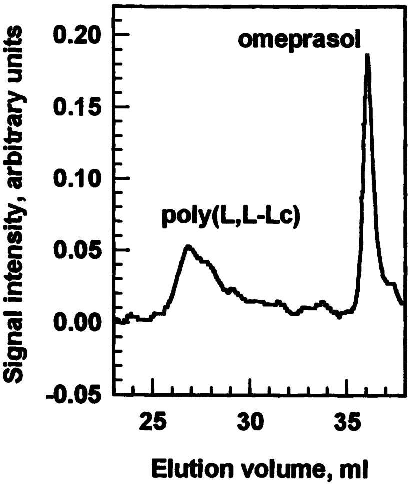

Figure 3 GPC trace of poly(L,L-Lc/omeprasol) microspheres dissolved in THF.

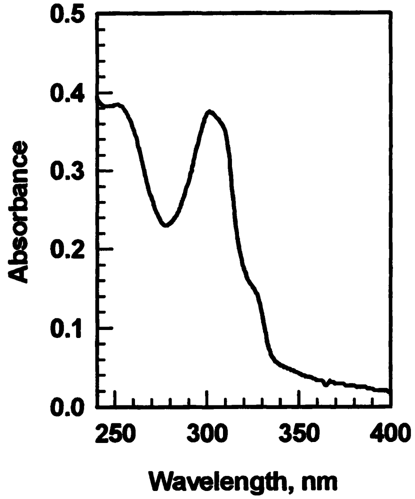

Figure 4 UV spectrum of poly(L,L-Lc/omeprasol) microspheres $8.4 \cdot 10^{-2}$ g/l, 1 cm cell.

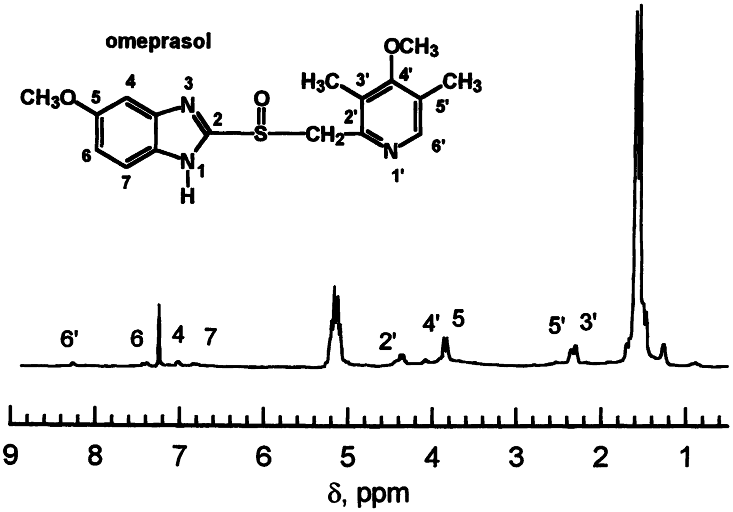

Figure 5 ^{1}H NMR spectrum of poly(L,L-Lc/omeprasol) in $CDCl_3$

Downloaded by UNIV OF GUELPH LIBRARY on October 31, 2012 | http://pubs.acs.org
Publication Date: September 24, 1998 | doi: 10.1021/bk-1998-0709.ch011

Crystallinity of poly(L,L-Lc) microspheres. DSC traces of poly(L,L-Lc) microspheres cooled rapidly to 50 °C, after synthesis at 95 °C, indicated that in the temperature region from 80 to 100 °C, polymer in microspheres crystallizes ("cold crystallization") *(26)*. Further increase of temperature results in complex endotherm (maxima at 131.8 and at 145.3 °C) characterizing melting. Determination of the enthalpy of cold crystallization (ΔH_c) and of the enthalpy of melting (ΔH_m) allowes estimation of the enthalpy of melting of the crystalline fraction present prior to the DSC run ($\Delta H_m(in) = \Delta H_m - \Delta H_c$). For the rapidly cooled particles, $\Delta H_m(in) = 2 \pm 3$ J/g. This indicated that they comprised the amorphous polymer. Annealing of poly(L,L-Lc) microspheres at 80 °C for 100 min gave crystalline particles ($\Delta H_m = 57.14$ J/g, $\Delta H_c = 0$ J/g, and therefore $\Delta H_m(in) = 57.14$ J/g). Thus, depending on the thermal treatment of poly(L,L-Lc) microspheres it was possible to obtain particles which were fully amorphous or partially crystalline. However, the DSC traces alone are not sufficient for determination of the degree of crystallinity of microspheres.

It was observed that in the solid state ^{13}C NMR spectra of highly crystalline polylactides, registered with sample spinning at magic angle (^{13}C MAS NMR), signals are split, indicating different location of the corresponding carbon atoms in the crystal cell *(37)*. In the case of amorphous polylactide ^{13}C MAS spectra are broad, without any fine structure. This effect was used for determination of degree of crystallinity of polylactides *(38)*. In the ^{13}C MAS spectrum of poly(L,L-Lc) microspheres, annealed at 80 °C for 80 min, (cf Figure 6a) splitting of the signals of carbonyl, methine, and methyl carbon atoms, indicating presence of crystalline fraction, can be clearly seen.

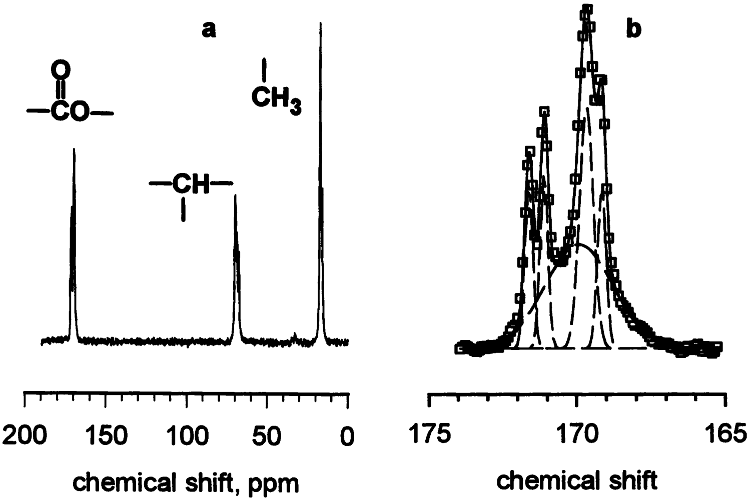

Figure 6 a - ^{13}C MAS NMR spectrum of poly(L,L-Lc) microspheres annealed at 80 °C for 80 min. b - Deconvolution of the signal of carbonyl carbon atoms into narrow signals due to the crystalline fraction and broad signal due to the amorphous fraction in poly(L,L-Lc) microspheres.

Figure 6b illustrates deconvolution of the signal of carbonyl carbon atoms into the narrow signals of crystalline fraction with maxima at 169.1, 169.7, 171.1, and 171.7 ppm and the broad signal due to the amorphous fraction of poly(L,L-Lc) in microspheres with maximum at 169.9 ppm. Integration of signals in Figure 6b indicated that fraction of crystalline phase in these microspheres was equal to 51.4%. Similar procedure performed for signal of methine carbon atom (two narrow signals with maxima at 15.8 and 17.1 ppm due to CH groups of the crystalline fraction and the broad signal at 16.7 ppm due to amorphous fraction) gave value of the degree of crystallinity equal 46%. Deconvolution of the signal due carbon atoms of CH_3 groups did not provide unique solution (results were dependent on the input parameters) and could not be used for analysis. Annealing at 80 °C for more than 80 min did not led to increase of the degree of crystallinity of poly(L,L-Lc) microspheres. Thus, depending on the thermal treatment we could obtain poly(L,L-Lc) particles with the degree of crystallinity controlled from 0 to ca 50%.

Poly(CL) and poly(L,L-Lc) microspheres with hydroxylic and carboxylic groups in their surface layers. Polyester microspheres formed during ring-opening polymerization in the heptane rich media have hydrophobic surfaces and aggregate when transferred to water. For medical applications, microspheres usually have to be suspended in water based media, and stability of such suspensions is of great importance. Moreover, local concentrations of functional groups, potentially useful for an attachment of targeting moieties, in surface layers of these microspheres is limited to hydroxyl groups and rather low. Thus, we decided to investigate whether a combination of partial hydrolysis of the polyesters in microspheres, leading to formation of carboxyl and hydroxyl polymer end-groups, and use of one of a typical low molecular weight surfactants for polymer dispersions in water, can give a solution to this problem.

It was obvious that for transferring microspheres from heptane to water we have to use an intermediate medium (heptane and water are not miscible). We chose ethanol for this purpose. As a surfactant we selected Triton X-405 (*t*-octylphenoxy-polyethoxyethanol with the average number of $-CH_2CH_2O-$ groups equal 30 and $\bar{M}_n$ = 1 550). We did try to hydrolyze microspheres with KOH in an ethanol or after transferring them (via ethanol containing Triton X-405) to water with 1% Triton X-405. The second method was found to be not suitable because in the KOH solution in water (pH adjusted to 11 and/or 13) microspheres aggregated irreversibly shortly after beginning of hydrolysis (within 10 to 20 min). The best results were obtained when hydrolysis was carried out in ethanol. The typical reaction mixture consists on addition of 50 μl of 1 M KOH in ethanol and 75 μl of suspension of microspheres (c = 5 wt%) in ethanol solution of Triton X-405 (2 wt%) to 1 ml of ethanol solution of Triton X-405 (2%). After the required time the microspheres were transferred to a phosphate buffer (pH = 7.5) containing Triton X-405. Diameters of particles in supension were measured by dynamic light scattering.

Dependence of poly(CL) microsphere diameters in suspension on time of hydrolysis is illustrated in Figure 7. From the plot in Figure 7, it follows that for time periods up to 100 min the basic hydrolysis did not affect diameters of particles either by decomposition or aggregation. After longer hydrolysis times microsphere aggregation was observed (diameters of particles exceeded 1 μm.

It was important to find out the lowest concentration of Triton X-405 at which suspensions of microspheres are still stable. Thus, poly(CL) microspheres were partially hydrolyzed in ethanol, according to the protocol described above, with concentrations of

Downloaded by UNIV OF GUELPH LIBRARY on October 31, 2012 | http://pubs.acs.org
Publication Date: September 24, 1998 | doi: 10.1021/bk-1998-0709.ch011

Triton X-405 varied from 0.1 to 3 wt%. After 45 min of hydrolysis microspheres were transferred into borate buffers (pH = 10) with the same concentrations of Triton X-405 as those in ethanol solutions used for hydrolysis. The dependencies of diameters of microspheres (measured 1 h, 30 h, and 1 week after transferring them to the buffer) on concentration of surfactant are shown in Figure 8. From this plot it is evident that for concentrations of Triton X-405 which are higher than 0.2 wt% the poly(CL) microspheres did not aggregate.

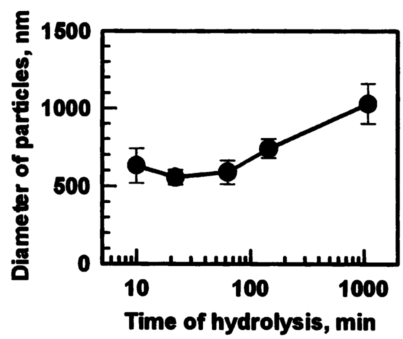

Figure 7 Dependence of diameter of poly(CL) microspheres suspended in ethanol on time of hydrolysis. Diameters determined after transferring microspheres into phosphate buffer (pH = 7.5).

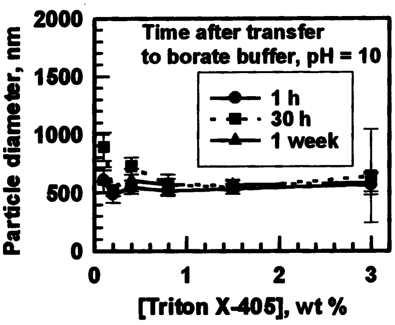

Figure 8 Dependence of diameters of poly(CL) particles on concentration of Triton X-405 during partial hydrolysis in ethanol.

Presence of carboxylic groups in the surface layers of poly(CL) and poly(L,L-Lc) microspheres subjected to partial hydrolysis during 45 min (carried out according to the recipe described previously) was detected by conductometric and pH-metric titration. In the case of partially hydrolyzed poly(CL) microspheres, the concentration of carboxylic groups in the surface layer of particles was found equal to $4.2 \cdot 10^{-4}$ mol/g and $3.6 \cdot 10^{-4}$ mol/g, respectively by acidic (HCl) and reciprocal basic (KOH) titrations. Acidic titration of poly(L,L-Lc) microspheres, hydrolyzed in the same manner as poly(CL) particles, gave value of concentration of carboxylic groups in the surface layer equal $1.3 \cdot 10^{-3}$ mol/g. These values are too high to be related directly to the surface of particles. For example, an assumption that all detected carboxylic groups are present on the surface would require the average distance between them equal ca 1 Å. Therefore, we have to consider that OH^- ions during hydrolysis and H^+ ions during titration diffuse into bulk of microspheres providing information also on -COOH groups which are present inside of particles. Measurements of ζ potential of poly(CL) and poly(L,L-Lc) microspheres at various pH revealed that the isoelectric point for these particles is at pH close to 3, i.e. close to pKa of carboxylic acids.

Downloaded by UNIV OF GUELPH LIBRARY on October 31, 2012 | http://pubs.acs.org
Publication Date: September 24, 1998 | doi: 10.1021/bk-1998-0709.ch011

Conclusions

- Poly(CL) and polylactide microspheres were obtained by ring-opening polymerizations of parent cyclic esters carried out in 1,4-dioxane/heptane mixtures in the presence of poly(dodecyl acrylate)-*g*-poly(ϵ-caprolactone) surface active agent.
- Poly(L,L-Lc) microspheres loaded with drug (omeprasol) were obtained directly in the polymerization process giving an example of a one pot process combining synthesis of polymer, formation of microspheres and their loading with drug.
- Crystallinity of poly(L,L-Lc) microspheres can be controlled by the required heat treatment after synthesis.
- Partial basic hydrolysis of poly(CL) and poly(L,L-Lc) microspheres, carried out in ethanol in the presence of Triton X-405, allows to obtain particles which after being transferred into the water based media give suspensions of nonagregated particles.

Downloaded by UNIV OF GUELPH LIBRARY on October 31, 2012 | http://pubs.acs.org
Publication Date: September 24, 1998 | doi: 10.1021/bk-1998-0709.ch011

Acknowledgements

This work was supported by KBN Grant 4P05F 021 10 and by French Research Ministry within the research network program between Poland, Latvia, and France.

References

1. P.Johnson, J.G.Lloyd-Jones (eds), *Drug Delivery Systems, Fundamentals and Techniques*, VCH, Weinheim, **1987**, pp. 1-282.
2. M.Rosoff (ed), *Controlled Release of Drugs: Polymers and Aggregate Systems*, VCH, New York, **1989**, pp 1-315.
3. A.J.Domb (ed), *Polymeric Site-specific Pharmacotherapy*, Wiley, New York, **1994**, pp 1-464.
4. R.J.Linhardt, in *Controlled Release of Drugs: Polymers and Aggregate Systems*, M.Rosoff (ed),VCH, New York, **1989**, p. 53.
5. J.P.Benoit, F.Puisieux, in *Polymeric Nanoparticles and Microspheres*, P.Guiot, P.Couvreur (eds), Boca Raton, FL, CRC Press, **1986**, p.137.
6. H.L.Gabelnick, *ACS Polym.Prep.*, **1990**, *31(2)*, 184.
7. T.R.Tice, F.Labrie, A.McRae-Deguerce,, D.L.Dillon, D.W.Mason, R.M.Giley, *ACS Polym.Prep.* **1990**, *31(2)*, 185.
8. Ch.G.Gebelein, M.Chapman, T.Mirza, in *Applied Bioactive Polymeric Materials*, Ch.G.Gebelein, Ch.E.Carraher, Jr., V.R.Foster, New York, N.Y., Plenum Press, **1987**, p. 151.
9. W.W.Thompson, D.B. Anderson, M.L.Heiman, *J. Controlled Release*, **1997**, *43*, 9.
10. M. Boisdron, P. Menei, J.P. Benoit, *J. Pharm. Pharmacol.*, **1995**, *47*, 108.
11. L. Chen, R.N. Apte, S.Cohen, *J. Controlled Release*, **1997**, *43*, 261.
12. J.H. Kim, I.C. Kwon, Y.H. Kim, S.B.La, Y.T. Sohn, S.Y. Jeong, *Arch. Pharm. Res.*, **1996**, *19*, 30.

13. R.L. Dunn, A.J. Tipton, G.L. Yewey, P.C. Reinhart, E.M. Menardi, J.A. Rogers, G.L. Southard, *ACS Polym. Prep.*, **1990**, *31(2)*, 189.
14. S. Staniscuaski Guterres, H. Fessi, G.Barratt, F.Puisieux, J.-P. Devissaguet, *Pharm. Res.*, **1995**, *12*, 1545.
15. E.S. Nuwayser, D.L. Williams, J.H. Kerrigan, W.A. Nucefora, J.C. Armstrong, in *Long-Acting Contraceptive Delivery Systems*, G.I. Zatuchni, A. Goldsmith, J.D. Shelton, J.J. Sciarra (eds), Harper and Row, Philadelphia, **1983**, p.64
16. D.H Lewis, T.R Tice, n *Long-Acting Contraceptive Delivery Systems*, G.I. Zatuchni, A. Goldsmith, J.D. Shelton, J.J. Sciarra (eds), Harper and Row, Philadelphia, **1983**, p.77
17. S. Cohen, A. Cochrane, E. Nardin, R. Langer, *ACS Polym. Mat. Sci. Eng.*, **1992**, *66*, 91.
18. T. Uchida, S. Goto, *Biol. Pharm. Bull.*, **1994**, *17*, 1272.
19. H.C.J. Ertl, I. Varga, Z.Q. Xiang, K. Kaiser, L. Tephens, L. Otvos, Jr., *Vaccine*, **1996**, *14*, 879.
20. H.K.Lee, J.H. Park, K.C. Kwon, *J. Controlled Release*, **1997**, *44*, 283.
21. T.L.Whateley, *Microencapsulation of Drugs*, Harwood Acad. Publ., Chur, **1992**, 1-306
22. J.-Z. Yang, S. Antoun, R.B. Ottenbrite, S.Milstein, *J. Bioact. Compat. Polym.*, **1996**, *11*, 219.
23. J.-Z.Yang, M. Wang, R.M. Ottenbrite, S.Milstein, *J. Bioact. Compat. Polym.*, **1996**, *11*, 236.
24. S.Sosnowski, M.Gadzinowski, S.Slomkowski, S.Penczek, *J. Bioact. Compat. Polym.*, **1994**, *9*, 345.
25. Polish Acad.Sci., Center Mol.Macromol.Studies, Polish patent, PL 171136 B1, **1993**
26. S.Sosnowski, M.Gadzinowski, S.Slomkowski,*Macromolecules*, **1996**, *29*, 4556.
27. M.Gadzinowski, S.Sosnowski, S.Slomkowski, *Macromolecules*, **1996**, *29*, 6404.
28. S.Slomkowski, *Macromol.Symp.*, **1996**, *103*, 213.
29. S.Slomkowski, S.Sosnowski, M.Gadzinowski, *Macromol. Symp.*, **1997**, *123*, 45.
30. A.Duda, Z.Florjanczyk, A.Hofman, S.Slomkowski, S.Penczek, *Macromolecules*, **1990**, *23*, 1640.
31. S.Sosnowski, S.Slomkowski, S.Penczek, Z.Florjanczyk, *Makromol. Chem.*, **1991**, *192*, 1457.
32. A.Duda, *Macromolecules*, **1994**, *27*, 576.
33. A.Duda, S.Penczek, *Macromolecules*, **1993**, *23*, 1636.
34. S.Penczek, A.Duda, S.Slomkowski, *Makromol.Chem., Macromol.Symp.* **1992**, *54/55*, 31.
35. J. Senn-Bilfinger, U. Krüger, E. Sturm, V. Figala, K. Klemm, B. Kohl, G. Rainer, H. Schaefer, T.J. Blake, D.W. Darkin, R.J. Ife, C.A. Leach, R.C. Mitchell, E.S. Pepper, C.J. Salter, N.J. Viney, G. Huttner, L. Zsolnai, *J. Org. Chem.*, **1987**, *52*, 4582.
36. U. Krüger, . Senn-Bilfinger, E. Sturm, V. Figala, K. Klemm, B. Kohl, G. Rainer, H. Schaefer, T.J. Blake, D.W. Darkin, R.J. Ife, C.A. Leach, R.C. Mitchell, E.S. Pepper, C.J. Salter, N.J. Viney, *J. Org. Chem.*, **1990**, *55*, 4163.
37. H.Tsui, F.Horii, M.Nagakawa, Y.Ikada, H.Odani, R.Kitamaru, *Macromolecules*, **1992**, *25*, 4114.
38. K.A.M. Thakur, T.T. Kean, J.M. Zupfer, N.U. Buehler, M.A. Doscotch, E.J. Munson, *Macromolecules*, **1996**, *29*, 8844.

Downloaded by UNIV OF GUELPH LIBRARY on October 31, 2012 | http://pubs.acs.org
Publication Date: September 24, 1998 | doi: 10.1021/bk-1998-0709.ch011

Downloaded by MONASH UNIV on October 31, 2012 | http://pubs.acs.org
Publication Date: September 24, 1998 | doi: 10.1021/bk-1998-0709.ch012

Chapter 12

Novel Bioadhesive Complexation Networks for Oral Protein Drug Delivery

A. M. Lowman[1], Nicholas A. Peppas[2], M. Morishita[3], and T. Nagai[3]

[1]Department of Chemical Engineering, Drexel University, Philadelphia, PA 19104
[2]School of Chemical Engineering, Purdue University, West Lafayette, IN 47907-1283
[3]Department of Pharmaceutics, Hoshi University, Tokyo, Japan

Copolymer networks of poly(methacrylic acid) grafted with poly(ethylene glycol), which exhibit pH-sensitive swelling behavior due to the reversible formation/dissociation of interpolymer complexes, are investigated as potential carriers for protein drugs. The ability of these gels to serve as oral carriers for proteins was examined. The release kinetics of insulin from complexed and uncomplexed gels was studied. The rate of insulin release from the gels was strongly dependent on the pH of the environmental fluid and the copolymer composition. Because of interpolymer compelxation, the release rate of the drug in acidic fluids simulating the conditions of the stomach was an order of magnitude greater than the release rate in fluids simulating that of the upper small intestine. Additionally, these materials exhibit favorable bioadhesive characteristics for oral protein delivery. The mucoadhesive interactions were significantly stronger between the highly swollen, uncomplexed gels and the mucosa.

Two problems exist in developing oral delivery systems for peptides and protein drugs, such as insulin. The major problem is the inactivation of the sensitive drugs by proteolytic enzymes in the gastrointestinal (GI) system, mainly in the stomach and the proximal regions of the small intestine (*1-5*). This can be overcome by designing carriers which can protect the insulin from the harsh environments of the stomach before releasing the drug into more favorable regions of the GI tract, specifically the upper small intestine or the colon (*1-7*). Additionally, researchers have attempted to incorporate protease inhibitors into oral formulations which serve to prevent degradation of the sensitive drug by the proteolytic enzymes (*4,5,8*).

The other major problem is the slow transport of the macromolecular drugs across the lining of the colon into the blood stream. Researchers have attempted to bypass this hurdle with the addition of compounds known as absorption enhancers which aid the transport of macromolecules across boundaries (*4,5*).

In Tailored Polymeric Materials for Controlled Delivery Systems; McCulloch, I., et al.;
ACS Symposium Series; American Chemical Society: Washington, DC, 1998.

We have experimented with a delivery system consisting of microparticles of crosslinked copolymers of poly(methacrylic acid) which are grafted by ethylene glycol (P(MAA-g-EG)) and contain insulin. These new systems function because the structure of the copolymers exhibits pH sensitive swelling behavior due to the reversible formation of interpolymer complexes stabilized by hydrogen bonding between the protons of the carboxylic acid group and the etheric groups on the grafted chains (*9*). The formation of the interpolymer complexes also serves to stabilize the insulin (*10,11*). Additionally, the presence of the PEG grafts helps maintain the biological activity of the insulin by stabilizing the drug and preventing binding to ionizable backbone chain (*12*). Complex formation in the insoluble copolymers is sensitive to the nature and pH of the surrounding fluid as well as the copolymer composition and graft chain length (*9*). In the acidic environment of the stomach, the gels are in the complexed state. Under these conditions insulin cannot readily diffuse through the membrane because of the small pore size, ξ, and is therefore protected from the harsh environment of the stomach. As the particles pass the stomach into the intestine, the environmental pH increases above the transition pH of the gel. The complexes immediately dissociate and the network pore size rapidly increases leading to the diffusive release of insulin.

Downloaded by MONASH UNIV on October 31, 2012 | http://pubs.acs.org
Publication Date: September 24, 1998 | doi: 10.1021/bk-1998-0709.ch012

Experimental Section

Material Preparation. In previous work with P(MAA-g-EG) hydrogels, the gels were prepared as films (thickness = 0.7 mm) by a solution polymerization technique (*9*). In order to increase the response of the hydrogels, it was desireable to prepare the hydrogels in the form of micron sized polymeric microparticles. Thus, P(MAA-g-EG) microspheres were prepared by a free-radical bulk, suspension polymerization.

The suspending phase, 250 ml of Silicon oil (Dow 200 fluid) was added to a three-necked flask and heated to 70° C while being agitated at 250 RPM using an overhead stirrer. A reflux condenser was attached to the flask. The flask was sealed and purged with nitrogen to ensure an inert atmosphere for the reaction vessel.

Vacuum distilled methacrylic acid (Sigma Chemical Co., St. Louis, MO) and poly(ethylene glycol) monomethacrylate containing PEG of molecular weight 1000 (Polysciences Inc., Warrington, PA) were mixed in appropriate molar ratios (20 g total monomers). The crosslinking agent, tetraethylene glycol dimethacrylate (Polysciences Inc., Warrington, PA), was added in the amount of 0.75 % moles of total monomers. Following complete dissolution of the monomers, nitrogen was bubbled through the well mixed solution for 30 minutes to remove dissolved oxygen, a free radical scavenger, which would act as an inhibitor. 2,2'-Azobisisobutyronitrile (AIBN) was added in the amount of 0.5% of the total monomers as the thermal reaction initiator. At elevated temperatures ($T > 50°$ C), AIBN degrades into a stable nitrogen molecule and two free radical containing compounds at a rate rapid enough to initiate the polymerization reaction (*13*). Poly(dimetyl siloxane-b-ethylene oxide) (Polysciences Inc., Warrington, PA) containing 25% DMS was added in the amount of 1% weight of total monomers as a surfactant to prevent microparticle aggregation during and after the reaction.

The monomer mixture was added to the oil phase, agitated at 350 rpm and allowed to react for 3 hours at 70° C. After 3 hours, the temperature was increased to 90° C and allowed to react for an additional 2 hours. Following the higher temperature reaction period, the solution was cooled to 37° C and the agitation rate was decreased to 250 RPM. Once the temperature reached 37° C, 20 ml of deionized water was added to polymer suspension and mixed for an additional 2 hours.

The suspension was allowed to settle and the oil was decanted. The reaction flask was filled with deionized water and the swollen particles were stirred for 24 hours at 100 RPM. After 24 hours, the particles were filtered and rinsed with deionized water. This process was continued until all of the silicon oil had been removed. Following the washing, the particles were stored in deionized water with the pH adjusted to 8 by the addition of NaOH

The equilibrium swelling of the particles was determined using laser light scattering. Dilute samples of particles were placed in dimethyl glutaric acid (DMGA) buffered solutions of pH = 3.2 and 7.4 and allowed to swell to equilibrium. The ionic strength was adjusted to 0.1 M with the addition of NaCl. Assuming isotropic swelling, the ratio of the volume swelling ratios in the complexed (pH = 3.2) and uncomplexed states (pH = 7.4) was determined as the ratio of the swollen diameters cubed.

Downloaded by MONASH UNIV on October 31, 2012 | http://pubs.acs.org
Publication Date: September 24, 1998 | doi: 10.1021/bk-1998-0709.ch012

Drug Loading. Drug loading was accomplished by equilibrium partitioning of the insulin into the P(MAA-g-EG) microparticles. Bovine pancreatic insulin (10 mg, 27.6 IU/mg, MW 5,743, Sigma Chemical Company, St. Louis, MO) was dissolved in 200 μl of 1 N HCl. The insulin solution was diluted with 20 ml of phosphate buffer solution (pH = 7.4) and normalized with 200 μl of 0.1 N NaOH. Loading was accomplished by soaking 150 mg of dry P(MAA-g-EG) microparticles, which had been dried under vacuum at 37° C, for 24 hours in the insulin solution. Additionally, some of the solutions included 5% weight aprotinin, a protease inhibitor. The concentration of insulin in the solution was monitored over time using HPLC. The particles were then filtered and washed with 100 ml of 0.1 N HCl solution to collapse the microparticles and "squeeze out" the remaining buffer solution. The drug loaded microspheres were dried under vacuum and stored at 4° C. The degree of loading was determined from HPLC analysis of the insulin concentrations of the initial solutions and the filtrate from the washings.

***In Vitro* Release Studies.** The *in vitro* release of insulin from P(MAA-g-EG) microspheres was also studied. Dry, insulin loaded polymer microparticles were swollen in 200 ml fluid of pH 1.2 and ionic strength of 0.1 M (simulated gastric fluid) for 2 hours and agitated at 125 RPM. The polymer microparticles were then transferred to pH = 6.8 phosphate buffered saline solutions. Samples were taken at discrete intervals and the insulin concentration in the solutions was monitored using HPLC.

Mucoadhesion Studies. Films of P(MAA-g-EG) (thickness = 0.9 mm) were prepared using a solution polymerization technique described previously (*9*). These copolymers contained equimolar amounts of MAA and EG and PEG grafts of molecular weight 1000. The copolymers were swollen to equilibrium in DMGA buffered saline solutions of pH = 3.2 and 7.4. Upon reaching equilibrium, the swollen gels were cut into disks with diameters of 19 cm. The polymer samples were adhered to the upper holder of a tensile tester (Instron Model 4301, 10 N load cell, Park Ridge, IL) at 25° C and 90% RH using cyanoacrylate medical adhesive, whereas a sample of gelled bovine submaxillary mucin (Sigma, St. Louis, MO) was affixed on the lower jaws. The two jaws were brought together for 15 min to allow for equilibration and then separated at 1 mm/min. The detachment force was measured as a function of displacement.

Results and Discussion

Equilibrium Swelling of Polymer Microparticles. The equilibrium volume swelling ratios of the polymer microspheres were determined using laser light scattering. The average diameter for swollen P(MAA-g-EG) microspheres containing a 1:1 MAA/EG ratio and graft PEG chains of molecular weight 1000 swollen in pH = 3.2 DMGA buffered solution was 10 ± 4 μm. The diameter for the microspheres swollen in pH = 7.4 buffer solution was 30 ± 12 μm. Assuming isotropic swelling, the ratio of the volume swelling ratios in the two states (Q_{uncom}/Q_{com}) was 30. The similar ratio for hydrogels prepared as films using a photo-initiated solution polymerization was 15. Thus, a greater transition existed between the uncomplexed and complexed states for the microparticles prepared by the suspension polymerization technique.

Downloaded by MONASH UNIV on October 31, 2012 | http://pubs.acs.org
Publication Date: September 24, 1998 | doi: 10.1021/bk-1998-0709.ch012

***In Vitro* Release Results.** The pulsatile release of insulin from P(MAA-g-EG) microparticles of different concentrations and PMAA microparticles is shown in Figure 1. For all of the gels studied, the rate of insulin release was significantly lower in the lower pH solution. Under these conditions, the PEG containing gels were in the collapsed state due to the formation of interpolymer complexes and the hydropholic nature of the gel in acidic media. In the collapsed state, the additional physical crosslinks were formed and the backbone chains were in the coiled conformation. The small mesh size or pore size of the gel served to hinder the diffusion of insulin through the gel. The PMAA gels were also in the collapsed state due to the hydrophobic nature of the gel in solutions of low pH. In these samples, the small network mesh size was due to the coiling of the polymer chains because of the poor compatibility between the swelling agent and the hydrophobic polymer chains.

When the gels were transferred to the higher pH solution, the release rates of insulin increased dramatically. In all of the gels, the acidic groups were ionized and the gels were swelled rapidly due to the large swelling force generated due to ionization of the pendant groups and increases in the osmotic swelling force. In the PEG-containing copolymers, ionization resulted in the dissociation of the interpolymer complexes. The most rapid release of insulin occurred in the gels containing the greatest amounts of PEG. In these gels, the tethered PEG chains served to prevent binding of the peptide to the charged groups along the polymer backbone. In the other gels, the release rates slowed due to ionic interactions between the backbone polymer (PMAA) and the insulin.

For the case of the gels swelling in the simulated gastric fluid, the largest amount of insulin was released from the PMAA gels, in which no complexation occured (Figure 2). However, the amount of insulin released from the gels was decreased by increasing the amount of PEG incorporated into the network structure. In gels containing PEG, interpolymer complexes formed in the gels swollen in pH = 1.2 solution. Due to the formation of complexes, the network mesh size was reduced resulting in a significant decrease in rate of release of the drug from the gels.

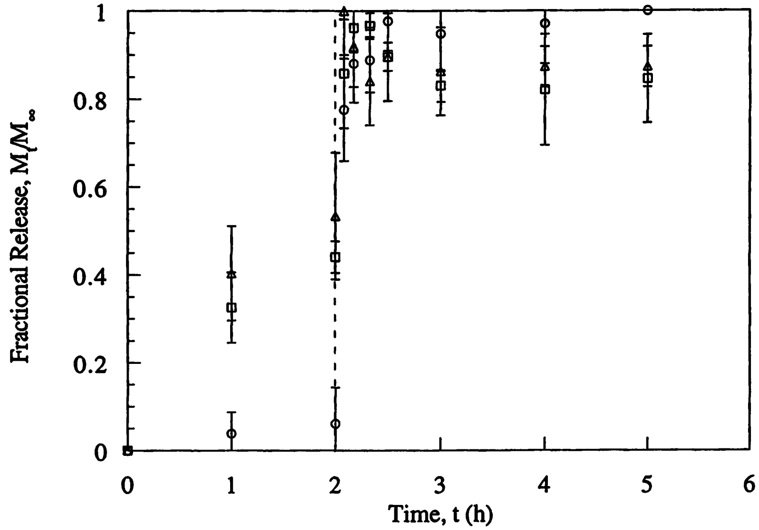

Figure 1. Pulsatile release of insulin *in vitro* from P(MAA-g-EG) microparticles containing graft PEG chains of molecular weight 1000 and MAA/EG ratios of (○) 1 and (□) 4 in simulated gastric fluid (pH = 1.2) for the first two hours and phosphate buffered saline solutions (pH = 6.8) for the remaining three hours at 37° C. The release from P(MAA) microparticles is represented by ▲.

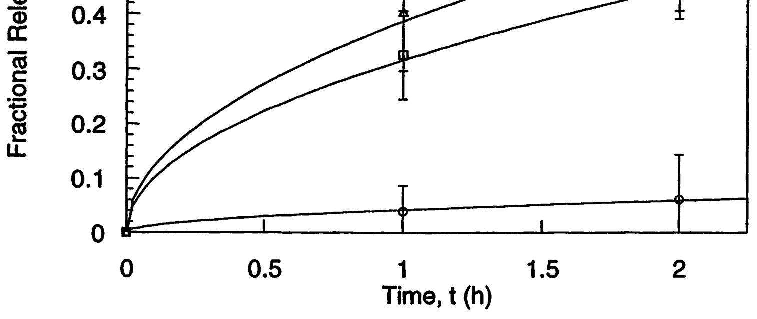

Figure 2. Controlled release of insulin *in vitro* from P(MAA-g-EG) microparticles containing graft PEG chains of molecular weight 1000 and MAA/EG ratios of (○) 1 and (□) 4 in simulated gastric fluid (pH = 1.2) at 37° C. The release from P(MAA) microparticles is represented by ▲.

Downloaded by MONASH UNIV on October 31, 2012 | http://pubs.acs.org
Publication Date: September 24, 1998 | doi: 10.1021/bk-1998-0709.ch012

Downloaded by MONASH UNIV on October 31, 2012 | http://pubs.acs.org
Publication Date: September 24, 1998 | doi: 10.1021/bk-1998-0709.ch012

Additionally, complexation was enhanced in gels containing equimolar amounts of MAA/EG and these gels had the smallest network mesh size due to the presence of the largest number of physical crosslinks in these materials. Accordingly, the least amount of insulin (< 10%) was released in the gastric fluid from gels containing a 1:1 ratio of MAA/EG.

In designing a device for oral delivery of a protein drug, it is important to protect the drug in the stomach and release the drug into the more favorable regions of the GI tract. Therefore, in an effective carrier the release rates and diffusion coefficients will be significantly greater in neutral or basic conditions than acidic conditions. One significant parameter in evaluating the viability of a particular hydrogel for oral delivery of proteins in peptides is the ratio of the diffusion coefficients of the drug in the carrier in the stomach (acid environment) and the intestine (neutral environment). This parameter can be calculated from the Fickian expression at short times where the fractional drug released is proportional to the square root of the diffusion coefficient. Therefore, the ratio of diffusion coefficients was calculated as:

$$\frac{D_{1.2}}{D_{6.8}} = \left[\frac{(M_t / M_\infty)_{1.2}\ \Delta t_{6.8}}{(M_t / M_\infty)_{6.8}\ \Delta t_{1.2}}\right]^2 \qquad (1)$$

The ratio of diffusion coefficients for insulin in the gels is shown in Table I. The greatest change in diffusion coefficients between the two pH solutions was for the gels containing a 1:1 ratio of MAA/EG due to the formation of complexes in the acidic media and the reduction of polymer/drug interactions in the high pH solution due to the presence of the PEG grafts. In these gels, the diffusion coefficients varied by greater than three orders of magnitude corresponding to greater than an order of magnitude difference in the release rate between the two solutions. In gels containing lower amounts of PEG, fewer complexes formed and increased drug/polymer binding occurred resulting in a significantly lower variation in release rates between the two solutions.

Table I. Ratio of diffusion coefficients of insulin in the complexed and uncomplexed hydrogels as compared to PMAA.

Composition	$D_{1.2}/D_{6.8}$
1:1 MAA/EG	1.79×10^{-3}
4:1 MAA/EG	0.152
PMAA	0.359

Mucoadhesive Behavior of P(MAA-g-EG) Hydrogels. The primary goal of bioadhesive controlled drug delivery is to localize a delivery device within the body to enhance the drug absorption process in a site-specific manner (*14-17*). Hydrogels of P(MAA-g-EG) exhibit mucoadhesive characteristics due to the presence of the graft PEG chains which serve as adhesion promoters. Adhesion promoters, such as polymer grafts or even linear polymers, function by penetrating the gel/mucosa or gel/gel interface and forming temporary anchors (*18,19*).

The mucoadhesive characteristics of P(MAA-g-EG) hydrogels were strongly dependent on the pH of the environmental fluid (Figure 3). The work of mucoadhesion was calculated as the area under the curves for each pH value (Table II). The work of adhesion was significantly higher at the pH value of 7.4. However, to truly compare the mucoadhesive characeteristics of the gels, the work of adhesion was normalized to account for the polymer gel fraction. The normalized work of adhesion was two-orders of magnitude greater for gels in the uncomplexed state (Table II). Accordingly, the gels would adhere to the mucosa of the intestine to a much greater extent than the stomach. Therefore, the residence of time of the gels would be much greater in regions where the insulin could be absorbed.

Downloaded by MONASH UNIV on October 31, 2012 | http://pubs.acs.org
Publication Date: September 24, 1998 | doi: 10.1021/bk-1998-0709.ch012

Table II. Work of adhesion for P(MAA-g-EG) gels containing a 1:1 MAA/EG ratio and graft PEG chains of molecular weight 1000.

pH	*Work of Adhesion, $W * 10^6 (J)$*	*Polymer Volume Fraction, $v_{2,s}$*	*Normalized Work of Adhesion, $W/(v_{2,s})^{2/3} * 10^6 (J)$*
3.2	5.38	0.693	62.1
7.4	9.34	0.049	6720

The differences in the adhesive characteristics of the gels at different pH values was due to differences in the mobility of the PEG chains in each material (Figure 4). In the highly swollen, uncomplexed state, the graft PEG chains were free and readily penetrated the mucosa to serve as anchors for adhesion. In the complexed state, the graft PEG chains in the P(MAA-g-EG) formed complexes with the backbone chains and were unable to penetrate the gel/mucosa interface and form termporary anchors.

Conclusions

The rate of insulin permeation through P(MAA-g-EG) gels was strongly dependent on the pH of the environmental fluid and the copolymer composition. Because of interpolymer compelxation, the release rate of the drug in acidic fluids simulating the conditions of the stomach was an order of magnitude greater than the release rate in fluids simulating that of the upper small intestine (pH = 6.8). Addtionally, the largest change in the release rates between the two fluids was greatest for gels containing equimolar amounts of MAA/EG in which the largest number of complexes formed in acidic media.

Additionally, the interactions between the mucosa and the gel were significantly stronger when the gel was in the highly swollen, uncomplexed state. Interpolymer complexation in acidic prevented penetration of the PEG grafts through gel/mucosa interface. Under complex breaking conditions, the tethered PEG chains were able to penetrate the gel/mucosa interface and serve as anchors to promote adhesion.

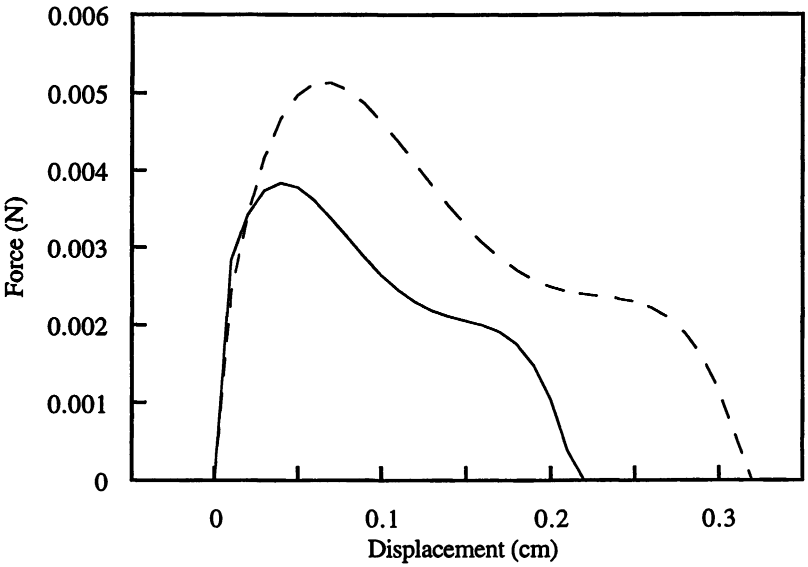

Figure 3. Adhesive behavior of P(MAA-g-EG) gels containing a 1:1 MAA/EG ratio and graft PEG chains of molecular weight 1000 at pH values of (----) 3.2 and (-- --)7.4 in contact with bovine submaxillary gland mucin.

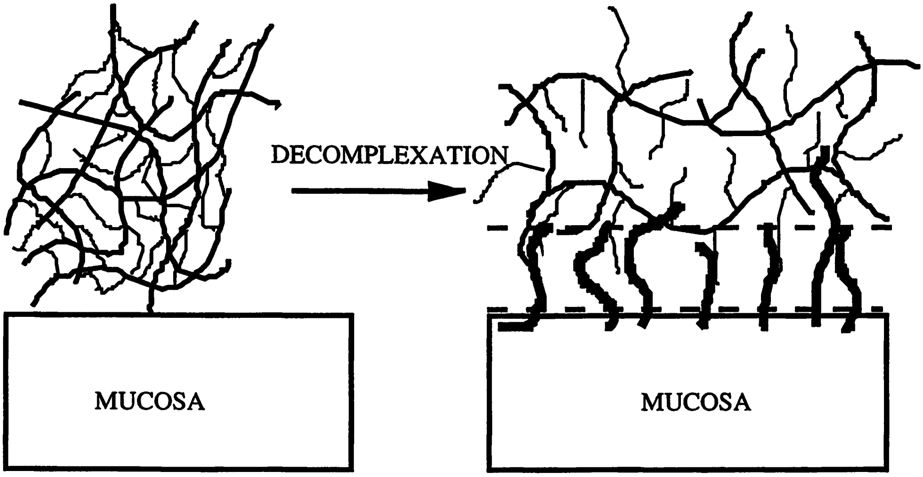

Figure 4. Proposed mechanism of adhesion between P(MAA-g-EG) hydrogels in the complexed and uncomplexed states and the mucosa.

Downloaded by MONASH UNIV on October 31, 2012 | http://pubs.acs.org
Publication Date: September 24, 1998 | doi: 10.1021/bk-1998-0709.ch012

Acknowledgments

This work was supported by grants from the National Institutes of Health and the Nagai Foundation, Tokyo.

Literature Cited

1. Saffran, M.; Sudesh Kumar, G.; Savariar, C.; Burnham, J.C.; Williams, F.; Neckers, D.C. *Science* **1986,** *233,* 1081-1084.
2. Lee, V.H.L. *Peptide and protein drug delivery;* Dekker: New York, 1991.
3. Saffran, M. Oral colon-specific drug delivery with emphasis on insulin. In *Oral Colon-Specific Drug Delivery;* Friend, D.R., Ed.; CRC Press: Boca Raton, Fla., 1992; 115-142.
4. Fix, J.A. *Pharm. Res.* **1996,** *13(12),* 1760-1764.
5. Wang, W. *J. Drug Targ.,* **1996,** *4(4),* 195-232.
6. Saffran, M.; Pansky, B.; Budd, G.C.; Williams, F.E. *J. Controlled Release* **1997,** *46,* 89-98.
7. Matiowitz, E.; Jacob, J.S.; Jong, Y.S.; Carino, G.P.; Chickering, D.E.; Chaturvedi, P.; Santos, C.A.; Vijayaraghavan, K.; Montgomery, S.; Bassett, M.; Morrel, C.; *Nature* **1997,** *386,* 410-414.
8. Langguth, P.; Bohner, V.; Heizmann, J.; Merkle, H.P.; Wolframm, S.; Almidon, G.L.; Yamashita, S. *J. Controlled Release* **1997,** *46,* 39-57.
9. Lowman, A.M.; Peppas, N.A. *Macromolecules,* **1997,** *30,* 4959-4965.
10. Bektorov, E.A.; Bimendina, L.A. *Adv. Polym. Sci.* **1981,** *41,* 99-147.
11. Samsonov, G.V. *Vysokomol. Soedin.* **1979,** *A21,* 723-733.
12. Harris, J.M. *Poly(ethylene glycol) Chemistry;* Plenum Press: New York, 1992.
13. Odian, G. *Principles of Polymerization,* 2nd ed.; Wiley: New York, 1970.
14. Lehr, C.M. *Crit. Revs. Therap. Drug Carrier Systems* **1994,** *11,* 119-160.
15. Lehr, C.M. *Europ. J. Drug Metab. Pharmacokin.* **1996,** *21,* 139-148.
16. Peppas, N.A.; Sahlin, J.J.; *Biomaterials* **1996,** *17,* 1553-1561.
17. am Ende; M.T.; Mikos, A.G. In *Protein delivery: Physical systems;* Samders, L.M., Hendren, R.N., Eds.; Plenum Press, New York, 1997; 139-165.
18. Mikos, A.G.; Peppas, N.A. In *Bioadhesive Drug Delivery Systems;* Lenaerts, V., Gurny, R., Eds,; CRC Press, Boca Raton, Fla., 1990; 25-42.
19. Sahlin, J.J.; Peppas, N.A. *J. Biomat. Sci., Polym. Ed.* **1997,** *8,* 421-436.

Downloaded by MONASH UNIV on October 31, 2012 | http://pubs.acs.org
Publication Date: September 24, 1998 | doi: 10.1021/bk-1998-0709.ch012

Downloaded by CORNELL UNIV on October 31, 2012 | http://pubs.acs.org
Publication Date: September 24, 1998 | doi: 10.1021/bk-1998-0709.ch013

Chapter 13

Shell Cross-Linked Knedels: Amphiphilic Core-Shell Nanospheres with Unique Potential for Controlled Release Applications

K. Bruce Thurmond II[1] and Karen L. Wooley[2]

Department of Chemistry, Washington University, One Brookings Drive, Campus Box 1134, St. Louis, MO 63130–4899

Shell cross-linked knedels (SCK's) are stable, covalently bound macromolecular assemblies that possess spherical shape, a core-shell morphology, and nanometer dimensions. The SCK's are prepared by a three-step procedure beginning with covalent construction of an amphiphilic diblock copolymer, followed by self-assembly into a three-dimensional structure and lastly, stabilization *via* covalent cross-links within selective regions. This is reminiscent of the method by which proteins are created. The chemistry is performed in water and the SCK's contain a hydrogel-like cross-linked surface layer that surrounds a hydrophobic core. Investigation of the SCK's for encapsulation and binding applications is discussed.

There is currently a great interest in the design, formation, and development of novel polymeric systems, including dendrimers, polymer micelles, etc. The motivation for the creation of novel three-dimensional macromolecular architectures comes from the ability of structures to affect properties, which then leads to different functions. It is not the goal of this chapter to debate which of these materials is the best or holds the most promise, but rather to provide information on the preparation, characterization, and potential applications of cross-linked polymer micelles, specifically shell cross-linked knedels (SCK's) (*1*).

Polymer micelles (*2-5*) consist of block copolymer chains that form a micellar structure in a selective solvent for one block or in solvent mixtures that have differing solubilities for the different blocks. Micellar systems exist in a constant dynamic equilibrium between mono- and multi-molecular micelles and in each case the micelle maintains a core-shell morphology, where the soluble block shields the insoluble portion from the solvent system. The ability to control or change the

---

[1] Current address: Monsanto Company, 800 North Lindbergh Boulevard, St. Louis, MO 63167.
[2] Corresponding author.

In Tailored Polymeric Materials for Controlled Delivery Systems; McCulloch, I., et al.;
ACS Symposium Series; American Chemical Society: Washington, DC, 1998.

Downloaded by CORNELL UNIV on October 31, 2012 | http://pubs.acs.org
Publication Date: September 24, 1998 | doi: 10.1021/bk-1998-0709.ch013

morphology allows for production of an assortment of polymeric micelle structures (*6,7*). Changes in the solvent system, the block copolymer content, or the ratios of the polymeric blocks leads to changes in the core, the shell, the surface, and the interface between the core and the shell thus providing some degree of control over these systems. The properties of the core and the shell enable encapsulation of molecules and subsequent release, which allows for polymer micelles to be studied as agents for pharmaceutical delivery. A variety of potential applications may be envisioned for these systems including areas such as drug delivery (*8*), gene therapy (*9*), and encapsulation technologies (*10-12*).

Polymer micelles are stable systems at concentrations above their critical micelle concentration (cmc), but destruction of the system once going below this concentration may be of great concern when trying to apply these systems. In addition to concentration effects upon polymer micelle structures, deformation can result under the action of shear forces. Nevertheless, the use of polymer micelles for *in vivo* drug delivery has been reported (*8*). For example, an anti-tumor drug, adriamycin, was covalently-attached to the poly(aspartic acid) block, PASP, of a block copolymer composed of poly(ethylene oxide), PEO, and PASP. Formation of the micelle with PASP-adriamycin nucleating to form the core of the polymer micelle was then carried out. Release of the adriamycin was accomplished by cleavage from the PASP chains making up the core. PEO is commonly used in the shell of polymeric micelles (*10,11*) and on the surface of cationic liposomes (*13*) for biological (*in vivo*) applications (*14*), because of its flexibility, high hydration, resistance to proteins through the steric exclusion mechanism, and its strong hydrogen bonding character, which may be important at the interface between the polymer micelle and the target site (*8*).

The properties of the polymer micelle core are also very important. Using polymer micelle systems with glassy cores (high T_g) can stabilize the multi-molecular micelles and prevent destruction of the micelles that can occur upon infinite dilution under *in vivo* conditions (*8*). However, such a high T_g and an impenetrable core may not be conducive to the loading or the release of guest molecules.

The emphasis here is on static SCK structures, which possess mechanical stability and also are not affected by changes in concentration. The design of these materials has gained much from the in-depth studies of polymer micelle synthesis, characterization, structure, and function. The SCK's are polymer micelles containing covalent cross-links that serve to reinforce the micellar architecture. The preparation of such structures requires only a three step approach: synthesis of a functionalized diblock copolymer, self-assembly into a micellar structure, and cross-linking the polymer chains to form a stable, covalently bound particle system as seen in Figure 1.

Examples of cross-linked polymer micelle systems in which the core is cross-linked have been reported with particle sizes typically between 0.02 and 1 µm (*15-18*). These materials contain hydrophobic polystyrene shells, which limits them to non-biological applications. Although core cross-linked micro- and nanoparticles are useful systems, the focus of this chapter is on polymer micelles with a hydrophobic polystyrene (PS) core and a cross-linked, hydrophilic, quaternized poly(4-vinylpyridine) (PVP) shell. These materials maintain water solubility and should provide additional volume in the non-cross-linked core for uptake or encapsulation of small molecules, thus allowing the SCK's to be envisioned for a variety of biological applications.

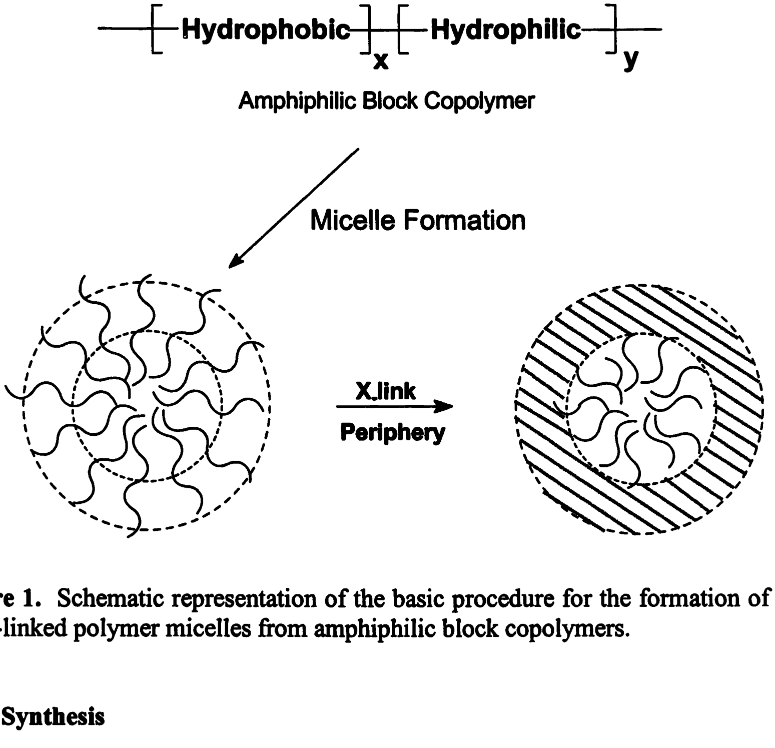

Figure 1. Schematic representation of the basic procedure for the formation of shell cross-linked polymer micelles from amphiphilic block copolymers.

Downloaded by CORNELL UNIV on October 31, 2012 | http://pubs.acs.org
Publication Date: September 24, 1998 | doi: 10.1021/bk-1998-0709.ch013

SCK Synthesis

The preparation of the SCK's begins by synthesizing the diblock copolymer, polystyrene-*b*-poly(4-vinylpyridine) (PS-*b*-PVP), under anionic conditions. Three different block copolymers were formed with PS:PVP ratios of 1:2, 1:1, and 2:1, and with molecular weights of 20700, 14600, and 14400, respectively. A percentage, 15% to 50%, of the pyridyl groups were quaternized with *p*-chloromethylstyrene to provide hydrophilicity to the VP portion of the block copolymer and to introduce the cross-linkable sites along the hydrophilic segment. The quaternized block copolymer was dissolved in a mixture of 30% tetrahydrofuran/H_2O at concentrations that allowed for formation of the polymer micelle. Under these conditions, the hydrophobic PS nucleated to form the core and the quaternized hydrophilic PVP comprised the surrounding shell. After formation of the polymer micelle, cross-linking through the *p*-chloromethylstyrene groups was carried out using a water-soluble radical initiator, 4,4'-azo*bis*(4-cyanovaleric acid), and irradiating for 24 hours. Polymerization of the styrene side groups along the VP chains resulted in cross-links within the shell and formation of the SCK's, Figure 2.

Following cross-linking, no cmc was detectable by pyrene excitation spectroscopy and the SCK's maintained spherical shape upon adsorption onto a mica substrate as observed by atomic force microscopy (AFM) (*19*). In contrast, polymer micelles exhibited cmc's at ~10^{-7} M and experienced severe deformation (flattening) upon mica. The SCK's were determined by AFM to be of narrow size dispersities with average diameters between 5 and 30 nm, depending upon the makeup of the SCK (*20*). For example, increasing relative hydrophobicity gave SCK's with increasing diameters, where the 1:2, PS:PVP block copolymers resulted in SCK's with average diameter of 9 ± 3 nm, the 1:1, PS:PVP gave 15 ± 2 nm, and the 2:1, PS:PVP system was 27 ± 5 nm.

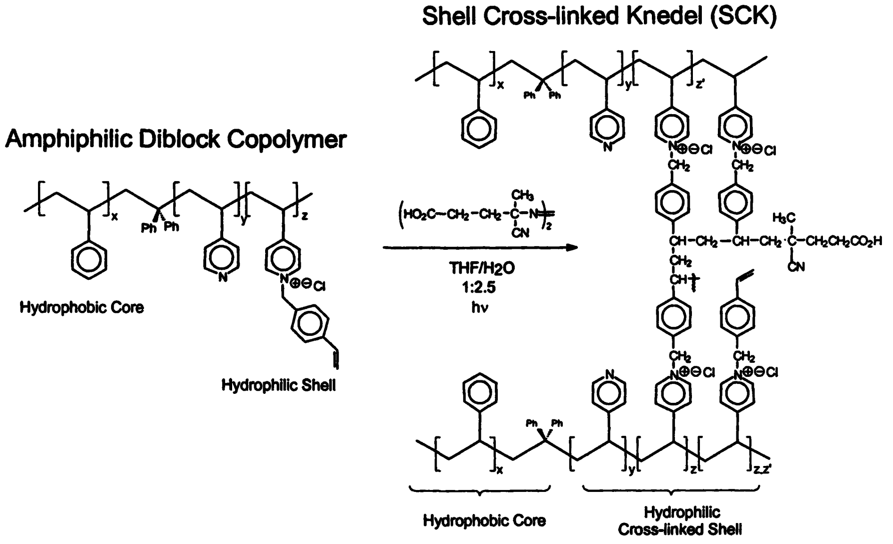
Shell Cross-linked Knedel (SCK)
Amphiphilic Diblock Copolymer
Hydrophobic Core
Hydrophilic Shell
THF/H2O
1:2.5
hv
Hydrophobic Core
Hydrophilic Cross-linked Shell

Figure 2. Chemistry involved in the synthesis of a shell cross-linked knedel (SCK), in which polystyrene comprises the core and the cross-linking is accomplished by radical polymerization of styrenyl side groups along the backbone of poly(4-vinylpyridine) located in the polymer micelle outer-shell.

The SCK's are a diverse material with a high degree of tailorability of the macromolecular structure and composition (Figure 3). It is possible to alter the shell surface, the shell layer, the core, and thus the interface between the two, either by selecting different starting block copolymers, using different cross-linking reactions or modifying regions of the SCK after construction. This ability to manipulate large facets of the structure of the SCK makes for a variety of potential applications.

Downloaded by CORNELL UNIV on October 31, 2012 | http://pubs.acs.org
Publication Date: September 24, 1998 | doi: 10.1021/bk-1998-0709.ch013

Specifically, encapsulation within the hydrophobic core and binding throughout the hydrophilic shell, where charge interactions are key, have been studied.

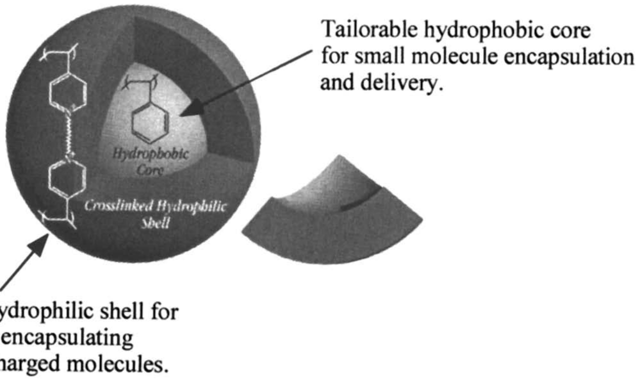

Tailorable hydrophobic core for small molecule encapsulation and delivery.

Tailorable hydrophilic shell for binding and encapsulating negatively charged molecules.

Figure 3. Schematic representation of an SCK displaying the diversity of the macromolecular structure and composition, selectively controlled within either the core domain, the shell layer, the surface, or any combination thereof.

Core Encapsulation

Excitation spectroscopy experiments showed that large hydrophobic molecules, such as pyrene, could be encapsulated within the core (*21*). Additionally, the solution-state ^{1}H NMR spectra obtained in D_2O indicated that tetrahydrofuran (THF) was able to penetrate the several nanometer thick cross-linked shell, migrate to the core, and solvate the mobile PS (*21*). A third molecule was investigated, α,γ-bisdiphenylene-β-phenylallyl radical or BDPA radical (**1**), a large hydrophobic molecule.

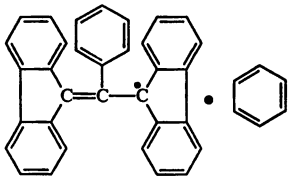

1

BDPA radical has no visually detectable solubility in a 10% THF/H_2O solution, and gives no absorbance by UV-Vis spectroscopy. However, addition of BDPA radical (10% by weight) to a solution of 10% THF/H_2O containing SCK (1:1, PS:PVP) results in complete dissolution. Encapsulation of **1** in the SCK's was also evident based upon the UV-Vis spectrum which gave a peak at 485 nm (Figure 4) and a change in color of the solution from pale yellow to a bright yellow/orange.

Downloaded by CORNELL UNIV on October 31, 2012 | http://pubs.acs.org
Publication Date: September 24, 1998 | doi: 10.1021/bk-1998-0709.ch013

Downloaded by CORNELL UNIV on October 31, 2012 | http://pubs.acs.org
Publication Date: September 24, 1998 | doi: 10.1021/bk-1998-0709.ch013

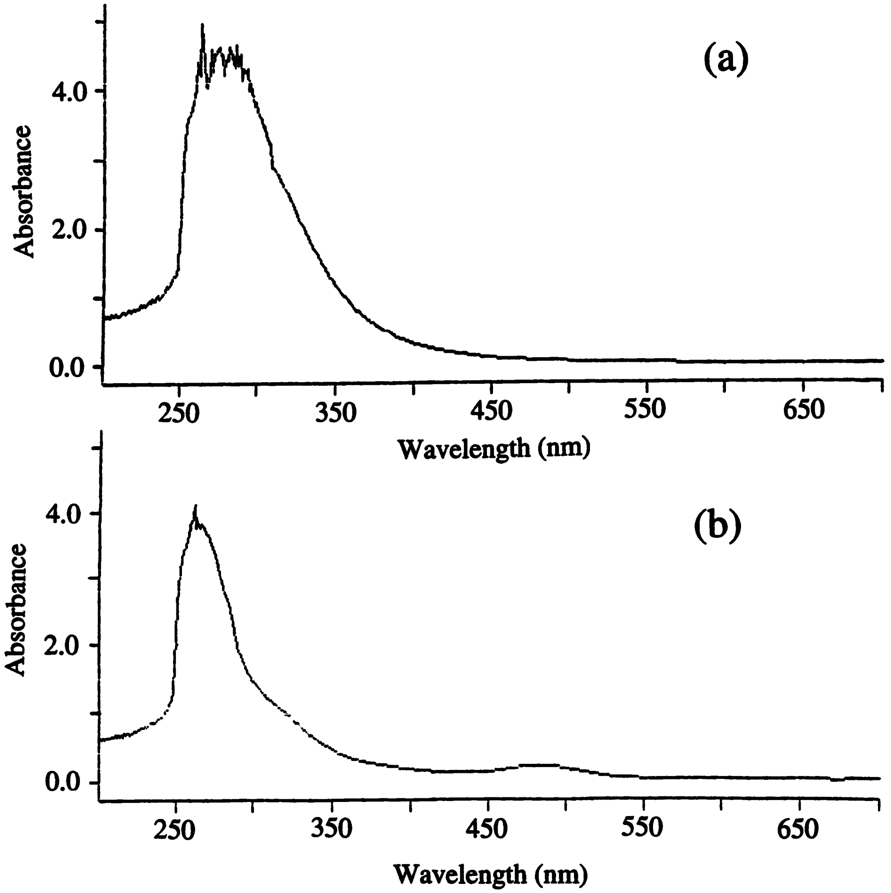

Figure 4. UV-Vis Spectra of (a) SCK and (b) SCK + BDPA radical, taken in 10% THF/H_2O.

Downloaded by CORNELL UNIV on October 31, 2012 | http://pubs.acs.org
Publication Date: September 24, 1998 | doi: 10.1021/bk-1998-0709.ch013

Shell Binding

The complexation of small molecules within the positively-charged shell layer of the SCK structure was also studied through binding interactions of SCK's with negatively charged small molecules. Specifically, the dye molecules Coomassie Blue **2** and Copper (II) phthalocyanine tetrasulfonic acid tetrasodium salt **3** were used.

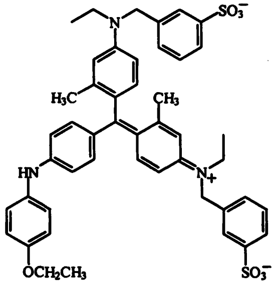

2

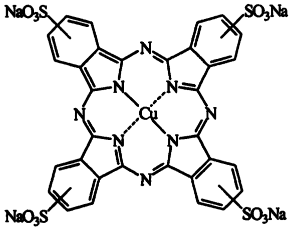

3

Binding experiments were carried out using a constant mass of SCK (PS:PVP, 1:1), 0.58 mg in 5 mL of water, and masses of dyes ranging from 0.05 - 1.1 mg. After allowing the solutions to stir for 24 h, UV-Vis spectra were obtained. The λ_{max} of **2** shifted from 585 nm in pure H_2O to 602 nm when in the presence of the SCK's, Figures 5a and 5b. This shift may be due to a solvatochromic effect upon binding of **2** to the SCK's, however, determination of binding could not be made from the UV-Vis spectra alone. Therefore, the sample was centrifuged to precipitate **2**/SCK complexes and measure the amount of dye remaining in solution, Figure 5c. The amount of binding/uptake was based upon the difference in intensities, at 602 nm for **2** and at 611 nm for **3**, of the spectra before and after centrifugation.

As shown in Figure 6, the amount of dye **2** uptake for the constant mass of SCK was plotted against the mass of the dye in the solution. The theoretical values in Figure 6 are based upon achievement of a charge balanced SCK-dye complex, which would occur at 0.43 mg **2** per 0.58 mg SCK. Charge balance can be described as the amount of dye needed to contain the same number of negative charges as there are positive charges in the SCK.

Since a constant mass of SCK was used, a plateau of uptake is expected, but as shown in Figure 6 this is not observed. The plot can be broken down into three areas, low, intermediate, and high dye concentration. There is a deviation between actual and theoretical uptake at low and high dye concentrations, but it is much more pronounced at the high masses of **2** added. At intermediate dye concentrations the actual and theoretical binding correspond rather well, Figures 5b, 5c, and 6. The hypothesis for the behavioral differences over the entire range of dye concentrations is as follows. At low dye concentrations there is not enough of **2** to form a neutral complex, thus complete precipitation does not occur and a portion of the SCK-dye complexes remain in solution, suspended by excess positive charges of the SCK's

Downloaded by CORNELL UNIV on October 31, 2012 | http://pubs.acs.org
Publication Date: September 24, 1998 | doi: 10.1021/bk-1998-0709.ch013

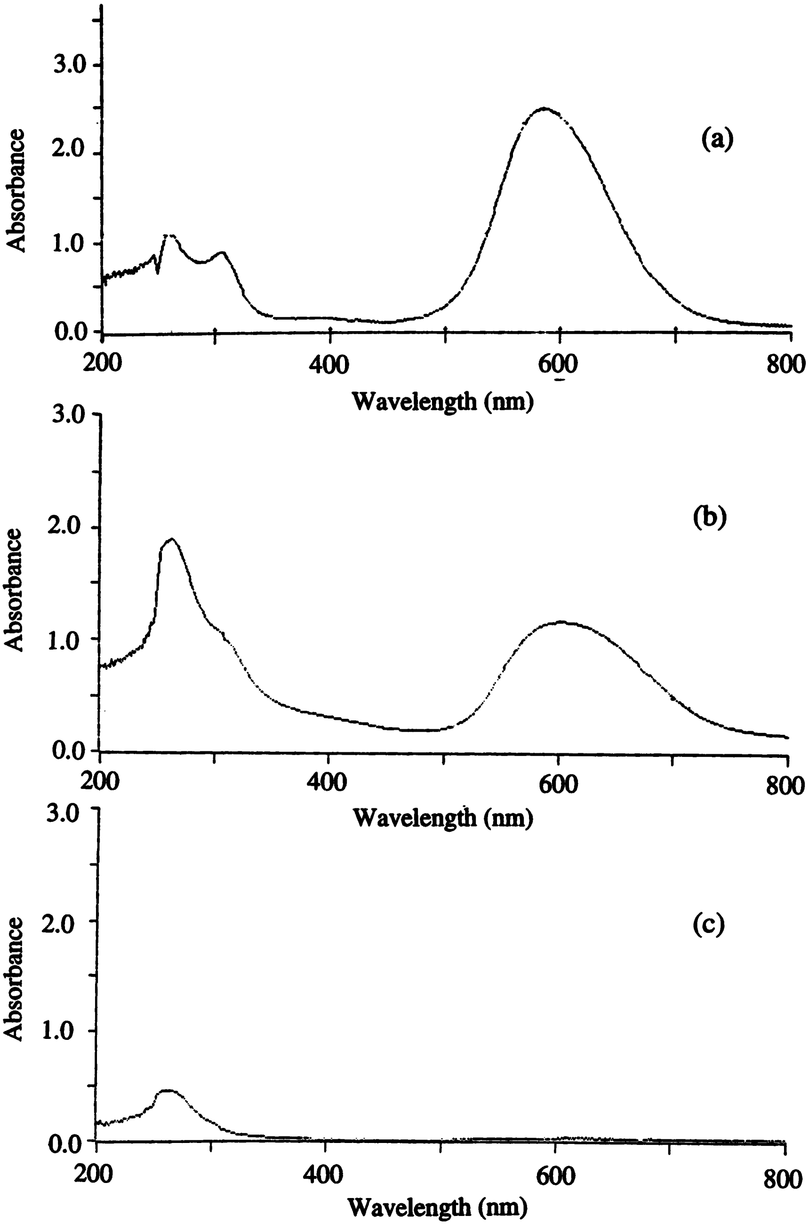

Figure 5. UV-Vis Spectra of (a) coomassie blue, **2**; (b) SCK + **2**; and (c) SCK + **2** after centrifugation, each collected in H_2O.

Downloaded by CORNELL UNIV on October 31, 2012 | http://pubs.acs.org
Publication Date: September 24, 1998 | doi: 10.1021/bk-1998-0709.ch013

(with chloride counterions). At intermediate dye concentrations, the hydrophilicity of the SCK is reduced by interaction with a significant number of the dye molecules.

This results in formation of an insoluble complex, which leads to comparable actual and theoretical binding values. At high dye concentrations the maximum uptake of **2** by the SCK is exceeded and provides an excess of **2**, which forms weak interactions with the SCK-dye complexes. This helps to maintain solubility of the SCK-dye complex to be detected by UV-Vis spectroscopy and reduce the amount of precipitate formed. Therefore, the deviation between the actual and theoretical data points is apparently observed due to the formation of soluble complexes, and the extent of SCK-dye binding is underestimated by this method. Further analysis of the complexation is in progress.

Strikingly similar data was observed when using **3** under the same conditions as the previous experiment (Figure 7). The dye molecule **3** contains two more negative charges per molecule than **2**, thus charge balance was achieved with a lesser mass. The results provide additional support for the SCK-dye complexes remaining in solution with an excess of dye or SCK, but when there are sufficient numbers of dye molecules interacting with each SCK to reduce the effective hydrophilicity, the complexes precipitate. Although these experiments do not provide quantitative measurements of binding, they do offer insight into the nature of binding and solubility properties for the complexes of SCK's with small negatively charged organic molecules. This is expected to be important for binding and release applications. For example, when an excess of negatively-charged guests bind to the SCK's, there must be differences in the binding strengths and a gradient of release kinetics may be observed. Further investigation of these behaviors is in progress.

The uptake of hydrophobic molecules within a hydrophilic system and the binding of negatively charged molecules are just two of the many unique characteristics of the SCK's. The results from these initial studies, in combination with the diversity of the SCK's structure and composition provides encouragement toward further evaluation and development of the SCK's for controlled release applications. The shell, the core, the surface, or any combination of these may be manipulated to provide a new system tailored to the desired environment. The core can be changed from a glassy polymer to a rubbery polymer and the charge within the shell can bear charges or be neutral (*22*). This allows for control of the shell surface as well as the interface between the core and the shell. The SCK's are prepared by a simple self-assembly process, but they possess increased stability over polymer micelles because of the covalent linkages between the polymer chains. This increased stability may allow for longer and highly controlled release times and provide protection for the guest molecule when used as a carrier vehicle. Degradable cores, shells, and cross-links are being investigated for post-delivery decomposition and release. The numerous methods in which an SCK can be tailored have shown promise in preliminary studies of areas such as encapsulation, drug delivery, and DNA compaction and transfection.

Downloaded by CORNELL UNIV on October 31, 2012 | http://pubs.acs.org
Publication Date: September 24, 1998 | doi: 10.1021/bk-1998-0709.ch013

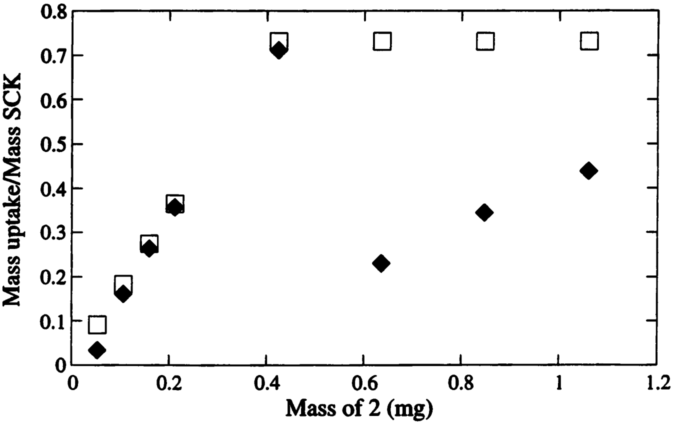

Figure 6. Plot of the mass of coomassie blue, 2, bound by the SCK (constant 0.58 mg mass in 5 mL H_2O) and precipitated as a charge balanced complex (♦), measured as the decrease in UV-vis intensity for the absorbance of 2 following binding and centrifugation. The theoretical binding (□) is based upon complete uptake of 2 until a charge balance between the dye molecules and the SCK's is reached. Deviation from theoretical values indicates that the 2/SCK complex remains suspended in the water, with excess 2 or excess SCK.

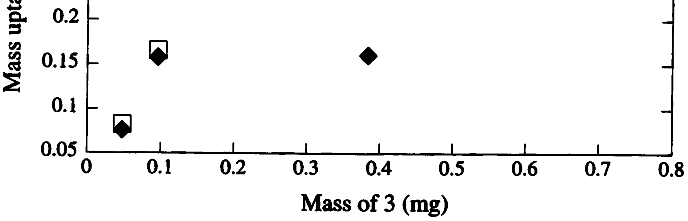

Figure 7. Plot of the mass of copper (II) phthalocyaninetetrasulfonic acid, tetrasodium salt, 3, bound by the SCK (constant 0.58 mg mass in 5 mL H_2O) and precipitated as a charge balanced complex (♦), measured as the decrease in UV-*vis* intensity for the absorbance of 3 following binding and centrifugation. The theoretical binding (□) is based upon charge balance between the dye molecules and the SCK's. Deviation from theoretical values indicates that the 3/SCK complex remains suspended in the water.

Downloaded by CORNELL UNIV on October 31, 2012 | http://pubs.acs.org
Publication Date: September 24, 1998 | doi: 10.1021/bk-1998-0709.ch013

Acknowledgements

Financial support for this work from the National Science Foundation National Young Investigator Award DMR-9458025 and Monsanto Company is gratefully acknowledged. Fellowship support (K.B.T.) was provided from the Department of Education, Graduate Assistance in Areas of National Need (P200A4014795). The authors thank Professor Tomasz Kowalewski for AFM studies and Mr. Christopher G. Clark, Jr. for structural drawings.

References:

1. (note: knedel is a Polish word to describe a dumpling-like food of filling surrounded by a dough layer; pronounced k·ned′ 'l)
2. Astafieva, I.; Zhong, X. F.; Eisenberg, A. *Macromolecules* **1993**, *26*, 7339.
3. Gao, Z.; Eisenberg, A. *Macromolecules* **1993**, *26*, 7353.
4. Qin, A.; Tian, M.; Ramireddy, C.; Webber, S.; Munk, P; Tuzar, Z. *Macromolecules* **1994**, *27*, 120.
5. Forder, C.; Patrickios, C. S.; Armes, S. P. Billingham, N. C. *Macromolecules* **1996**, *29*, 8160.
6. Zhang, L.; Eisenberg, A. *Science* **1995**, *268*, 1728.
7. Spatz, J. P.; Mößmer, S.; Möller, M. *Angew. Chem. Int. Ed. Engl.* **1996**, *35*, 1510.
8. Kataoka, K.; Kwon, G. S.; Yokoyama, M.; Okano, T.; Sakurai, Y. *J. Controlled Release* **1993**, *24*, 119.
9. Friedmann, T.; Felgner, P. L.; Blaese, R. M.; Ho, D. Y.; Sapolsky, R. M.; Mirsky, S.; Rennie, J. *Scientific American* **June 1997**, *276* , 95.
10. Gref, R.; Minamitake, Y.; Peracchia, M. T.; Trubetskoy, V.; Torchilin, V.; Langer, R. *Science* **1994**, *263*, 1600.
11. Peracchia, M. T.; Gref, R.; Minamitake, Y.; Domb, A.; Lotan, N.; Langer, R. *J. Controlled Release* **1997**, *46*, 223.
12. Kriz, J.; Masar, B.; Doskocilova, D. *Macromolecules* **1997**, *30*, 4391.
13. Lasic, D. D. *ACS Polym. Prepr.* **1997**, *38*, 543.
14. Harris, J. M. *ACS Polym. Prepr.* **1997**, *38*, 520.
15. Procházka, K.; Baloch, M. K.; Tuzar, Z. *Makromol. Chem.* **1979**, *180*, 2521.
16. Wilson, D. J.; Riess, G. *Eur. Polym. J.* **1988**, *24*, 617.
17. Ishizu, K.; Saito, R. *Polym.-Plast. Technol. Eng.* **1992**, *31*, 607.
18. Guo, A.; Liu, G.; Tao, J. *Macromolecules* **1996**, *29*, 2487.
19. The SCK shapes were found to be spherical with equivalent height-to-diameter ratios, after deconvolution of AFM tip effects. All SCK diameters were determined as the particle heights from tapping mode AFM images of SCK's adsorbed onto mica, and were averaged over measurement of *ca.* 300 SCK particles.
20. Thurmond II, K. B.; Kowalewski, T.; Wooley, K. L. *J. Am. Chem. Soc.* **1997**, *119*, 6656
21. Thurmond II, K. B.; Kowalewski, T.; Wooley, K. L. *J. Am. Chem. Soc.* **1996**, *118*, 7239.
22. Huang, H.; Kowalewski, T.; Remsen, E. E.; Gertzmann, R.; Wooley, K. L. *J. Am. Chem. Soc.* **1997**, *119*, 11653.

Chapter 14

Multilayered Semicrystalline Polymeric Controlled Release Systems

Surya K. Mallapragada and Shook-Fong Chin

Department of Chemical Engineering, Iowa State University, Ames, IA 50011–2230

Downloaded by NORTH CAROLINA STATE UNIV on October 31, 2012 | http://pubs.acs.org
Publication Date: September 24, 1998 | doi: 10.1021/bk-1998-0709.ch014

Novel multilayered polymeric controlled release devices were fabricated to facilitate controlled release of one or more compounds. These devices belong to the class of crystal dissolution-controlled release systems where the change of polymer phase from crystalline to amorphous controls the release of the drug. Multilayered semicrystalline poly(vinyl alcohol) devices were developed using a completely benign technique. Metronidazole was incorporated in one layer and gentisic acid ethanolamide (GAE) in a second layer formed by a solvent casting technique. Annealing conditions were varied to control the polymer degree of crystallinity, thereby controlling the release rates of metronidazole and GAE. The added advantage of these devices is that they can incorporate larger amounts of drugs compared to single layered crystal dissolution-controlled release systems.

Multidrug therapy is recommended for treatment of several diseases, particularly in the case of patients with acquired immune deficiency syndrome. The efficacy of combinations of drugs has been tested and proved in many cases such as for the treatment of rheumatism, toxoplasmosis, pneumocytosis, and hypertension *(1-3)*. Emerging resistance of organisms to standard antibiotic therapy has forced clinicians to use combinations of drugs *(4)*.

Polymeric controlled release systems with different mechanisms for obtaining zero-order drug release or constant release rates have been investigated in the past. Such systems help to maintain concentration of drugs in the body between therapeutic limits for extended periods of time. The other advantage is that these systems typically require smaller and less frequent drug dosages than conventional formulations, thereby minimizing side-effects. The polymer carrier also serves to act as a protective carrier for drugs with very short half-lives. The fabrication of a zero-order system to release one or more drugs simultaneously is described in this paper.

Rationale

Novel multilayered semicrystalline poly(vinyl alcohol) (PVA) devices were developed for controlled release of one or more compounds. These devices were fabricated by solvent casting aqueous PVA solutions containing different drugs, layer by layer. Semicrystalline PVA systems were developed for controlled release of metronidazole and gentisic acid ethanolamide (GAE). Multilayered systems were developed in the past for controlled drug release. However, the additional layers used were largely made of material impermeable to the drug to obtain zero-order release and not as another unit to release drugs *(5, 6)*. In contrast, the multilayered PVA crystal dissolution systems fabricated were focused primarily on releasing two or more active agents simultaneously from a single device. Since different drugs were incorporated in different layers, the processing conditions for each layer could be altered to control release rates of the different drugs.

Drug release from polymeric controlled release devices can be diffusion-controlled, swelling/dissolution controlled, chemically controlled or magnetically controlled *(7)*. The multilayered controlled release devices described here fall under the category of crystal dissolution-controlled release systems *(8, 9)*, a class of phase-erosion systems *(10)*, where the rate of release of drug from the polymer matrix is controlled by the rate of change of phase from crystalline to amorphous polymer (Figure 1). The diffusion coefficient of a drug through a crystalline portion of the polymer is much lower than diffusion through an amorphous portion *(11)*. Therefore, a decrease in the degree of crystallinity of the polymer causes an increase in the diffusion coefficient of the drug. However, the concentration gradient for drug diffusion decreases as a function of time. These two compensating effects contribute to produce zero-order release of the drug in crystal-dissolution controlled systems.

In addition, these devices were fabricated with two or more layers of polymer matrix loaded with the same or different drugs. Each layer had a different initial drug concentration so as to provide zero-order release. As shown by Lee *(12)* the initial spatial concentration profile of the drug in the polymer has a pronounced effect on the release profile. These multilayered systems enable tailoring the initial drug distribution profile in the polymer in order to obtain zero-order release. These PVA devices were also fabricated using a benign annealing technique, thereby eliminating the use of toxic additives or crosslinking agents which might subsequently leach out. The initial degree of crystallinity of the polymer, which can be easily controlled by changing the annealing conditions *(13)*, influences the crystal dissolution, and thereby the rate of drug release. Multilayered systems facilitate release of larger quantities of drugs in the body without encountering problems such as uniform drying and burst release due to the drug interference with polymer crystallization, which arises in single layered systems.

Materials and Methods

Multilayered Controlled Release Devices Loaded with a Single Drug. Poly(vinyl alcohol) with $\overline{M_n}$ =64,000 (Elvanol grades, E. I. duPont de Nemours, DE) with a degree of hydrolysis of 99.8%, and polydispersity index of 2.15 was used for the experiments. Metronidazole (Sigma Chemical, St. Louis, MO), an antitrichomonal drug, and gentisic acid ethanolamide (GAE), a formulating agent, were used for the release studies.

Two 10 % (w/v) aqueous solutions of PVA containing 2 wt% and 4 wt% metronidazole were prepared. Film samples of thickness 0.05 mm were prepared by casting the polymer solution containing the 4 wt% drug on siliconized glass plates and drying them at room temperature for 2 days. The films were crystallized by annealing at temperatures ranging from 90°C to 130°C and for various times ranging from 10 minutes to 1 hour. Samples of size 1 sq. cm were cut and coated with polymer solution containing 2 wt% metronidazole and allowed to dry at room temperature for 2 days. The multilayered sample was crystallized again by annealing at temperatures ranging from 90°C to 130°C for various times. In some cases, the

Downloaded by NORTH CAROLINA STATE UNIV on October 31, 2012 | http://pubs.acs.org
Publication Date: September 24, 1998 | doi: 10.1021/bk-1998-0709.ch014

sample was not crystallized prior to coating. Therefore, two kinds of samples - those that were crystallized only after coating (single-crystallized) and those that were crystallized twice (double-crystallized), were formed. The procedure was extended to make triple-crystallized samples made up of three layers of polymer containing the drug, to extend release periods and release larger amounts of the drug.

Multilayered Controlled Release Devices Loaded with Two Compounds. Two 10 % (w/v) aqueous solutions of PVA containing 4 wt% of metronidazole and 4 wt% of GAE, respectively were prepared. Films of thickness 0.05 mm were prepared by casting the PVA solution containing metronidazole on siliconized glass plates and drying them at room temperature for 2 days. The films were crystallized by annealing at temperatures ranging from 90°C to 130°C for various times. Samples of size 1 sq. cm were cut and coated with PVA solution containing GAE and allowed to dry at room temperature. The multilayered polymer samples loaded with the two different compounds was crystallized a second time by annealing at the same temperature at which the inner core was initially crystallized.

Differential Scanning Calorimetry. The PVA samples were analyzed using differential scanning calorimetry (DSC). A DSC (DSC 7, Perkin-Elmer) was used to record the melting endotherm of the PVA samples. A scanning rate of 10°C/min was used to heat the samples from 30°C to 250°C. Using DSC plots, the degrees of crystallinities of the samples *(14)* annealed under different conditions were compared.

Release Studies. Release kinetics from these systems were measured *in vitro* using a United States Pharmacopoeia (USP) specified dissolution apparatus (Hanson Research, CA). Multilayered PVA samples loaded with one or two compounds were placed in baskets attached to stirring rods. The stirring rate was fixed at 20 rpm. These baskets were immersed in cells containing 500 mL of deionized water at 37°C. Metronidazole and GAE release were monitored by measuring the absorbances of the solution using an ultraviolet spectrophotometer (Model 1601, Shimadzu, Japan) at 317 nm and 294 nm respectively and at various times. Influence of parameters such as annealing temperature and time, as well as the number of layers constituting the controlled release device were investigated.

The weight of PVA dissolved was also monitored simultaneously by complexing 50 mL of the solution with 25 mL of 0.65M boric acid solution and 3 mL of 0.05M I_2/0.15M KI solution at 25 °C. The concentration of the complexed PVA in the solution was obtained by measuring the absorbance of visible light at 671 nm. From the absorbance value, the weight of PVA dissolved at regular intervals was calculated *(15)*.

Results and Discussion

All experimental points in the figures are the average values of three sets of data and the error bars represent standard deviations. Multilayered PVA based controlled release devices were found to have higher degrees of crystallinities when crystallized at higher temperatures and for longer periods of time. However, crystallization times greater than 2 hours or crystallization temperatures greater than 130°C were avoided to prevent polymer degradation. Figure 2 shows the influence of crystallization temperature on the release rate of metronidazole from two-layered double-crystallized PVA films. The sample crystallized at 120°C exhibited much faster release than the sample crystallized at 130°C, all other conditions being the same. The rate of crystal unfolding is significantly lower for films crystallized at higher temperatures *(8)*, thereby leading to slower drug release rates. During the release, the polymer degree of crystallinity dropped from about 30% to 20%, facilitating zero-order release.

Downloaded by NORTH CAROLINA STATE UNIV on October 31, 2012 | http://pubs.acs.org
Publication Date: September 24, 1998 | doi: 10.1021/bk-1998-0709.ch014

Downloaded by NORTH CAROLINA STATE UNIV on October 31, 2012 | http://pubs.acs.org
Publication Date: September 24, 1998 | doi: 10.1021/bk-1998-0709.ch014

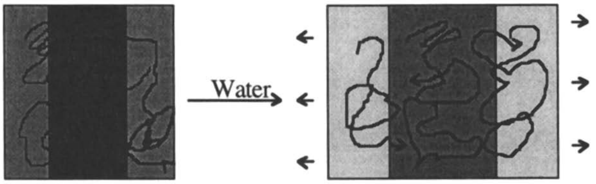

Figure 1. Schematic representation of multilayered crystal dissolution-controlled systems. Shading intensity is directly proportional to drug concentration. Folded chains represent polymer crystals.

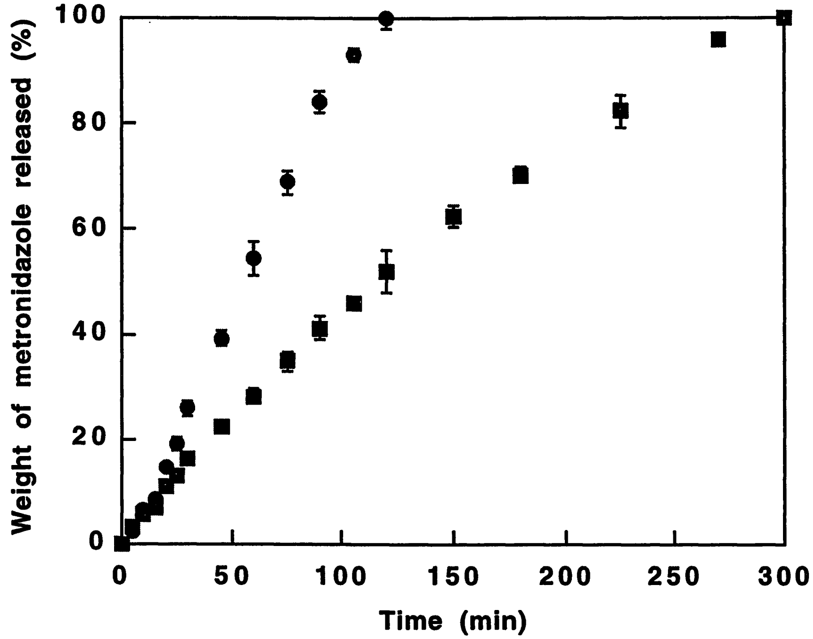

Figure 2. Percentage of metronidazole released as a function of time from a double-layered PVA sample crystallized at (●) 120⁰C for 45 minutes and (■) 130⁰C for 45 minutes.

Downloaded by NORTH CAROLINA STATE UNIV on October 31, 2012 | http://pubs.acs.org
Publication Date: September 24, 1998 | doi: 10.1021/bk-1998-0709.ch014

Double-crystallized PVA films were found to exhibit significantly lower release rates, compared to single-crystallized PVA films. This is clearly seen in Figure 3, where double-crystallized films of PVA loaded with metronidazole and crystallized at 130°C released the drug completely in 7 hours while single-crystallized films released the drug in 5 hours. Double crystallization increases the degree of crystallinity of the polymer and the size of the crystals (obtained from DSC measurements), thereby slowing the crystal-dissolution rate. This, in turn, accounts for the slower drug release rates.

Triple-crystallized films exhibited even slower release rates (Figure 4). This is to be expected because of the combination of higher degrees of crystallinities and greater resistance to drug diffusion because of the presence of an additional layer. The advantage of triple-crystallized systems is the capability of releasing greater amounts of drug using these devices without interfering with the crystallization process of the polymer or facing the solvent removal problems associated with very thick monolithic samples. In all the cases, nearly zero-order drug release was obtained because of the phase erosion mechanism of drug release and the initial drug distribution profiles.

The release kinetics of GAE from PVA devices loaded with both metronidazole and GAE are shown in Figure 5. As the crystallization temperature increased, the slope of the curve decreased, indicating a decrease in the rate of release. The sample crystallized at 130°C showed significantly slower release than the one crystallized at 120°C. The shape of the release curve for the 130°C was also non-Fickian and exhibited nearly zero-order behavior. The release of metronidazole from PVA devices containing two compounds also showed a similar dependence on crystallization conditions. As the crystallization temperature was increased, the slope of the drug release curve was found to decrease, as in the case of multilayered devices containing a single drug.

The release of GAE and metronidazole from PVA devices crystallized at 90°C is shown in Figure 6. As seen from the figure, the release of both compounds was almost simultaneous. The thickness of the layers in this case was very small and the water penetration into the polymer was very fast. As a result, there did not appear to be any significant difference between GAE and metronidazole release kinetics. This behavior was slightly altered in the case of the sample crystallized at 120°C (Figure 7) where initially, the release of GAE was slightly faster than that of metronidazole as it was present in the outer layer. In this case, since the sample was crystallized at higher temperatures, greater resistance to water penetration was expected, leading to the small difference in initial release rates. By controlling the crystallization conditions, thickness of the layers and the drug loading in each layer, the individual release of drugs from the device can be controlled. In all the cases, less than 3% of the polymer was found to have dissolved during the duration of release of the compounds.

Conclusions

Multilayered crystal dissolution-controlled release PVA systems were found to exhibit nearly zero-order release of metronidazole. The change of phase of the polymer from crystalline to amorphous was found to control the release rates of drugs from these systems. These devices were relatively easy to fabricate using benign techniques and the drug release rates could be easily controlled by changing the crystallization conditions or changing the number of polymer layers. Higher crystallization times were found to produce slower release rates. Multiple layers also slowed down the release rate from these devices. Changing drug concentration in the different layers was also found to alter the drug release profiles. Crystallizing each the individual layer before coating was found to contribute toward slowing down the drug release rate from these systems. The multilayering technique increased the amount of

Downloaded by NORTH CAROLINA STATE UNIV on October 31, 2012 | http://pubs.acs.org
Publication Date: September 24, 1998 | doi: 10.1021/bk-1998-0709.ch014

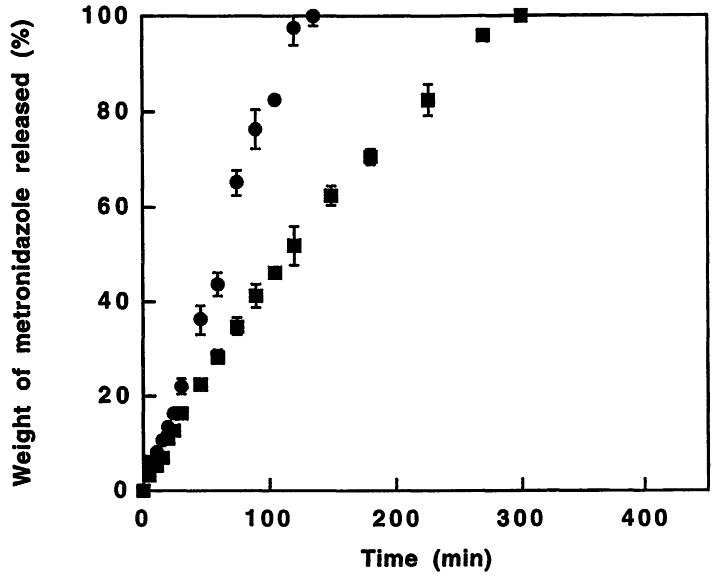

Figure 3. Percentage of metronidazole released as a function of time from a PVA sample (●) single crystallized and (■) double crystallized at 130^{0}C for 45 minutes.

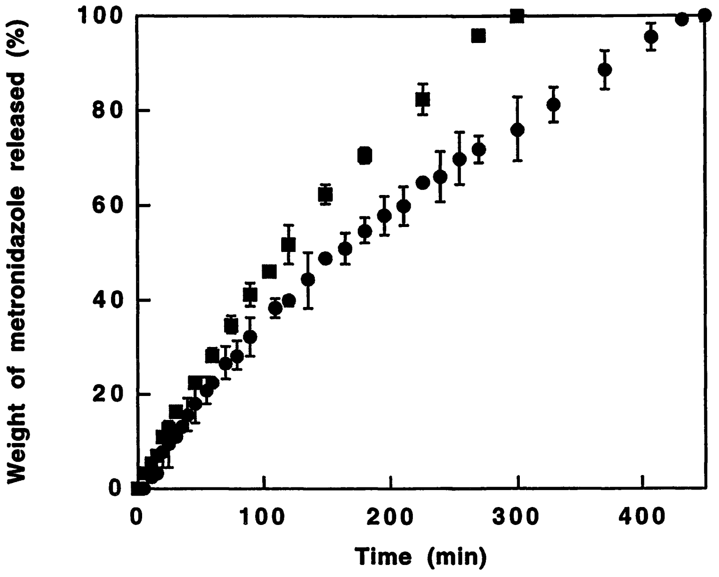

Figure 4. Percentage of metronidazole released as a function of time from a PVA sample with (■) two layers and (●) three layers.

Downloaded by NORTH CAROLINA STATE UNIV on October 31, 2012 | http://pubs.acs.org
Publication Date: September 24, 1998 | doi: 10.1021/bk-1998-0709.ch014

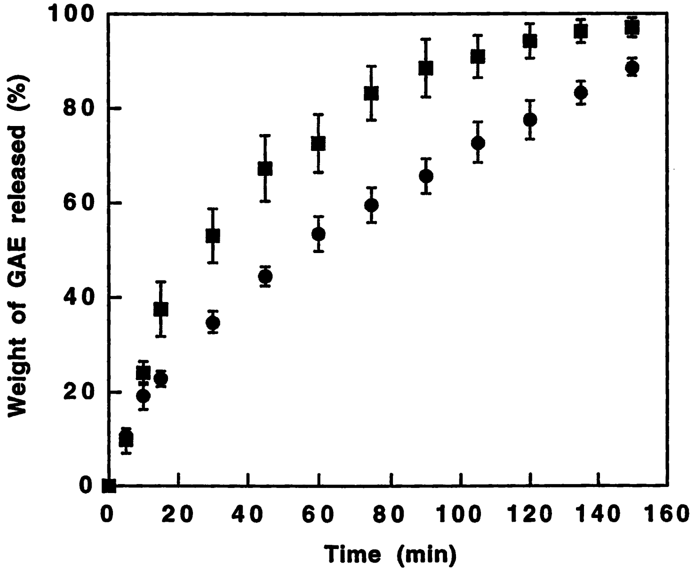

Figure 5. Percentage of GAE released as a function of annealing temperature from a PVA sample crystallized at (■) 120°C and (●) 130°C for 45 minutes.

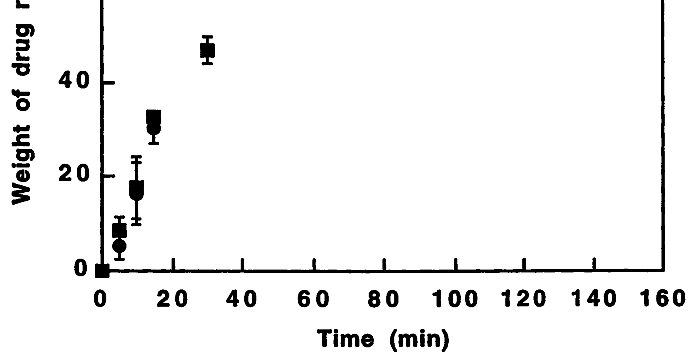

Figure 6. Percentages of (■) GAE and (●) metronidazole released from a PVA device crystallized at 90°C for 45 minutes.

Downloaded by NORTH CAROLINA STATE UNIV on October 31, 2012 | http://pubs.acs.org
Publication Date: September 24, 1998 | doi: 10.1021/bk-1998-0709.ch014

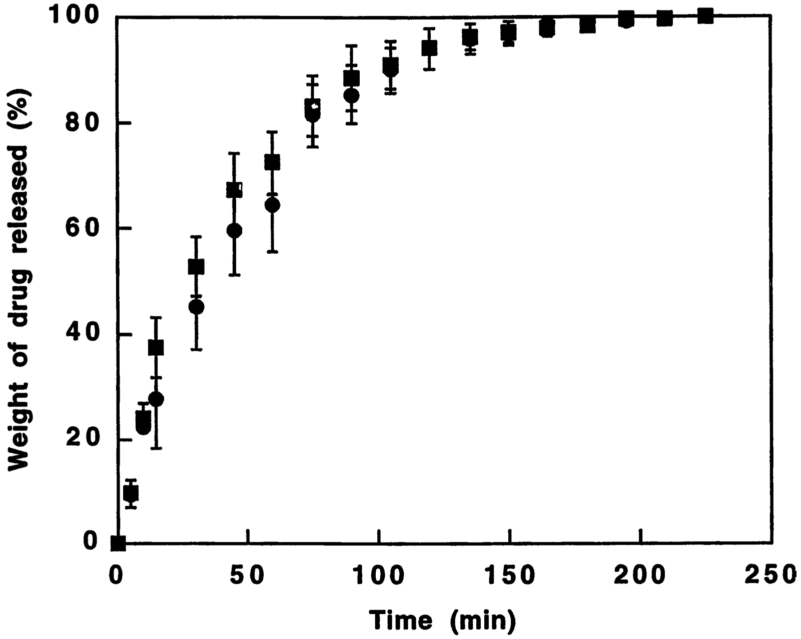

Figure 7. Percentages of (■) GAE and (●) metronidazole released from a PVA device crystallized at 120°C for 45 minutes.

drug that could be delivered from such a device without interfering with the polymer crystallization.

These multilayered systems were also used to load different compounds in the different layers. Two different compounds, GAE and metronidazole, were released simultaneously from a single device. The crystallization conditions were found to control the release kinetics of each compound and increase in crystallization temperatures led to slower release rates. The thicknesses of the two layers and the crystallization conditions of each layer can be controlled to obtain either simultaneous or staggered release of the two compounds. The same principle can potentially be extended to release more than two active substances in the body.

Acknowledgments

This work was supported partly by the Program for Women in Science and Engineering at Iowa State University. We would like to thank Melinda Madgett, Laura Marsh and Sean McDermott for their help in the laboratory.

Literature Cited

1. Yajko, D. M.; Sanders, C. A.; Madej, J. J.; Cawthon, V. L.; Hadley, W. K., *Microb. Agents Chemotherapy*, **1996**, *40*, 743.
2. Haagsma, C. J.; Reil, P. L. C. M., *Annals. Med.*, **1997**, *29*, 169.
3. Deleeuw, P. W.; Notter, T.; Zilles, P., *J. Hypertension*, **1997**, *15*, 87.
4. Roth, D. B.; Flynn, H. W. Jr., *Surv. Opthalmol.*, **1997**, *41*, 395.
5. Conte, U.; Maggi, L., *Biomaterials*, **1997**, *17*, 889-896.
6. Conte, U.; Maggi, L.; Colombo, P.; La Manna, A., *J. Contr. Rel.*, **1993**, *38*, 39-47.
7. Park, H.; Park., K., In *Polymers of Biological and Biomedical Significance*; Shalaby, W. S.; Ikada, Y.; Langer, R.; Williams, J., Eds.; ACS Symp. Ser. 540; American Chemical Society: Washington, DC, 1992; pp 2-15.
8. Mallapragada, S. K.; Peppas, N. A., *J. Contr. Rel.*, **1997**, *45*, 87.
9. Mallapragada, S. K.; Peppas, N. A.; Colombo, P., *J. Biomed. Mater. Res.*, **1997**, *36*, 125.
10. Lee, P. I., *J. Membr. Sci.*, **1980**, *7*, 255.
11. Harland R. S. ; Peppas, N. A., *Coll. Polym. Sci.*, **1989**, *267*, 218.
12. Lee, P. I., *J. Contr. Rel.*, **1986**, *4*, 1.
13. Mallapragada, S. K.; Peppas, N. A., *J. Polym. Sci. Polym. Phys.*, **1996**, *34*, 1339.
14. Peppas, N. A.; Hansen, P. J, *J. Appl., Polym. Sci.*, **1982**, *27*, 4787.
15. Baumgartner, C. E., *Anal. Chem.*, **1987**, *59*, 2716.

Downloaded by NORTH CAROLINA STATE UNIV on October 31, 2012 | http://pubs.acs.org
Publication Date: September 24, 1998 | doi: 10.1021/bk-1998-0709.ch014

Chapter 15

Electroconductive Gels for Controlled Electrorelease of Bioactive Peptides

Anthony Guiseppi-Elie, Ann M. Wilson, and Andrew S. Sujdak

Research and Development Department, ABTECH Scientific, Inc., P.O. Box 376, Yardley, PA 19067–8376

Downloaded by CORNELL UNIV on October 31, 2012 | http://pubs.acs.org
Publication Date: September 24, 1998 | doi: 10.1021/bk-1998-0709.ch015

We have synthesized highly hydrophilic, chemically responsive materials we call electroconductive gels. They are formed as an interpenetrating network of an electroconductive polymer and a hydrophilic hydrogel. Polymers were formulated form UV polymerizable hydrophilic monomer such as hydroxyethyl methacrylate (HEMA), N-[tris(hydroxymethyl)methyl] acrylamide (HMMA), and tetraethylene glycol diacrylate (TEGDA), and oxidatively polymerizable electroactive monomer such as aniline and dianiline. The hydrogel network was formed by UV-photoinitiated polymerization and the electroconductive polymer subsequently formed by chemical oxidative coupling induced by immersion in aqueous $FeCl_3$ solutions, by electropolymerization, or by a combination of these methods. Interaction between both networks was accorded by the difunctional 3-sulfopropylmethacrylate (SPM). These materials retain more electroactivity and display fast cation transport with K^+ diffusivity (D_O=5.31×10^{-7} cm^2 s^{-1}) that are an order of magnitude larger than that of electropolymerized polyaniline (D_O=3.12×10^{-8} cm^2 s^{-1}). The electroconductive polyaniline gels are shown to be more stable under ambient conditions and to efficiently imbibe and release Ca^{++} under electrostimulation.

Hydrogels have been established as controlled release materials suitable for the passive delivery of bioactive peptides (*1*). Electroconductive hydrogels are now being developed as controlled release materials for the programmable delivery of bioactive peptides to cells and tissues grown in culture. Our goal is to address the challenge of maintaining control over cell metabolism, differentiation, and proliferation by providing for the precisely controlled (quantity, timing, and duration) delivery of bioactive agents and peptides.

In Tailored Polymeric Materials for Controlled Delivery Systems; McCulloch, I., et al.;
ACS Symposium Series; American Chemical Society: Washington, DC, 1998.

These materials have been integrated into single well and 24-well controlled electrorelease cell culture vessels (*2*). These devices are suitable for the study of the potentiation of insulin secretion by HIT-T15 cells under the influence of electroreleased bradykinin (*3*).

Electroconductive polymers have emerged as field-responsive materials suitable for controlled electrorelease (*4*), as transducer-active elements in gas, chemical and biological sensors (*5*), as responsive films in solid state devices, and as mechanical actuators (*6*). Indeed, electroconductive membranes have been shown to release bioactive molecules such as adenosine-5′-triphosphate (ATP) (*7*) and the 11 amino acid peptide, insulin, as well as organic molecules such as 2,6-anthraquinone disulfonate (*8*). Electrorelease applications are based on chemically or electrochemically induced changes in oxidation state of the polymer, concomitant changes in the charge density of the material, and consequent diffusive egress of charge-neutralizing "dopants" previously held in association with the electroactive polymer. Both anionic and cationic molecules may be electroreleased (*9*). The preparation of water-containing electroconductive polymers has been generally achieved by the electropolymerization of the electroactive monomer form a solution that contained suitable anionic polyelectrolytes (*10,11*). Other types of hydrogels have been found useful in the controlled release of bioactive molecules (*12*). By formulating and/or synthesizing an electroconductive hydrogel, we believe that such a composite material will facilitate diffusion, provide a biocompatible environment for the retained bioactivity of amino acid, peptide, or protein agents, accelerate redox switching times, and offer increased loading capacity for the bioactive molecules of interest.

The electroconductive polymers of this study are interpenetrating networks of inherently conductive polymers, such as *polyaniline* or *polypyrrole,* formed within water-swellable, electrode-supported or freestanding, HEMA-based hydrogels. We conceptualize these smart materials as precursors to artificial endocrine organs, capable of delivering function-regulating peptides to cells and tissues grown in culture and hypothesize that precise quantities of bradykinin will be electroreleased into cell culture media after programmed electric pulses are delivered to the electroconductive polymer film.

Experimental

Materials. The hydrogel membranes were formulated from hydrophilic, UV-polymerizable monomer and electroactive aniline monomer. The hydrophilic and UV-polymerizable components consisted of ophthalmic grade 2-hydroxyethyl methacrylate (HEMA) (Polysciences), N-[tris(hydroxymethyl)methyl] acrylamide (HMMA) (Aldrich), poly(ethylene glycol)(200) monomethacrylate (PEG200MMA) (Polysciences), potassium salt of 3-sulfopropylmethacrylate (SPM) (Sigma), and poly-(2-hydroxyethyl methacrylate) (pHEMA) (MW = 300,000) (Polysciences). The formulation was also made to contain tetraethylene glycol diacrylate (TEGDA) which served as

Downloaded by CORNELL UNIV on October 31, 2012 | http://pubs.acs.org
Publication Date: September 24, 1998 | doi: 10.1021/bk-1998-0709.ch015

the UV-polymerizable cross-linker and 2,2-dimethoxy-2-phenylacetophenone (DMPA) which served as the photoinitiator. Aniline (An), dianiline (DAn), 3-aminopropyltrimethoxysilane (γ-APS), 3-methacryloxypropyltrimethoxysilane (γ-MPS), and dodecyltrichlorosilane were obtained form Aldrich (Milwaukee, WI). Prior to formulation, HEMA , HMMA, and TEGDA were each passed over inhibitor remover columns (Aldrich) to remove the polymerization inhibitor, hydroquinone monomethyl ether (MEHQ), purged with dry argon, and stored in dark bottles at 4°C. All other reagents were used as received. Table I shows the formulae for a typical electroconductive gel dope. To each 5 g batch of the foregoing formulation was added 20% by weight of DI water (1 g) and ethylene glycol (1 g) as mixed solvent.

Table I. Formulation of an electroconductive gel dope based on polyaniline.

Compounds in Formulation	**Mole %**	**g %**
2-Hydroxyethyl methacrylate (HEMA)	57.85	50.44
N-[Tris(hydroxymethyl)methyl] acrylamide (HMMA)	10	11.74
Poly(ethyleneglycol)(200)monomethacrylate (PEG200MMA)	5	8.78
3-sulfopropylmethacrylate (SPM)	5	8.25
Tetraethylene glycol diacrylate (TEGDA) (cross-linker)	3	6.077
Poly-(2-hydroxyethyl methacrylate) (pHEMA) 300,000	2	1.74
2,2-Dimethoxy-2-phenylacetophenone (DMPA) (photoinitiator)	2	3.43
Aniline (An)	15	9.36
Dianiline (DAn)	0.15	0.19
Total of Reagents	100	100
Water (solvent)		20
Ethylene glycol (solvent)		20

Electrodes. Electrode-supported hydrogel membranes (10 µm - 30 µm thick) were cast onto 1.00 cm x 1.75 cm x 0.05 cm planar metal gold electrodes (PME Au-118, ABTECH Scientific, Yardley, PA), microlithographically fabricated Interdigitated Microsensor Electrode (IME) arrays (IME 1050-M-Au-P, ABTECH) or onto 7 mm x 50 mm x 0.5 mm ITO-coated (<10 Ω/☐) borosilicate glass plates (ABTECH Scientific, Yardley, PA). The PGEs and IMEs were fabricated from 1,000 Å of magnetron sputtered gold over 200 Å of adhesion promoting titanium/tungsten (Ti/W) on a chemically resistant, electronics quality, Schott D263 borosilicate glass. The IME array possessed lines and spaces that were 10 µm each and consisted of 50 digit pairs that were 0.5 cm long. An electroactive window that was 0.425 cm diameter was defined on each PGE (0.142 cm^2), ITO (0.142 cm^2), and IME (0.05 cm^2) using adhesive backed polyimide tape (Kapton 102, Furon CHR, New Haven, CT).

Downloaded by CORNELL UNIV on October 31, 2012 | http://pubs.acs.org
Publication Date: September 24, 1998 | doi: 10.1021/bk-1998-0709.ch015

Surface Preparation and Functionalization of Electrodes. The windowed electrodes were each separately and differently surface modified and functionalized for receiving the electroconductive gel dope. The windowed gold electrodes were first surface modified with 4-aminothiophenol and the primary amine subsequently derivatized with methoxy-PEG(5000)-epoxide (Shearwater Polymers, Huntsville, AL) by reaction at 110 °C for 10 min. The exposed glass of the interdigit spaces of the windowed IMEs were surface modified with 3-methacryloxypropyltrimethoxysilane. The windowed ITO was first surface modified with 3-aminopropyltrimethoxy silane and the primary amine subsequently derivatized with methoxy-PEG(5000)-epoxide by reaction at 110 °C for 10 min.

Downloaded by CORNELL UNIV on October 31, 2012 | http://pubs.acs.org
Publication Date: September 24, 1998 | doi: 10.1021/bk-1998-0709.ch015

Preparation of Gels. Electroconductive and blank (containing no electroactive monomers) gel membranes were solvent cast onto the windowed area of the various types of electrodes. Where freestanding gels were required, the films were cast onto dodecyltrichlorosilane treated microscope glass slides or petri dishes. Electrodes or slides were placed in a UV-crosslinker, purged with argon, and then exposed for 30 min. of ultraviolet light from a low pressure mercury lamp (12 mW/cm^2). Where appropriate, unpolymerized monomer was removed by sequential washing for 30 min. in each of 100% ethanol, 75%, 50%, 25% ethanol-water mixtures, and finally in DI water.

Electroactivity Measurements. Electroactivity was measured by multiple scan rate cyclic voltammetry using an EG&G PAR 273 Potentiostat/Galvanostat. Four-point electrical conductivity was measured using a Keithley Instruments 2010 Multimeter. Electrochemical Impedance Spectroscopy (EIS) was performed using a Solartron 1255 FRA (Slumberger, Hampshire, England) interfaced to the EG&G PAR 273. Each instrument was equipped with computerized control and data acquisition. Electropolymerized polyaniline hydrogels were prepared by potentiostatic electropolymerization (+ 0.70 V *vs.* Ag°/AgCl, 3 M Cl^-) form deaerated 1.0 M An, 0.01 M DAn, and 2.0 M HCl held at 20 °C. Oxidatively polymerized polyaniline hydrogels were prepared by exposure (1 hr) of the aniline-containing hydrogel to 0.10 M $FeCl_3$ at 20 °C. The interdigit spaces of the IME devices were chemically modified with γ-APS or γ-MPS to improve adhesion prior to hydrogel casting. The film was allowed to grow on each electrode and also between the digits of the pair of electrodes such that it formed a fully contiguous membrane.

Results and Discussion

Electroconductive Gel Synthesis. The synthesis of electroconductive hydrogels proceeds form two separate polymerization reactions. The first reaction is the UV-initiated polymerization of the hydrophilic polymer network formed from acrylate and methacrylate monomers in the formulation. The second reaction is the oxidative polymerization of electroactive monomers that are trapped within the pre-polymerized hydrophilic network. Figure 1 shows the structure of the various monomers used in this work. The first reaction produces a clear, optically transparent membrane of controlled thickness supported on the chosen conductive or insulating substrate. Membranes containing aniline and dianiline monomer of molar concentrations used in this study were visibly indistinguishable from blank membranes. That is, they were visibly colorless and optically transparent. The formation of the electroconductive network by oxidative polymerization was done by three separate schemes.

The first scheme (**I**) was via chemically based, oxidative polymerization of aniline that was formulated and trapped within the pre-polymerized hydrophilic hydrogel membrane. Contact of the 20 - 35 μm thick and 0.142-cm^2 area gel membrane with 25 μl of aq. 0.1 M $FeCl_3$ at a pH of 1.4 produced a clear, emerald green colored solution and a more intense emerald green membrane. The color developed on the time-scale of minutes, reaching an unchanging intensity after about 10 min. Other oxidizing agents used included acidified hydrogen peroxide (pH 2, ca. 30 % H_2O_2), ammonium peroxydisulphate, and dilute acidified potassium permanganate. In all cases there was visible evidence for diffusion of some aniline and/or dianiline out of the gel membrane into the aqueous bathing solution, as both hydrogel swelling and aniline oxidative coupling occurred. This synthesis scheme produces a somewhat un-controlled reaction as several competing forces are simultaneously at work. Contact of the aqueous $FeCl_3$ solution with the membrane causes its immediate swelling with concomitant influx of water, transport of ions into and out of the gel, and transport of unreacted monomer and glycerol out of the gel. Ferric ions react with aniline and dianiline monomers to produce cation-radicals that couple within the gel matrix and also diffuse out of the gel. The latter possibly accounting for the development of the pale green color in the bathing solution. For aniline oligomers of increasing molecular weight, diffusion out of the gel becomes restricted and future molecular weight increases occurs within the gel, favoring larger molecular weight chains of polyaniline within the gel. The result is polyaniline (likely the emeraldine salt) formed within the matrix of the hydrophilic hydrogel network.

The second scheme (**II**) was via electropolymerization of aniline within the electrode-supported, pre-polymerized hydrogel membrane. In this scheme, the electrode-supported membrane was placed in an electrochemical cell containing deaerated 1.0 M An, 0.01 M DAn, and 2.0 M HCl held at 20 °C. The aniline was then potentiosticly (0.70 V *vs.* Ag°/AgCl, 3 M Cl^-) electropolymerized until the passage of a total of 200 mC cm^{-2} of charge. Of course, such a reaction may be performed on a blank electrode leading to the familiar potentiosticly electropolymerized polyaniline, on a blank hydrogel membrane i.e. one containing no aniline or dianiline monomer within the gel, on a membrane containing electroactive monomer within the gel, or on a membrane containing electroactive monomer that had been exposed to $FeCl_3$

Downloaded by CORNELL UNIV on October 31, 2012 | http://pubs.acs.org
Publication Date: September 24, 1998 | doi: 10.1021/bk-1998-0709.ch015

Downloaded by CORNELL UNIV on October 31, 2012 | http://pubs.acs.org
Publication Date: September 24, 1998 | doi: 10.1021/bk-1998-0709.ch015

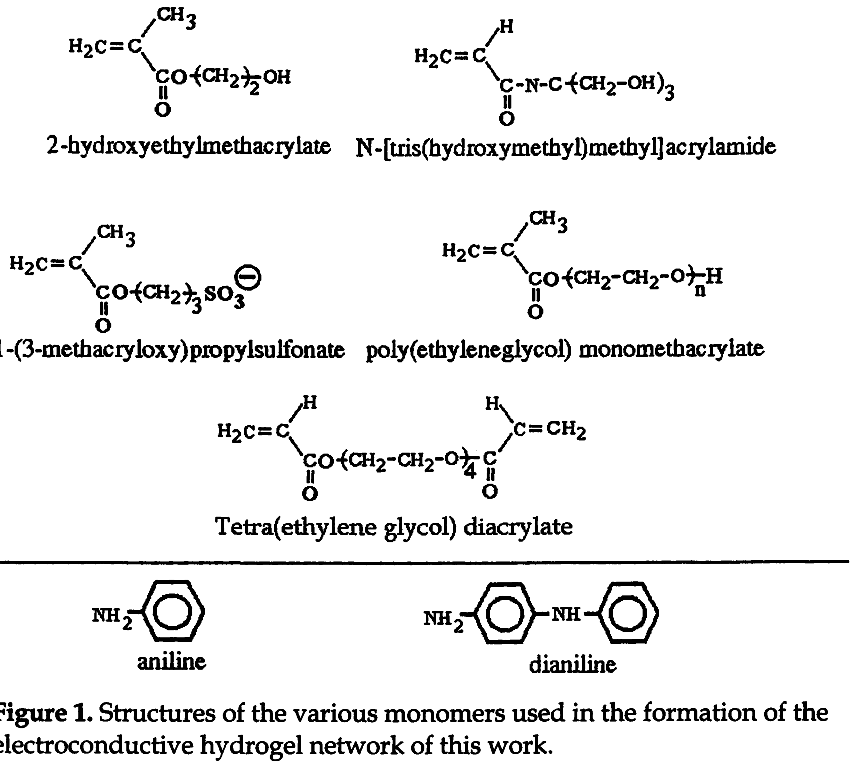

2-hydroxyethylmethacrylate

N-[tris(hydroxymethyl)methyl]acrylamide

1-(3-methacryloxy)propylsulfonate

poly(ethyleneglycol) monomethacrylate

Tetra(ethylene glycol) diacrylate

aniline

dianiline

Figure 1. Structures of the various monomers used in the formation of the electroconductive hydrogel network of this work.

treatment as described in scheme I. The three types of hydrogel-modified electrodes gave vastly different performance under electropolymerization conditions. The blank membrane produced no evidence of electropolymerization after 30 minutes under the mentioned conditions. Polyaniline did not form at such an electrode even with aniline/dianiline monomer in the solution. The aniline/dianiline containing gel membrane produced electropolymerized polyaniline that required 13 min to achieve the requisite 200 mC cm^{-2} of electropolymerization charge. During electropolymerization, green clouds could be seen streaming away from the electrode surface. The result however was a dark green membrane film adhered to and supported by the electrode.

Downloaded by CORNELL UNIV on October 31, 2012 | http://pubs.acs.org
Publication Date: September 24, 1998 | doi: 10.1021/bk-1998-0709.ch015

The third scheme (III) was via scheme II augmented by scheme I -- This combined approach produces a membrane visibly indistinguishable from that of II. However, its electropolymerization required only 13 s to achieve the desired 200 mC cm^{-2} of electropolymerization charge and no green clouds were seen streaming away from the electrode surface during electropolymerization. Electropolymerization, when performed at the gel-supported interdigitated electrode array (IME) devices, produced the dark green polyaniline only in the region of interdigitation (*13*). Inspection under an optical microscope and electrical conductivity measurements confirmed sufficient polyaniline formation to bridge the 10 μ interdigit space of the device. This was true whether the film was pretreated with $FeCl_3$ or not. The three foregoing schemes gave rise to materials with vastly different electrochemical, electrochemical impedance, hydration, electrical, environmental stability, and optical properties. Figure 2 is a simple schematic of the processes and results of the foregoing synthetic schemes.

Electrochemical Characterization. Electrochemical characterization of the oxidatively prepared (I), electrochemically prepared (II), and the mixed-mode prepared (III) hydrogels was done by multiple scan rate cyclic voltammetry (CV) in deaerated 0.10 M KCl, pH 7.2 50 mM tris(hydroxymethyl)aminomethane (TRIZMA) buffer, and in 0.1 M HCl at 20 °C. We were concerned in these analyses with the electrochemical properties of the electroactive component of the electroconductive gel and with the transport characteristics of ions within the gel. We were also concerned with the influence of oxidation/reduction and the attendant generation of charge (ionogenecity) on the consequent swelling and deswelling of these hydrogels. Where appropriate, comparisons were made to the behavior of the blank gel (no polyaniline) or to pure electropolymerized polyaniline. CV scans were performed at 5, 10, 20, 50, 100, 200, and 500 mV s^{-1} over the range - 0.5 V to + 0.9 V *vs.* Ag°/AgCl, 3 M Cl$^-$. The properties of these films were compared to pristine polyaniline that was directly electropolymerized at a bare gold electrode to the same extent of electropolymerization charge.

The first CV scans obtained at 5 mV s^{-1} for these three electroconductive gels are shown in Figure 3a. The scans display the expected two anodic half

Downloaded by CORNELL UNIV on October 31, 2012 | http://pubs.acs.org
Publication Date: September 24, 1998 | doi: 10.1021/bk-1998-0709.ch015

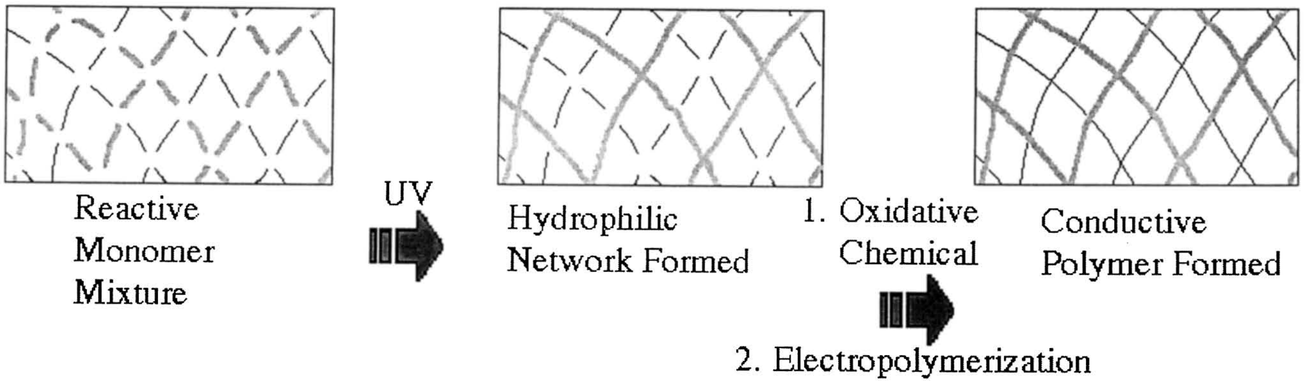
Reactive
Monomer
Mixture
UV
Hydrophilic
Network Formed
1. Oxidative
Chemical
2. Electropolymerization
Conductive
Polymer Formed

Figure 2. Schematic illustration of the two reactions involved in the production of electroconductive hydrogels.

waves characteristic of polyaniline (*14*). However, the second anodic half wave, for the case of the various polyaniline hydrogels, is shifted over to higher oxidation potentials. This indicates a higher overpotential for oxidation to the pernigraniline form and a wider potential range over which the emeraldine salt exists. However, there was in all cases only one broad cathodic half wave indicating lack of reversibility. All subsequent voltammograms were dominated by a single redox reaction of considerably attenuated current, with apparent reversibility, but of large $\Delta E \cong 400$ mV. Figure 3b shows the second CV scans obtained at 10 mV s^{-1} for these materials. The considerable difference in the anodic current densities, the shape of the anodic half waves, the lack of reversibility in the first scan, apparent reversibility in subsequent scans, and the increased overpotential for redox reactions in subsequent scans suggests considerable microstructural reorganization of the electroactive component upon going through the oxidation-reduction cycle. There is implied in these observations that the electroactive component of the gel is initially highly accessible to ions and readily oxidizable. Oxidation to above 0.8 V, known to produce the quiniodal imine form of polyaniline, however imposes irreversibility in most of the electroconductive polymer component. This is not observed in polyanilines formed with small counter anions such as Cl^- and NO_3^- which are freely electrochemically reversible between the various oxidation states.

In Figure 4 is shown the initial anodic charge density for the four materials studied. The anodic charge density is the area beneath the anodic curve and is taken as a measure of the electroactivity of the gel membrane. The electropolymerized hydrogels are similar in anodic charge capacity to pristine polyaniline, although, there is considerable overpotential for the second oxidation reaction within the gels when compared to the electropolymerized polyaniline. The gel formed by $FeCl_3$ induced polymerization only, displays very little anodic capacity, consistent with its weak color development. Figure 5 shows the cathodic charge densities measured from the second CV scan and expressed as a function of scan rate. At 5 mV s^{-1} the electropolymerized hydrogels display very similar cathodic charge capacities and is similar to pristine electropolymerized polyaniline. However, with increasing scan rate the PAn gel formed by **scheme III** consistently shows higher retained charge capacity compared to that formed by **scheme II** and pristine polyaniline. PAn gel formed by **scheme I** shows little electroactivity, again, consistent with its weaker color development.

The cathodic charge capacity of each membrane reflects the total number of reducible equivalents within the membrane. The evolution of this with scan rate reflects the impact of cation transport on the facility with which these reducible equivalents are reduced. Analysis of the peak cathodic current (i_{cp}) as a function of scan rate reveals the diffusivity for K^+ that is 5.81×10^{-7} cm^2 s^{-1} in polyaniline hydrogels **(III)** compared to 3.12×10^{-8} cm^2 s^{-1} in electropolymerized polyaniline.

Downloaded by CORNELL UNIV on October 31, 2012 | http://pubs.acs.org
Publication Date: September 24, 1998 | doi: 10.1021/bk-1998-0709.ch015

Downloaded by CORNELL UNIV on October 31, 2012 | http://pubs.acs.org
Publication Date: September 24, 1998 | doi: 10.1021/bk-1998-0709.ch015

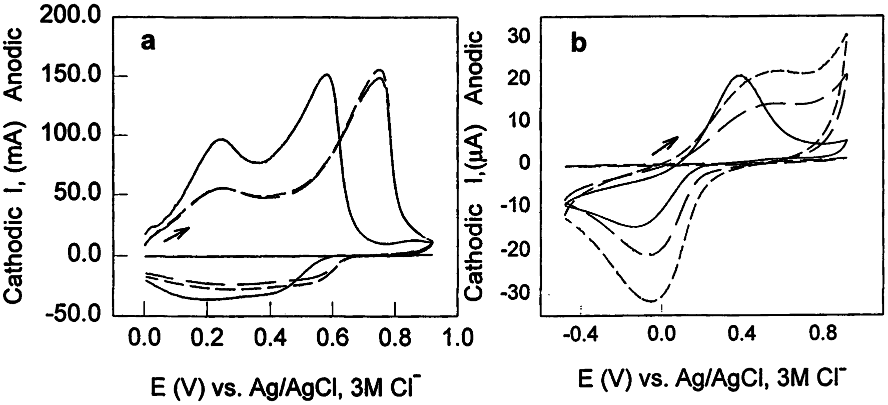

Figure 3. Cyclic voltammograms of electropolymerized PAn and PAn hydrogels in deaerated 0.1M KCl at 20 °C. a) First scan obtained at 5 mV s^{-1}. b) Second scan obtained at 10 mV s^{-1}.

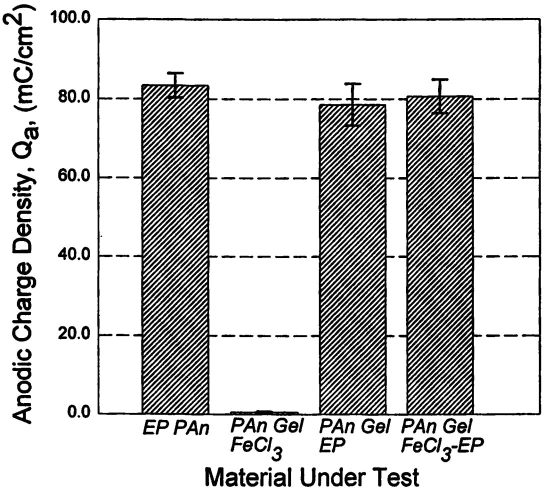

Figure 4. Anodic charge density of electropolymerized PAn and PAn hydrogels calculated from the 1st CV scan obtained at 5 mV s^{-1} in deaerated 0.1M KCl at 20 °C over the range 0.00 V to 0.90 V vs. g/AgCl, 3M Cl⁻.

Electrochemical Impedance Spectroscopic Characterization. Electrochemical impedance spectroscopy (EIS) was performed on polymer coated IMEs immersed in deaerated 0.10 M KCl at 20°C. EIS interrogation was done over the range 0.10 mHz to 100 kHz using a sine wave voltage pattern of 100 mV peak voltage. The two-electrodes of the interdigitated array served as working and auxiliary/counter electrodes respectively while the reference electrode (Ag/AgCl) was placed in the electrolyte and in close proximity to the hydrogel surface. In this configuration the impedance measured was the in-plane impedance of the solvent-cast hydrogel membrane. On un-treated IME devices, immersion in 0.10 M KCl solution lead to swelling of the hydrogel and often also lead to hydrogel disbondment from the IME device. This we believed to be the result of interfacial shear stress incident to swelling of the gel. Surface modification of the IME device with 3-aminopropyltrimethoxy silane followed by derivatization of the primary amine with methoxy-PEG(5000)-epoxide eliminated all evidence of adhesion loss. Hydrogel-coated IME devices, having achieved equilibrium, could be immersed in electrolyte for extended periods. Figure 6 shows a Bode plot of the impedance (magnitude and phase) of pristine electropolymerized PAn and various PAn hydrogel coated IMEs. The polyaniline-free hydrogel was found to give an impedance spectrum similar to that of aqueous 0.1 M KCl (*15*). This reflects the "solution like" character of the hydrogel membrane and indicates an ion concentration and ion mobility within the gel that is on the order of the bathing solution (*16*). There are subtle differences at the extremes of frequency that clearly distinguishes these media but these shall be overlooked for the purpose of this discussion. The influence of the polyaniline formed within the gel by the action of exposure to 0.1 M $FeCl_3$ is to appreciably reduce the low frequency impedance of the gel but also to increase the high frequency (> 1 Hz) impedance magnitude and produce a significant change in the phase behavior. Consistent with the electrochemical data, the development of color, and the change in gel hydration, this clearly supports the formation of polyaniline within the gel matrix. Electropolymerization within the gel results in a significant further reduction in impedance magnitude and produces frequency independence of both magnitude and phase. The combined action of treatment with $FeCl_3$ and electropolymerization is to produce still further reduction in the impedance magnitude and frequency independence. The impedance behavior of such a gel (III) is similar to that of pristine polyaniline that is formed by direct electropolymerization. Neither $FeCl_3$ nor electropolymerization, performed separately on the hydrogel, produces this polymer impedance character.

Hydrogel Hydration. The water content of electroconductive hydrogels was studied gravimetrically by casting films of the gel dope into pre-weighted glass weighing boats. The UV-polymerized gel membranes were subsequently reacted for 30 min with 0.1 M $FeCl_3$ prepared in 10% ethanol-water. The unreacted monomer and the ethylene glycol co-solvent were subsequently

Downloaded by CORNELL UNIV on October 31, 2012 | http://pubs.acs.org
Publication Date: September 24, 1998 | doi: 10.1021/bk-1998-0709.ch015

Downloaded by CORNELL UNIV on October 31, 2012 | http://pubs.acs.org
Publication Date: September 24, 1998 | doi: 10.1021/bk-1998-0709.ch015

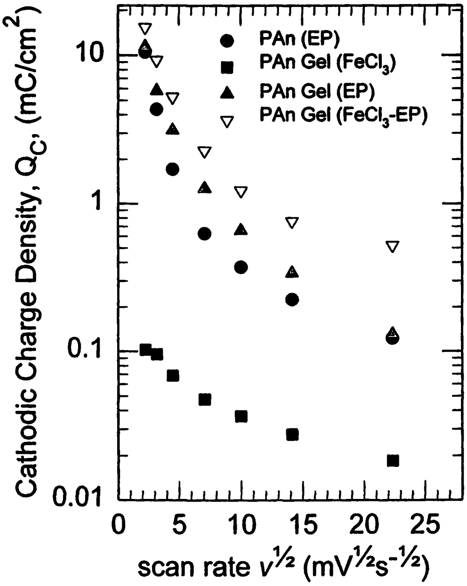

Figure 5. Cathodic charge density of electropolymerized PAn and PAn hydrogels calculated form the 2nd CV scan as a function of scan rate in deaerated 0.1M KCl at 20 °C over the range -0.5 to 0.9 V vs. Ag/AgCl, 3M Cl⁻.

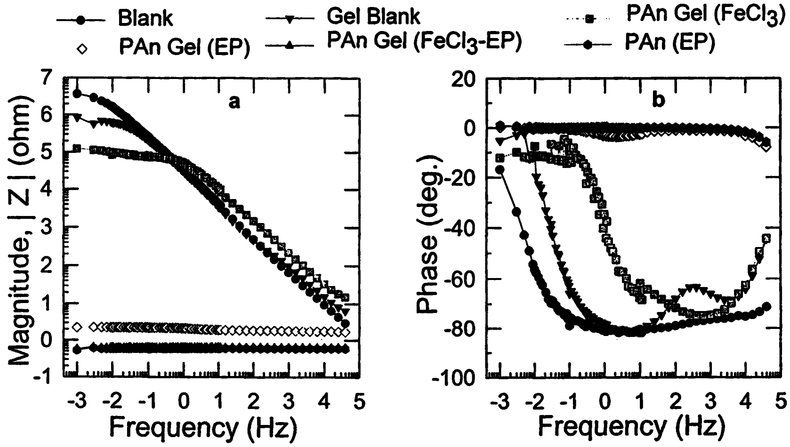

Figure 6. Bode plot (a) magnitude and b) phase angle) of the in-plane electrochemical impedance of electropolymerized PAn and PAn hydrogels in deaerated 0.1M KCl, 20 °C.

removed by sequential washing, each for 30 min, with 100% ethanol, 75%, 50% and 25% ethanol-water mixtures, and finally, with pure DI water. The resulting fully hydrated gel was scrupulously sapped dry with lint free Kimwipes and then weighed to obtain the hydration weight. Samples were then dried to constant weight by the application of repeated 3-hr drying periods in a Turbo Vac 500 dryer (Zymark, Hopkinton, MA) followed by re-weighing after each drying period. The Turbo Vac was set with a temperature differential corresponding to 35 °C in the sample chamber and 10 °C in the condenser. Constant weight was often reached within 4 such drying cycles. Repeated hydration and dehydration cycles revealed the polyaniline-free gel (I) and the electroconductive polyaniline gel (II) to contain 57 ±8% and 80 ±2% hydration respectively. The difference between the dry weight of the gel and weight immediately following UV polymerization yields the monomer extractables. The polyaniline-free gel and the electroconductive polyaniline gel were found to contain 28 % and 33 % extractables respectively. The extractables content calculated from the monomer dope formulae and assuming 100% conversion of acrylate monomer to polymer for these two materials was 30.7 % and 28.6% respectively.

Electrical Conductivity Characterization. The electrical conductivity of the various solvent-cast gel membranes was determined directly on the polymer-coated IMEs and also on freestanding electroconductive gels. The latter measurements were judged unreliable as the probe tip readily penetrated the gel thereby giving rise to spurious results. The four point technique yielded the resistance values for the various materials measured on the IME device: PAn (EP) = 3.2 S cm^{-1}, PAn Gel ($FeCl_3$) = 4.6 x 10^{-5} S cm^{-1}, PAn Gel (EP) = 8.4 x 10^{-1} S cm^{-1}, and PAn Gel ($FeCl_3$-EP) = 3.9 x 10^{-1} S cm^{-1}. These DC resistances correlate well with the above reported impedance measurements.

Environmental Stability. The stability of the electroconductive gels was studied by monitoring the four-point resistance over time during exposure to ambient laboratory air. The relative humidity and temperature were simultaneously monitored with each conductivity measurement. No attempts were made to normalize or correct the resistance data for variations in either RH or temperature. Relative humidity varied between 55 % and 68 % over the course of the reported measurement and were typically 66% RH. Temperature varied from 20 to 24 degrees and showed an upward trend into the summer months. Figure 7 shows a plot of the resistance expressed as sheet resistance and normalized resistance (R_t-R_o/R_o) over an approximate 100-day period. The electroconductive gel formed exclusively by electropolymerization shows the most dramatic loss of conductivity. The electropolymerized polyaniline shows excellent well-documented stability but with still some evidence of decay in its conductivity over the 100-day period. The electroconductive gel formed by the process of oxidative chemical polymerization followed by

Downloaded by CORNELL UNIV on October 31, 2012 | http://pubs.acs.org
Publication Date: September 24, 1998 | doi: 10.1021/bk-1998-0709.ch015

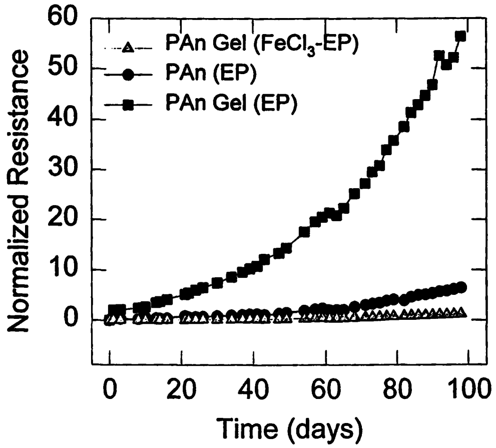

Figure 7. Stability of electropolymerized PAn and PAn hydrogels measured over a 100-day period under laboratory conditions.

Downloaded by CORNELL UNIV on October 31, 2012 | http://pubs.acs.org
Publication Date: September 24, 1998 | doi: 10.1021/bk-1998-0709.ch015

electropolymerization (III) shows almost imperceptible change in electrical conductivity over the 100 day period.

UV/Visible Spectrophotometry. UV-Vis spectra were taken on a Beckman DU-7 High-Speed spectrophotometer equipped with a water-jacketed six-cell changer. The gel was cast onto ITO-coated borosilicate glass plates (0.7 cm x 5 cm x 0.05 cm) that fitted directly into the 1 cm path-length cuvette and were set perpendicular to the beam direction. The cuvette was filled with 0.1 M $FeCl_3$ solution, equilibrated to 20 °C, and the glass plates introduced at time zero. Spectra were obtained in the rapid scan mode at 1200 nm/min (15 s each) with 1 minute intervals between scans. Figure 8 shows UV-Vis spectra over the range 400 nm to 700 nm of the gel membrane during exposure to 0.1 M $FeCl_3$. The reaction was followed in this way for a total of 13 min. The development of polyaniline within the gel membrane could be clearly seen from the change in absorbance over the range 400 - 700 nm. This could be compared with a blank gel studied in the same manner and also presented in Figure 8.

Electrorelease. Electrorelease using the electroconductive gel formed by the process of oxidative chemical polymerization followed by electropolymerization (III) was performed using the method described by Schlenoff et al. (*17*). The gel was cast, UV polymerized, and electropolymerized on gold-coated (1,000Å) polystyrene scintillator electrodes. The divinylbenzene (2%) cross-linked polystyrene substrate contains dissolved primary and secondary fluorescent dyes (<1%) that produce emissions in the visible. $^{45}Ca^{++}$ is a β-emitter (0.25 MeV) from which b-particles of sufficient energy travel through the scintillator polymer and induce emissions that may be measured with a photomultiplier tube (PMT) and frequency counter. The electrodes were immersed in $^{45}Ca^{++}$ (0.1 M $CaCl_2$) and electrochemically cycled over the range -0.8 V to +0.8 V vs. Ag/AgCl. Ingress and egress of hot Ca was monitored by the photon count produced by the scintillator. Figure 9 shows the photon count (cps) produced by hot Ca and the corresponding cyclic voltammogram. Under the initially reducing conditions (-80V), $^{45}Ca^{++}$ are slowly exchanged with K^+ ions within the gel. Sweeping anodicly oxidizes the polyaniline component of the gel. Upon achieving the oxidation potential, the population of oxidized polyaniline chain segments becomes large enough to cause the exclusion of mobile cations from within the gel. The photon count associated with $^{45}Ca^{++}$ therefore falls as $^{45}Ca^{++}$ are excluded form the electroconductive gel. Upon sweeping cathodicly, the $^{45}Ca^{++}$ signal shows a sharp increase corresponding to ingress of cations to maintain charge neutrality. The $^{45}Ca^{++}$ ingress-egress curve does not follow a smooth continuous pattern but rather clearly displays changes in slopes corresponding to the redox transitions. This indicates the capacity for electrode potential control of cation release kinetics.

Downloaded by CORNELL UNIV on October 31, 2012 | http://pubs.acs.org
Publication Date: September 24, 1998 | doi: 10.1021/bk-1998-0709.ch015

Downloaded by CORNELL UNIV on October 31, 2012 | http://pubs.acs.org
Publication Date: September 24, 1998 | doi: 10.1021/bk-1998-0709.ch015

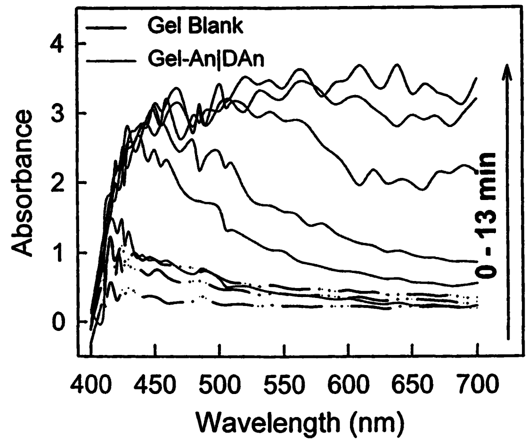

Figure 8. Progress in the UV-Vis absorbance spectra of an electroconductive polyaniline hydrogel during exposure to 0.1 M $FeCl_3$.

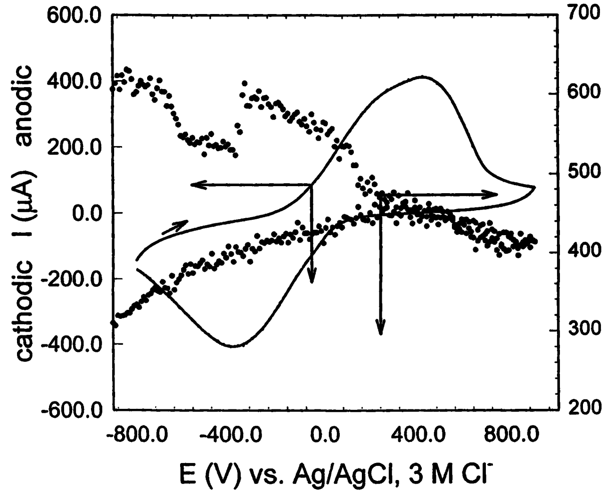

Figure 9. Electrorelease of $^{45}Ca^{++}$ and the corresponding cyclic voltammogram obtained by sweeping over the range – 800 mV to + 800 mV vs. Ag/AgCl, 3M Cl^- at 1 mV s^{-1} in 0.1 M $^{45}CaCl_2$ at room temperature and at 10 mV s^{-1} in deaerated 0.1M KCl, 20 °C respectively.

Summary and Conclusions

A class of electroconductive hydrogels have been formulated and fabricated by the sequential UV polymerization of acrylate and methacrylate monomers and oxidative chemical and/or electropolymerization of monomers such as aniline. Incorporating 3-sulfopropylmethacrylate as a difunctional monomer results in a virtual single macroanion, which when combined with the electrochemically reversible oxidation and reduction of polyaniline; a) creates ionic links between the two polymer networks that may alter network density, and b) allows the low voltage electro-stimulated release of bioactive cations trapped within the gel. These electroconductive hydrogels have been shown to retain more electroactivity than corresponding electropolymerized polyaniline, to allow faster cation transport into and out of the gel with K^+ diffusivity that is an order of magnitude greater in the gel than in electropolymerized polyaniline. In addition, the electrical conductivity, while somewhat lower is non-the less comparable to electropolymerized polyaniline. The electroconductive polyaniline gels are also shown to be more stable under ambient conditions and to efficiently imbibe and release Ca^{++} under electrostimulation.

Downloaded by CORNELL UNIV on October 31, 2012 | http://pubs.acs.org
Publication Date: September 24, 1998 | doi: 10.1021/bk-1998-0709.ch015

Acknowledgments

The authors thank Dr. Norman Sheppard, Jr., Mr. Matt Lesho (Biomedical Engineering, JHU), Dr. Kimberly Brown (Biological Resource Engineering, UMCP), and Prof. Joseph Schlenoff (Chemistry, University of Florida) for useful discussions and Prof. Schlenoff for electrorelease measurements.

References and Notes

1. Lowman, A. M. and Peppas, N. A. *Macromolecules* **1997**, 30, 4959-4965.
2. Guiseppi-Elie, A.; Wilson, A. M.; Sujdak, A. R.; Brown, K.E. *Polymer Preprints* **1997**, 38(2), 608-611.
3. Saito, Y.; Masakatsu, K.; Kubohara, Y.; Kobayashi, I.; Tatemoto, k. *Biochem. Biophys. Res. Commun.* **1996**, 221, 577-580.
4. Tierney, M. J.; Martin, C. R. *J. Electrochem. Soc.* **1990**, 137(12), 3789-3793
5. Guiseppi-Elie, A.; Wallace, G. G.; Matsue, T. **In** *Handbook of Conducting Polymers*; Skotheim, T.; Elsenbaumer, R..; Reynolds, J. R.., Eds.; Marcel Dekker: New York, NY 1997, Ch. 34, pp 963–991.
6. Otero, T. F.; Grande, H.-J. **In** *Handbook of Conducting Polymers*; Skotheim, T.; Elsenbaumer, R..; Reynolds, J. R.., Eds.; Marcel Dekker: New York, NY 1997, Ch. 36, pp 1113 - 1134.
7. Pyo, M.; Reynolds, J. R. *Chem. Mater.* **1996**, 8(1), 128-132.
8. Lin, Y.; Wallace, G. G. *J. Controlled Rel.* **1994**, 30, 137-142.
9. Hepel, M.; Dentrone, L. *Electroanalysis* **1996**, 8(11), 996-1005.

10. Hodgson, A. J.; John, M. J.; Campbell, T.; Georgevich, T.; Woodhouse, S.; Aoki, T.; Ogata, N.; Wallace, G. G. *Smart Materials Technologies and Biomimetics,* SPIE Proceedings Series; Society of Photo-Optical Instrumentation Engineers: Bellingham, WA, 1996; Vol. 2716, pp 164-176.
11. Small, C. J.; Too, C.O.; Wallace, G.G. *Polymer Gels and Networks* **1997,** 5 (3), 251-265.
12. Yu, H.; Grainger, D. W. *J. Controlled Release* **1995,** 34, 117-127.
13. Guiseppi-Elie, A.; Wilson, A. M.; Tour, J. M.; Brockman, T. W.; Zhang, P.; Allara, D. L. *Langmuir* **1995,** 11(45), 1768.
14. Guiseppi-Elie, A.; Pradhan, S. P.; Wilson, A. M.; Allara, D. L.; Zhang, P.; Collins, R. W.; Kim, Y.-T. *Chem. Mat.* **1993,** 5(10), 1474.
15. Sheppard Jr., N. F.; Lesho, M. J.; McNally, P.; Francomacaro, A. S. *Sens. and Act. B* **1995,** 28, 95-102.
16. Guiseppi-Elie, A.; Lesho, M.; Sheppard, Jr., N. F. In *Electrical and Optical Polymer Systems: Fundamentals, Methods, and Applications*; Wise, D. L.; Wnek, G. E.; Trantolo, D. J.; Gresser, J. D.; Cooper, T. M. Eds.; Marcel Dekker: New York, NY, 1997, Ch. 34, pp 1187-1211.
17. Li, M. and Schlenoff, J. B. *Anal. Chem.* **1994** 66(6), 824-829.

Downloaded by CORNELL UNIV on October 31, 2012 | http://pubs.acs.org
Publication Date: September 24, 1998 | doi: 10.1021/bk-1998-0709.ch015

Chapter 16

Thermally Triggered Gelation of Alginate for Controlled Release

H. Cui and P. B. Messersmith

Division of Biological Materials, Northwestern University, 311 East Chicago Avenue, Chicago, IL 60612

Downloaded by NORTH CAROLINA STATE UNIV on October 31, 2012 | http://pubs.acs.org
Publication Date: September 24, 1998 | doi: 10.1021/bk-1998-0709.ch016

Thermally responsive Ca-loaded lipid vesicles, designed to release Ca^{2+} when heated to body temperature, were employed along with Na-alginate to form a fluid suspension that rapidly gelled when heated to body temperature. The liposomes were exploited to prevent alginate hydrogel formation at room temperature by isolating intravesicular Ca^{2+} from extravesicular Na-alginate. Heating of the fluid liposome/alginate mixture to 37°C resulted in release of Ca^{2+} from the liposomes and formation of Ca-alginate hydrogel. The 37°C gelation time was found to be dependent on the lipid composition used to prepare the liposomes, and the liposome/alginate ratio. Optimized formulations gelled within 30 seconds at 37°C. The addition of drug-filled liposomes to the formulation resulted in a thermally gelled hydrogel that released entrapped drug in a controlled manner. The kinetics of drug release was affected by lipid composition, which permitted the systematic control of drug release rate. This approach may prove advantageous to the use of pre-crosslinked alginate spheres for certain local drug delivery applications in which *in-situ* gelation is desired.

Liposomes have been extensively explored for use as delivery vehicles for a wide variety of therapeutic agents, including antibiotics, chemotherapy drugs, and growth factors (1). The most common route of liposome administration is by intravenous injection, an approach which is hampered by problems such as rapid clearance by the reticuloendothelial system and poor targeting to specific tissues and organs. In some cases, it may be possible to achieve a desirable therapeutic outcome by direct local delivery of liposomes to a target site (2-5). Direct local administration of liposomal drugs has the potential advantages of prolonged local drug release, reduced systemic exposure of drugs, and enhanced drug efficacy (6). For example, Lagace and coworkers (2,3) have employed direct administration of liposome-encapsulated antibiotic for the treatment of bacterial pulmonary infections.

In Tailored Polymeric Materials for Controlled Delivery Systems; McCulloch, I., et al.;
ACS Symposium Series; American Chemical Society: Washington, DC, 1998.

Downloaded by NORTH CAROLINA STATE UNIV on October 31, 2012 | http://pubs.acs.org
Publication Date: September 24, 1998 | doi: 10.1021/bk-1998-0709.ch016

Although local retention of liposome-entrapped drugs is likely to be longer than that of free drugs, it may not always be long enough to maintain local therapeutic drug levels, due in part to rapid clearance of vesicles by macrophages and other cells. A possible solution to this problem may be to entrap drug-containing liposomes within a bioinert hydrogel matrix that isolates the liposomes from cellular attack, yet permits the controlled release of liposome-entrapped therapeutic agents (7). Ionically crosslinked polysaccharide hydrogels, such as Ca-alginate, have been investigated for entrapping drug-containing liposomes (7-9) as well as cells (10). Alginates are linear, water-soluble polysaccharides composed of 1,4-linked β-D-mannuronic and α-L-guluronic acid units in varying proportions and arranged in a blockwise pattern along the linear chain, which form viscous solutions at a few weight percent in water (11). One of the main biofunctional characteristics of alginates is their ability to form transparent or translucent gels in the presence of Ca^{2+} ions (12). Spherical alginate hydrogel particles, including those containing entrapped liposomes (7-9), are typically made by dripping or spraying a Na-alginate solution into a rapidly stirred solution containing a high concentration of Ca^{2+} ions. Under these conditions alginate crosslinking is extremely rapid, resulting in spherical hydrogel particles, which can be injected *in-vivo* via syringe.

For some applications, such as drug delivery to the eye (13) or to the periodontal pocket (14), it is desirable for the precursor solution to infiltrate a tissue or assume the shape of a cavity prior to *in-situ* gelation, forming a reservoir from which a therapeutic agent is released. Cohen and coworkers (13) recently reported an *in-situ* gelling alginate system which relies on diffusion of Ca^{2+} from adjacent body fluid (e.g. lacrimal fluid of the eye) to form Ca-alginate hydrogels. Instead of relying on diffusion of Ca^{2+} from the extracellular fluid, our strategy for *in-situ* gelation of alginate is to employ stimuli responsive lipid vesicles to isolate Na-alginate (extravesicular) from Ca^{2+} (intravesicular) as shown in Figure 1. Utilizing the compartmentalization ability of liposomes in this manner permits us to design a system that remains fluid under certain conditions but which rapidly forms a homogeneous Ca-alginate hydrogel when Ca^{2+} is released from the liposomes in response to an applied stimulus, such as a change in temperature or exposure to light. In this paper we describe the use of thermally triggered Ca^{2+} release from liposomes as a means for rapidly gelling alginate *in-situ*. We also report on the release of liposome-entrapped drugs from these hydrogels. The long term goal of our research is to develop a liposome-containing alginate drug delivery system which can be manipulated as a fluid before gelling rapidly in-situ.

Experimental

Materials. 1,2-bis(palmitoyl)-sn-glycero-3-phosphocholine (DPPC,>99%) and 1,2-bis(myristoyl)-sn-glycero-3-phosphocholine (DMPC, > 99%) were obtained from Avanti Polar Lipids and used as received. The Na-alginate was obtained from Sigma Chemical Co. in low, medium, and high viscosity grades extracted from macrocystis pyrifera. Metronidazole was also purchased from Sigma. All other chemicals were reagent grade and used as received.

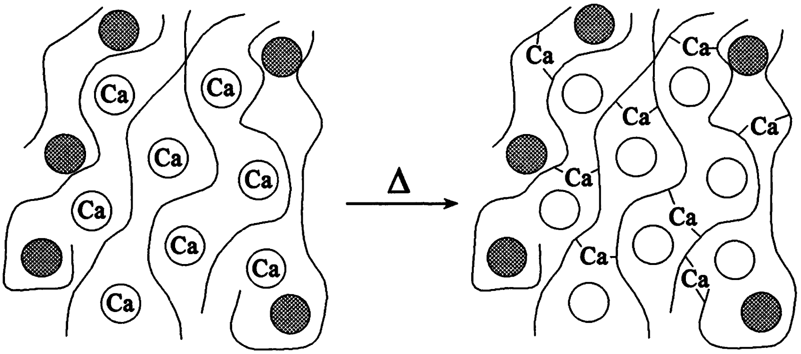

Figure 1. Schematic illustration of thermally triggered hydrogel formation from a suspension containing Ca-loaded liposomes (open circles), drug-filled liposomes (shaded circles), and alginate (lines). The Ca-loaded vesicles are designed to rapidly release Ca^{2+} in response to a change in temperature, crosslinking the alginate to form a hydrogel containing entrapped drug-filled liposomes.

Liposome Preparation. The interdigitation-fusion (IF) approach (15) was used to prepare both Ca-loaded and drug-loaded phospholipid vesicles. Briefly, DPPC alone or DPPC:DMPC (9:1 molar ratio) in $CHCl_3$ stock solution was placed in a round bottom flask, the solvent was removed in a rotary evaporator, and then dried in vacuo. Lipid films were hydrated (lipid concentration 20mg/ml) with either $CaCl_2$ (.2M) or drug (10-30mg/ml in .3M NaCl) solution and sonicated to form small unilamellar vesicles. Ethanol was added to the SUV suspension to a final concentration of 4M, to form the viscous interdigitated phase (15). This suspension was then incubated at room temperature for 30 minutes followed by an additional 30 minutes at 50°C. Finally, the ethanol was removed from the liposome suspension by sparging with a gentle stream of nitrogen gas at 50cc/min for 20-30 minutes. This process was used for encapsulation of both $CaCl_2$, and metronidazole within liposomes of composition 90%DPPC/10%DMPC. Metronidazole was also encapsulated within liposomes composed of pure DPPC. Free (unencapsulated) Ca^{2+} or drug was removed from the liposome suspensions as follows. 1.5-2.0 ml of liposome suspension was diluted to 8ml total with .3M NaCl and the suspension was vortexed. This suspension was centrifuged at 16,000xG for 3 minutes, and the supernatant decanted. This process was repeated a minimum of 5 times to fully remove unentrapped material. Encapsulation efficiency ranged from 60-75% of the total available encapsulant.

Calcium Release Assay. Thermally triggered release of Ca^{2+} from liposomes was detected using the Ca^{2+} sensitive dye arsenazo III (AIII). A 10μl aliquot of Ca-loaded liposome suspension was added to 3ml of an iso-osmotic AIII solution (20μM), and the absorption at 650nm measured during heating from room

Downloaded by NORTH CAROLINA STATE UNIV on October 31, 2012 | http://pubs.acs.org
Publication Date: September 24, 1998 | doi: 10.1021/bk-1998-0709.ch016

temperature to 50°C. A circulating water bath and a jacketed quartz cuvette were used to heat the suspensions at a rate of 1°C/minute during measurement.

Preparation of Hydrogel Precursor Suspension. At room temperature, one part of Ca-loaded liposomes was combined with 1-20 parts Na-alginate (2-2.67% in .3M NaCl) to form a thermally sensitive hydrogel precursor. For drug-containing hydrogel formulations, one part each of drug-loaded and Ca-loaded liposomes were combined with 3 parts Na-alginate to make the precursor suspension.

Determination of Gel Time. Thermal hydrogel formation was determined semi-quantitatively by loading the room temperature liposome/alginate precursor solution into thin-walled glass capillaries (1mm i.d. by 75mm long), sealing the ends with a plug of vacuum grease, and then immersing the capillary into a thermostated water bath for a specified length of time. Upon removal from the water bath, pressure was applied to one end of the capillary to expel the sample. Samples that gelled due to release of Ca^{2+} from the liposomes were able to be removed from the capillaries as intact cylinders; samples that did not gel were still fluid when removed from the capillary. Preliminary experiments demonstrated this method to be a rapid and accurate way of determining gelation time.

Drug Release Experiments. .2-.4ml of drug-containing precursor suspensions were loaded into syringes and injected into pre-wet dialysis tubing (4mm diameter; 8,000 MW cutoff), and the ends of the bags sealed with closures. Hydrogel formation was initiated by inserting the loaded dialysis bags into vials containing 30ml of pH 7.4 buffer solution (.3M NaCl, 10mM HEPES) equilibrated at 37°C. At predetermined time intervals, the dialysis bags were transferred to 30ml of fresh buffer solution pre-warmed to 37°C. The amount of drug released into the buffer solution at each time interval was measured spectrophotometrically (320 nm). All reported data represent the mean values of at least three identical trials.

Results and Discussion

A useful means of releasing liposome-entrapped reagents at a specific temperature is to take advantage of temperature-induced changes in lipid bilayer permeability. It is well known that the permeability of phospholipid bilayers is strongly temperature-dependent (16,17). At temperatures below the lipid chain melting transition (T_m) ("gel" state) phospholipid bilayers are relatively impermeable to multivalent ions (18-20). However, bilayer permeability has been shown to be several orders of magnitude higher at T_m (16), a phenomenon which has been attributed to the presence of highly permeable interfacial regions between coexisting gel ($<T_m$) and liquid crystalline ($>T_m$) domains (17). This characteristic of lipid bilayers allows the design of liposomes which are relatively impermeable to encapsulant at one temperature but highly permeable at another temperature. Early work by Yatvin et al (21) demonstrated that liposomes formulated to release their contents a few degrees above 37°C can be used in conjunction with local hyperthermia for targeted drug delivery to tumors.

Downloaded by NORTH CAROLINA STATE UNIV on October 31, 2012 | http://pubs.acs.org
Publication Date: September 24, 1998 | doi: 10.1021/bk-1998-0709.ch016

We have adopted a similar approach for releasing, in a temperature-dependent manner, liposome-entrapped Ca^{2+} for the purposes of *in-situ* formation of biomaterials (22-24). Using saturated phospholipids and aqueous $CaCl_2$ as the encapsulating solution, we have encapsulated up to 75% of available Ca^{2+} within large unilamellar liposomes (22,23). Due to low bilayer permeability in the gel state ($<T_m$), removal of free (i.e. unentrapped) Ca^{2+} is possible while maintaining high internal Ca^{2+} concentration (.2M). Using scanning calorimetry to detect the T_m of liposome suspensions, we previously showed that while the T_m of DPPC was several degrees too high (42°C) for Ca^{2+} release at physiologic temperature, the T_m of Ca^{2+}-loaded liposomes could be tailored to approximately 37°C by the addition of a small amount of DMPC (10%) to DPPC (23). As shown in Figure 2, the absorbance at 650nm of a Ca-loaded liposome/AIII solution (DPPC/DMPC = 9/1) increased significantly at approximately 36°C, indicating the release of entrapped Ca^{2+} and formation of Ca^{2+}-AIII complex (25). This result suggests that the liposome membrane is relatively impermeable to Ca^{2+} below T_m, but that the bilayer becomes highly permeable to Ca^{2+} as T_m is approached.

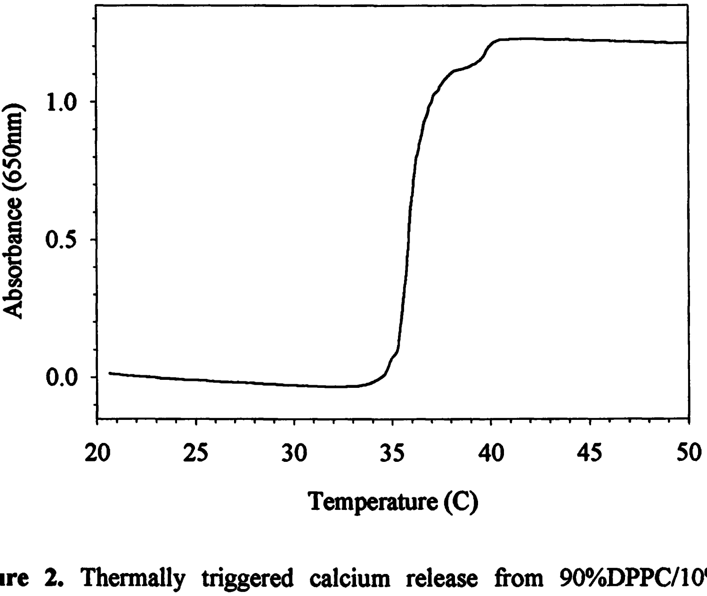

Figure 2. Thermally triggered calcium release from 90%DPPC/10%DMPC liposomes suspended in AIII solution. Sample was heated at 1°C/minute. Formation of Ca^{2+}-AIII complex is indicated by an increase in absorbance at 650nm (25).

When Ca-loaded liposomes were combined with 2% Na-alginate solution, a fluid-like mixture resulted which possessed a viscosity similar to that of pure Na-alginate solution. The liposome/alginate mixture remained fluid during storage at room temperature, although some thickening was observed after several days.

Downloaded by NORTH CAROLINA STATE UNIV on October 31, 2012 | http://pubs.acs.org
Publication Date: September 24, 1998 | doi: 10.1021/bk-1998-0709.ch016

However, it was found that incubation of the alginate/liposome suspension at 37°C resulted in rapid gelation, due to thermally triggered release of Ca^{2+} and subsequent formation of Ca-alginate hydrogel. Table I shows the physical consistency of the alginate hydrogels with a liposome/alginate mixing ratio of 1 to 3. It was found that the low viscosity alginate yielded more robust gels than the medium and high viscosity grades. Further experiments revealed that increasing the alginate solution concentration from 2% to 2.67% yielded gels with excellent rigidity. It should be pointed out that using the 2.67% alginate solution at a 1/3 liposome/alginate ratio results in a final alginate concentration of 2%, which is similar to that used by other investigators for entrapment of liposomes within alginate hydrogels (7-9).

Downloaded by NORTH CAROLINA STATE UNIV on October 31, 2012 | http://pubs.acs.org
Publication Date: September 24, 1998 | doi: 10.1021/bk-1998-0709.ch016

Table I. Composition and physical consistency of thermally gelled liposome/alginate hydrogels.*

Na-Alginate	Physical Consistency‡
2% high viscosity	+
2% medium viscosity	++
2% low viscosity	+++
2.67% low viscosity	++++

*1 part liposome/3 parts Na-alginate, incubated at 37°C for 30 minutes; lipid composition 90%DPPC/10%DMPC.

‡qualitative measure of physical consistency of the hydrogel from soft (+) to rigid (++++) gel.

The capillary method used in this study to determine gelation time was found to be reproducible and permitted the measurement of gel status of samples incubated at a specific temperature for as little as 10 seconds. Using this method, we also investigated the effect of liposome/alginate ratio on gelation time at several temperatures. For example, we found that while samples did not gel within several hours at temperatures between 25 and 30°C, gelation caused by thermally-induced leakage of Ca^{2+} from the liposomes occurred within minutes or even seconds at temperatures as low as 33°C (Table II). In fact, all liposome/alginate mixing ratios between 1/3 and 1/8 were found to have gelled after only 10 seconds of incubation at 37°C.

Drug-filled liposomes were processed using the same approach as the Ca-loaded liposomes, and free drug removed from the suspension. Two different lipid compositions were used to prepare the drug-filled liposomes; pure DPPC and 90%DPPC/10%DMPC. Due to the relationship between T_m and bilayer permeability, these two compositions are expected to yield vesicles of low and high permeability, respectively, at body temperature. The formulation used for the drug release studies was a mixture of Ca-loaded liposomes/drug-filled liposomes/alginate in a 1/1/3 ratio. The formulations containing drug-filled liposomes were found to have gelling characteristics similar to the drug-free formulations.

Downloaded by NORTH CAROLINA STATE UNIV on October 31, 2012 | http://pubs.acs.org
Publication Date: September 24, 1998 | doi: 10.1021/bk-1998-0709.ch016

Table II. Gelation time of liposome/alginate mixtures at 33°C.

Liposome/Alginate Ratio	Gelation Time* (seconds)
1/2	DNG[‡]
1/3	30
1/4	30
1/6	60
1/8	60
1/10	DNG
1/20	DNG

*Determined using the capillary method by immersion in a thermostated water bath; lipid composition 90%DPPC/10%DMPC.

[‡] Did not gel within 1 minute.

The release of metronidazole from thermally crosslinked liposome/alginate hydrogels is shown in Figure 3. For the purposes of comparison, a liposome-free 2% Ca-alginate hydrogel loaded with 10mg/ml metronidazole was also prepared. Drug release from the liposome-free hydrogel was most rapid, with greater than 90% released within the first few hours. Both liposome-containing samples exhibited a rapid "burst"-type release, in which approximately 20% of the drug was immediately released from the hydrogel with kinetics similar to that of drug release from liposome-free Ca-alginate. The rapid burst-type release of drug from the drug-filled liposomes could be due to the increased permeability of lipid bilayers to drug in the presence of alginate (26). Nevertheless, the initial burst release of drug was followed by slower release, the kinetics of which were found to be dependent on the lipid composition of the drug-filled liposomes. For example, metronidazole was released more rapidly from the 10% DMPC liposome than from the pure DPPC liposme (Figure 3). This difference may be due to the difference in bilayer permeability of the two compositions at the experimental temperature (37 °C). At this temperature, pure DPPC liposomes are in the gel state and are therefore less permeable to drug. On the other hand, the drug-filled liposomes containing 10%DMPC, having a T_m of approximately 37°C, are more permeable and therefore release drug more rapidly. Changes in lipid composition, such as those described above, could be useful for tailoring the release rate of liposome-encapsulated drugs.

Conclusions

We have developed a method which employs the liposome compartment to segregate reactive Ca^{2+} and alginate at room temperature, yet permits the release of Ca^{2+} to rapidly crosslink alginate into a hydrogel at body temperature. In-situ gelling liposome/alginate formulations containing entrapped drug-filled liposomes were also developed. These formulations also gelled rapidly at 37°C and released drug in a controlled manner. Drug release was characterized by a rapid burst-type release followed by a slower controlled release of drug from the hydrogel matrix. The rate of release could be modulated by the composition of the liposomes used to entrap the drug. This approach may prove advantageous to the use of pre-crosslinked alginate spheres for certain local drug delivery applications in which in-situ gelation is required.

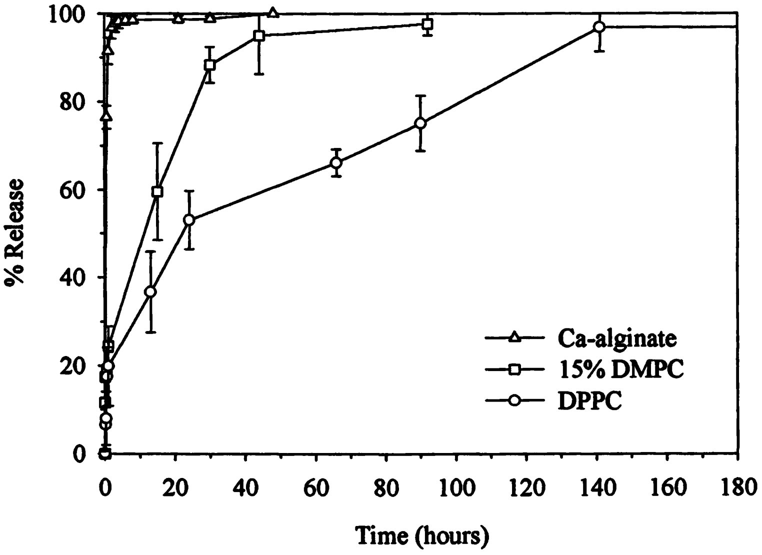

Figure 3. Release of metronidazole from thermally gelled liposome/alginate hydrogels. Sealed dialysis bags containing one part Ca-loaded liposomes, one part drug-loaded liposomes (DPPC or 15% DMPC), and three parts Na-alginate (2%) were inserted into 37°C buffer at time zero. The control was a metronidazole-infused Ca-alginate hydrogel (2%).

Acknowledgments

The authors gratefully acknowledge the support of this research by the Whitaker Foundation.

Literature Cited

1. *Liposome Technology*, Gregoriadis, G., Ed.; CRC press: Boca Raton, FL, 1984; Vol. III.
2. Beaulac, C.; Clement-Major, S.; Hawari, J.; Lagace, J. *Antimicrob. Agents and Chemotherapy* **1996**, *40*, 665-9.
3. Omri, A.; Beaulac, C.; Bouhajib, M.; Montplaisir, S.; Sharkawi, M.; Lagace, J. *Antimicrob. Agents and Chemotherapy* **1994**, *38*, 1090.

Downloaded by NORTH CAROLINA STATE UNIV on October 31, 2012 | http://pubs.acs.org
Publication Date: September 24, 1998 | doi: 10.1021/bk-1998-0709.ch016

4. Fountain, M. W.; Weiss, S.J.; Fountain, A.G.; Shen, A.; Lenk, R.P. *J. Infect. Dis.* **1985**, *152*, 529.
5. Price, C.I.; Horton, J.W.; Baxter, C.R. *Surg. Gynecol. Obstet.* **1992**, *174*, 175.
6. Nacucchio, M.C.; Bellora, M.J.G.; Sordelli, D.O.; D'Aquino, M. *J. Microencaps.* **1988**, *5*, 303.
7. Kibat, P.G.; Igari, Y.; Wheatley, M.A.; Eisen, H.N.; Langer, R. *FASEB J.* **1990**, *4*, 2533.
8. Takagi, I.; Shimizu, H.; Yotsuyanagi, T. *Chem. Pharm. Bull.* **1996**, *44*, 1941.
9. Machluf, M.; Gegev, O.; Peled, Y.; Kost, J.; Cohen, S. *J. Controlled Rel.* **1996**, *43*, 35.
10. Lim, F.; Sun, A.M. *Science* **1980**, *210*, 908.
11. Smidsrod, O. *Carbohyd. Res.* **1973**, *27*,107.
12. Grasdalen, H.; Larsen, B.; Smiderod, O. *Carbohyd. Res.* **1979**, *68*, 23.
13. Cohen, S.; Lobel, E.; Trevgoda, A.; Peled, Y. *J. Controlled Rel.* **1997**, *44*, 201.
14. Soskolne, W.A. *Crit. Rev. Oral Biol. Med.* **1997**, *8*, 164.
15. Ahl, P.L.; Chen, L.; Perkins, W.R.; Minchey, S.R.; Boni, L.T.; Taraschi, T.F.; Janoff, A.S. *Biochim. et Biophys. Acta* **1994**, *1195*, 237.
16. Papahadjopoulos, D.; Jacobsen, K.; Nir, S.; Isac, T. *Biochim. Biophys. Acta* **1973**, *311*, 330.
17. Marsh, D.; Watts, A.; Knowles, P.F. *Biochim. Biophys. Acta* **1976**, *858*, 161.
18. Cevc, G. in *Phospholipids Handbook*, Cevc, G., Ed.; Marcel Dekker, New York, NY, 1993: pp. 639-661.
19. Bangham, A.D.; Standish, M.M.; Watkins, J.C.; Weissmann, G. *Protoplasma* **1967**, *63*, 183.
20. Deamer, D.W.; Bramhall, J.; *J. Chem. Phys. Lipids* **1986**, *40*, 167.
21. a)Yatvin, M.B.; Weinstein, J.N.; Dennis, W.H.; Blumenthal, R., *Science* **1978**, *202*, 1290; b) Weinstein, J.N.; Magin, R.L.; Yatvin, M.B.; Zaharko, D.S., *Science* **1979**, *204*, 188.
22. Messersmith, P.B.; S. Vallabhaneni; Nguyen, V., "Preparation of Calcium-Loaded Liposomes and Their Use in Calcium Phosphate Formation", *Chem. Mater.* **1998**, *10*, 109.
23. Messersmith, P.B.; Starke, S., "Thermally Triggered Calcium Phosphate Formation From Calcium-Loaded Liposomes", *Chem. of Mater.* **1998**, *10*, 117.
24. Cui, H.; Messersmith, P.B., *Polym. Prepr.* **1997**, *38*, 616.
25. (a) Sokolove, P.M.; Kester, M.B. *Anal. Biochem.* **1989**, *177*, 402. (b) Weissmann, G.; Collins, T.; Evers, A.; Dunham, P. *Proc. Natl. Acad. Sci. U.S.A.* **1976**, *73*, 510.
26. Cohen, S.; Bano, M.C.; Chow, M.; Langer, R. *Biochim. Biophys. Acta* **1991**, *1063*, 95.

Downloaded by NORTH CAROLINA STATE UNIV on October 31, 2012 | http://pubs.acs.org
Publication Date: September 24, 1998 | doi: 10.1021/bk-1998-0709.ch016

Downloaded by CORNELL UNIV on October 31, 2012 | http://pubs.acs.org
Publication Date: September 24, 1998 | doi: 10.1021/bk-1998-0709.ch017

Chapter 17

Effect of Surfactants on the Release of Griseofulvin from Polyvinylpyrrolidone Dispersions

Hanife Akin, Jeorge Heller[1], and Frank W. Harris

The Maurice Moron Institute and Department of Polymer Science, The University of Akron, Akron, OH 44325–3909

The overall objective of this work was to increase the apparent water-solubility and dissolution rate of the water-insoluble drug griseofulvin (gris) so as to enhance its bioavailability, absorption and therapeutic efficacy. This was to be accomplished by incorporating the drug in polyvinylpyrrolidone (PVP) solid dispersions. Thus, gris and PVP were dissolved in a common solvent and then isolated as an intimate mixture or complex. In this work, the effect of several surfactants on the dissolution rates of gris from the gris/PVP solid dispersions was determined. The anionic surfactant sodium dodecyl sulfate (SDS), the cationic surfactant deodecyltrimethylammonium bromide (DTAB) and the non-ionic surfactant polyoxyethylene dodecylether (Brij-35) were added in equivalent amounts (0.01% w/v) to the release media. The anionic surfactant greatly enhanced the dissolution rate of gris. The non-ionic and cationic surfactants showed a less pronounced positive influence on the release of gris.

Drugs with low water solubilities are often characterized by low absorption and poor oral bioavailability. Thus, many studies have been carried out aimed at increasing the dissolution rates and solubilities of such drugs to increase their total bioavailability in gastrointestinal (GI) absorption. For example, hydrophobic drugs have been dispersed in water-soluble polymers to form so-called "solid dispersions"(*1*). A solid dispersion is a multi-particulate delivery system that consists of one or more active ingredients dispersed in an inert carrier or matrix. The use of solid dispersions to increase the rate of dissolution of drug was first demonstrated by Sekiguchi and Obi *(2)*.

The enhanced dissolution rates observed from many of these formulations has been attributed to several different factors including : a) the existence of a metastable form of the drug that can be stabilized by specific interactions with the polymer, such as, hydrogen bonds *(3,4)*; b) a reduction in particle size or particle agglomeration due to the presence of the polymer *(5-7)*; c) an increase in the surface wetting of the drug; and d) the formation of water-soluble drug/polymer complexes *(8)*.

---

[1] Current address: Advanced Polymer Systems, 3696 Haven Avenue, Redwood City, CA 94063.

The physical forms of the drug and the dispersions produced depends on factors such as: a) the method of preparation, b) the solvent used c) the molecular weight of the polymer d) the drug loading, and e) the physico-chemical properties of the drug. Drug-carrier interactions must be carefully evaluated during preformulation studies, since they can significantly affect the system's biopharmaceutical properties. Therefore, a through understanding of these interactions is necessary to formulate an effective solid dispersion dosage form or particular drug.

In the solid dispersion technology, an ideal carrier should meet the following criteria:

- it should be freely water soluble with intrinsic rapid dissolution properties;
- it should be non-toxic;
- it should be chemically compatible with the drug;
- it should not form strongly-bonded complexes with high association constants that will reduce dissolution rates; and
- it should be pharmacologically inert.

Polyvinylpyrrolidone (PVP) is a water soluble synthetic polymer that fully meets these criteria. Polyvinylpyrrolidone (PVP) is a water soluble synthetic polymer that has been used in the formation of several solid dispersions *(3-8)*. PVP is good matrix material because it undergoes rapid dissolution; it is non-toxic; it is compatible with many drugs; and it is pharmacologically inert.

PVP appears to aid in bioavailability in three ways: First, the dissolution rates of many poorly soluble drugs are faster from PVP dispersions. Second, PVP appears to form water soluble or water dispersible complexes of indefinite composition with many insoluble or slightly soluble drugs. Third, PVP appears to inhibit or retard the nucleation and crystal growth of drugs once they are dissolved, thus, allowing for the formation of supersaturated solutions. PVP is also notable for the ease with which it forms "complexes" in the solid state with a diversity of drugs. Hydrophobic and hydrogen bonding can play a role in the complexation process because PVP contains hydrophilic (pyrrolidone ring) and hydrophobic (vinyl chain) groups. In most cases, these complexes have a high aqueous solubility depending on copolymer ratio.

The objective of this ongoing project is to increase the dissolution rate of griseofulvin (gris), which is an antibiotic, antifungal agent used in the treatment of mycotic diseases of the skin, hair and nails *(9)*. Gris has been shown to be incompletely and irregularly absorbed after oral administration because of its slow dissolution rate in the GI tract *(10)*. In order to improve absorption from the GI tract, tablets and capsules are formulated to contain microsize crystals of gris. Erratic and incomplete absorption with these formulations can still occur as shown by the sensitivity of gris bioavailability to the dissolution rate of tablets *(9)*. Therefore, a convenient, acceptable and improved dosage form of gris is needed from which the drug is uniformly, rapidly and maximally absorbed in humans. In the present study , the dissolution of gris from PVP dispersions was studied in solutions containing charged and non-charged surfactants. The effect of surfactants was investigated because of their potential to aid in the release of

Downloaded by CORNELL UNIV on October 31, 2012 | http://pubs.acs.org
Publication Date: September 24, 1998 | doi: 10.1021/bk-1998-0709.ch017

drugs. Since the length of carbon chains in a surfactant influences its behavior, all the surfactants used contained a dodecyl chain.

Experimental

Materials. Griseofulvin (gris) (Aldrich, USA) with the formula $C_{17}H_{17}ClO_6$ was used as a hydrophobic model drug. Polyvinylpyrrolidone (PVP) (Sigma, USA) with a number-average molecular weight of 40,000 was used as the carrier. Both gris and PVP were in powder form when received form the companies and used as received. Methylene chloride (MeCl, Fisher, U.S.A) was used as the solvent in the preparation of the solid dispersions. Sodium dodecyl sulfate (SDS, Aldrich, U.S.A), is an anionic surfactant with the formula of $C_{12}H_{25}SO_4Na$, polyoxyethylene dodecylether (Brij-35, Aldrich, U.S.A), is a nonionic surfactant with the formula $CH_3(CH_2)_{11}(OCH_2CH_2)_yOH$ and with y=23, dodecyltrimethylammonium bromide (DTAB, Aldrich, U.S.A), is a cationic surfactant with the formula $(CH_3)N(CH_2)_{11}CH_3Br$, were evaluated in the release studies.

Methods. The required amount of polymer and drug were weighed, dissolved in a minimum amount of solvent to obtain a homogeneous solution. Then, the solvent was removed under reduced pressure at 50 ± 2°C on a rotary evaporator. The residue was dried in a vacuum oven at 70 °C overnight. Solid dispersions were prepared from various drug-to-PVP ratios. MeCl had previously been shown to be the best solvent for the preparation of gris-PVP dispersions (H. Akin, J. Heller and F.W.Harris, University of Akron, unpublished data). The each batch of the prepared dispersions was tested for content of the drug. This was done by dissolving a weighed amount of the dispersion in MeCl and the content of the gris was determined spectrophotometrically at 294 nm.

Gris was also treated with MeCl to investigate the solvent effect on the drug. Thus, the drug was dissolved in the solvent and then recovered by removing the solvent under reduced pressure. Physical mixtures were also prepared by simply mixing the drug and the PVP in various proportions.

Solid Dispersion Characterization

Physicochemical Analysis. The physical nature, solid-solid interactions and homogeneity of the solid dispersion systems and physical mixtures were evaluated by differential scanning calorimeter (DSC) and wide angle X-ray diffractometry (WAXD).

DSC thermograms were obtained using a DuPont 1090 Differential Scanning Calorimeter equipped with a DuPont 9900 thermal analyzer. Samples contained in DSC aluminum pans (5-10 mg) were heated at a rate of 10 °C/min under a nitrogen atmosphere.

WAXD powder patterns were obtained using a Rigaku X-ray generator (40 kV, 150 mA) with a scanning rate of 4°/min. A rotating anode was the source of the incident X-ray beam. The WAXD pattern was acquired at the diffraction angles, 2θ, of 10 to 35°. The dried samples were compressed in 4 mm diameter hole of the aluminum sample holder.

Release Experiments. Release rate experiments were carried out under nonsink conditions. A powdered sample equivalent to 20 mg of gris was dispersed in 400

Downloaded by CORNELL UNIV on October 31, 2012 | http://pubs.acs.org
Publication Date: September 24, 1998 | doi: 10.1021/bk-1998-0709.ch017

ml of a pH=6.4 phosphate buffer solution. At appropriate intervals, 3 ml samples were withdrawn, filtered through a 0.22 μm membrane, and analyzed for gris with UV spectroscopy. All of the release experiments were carried out at 37 °C in a shaker water-bath at 70 strokes/min. For comparison purposes, solvent treated samples of gris were also used in the release experiments. To determine the effect of surfactant on gris dissolution, anionic SDS, cationic DTAB and nonionic Brij-35 surfactants (0.01%) were also added to the release media of the MeCl-treated gris sample and solid dispersions

Result and Discussion

Physicochemical Studies. Pure gris and PVP displayed crystalline and amorphous X-ray patterns, respectively. The sharp diffraction peaks attributed to the gris crystals were maintained in all the physical mixtures. The intensity of the diffraction peaks was dependent on the ratio of gris to PVP.

DSC thermograms of gris-PVP physical mixtures exhibits a broad endothermic peak around 70-100 °C, which was attributed to the vaporization of moisture, and an endothermic peak near 220 °C corresponding to the melting point of gris. The intensity of the peak at 220 °C decreased and shifted to lower temperatures with increasing PVP content.

Polymorphism was not apparent in the gris samples recovered from MeCl. The X-ray diffraction peaks and the melting points of the gris crystals obtained in this manner were consistent with those of the original crystal powder.

The X-ray patterns and DSC thermograms of the solid dispersions are presented in Figures 1 and 2. The sharp diffraction peaks attributed gris crystals disappeared in the X-ray diffraction patterns of the dispersions composed of different gris-to-PVP (w/w) ratios such as 1:3, 1:5, 1:7 and 1:10. The peak at 220 °C which corresponds to the melting point of gris was disappeared in the DSC thermograms of these dispersions. The absence of gris diffraction peaks and the melting peak in X-ray pattern and DSC thermograms, respectively, indicates that was only obtained from the 1:1 ratio of gris-to-PVP. Thus, the ratio of gris-to-PVP had to be less than 1:1 in order to obtain amorphous solid dispersions to get better dissolution and water solubility.

Downloaded by CORNELL UNIV on October 31, 2012 | http://pubs.acs.org
Publication Date: September 24, 1998 | doi: 10.1021/bk-1998-0709.ch017

Release Rate Studies. The release rate of gris from all studied physical mixtures was faster than from those of commercial and MeCl treated gris samples alone. But the initial release of drug from the mixtures was independent of their PVP content. Approximately 26% of the gris in the physical mixtures dissolved in 10 min. However, after this point no additional gris dissolved. The increase in the release rate of gris from the physical mixtures may have been due to a surfactant effect of PVP, which increased the wetting of the drug particles.

The solvent treated gris samples dissolved slower than commercial gris (received one). Approximately 19.0 % of the commercial gris sample dissolved in 30 min, while only 5.3% of the MeCl-treated samples dissolved during this time.

The solid dispersions provided significantly faster drug dissolution than the commercial gris and physical mixtures (Figure 3). In fact, there was rapid saturation of the release medium due to the non-sink conditions. The concentration of the drug exceeded its reported solubility limit (15 mg/L) within a

Downloaded by CORNELL UNIV on October 31, 2012 | http://pubs.acs.org
Publication Date: September 24, 1998 | doi: 10.1021/bk-1998-0709.ch017

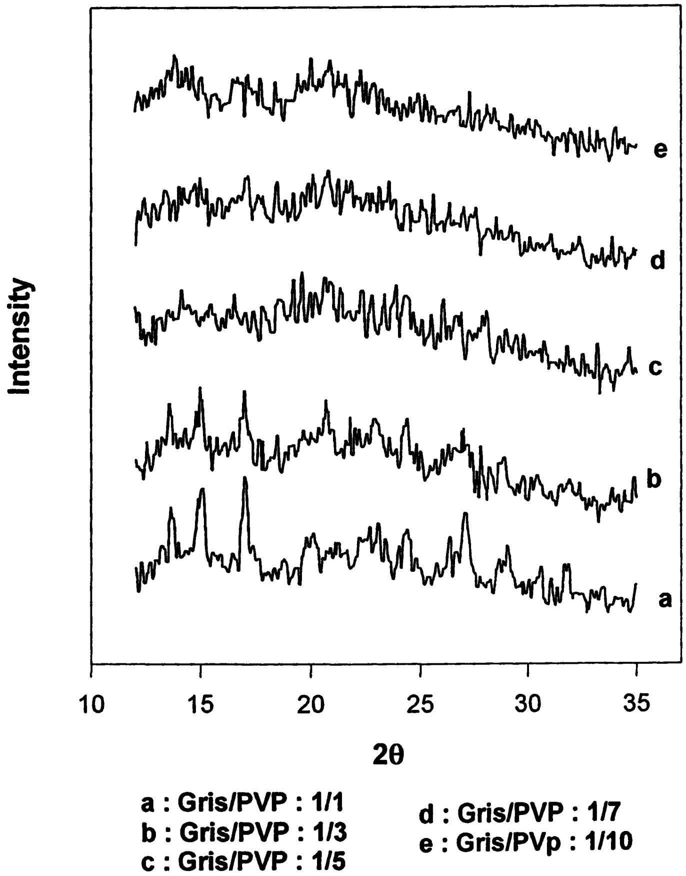

Figure 1. The X-ray pattern of the solid dispersions

few minutes, peaked and then decreased gradually. The faster dissolution rates can be attributed to the presence at amorphous drug and drug co-dissolution with the water-soluble PVP. Dissolved PVP is also known to inhibit or retard the crystallization of the drug. Thus, the apparent dissolution curves of the solid dispersions represent the difference between the rate of dissolution and the rate of crystallization. When the rate of dissolution is greater than the rate of recrystallization, the slope is positive. At the maximum, the rates of dissolution and recrystallization are equal. The slope becomes negative when the rate of recrystallization exceeds the rate of dissolution. In this case, PVP in solution helped maintain the supersaturated condition for 6 h. Only the solid dispersion prepared from a 1:1 (w/w) gris-to-PVP ratio, which had been shown to be semicrystalline, released gris slower than the corresponding 1:1 (w/w) gris-to-PVP physical mixture.

The amount of gris released from the dispersions was dependent on the PVP content of the dispersions. The amount of gris that was released increased as

Downloaded by CORNELL UNIV on October 31, 2012 | http://pubs.acs.org
Publication Date: September 24, 1998 | doi: 10.1021/bk-1998-0709.ch017

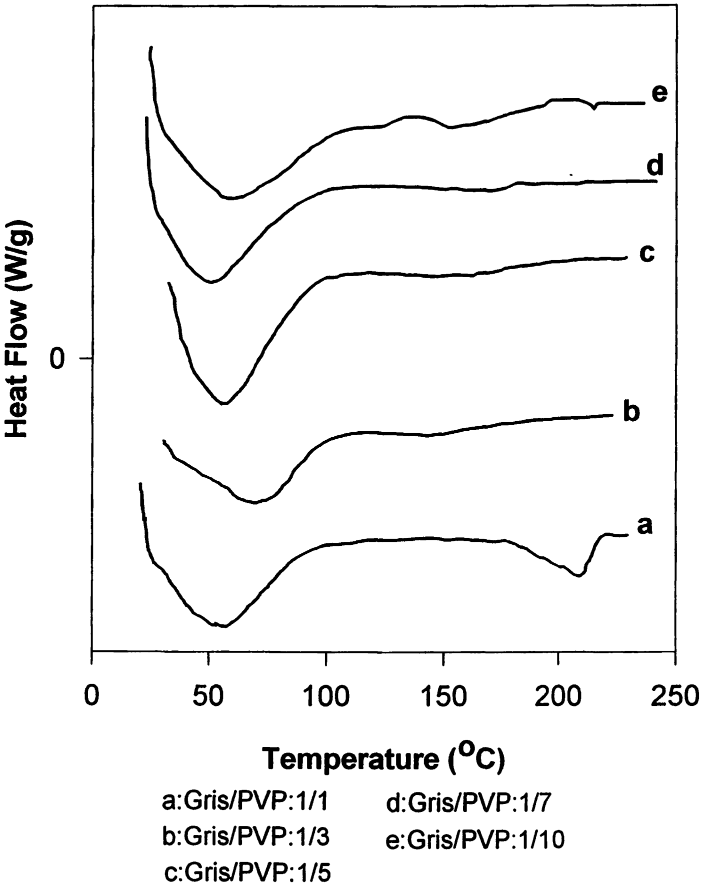

Figure 2. The DSC thermograms of the solid dispersions

the PVP content was increased. The maximum release was obtained with a dispersion prepared from a gris-to-PVP (w/w) ratio of 1:5. A further increase in the gris-to-PVP ratio to 1:7 did not result in more gris being released.

The surfactant effects on the release of gris from the solid dispersions are shown in Figures 4-6. The charged and non-charged surfactants enhanced the dissolution rates and the amount of gris that dissolved. In the case of the anionic surfactant (SDS), approximately 70% of gris dissolved in 30 min while only 40% of the gris dissolved from 1/5 gris-to-PVP solid dispersions without surfactant during this time. The most dramatic increases in the dissolution rate of gris were observed for 1/7 and 1/10 gris-to-PVP solid dispersions. Complete gris dissolution was obtained in 30 min from the 1/10 gris-to-PVP solid dispersion and in 400 min from the 1/7 gris-to-PVP dispersion. Although the cationic (DTAB) and nonionic (Brij-35) surfactants did not enhance the gris release rate as much as

Downloaded by CORNELL UNIV on October 31, 2012 | http://pubs.acs.org
Publication Date: September 24, 1998 | doi: 10.1021/bk-1998-0709.ch017

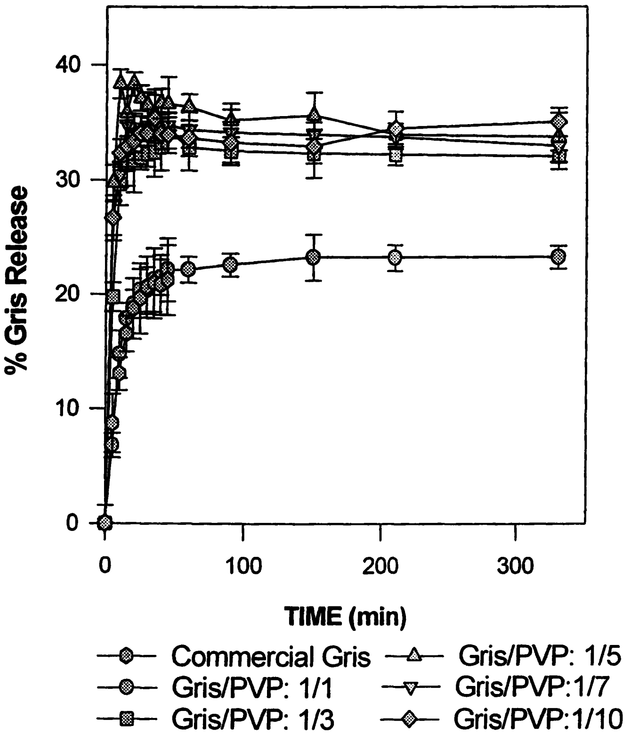

Figure 3. Gris dissolution from solid dispersions

Downloaded by CORNELL UNIV on October 31, 2012 | http://pubs.acs.org
Publication Date: September 24, 1998 | doi: 10.1021/bk-1998-0709.ch017

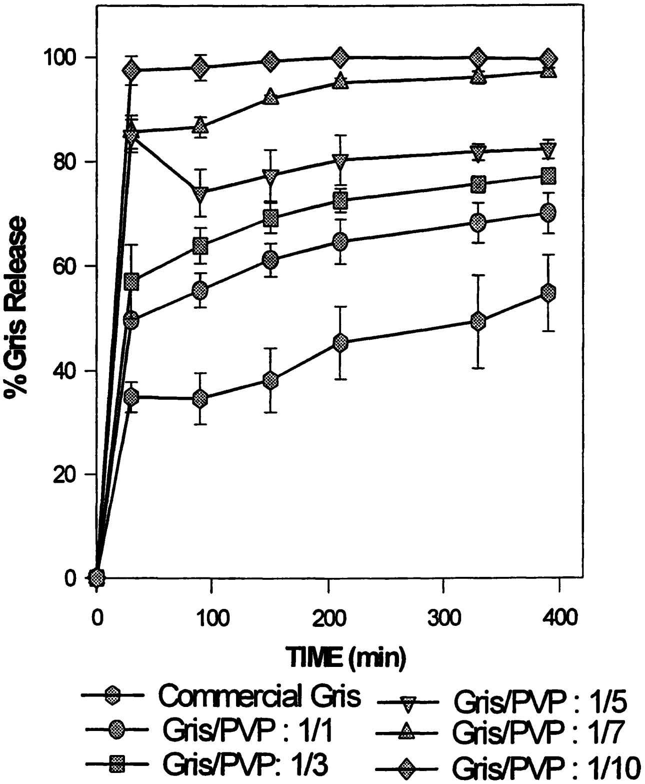

Figure 4. Effect of an anionic surfactant on the release of gris

In Tailored Polymeric Materials for Controlled Delivery Systems; McCulloch, I., et al.;
ACS Symposium Series; American Chemical Society: Washington, DC, 1998.

Downloaded by CORNELL UNIV on October 31, 2012 | http://pubs.acs.org
Publication Date: September 24, 1998 | doi: 10.1021/bk-1998-0709.ch017

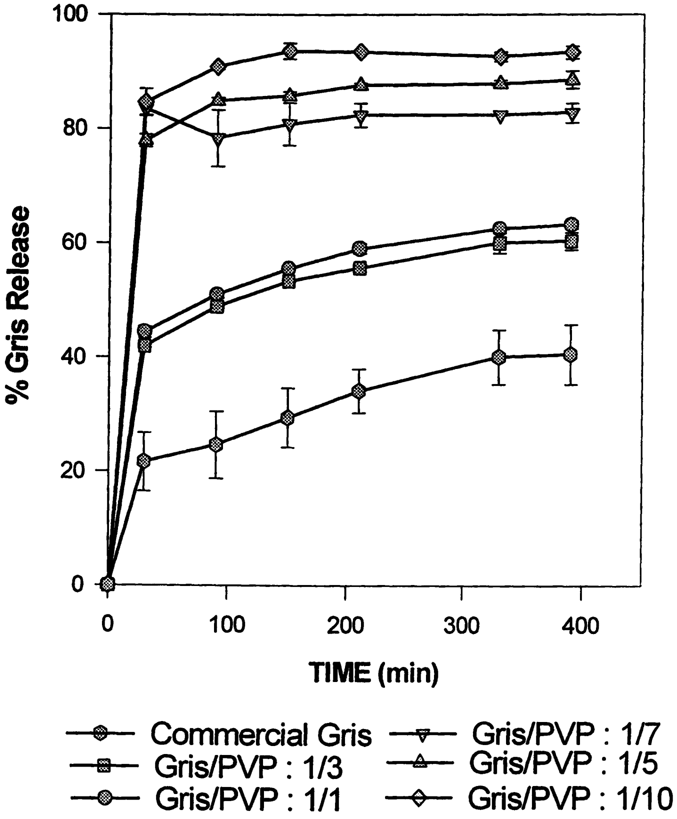

Figure 5. Effect of a cationic surfactant on the release of gris

Downloaded by CORNELL UNIV on October 31, 2012 | http://pubs.acs.org
Publication Date: September 24, 1998 | doi: 10.1021/bk-1998-0709.ch017

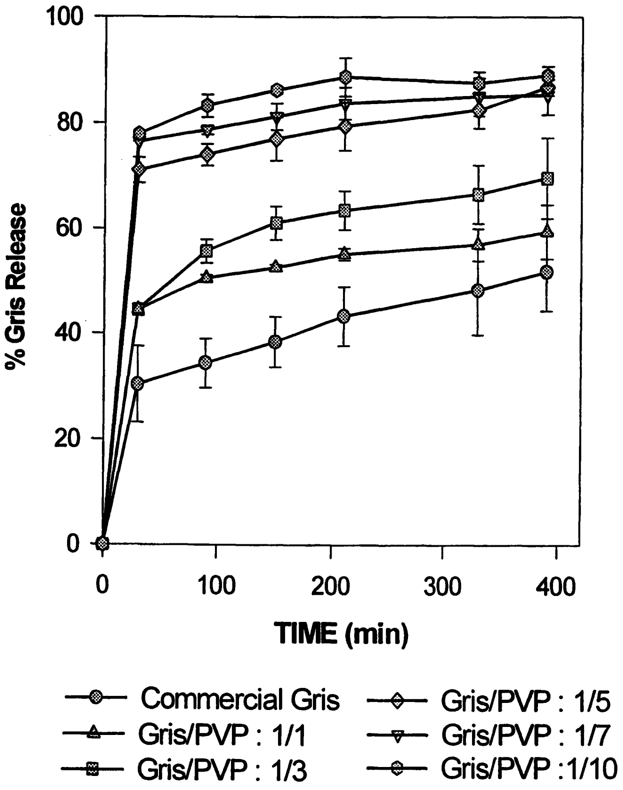

Figure 6. Effect of a non-charged surfactant on the release of gris

the anionic surfactant, the rates were still significantly increased. The effect was noticeable for the 1/5, 1/7, and 1/10 gris-to-PVP solid dispersions where the amount of gris released was twice that of the gris released in the absence of the surfactants.

Conclusion

Amorphous dispersions of gris in PVP can be prepared from MeCl solutions. However, the ratio of gris-to-PVP has to be less than 1:1 (w/w) in order to prevent the gris from undergoing crystallization. The T_g of the PVP is significantly decreased in the dispersions suggesting that there are strong interactions between the drug and PVP. The amount of gris released from the dispersions in a phosphate buffer solution increases as the ratio of gris-to-PVP decreases from 1:1 to 1:5. The amount of gris released is not increased by further increases in the amount of PVP. The maximum amount of gris released in % 40 in 400 minutes is 2 times greater than the amount of gris released from pure gris powder in the same time period. Anionic, cationic and non-charged surfactants in the buffer enhance the dissolution rate and increase the amount of gris released.

Acknowledgement

The support of this research by Advanced Polymer Systems is gratefully acknowledged.

References

1. W.L.Chiou and S.Riegelman, J.Pharm.Sci., 1971, 60, 1281.
2. K. Sekiguchi and N. Obi, *Chem. Pharm. Bull.*, 9, 866-872, 1961.
3. B.J.Hargreaves, J.E.Pearson, P.Connor, J.Pharm.Pharmacol., 1979, 31, 47P.
4. A.P.Simonelli, S.C.Mehta, W.I.Higuchi, J.Pharm. Sci., 1969, 58, 538.
5. B.A.Bolton, P.N.Prasad, J.Pharm.Sci., 1984, 73(12), 1849.
6. R.Jachowicz, Int.J.Pharm., 1987, 35, 1.
7. A.Hoelgaard, N.Moeller, Arch.Pharm.Chemi., Sci.Ed., 1975, 3(3), 67.
8. A.P.Simonelli, S.C.Mehta, W.I.Higuchi, J.Pharm.Sci., 1976, 65(3), 355.
9. N. Aoyagi, H. Ogata, N. Kaniwa, M. Koibuchi, T. Shibazaki, A. Ejima, J.Pharm.Sci, 1982, 71(10), 1165.
10. H. Blank, Am. J. Medicine, 39, 831, 1965.

Downloaded by CORNELL UNIV on October 31, 2012 | http://pubs.acs.org
Publication Date: September 24, 1998 | doi: 10.1021/bk-1998-0709.ch017

Downloaded by NORTH CAROLINA STATE UNIV on October 31, 2012 | http://pubs.acs.org
Publication Date: September 24, 1998 | doi: 10.1021/bk-1998-0709.ch018

Chapter 18

Self-Diffusion of Solvents and Solute Probes in Polymer Solutions and Gels: The Use of a New Physical Model of Diffusion

X. X. Zhu[1], L. Masaro[1], J.-M. Petit[1], B. Roux[1], and P. M. Macdonald[2]

[1]**Département de Chimie, Université de Montréal, C. P. 6128, Succursale Centre-ville, Montréal, Québec H3C 3J7, Canada**
[2]**Department of Chemistry and Erindale College, University of Toronto, 3359 Mississauga Road, Mississauga, Ontario L5L 1A2, Canada**

We have proposed a new physical model for the interpretation of the diffusion of solvent and other solute molecules in polymer solutions. In this model, the polymer solution is regarded as a network where the diffusing molecules have to overcome periodic energy barriers of equal magnitude, and the distance between the barriers corresponds to the correlation length in polymer solutions. The new diffusion model has been used successfully to describe the effects of polymer concentration, temperature and molecular size of the diffusants on the self-diffusion coefficients of various molecular probes in several polymer systems. It has been shown that this model applies to the diffusion of small molecules in polymer matrices, such as ternary aqueous systems of poly(vinyl alcohol) (PVA) and binary organic solutions of poly(methyl methacrylate). In an effort to link the diffusion properties of small and large molecules in polymer systems, we have measured the self-diffusion coefficients of a series of solute probes, including ethylene glycol and its oligomers and polymers in aqueous solutions and gels of PVA using the pulsed-gradient spin-echo NMR technique. The self-diffusion coefficients of the solute probes decrease with increasing PVA concentrations and with increasing molecular size of the probes. The effect of temperature on the self-diffusion coefficients has also been studied with selected probe molecules. The dependence of the physical parameters in the diffusion model on the molecular size of the diffusant and on temperature is also discussed.

In Tailored Polymeric Materials for Controlled Delivery Systems; McCulloch, I., et al.;
ACS Symposium Series; American Chemical Society: Washington, DC, 1998.

The release of drugs from polymer matrices is a typical diffusion process, which is dependent on various physical parameters of the system. This process may also be coupled with chemical reactions such as the degradation of the polymer matrix. The addition of plasticizers in polymers, the permeability through polymer membranes and the miscibility of polymers are all related to diffusion in polymers (*1-3*). Therefore, the understanding of the diffusion process is important to the application of polymer materials. With the development of pulsed field-gradient NMR spectroscopic methods (*4,5*), self-diffusion of various diffusants in polymer systems can now be easily determined. The diffusion of solvent and solute molecules in polymer gels may be influenced by many factors: polymer concentration, size and shape of the diffusant, temperature, and any specific interactions in the polymer networks. The elucidation of these effects are useful in the application of the polymer gels in the controlled release technology.

To understand the diffusion in polymers, physical models describing self-diffusion of solvents and solutes in polymer systems are needed. It would be interesting and useful to be able to predict or to estimate the diffusion rates of a component such as a drug molecule in a given polymer mixture. Various theoretical descriptions of solvent diffusion in polymers have been proposed. Diffusion of small solute molecules in organic polymer solutions is readily handled using the models based on the free volume theory (*6,7*) or microscopic friction coefficients (*8*). When the solute is an electrolyte, its diffusion can be described by using an adaption of Fujita's free volume theory for pseudo-binary systems, as shown by Yasuda (*9*). When the solute is a larger molecule such as poly(ethylene glycol), free volume theory proves to be limited as a means of predicting diffusion bahavior (*10*). Such a model can reproduce the polymer concentration dependence of the self-diffusion of small solute molecules in a poly(vinyl alcohol) (PVA)-water system (*10*), but fails to account for the temperature dependence. The obstruction theory set out by Mackie and Meares (*11*) includes aqueous systems, but is strictly limited to small solvent molecules and does not account for the size effects of the diffusants as observed by Waggoner *et al* (*12*). Obstruction theories have been modified to describe the diffusion of larger spherical molecules in dilute media (*13,14*), they still do not apply in concentrated solutions. To explain the molecular size effects, a model based on kinetic theory has been proposed (*15*), but proved to be less than satisfactory at higher polymer concentrations. Various hydrodynamic models of the interactions between solute and polymer (*16-21*) can help in the interpretation of the diffusion behavior in polymers. The use and limitations of the models have been shown previously in the treatment of the diffusion data obtained for aqueous solutions of poly(vinyl alcohol) (*10,22*). The reptation theory of diffusion established by de Gennes (*23,24*) relates the diffusion coefficient with the molecular weight of the diffusant and the concentration of the polymer and has been used widely for gel electrophoretic separations of biopolymers such as DNA (*25,26*). The dependence of the self-diffusion coefficient on polymer concentration as stipulated by the theory did not always hold, especially for the continuous diffusion data over a large range of polymer concentrations (*27,28*).

It may be difficult, if not impossible, to find a single physical model of diffusion which can successfully treat solute diffusion in polymer solutions over a wide range of physical situations (solute size and shape, polymer concentration, temperature, etc.). Any

Downloaded by NORTH CAROLINA STATE UNIV on October 31, 2012 | http://pubs.acs.org
Publication Date: September 24, 1998 | doi: 10.1021/bk-1998-0709.ch018

Downloaded by NORTH CAROLINA STATE UNIV on October 31, 2012 | http://pubs.acs.org
Publication Date: September 24, 1998 | doi: 10.1021/bk-1998-0709.ch018

physical model capable of bridging the gap between the diffusion behavior of small versus large solute molecules needs first to distinguish small molecules from large. In semidilute polymer solutions a convenient discriminator of large versus small molecules is the mesh size ξ introduced by de Gennes to describe the correlation length in his representation of the semidilute polymer solution as a statistical network (*29*). We have proposed a new physical model for the diffusion of solvent and solute molecules in polymer solutions. By treating the polymer solution as a statistical network through which the solute diffuses in a series of jumps over potential barriers determined by the correlation length, we find that we can describe the diffusion bahavior of both small and large solutes, in both dilute and more concentrated polymer solutions in water and organic solvents (*10,22,30,31*), and over a range of temperatures.

In order to make a link between the diffusion of small molecules and that of larger diffusants such as oligomers and polymers, we selected a series of solute probes including ethylene glycol and its oligomers and polymers and measured their self-diffusion coefficients in aqueous solutions and gels of PVA using the pulsed-gradient spin-echo (PGSE) NMR techniques. By examining the effects of polymer concentration, probe size and temperature on the self-diffusion of these probe molecules, we have tested the validity of the new model of diffusion for the case of larger diffusant molecules such as oligomers and polymers.

The Physical Model

In the scaling theory of de Gennes, a semidilute polymer solution is represented by a transient statistical network with mesh size ξ, known as the correlation length (*29*). We regard the polymer matrix through which the diffusant moves as a statistical network with a certain mesh size. The diffusing molecule, either the solvent or the solute, is considered as a particle residing temporarily in a potential energy well and the diffusion occurs when the particle has enough energy to overcome a certain potential barrier and jump into the adjacent potential energy well. An illustration of a one-dimensional diffusion through a periodic energy potential is shown in Figure 1. The energy potentials are assumed to be of equal amplitude ΔE and spaced at intervals equal to ξ, a certain average mesh size in the polymer networks over a much larger concentration range.

Applying Fick's first law of diffusion to a lattice model leads to the well known relation for the diffusion coefficient:

$$D = k\,\xi^2 \qquad (1)$$

where k is the jump frequency, which is expected to depend on temperature and size of the diffusant. For an ensemble of non-interacting particles moving in a matrix such as represented in Figure 1, this jump frequency over the periodic energy barriers, or escape rate as it is termed by Kramers (*32*), can be written in an Arrhenius form:

$$k = F_p \exp\left(-\frac{\Delta E}{k_B\,T}\right) \qquad (2)$$

Downloaded by NORTH CAROLINA STATE UNIV on October 31, 2012 | http://pubs.acs.org
Publication Date: September 24, 1998 | doi: 10.1021/bk-1998-0709.ch018

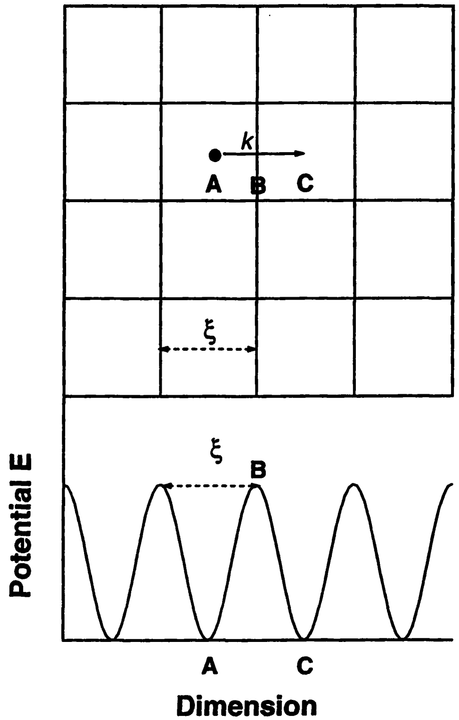

Figure 1. Representation of a polymer solution as a network of mesh size ξ and potential E for the diffusion process of a molecule in a polymer solution. (Reproduced with permission from ref. 22, Copyright 1996 ACS.)

Downloaded by NORTH CAROLINA STATE UNIV on October 31, 2012 | http://pubs.acs.org
Publication Date: September 24, 1998 | doi: 10.1021/bk-1998-0709.ch018

where F_p is a frequency prefactor, ΔE is the height of the potential barrier, k_B is the Boltzmann constant, and T is the temperature. The parameter k is the rate at which a particle originally residing in the potential energy well at A jumps into C crossing the barrier at B as a consequence of Brownian motion (Figure 1). The potential barrier ΔE is a free energy arising from both enthalpic and entropic contributions. We assume that it is more or less a constant within a certain temperature range. The dependence of ξ on the polymer concentration in the semidilute regime can be described by the equation (*29*)

$$\xi = \beta c^{-v} \qquad (3)$$

where c is the polymer concentration, β and v are constants of the system. When the polymer chains are longer than the mesh size and in a solution where the concentration is sufficiently high, ξ depends only on the concentration and not on the the molecular weight of the polymer.

It is generally assumed that the total friction coefficient, f, experienced by a diffusing molecule results from an additive contribution from the liquid solvent background, f_0, and from the polymer network, f_p (*33,34*):

$$f = f_0 + f_P \qquad (4)$$

where the term f_p represents the excess of friction due to the polymer. Using the Stokes-Einstein relation, $D = k_B T / f$, and equation 1, we can rewrite equation 4 as the following:

$$\frac{1}{D} = \frac{1}{D_0} + \frac{1}{k\xi^2} \qquad (5)$$

where D_0 is the diffusion coefficient of the diffusing molecule in the absence of the polymer. Substituting equation 3 into 5 followed by rearrangements gives equation 6:

$$\frac{D}{D_0} = \frac{1}{1 + a c^{2v}} \qquad (6)$$

where

$$a = \frac{D_0}{k\,\beta^2} \qquad (7)$$

and $k\beta^2$ and v are the characteristic parameters of the model. The parameter v should depend on the quality of the solvent and β should not vary as a function of polymer concentration or the molecular weight of the polymer. The parameter k denpends on F_p and ΔE, which should both be functions of the polymer concentration, and this dependence will be evident over a large range of polymer concentrations. To simplify the treatment, we assume that, to a first approximation, k remains constant within a certain concentration range, i.e., k does not change although the mesh size of the polymer network does with varying polymer concentration. For a given polymer-solvent system, it is expected that β remains constant so that $k\beta^2$ depends only on the size of the diffusing molecule and on the temperature.

Experimental

The samples for the diffusion studies include binary poly(methyl methacrylate) (PMMA)-organic solvent (*30,31*) and ternary PVA-water-solute systems (*10,22*). The PMMA used has a molecular weight of 60,000. PVA samples of different degrees of hydrolysis (DH) and molecular weights (M) were used (*10*), which include PVA1 (DH = 99 % and M = 50,000), PVA2 (DH = 99 % and M = 115,000) and PVA3 (DH = 87 - 89 % and M = 115,000). For the binary systems, a series of ketones and esters with varying molecular size and shape were selected as the solvent for PMMA. For the aqueous ternary systems, a series of small molecules including alcohols, acid, amine and amide were selected as the solute probes. Ethylene glycol (EG) and its oligomers (OEG) and polymers (PEG) were also used as probes. Size exclusion chromatography (SEC) of the oligo- and poly(ethylene glycol)s showed that the molecular weights (M_n and M_w) of each of the OEG and PEG samples are quite narrowly distributed ($M_w/M_n < 1.1$). The PEG samples were PEG-200, PEG-400, PEG-600, PEG-1000, PEG-2000 and PEG-4000. The molecular weight of PEG is represented by the number following PEG.

The preparation of the samples for NMR experiments has been described (*10,22,30,31*). For the ternary aqueous systems, PVA was dissolved in D_2O containing 1 wt% solute probe. The concentration of polymer ranged from 0.03 to 0.38 g/mL. The NMR tubes containing the samples were sealed to avoid evaporation of the solvent and then heated to about 100 °C. The heating of the samples is necessary to help the mixing and also to prevent gelation effects. The NMR measurements were made within the three following days.

The self-diffusion coefficients were measured by the use of the PGSE NMR technique developed by Stejskal and Tanner ($90°_x$ - τ - $180°_y$ - τ - echo, with gradient pulses during the half echo time τ) (*35*) on a Chemagnetics CMX-300 NMR spectrometer operating at 300 MHz for protons. A magnetic resonance imaging probe with actively shielded gradients coils (Doty Scientific, Columbia, SC) and a Techron gradient amplifier were used. The details of the experiment have been described previously (*10,30,36*). Gradient was applied only in the z direction. The gradient strengths used in this study were between 0.3 and 0.6 T/m, calibrated with a sample of known self-diffusion coefficient (*37*). Variable temperature NMR experiments were performed at 23, 33, 43 and 53 °C. The self-diffusion coefficient D can be extracted from the attenuation of the NMR signals due to the application of the gradient pulse of various durations (*4*). The error of the measured self-diffusion coefficients was estimated as less than 5%. A nonlinear least-square fitting method was used to fit the experimental data to the diffusion model (equation 6) and the errors listed in the tables are expressed as the root-mean-square (RMS) fractional errors.

Downloaded by NORTH CAROLINA STATE UNIV on October 31, 2012 | http://pubs.acs.org
Publication Date: September 24, 1998 | doi: 10.1021/bk-1998-0709.ch018

Downloaded by NORTH CAROLINA STATE UNIV on October 31, 2012 | http://pubs.acs.org
Publication Date: September 24, 1998 | doi: 10.1021/bk-1998-0709.ch018

Results and Discussion

PMMA-Organic Solvent Binary Systems. To verify the validity of the proposed model in polymer-organic solvent binary systems, we used the model to fit our previously reported solvent diffusion data in PMMA solutions for a series of ketones and esters varying in size and shape (*30,31*). The parameters from the fittings are listed in Table 1. Selected examples are shown in Figure 2 and it is clear that equation 6 provides excellent fits to the experimental self-diffusion coefficients as a function of PMMA concentration over a wide range of concentrations. The root mean square (RMS) errors are somewhat greater than those listed in Tables 2-4 for the aqueous systems, possibly due to the fact the ketone and ester diffusion data cover a much larger concentration range. In addition, the experimental error involved in diffusion measurements of the more concentrated samples was usually higher than the dilute ones due to the limitations of the NMR technique (*30,36*).

As shown in Table 1, the parameter ν is approximately the same for all the ester and ketone solvents investigated, with a mean value of 0.67 for the esters and 0.68 for the ketones. The values of $k\beta^2$ of the diffusants in Table 1 are calculated from equation 7 with the D_0 values obtained from the Stokes-Einstein equation. Figure 3 shows that the values of $k\beta^2$ is inversely proportional to the hydrodynamic radius of the diffusing solvent molecules. It should be noted that the solvents are different and the β values are expected to be also different. However, since each series of the solvents (ketones and esters, respectively) consists of similar solvents, we assume that, within each series, the value of β does not vary significantly so that its effect on $k\beta^2$ is minor. Thus, in general, for both ketone and ester solvents, k decreases as the size of the diffusing molecule increases. Parameter k is the jump frequency of the diffusing molecule from the potential energy well and should depend on the nature of the molecules, especially the molecular size. It is reasonable to expect that the larger molecules will have a lower jump frequency. Therefore, according to equation 2, the potential barrier ΔE should be higher for larger diffusant molecules.

PVA-Water Ternary Systems. For the PVA-water-solute-probe ternary systems, we have verified the influence of the molecular weight and concentration of PVA, the molecular size of the the diffusant, and temperature on the self-diffusion coefficients of the solute probes.

(1) Effect of molecular weight of the polymer. The polymer concentration of the aqueous ternary systems ranged from 0 to about 0.4 g/mL. At the higher end, the samples were in fact viscous gels. Clearly, the self-diffusion coefficients of the solvent (water) and solute probes depend on the polymer concentration, as we have reported previously (*10,30,31*). We have measured the self-diffusion coefficients of two solute probes (MeOH and *t*BuOH) in PVAs of different molecular weights and the fit parameters obtained for these and all other solute probes are listed in Table 2. The exponent ν appears to be characteristic of a given polymer system, remaining more or less a constant for each group of the PVA samples. Mean values of ν are 0.52 for PVA1, 0.37 for PVA2, and 0.42 for PVA3. Therefore, the parameter ν can be regarded as a constant

Downloaded by NORTH CAROLINA STATE UNIV on October 31, 2012 | http://pubs.acs.org
Publication Date: September 24, 1998 | doi: 10.1021/bk-1998-0709.ch018

Table 1. Molecular sizes, self-diffusion coefficients and parameters ν and $k\beta^2$ obtained from the solvent diffusion data at 23 °C in PMMA systems by curve fitting to equation 6.

Solvent	D_0 (10^{-9} m^2/s)	R_H (Å)	ν	$k\beta^2 \times 10^{10}$	RMS Error
ACT	4.65	1.45	0.65	12.2	0.084
MEK	3.58	1.49	0.72	7.52	0.055
MPK	2.76	1.62	0.68	5.70	0.110
MiPK	2.68	1.72	0.68	2.72	0.061
MBK	2.17	1.66	0.70	4.00	0.047
MtBK	1.58	2.01	0.67	2.19	0.019
MiBK	2.11	1.84	0.70	3.33	0.021
MeAc	3.71	1.57	0.64	9.34	0.248
EtAc	3.04	1.63	0.57	6.77	0.204
PrAc	2.23	1.72	0.66	4.00	0.056
iPrAc	2.41	1.69	0.71	2.81	0.127
MePr	3.01	1.63	0.62	8.24	0.058
MeBu	2.36	1.65	0.68	5.54	0.024
MeiBu	2.42	1.77	0.78	3.81	0.064

Source: Reprinted with permission from ref. 22, Copyright 1996 ACS.

Abbreviations in this table: acetone (ACT), methyl ethyl ketone (MEK), methyl propyl ketone (MPK), methyl isopropyl ketone (MiPK), methyl butyl ketone (MBK), methyl *t*-butyl ketone (MtBK), methyl isobutyl ketone (MiBK), methyl acetate (MeAc), ethyl acetate (EtAc), propyl acetate (PrAc), isopropyl acetate (iPrAc), methyl propionate (MePr), methyl butyrate (MeBu) and methyl isobutyrate (MeiBu).

Downloaded by NORTH CAROLINA STATE UNIV on October 31, 2012 | http://pubs.acs.org
Publication Date: September 24, 1998 | doi: 10.1021/bk-1998-0709.ch018

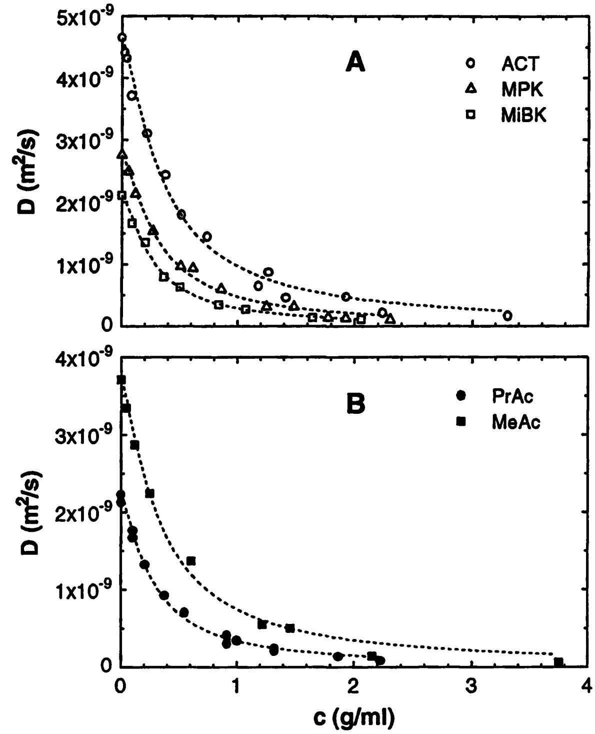

Figure 2. Self-diffusion coefficients of selected solvents in PMMA solutions as a function of PMMA concentration at 23 °C for ketones (A) and esters (B). Dashed lines are fittings to equation 6. Abbreviations: acetone (ACT), methyl propyl ketone (MPK), methyl isobutyl ketone (MiBK), methyl acetate (MeAc), propyl acetate (PrAc). (Reproduced with permission from ref. 22, Copyright 1996 ACS.)

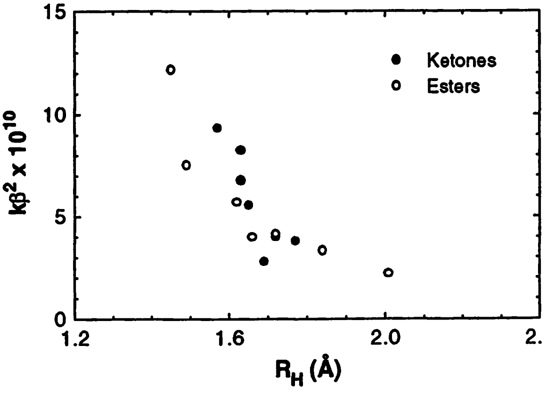

Figure 3. Semi-logarithmic plot of the parameter of the model, kβ^2 plotted as a function of the hydrodynamic radius of the solvent in PMMA-solvent binary systems. (Reproduced with permission from ref. 22, Copyright 1996 ACS.)

within the concentration range of the polymer under study for a given PVA-water system, while the other fitting parameter $k\beta^2$ changes as a function of molecular size of the diffusant, which will be further discussed below. The difference in ν values of PVA1 and PVA2 should be a result of the difference in molecular weight of the polymers, and the difference between PVA2 and PVA3 should result from the difference in the degree of hydrolysis. Apparently, an increase in molecular weight of the polymer leads to a smaller ν value as does an increase in DH of PVA. The changes seem to be logical since an increase in DH should lead to increased hydrogen-bonding of PVA, which implies an increase in the apparent molecular weight of the polymer. However, the proposed physical model in its present form cannot explain the effects of the molecular weight and the degree of hydrolysis of the polymer. The origin of the differences in the fitting parameter ν for PVAs of different molecular weights and structures (namely, DH) remain to be elucidated.

Downloaded by NORTH CAROLINA STATE UNIV on October 31, 2012 | http://pubs.acs.org
Publication Date: September 24, 1998 | doi: 10.1021/bk-1998-0709.ch018

Table 2. Molecular sizes, self-diffusion coefficients and parameters $k\beta^2$ and ν obtained for selected solute probes in PVA1-water systems at 23°C by curve fitting to equation 6.

PVA	Solute	D_0 (10^{-10} m^2/s)	R_H (Å)	ν	$k\beta^2\times10^{10}$	RMS Error
PVA1:	H_2O	19.5	1.20	0.51	5.21	0.006
M = 50,000	MeOH	13.3	1.75	0.47	3.73	0.012
DH = 99%	*t*BuOH	7.07	3.30	0.56	0.98	0.010
	$N(CH_3)_3$	7.96	2.93	0.50	1.68	0.007
	$^+N(CH_3)_4$	9.79	2.38	0.54	1.73	0.004
	HAc	10.35	2.25	0.53	1.73	0.010
	$HCONH_2$	7.37	3.16	0.52	1.27	0.007
PVA2:	MeOH	13.3	1.75	0.35	5.8	0.011
M = 115,000	*t*BuOH	7.07	3.30	0.38	2.0	0.009
DH = 99%						
PVA3:	MeOH	13.3	1.75	0.43	4.9	0.010
M = 115,000	*t*BuOH	7.07	3.30	0.42	1.7	0.007
DH = 87-89%						

Source: Reprinted with permission from ref. 22, Copyright 1996 ACS.

Abbreviations in this table: methanol (MeOH), *t*-butanol (*t*BuOH), acetic acid (HAc), trimethylamine ($N(CH_3)_3$), tetramethylammonium ($^+N(CH_3)_4$), and formamide ($HCONH_2$).

Downloaded by NORTH CAROLINA STATE UNIV on October 31, 2012 | http://pubs.acs.org
Publication Date: September 24, 1998 | doi: 10.1021/bk-1998-0709.ch018

(2) Effect of polymer concentration. The measured self-diffusion coefficients for several series of solute probes as a function of PVA concentration are shown in Figure 4 and the fit parameters are listed in Tables 2 and 3. It is evident that there is a decrease of the values of D with increasing PVA concentration for each of the solute probes. The PVA concentration ranged from dilute solutions to viscous gels. The difference of the self-diffusion coefficients of the solute probes at lower PVA concentrations are greater and it appears that all of the measured D values approach a common low value at high PVA concentrations. In all cases, the proposed model of diffusion seems to be able to reproduce closely the measured D values as a function of the polymer concentration.

Table 3. Molecular sizes, self-diffusion coefficients and parameters $k\beta^2$ and ν obtained for EG and PEG diffusants in PVA1-water systems at 23°C by curve fitting to equation 6.

Sample	D_0 (10^{-10} m^2/s)	R_H (Å)	ν	$k\beta^2 \times 10^{-10}$	RMS Error
EG	9.37	2.43	0.76	0.28	0.13
$(EG)_3$	5.95	3.91	0.60	0.23	0.08
$(EG)_4$	5.38	4.32	0.59	0.24	0.05
$(EG)_5$	4.58	5.08	0.60	0.25	0.04
$(EG)_6$	4.08	5.70	0.63	0.21	0.06
PEG-200	4.84	4.81	0.60	0.24	0.08
PEG-400	3.31	7.00	0.56	0.23	0.04
PEG-600	1.86	12.48	0.58	0.12	0.002
PEG-1000	1.66	13.99	0.49	0.12	0.02
PEG-1500	1.13	20.59	0.54	0.068	0.02
PEG-2000	1.07	22.69	0.53	0.053	0.001
PEG-4000	0.958	24.35	0.50	0.047	0.01

Matsukuwa and Ando studied the diffusion of PEG in water and poly(N,N-dimethylacrylamide) gels by ^1H PGSE NMR spectroscopy (*38*). The D value for PEG-4250 (ca. 1.2 × 10^{-10} m^2/s, for 1 wt% aqueous solution at 303 K) is comparable with the D_0 value determined for PEG-4000 (0.95 × 10^{-10} m^2/s) at 23 °C in this report. Their experimental temperature is about 7 °C higher, and their PEG samples seemed more polydisperse ($M_w/M_n < 1.19$) than the sample used in this study. They have also observed decreases in D values as the degree of swelling of the gels decreased, which corresponds to a higher concentration of the polymers (*38*).

(3) Effect of Molecular Size of the Diffusant. In Figure 4, we can observe the dependence of the measured D values of the solute probes on their molecular sizes. In

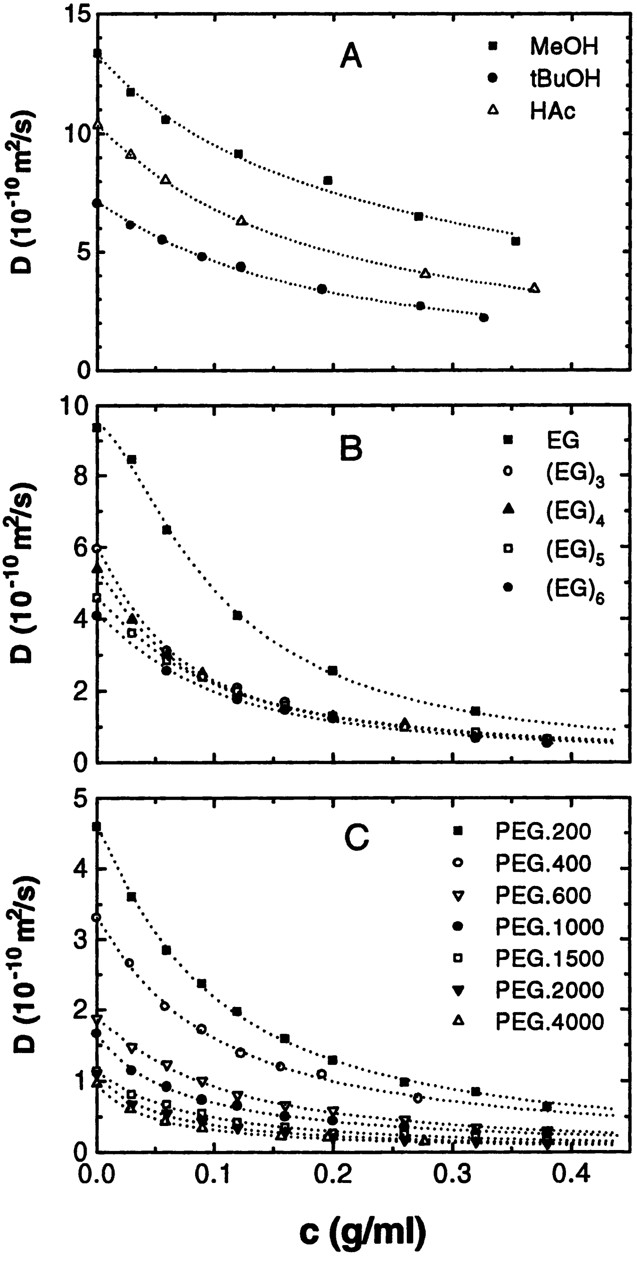

Figure 4. Self-diffusion coefficients of solute probes in PVA1 solutions as a function of PVA concentration at 23 °C. (A) Solute probes, (B) EG and OEG and (C) PEG. Dashed lines are fittings to equation 6.

In Tailored Polymeric Materials for Controlled Delivery Systems; McCulloch, I., et al.;
ACS Symposium Series; American Chemical Society: Washington, DC, 1998.

Downloaded by NORTH CAROLINA STATE UNIV on October 31, 2012 | http://pubs.acs.org
Publication Date: September 24, 1998 | doi: 10.1021/bk-1998-0709.ch018

general, the D values decrease as the molecular size of the diffusant increases for the entire PVA concentration range studied. The self-diffusion coefficients of EG measured at different concentrations of PVA are significantly higher than the oligomers and polymers (Figure 4B). As the molecular weight (MW) or the molecular size of the diffusant increases, the measured D value decreases. The difference in D values of PEGs with different MWs becomes less significant as the MW of PEG increases, especially at higher PVA concentrations (Figure 4C). The calculated hydrodynamic radii of the diffusants, R_H, give an indication of the relative size of the diffusants. The effect of the molecular size of the diffusant on self-diffusion observed here is similar to those observed in other types of gels and solutions by the radioactive tracer method (*39*) and the results of another study in cellulose gels and membranes (*40*). It is to be noted that the D values measured by the PGSE NMR methods here and in the study of Matsukuwa and Ando (*38*) are in the same order of magnitude with the results obtained by other methods (*39,40*), but they are shown to be consistently lower in values.

The combined parameter $k\beta^2$ is related to the jump frequency, k, of the diffusant while β is a characteristic constant. Clearly, the jump frequency should be inversely related to the molecular size of the diffusant. Values of $k\beta^2$ can be obtained from fittings of the experimental data to equation 6, but a separate value for k cannot be extracted since the value of β is not known. The logarithm of the parameter $k\beta^2$ as a function of the hydrodynamic radii of the diffusants (R_H) has more or less a linear relationship for the OEG and PEG solute probes (Figure 5A), which confirms that an increase in the molecular size of the diffusant leads to a lower jump frequency, k. Table 2 also shows that the parameter $k\beta^2$ is inversely proportional to the molecular size (R_H) of the diffusing solute molecules.

The second fitting parameter, ν, should remain more or less a constant for a given polymer system. Figure 5B shows that indeed ν can be regarded as characteristic of the PVA-water system since the variation of ν is small for the series of OEG and PEG studied. The average value of ν (ca. 0.58) obtained for these diffusants is similar to that of the other diffusants obtained for the same system (Table 2) (*22*). A certain deviation was observed for the very small molecules such as ethylene glycol itself ($\nu = 0.76$).

(4) Effect of Temperature. We have studied the variable temperature effect on the self-diffusion coefficients of selected solute probes such as *tert*-butanol (*t*BuOH), EG, PEG-600 and PEG-2000. As one may expect, the D values increase for a given diffusant as the temperature rises. An example of the plots of D values as a function of PVA concentration at different temperatures (PEG-600) is shown in Figure 6. The ability of the proposed diffusion model to reproduce the temperature dependence of solute diffusion in PVA-water systems is demonstrated in this figure and the experimental data can be fitted very well to equation 6 for each of the temperatures studied and for all the probes used.

The fitting parameters obtained from the variable temperature studies of *t*BuOH diffusion in the PVA1-water system are listed in Table 4. The parameter ν does not depend on temperature and falls very close to the average value of 0.52 obtained for PVA1 with the various solutes shown in Table 2, while the dependence of $k\beta^2$ on temperature is clear (Table 4).

Downloaded by NORTH CAROLINA STATE UNIV on October 31, 2012 | http://pubs.acs.org
Publication Date: September 24, 1998 | doi: 10.1021/bk-1998-0709.ch018

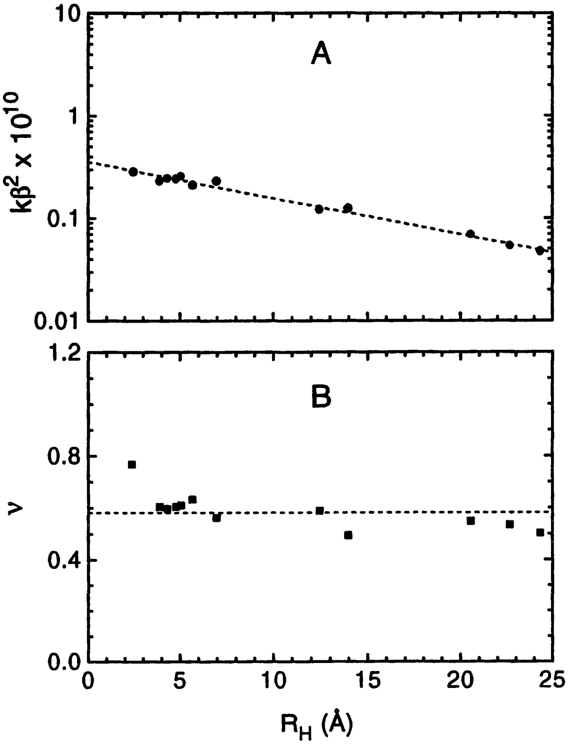

Figure 5. (A) Semilogarithmic plot of $k\beta^2$ and (B) plot of the parameter ν, as a function of the hydrodynamic radius, R_H, of EG, OEG and PEG diffusants in PVA1-water systems at 23 °C.

Downloaded by NORTH CAROLINA STATE UNIV on October 31, 2012 | http://pubs.acs.org
Publication Date: September 24, 1998 | doi: 10.1021/bk-1998-0709.ch018

Downloaded by NORTH CAROLINA STATE UNIV on October 31, 2012 | http://pubs.acs.org
Publication Date: September 24, 1998 | doi: 10.1021/bk-1998-0709.ch018

Table 4. Parameters ν and $k\beta^2$ obtained from the self-diffusion data of *t*BuOH in a PVA1-water system at different temperatures by fitting the experimental data to equation 6.

Temperature (°C)	D_0 ($10^{-10}m^2/s$)	ν	$k\beta^2 \times 10^{10}$	RMS Error
23	7.07	0.56	0.98	0.010
33	8.18	0.57	1.25	0.006
43	10.7	0.58	1.54	0.004
53	13.9	0.58	2.21	0.003

Source: Reprinted with permission from ref. 22, Copyright 1996 ACS.

As shown in equation 2, the jump frequency k for a given diffusant is expected to be dependent on the temperature. The $k\beta^2$ values can be obtained from fittings to equation 6 at each temperature. Since we assume that β is a constant within the temperature range studied here, the relationships between $k\beta^2$ and T shown in Figure 7 can be regarded as the relationship between k and T. The Arrhenius plots (log $k\beta^2$ vs 1/T, as in equation 2) in Figure 7 show excellent linear relationships. The energy barrier ΔE can be calculated from the slopes of the linear plots when we assume that both β and F_p are independent of temperature. We have obtained ΔE values of 21, 30, 36.5 and 39 kJ/mol, respectively, for the diffusants *t*BuOH, EG, PEG-600 and PEG-2000. These values represent the heights of the potential barrier that the diffusant has to overcome for the diffusion to take place. The molecular weight of *t*BuOH is higher than that of EG, but the energy barrier for the diffusion of *t*BuOH is lower. The higher facility of EG in forming hydrogen bonds with the polymer matrix and with the aqueous environment, which causes increased friction with the environment as shown by equation 4, is probably the reason for its higher energy barrier of diffusion than that of *t*BuOH. The effect of hydrogen bonds on diffusion of small molecules was also evidenced when trimethylamine was compared with tetramethylammonium cation (*10*). Since PEG is a flexible linear polymer, the increase in molecular weight of PEG does not seem to increase the energy barrier of diffusion to a great extent. It is clear, however, that there is a trend that the energy barrier of diffusion increases with increasing molecular size of the diffusant, which leads to smaller self-diffusion coefficients.

The mesh size of the network ξ is calculated to be in the order of 5-15 Å for PVA in the concentration range of interest, decreasing as the the polymer concentration increases (*10*). The size of the pseudo-spherical diffusant *t*BuOH (3.3 Å) is relatively small compared to the mesh sizes for a large part of the concentration range. Consequently, $2R_H < \xi$, and the polymer network does not create an effective barrier to diffusion of small molecules, which explains the relatively low activation energy. At the high concentration extremity studied here, the mesh size is similar or slightly smaller than the hydrodynamic diameter of *t*BuOH, but the flexibility of the polymer network and the

Downloaded by NORTH CAROLINA STATE UNIV on October 31, 2012 | http://pubs.acs.org
Publication Date: September 24, 1998 | doi: 10.1021/bk-1998-0709.ch018

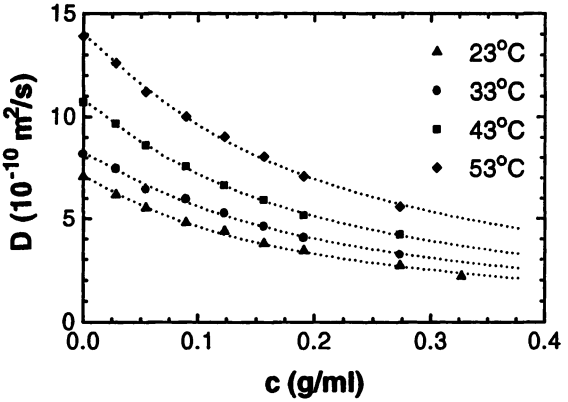

Figure 6. Self-diffusion coefficients of *t*-butanol in PVA1 aqueous solutions plotted as a function of PVA concentration at four different temperatures. Dashed lines are fittings to equation 6.

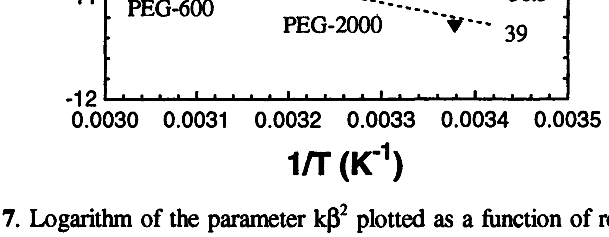

Figure 7. Logarithm of the parameter kβ^2 plotted as a function of reciprocal temperature for selected diffusants. The potential energy barriers (ΔE) are calculated from the slopes of these lines by the use of equation 2.

imperfection of this pseudo-spherical diffusant still seem to allow its passage. Larger diffusants ($2R_H \approx \xi$) exhibit a concentration dependence of the apparent activation energy. Johnson *et al* (*41*) studied the diffusion of a larger probe molecule, 9,10-diphenylanthracene, in tetrahydrofuran (THF) solutions of polyisoprene (PI) at three different temperatures. It appears that the apparent activation energy depends on the polymer concentration (*22*). Although the hydrodynamic radii R_H of certain PEG samples are calculated to be rather large, these are flexible linear polymers so that the diffusion should be easier than more spherical diffusants of similar sizes. For these diffusants, the values of R_H can be regarded as a molecular size parameter rather than an indication of the real size of a hard sphere. We might speculate that when a more spherical diffusant molecule is much greater than the mesh size of the polymer network ($2R_H >> \xi$), the diffusion mechanism may be very different.

Concluding Remarks

In the proposed physical model of diffusion, the polymer solution is regarded as a network where the diffusing molecules have to overcome certain periodic energy barriers of equal amplitude. The wide range of molecular weight of the selected diffusants enables us to link the diffusion behavior of small to large molecules in the polymer system. The newly proposed physical model of diffusion is used successfully in the treatment of the self-diffusion data of these molecules. We have shown here that such a model can reproduce the effects of polymer concentration and of the molecular size of the diffusants on the self-diffusion of solute molecules in aqueous-polymer solutions and that of solvent molecules in organic solvent-polymer solutions. The temperature effect can also be described adequately by the model. The jump frequency, k, a physical parameter defined in the model, is shown to depend on the size of the diffusant as well as on temperature, while the parameter ν in the model remains more or less a constant for a given system. In this study, the hydrodynamic radii of the diffusants have been used as the molecular size parameter. The energy barriers of diffusion have been obtained from the variable temperature studies for selected diffusants of different sizes. Further studies are needed to elucidate the importance of hydrogen-bonding and other chemical or physical interactions that may occur in the diffusion of solutes in polymer systems. The effects of molecular weight and structure (such as degree of hydrolysis and crosslinking) of the polymers also need to be examined in detail. The understanding of the diffusion properties of the various diffusants in polymers would help to establish a correlation between the measured diffusion coefficient of a given diffusant and the real-time release and migration in the controlled release systems.

Acknowledgments

Financial support from Natural Sciences and Engineering Research Council (NSERC) of Canada and from the Province of Quebec (Fonds FCAR and a Quebec-Ontario collaboration travel grant) is gratefully acknowledged.

Downloaded by NORTH CAROLINA STATE UNIV on October 31, 2012 | http://pubs.acs.org
Publication Date: September 24, 1998 | doi: 10.1021/bk-1998-0709.ch018

References

1. Kosmeyer, R.W.; von Meerwall, E.D.; Peppas, N.A. *J. Polym. Sci., Polym. Phys. Ed.* **1986**, *24*, 409.
2. Waggoner, A.; Blum, F.D. *J. Coatings Technol.* **1989**, *61*, 768.
3. Clericuzio, M.; Parker, W.O.; Soprani, M.; Andrei, M. *Solid State Ionic* **1995**, *77*, 685.
4. Stilbs, P. *Prog. Nucl. Magn. Reson. Spectrosc.* **1987**, *19*, 1.
5. Price, W.S. *Annual Reports on NMR Spectroscopy* **1996**, *32*, 51.
6. Fujita, H. *Adv. Polym. Sci.* **1961**, *3*, 1.
7. Vrentas, J.S.; Duda, J.L.; Ling, H.C.; Hou, A.C. *J. Polym. Sci., Polym. Phys. Ed.* **1985**, *23*, 289.
8. von Meerwall, E.D.; Amis, E.J.; Ferry, J.D. *Macromolecules* **1985**, *18*, 260.
9. Yasuda, H.; Lamaze, C.E.; Ikenberry, L D. *Makromol. Chem.* **1968**, *118*, 19.
10. Petit, J.-M.; Zhu, X.X.; Macdonald, P.M. *Macromolecules* **1996**, *29*, 70.
11. Mackie, J.S.; Meares, P. *Proc. Royal Soc. Lond.,* A **1955**, *232*, 498.
12. Waggoner, R.A.; Blum, F.D.; MacElroy, J.M.D. *Macromolecules* **1993**, *26*, 6841.
13. Ogston, A.G.; Preston, B.N.; Wells, J.D. *Proc. Royal Soc. Lond., A* **1973**, *333*, 297.
14. Johansson, L.; Elvingson, C.; Löfroth, J.-E. *Macromolecules* **1991**, *24*, 6024.
15. MacElroy, J.M.D.; Kelly, J.J. *AIChE J.* **1985**, *31*, 35.
16. Cukier, R.I. *Macromolecules* **1984**, *17*, 252.
17. Phillies, G.D.J. *Macromolecules* **1987**, *20*, 558.
18. Altenberger, A.R.; Tirrell, M. *J. Chem. Phys.* **1984**, *80*, 2208.
19. Chang, T.; Kim, H.; Yu, H. *Macromolecules* **1987**, *20*, 2629.
20. Furukawa, R.; Arauz-Lara, J.L.; Ware, R.R. *Macromolecules* **1991**, *24*, 599.
21. Park, I.H.; Johnson, C.S. Jr.; Gabriel, D.A. *Macromolecules* **1990**, *23*, 1548.
22. Petit, J-M.; Roux, B.; Zhu, X.X.; Macdonald, P.M. *Macromolecules* **1996**, *29*, 6031.
23. de Gennes, P.G. *J. Chem. Phys.* **1971**, *55*, 572.
24. de Gennes, P.G. *Macromolecules* **1976**, *9*, 594
25. Viovy, J.-L. *Molecular Biotechnology* **1996**, *6*, 31.
26. Alon, U.; Mutamel, D. *Phys. Rev. E* **1997**, *55*, 1783.
27. Phillies, G.D.J. *Macromolecules* **1986**, *19*, 2367.
28. Phillies, G.D.J. *J. Phys. Chem.* **1989**, *93*, 5029.
29. de Gennes, P.G. *Scaling Concepts in Polymer Physics*; Cornell University Press: Ithaca, NY, 1979.
30. Zhu, X.X.; Macdonald, P.M. *Macromolecules* **1992**, *25*, 4345.
31. Zhu, X.X.; Wang, F.; Nivaggioli, T.; Winnik, M.A.; Macdonald, P.M. *Macromolecules* **1993**, *26*, 6397.
32. Kramers, H.A. *Physica* **1950**, *7*, 248.
33. Golden, K.; Goldstein, S.; Lebowitz, J.L. *Phys. Rev. Letters* **1985**, 55, 2629.
34. Zwanzig, R.W. *Proc. Natl. Acad. Sci. USA* **1988**, 85, 2029.
35. Stejskal, E.O.; Tanner, J.E. *J. Chem. Phys.* **1965**, *42*, 288.

Downloaded by NORTH CAROLINA STATE UNIV on October 31, 2012 | http://pubs.acs.org
Publication Date: September 24, 1998 | doi: 10.1021/bk-1998-0709.ch018

36. Zhu, X.X.; Macdonald, P.M. *Solid State NMR* **1995**, *4*, 27.
37. James, T.L.; McDonald, G.G. *J. Magn. Reson.* **1973**, *11*, 58.
38. Matsukawa, S.; Ando, I. *Macromolecules* **1996**, *29*, 7136.
39. Johansson, L.; Skantze, U.; Löfroth, J.-E. *Macromolecules* **1991**, *24*, 6019.
40. Brown, W.; Honsen, R.M. *J. Appl. Polym. Sci.* **1981**, *26*, 4135.
41. Johnson, B.S.; Ediger, M.D.; Kitano, T; Ito, K. *Macromolecules* **1992**, *25*, 873.

Downloaded by NORTH CAROLINA STATE UNIV on October 31, 2012 | http://pubs.acs.org
Publication Date: September 24, 1998 | doi: 10.1021/bk-1998-0709.ch018

Chapter 19

Biodegradation of Lactic–Glycolic Acid Oligomers

Nuo Wang[1], Jin Song Qiu[1], and Xue Shen Wu[1,2]

[1]Division of Pharmaceutics and Industrial Pharmacy, Arnold and Marie Schwartz
College of Pharmacy and Health Sciences, Long Island University,
Brooklyn, NY 11201
[2]Herman F. Mark Polymer Research Institute, Polytechnic University,
Brooklyn, NY 11201

Downloaded by CORNELL UNIV on October 31, 2012 | http://pubs.acs.org
Publication Date: September 24, 1998 | doi: 10.1021/bk-1998-0709.ch019

The biodegradation of lactic/glycolic acid (LGA) oligomers having different composition and molecular weight has been investigated. The results of this investigation show that composition and molecular weight of LGA oligomers and pH of incubating media all affect biodegradation of LGA oligomers. A higher content of glycolic acid residue in an LGA oligomer results in a higher biodegradation rate of the oligomer. For oligomers having the same composition and in a constant pH medium, the weight loss of a higher molecular weight LGA oligomer is slower than that of a lower molecular weight counterpart. The weight loss of the LGA oligomers is faster in an alkaline incubating medium (pH 9.4) than that in a neutral incubating medium (pH 7.4). When distilled water is used as an incubating medium, the pH of the incubating medium drops rapidly along with the biodegradation of the LGA oligomers. A three-step biodegradation mechanism is proposed for the LGA oligomers. These three steps are hydration, matrix bulk degradation, and surface erosion-controlled solubilization. The controllable biodegradation properties of the LGA oligomers have useful applications to controlled-release drug delivery.

Lactic/Glycolic acid (LGA) polymers, including poly(lactic acid), poly(glycolic acid) as well as their co-polymers are one of the most promising biomaterials in the medical and pharmaceutical area because of not only their outstanding biocompatibility but also their controllable or programmable biodegradation behavior. The biodegradation products of these polymers are lactic and/or glycolic acid that are (is) readily metabolized and eliminated from the body. Many researchers (1-7) have investigated these polymers in the molecular weight range from 5,000 to 320,000. Biodegradation of these polymers is believed to undergo bulk hydrolysis throughout the polymer matrix (8). The in vitro and in vivo experiments reveal that many factors may influence the biodegradation of LGA polymers. These factors include polymer composition (ratio of lactic to glycolic acid in a copolymer) (9), molecular weight of polymers (10, 11), pH

In Tailored Polymeric Materials for Controlled Delivery Systems; McCulloch, I., et al.;
ACS Symposium Series; American Chemical Society: Washington, DC, 1998.

of an incubating medium (12, 13), buffer effect (13, 14), and ionic strength of an incubating medium (13).

However, little data are available for biodegradation of low molecular weight lactic/glycolic acid polymers or LGA oligomers. The biodegradation mechanism, kinetics, and factors affecting the biodegradation of LGA oligomers are still not well studied. To clearly understand the behavior of LGA oligomers in an aqueous medium, we investigate the in vitro biodegradation mechanism, kinetics, and factors affecting the biodegradation of LGA oligomers. The factors affecting the biodegradation are investigated with regards to oligomer composition, molecular weight of oligomers, and pH of an incubating medium.

Downloaded by CORNELL UNIV on October 31, 2012 | http://pubs.acs.org
Publication Date: September 24, 1998 | doi: 10.1021/bk-1998-0709.ch019

Experimental

Materials. LGA oligomers having three different compositions were synthesized and characterized in our laboratory and previously reported (15). The three compositions of the LGA oligomers were LGAO46/54 having molar ratio of lactic to glycolic acid moiety of 46 to 54 (Mn: 990), LGAO65/35 having that of 65 to 35 (Mn: 912), and LGAO72/28 having that of 72 to 28 (Mn: 1317 and 3025). The variation of the number average molecular weight of LGAO72/28 was generated by varying the polymerization time. The oligomers were ground into small pieces having approximately 5 mm in diameter before use. All other chemicals were purchased from Spectrum Chemical Manufacturing Corp. (Gardena, CA).

Investigation of Composition Effect on Biodegradation of the LGA Oligomers. Three oligomer samples with different compositions, LGAO46/54, LGAO65/35, and LGAO72/28, were used in this experiment. For each composition, ten oligomer samples (0.5 g for each sample) were weighed and placed in ten test tubes. All test tubes containing the oligomers were incubated in a phosphate buffer (0.2 M, pH 7.4) and placed in a 37 °C water bath shaking at 30 rpm. At predetermined time intervals, one test tube in each sample group was taken out of the water bath and centrifuged for 10 min at 1000×g. The supernatant was discarded and the test tubes were dried in vacuo to a constant weight at 40 °C. The weight of the test tubes was recorded after drying. The weight loss of the LGA oligomers was calculated using the following equation:

$$\text{Weight Loss (\%)} = (W_O - W_R)/W_O = 1 - W_R/W_O = 1 - (W_T - W_E)/W_O \qquad (1)$$

where W_O is the original weight of an oligomer, W_R is the remaining weight of an oligomer after incubation or biodegradation, W_T is the weight of a test tube plus the remaining oligomer, and W_E is the weight of the test tube, respectively. The biodegradation profile for each oligomer was obtained by plotting percent weight loss of the oligomer versus time.

Assay of Molecular Weight Effect on Biodegradation of the LGA Oligomers. LGAO72/28 having molecular weight of 1,317 and 3,025 were used in this experiment. Ten oligomer samples for each molecular weight were weighed (0.5 g for each sample) and placed in test tubes with known weight. All test tubes were incubated in a phosphate buffer (0.2 M, pH 7.4) and placed in a 37 °C water bath shaking at 30 rpm. At predetermined time intervals, one test tube in each molecular weight sample was taken out of the water bath and processed following the same procedures described in the section of "Investigation of Composition Effect on Biodegradation of the LGA Oligomers".

Measurement of pH Change of the Incubating Medium during Biodegradation of the LGA Oligomers. The LGA oligomers with the three different compositions (LGAO46/54, LGAO65/35, and LGAO72/28) were incubated in distilled water separately in three test tubes. The test tubes were shaken at 30 rpm in a 37 °C water bath. At predetermined time intervals, the pH of the incubating medium in each sample was measured and recorded. The pH of the incubating medium was then plotted versus incubating time.

Downloaded by CORNELL UNIV on October 31, 2012 | http://pubs.acs.org
Publication Date: September 24, 1998 | doi: 10.1021/bk-1998-0709.ch019

Study of pH Effect on Biodegradation of the LGA Oligomers. The effect of pH on biodegradation of the LGA oligomers was determined by comparing the biodegradation of LGA oligomers in two different pH conditions. The LGAO72/28 having a number average molecular weight of 3,025 was chosen for this study. The oligomer was divided into two sample groups. Each sample group has ten oligomer samples (0.5 g oligomer for each sample). Each oligomer sample was placed in a test tube. One group of the samples was incubated in a phosphate buffer (200 mM, pH 7.4) and the other group was incubated in a $Na_2B_2O_7 \cdot 10\ H_2O$ buffered solution (100 mM, pH 9.4). These two buffer solutions had the capability to maintain a constant pH throughout the experiments. All samples were placed in a 37 °C water bath shaking at 30 rpm. At predetermined time intervals, one test tube in each sample group was taken out of the water bath and processed following the same procedures described in the section of "Investigation of Composition Effect on Biodegradation of the LGA Oligomers".

Results and Discussion

Composition Effect on Oligomer Biodegradation. The changeable biodegradation rate by changing the composition is one of the advantages of LGA polymers/oligomers. The ratio of lactic to glycolic acid moiety determines the hydrophobicity of the LGA polymers/oligomers (16). Lactic acid moiety is more hydrophobic than glycolic acid moiety because of the pendant methyl group in the lactic acid residue. The hydrophobicity controls the water accessibility to the LGA polymer/oligomer matrix and further influences the biodegradation of the LGA polymers/oligomers. By changing the composition of LGA polymers/oligomers, desirable biodegradation duration can be obtained, which can be used to control the release time of a drug delivery system made from an LGA polymer/oligomer. This programmable biodegradation characteristic completely applies to LGA oligomers. Although an LGA oligomer is more hydrophilic than its high molecular weight counterpart, the composition effect on the biodegradation is still clearly observed as shown in Figure 1. Figure 1 shows the weight loss of the LGA oligomers having varying compositions versus time. As shown in the figure, the weight loss of all three oligomers has a linear dependence on time after a

Downloaded by CORNELL UNIV on October 31, 2012 | http://pubs.acs.org
Publication Date: September 24, 1998 | doi: 10.1021/bk-1998-0709.ch019

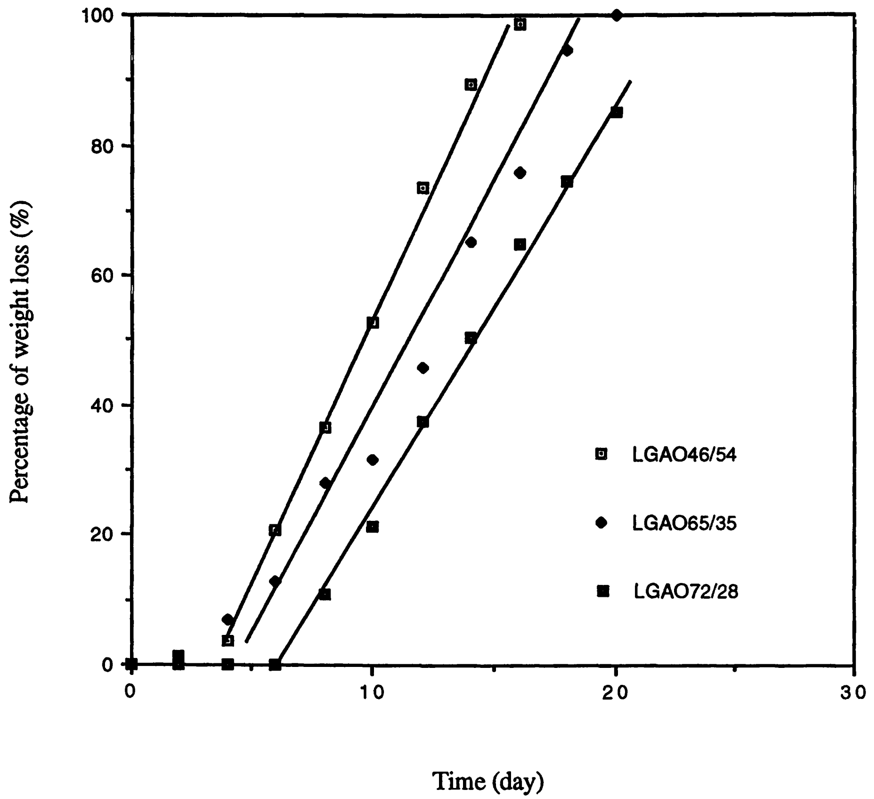

Figure 1 Effect of oligomer composition on the biodegradation of the LGA oligomers.

hydration period. The rate of weight loss can be observed from the slope of the linear part of the data points. As one can see, the rate of weight loss is influenced by the composition of the LGA oligomer. An increase of glycolic acid residue in the oligomers accelerates the rate of weight loss. The LGAO46/54 has the highest rate of weight loss while the LGAO72/28 has the lowest rate of weight loss. This property can be used to control the drug release duration of a drug delivery system prepared from the LGA oligomers.

Molecular Weight Effect on Oligomer Biodegradation. The molecular weight of LGA polymers/oligomers affects their biodegradation mainly through influencing their hydrophobicity (16). The molecular weight of LGA polymers/oligomers determines the number of carboxylic end groups in the polymer/oligomer matrix. For the same amount of material, a low molecular weight LGA polymer/oligomer contains more carboxylic end groups per unit weight than a high molecular weight counterpart. Therefore, a low molecular weight LGA polymer/oligomer is more hydrophilic than its high molecular weight counterpart and has a faster biodegradation rate. Figure 2 shows the weight loss of two LGA oligomers having the same composition but different molecular weights. These two oligomers have a similar hydration period of 6 days. But the oligomer having high molecular weight has lower biodegradation rate than that having lower molecular weight.

In addition to the hydrophilicity of the LGA oligomers, another parameter frequently influenced by molecular weight is glass transition temperature (T_g). The T_g of high molecular weight LGA polymers is usually higher than the physiological temperature, i.e. 37 °C (17). However, the T_g of LGA oligomers is lower than the physiological temperature (15). At 37 °C, an LGA oligomer is in a rubbery state and can absorb much more water than a LGA polymer in a glassy state, which may be one reason that LGA oligomers biodegrade much faster than high molecular weight LGA polymers (17).

pH Effect on Oligomer Biodegradation. It is reported that LGA polymers/oligomers degrade in an aqueous medium following the mechanism of ester hydrolysis (14,16). The hydrolysis of a polymer/oligomer increases the number of carboxylic end groups and decreases the molecular weight of the polymer/oligomer. The polymer/oligomer eventually degrades to free acids, lactic and/or glycolic acid. As the number of the carboxylic end groups increases, protons or hydronium ions are released to the incubating medium and, if the incubating medium is not buffered, the pH of the incubating medium is lowered.

During the biodegradation of the LGA oligomers, this lowering of pH of the incubating medium can be clearly observed. Figure 3 shows the pH change of the incubating medium with time for the three oligomers (LGAO46/54, LGAO65/35, and LGAO72/28). As shown in the figure, the pH of the incubating medium drops rapidly with time and finally reaches the value of approximately 2. This quick pH drop of the incubating medium suggests that a large amount of protons or hydronium ions have been produced during the biodegradation of the oligomers, which suggests that the LGA oligomers have a fast biodegradation rate.

In contrast to the experiment shown in Figure 3, if the pH of the incubating medium is controlled or the incubating medium is buffered, one can see the effect of pH

Downloaded by CORNELL UNIV on October 31, 2012 | http://pubs.acs.org
Publication Date: September 24, 1998 | doi: 10.1021/bk-1998-0709.ch019

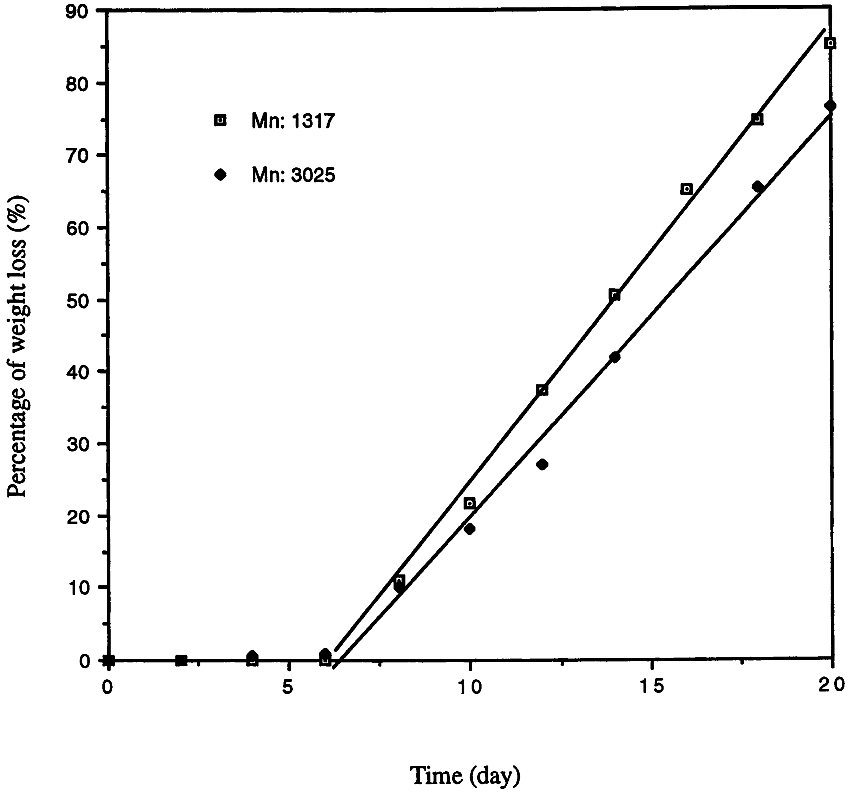

Figure 2 Effect of molecular weight on the biodegradation of the LGA oligomers (molar ratio of lactic to glycolic acid: 72/28).

Downloaded by CORNELL UNIV on October 31, 2012 | http://pubs.acs.org
Publication Date: September 24, 1998 | doi: 10.1021/bk-1998-0709.ch019

In Tailored Polymeric Materials for Controlled Delivery Systems; McCulloch, I., et al.;
ACS Symposium Series; American Chemical Society: Washington, DC, 1998.

Downloaded by CORNELL UNIV on October 31, 2012 | http://pubs.acs.org
Publication Date: September 24, 1998 | doi: 10.1021/bk-1998-0709.ch019

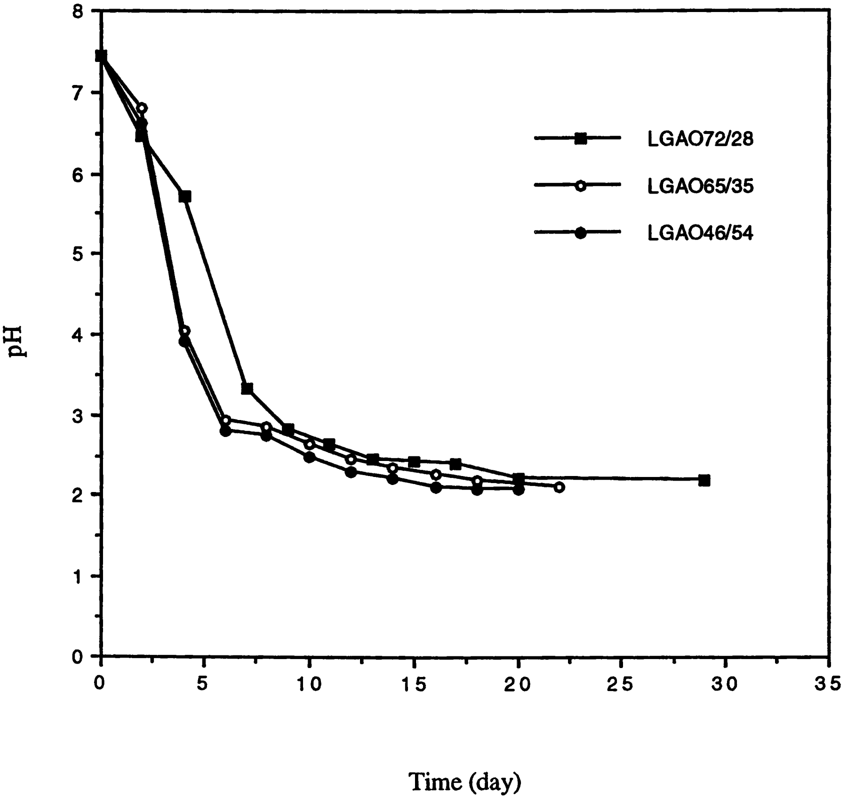

Figure 3 Change of pH of the incubating medium during the biodegradation of the LGA oligomers of three different compositions.

of the incubating medium on biodegradation of the LGA oligomers (Figure 4). Figure 4 shows that the biodegradation of the oligomer is faster at pH 9.4 than at pH 7.4. The percent weight loss of the oligomer in the basic medium (pH 9.4) is 56% after 14 days of incubation, while that of the same oligomer in the neutral medium (pH 7.4) is only 42%.

The pH influence on biodegradation of LGA polymers has been studied by some researchers (6, 10, 11, 18, 19). The hydrolysis of LGA polymers/oligomers can be catalyzed by an acid or a base as shown in Figure 5. In the basic pH range (pH 7.4-9.4), the base catalysis may be dominant. It is known that the hydrolysis of a carboxylic ester is an equilibrium reaction (20). Therefore, a basic incubating medium favors shifting the reaction of the biodegradation of LGA polymers/oligomers (Figure 5) towards the right because one of the hydrolysis products of the LGA polymers/oligomers has free carboxylic group. The free carboxylic group is neutralized by the alkaline buffer. The pH 9.4 buffer can neutralize more free carboxylic groups than the pH 7.4 buffer. Therefore, the biodegradation of the LGA oligomers in pH 9.4 buffer is faster than in pH 7.4 buffer.

Downloaded by CORNELL UNIV on October 31, 2012 | http://pubs.acs.org
Publication Date: September 24, 1998 | doi: 10.1021/bk-1998-0709.ch019

Proposed Mechanism for Oligomer Biodegradation. A lag time can be observed in the weight loss of the LGA oligomers as shown in Figure 2 and 4. Significant weight loss starts 6 days after the incubation. After the 6-day lag time, a massive weight loss starts, having a linear relationship to the incubating time. This biodegradation behavior suggests a different biodegradation mechanism for the LGA oligomers from their high molecular weight counterpart. The biodegradation of LGA polymers follows a four-step process: hydration, initial degradation, further degradation and solubilization (16). For the LGA oligomers, only three biodegradation steps were observed as schemed in Figure 6. The first step is the hydration of LGA oligomers. In this period, the LGA oligomer matrix absorbs water and swells. There is no weight loss occurring but the pH of the incubating medium starts declining due to the release of protons from the carboxylic end group of the oligomer chain in the oligomeric matrix to the incubating medium (as shown in Figure 3 between 0-2 days). After the hydration period, the biodegradation starts all over the hydrated matrix, which is believed to undergo bulk degradation. This period is characterized by a rapid decline of the pH of the incubating medium and a slight weight loss of the oligomer matrix (as shown in Figure 3 between 2-6 days). After this bulk degradation period, a massive weight loss period takes over and follows a linear dependency with respect to incubating time. This linear weight loss period may suggest a surface erosion-controlled solubilization mechanism. This solubilization mechanism may be speculated as follows. After the bulk degradation period, the pH inside the oligomer matrix may have approached to an acidic value. This acidic micro-environment may retard the hydrolysis or biodegradation inside the oligomeric matrix. The surface of the oligomeric matrix is still exposed to the buffered incubating medium that has a basic pH. Therefore, the matrix surface undergoes biodegradation at a much faster rate than the matrix core. This difference of biodegradation rate between the matrix surface and the matrix core brings about a surface erosion-controlled solubilization of the LGA oligomer after the stage of bulk degradation. The proposed surface erosion-controlled solubilization mechanism may be characterized by a slower rate of pH decrease after 8 days of incubation (see Figure 3). This surface erosion results in a linear relationship of weight loss with time.

Downloaded by CORNELL UNIV on October 31, 2012 | http://pubs.acs.org
Publication Date: September 24, 1998 | doi: 10.1021/bk-1998-0709.ch019

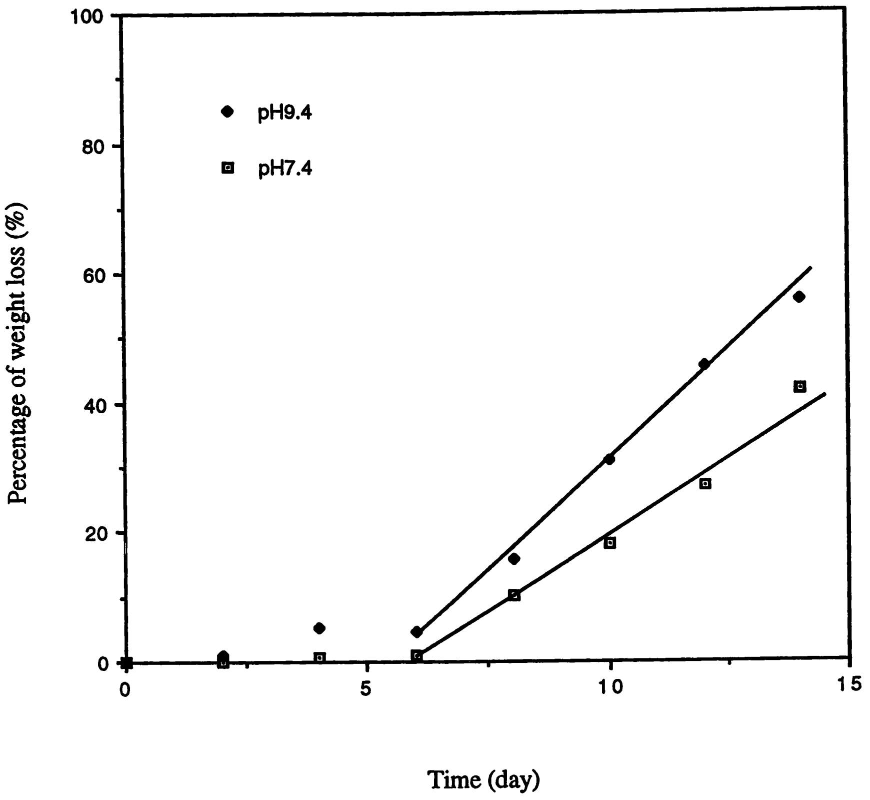

Figure 4 Effect of pH of the incubating medium on the biodegradation of the LGA oligomers. (LGAO72/28, Mn: 3,025).

Downloaded by CORNELL UNIV on October 31, 2012 | http://pubs.acs.org
Publication Date: September 24, 1998 | doi: 10.1021/bk-1998-0709.ch019

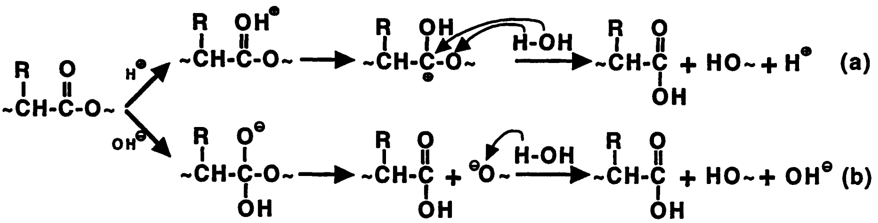
(a)
(b)
H-OH
+ HO~ + H⊕
+ HO~ + OH⊖

Figure 5 Hypothetical mechanisms of hydrolysis of LGA polymers/oligomers. (a) at pH < 7; (b) at pH > 7.

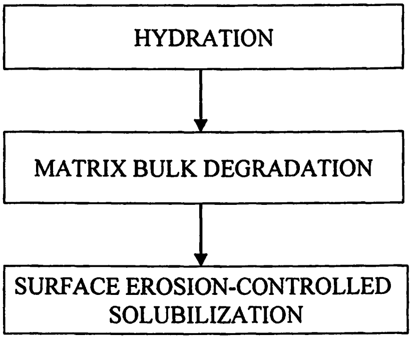
HYDRATION
MATRIX BULK DEGRADATION
SURFACE EROSION-CONTROLLED SOLUBILIZATION

Figure 6. Scheme of the three steps proposed for the biodegradation of LGA oligomers.

Conclusions

The factors affecting the biodegradation of the LGA oligomers have been separately investigated. The experimental data show that the biodegradation of LGA oligomers is influenced by the composition and the molecular weight of the LGA oligomers, and the pH of the incubating medium. A higher content of glycolic acid residue in an LGA oligomer results in a higher biodegradation rate of the oligomer. In a constant pH medium and for the oligomers having the same composition, the weight loss of a higher molecular weight LGA oligomer is slower than that of a lower molecular weight counterpart. The weight loss of the LGA oligomers is faster in an alkaline incubating medium (pH 9.4) than that in a neutral incubating medium (pH 7.4). When distilled water is used as an incubating medium, the pH of the incubating medium drops rapidly along with the biodegradation of the LGA oligomers. A three-step biodegradation mechanism is proposed for the LGA oligomers. These three steps are hydration, matrix bulk degradation, and surface erosion-controlled solubilization. The controllable biodegradation properties of the LGA oligomers have useful applications to controlled-release drug delivery.

Downloaded by CORNELL UNIV on October 31, 2012 | http://pubs.acs.org
Publication Date: September 24, 1998 | doi: 10.1021/bk-1998-0709.ch019

Literature Cited

1. Park, T. G. *J. Controlled Release* **1994**, 30, 161-173.
2. Visscher, G.E.; Robison, R.L.; Maulding, H.V.; Fong, J.W.; Pearson, J.E. and Argentieri, G.J. *J. Biomed. Mater. Res.* **1986**, 20, 667-676.
3. Bodmer, D.; Kissel, T. and Traechslin, E. *J. Controlled Release* **1992**, 21, 129-138.
4. Spenlehauer, G.; Vert, M.; Benoit, J.P. and Boddaert, A. *Biomaterials* **1989**, 10, 557-563.
5 Wang,. H.T.; Palmer, H.; Linhardt, R.J.; Flanagan, D.R. and Schmitt, E. *Biomaterials* **1990**, 11, 679-685.
6. Ginde, R.M. and Gupta, R.K. *J. Appl. Polym. Sci.* **1987**, 33, 2411-2429.
7. Zhu, J.H.; Shen, Z.R.; Wu, L.T. and Yang, S.L. *J. Appl. Polym. Sci.* **1991**, 43, 2099-2106.
8. Thies, C. and Bissery, M.C. In *Biomedical Applications of Microencapsulation*; Lim, F. Ed.; CRC Press: Boca Raton, FL, **1984**, pp. 53-74.
9. Kaetsu, I.; Yoshida, M.; Asano, M.; Yamanaka, H.; Imai, K.; Yuasa, H.; Mashimo, T.; Suzuki, K.; Katakai, R. and Oya, M. *J. Controlled Release* **1987**, 6, 249-263.
10. Asano, M.; Fukuzaki, H.; Yoshida, M.; Kumakura, M.; Mashimo, T.; Yuasa, H.; Imai, K. and Yamanaka, H. *Drug Design and Delivery* **1990**, 5, 301-320.
11. Huffman, K.R. and Casey, D.J. *J. Polym. Sci. Polym.: Chem. Ed.* **1985**, 23, 1939-1954.
12. Chu, C.C. *J. Biomed. Mater. Res.* **1981**, 15, 795-804.
13. Makino, K.; Ohshima, H. and Kondo, T. *J. Microencapsulation* 1986, 3, 203-212.
14. Chu, C.C. *J. Biomed. Mater. Res.* **1981**, 15, 19-27.
15. Wang, N.; Wu, X.S.; Upton, H.L.; Donahue, E. and Siddiqui, A. *J. Biomat. Sci.: Polym. Ed.*, **1997**, 8, 905-917.
16. Wu, X.S. In *Encyclopedic Handbook of Biomaterials and Bioengineering, Part A: Materials*; Wise, D.L.; Trantolo, D. J.; Altobelli, D. E.; Yaszemski, M.J.; Gresser, J. D. and Schwartz, E. R., Ed.; Marcel Dekker: New York, NY, **1995**, pp. 1015-1054.
17. Vert, M., Li, S. and Garreau, H., *J. Controlled Release* **1991**, 16, 15-26.

18. Kishida, A.; Yoshioka, S.; Takeda, Y. and Uchiyama, M. *Chem. Pharm. Bull.* **1989**, 37, 1954-1956.
19. Williams, D. F. *J. Biomed. Mater. Res.* **1980**, 14, 329-338.
20. March, J. *Advanced Organic Chemistry*, Fourth Edition, John Wiley & Sons: New York, NY, **1992;** p. 378.

Downloaded by CORNELL UNIV on October 31, 2012 | http://pubs.acs.org
Publication Date: September 24, 1998 | doi: 10.1021/bk-1998-0709.ch019

Downloaded by UNIV OF GUELPH LIBRARY on October 31, 2012 | http://pubs.acs.org
Publication Date: September 24, 1998 | doi: 10.1021/bk-1998-0709.ch020

Chapter 20

Lactic–Glycolic Acid Oligomeric Microgranules for Aspirin Delivery and Stabilization

Nuo Wang[1] and Xue Shen Wu[1,2]

[1]**Division of Pharmaceutics and Industrial Pharmacy, Arnold and Marie Schwartz College of Pharmacy and Health Sciences, Long Island University, Brooklyn, NY 11201**
[2]**Herman F. Mark Polymer Research Institute, Polytechnic University, Brooklyn, NY 11201**

Injectable lactic/glycolic acid (LGA) oligomeric micro-granules have been prepared for aspirin delivery and stabilization. Aspirin is incorporated with LGA oligomers having different compositions, by a thermal blending method. The thermal blending method has advantages of easy processing and high drug loading efficiency. The LGA oligomeric micro-granules have a size range between 50 and 200 μm. The in vitro release experiment shows that the drug release is affected by the oligomer composition as well as the drug content. The oligomeric matrix has the capability to retard aspirin hydrolysis.

Much work has been performed in the fabrication of biodegradable polymers into drug delivery systems that can release drugs in a sustained, controlled, or programmed way (1). Among these, the use of lactic/glycolic acid (LGA) polymers as a drug carrying matrix and the formulation of this polymer into microparticles show some promising results (2). LGA polymers have a long history of being safely used as surgical suture materials. The polymers themselves as well as their ultimate biodegradation products, i.e., lactic and glycolic acid, have great biocompatibility (3). When LGA polymer is fabricated into a microparticulate drug delivery system, it not only has the advantage of easy administration, but also avoids the retrieval of the drug carrier after drug is depleted.

Most work involving this type of drug delivery system is based on high molecular weight LGA polymers (4-6). The high molecular weight LGA polymers have the problem of high production cost and prolonged biodegradation and bioelimination duration. In addition, the formation of most of the microparticulate drug delivery systems based on the high molecular weight LGA polymers utilizes organic solvents to dissolve the polymers. Removal of the organic solvent frequently results in formation of pores or channels and leaves behind a porous polymer matrix, which complicates the

In Tailored Polymeric Materials for Controlled Delivery Systems; McCulloch, I., et al.;
ACS Symposium Series; American Chemical Society: Washington, DC, 1998.

drug release mechanism and kinetics as well as the biodegradation of the LGA polymers (7). The drug release from such a porous system is usually much faster than the degradation of the polymer matrix, which results in a drug-depleted polymer matrix being formed. From a compliance point of view, this is not preferred.

To avoid these problems, we have used LGA oligomers to prepare biodegradable drug delivery systems. These systems are formulated as micro-granules by using a thermal blending method. These biodegradable, micro-granular drug delivery systems have many advantages. The LGA oligomers degrade faster in a biological environment (8). The preparation of the micro-granules does not involve any organic solvent. A model drug is incorporated in LGA oligomers by blending an oligomer and the drug at an elevated temperature. Instead of forming a porous matrix, a solid, compact oligomeric matrix is formed. The potential uses of this drug delivery system may be the weekly or biweekly pain-relief in the recovery period after dental repair, bone fixation, and surgeries. The system can be easily extended for the delivery of many other analgesics or antipyretics.

Aspirin is used as a model drug to conduct the research of this drug delivery system. The LGA oligomers and aspirin are blended at 120 °C, molded into rods at –5 °C, and ground into micro-granules at 5 °C. The thermal blending preparation method has a high drug loading efficiency. The in vitro release experiment results show that the LGA oligomer micro-granules can release aspirin for 9-14 days, depending on the oligomer composition and the drug content. Aspirin is significantly stabilized in the LGA oligomer micro-granules. The LGA oligomer micro-granules have potential to be used as a controllable, biodegradable drug delivery system

Experimental

Materials. The LGA oligomers used in this experiment have four different compositions: LGAO85/15 having molar ratio of lactic to glycolic acid moiety of 85 to 15 (Mn: 1107), LGAO72/28 having that of 72 to 28 (Mn: 1317), LGAO65/35 having that of 65 to 35 (Mn: 912), and LGAO46/54 having that of 46 to 54 (Mn: 990). They were synthesized and characterized by a previously reported method (9). Aspirin powder (U.S.P./N.F. grade) and all other chemicals and solvents were from Spectrum Chemical Manufacturing Corp. (Gardena, CA).

Preparation of Aspirin-containing LGA Oligomer Micro-Granules. The preparation of aspirin-containing LGA oligomer micro-granules followed the method reported by Y. Tabata et al. (10) with minor modification. Five grams of each LGA oligomer (LGAO85/15, LGAO72/28, LGAO65/35, and LGAO46/54) were weighed, and then melted at 120 °C using a silicone oil bath, separately. When the oligomer became a viscous liquid, ground aspirin fine powder was added. The aspirin powder and the oligomer liquid were well mixed using a glass-stirring rod, at 120 °C. The resulting mixture was molded into a rod by cooling the aspirin-containing oligomer liquid in a cylindrical mold in a freezer (-5 °C). The aspirin-containing oligomeric rods were then ground into micro-granules using a glass mortar and pestle at 5 °C. The micro-granules were sieved using a stainless steel sieve (200 μm). The aspirin-containing LGA oligomer micro-granules were stored at –5 °C. For the LGA oligomer

Downloaded by UNIV OF GUELPH LIBRARY on October 31, 2012 | http://pubs.acs.org
Publication Date: September 24, 1998 | doi: 10.1021/bk-1998-0709.ch020

micro-granules made from LGAO72/28, three batches of micro-granules were prepared with 10%, 15%, and 20% aspirin content for the investigation of the effect of drug content on aspirin release.

Observation of Morphology and Size of the Aspirin-Containing LGA Oligomer Micro-Granules. The morphology and size of the aspirin containing LGA oligomer micro-granules were examined using an Olympus optical microscope with a Polaroid instrument camera attached (Model MF-10, Newton, MA). The size of the micro-granules was measured using an eyepiece micrometer disc, pre-calibrated using an objective micrometer.

Downloaded by UNIV OF GUELPH LIBRARY on October 31, 2012 | http://pubs.acs.org
Publication Date: September 24, 1998 | doi: 10.1021/bk-1998-0709.ch020

Determination of Aspirin Loading Efficiency. The aspirin-containing LGA oligomer micro-granules, 20 mg, were dissolved in 2 ml co-solvent of ethyl acetate and absolute ethanol (1 to 1 volume ratio). A phosphate buffered saline (PBS, 20 mM, pH 7.4, containing 0.02% sodium azide as a bactericide), 1 ml was then added. Due to the presence of ethanol, the organic solvent phase and the aqueous phase became miscible. A 0.5 ml sample was taken and quantitated using a Spectra Phoresis 1000 high performance capillary electrophoresis system (HPCE, Spectra Physics Analytical, Inc., San Jose, CA) with a 44 cm×50 μm open type fused silica capillary at a detecting wave length of 236 nm. A phosphate buffer (40 mM, pH 10.5) was used as the mobile phase. Operating temperature was 25 °C. Peak areas were used for the quantitation of aspirin and salicylic acid. The loading efficiency of aspirin in the LGA oligomer micro-granules was defined in the following formula:

$$\text{Loading efficiency (\%)} = \frac{C_a}{C_t} \times 100$$

where C_a is the actual content of the aspirin in the LGA oligomer micro-granules determined experimentally and C_t is the theoretical content of the aspirin in the LGA oligomer micro-granules based on the amount of aspirin used in the preparation of the micro-granules.

Study of In Vitro Aspirin Release. The aspirin-containing LGA oligomer micro-granules, 50 mg of each sample, were suspended in 2 ml PBS (20 mM, pH 7.4, containing 0.02% sodium azide as a bactericide) in test tubes. The test tubes were placed in a 37 °C water bath, shaking at 30 rpm. At predetermined time intervals, the tubes were taken out of the water bath and centrifuged for 5 minutes at 700×g. Samples of 1.8 ml supernatant were taken and replaced with the same amount of PBS. The release samples were then analyzed using the same HPCE system described earlier under the same operating conditions. The cumulative amount of drugs released, i.e., aspirin and salicylic acid, is calculated by the following equation:

$$\text{Cumulative amount of drug released (\%)} = \frac{M_a + M_s}{C_a} \times 100$$

where M_a and M_s are the amount of aspirin and salicylic acid released at time t, respectively.

Downloaded by UNIV OF GUELPH LIBRARY on October 31, 2012 | http://pubs.acs.org
Publication Date: September 24, 1998 | doi: 10.1021/bk-1998-0709.ch020

Assay of Effect of LGA Oligomer Matrix on Aspirin Stability. Aspirin-containing LGAO72/28 micro-granules having drug content of 10% were used in this experiment. Four micro-granule samples, 20 mg of each, were investigated using the following procedures. The amount of aspirin in sample 1 was determined at day 0 by dissolving the micro-granules in the ethyl acetate-ethanol-PBS mixture right after weighing. The drug was quantitated using the same HPCE described above. Samples 2, 3, and 4 were suspended in 2 ml PBS in test tubes and placed in a water bath shaking at 30 rpm at 37 °C. At Days 2, 6, and 8, one tube was taken out of the water bath and the supernatant in the test tube was discarded. The remaining micro-granules in the test tube were rinsed with distilled water. The rinsing water was discarded. The amount of aspirin in the remaining micro-granules was determined using the same HPCE.

A control experiment was conducted for the purpose of comparison by placing five pure aspirin samples, 2 mg of each (the same amount of aspirin as that loaded in 20 mg PLGA micro-granules), in test tubes containing 2 ml PBS. The test tubes were placed in a shaking water bath at 37 °C. At time of 2, 4, 6, 8, and 24 hours, one sample was taken out of the water bath and centrifuged for 5 minutes at 700×g. A sample of 0.5 ml supernatant was taken and analyzed using the same HPCE.

The stability of aspirin was expressed as the percentage of aspirin unhydrolyzed, which was calculated using the following equation:

$$\text{Aspirin unhydrolyzed (\%)} = [W_a/(W_a+W_s)] \times 100$$

where W_a is the weight of aspirin and W_s is the weight of salicylic acid that is the hydrolysis product of aspirin.

Results and Discussion

Morphology and Size of the LGA Oligomer Micro-granules. Micro-granules are among the most convenient drug delivery systems in terms of fabrication and administration. Drugs can be incorporated with matrix forming materials by thermal blending at a temperature above the glass transition temperature (T_g) and/or the melting temperature (T_m) of the matrix forming material. Figure 1 shows a microscopic photograph of the LGA oligomer micro-granules. The LGA oligomer micro-granules have an irregular shape. Interestingly, a transparent matrix is formed although the aspirin has been blended at a temperature below the T_m of aspirin. The reason for the transparency may be that the aspirin molecules have been dissolved in the LGA oligomer matrix.

The size of the LGA oligomer micro-granules is approximately 50-200 μm. This size range is feasible to be administrated by injection, including subcutaneous and intramuscular injections.

Loading Efficiency. One of the advantages of the thermal blending preparation method is its high drug loading efficiency. Since only a few steps are involved in this method, there is little possibility for drug loss. As shown in Table 1, the loading efficiency of the LGA oligomer micro-granules has an average number of 92.3%. The 7.7% drug loss may be due to the hydrolysis of aspirin to salicylic acid during the

Downloaded by UNIV OF GUELPH LIBRARY on October 31, 2012 | http://pubs.acs.org
Publication Date: September 24, 1998 | doi: 10.1021/bk-1998-0709.ch020

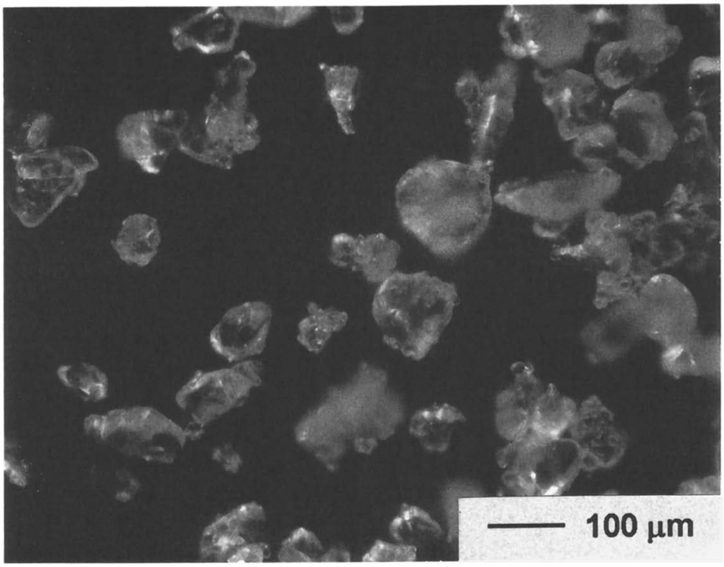

Figure 1. A micrograph of aspirin-containing LGAO72/28 micro-granules.

TABLE I. Drug Loading Efficiency of the LGA oligomer Micro-Granules

Micro-granule	Loading efficiency (%)
LGAO85/15	91.6
LGAO72/28	93.9
LGAO65/35	90.3
LGAO46/54	93.3

preparation, because only aspirin has been quantitated and used to calculate the loading efficiency. The aspirin was quantitated using capillary electrophoresis. The capillary electrophoresis can separate aspirin from salicylic acid due to the difference in the charge-to-mass ratio of these two different species. The different charge-to-mass ratio gives different electrophoretic mobility. Table 1 also shows that the oligomer composition has almost no effect on the drug loading efficiency.

Effect of Oligomer Composition on In Vitro Drug Release. Figure 2 shows the cumulative amount of drug released from the LGA oligomer micro-granules having different compositions. As shown in the figure, the drug release is affected by the oligomer composition. The difference of drug release between LGAO46/54 micro-granules and LGAO65/35 micro-granules or LGAO72/28 micro-granules and LGAO85/15 micro-granules is not significant. However, if one compares the drug release between micro-granules made from high glycolic acid content oligomers (i.e., LGAO46/54 and LGAO65/35) and that made from low glycolic acid content oligomers (i.e., LGAO72/28 and LGAO85/15), a noticeable difference can be observed. The drug release from the micro-granules made from the high glycolic acid content oligomers is generally faster than that from the micro-granules made from the low glycolic acid content oligomers.

The drug release from the LGA oligomer micro-granules can be explained from the effect of the oligomer composition on biodegradation rate of the oligomers. The higher content of glycolic acid in the oligomers increases the hydrophilicity of the oligomers, which is responsible for the faster biodegradation rate of the oligomers (3). The faster biodegradation of the high glycolic acid content oligomers promotes the drug release from the LGA oligomer matrices.

The in vitro release of many drugs, including hydrophobic and hydrophilic drugs, from lactic/glycolic acid polymer matrix has been widely investigated (11-13). The drug release mechanism can be different for different types of drugs and different types of lactic/glycolic acid polymers. Aspirin and its hydrolysis product, salicylic acid, are small molecules. They can be released by the mechanism of drug diffusion, particularly in a hydrated matrix. However, the biodegradation of the LGA oligomer still contributes to the drug release (14). Therefore, the release of aspirin from the LGA oligomer micro-granules is probably controlled by the diffusion of drug molecules together with the biodegradation of the oligomer matrix.

Effect of Drug Content on In Vitro Drug Release. The drug content in a microparticlate formulation has a considerable effect on the rate and duration of drug release (14). Figure 3 shows the influence of different drug content on the in vitro drug release. As the figure illustrates, different drug content may cause a noticeable change of drug release behavior. Firstly, the micro-granules having higher drug content possess a larger initial burst drug release than that having lower drug content. This is due to the smaller oligomer-to-drug ratio in the high-drug-content micro-granules, for the same amount of micro-granules. More drug molecules are exposed to the release medium in the high-drug-content micro-granules. Secondly, high drug loading induces faster drug release. The drug release from the micro-granules having 15% and 20% drug content is faster than those having 10% drug content. This is because high-drug-content micro-granules have less oligomer for the same amount of micro-granules. The oligomer is

Downloaded by UNIV OF GUELPH LIBRARY on October 31, 2012 | http://pubs.acs.org
Publication Date: September 24, 1998 | doi: 10.1021/bk-1998-0709.ch020

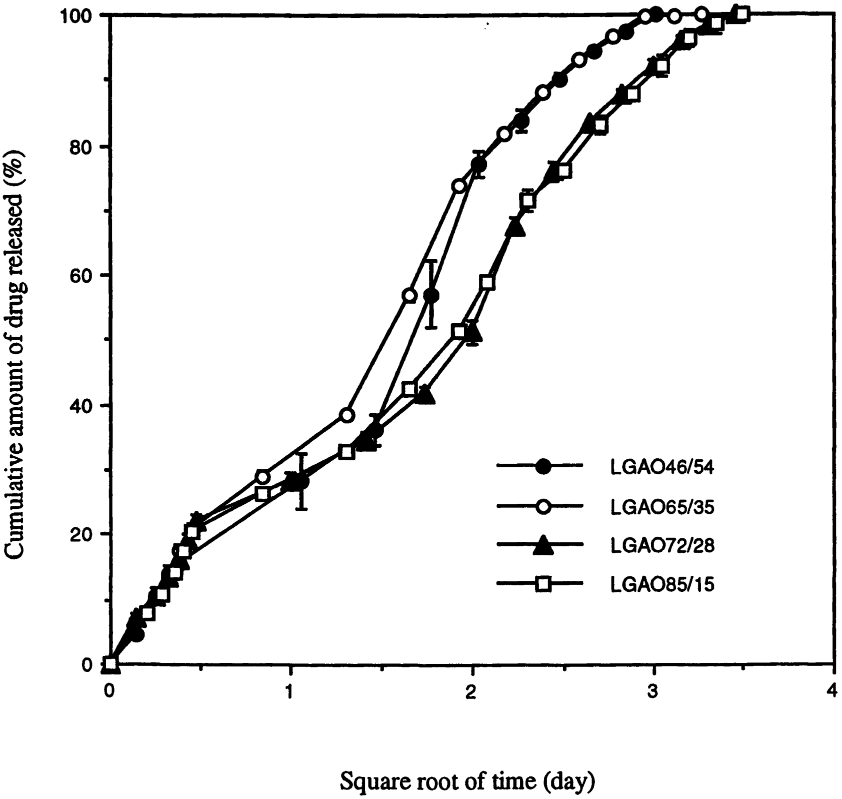

Figure 2. In vitro drug release from the LGA oligomer micro-granules comprised of oligomers with different compositions.

Downloaded by UNIV OF GUELPH LIBRARY on October 31, 2012 | http://pubs.acs.org
Publication Date: September 24, 1998 | doi: 10.1021/bk-1998-0709.ch020

Downloaded by UNIV OF GUELPH LIBRARY on October 31, 2012 | http://pubs.acs.org
Publication Date: September 24, 1998 | doi: 10.1021/bk-1998-0709.ch020

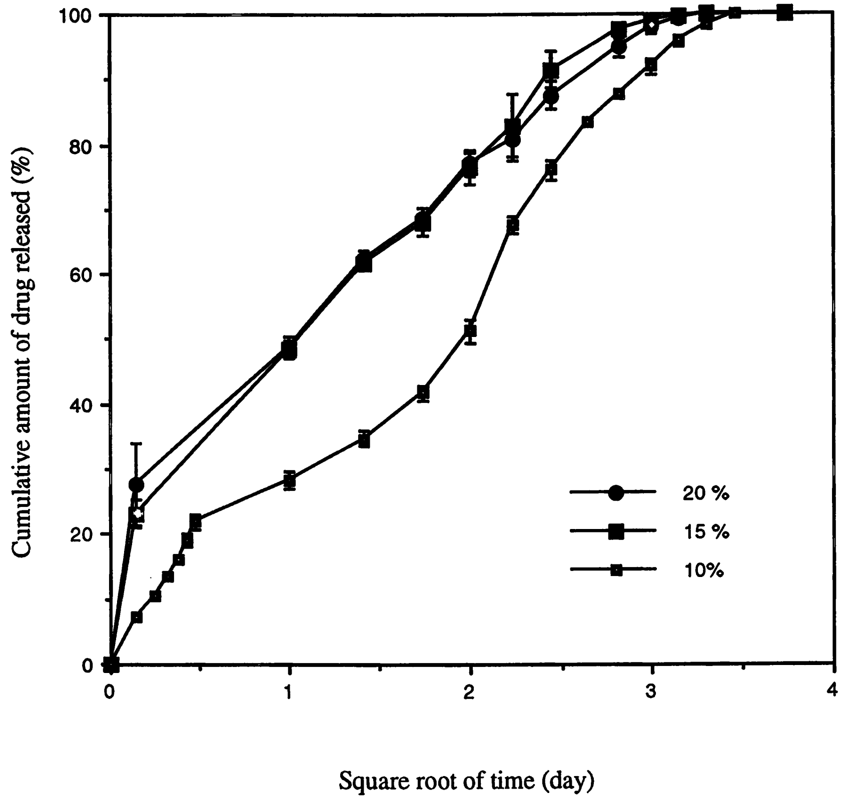

Figure 3. Effect of drug content on the in vitro drug release profile from LGAO72/28 micro-granules.

the main factor that retains the drug release. Less fraction of oligomer in the system results in faster drug release. However, this drug content effect disappears when the drug content reaches certain level. There is no significant release rate difference in drug release between the micro-granules having 15% and 20% drug content.

Effect of LGA Oligomer Matrix on Aspirin Stability. Figure 4 shows the comparison of hydrolysis of aspirin in the buffer and LGA oligomer matrix. As shown in the figure, the hydrolysis of aspirin in the hydrated LGA oligomer matrix is much slower than that in the buffer. The aspirin has been completely hydrolyzed within 24 hours when incubated in the buffer. In contrast, inside the LGA oligomer matrix incubated in the buffer, aspirin hydrolysis is significantly reduced. This result suggests that the LGA oligomer matrix inhibit the aspirin hydrolysis. Two aspects may contribute to the inhibition of the aspirin hydrolysis. Firstly, the oligomer molecules keep the aspirin molecules inside the matrix where there is less amount of water available to hydrolyze the drug. Secondly, the acidity of the oligomer matrix or the acidic microenvironment may be considered. Although a measurement is difficult, the pH of the oligomer matrices is generally considered acidic because of the presence of one carboxylic end group on each oligomer chain, particularly when the degradation of the oligomer has started. pH monitoring during biodegradation of the oligomer has revealed that the free acids (i.e., lactic and glycolic acid) generated by the oligomer degradation results in a pH of the incubating medium to approximately 2 (8). The acidic matrix may retard the hydrolysis of aspirin. Whitworth et al (15) found that aspirin decomposition was inhibited in presence of 1% citric or tartaric acid. An increase in concentration of the acids to 5% further decreases the aspirin decomposition rate. An explanation of the acid inhibition to aspirin hydrolysis may be described below. One byproduct of the aspirin hydrolysis is acetic acid that dissociates to hydronium and acetate ion in water. This dissociation is pH controlled. Therefore, pH has an effect on the formation of acetic acid. A lower pH or acidic micro-environment inhibits formation of the acetic acid and consequently retards the hydrolysis of aspirin.

Downloaded by UNIV OF GUELPH LIBRARY on October 31, 2012 | http://pubs.acs.org
Publication Date: September 24, 1998 | doi: 10.1021/bk-1998-0709.ch020

Conclusion

An injectable lactic/glycolic acid oligomeric micro-granules has been prepared for the aspirin delivery and stabilization. Aspirin is incorporated with the LGA oligomer having different compositions by a thermal blending method. The thermal blending method has the advantage of easy processing and high loading efficiency. The LGA oligomer micro-granules have a size range between 50 and 200 μm. The in vitro release experiment shows that the drug release is affected by the oligomer composition as well as the drug content. The oligomer matrix has capability to inhibit aspirin from hydrolysis.

Downloaded by UNIV OF GUELPH LIBRARY on October 31, 2012 | http://pubs.acs.org
Publication Date: September 24, 1998 | doi: 10.1021/bk-1998-0709.ch020

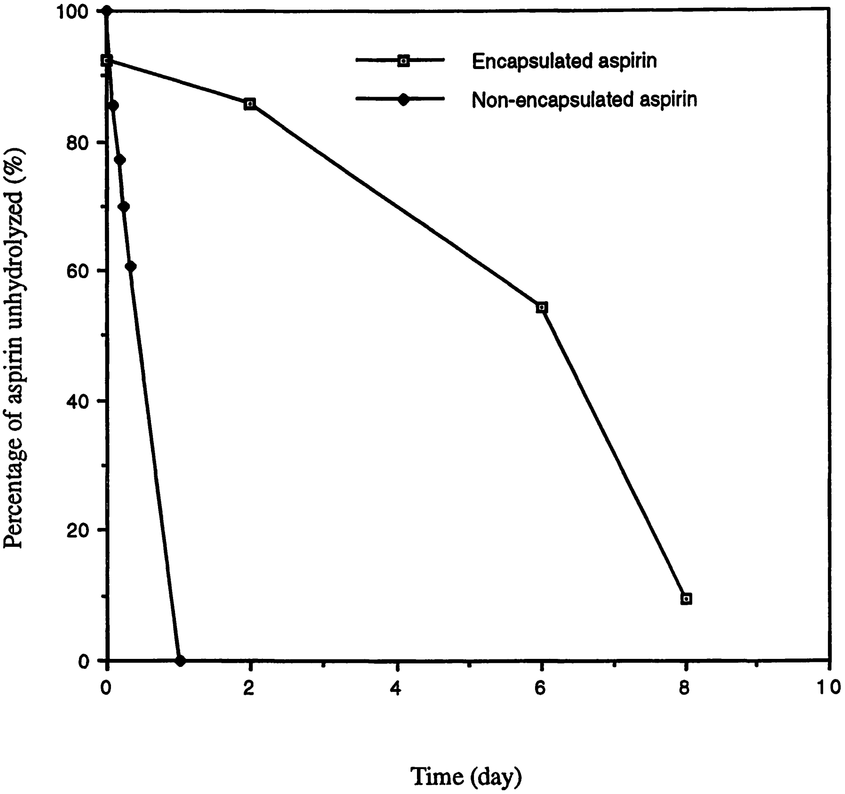

Figure 4 Comparison of the aspirin hydrolyzing profile between the non-encapsulated and encapsulated one (LGAO72/28 micro-granules with 10% drug content).

Literature Cited

1. Nitsch, M. J. and Banakar, U. V. In *Advances in Controlled Delivery of Drugs*; Kohudic, M. A. Ed.; Technomic Publishing Company, Inc.: Lancaster, PA, **1994**, p. 22.
2. Scholes, P. D.; Coombes, A. G. A.; Davies, M. C.; Illum, L. and Davis, S. S. In *Controlled Drug Delivery-Challenges and Strategies*; Park, K., Ed.; American Chemical Society: Washington, DC, **1997**, pp. 87-89.
3. Wu, X. S. In *Encyclopedic Handbook of Biomaterials and Bioengineering, Part A: Materials*; Wise, D. L.; Trantolo, D. J.; Altobelli, D. E.; Yaszemski, M. J.; Gresser, J. D. and Schwartz, E. R., Eds.; Marcel Dekker: New York, New York, **1995**, pp. 1015-1054.
4. Spenlehauer, G.; Vert, M.; Benoit, J. P. and Boddaert, A. *Biomaterials* **1989**, 10, 557-563.
5. Cohen, S.; Yoshioka, T.; Lucarelli, M.; Hwang, L. H. and Langer, R. *Pharm. Res.* **1991**, 8, 713-720.
6. Mehta, R. C.; Jeyanthi, R.; Calis, S.; Thanoo, B. C.; Burton, K. W.; DeLuca, P. P. *J. Controlled Release* **1994**, 29, 375-384.
7. Sah, H. K. and Chien, Y. W. *Drug Dev. Ind. Pharm.* **1993**, 19, 1243-1263.
8. Wang, N.; Wu, X.S, *J. Biomat. Sci.: Polym. Ed.*, **1997**, 9, 75-87.
9. Wang, N.; Wu, X.S.; Upton, H.L.; Donahue, E. and Siddiqui, A. *J. Biomat. Sci.: Polym. Ed.*, **1997**, 8, 905-917.
10. Tabata, Y.; Takebayashi, Y.; Ueda, T. and Ikada, Y. *J. Controlled Release* **1993**, 23, 55-64.
11. Yolles, S.; Sartori, M. F. In *Drug Delivery Systems: Characteristics and Biomedical Applications*; Juliano, R. L. Ed.; Oxford University Press: New York, NY, **1980**, pp. 84-111.
12. Wise, D. L.; Rosenkrantz, H.; Gregory, J. B.; and Esber, H. J. *J. Pharm. Pharmcol.* **1980**, 32, 399-403.
13. Wang, H. T.; Palmer, H.; Linhardt, R. J.; Glanagan, D. R. and Schmitt, E. *Biomaterials* **1990**, 11, 679-685.
14. Wu, X. S. In *Encyclopedic Handbook of Biomaterials and Bioengineering, Part A:_Materials*; Wise, D. L.; Trantolo, D. J.; Altobelli, D. E.; Yaszemski, M. J.; Gresser, J. D. and Schwartz, E. R., Eds.; Marcel Dekker: New York, New York, **1995**, pp. 1151-1200.
15. Whitworth, C. W., Jun H. W., Luzzi, L.A., *J. Pharm. Sci.* **1973**, 62, 1721-1722.

Downloaded by UNIV OF GUELPH LIBRARY on October 31, 2012 | http://pubs.acs.org
Publication Date: September 24, 1998 | doi: 10.1021/bk-1998-0709.ch020

Downloaded by YORK UNIV on October 31, 2012 | http://pubs.acs.org
Publication Date: September 24, 1998 | doi: 10.1021/bk-1998-0709.ch021

Chapter 21

Antitumor Drug Delivery by Dextran Derivatives Immobilizing Platinum Complex (II) Through Coordination Bond

Yuichi Ohya[1], Tatsunori Masunaga[1], Tatsuro Ouchi[1], Katsuro Ichinose[2], Mikirou Nakashima[3], Masataka Ichikawa[3], and Takashi Kanematsu[2]

[1]Department of Applied Chemistry, Faculty of Engineering, Kansai University, Suita, Osaka 564, Japan
[2]Second Department of Surgery and [3]Department of Hospital Pharmacy, Nagasaki University School of Medicine, 1-7-1 Sakamoto, Nagasaki 852, Japan

cis-Dichloro(cyclohexane-*trans-l*-1,2-diamine)platinum (II) : Dach-Pt(chlorato) is a platinum complex which is expected to exhibit higher antitumor activity than typical antitumoral platinum complexes. However, its strong side-effects and low water-solubility have been noted. We have reported that polymer/antitumor drug conjugates showed reduced side-effects and high antitumor activity. In order to provide a macromolecular prodrug of Dach-Pt having reduced side-effects and high water-solubility, we synthesized polymer conjugate of Dach-Pt by immobilizing Dach-Pt via a chelate-type coordination bond to dextran derivatives containing dicarboxylic acid groups, oxidized-dextran(OX-dextran)/Dach-Pt conjugate and dicarboxymethyl-dextran(DCM-Dex)/Dach-Pt conjugate. We investigated the release behavior of the platinum complex from the conjugates and the cytotoxic activity of the conjugates against p388D_1 *lymphocytic leukemia* cells *in vitro* compared with the carboxymethyl-dextran(CM-Dex)/Dach-Pt conjugate. The conjugates showed almost the same level of cytotoxic activity as free Dach-Pt(chlorato) or Dach-Pt(malonato). Although the cytotoxic activity of free Dach-Pt(chlorato) was decreased by incubation in a medium with serum, the conjugates kept their cytotoxic activity in higher level after certain period of incubation in a medium with serum. Moreover, we investigated *in vivo* antitumor activity of OX-Dex/Dach-Pt conjugate against colon 26 tumor bearing mice. The conjugate showed effective growth inhibitory effect against tumor cells.

In Tailored Polymeric Materials for Controlled Delivery Systems; McCulloch, I., et al.;
ACS Symposium Series; American Chemical Society: Washington, DC, 1998.

cis-Dichlorodiamineplatinum (II) (CDDP) (Figure 1) (*1*) has been widely used for clinical cancer chemotherapy in spite of its severe renal toxicity. Many approaches have been attempted to synthesize new platinum complexes having a broader spectrum of antitumor activity, reduced side-effects, greater solubility, and effective cytotoxic activity against tumor cells acquiring resistance to CDDP (*2-8*). Some platinum (II) complexes having 1,2-cyclohexanediamine (Dach) group as a chelating-ligand were reported to have favorable characteristics as anticancer agents (*3, 5-8*). Among them, *cis*-dichloro(cyclohexane-*trans-l*-1,2-diamine)-platinum(II), Dach-Pt(chlorate) (Figure 1), is one of the platinum complexes which is reported to exhibit higher antitumor activity than CDDP and also show effective cytotoxic activity against tumor cells having CDDP resistance (*8-10*). However, its strong side-effects and low water-solubility have also been cited.

Recently, drug delivery systems (DDS) using polymers as drug carriers have been investigated to achieve efficient delivery of anticancer agent to tumor cells. In comparison with a low-molecular-weight prodrug, a macromolecular prodrug is expected to overcome the problem of side-effects by improving the body distribution of drugs and prolongation of their activities (*11*). In recent years, macromolecular prodrug systems using polymers, such as poly[N-(2-hydroxypropyl)methacrylamide] (HPMA) (*12*), poly(L-glutamic acid) (*13*), poly(ethylene glycol)-*block*-poly(aspartic acid) (*14*), oxidized dextran (*15*), copolymer of divinylether and maleic anhydride (DIVEMA) (*16*), poly(α-malic acid) (*17*) and chitin (*18*) as drug carriers have been reported. Schechter *et al.* reported the usage of water soluble polymers, such as poly(L-glutamic acid), DIVEMA and carboxymethyl(CM)-dextran, as carriers of CDDP to reduce its side-effects (*19*). They reported that the increase in water-solubility of CDDP was achieved by complex formation with water-soluble polymers.

The potential of antitumor activity Dach-Pt(chlorato) is higher than that of CDDP, although one of its disadvantages compared with CDDP is its lower water-solubility. This disadvantage should be overcome by conjugation of Dach-Pt with water-soluble polymers to give high water-solubility. In this paper, we report on the syntheses of polymer complexes of Dach-Pt and dextran derivatives having dicarboxylic acid groups, oxidized-dextran(OX-Dex)/Dach-Pt conjugate and dicarboxymethyl-dextran(DCM-Dex)/Dach-Pt conjugate (Figure 2), to achieve reduced side-effects and high water-solubility of Dach-Pt. We investigated the release behavior of the platinum complex from the conjugates in phosphate buffer solution (PBS) (pH = 7.4) and the cytotoxic activity of the conjugates against p388D_1 *lymphocytic leukemia* cells *in vitro* compared with carboxymethyl-dextran(CM-Dex)/Dach-Pt conjugate (Figure 2), which has monocarboxylic acid group. The cytotoxic activity of platinum complex is decreased in blood stream, because of ligand exchange reactions with substances having amino groups in the serum, such as proteins, amino acids, and so on. The polymer/Dach-Pt complexes are expected to keep the platinum complex away from these deactivating factors and maintain their cytotoxic activity during circulation in blood stream. Therefore, we investigated residual cytotoxic activity of the conjugates and free Dach-Pt against tumor cells after incubation in the medium with serum. Moreover, we investigated *in vivo* antitumor activity of OX-Dex/Dach-Pt conjugate against colon 26 tumor bearing mice by intravenous injection.

Downloaded by YORK UNIV on October 31, 2012 | http://pubs.acs.org
Publication Date: September 24, 1998 | doi: 10.1021/bk-1998-0709.ch021

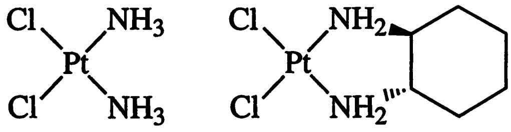
Cl
NH3
Pt
Cl
NH3
Cl
NH2
Pt
Cl
NH2

CDDP

Dach-Pt(chlorato)

Figure 1. Structure of *cis*-dichlorodiaminеplatinum (II): CDDP and *cis*-dichloro(cyclohexane-*trans*-*l*-1,2-diamine)platinum (II): Dach-Pt(chlorato).

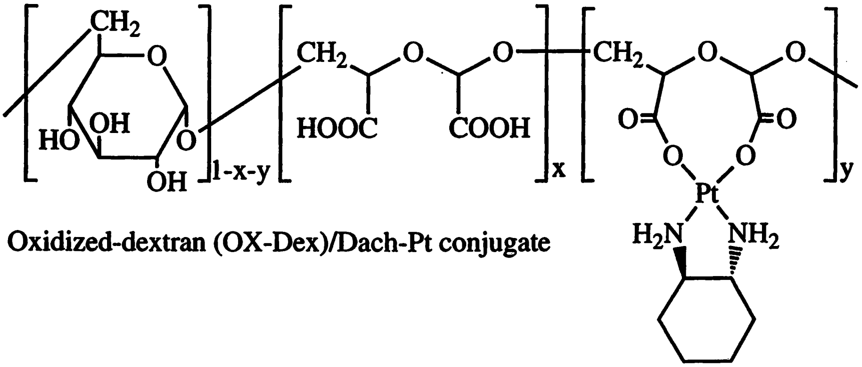
CH2
O
HO
OH
O
OH
1-x-y
CH2
O
O
HOOC
COOH
x
CH2
O
O
O
O
O
O
Pt
H2N
NH2
y

Oxidized-dextran (OX-Dex)/Dach-Pt conjugate

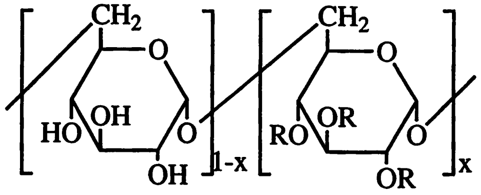
CH2
O
HO
OH
O
OH
1-x
CH2
O
RO
OR
O
OR
x

Dicarboxymethyl-dextran (DCM-Dex)/Dach-Pt conjugate

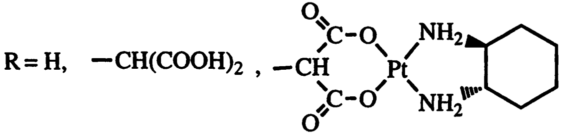
R = H, —CH(COOH)2 , —CH
O
C-O
NH2
Pt
C-O
NH2
O

Carboxymethyl-dextran (CM-Dex)/Dach-Pt conjugate

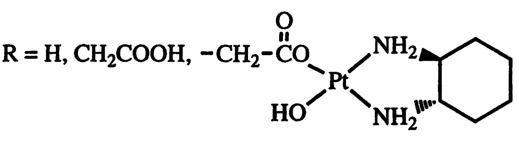
R = H, CH2COOH, -CH2-CO
O
NH2
Pt
HO
NH2

Figure 2. Structure of the dextran derivative/Dach-Pt conjugates.

Downloaded by YORK UNIV on October 31, 2012 | http://pubs.acs.org
Publication Date: September 24, 1998 | doi: 10.1021/bk-1998-0709.ch021

Experimental

Materials. Dach-Pt(chlorato) was obtained from Sumitomo Pharmaceuticals Co. Ltd. Dextran (Mw = 6.0×10^4) was purchased from Wako Pure Chemical Industry. The organic solvents were purified by the usual distillation methods. The other materials were of commercial grades and used without further purification. A low-molecular-weight chelate-type platinum complex, Dach-Pt(malonato), was prepared according to a method reported previously (*20*), as a control reagent.

Preparation of the conjugates. The syntheses of OX-Dex/Dach-Pt conjugate, DCM-Dex/Dach-Pt conjugate and CM-Dex/Dach-Pt conjugate were carried out according to methods in the references (*21, 22*) and were described as follows.

OX-Dex. Dextran (500 mg) was dissolved in 20ml of 0.06 M sodium periodate aq. and stirred at 0°C for 6 h in the dark. After the addition of 5 ml of ethylene glycol, the solution was dialyzed in distilled water using a cellulose tube (Seamless Cellulose Tubing, Small Size 30, Viskase Sales Co.) (Cut off : MW = 1.0×10^4) for 3 days and was freeze dried to yield 320 mg of dextran-dialdehyde as a white powder. The obtained dextran-dialdehyde (320 mg) was dissolved in 20 ml of 0.6 M sodium chlorite aq. The pH of the solution was adjusted to 4 by the addition of acetic acid and stirred at room temperature for 24 h. Nitrogen gas was then passed through the solution until a colorless solution was obtained. The pH of the solution was raised to 9 by the addition of 1 M NaOHaq. which was dialyzed in distilled water for 7 days. The obtained solution was passed through a column packed with an cation exchange resin (Amberlite 120B, Organo Co.) and freeze dried to yield 292 mg of OX-Dex as a white powder. The degree of introduction of carboxylic acid group per sugar unit (DCA) for OX-Dex was estimated by a neutralization titration method. Molecular weight of was determined by gel-permeation chromatography (GPC).

DCM-Dex and CM-Dex. Dextran (500 mg) was dissolved in 8.8 M NaOHaq. (10 ml). Bromodiethylmalonate (10 g) dissolved in 10 ml tetrahydrofuran was added to the solution at 0°C. The solution was stirred at room temperature for 20 hours. The reaction mixture was dialyzed in distilled water using cellulose tubing for 7 days. The solution obtained was passed through a column packed with a cation exchange resin (Amberlite 120B, Organo Co.) and freeze dried to give DCM-Dex in 480 mg yield as a white powder. CM-Dex was prepared by the similar methods descried above by using chloroacetic acid instead of bromodiethylmalonate. The yield was 420 mg. The DCA values and molecular weights for DCM-Dex and CM-Dex obtained were determined by the same methods descried above.

Conjugates. Dach-Pt(chlorato) (50 mg) was dissolved in 30 ml of water and stirred at 60°C for 3 h, whereupon aqueous silver nitrate solution (0.1 M, 0.22 ml) was added and stirred at 60°C for 6h. The precipitates of silver chloride were removed by filtration. The filtrate containing Dach-Pt(nitrato) was passed through a column packed with an anion exchange resin (Diaion SA-10A OH^- type) to convert it to Dach-Pt(hydroxo). The obtained solution was added to OX-Dex, DCM-Dex or CM-Dex (226 mg) in water and stirred at 60°C for 24h. The product was purified by gel-filtration chromatography (Sephadex G-25, eluent: water). The high molecular-weight fraction was collected and freeze dried to give

Downloaded by YORK UNIV on October 31, 2012 | http://pubs.acs.org
Publication Date: September 24, 1998 | doi: 10.1021/bk-1998-0709.ch021

Dextran/Dach-Pt conjugates. The degree of introduction of Dach-Pt (DPt) per sugar unit was determined by atomic absorption spectrometry.

Determination of release of platinum complex from the conjugates. The release behavior of the platinum complex from the conjugates was investigated in PBS *in vitro*. The conjugates (10 mg) were dialyzed in PBS (pH = 7.4, 20 ml) containing 1M NaCl using a cellulose tube (Seamless Cellulose Tubing, Small Size 30, Viskase Sales Co.) (Cut off : MW = 1.0×10^4). The solution outside of the cellulose tube was periodically replaced with fresh PBS. The amount of platinum complex released to the medium from the carrier polymer was estimated using atomic absorption spectrometry.

Measurement of cytotoxic activity of the conjugates. The *in vitro* cytotoxic activity of the conjugates against p388D_1 *lymphocytic leukemia* cells was measured according to methods described previously (*23*). The cell line of p388D_1 *lymphocytic leukemia* was maintained in RPMI-1640 medium (*24*) containing 10% (w/w) heat inactivated fetal calf serum (FCS), 2 mmol/l L-glutamine, 18 mmol/l sodium bicarbonate and 60 mg/l kanamycin. The tumor cell suspension (10 ml) containing 1.0×10^6 cells in culture medium containing 10% FCS (w/w) was distributed in a 96-well multi-plate (Corning 25860MP) and incubated with the conjugates or free Dach-Pt in a humidified atmosphere containing 5% CO_2 at 37°C for 24 h. The number of viable cells was determined by means of MTT [3-(4,5-dimethylthiazol-2-yl)-2,5-diphenyltetrazolium bromide] assay (25) using a microplate reader (MTP-120, Corona Electric Co.). The cytotoxic activity was calculated by the following equation:

> Cytotoxic activity (%) = (C-T) / C × 100
> where C is the number of viable cells after 24h incubation without drug and T is the number of viable cells after 24h incubation with drug.

The residual cytotoxic activity of the conjugates was also measured against p388D_1 *lymphocytic leukemia* cells *in vitro*. The conjugates, free Dach-Pt(chlorato) or Dach-Pt(malonato) (Pt concentration = 2.0×10^{-5} mol/l) were preincubated in RPMI-1640 medium containing 10% FCS at 37°C for certain periods before measurements of cytotoxic activity. The cytotoxic activity of the samples was measured by the same method as described above. The residual activity was calculated by the following equation:

> Residual cytotoxic activity (%) = $(C_0\text{-}C_t)/C_0 \times 100$
> where the C_t is the cytotoxic activity of the drug after preincubation in medium at 37°C and C_0 is the cytotoxic activity of the drug without preincubation.

In vivo antitumor activity. The *in vivo* tumor growth inhibitory effect of OX-Dex/Dach-Pt conjugate was investigated against colon 26 tumor cells in mice. Colon 26 tumor cells (2×10^5), which were maintained in RPMI-1640 culture medium containing 10% FCS, were inoculated subcutaneously into the dorsum of the six week old male CDF_1 mice. Six mice with tumor sizes of approximately 5mm in diameter were given intravenously 3 repeated injections of Dach-Pt or

Downloaded by YORK UNIV on October 31, 2012 | http://pubs.acs.org
Publication Date: September 24, 1998 | doi: 10.1021/bk-1998-0709.ch021

OX-Dex/Dach-Pt conjugate at each dose of 8 mg/kg Dach-Pt per injection or saline as a control at 4 days intervals. To evaluate the tumor growth inhibitory effect of Dach-Pt and OX-Dex/Dach-Pt, size of the tumor was recorded every 4 days after first injection. Tumor weight was estimated with the following formula based on Battelle Columbus Laboratory's protocol:

$$\text{Estimated tumor weight} = \text{length} \times \text{width}^2 \times 1/2$$

The relative increase in tumor weight was expressed as a percent increase at indicated times, compared with the base line value. The mice were killed 18 days after the first injection, and tumors were excised to compare the actual tumor weight among the 3 groups.

Measurements. The molecular weights of polymers were measured by gel-permeation chromatography (GPC) (column : Shodex OHpack KB-803, Showa Denko K.K., eluent : 1/15 M phosphate buffer, standard : pullulan). Atomic absorption spectra were measured on a Nippon Jarrell Ash AA-855.

Results and Discussion

Release behavior of platinum complex from the conjugates. The structural characteristics of the conjugates obtained are shown in Table I. The determination of extent release of platinum the complex from the conjugates was measured in PBS (pH = 7.4) containing 0.1M NaCl *in vitro*. The results are shown in Figure 3. It took about 2 and 4 days to release all of platinum complexes immobilized in OX-Dex/Dach-Pt conjugate and DCM-dextran/Dach-Pt conjugate, respectively. Sustained release of platinum complex from the carrier polymers was achieved. The release rate from OX-Dex/Dach-Pt conjugate and CM-Dex/Dach-Pt conjugate was almost same and faster than that from DCM-Dex/Dach-Pt conjugate. These results mean that the coordination bond between Dach-Pt moiety and carrier polymer for DCM-Dex/Dach-Pt conjugate was stable than that for OX-Dex/Dach-Pt conjugate and CM-Dex/Dach-Pt conjugate. The fact also support that the stable 6-membered chelate-type coordination bond formed in DCM-Dex/Dach-Pt conjugate. From these results, these all conjugates, especially DCM-Dex/Dach-Pt conjugate, are expected to show sustained release of platinum complex in blood stream or organs after intravenous injection *in vivo*.

Cytotoxic activity of the conjugates *in vitro*. The cytotoxic activity of the conjugates was investigated against p388D$_1$ *lymphocytic leukemia* cells *in vitro*. The results were shown in Table I as IC$_{50}$ values for each conjugates and low-molecular weight platinum complexes. The cytotoxic activity of the CM-Dex/Dach-Pt conjugate was very low compared with free Dach-Pt(chlorato) and the other conjugates. The OX-Dex/Dach-Pt conjugates and DCM-Dex/Dach-Pt conjugate showed almost the same level of cytotoxic activity as that of free Dach-Pt(chlorato). These results show that the immobilization of Dach-Pt to OX-Dex and DCM-Dex did not have fatal effect on the cytotoxic activity of Dach-Pt.

It is well known that the cytotoxic activity of platinum complex gradually decreased in blood stream because of ligand exchange reactions with compounds having amino groups in the serum, such as proteins, amino acids, and so on. The polymer/Dach-Pt conjugates are expected to keep the platinum complex away from these deactivating factors and maintain their cytotoxic activity during circulation in blood stream due to the immobilization by a stable, chelate-type

Downloaded by YORK UNIV on October 31, 2012 | http://pubs.acs.org
Publication Date: September 24, 1998 | doi: 10.1021/bk-1998-0709.ch021

Downloaded by YORK UNIV on October 31, 2012 | http://pubs.acs.org
Publication Date: September 24, 1998 | doi: 10.1021/bk-1998-0709.ch021

Table I. Structural data and cytotoxic activity of dextran derivatives/Dach-Pt conjugates and platinum complexes (Adatted from ref. 21 and 22)

samples	*MW of dextran derivatives*	*DCA*[a] *(mol% per sugar unit)*	*DPt (mol%)*[b]		*IC_{50}(mol/l)*[c]
			per sugar unit	*per carboxylic acid group*	
OX-Dex/Dach-Pt	1.1×10^4	58.4	11.4	19.0	2.5×10^{-6}
DCM-Dex/Dach-Pt	1.0×10^4	23.4	2.4	20.5	8.0×10^{-6}
CM-Dex/Dach-Pt	1.2×10^4	58.2	16.4	27.3	5.0×10^{-5}
Dach-Pt(chlorato)	-	-	-	-	7.2×10^{-6}
Dach-Pt(maolonato)	-	-	-	-	1.6×10^{-5}

a) Degree of introduction of carboxylic acid group per sugar unit.

b) Degree of introduction of platinum complex.

c) Concentration of platinum complex at which the cytotoxic activity reaches 50%.

Downloaded by YORK UNIV on October 31, 2012 | http://pubs.acs.org
Publication Date: September 24, 1998 | doi: 10.1021/bk-1998-0709.ch021

coordination bond and steric hindrance of polymer chain. Therefore we investigated the residual cytotoxic activity of the conjugates, Dach-Pt(chlorato) and Dach-Pt(malonato) against tumor cells after a certain preincubation period in medium containing serum. The results are shown in Figure 4. While the cytotoxic activity of Dach-Pt(chlorato) decreased gradually with preincubation time in the medium, OX-Dex/Dach-Pt conjugate, DCM-Dex/Dach-Pt conjugate and Dach-Pt(malonato) maintained higher residual cytotoxic activities. Especially, DCM-Dex/Dach-Pt conjugate kept its cytotoxic activity in almost 100% after 18 h preincubation in the medium. On the other hand, the cytotoxic activity of the CM-Dex/Dach-Pt conjugate decreased drastically with preincubation time and it showed no cytotoxic activity after 18 h preincubation. These results suggest that the dextran derivative containing dicarboxylic acid groups kept the cytotoxic activity of immobilized platinum complex by protecting it from deactivating factors in the medium containing serum. The resistance of the platinum complex against deactivating factors (protein or amino acid) in serum is due to both of the strength of coordination bond of platinum atom with carrier polymer and steric hindrance of carrier polymer. The coordination bond of platinum complex with carboxylic acid is generally weaker than that with amino group. However, DCM-Dex can form 6-membered chelate-type coordination bond with Dach-Pt as shown in Figure 2. The strength of the chelate-type coordination bond in DCM-Dex/Dach-Pt conjugate is higher than that in and OX-Dex/Dach-Pt conjugate or CM-Dex/Dach-Pt conjugate and may be comparable with that of single coordination bond of platinum complex with amino groups of deactivating factors. Moreover, the polymer chain in the conjugates can protect Dach-Pt moiety from deactivating factors by its steric hindrance. These are the reason why the DCM-Dex/Dach-Pt conjugate showed a longer maintenance of cytotoxic activity in the medium containing serum.

Although CM-Dex/Dach-Pt conjugate showed almost same release behavior as OX-Dex/Dach-Pt conjugate in PBS (Figure 3), CM-Dex/Dach-Pt conjugate showed lower cytotoxic activity (Table I) and lower stability in culture medium containing serum. The Dach-Pt moiety in CM-Dex/Dach-Pt conjugate must be immobilized by single coordination bond (Figure 2). The other coordination cite is free and can be easily converted aquo-type complex. This may easily lead deactivation of Dach-Pt moiety in CM-Dex/Dach-Pt conjugate. Moreover, the solubility of CM-Dex/Dach-Pt conjugate was much lower than the other two conjugates, possibliliy because of partial cross-linking. It took about 6h to dissolve the conjugate in buffer solution before the measurements of cytotoxic activity and residual cytotoxic activity. In this dissolution process, large amount of Dach-Pt immobilized should be converted to the aquo-type complex and released from CM-Dex. This is another possible reason why that CM-Dex/Dach-Pt conjugate showed lower cytotoxic activity and more rapid deactivation than the other conjugates.

***In vivo* antitumor activity.** The *in vivo* tumor growth inhibitory effect of OX-Dex/Dach-Pt conjugate was investigated against colon 26 tumor cells in mice by intravenous injection. The results are shown in Figure 5. Figure 6 shows a photograph of the tumors excised from the treated and control mice 28 days after inoculation. The actual tumor weights for control group, OX-Dex/Dach-Pt treated group and Dach-Pt(chlorato) treated group were 1327 ± 242, 519 ± 65 and 814 ± 99 mg±SD, respectively. The OX-Dex/Dach-Pt conjugate and Dach-Pt(chlorato) showed effective growth inhibitory effects against colon 26 tumor cells. The growth inhibitory effect of OX-Dex/Dach-Pt conjugate was larger than that of

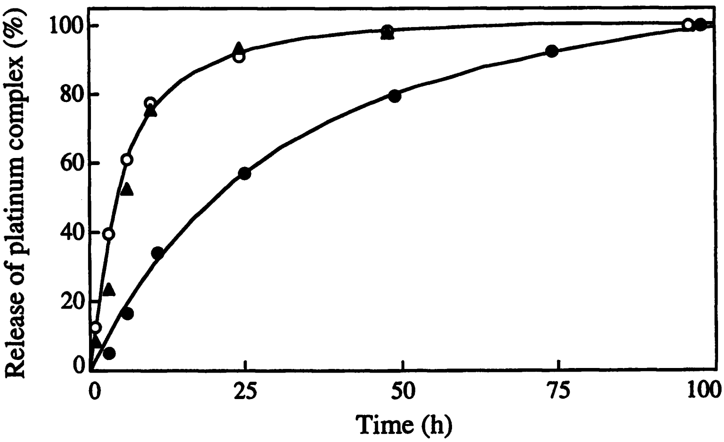

Figure 3. Release behavior of platinum complex from the conjugates in PBS (pH=7.4) containing NaCl (0.1M) at 37°C. (●): DCM-Dex/Dach Pt conjugate, (○): OX-Dex/Dach-Pt conjugate, (▲): CM-Dex/Dach-Pt conjugate. (Adapted from ref. 21 and 22).

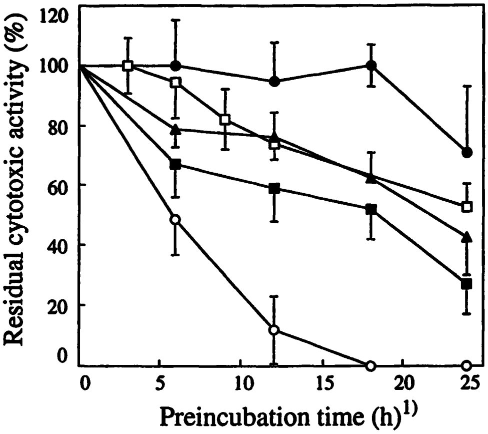

Figure 4. Residual cytotoxic activity of the conjugates and free platinum complexes after preincubation in the medium containing fetal calf serum (FCS) against p388D$_1$ *lymphocytic leukemia* cells for 24 h *in vitro.*

(●): DCM-Dex/Dach Pt conjugate, (□): OX-Dex/Dach-Pt conjugate, (○): CM-Dex/Dach-Pt conjugate, (■): Dach-Pt (chlorato), (▲): Dach-Pt (malonato). (Partially adapted from ref. 21 and 22).

1) Preincubation time of conjugates or free platinum complexes in RPMI-1640 medium containing 10% FCS at 37°C. The residual cytotoxic activity was measured by 24 h incubation with p388D$_1$ *lymphocytic leukemia* cells using drugs which were preincubated in RPMI-1640 medium containing 10% FCS at 37°C for cetain periods.

Downloaded by YORK UNIV on October 31, 2012 | http://pubs.acs.org
Publication Date: September 24, 1998 | doi: 10.1021/bk-1998-0709.ch021

Downloaded by YORK UNIV on October 31, 2012 | http://pubs.acs.org
Publication Date: September 24, 1998 | doi: 10.1021/bk-1998-0709.ch021

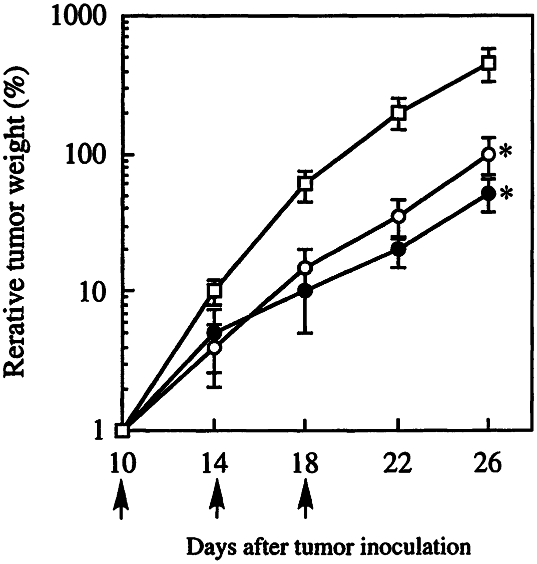

Figure 5. Growth inhibitory effects of OX-Dex/Dach-Pt conjugate and free Dach-Pt against Colon 26 tumor cells inoculated in CDF_1 mice. (●): OX-Dex/Dach-Pt conjugate, (○): Dach-Pt (chlorato), (□): control. The samples were injected intravenously to CDF_1 mice at the days indicated by arrows. $*P < 0.01$, compared with the control experiment by student *t* test.

Downloaded by YORK UNIV on October 31, 2012 | http://pubs.acs.org
Publication Date: September 24, 1998 | doi: 10.1021/bk-1998-0709.ch021

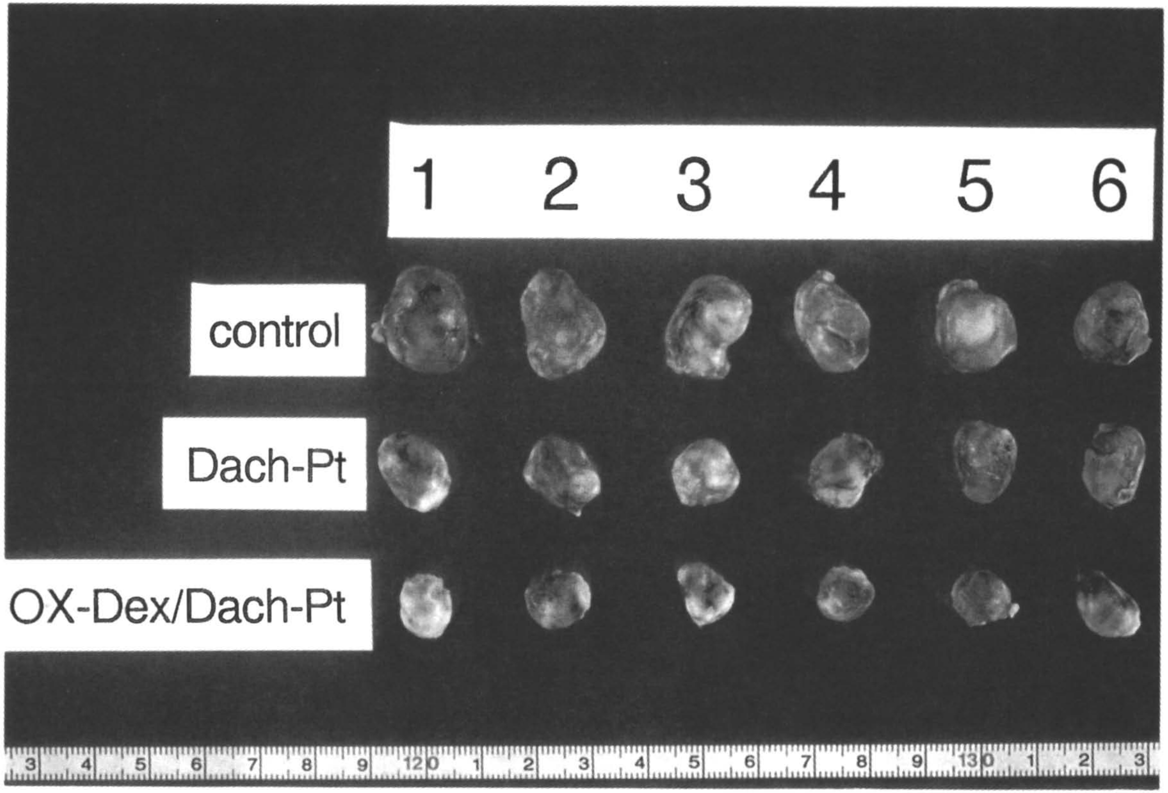
1
2
3
4
5
6
control
Dach-Pt
OX-Dex/Dach-Pt
3 4 5 6 7 8 9 120 1 2 3 4 5 6 7 8 9 130 1 2 3

Figure 6. Photograph of the tumors excised from CDF_1 mice 28 days after inoculation.

Dach-Pt(chlorato). This is because slow release of active platinum complex from carrier polymer and longer maintenance of the activity in blood stream.

Conclusion

Highly water-soluble OX-Dex/Dach-Pt conjugates and DCM-Dex/Dach-Pt conjugates could be synthesized by ligand exchange reaction using oxidized-dextran and dicarboxymethyl-dextran with Dach-Pt(chlorato). The obtained conjugates showed high level cytotoxic activity *in vitro*, which was comparable to free Dach-Pt(chlorato), parent drug. While the cytotoxic activity of Dach-Pt(chlorato) and CM-Dex/Dach-Pt conjugate decreased in the medium with serum, the obtained conjugates, especially DCM-Dex/Dach-Pt conjugate, maintained their cytotoxic activity for longer period. Moreover, OX-Dex/Dach-Pt showed effective *in vivo* growth inhibitory effect against colon 26 tumor cells in mice by intravenous injection.

Since the conjugates have much larger molecular size compared with the typical low-molecular-weight anticancer platinum complexes, these conjugates should presumably have a longer half-life in body and larger accumulation at the inflammatory tumor site than low-molecular-weight platinum complexes by enhanced permeability and retention (EPR) effect (*11*). This may be also because OX-Dex/Dach-Pt conjugate showed greater tumor growth inhibitory effect than free Dach-Pt(chlorato) in mice. A much better *in vivo* therapeutic index against tumors should be expected for the DCM-Dex/Dach-Pt conjugate having stable 6-membered chelate-type coordination bonds by keeping its cytotoxic activity during long circulation in body fluid. We shall report the *in vivo* antitumor activity of DCM-Dex/Dach-Pt conjugate in a subsequent paper.

Acknowledgment

The authors wish to express their sincere appreciation to Sumitomo Pharmaceuticals Co. Ltd. for providing Dach-Pt(chlorato). This research was financially supported by a Grant-in-Aid for Scientific Research (09240103) from the Ministry of Education, Science, Culture and Sports , Japan, and the Naito Foundation.

References

1. Rosenberg, R.; VanCamp, L.; Trosko J.; Mansour. V. H. *Nature* **1969,** *222*, 385.
2. Cleare, M. J.; Hoechele, J. D. *Platinum Metals Rev*. **1979,** *6*, 17.
3. Hacker, M. P.; Khokhar, A. R.; Brown, D. B.; McCormack, I. J.; Krakoff, I. H. *Cancer Res*. **1985,** *45*, 4748.
4. Kuramochi, H.; Motegi, A.; Maruyama, S.; Okamoto, K.; Takahashi, K.; Kogawa, O.; Nowatari, H.; Hayami, H. *Chem. Pharm. Bull.* **1990,** *38*, 123.
5. Maeda, M.; Takatsuka, N.; Suga, T.; Sasaki, T. *Jpn. J. Cancer Res.* **1990,** *81*, 567.
6. Kidani, Y.; Inagaki, K. *J. Med. Chem.* **1978,** *21*, 1315.
7. Kidani, Y.; Inagaki, K.; Yashiro, T.; Tashiro, T.; Tsukagoshi, S. *Chem. Pharm. Bull.* **1979,** *27*, 819.
8. Kidani, Y.; Noji, M.; Tashiro, T. *Gann* **1980,** *71*, 637.
9. Mauldin, S. K.; Husain, I.; Sancar, A.; Chaney, S. G. *Cancer Res.* **1986,** *46*, 2876.

Downloaded by YORK UNIV on October 31, 2012 | http://pubs.acs.org
Publication Date: September 24, 1998 | doi: 10.1021/bk-1998-0709.ch021

10 Gibbons, G. R.; Page, J. D.; Mauldin, S. K.; Husain, I.; Chaney, S. G. *Cancer Res.* **1986,** *50,* 6497.

11. Maeda, M.; Oda, T.; Matsumura, Y.; Kimura, M. *J. Bioact. Compat. Polym.* **1988,** *3,* 27.

12. Duncan, R.; Seymour, L. W.; O'Hare, K. B.; Flanagan, P. A.; Wedge, S.; Hume, I. C.; Ulbrich, K.; Strohalm, J.; Sabr, V.; Spreafico, F.; Grandi, M.; Ripamonti, M.; Farao, M.; Suarato, A. *J. Controlled Rel.* **1992,** *19,* 133.

13. Hoes, C. J. T.; Grootoonk, J.; Duncan, R.; Hume, I. C.; Bhakoo, M.; Bouma, J. M. W.; Feijen, J. *J. Controlled Rel.* **1993,** *23,* 37.

14. Kataoka, K.; Kwon, G. S.; Yokoyama, M.; Okano, T.; Sakurai, Y. *J. Controlled Rel.* **1993,** *24,* 119.

15 Ueda, Y.; Munechika, K.; Kikukawa, A.; Kanoh, Y.; Yamanouchi, K.; Yokoyama, K. *Chem. Pharm. Bull.* **1989,** *37,* 1639.

16 Hirano, T.; Ohashi, S.; Morimoto, S.; Tsuda, K.; Kobayashi, T.; Tsukagoshi, S. *Makromol. Chem.* **1986,** *187,* 2815.

17. Ohya, Y.; Hirai, K.; Ouchi, T. *Makromol. Chem.* **1992,** *193,* 1881.

18. Ohya, Y.; Nonomura, K.; Ouchi, T. *J. Bioact. Compat. Polym.* **1995,** *10,* 223.

19. Schechter, B.; Pauzner, R.; Wichek, M. *Cancer Biochem. Biophys.* **1986,** *8,* 277.

20. Hall, J. M.; Speer, R. J.; Ridgway, H. J.; Stewart, D. P.; Newman, A. D.; Hill, J. M. *J. Clin. Hematol. Oncol.* **1977,** *1,* 231.

21. Ohya, Y.; Masunaga, T.; Baba, T.; Ouchi, T. *J. Macromol. Sci.-Pure Appl. Chem.* **1996,** *A33,* 1005.

22. Ohya, Y.; Masunaga, T.; Baba, T.; Ouchi, T. *J. Biomater. Sci. Polymer Edn.* **1996,** *7,* 1085.

23. Ohya, Y.; Nonomura, K.; Hirai, K.; Ouchi, T. *Macromol. Chem. Phys.* **1994,** *195,* 2839.

24. Moore, G. E. *J. Natl. Cancer Inst.* **1966,** *36,* 405.

25. Mosmann, T. *J. Immunol. Methods* **1983,** *65,* 55.

Downloaded by YORK UNIV on October 31, 2012 | http://pubs.acs.org
Publication Date: September 24, 1998 | doi: 10.1021/bk-1998-0709.ch021

Downloaded by UNIV OF GUELPH LIBRARY on October 31, 2012 | http://pubs.acs.org
Publication Date: September 24, 1998 | doi: 10.1021/bk-1998-0709.ch022

Chapter 22

Potential Role of Controlled Drug Delivery in Tissue Engineering

K. J. L. Burg[1] and S. W. Shalaby[2]

[1]Department of General Surgery Research, Carolinas Medical Center, Charlotte, NC 28232–2861
[2]Poly-Med Inc., Center for Applied Technology, Westinghouse Road, Pendleton, SC 29670

This communication discusses the pertinence of controlled release of bioactive agents/drugs to the success of the fast-growing tissue engineering technology. Key aspects of the control release mode and processing of polymeric scaffolds for three-dimensional cell growth are analyzed. Contemporary trends in scaffold developments and future perspectives of controlled delivery systems/tissue engineering are noted.

The success of a tissue engineered construct, as with all biomaterial implants, is heavily dependent on the interaction of the material with the tissue. Additionally, since many tissue engineered constructs involve the replacement of an absorbable biomaterial with newly developing tissue, the success also hinges on cellular growth into the material, timely tissue growth, the development of a viable, structurally and biologically functional tissue, and its controlled growth to the final dimensions of the tissue. Many biomaterial designs allow the incorporation of bioactive agents/drugs for such purposes as infection control (antibiotics), cartilage and bone formation, angiogenic stimulation, and a variety of other tissue stimulating goals. Tissue engineering currently has areas to which drug delivery may be useful (*1-4*). First, one major area critical to progress of the field is the development of vasculature to support a relatively thick tissue (*5*). Angiogenesis is a complicated process, modulated by growth factors, extracellular matrices, and proteases (*6-14*). Development of a relatively thick tissue could potentially require additional angiogenic growth factors incorporated alone in the biomaterial or could potentially require additional incorporation of cells derived from vasculature (i.e., endothelial cells) to induce formation of tubular structures (*15*). Additionally, the surrounding tissue or cells incorporated within the material complex may require additional factors or a combination of factors to signal the appropriate cellular growth in a controlled fashion (*16-19*). Drug delivery is complicated by the fact that the

In Tailored Polymeric Materials for Controlled Delivery Systems; McCulloch, I., et al.;
ACS Symposium Series; American Chemical Society: Washington, DC, 1998.

behavior of the cellular component to the particular drug will depend largely also on the drug-material interaction and the resulting microenvironment (*14,20*).

Pertinent Modes of Controlled Release of Bioactive Agents

The most pertinent controlled release mode for future applications in tissue engineering is the diffusion controlled type, where the release involves a matrix or a reservoir system. The development of a reservoir system entails encapsulation of the drug by a polymer membrane, potentially microporous. In a tissue engineering design, this may involve encapsulation of specific cells individually or incorporation of multiple cells in a carrier for the purposes of releasing desired factors or it may involve direct encapsulation of the drug. These systems can have a release lag time as the surrounding polymer saturates with drug and as its release to the surrounding medium gradually reaches a steady state. If the encapsulating polymer is saturated with the drug prior to implantation, the surrounding medium will encounter a burst release followed by a gradual decline to a steady state (*20*).

The matrix system is one in which drug is incorporated in or throughout the polymer. In this system, the drug release gradually decreases with time as the distance of travel for the drug to go from the core to the surrounding medium increases. This can be adjusted by loading the drug, incrementally increasing towards the core. To be effective, this does require that the drug will not redisperse prior to implantation. The concentration of drug in the system will have an influence on the release profile. Isolated drug, or drug surrounded by a solid, nonporous polymer, will not release and will remain entrapped in the material until the material absorbs. The drug in the matrix system may either be physically dispersed throughout the matrix or chemically attached to the polymer. If the surface area of the material remains relatively constant throughout absorption period, the release rate will remain essentially constant. Porous polymeric structures, as are commonly exploited in tissue engineering, may release loaded drug with a minimized initial burst followed by a slow release rate.

The drug release may also be controlled through a swelling mechanism, as in the case of hydrogel systems, such as modified collagen or gelatin. The drug is incorporated into the gel; as water diffuses into the system swelling occurs, thus unlocking the drug and causing its release to the surrounding medium. Hydrogel systems are commonly used in tissue engineering constructs and have the positive attribute of providing a surgically minimally invasive option (*21-25*).

Processing Considerations in Tissue Engineering

There are many processing factors that affect the release rate of bioactive agents, including the type of polymeric carrier, substrate porosity, and the mode of delivery. Release of the drug may take place by physical means such as diffusion or osmosis. It may also be impacted by matrix swelling, which is in turn induced by enzymatic or hydrolytic means (*26*). The drug may be directly loaded into a polymeric material or it may be synthesized by and released from cells which are encapsulated in such polymeric material (*27,28,29*).

Downloaded by UNIV OF GUELPH LIBRARY on October 31, 2012 | http://pubs.acs.org
Publication Date: September 24, 1998 | doi: 10.1021/bk-1998-0709.ch022

The release of drugs from a three-dimensional system is complicated, particularly in a dynamic, absorbable one. The morphology of a tissue engineered foam scaffold may vary through its volume due to processing limitations or purposeful design (*30*). Similarly, the crystalline content and molecular weight parameters of the material may also vary. As the absorption process occurs, the material may preferentially absorb (*31*), depending on accessibility of water and enzymes to the site, which complicates drug release considerably. Additionally, as tissue and supporting vasculature develops throughout the scaffold, the kinetics of drug delivery may change. As engineered tissue develops and factors are produced *in situ*, the additional drug requirements of the area may subsequently change.

Some fabrication complications include thermal and chemical stability of the drug, since many fabrication processes involve either solvents or high temperatures. Proteins, for example, can readily denature so less destructive methods such as photopolymerization (*32*) are more desirable for their processing. Photopolymerization also leads to an initial nonuniform distribution of drug (*32*) which could be particularly useful in large tissue constructs, where nonuniform growth may be an important issue. Low melting solid solvents, such as napthalene, which have been successfully utilized in the manufacture of porous constructs, can be readily removed by extraction or sublimation from the solidified bicontinuous phases to provide continuous cell structure. This alleviates the need for more traditional processing methods which can cause protein denaturing (*33*). Additionally, many of the common methods of foam fabrication involve the addition of porogens which are later leached to form the porous structure. This leaching step can actually cause the leaching of any preloaded drug; so, use of these type foams typically involves later addition of bioactive agents; for example, the addition of drug delivery beads to a porous matrix (*34*). It may, however, be complicated to uniformly distribute the beads throughout the scaffold, particularly as thicker scaffolds are utilized and become potentially increasingly nonhomogeneous. Other important processing factors can include the physical state of the drug and its solubility in polymer, the shape and dimensions of the engineered construct, and the hydrophobicity of both the polymer and drug.

Contemporary Trends in Scaffold Development

There are several key factors which influence the performance of an absorbable scaffold, both as a substrate for three-dimensional cell growth and as a carrier of bioactive agents which modulate relevant complex biological events. These factors include (1) the continuity of the cellular structure in a microporous substrate and ease of nutrient and metabolic by-product transport through the engineered construct; (2) the surface energy, activities, and chemical environment presented initially to living cells; (3) the ability to synchronize the absorption and strength loss properties of the substrate with the gradual three-dimensional growth of the engineered tissue; and (4) injectability of the polymeric carrier for cells and bioactive agents. Study of these factors was initiated several years ago by Shalaby and his co-workers at Clemson University and, more recently, at Poly-Med, Inc. (*35-39*). Formation of continuous-cell microporous foams for housing living cells has been achieved with certain absorbable and non-absorbable polymers using the

Downloaded by UNIV OF GUELPH LIBRARY on October 31, 2012 | http://pubs.acs.org
Publication Date: September 24, 1998 | doi: 10.1021/bk-1998-0709.ch022

principle of crystallization-induced microphase separation denoted as CIMS (*35*). A typical CIMS process entails (1) co-melting of an absorbable crystalline thermoplastic polymer, such as poly(lactide-co-glycolide) or poly(,-caprolactone-co-glycolide), with certain low-melting organic solids (or diluents), such as naphthalene, to form a one-phase melt; (2) rapid cooling of the one-phase systems which results in simultaneous crystallization of the organic diluent and polymer to form two bicontinuous microphases; and (3) sublimation or extraction of the diluent phase to produce a continuous-cell microporous foam. The porosity and surface area of the foam can be controlled by varying the diluent/polymer ratio and cooling rate of the molten system. Depending on the type of cells involved in tissue engineering, the internal and external surface of the porous constructs can be functionalized to impart hydrophilicity and/or ionic character. In a typical construct for use in bone regeneration, the surface can be phosphonylated to develop suitable functionality for the deposition of hydroxyapatite, a key component in bone formation (*36-37*). To modulate the absorption profile of polymers pertinent to tissue-engineering, the concept of constructing polyester chains with amine functionalities for auto-catalyzed hydrolysis has been successfully tested (*38*). A simple foam of these systems is based on carboxy-terminated polyester chains which are conjugated ionically with a basic amino acid, such as lysine. Exploiting the proven biocompatibility of polyethylene glycol (PEG), Shalaby (*39*) developed a family of absorbable, injectable liquid PEG-polyester copolymers that transform to insoluble gels in aqueous media. Such gel-formers have been proposed as transient carriers for living cells as well as bioactive agents/drugs intended for injection to the specific biological site in need of repair.

Future Perspective

The potential for tissue engineering drug delivery systems is great. With careful consideration to avoid overloading an area with factors and potentially causing uncontrolled, undesired cellular growth (*40*), this indeed may provide a currently missing link in development of viable tissue replacement. As tissues are indeed composed of a mixture of different cells and factors rather than a purified population, it seems logical that additional signals generated through drug delivery (either by the appropriate combination of factor secreting cells or appropriate combination of growth factors) potentially remain the key to successfully engineered tissue and organs. As scientists continue to address scaffold design, the considerations associated with drug incorporation will remain key.

Literature Cited

1. Sato, T.; Kanke, M.; Schroeder, H.G.; DeLuca, P.P. *Pharm. Res.* **1988,** *5*, pp. 21-30.
2. Thomson, R.C.; Yaszemski, M.J.; Powers, J.M.; Mikos, A.G. In *Biomaterials for Drug and Cell Delivery*; Mikos, A.G.; Murphy, R.M.; Bernstein, H.; Peppas, N.A., Eds.; Materials Research Society Symposium Proceedings: Pittsburgh, PA, 1994, Vol. 331.

Downloaded by UNIV OF GUELPH LIBRARY on October 31, 2012 | http://pubs.acs.org
Publication Date: September 24, 1998 | doi: 10.1021/bk-1998-0709.ch022

3. Elema, H.; DeGroot, J.H.; Nijenhuis, A.J.; Pennings, A.J.; Veth, R.P.H.; Klompmaker, J. *Colloid Polym. Sci.* **1990**, *268*, pp. 1082-1088.
4. Hsu, Y.-Y; Gresser, J.D.; Trantolo, D.J.; Lyons, C.M.; Gangardharam, P.R.J.; Wise, D.L. *J. Control. Rel.* **1996**, *40*, pp. 293-302.
5. Mikos, A.G.; Sarakinos, G.; Lyman, M.D.; Ingber, D.E.; Vacanti, J.P.; Langer, R. *Biotechnol. Bioeng.* **1993**, *42*, pp. 716-723.
6. Connolly, D.T.; Heuvelman, D.M.; Nelson, R.; Olander, J.V.; Eppley, B.L.; Delfino, J.J.; Siegel, N.R.; Leimgruber, R.M.; Feder, J. *J. Clin. Invest.* **1989**, *84*, pp. 1470-1478.
7. Montesano, R.; Vassali, J.D.; Baird, A.; Guillemin, R.; Orci, L. *Proc. Natl. Acad. Sci. USA*. **1986**, *83*, pp. 7297-7301.
8. Kubota, Y.; Kleinman, H.K.; Martin, G.R.; Lawley, T.J. *J. Cell Biol.* **1988**, *107*, pp. 1589-1598.
9. Mignatti, P.; Robbins, E.; Rifkin, D.B. *Cell.* **1986**, *47*, pp. 487-498.
10. Montesano, R.; Orei, L.; Vassali, P. *J. Cell Biol.* **1983**, *97*, pp. 1648-1652.
11. Nicosia, R.F.; Bonanno, E.; Smith, M. *J. Cell Physiol.* **1993**, *154*, pp. 654-661.
12. Yang, E.Y.; Moses, H.L. *J. Cell Biol.* **1990**, *111*, pp. 731-741.
13. Yasunaga, C.; Nakashima, Y.; Sueishi, K. *Lab. Invest.* **1989**, *61*, pp. 698-704.
14. Greisler, H.P.; Gosselin, C.; Ren, D.; Kang, S.S.; Kim, D.U. *Biomater.* **1996**, *17*, pp. 329-336.
15. Fournier, N; Doillon, C.J. *Biomater.* **1996**, *17*, pp. 1659-1665.
16. Toolan, B.C.; Frenkel, S.R.; Pachence, J.M.; Yalowitz, L.; Alexander, H. *J. Biomed. Mater. Res.* **1996**, *31*, pp. 273-280.
17. Fujisato, T.; Sajiki, T.; Liu, Q.; Ikada, Y. *Biomater.* **1996**, *17*, pp. 155-162.
18. Isobe, M.; Yamazaki, Y., Oida, S.; Ishihara, K.; Nakabayashi, N.; Amagasa, T. *J. Biomed. Mater. Res.* **1996**, *32*, pp. 433-438.
19. Kim, K.J.; Itoh, T.; Kotake, S. *J. Biomed. Mater. Res.* **1997**, *35*, pp. 279-285.
20. Leong, K.W. In *Synthetic Biodegradable Polymer Scaffolds*; Atala, A.; Mooney, D; Vacanti, J.P.; Langer, R., Eds.; Birkhäuser: Boston, MA, 1997, pp. 97-119.
21. Spargo, B.J.; Rudolph, A.S.; Rollwagen, F.M. *Biomater.* **1994**, *15*, pp. 853-858.
22. Paige, K.T.; Cima, L.G.; Yaremchuk, M.J.; Schloo, B.L.; Vacanti, J.P.; Vacanti, C.A. *Plast. Reconstr. Surg.* **1996**, *97*, pp. 168-178.
23. Paige, K.T.; Cima, L.G.; Yaremchuk, M.J.; Vacanti, J.P.; Vacanti, C.A. *Plast. Reconstr. Surg.* **1995**, *96*, pp. 1390-1398.
24. Atala, A.; Cima, L.G.; Kim, W.; Paige, K.T.; Vacanti, J.P.; Retik, A.B.; Vacanti, C.A. *J. Urol.* **1993**, *150*, pp. 745-747.
25. Schuman, L.; Buma, P.; Versleyen, D.; de Man, B.; van der Kraan, P.M.; van den Berg, W.B.; Homminga, G.N. *Biomater.* **1995**, *16*, pp. 809-814.
26. Fan, L.T. *Controlled Release: A Quantitative Treatment*; Springer-Verlag: New York, NY, **1989**.
27. Davis, M.W.; Vacanti, J.P. *Biomater.* **1996**, *17*, pp. 365-372.
28. Demetriou, A.A.; Whiting, J.F.; Feldman, D.; Levenson, S.M.; Chowdhury, N.R.; Moscioni, A.D.; Kram, M.; Chowdhury, J.R. *Science.* **1986**, *233*, pp. 1190-1192.
29. Nyberg, S.L.; Peshwa, M.V.; Payne, W.D.; Hu, W.-S.; Cerra, F.B. *Amer. J. Surg.* **1993**, *166*, pp. 512-521.

Downloaded by UNIV OF GUELPH LIBRARY on October 31, 2012 | http://pubs.acs.org
Publication Date: September 24, 1998 | doi: 10.1021/bk-1998-0709.ch022

30. Wake, M.C.; Patrick, Jr., C.W.; Mikos, A.G. *Cell Transplant.* **1994,** *3*, pp. 339-343.
31. Grizzi, I.; Garreau, H.; Li, S.; Vert, M. *Biomater.* **1995,** *16*, pp. 305-311.
32. Lu, S.; Anseth, D.S. In *Proceedings of the Topical Conference on Biomaterials, Carriers for Drug Delivery, and Scaffolds for Tissue Engineering;* Peppas, N.A.; Mooney, D.J.; Mikos, A.G.; Brannon-Peppas, L., Eds.; American Institute of Chemical Engineers: New York, NY, 1997; pp. 181-183.
33. Roweton, S.; Shalaby, S.W. *Proc. of the Fifth World Biomaterials Congress,* **1996,** *2*, p. 95.
34. Yuksel, E.; Ray, B.; Widmer, M.; Weinfeld, A.B.; Waugh, J.; Jensen, J.; Cleek, R.; Mikos, A.G.; Shenaq, S.; Spira, M. In *Proceedings of the Topical Conference on Biomaterials, Carriers for Drug Delivery, and Scaffolds for Tissue Engineering;* Peppas, N.A.; Mooney, D.J.; Mikos, A.G.; Brannon-Peppas, L., Eds.; American Institute of Chemical Engineers Proceedings: New York, NY, **1997**; pp. 341-343.
35. Shalaby, S.W.; Roweton, S.L. U.S. Patent 5,677,218, **1997**.
36. Shalaby, S.W.; McCaig, M.S. U.S. Patent (to Clemson University) 5,491,198, **1996**.
37. Shalaby, S.W.; Rogers, K.R. U.S. Patent (to Clemson University) 5,558,517, **1996**.
38. Shalaby, S.W. U.S. Patent (to Poly-Med, Inc.) 5,522,842, **1996**; U.S. Patent (to Poly-Med, Inc.) to be issued in 1998.
39. Shalaby, S.W. U.S. Patent (to Poly-Med, Inc.) 5,612,052, **1997**; U.S. Patent (to Poly-Med, Inc.) to be issued 1998.
40. Heldin, C.-H.; Westermark, B. In *The Molecular and Cellular Biology of Wound Repair, 2nd ed.*; Clark, R.A.F., Ed.; Plenum Press: New York, NY, **1996** pp. 249-273.

Downloaded by UNIV OF GUELPH LIBRARY on October 31, 2012 | http://pubs.acs.org
Publication Date: September 24, 1998 | doi: 10.1021/bk-1998-0709.ch022

Chapter 23

Direct Measurement of Multiphase Flow Using Controlled Release of Polymers Soluble in Single Phase

Roman Bielski and Dorsey Montenecourt

PetroTraces, Inc., 115 Research Drive, Suite 136, Bethlehem, PA 18015

Downloaded by YORK UNIV on October 31, 2012 | http://pubs.acs.org
Publication Date: September 24, 1998 | doi: 10.1021/bk-1998-0709.ch023

Polymeric inserts containing minute amounts of radioactive substances (at safe levels) can be applied to measuring multi phase flows in pipelines, including those carrying crude oils. Several water and oil soluble polymeric systems were tested, and some were found to be applicable to the described measurements. The tests were performed under field conditions with varying pressures, temperatures, composition and flows of liquid phases. This novel, *on line*, direct measuring methodology is very simple, accurate and does not require sample collection.

The measurements of single phase fluids pumped through the pipelines are easy and accurate. Nonetheless, some important mixtures that fill the pipelines consist of more than one phase. For example, crude oil is almost always accompanied by significant amounts of water and gaseous phases.

Often, the existing techniques, measuring the mass flow of the multi phase systems, are not sufficiently precise or definitive. They either try to take advantage of the static situation (separation of phases), or measure properties which are not directly related to the mass flow of each phase. Moreover, most techniques are spot checks of fluid flow averages. The error is particularly high when the gaseous phase concentration is elevated to 80 percent or more. In some cases this error can be as high as 100% or more (1).

Recently, we devised two new methods for crude oil pipeline measurements, each involving the introduction of a foreign substance to the flow. The substance should dissolve proportionally to the flow of an individual phase. Here we describe some of our results related to the system where the dissolving substance is a polymer.

It is advantageous to observe the disappearance of the measured substance from a given insert *on line*. Hence, it is natural to use a methodology which can detect small, non-regulated amounts of radiation from the outside of the pipeline. Probably the most significant property of radioactivity is its ability to penetrate various materials, *i.e.*, radioactivity present inside a pipeline can be detected from outside of the pipeline. Additionally, the methods employing radiation can be extremely sensitive. Radioactivity, however, has its drawbacks including the existence of natural, radioactive background (NORM - naturally occurring radioactive material), serious problems with the radioactive waste disposal, and the fact that radiation is bio-hazardous.

Multi phase flow measurements do not usually take advantage of radioactivity. Recently, however, a method measuring dilution of three injected radio-tracers has been proposed (2).

In the last few years, a new detection technique, called **multi photon detection (MPD)** has been developed by BioTraces, Inc. (Drukier A.K. *et al.*, A new supersensitive technique for biomedical applications: Multi Photon Detection; *Proceedings of NIST Workshop on Supersensitive Biomedical Methods*, **1997**, in press). It uses only man made radio-isotopes and only these, which produce at least two energetic photons during the radioactive event. Employing rather sophisticated hardware and software, the MPD instrument can distinguish between events produced by the radio-isotope of interest and all other events. Thus, it enables almost perfect rejection of any radioactive background. Because of the instrument's extraordinary sensitivity, it needs a few orders of magnitude smaller amounts of radioactivity than prior art techniques.

The MPD methodology is particularly suitable for our purpose, not only because it requires very small amounts of radioactivity, but also because it can measure several radio-isotopes concurrently. If each substance to be washed by an individual phase contains a different radio-isotope, the MPD unit can independently measure each radioisotope's disappearance and, thus, the flow of each phase.

Method

The method involves the insertion of a metal plate, coated with the polymeric substance, into the pipeline. The rate the flow dissolves the polymer from the plate is directly related to the flow of the individual phase. In other words, the wash out time of the polymer layer must be related to the number and rate of molecules of a given fluid phase which were in contact with the surface of the polymer and, thus, to the mass flow of this phase. If we use three different polymers, each soluble only in a single phase, then each polymer can be washed out proportionally to the flow of the phase, in which it is soluble. If we independently and simultaneously measure the time required to wash the known amount of each radio-isotope doped polymer, we shall be able to determine the flow of each phase. Actually, the above described measurements of the mass flow of only two phases should be sufficient. The mass flow of the third phase could be determined from two additional, simple measurements - volumetric flow and density.

One can consider several, practical options to execute the above described idea:

1. The radioactive compound is located under the layer of the polymer. The polymer layer dissolves in the flow and, then, the radioactive salt rapidly disappears from the insert plate. Thus, multi photon detectors placed closely to the inserted sample can establish precisely the time needed for the washout of the radioactive compound and the polymer.

Downloaded by YORK UNIV on October 31, 2012 | http://pubs.acs.org
Publication Date: September 24, 1998 | doi: 10.1021/bk-1998-0709.ch023

2. A sample comprises of a single phase soluble polymer with covalently bonded radioactive atoms; gradual disappearance of radioactivity from the insert is measured.
3. The polymeric sample is dissolved in the solvent containing the radioactive compound. Solvent evaporation gives a polymer layer with homogeneously distributed radioactivity. Detectors located near the insert measure gradual disappearance of radioactivity.
4. A variation of the second and third approach avoids the necessity of mounting the detectors on the pipeline. In this case, the sample radioactivity is measured first, prior to insertion into the flow. Next, the sample is introduced to the pipeline for a precisely known period of time. After removal of the sample from the pipeline, it is re-measured in the laboratory to find out how much radioactivity and, thus, the polymer remained on the metal plate.

The described methodology requires materials which can be washed out proportionally to the flow of individual phases *i.e.* oil, water and gas. We set out to find appropriate polymers which are soluble in the water phase and the oil phase. The following is the first presentation of this unique and novel measuring technique and shows some of our preliminary results.

Downloaded by YORK UNIV on October 31, 2012 | http://pubs.acs.org
Publication Date: September 24, 1998 | doi: 10.1021/bk-1998-0709.ch023

Experimental

Isotopes. More than one hundred radioactive isotopes are compatible with the MPD technique. We selected cobalt-60 (^{60}Co, half life 5.2 y) and sodium-22 (^{22}Na, half life - 2.58 y). Both of these radio-isotopes are commercially available, inexpensive, and produce photons of relatively high energy (above 0.5 MeV). Since their half-lives are relatively long, no compensation for the half life decay during the short test duration is required. Our selection was based also on chemical and physical properties of available salts of these radio-isotopes, including solubility in matrices of interest (crude oil, brine). Both of these radio-isotopes are available in the form of water solutions of their chlorides. Both cations are known to form complexes with appropriate crown ethers (coronands), and therefore can be made soluble in either water or hydrocarbons. In most our experiments, we used solutions of (^{22}Na)sodium chloride.

Selection of Water Phase Soluble Polymers. The market for various water soluble polymers has grown very fast in recent years (4). In particular, controlled delivery of specific drugs into the blood system using water soluble or biodegradable polymers has been studied for several years. Unfortunately, the flows in veins and in pipelines are not always the same. Thus, polymers to be used in pipelines must be resistant to very high pressures and temperatures. Mechanical and thermal properties of polyethyleneglycols or polyvinylpyrrolidones are not sufficient for our purposes. We tried about two dozen different, commercially available polymers belonging to polysaccharides, polyacrylic and polymethacrylic acids, polyacrylic and polymethacrylic amides, polyvinylbenzenesulfonic acids and some relevant copolymers. The studied polymers differed not only in their structure but, also, in molecular weight. Careful experiments in the lab and, then, in the field led to selection of three water soluble polymers belonging to polyacrylic acids and amides, which met our criteria. These polymers can be easily prepared to contain the required, non-regulated amount of radioactive substance and are soluble in the flow of brine (in case of crude oils, so called water phase actually contains a few percent of various salts, mostly NaCl). It should be added, that in most cases the water phase soluble polymers can be attached directly to the metal plate and the system exhibits very good mechanical properties.

Selection of Oil Phase Soluble Polymers. We are not aware of any studies on the controlled release of drugs to crude oils in veins or pipelines. Thus, we tried several polymers based on general knowledge of polymers solubility. We experimented with various polyacrylates and polymethacrylates, polyalkenes, polystyrene and its substituted derivatives, and blends of some of these polymers. The measured polymers (about two dozens) differed in their chemical structure and molecular weight. We tried to select polymers which are applicable to any system consisting of water and oil phase. The selected polymers belong to substituted polystyrenes.

Preparation of Polymeric Samples. As it was already mentioned we considered four different ways of measuring flow using radioactive inserts. The approach # 1 (radioactivity under the polymer) happened to be impractical. The washout of the polymer was not as homogeneous as we hoped for, particularly in the final moments. It resulted in relatively long time, the radioactive substance disappeared from the insert. We discontinued this method after a few experiments. Also, we did not try to synthesize polymers containing radioactive atoms (approach # 2).

Downloaded by YORK UNIV on October 31, 2012 | http://pubs.acs.org
Publication Date: September 24, 1998 | doi: 10.1021/bk-1998-0709.ch023

Preparation of Water Phase Soluble Inserts. First, the required amount of the polymer was dissolved in appropriate solvent to form 10 -15 % solution. Water or methanol were used as solvents. Next, the water solution of sodium (^{22}Na) chloride (2 - 30 nanoCuries) was added to the mixture and vortexed. The mixture was transferred with a pipette onto the stainless steel plate to fill a circular area limited by a plastic or metal ring of appropriate diameter. The polymer solution was dried by evaporation of the solvent using nitrogen at room temperature. Additional layers of polymer were added, using the same procedure until the required thickness was achieved. This thickness was calculated from the measured mass of the polymer, measured diameter of the polymeric layer and known density of the polymeric system. After the insert preparation was complete, the ring was removed from the metal plate.

Preparation of Oil Phase Soluble Inserts. The polymeric inserts were prepared as described for water soluble polymers. In this case chloroform or methylene chloride served as solvents. Benzo-15-crown-5 was used to solubilize ^{22}NaCl in an organic solvent. To ensure that a sufficient amount of radioactivity was introduced to the polymeric system, the commercially available water solution of the radioactive material was evaporated almost to dryness and, then, the residue was dissolved in an organic solvent containing several times excess of the crown ether. The experiments showed that oil soluble polymers are not compatible with the metal (stainless steel) plate and, sometimes, under high flow conditions did not stay on the plate. Additionally, they are brittle and must be attached to the metal holder *via* the appropriate membrane or *via* the neutral polymer which is compatible with the metal and with the oil phase soluble polymer. Thus, in most cases we introduced small amount of metal plate compatible polymers between a plate and an oil soluble polymer.

In some experiments the metal plates with mesh were used. In such a case the solution of the selected polymer containing no radioactive additives was transferred to the meshed ring until the layer after evaporation reached the level of mesh. The mass of this product was measured. Next, the radioactive solution of the same polymer was gradually transferred onto the plate and evaporated until the required thickness of the polymer containing radioactive substance was achieved. After thorough evaporation of solvents the mass of the resulting insert was measured again.

Measurements. For obvious reasons most experiments could not be carried out in the laboratory. They were conducted at the Conoco facility in Lafayette, LA. The pipeline diameter was 2 or 3 inch. The most advantageous way of introducing polymeric sample into the flow was to attach it to the metal coupon, which was placed into a specially designed holder (Teflon) and inserted in the pipe. In most experiments, the coupon was introduced into the pipe in such a way that the polymeric insert was parallel to the flow. It was important not to affect the flow cross-section. Additionally, we checked if it was beneficial to place inserts at a small angle with respect to the flow. An appropriate device has been designed, built and tested. The Gallager mixing device was placed in the flow immediately before the insert to ensure as homogenous flow as possible. For water soluble polymers the water cut was between 2 and 40%, for oil soluble polymers the oil cut was 5 - 60%. The system contained small amounts of gas but no gas measuring experiments were performed. The flows in the pipeline were between 200 and 600 L/min and the temperature was between 30°C and 80°C. All these parameters were programmed, controlled and constantly measured using entirely independent methods available at the Lafayette facility. Close to a hundred different inserts were introduced to the flow.

The MPD detectors were mounted at the pipeline as close as possible to the radioactive insert. The sample radioactivity was measured for a few minutes with no flow and, then, radioactivity was measured constantly in 5, 10 or 20 second intervals until the background radiation levels were reached. The wash out time was determined as the time needed to obtain background level radiation of the insert. In some recent experiments the radioactivity of the sample was measured before introduction and after removal of the sample from the pipeline. In these cases, the radioactivity of the sample was also measured *on line* after the flow was introduced to the pipeline system. The *on line* measurements were necessary to determine the precise time at which the sample radioactivity diminished to about 50 - 60 % of its initial value. We assumed that the decrease in radioactivity was fully proportional to the decrease of the polymer layer thickness.

Results and Discussion

It was found that the solubility of most of the tested polymers in crude oil was lower than originally expected. The crude oil used in the Conoco facility in Lafayette is a typical light crude oil containing significant amounts of aromatic hydrocarbons. For example, poly(benzyl methacrylate) and poly(methyl methacrylate) of rather low molecular weight

Downloaded by YORK UNIV on October 31, 2012 | http://pubs.acs.org
Publication Date: September 24, 1998 | doi: 10.1021/bk-1998-0709.ch023

were practically insoluble in the system consisting of crude oil and brine. Additionally, some of these polymers showed much lower thermal resistance under real life (high pressure, brine) conditions than expected (based on producers Tg numbers). For example, poly (octadecyl methacrylate) shows Tg of 100°C (212°F). It turned out to be an excellent oil soluble polymer until we performed experiments with fluids in the pipeline at temperatures as high as 75°C (167°F). Soon after the flow was introduced to the system, the polymeric substance melted out of the metal plate.

In our first experiments we measured time necessary for total disappearance of radioactivity. Not surprisingly, the reproducibility of results was not satisfactory. It seems likely that with the layer of polymer becoming thinner and thinner new mechanisms related to the presence of the metal support start to play important role in the washout of the polymer.

In the next experiments we took into account the time needed to wash out 50 or 67% of the original amount of radioactivity. We calibrated the insert against the independent measurement. Then, we changed usually one parameter such as the ratio of liquid phases or the flow of all phases. It enabled estimation of the flow of the given phase with reasonable accuracy (about 2-5%). Pictures 1 and 2 show typical pattern of radioactivity disappearance as measured with MPD instrument *on line*.

The most encouraging results were obtained when the radioactivity of the polymer/isotope insert was measured before and after insertion to the pipeline flow. The polymer/isotope insert was kept in the flow for a precisely measured period of time. Since radioactivity is a random phenomenon, the length of time of the polymeric samples measurement (before and after insertion) was very important. The inserts were measured until the number of detected events reached 10,000. Here, the Poisson distribution predicts a standard deviation of 1% with 68 % confidence (5). Thus, each measurement required a few minutes for samples before the washout and about 10 minutes for samples after the washout. In most cases, the difference between our results (based on the MPD measurements) and independent results was below 2% both for water and oil soluble polymers. At this stage of research, we were often not able to predict the washout time of prepared polymeric inserts. Thus, it was necessary to carry out measurements *on line* to be able to stop the flow when the washout reached about 50-60 %.

What is of particular importance, the single phase measurement results do not depend on the composition of the other two phases (oil and gas or water and gas). Moreover, if the insert was left in the pipeline containing the oil and water phase with no flow for about 16 hours, the radioactivity of the insert did not change significantly. Apparently, the flow is responsible for the washout and the rate of dissolving of the polymer due to diffusion is negligible.

Figures 1 and 2 show typical pictures representing *on line* measurements of the washout of the radioactive substance from the polymeric insert. The starting count rate was measured for a few minutes before the flow was introduced to the bypass with the insert. The pressure, the flow and the ratio of liquid phases were constant during the measurement. As it was already mentioned the time required for the disappearance of 50 or 67 percent of the original amount of the sample radioactivity [the starting amount (counts) of radioactivity minus the final amount (counts) of radioactivity] was taken into account in the most accurate measurements. As the pictures show the pattern is similar for water and oil soluble inserts.

Downloaded by YORK UNIV on October 31, 2012 | http://pubs.acs.org
Publication Date: September 24, 1998 | doi: 10.1021/bk-1998-0709.ch023

Downloaded by YORK UNIV on October 31, 2012 | http://pubs.acs.org
Publication Date: September 24, 1998 | doi: 10.1021/bk-1998-0709.ch023

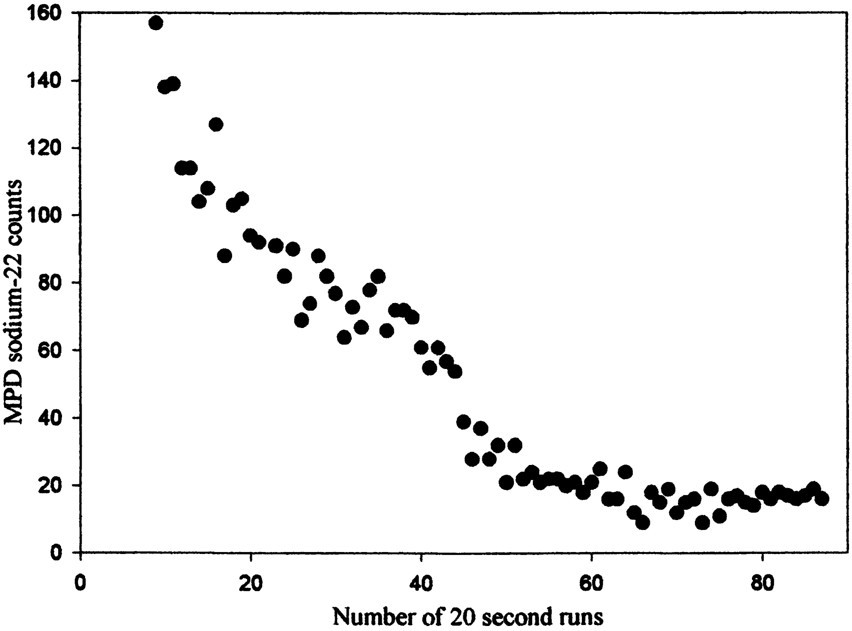

Figure 1. Water Soluble Polymer Z-21
Starting counts = 148 c/20 sec; Final counts = 18 c/20 sec;
Pressure =106 psi; Temperature = 151°F;
Flow = 60 gal/min; Water Flow = 36 gal/min

Downloaded by YORK UNIV on October 31, 2012 | http://pubs.acs.org
Publication Date: September 24, 1998 | doi: 10.1021/bk-1998-0709.ch023

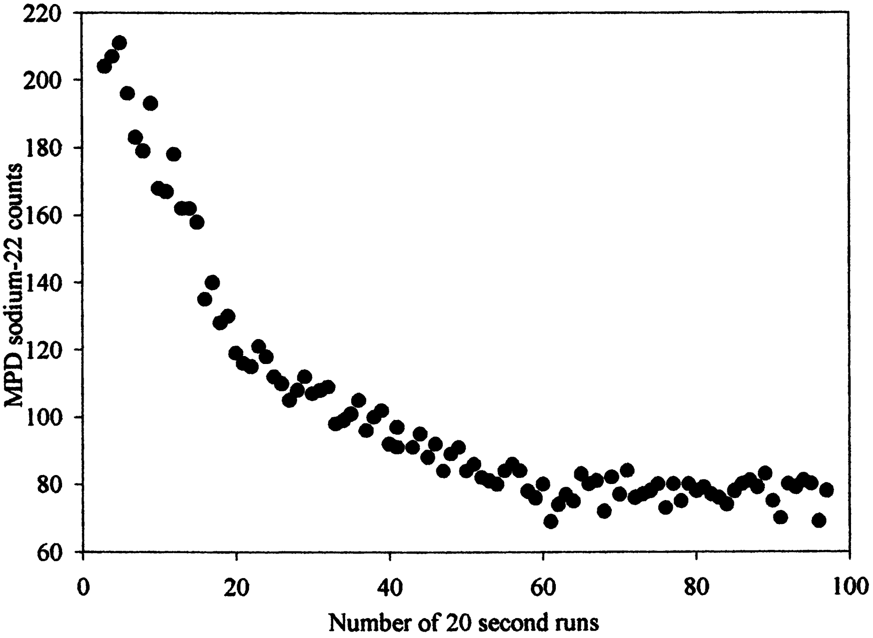

Figure 2. Oil Soluble Polymer A-19
Starting counts = 211 c/20 sec; Final counts = 79 c/20 sec;
Pressure = 106 psi; Temperature = 135°F;
Flow = 60 gal/min; Oil Flow = 48 gal/min

The following tables I and II briefly summarize the results obtained using various polymeric compounds:

Table I. Water Soluble Polymers

STRUCTURE	USEFULNESS	COMMENT
Polyethyleneglycols	No	Poor mechanical properties
Polyvinylpyrrolidones	No	Poor mechanical properties
Polysaccharides	No	Solubility and viscosity problems
Polyacrylic & polymethacrylic acids	Yes	Good mechanical and thermal properties
Polyacrylic & polymethacrylic amides	Yes	Good mechanical and thermal properties
Copolymers of PAAcids and PAAmides (Mw about 200,000)	Yes	Good mechanical and thermal properties
Polyvinylbenzenesulfonic acids	No	Solubility problems

Table II. Oil Soluble Polymers

STRUCTURE	USEFULNESS	COMMENT
Polyacrylates	No	Thermal properties not sufficient
Polymethacrylates	No	Thermal properties not sufficient
Polyalkenes	No	Insufficient solubility
Polystyrene	No	Solubility Problems
Poly(4-methylstyrene)	No	Solubility Problems
Poly(4-*t*-butylstyrene) (Mw below 100,000)	Yes	Good mechanical and thermal properties

Although this was only a feasibility study, it did define the direction for future development of this measuring technique. At this point we consider our feasibility studies finished. We expect that the measuring devices based on the approach described will be particularly useful in measuring the water cut (water content) of the multi phase flow system. It should be emphasized that the described analytical methodology requires

Downloaded by YORK UNIV on October 31, 2012 | http://pubs.acs.org
Publication Date: September 24, 1998 | doi: 10.1021/bk-1998-0709.ch023

no sample collection, uses no moving parts and is the only *on line* approach measuring two of the three phases inside the pipeline. Due to the high sensitivity of the MPD measurement technology the amounts of the radioactive substance in the insert will be very small and will require no radioactive licenses. Experiments to measure small amounts of oil in water and small amount of water in crude oil (below 1%) are in progress. We tried several statistical methods to find the optimum way to determine the washout time but we did not optimize the process yet. We initiated some measurements related to the properties of the polymeric films that had been used in the described experiments. several statistical methods to find the optimum way to determine the washout time but we did not optimize the process yet.

Downloaded by YORK UNIV on October 31, 2012 | http://pubs.acs.org
Publication Date: September 24, 1998 | doi: 10.1021/bk-1998-0709.ch023

Conclusion

The new methodology enables accurate and reliable measurements of the flow rate of oil and aqueous phases within a pipeline. Our approach employs the insertion of a coupon covered with single phase polymers doped with appropriate non-regulated quantities of radioactive substances into the flow. The polymers dissolve in the flow over a period of time and their loss of radioactivity is dependent upon flow rate, temperature, and fluid composition. The loss of the sample radioactivity, which is proportional to the flow of the measured phase, is measured using the ultra sensitive technique called MPD. No interference with the other liquid phase has been observed.

The results show that selected polymers survive well in the dynamic conditions of the flow. Easy to prepare polymer films show good reproducibility. In some cases the flow measurement accuracy was better than 2%.

Acknowledgments:

The authors would like to thank John Carter, late Bernie Tuss, Vladimir Gorodetsky and Dennis Perry for their valuable contribution and technical assistance. This work was partially supported by Conoco and SGS CSI, Inc.

Literature Cited:

1. Tuss, B.M. Status of Multi-Phase Flow Measurement Research, *Proceedings of the 71st International School of Hydrocarbon Measurements*, Oklahoma, OK **1996**, p 683.
2. Sevel T.; Pedersen N.H.; Weinell C.E.; Lind-Nielsen B. Development of an in-situ Calibration Method for Multiphase Flow Meters Using a Radioactive Tracer Technique, *North Sea Flow Measurement Workshop*, **1995**.
3. *Industrial Water Soluble Polymers*, Finch C.A., Ed.; The Royal Society of Chemistry, Special Publication # *186*, Thomas Graham House, Cambridge **1996**.
4. Whitehouse W.J.; Putman J.L. *Radioactive Isotopes*, Clarendon Press, Oxford **1953**.

Downloaded by UNIV OF GUELPH LIBRARY on October 31, 2012 | http://pubs.acs.org
Publication Date: September 24, 1998 | doi: 10.1021/bk-1998-0709.ch024

Chapter 24

Structural Characterization and Effects of Gibberellic Acid-Containing Organotin Polymers on Sawgrass and Cattail Germination and Seedling Growth for Everglades Restoration

Charles E. Carraher, Jr.[1,2], Anupam Gaonkar[1], Herbert H. Stewart[1], Shi Li Miao[3], and Shawn M. Carraher[4]

[1]Departments of Chemistry and Biological Sciences, Florida Atlantic University, Boca Raton, FL 33431
[2]Florida Center for Environmental Studies, NorthCorp Center, Palm Beach Gardens, FL 33410
[3]Everglades System Research Division, South Florida Water Management District, West Palm Beach, FL 33406
[4]Department of Management and Finance, Indiana State University, Terre Haute, IN 47809

The Florida Everglades is undergoing rapid change with much of the change associated with displacement of sawgrass by cattail. A major part of the Everglades restoration involves the growth of sawgrass plants from seeds. Polymers containing gibberellic acid, GA3, were synthesized from reaction with diorganotin dichlorides. Structural analysis emphasizing mass spectroscopy and infrared spectroscopy are consistent with the products containing tin-oxygen bonds. Through the use of GA3 and polymers containing the GA3 moiety, the percentage germination was increased from about 2-4% to 4-19% and the time required for germination decreased from about 4 weeks to 10-21 days.

The Florida Everglades is called the "River of Grass". The "grass" is actually a sedge called sawgrass (Cladium jamaicense Crantz). The Everglades is a subtropical, freshwater wetland ecosystem that is about 180 miles long and 90 miles wide. It is dominated by monospecific sawgrass marshes that historically covered about 70% of the land (1,2). It is undergoing rapid change with sawgrass being displaced by cattail (mainly Typha domingensis Pers.). For instance, in Water Conservation Area 2A, located in the heart of the northern Everglades with about 45,000 ha cattail dominated about 2,000 ha, in the early 1980's. In 1992 this was increased to over 7,000 ha and the cattail dominance is continuing to spread (3-6).

Various legislative mandates have recognized the need to halt the recent changes and to re-establish the Everglades as an ongoing, self sustaining and healthy ecosystem (for instance Douglas Act-Chapter 373.4592 and Everglades

Forever Act-Chapter 94-115). A major part of this restoration involves the "River of Grass".

The natural re-establishment of sawgrass after soil disturbances (such as fire) is known to be difficult (7). One of the difficulties of re-establishing sawgrass is their low seed germination (for instance 7,8). Seed germination has only rarely been observed in the field (7).

Both sawgrass and cattail replicate through rhizome development and seeds. Reproduction through seeds allows the retention of genetic diversity that is important in the Everglades since the Everglades is a system of extremes where adaptability is a necessary feature for long term survival. The successful transplanting of sawgrass plants into the Everglades has been reported (9).

Sawgrass seed germination is a critical part of the restoration of the Everglades either through growth of plants under controlled conditions and their subsequent introduction into the Everglades or through aerial (or other) dispersion of seeds. The latter is lower cost and offers the ability to cover large areas of space at a relatively low cost. In both cases, creation of conditions that favor sawgrass germination is advantageous.

The current study is part of a major undertaking aimed at stabilizing and re-establishing the Everglades. One of the areas of study involves the treatment of sawgrass seeds in an attempt to increase their germination percentage.

Seed treatments are a common practice in the seed industry. One of the major reasons for seed treatments is to increase seed germination mainly through seed protection and/or germination enhancement. The present report involves germination enhancement through treatment of seeds with plant growth regulators.

Plant growth regulators, PGRs, have been divided into groups-auxins (such as indole-3-acetic acid), cytokinins (including kinetin, zeatin, zeatin riboside and benzyladenine), gibberellins, ethylene and abscisic acid; and ancillary compounds such as polyamines (such as putrescine, spermidine and spermine) and phenolics. Here, we will focus our attention on gibberellins.

Gibberellins are cyclic diterpenes with the ability to induce a number of plant responses including cell elongation and cell division. While they are widespread in nature only a few have been shown to be active and only one, called gibberellic acid or GA3, is commercially available.

In general, controlled release formulations can offer

*longer "shelf life" and

*sustained release

For the present study, the controlled release polymer can offer

*greater retention of the active agent due to the lowered solubility of the polymer and

*the "co-reactant" can offer additional properties such as antifungal activity.

Each of these advantages can result in a greater activity with less active agent and by-products in the environment.

A "by-product" from the current work is the evaluation of the ability of the polymer to "deliver" through hydrolysis (or other mechanism) the active agent, here GA3. While there are a large number of gibberellins, only one of these,

Downloaded by UNIV OF GUELPH LIBRARY on October 31, 2012 | http://pubs.acs.org
Publication Date: September 24, 1998 | doi: 10.1021/bk-1998-0709.ch024

gibberellic acid, has found commercial application and almost all of the other gibberellins are inactive. GA3 is known to play a key role in the germination of most seeds. The most direct effect is in inducing the expression of the gene for a-amylase in germinating seeds (for instance 12). As seen, the polymer is active in regulating the germination and growth of both cattail and sawgrass seeds similar to but not the same as GA3 itself. This is consistent with an active moiety, presumably GA3 itself, being released through either enzymatic or physical hydrolysis of the polymer.

The present paper describes the structural characterization of the products emphasizing the product derived from the reaction of GA3 and diorganostannane dichlorides. Further, preliminary seed germination and seedling development results will be presented for GA3 itself and the polymer derived from reaction of dimethyltin dichloride and GA3, designated as DMT-GA3.

Downloaded by UNIV OF GUELPH LIBRARY on October 31, 2012 | http://pubs.acs.org
Publication Date: September 24, 1998 | doi: 10.1021/bk-1998-0709.ch024

Experimental

The polymers were synthesized utilizing the (aqueous) interfacial polycondensation process. Reactions were conducted employing a one quart Kimex emulsifying jar placed upon a Waring Blender (Model 7011G) with a "no-load" stirring rate of 18,000 rpm. The diorganostannane dichloride (1.00 mmole; Aldrich Chemical Company, Milwaukee, WI) was dissolved in 50 cc chloroform. This was added to a stirred solution of water (50 cc) containing gibberellic acid (1.00 mmole; Aldrich Chemical Company) containing sodium hydroxide (2.00 mmole). The product was collected as a precipitate employing suction filtration. The solid was repeatedly washed using water and chloroform to remove unreacted materials. The solid was allowed to dry in the open. Percentage yields were in the range of 20 to 50%.

Infrared spectral analysis was achieved using a Mattson Model 4020 Fourier Transform Infrared Spectrometer utilizing KBr pellets. Mass spectra were provided by the Midwest Center for Mass Spectroscopy, Lincoln, NE (Grant Number DIR9017262) using high resolution electron impact mass spectrometry with the samples placed on a heating stage with heating occurring rapidly to the 400 C range.

Germination and seedling development experiments were carried out in a greenhouse. "Tap" water was used. The pH of the water-soil combination was about 7 consistent with what is found in the Everglades.

Seeds were collected within a 45,000 hectare area in the northern Everglades referred to as Water Conservation Area 2A (WCA 2A). Sawgrass and cattail seeds were collected at a collection and measuring site referred to as F1 within a high phosphorus area. The plants were selected randomly and were separated by at least one meter to ensure that plants were of different clones.

Once seeded cattail fruits were separated from spikes, seeds were further isolated by gently grinding in a blender. The seeds underwent further preparatory procedures previously described by us (10). For cattails, viable seeds were identified as those that sank to the bottom of the blender that was used to separate the seed from the fruit parts (11). Cattail viability was 100% using growth percentages found for the seeds germinated in a petri dish. For sawgrass, seeds were separated from the seed parts using a mortar and pestle. Mature seeds were identified by visual observation. Viability was determined using a standard tetrazolium staining technique (12). Viability was found to be 46%.

Rectangular plastic trays (24X40X15(deep) cm) offering a soil surface area of about 860 square cms were used. Holes were drilled in the bottom of the trays to allow exchange of water. Ten cms of potting soil (Jungle Growth Potting Soil) was added to allow for seedling development to occur without need for immediate replanting.

A combined seed arrangement was used where 100 seeds of each cattail and sawgrass were used. Seeds were treated with talc-mixtures containing varying amounts of test material. The levels chosen have previously been reported to produce results for other seeds (13). Three replicates were run.

The trays were placed in "table top" trenches. The water level was maintained at about 10 cms, presenting what is referred to as "saturated" conditions. The water-filled trenches act to moderate temperatures and temperature changes more closely approximating field conditions. As noted above, the experiment was conducted within a covered greenhouse and watering was done by simply adding waster as needed to the trenches. This allowed water to reach the location of the seeds from below minimizing the "washing-away" of the seed treatments.

Talc mixtures containing GA3 or GA3-containing polymer, DMT-GA3, were made up prior to administration of the mixtures to the seeds. The seeds were treated with these known amounts of talc mixtures. The seeds were wetted to allow the talc mixtures to adhere to the seeds.

The seeds were spread over the surface of the trays. Germination was defined as the appearance of a small green shoot emanating from the seed. Observations of germination were made three times a week while leaf height measurements were made as indicated in the tables.

Results and Discussion

Structural Characterization. Gibberellic acid has three groups that can react with diorganotin dichlorides-two alcohol groups and one acid group. We have already reported the synthesis of a number of organotin-containing polyethers and polyesters from the analogous reaction of diols and salts of diacids with organotin dichlorides (for instance 14-18).

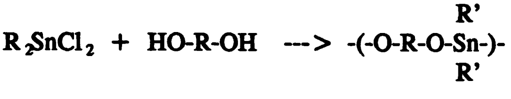

$$R_2SnCl_2 + HO\text{-}R\text{-}OH \text{ ---> } \text{-(-}O\text{-}R\text{-}O\text{-}\underset{R'}{\overset{R'}{Sn}}\text{-)-}$$

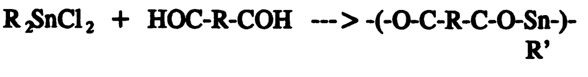

$$R_2SnCl_2 + HO\overset{O}{C}\text{-}R\text{-}\overset{O}{C}OH \text{ ---> } \text{-(-}O\text{-}\overset{O}{C}\text{-}R\text{-}\overset{O}{C}\text{-}O\text{-}\underset{R'}{\overset{R'}{Sn}}\text{-)-}$$

In Tailored Polymeric Materials for Controlled Delivery Systems; McCulloch, I., et al.;
ACS Symposium Series; American Chemical Society: Washington, DC, 1998.

Downloaded by UNIV OF GUELPH LIBRARY on October 31, 2012 | http://pubs.acs.org
Publication Date: September 24, 1998 | doi: 10.1021/bk-1998-0709.ch024

Thus, the products are probably cross-linked containing Sn-O-R and Sn-O-C(O)-R bonding between the organostannane moiety and the GA3 moiety with a repeat unit approximating that shown below.

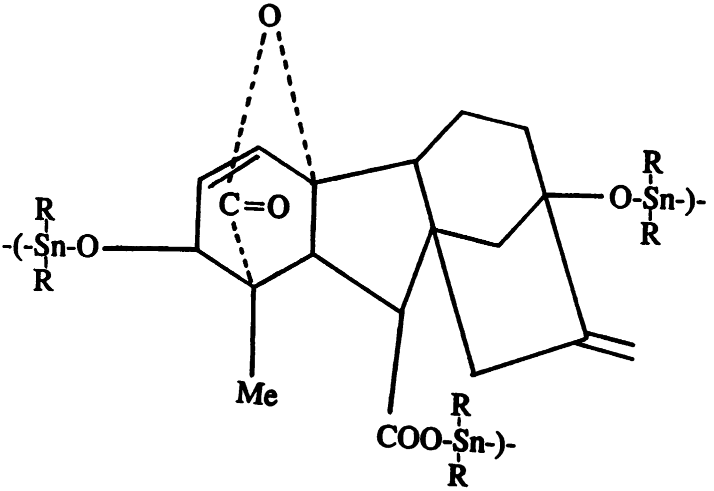

The products are insoluble in all attempted liquids consistent with the presence of some crosslinking. The liquids tested included those that are commonly used to solubilize analogous tin-containing non-crosslinked polymers (for instance 19-21).

Infrared spectral results are consistent with the formation of the proposed product. A new band about 600 (all band locations are given in 1/cm) is assigned to the symmetric Sn-O-R (Sn-O) stretch. A new band about 625 is attributed to the combination skeletal Sn-O and O-CO-R stretching in tin esters (22,23). New bands about 970 and 1000 are assigned to the Sn-O stretch in tin esters.

A strong band centering about 3400 is probably due to the presence of unreacted alcohol groups. Bands are present on both sides of 3000 derived from the C-H stretching (aromatic-above; aliphatic-below).

The carbonyl-tin bond can be either bridging or non-bridging (22,23). Bridging carbonyl stretching-associated bands appear about 1570 (asymmetric) and 1420 (symmetric) while non-bridging bands appear at about 1610-1650 (asymmetric) and 1360 (symmetric). Large bands about 1610 are consistent with the majority of the bonding being of the non-bridging type. Regions where the symmetrical stretching should appear have other bands present making assignments in these regions difficult.

While most organotin polyesters form bridged structures, those derived from reactants with two types of functional groups (such as amino acids) are found to favor non-bridged structures as found here (24,25).

Downloaded by UNIV OF GUELPH LIBRARY on October 31, 2012 | http://pubs.acs.org
Publication Date: September 24, 1998 | doi: 10.1021/bk-1998-0709.ch024

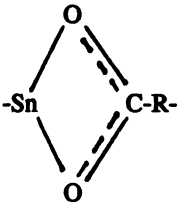

Bridging

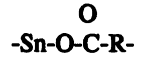

$$-Sn-O-\overset{O}{C}-R-$$

Non-bridging

Mass spectral analysis is consistent with the proposed structure. Table I contains the most abundant ion fragments from the product from dimethyltin dichloride and GA3. Unlike other products produced in this study that gave ion fragments to m/e = 500 Daltons, the product from dimethyltin dichloride only gave ion fragments to 208. There are no bands in the 35-38 range consistent with the absence of unreacted Sn-Cl groups.

Bands are present consistent with the formation of Sn-O- and Sn-OCO linkages with the GA3. Thus ion fragments are present at 138 (Sn-O), 152 (O-Sn-O), 165 (Me_2Sn-O), 185 (O-Me_2Sn-O), 197 (Me_2Sn-OCO), and 208 (O-Me_2Sn-OCO). Ion fragments containing tin are also present at 120 (Sn), 142 (SnMe) and 159 ($SnMe_2$). Ion fragments are also present derived from the breakage of the GA3 into two ring systems-one of the ring systems will be referred to as the "Gibb" unit and the other the "Lactone" unit as pictured below. For the "Gibb" portion ion fragments are found at 135 (Gibb itself) and 122 (Gibb minus methylene). For the lactone portion, ion fragments are found at 151 (Lactone portion itself), 136 (Lactone minus methyl), 135 (Lactone portion minus OH), 120 (Lactone minus methyl and OH), 107 (Lactone minus OCO), 90 (Lactone minus OCO and OH and 75 Lactone minus OCO, OH and methyl).

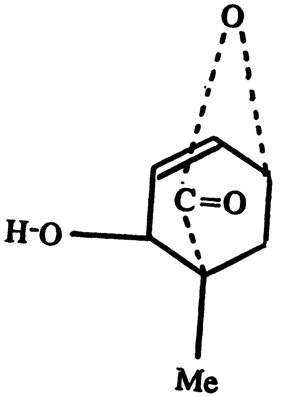

Lactone

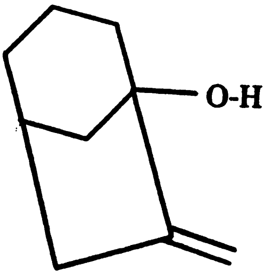

Gibb

Downloaded by UNIV OF GUELPH LIBRARY on October 31, 2012 | http://pubs.acs.org
Publication Date: September 24, 1998 | doi: 10.1021/bk-1998-0709.ch024

Tin has ten natural isotopes. Of these seven can be considered significant with respect to abundance. These seven isotopes comprise over 98% of the natural occurring isotopic fraction and these seven isotopes were used in making isotopic abundance ratio compairsons. Table II contains isotopic matches for Me_2Sn-O (161-169), O-Me_2Sn-O (181-189) and O-Me_2Sn-OCO (201-209).

Thus, mass spectral results are consistent with the proposed structure with the organotin moiety connected to the GA3 moiety through the hydroxyls and carboxyl groups.

Control reactions were carried out where one of the reactants was omitted. No precipitation was found for these control reactions consistent with the precipitate containing portions derived from both reactants.

In summary, mass spectral, control reactions, the results from analogous reactions and infrared spectral analyses are consistent with the product containing both Sn-O and Sn-OCO linkages to the GA3 moiety. Biological activity results, given in the following section, are also consistent with the product containing both a tin-containing moiety (reduction in the formation of microorganisms) and GA3-containing moiety (effect of polymer on germination rate and seedling growth).

Biological Characterization. We previously described the synthesis and some biological characterization of GA3-containing polymers derived from the reaction of titanocene dichloride and GA3 (26). Rooting experiments were conducted using Anderson's Crepe Pink hibiscus. Briefly, those stocks treated with both talc mixtures of GA3 and the polymers formed substantially fewer roots than the stock simply treated with talc alone and without any treatment. Of interest is the number of stocks that formed roots along the stem, but above the treated portion at sites where small branches had been removed from the stocks.

Seedling development was studied for Kentucky Wonder and Red Kidney pole beans. Results for both bean types were similar. Those plants treated with GA3 and polymer grew at a much faster rate with the rate increasing with increased concentration of GA3 or polymer. For the Kentucky Wonder beans treated with 1000 ppm of the GA3 or polymer, the plants grew so fast that after about two weeks, the stem could not support the growth and the plant "fell over" and subsequently died. By comparison, plants treated with 100 ppm polymer show more rapid growth and height through out the test period of four weeks being able to support the growth.

Red Kidney bean stocks treated with GA3 and polymer both showed enhanced growing rates. For instance, plants treated with 1000 ppm polymer or 1000 ppm GA3 showed an increased height of about 50% greater than non-treated beans.

Here we will briefly describe results related to the germination and seedling development of the polymer derived from reaction of GA3 and dimethyltin dichloride, designated as DMT-GA3.

For sawgrass re-establishment to be successful, a number of factors need to be considered. These factors include:

*favorable conditions for sawgrass germination and seedling development (relative to cattail)

Downloaded by UNIV OF GUELPH LIBRARY on October 31, 2012 | http://pubs.acs.org
Publication Date: September 24, 1998 | doi: 10.1021/bk-1998-0709.ch024

Downloaded by UNIV OF GUELPH LIBRARY on October 31, 2012 | http://pubs.acs.org
Publication Date: September 24, 1998 | doi: 10.1021/bk-1998-0709.ch024

Table I. Most abundant ions from the product of dimethyltin dichloride and GA3, DMT-GA3.

m/e	Relative Intensity (%)	(Possible) Assignment
55	9	C_4H_y
57	16	Above
69	9	C_5H_y
71	11	Above
83	7	C_6H_y
85	7	Above
97	7	C_7H_y
134	6	Gibb unit
150	5	Gibb unit + CH
161	8	Me_2SnO
163	13	Above
165	18	Above
181	9	O-Me_2Sn-O
183	16	Above
185	22	Above
187	9	Above

Table II. Tin isotopic ratios for selected high molecular weight ion fragments of the product from GA3 and dimethyltin dichloride.

Tin Isotope	116	117	118	119	120	122	124
%-Nat. Abundance	14	8	24	9	33	5	6
Ion Fragment	161	162	163	164	165	167	169
%-Abundance	11	10	20	11	39	2	2
Ion Fragment	181	182	183	184	185	187	189
%-Abundance	12	6	22	9	33	12	6
Ion Fragment	201	202	203	204	205	207	209
%-Abundance	8	5	23	8	35	12	8

*time of germination
*fraction of germination
*mortality
*plant reproduction and
*vitality.

Cattails and most weeds typically found in the Everglades begin to germinate within 3 to 10 days and to a high percentage (generally >30%). A single cattail produces in the range of 3,000,000 seeds (10). By comparison, sawgrass requires between 4 to 8 weeks, with germination percentages typically in the 0 to 5% range. A single sawgrass produces on the order of 3,000 seeds. Thus, increased germination fraction and decreased germination time are important factors with respect to re-establishment of sawgrass in the Everglades.

While a number of organotin-GA3 containing products were made, the dimethyltin-GA3 polymer, DMT-GA3, was chosen for initial study since it is the least hydrophobic of the diorganotin moieties used and should hydrolyze most rapidly. The evidence for degradation is circumstantial and is based on the ability of the polymer to influence the germination and seedling development of sawgrass and cattail and on the fact that while there are many gibberellins, only a few are active so that in order for the polymer to exhibit activity, it (most likely) must degrade giving the GA3 moiety in an "active" form. It is believed that release of the GA3 "active" moiety occurs through simple physical (rather than enzymatic-catalyzed) hydrolysis of the polymer.

Organotin compounds are known to inhibit microorganisms. While "free" or monomeric organotin compounds are illegal for commercial use, "bound" tin compounds are legal and are used for many applications including marine applications where adverse effects to marine life are unwanted (for instance 27) "Bound" tin compounds are defined as those that are chemically bound within polymers. The polymer tested here, DMT-GA3, is a "bound" organotin compound since the tin moiety is chemically bound as part of a polymer. The amount of organotin involved in the treatment (100 ppm) of a single seed is 5 micrograms or 30 nanomoles. Upon hydrolysis, small amounts of "free" organotin are released.

Algae began growing several days after the experiment began in all of the containers except those containing seeds treated with DMT-GA3 polymer. For trays containing seeds treated with DMT-GA3 polymer noticeable algae growth was delayed for four weeks. This is consistent with the effect of the DMT-GA3 polymer lasting at least about three to four weeks longer than GA3 itself.

As noted above, gibberellins influence seed germination and they are also endogenous regulators of growth (26). GA3 acts to increase cell wall extensibility for some plants thus functioning as a growth accelerator.

Tables III-VI contain mean values as a function of GA3 and DMT-GA3 polymer concentration. Table VII contains summation statistical resluts for the informaiton given in Tables III-VI. The results are treated in two ways with respect to the influence of concentration. First, each of the five concentrations were considered independently. This scenario will be referred to as "non-grouped". Second, the results were "grouped" into two groupings based on concentration-a "low" concentration (0.1, 1.0, and 10 ppm) and a "high" (100 and

Downloaded by UNIV OF GUELPH LIBRARY on October 31, 2012 | http://pubs.acs.org
Publication Date: September 24, 1998 | doi: 10.1021/bk-1998-0709.ch024

Downloaded by UNIV OF GUELPH LIBRARY on October 31, 2012 | http://pubs.acs.org
Publication Date: September 24, 1998 | doi: 10.1021/bk-1998-0709.ch024

Table III. Onset of germination*.

PGH	SAWGRASS	CATTAIL
CONTROL	29	8
GA3	11	7
DMT-GA3 Polymer	20	7

* in days.

Table IV. Germination percentages of sawgrass as a function of PGH concentration.

CONCENTRATION (PPM)	0.01	1.0	10.0	100.0	1000.0
PGH					
CONTROL-2					
GA3	9	11	12	11	19
DMT-GA3 Polymer	8	4	9	7	6

Table V. Germination percentages of cattail (T. domingensis) as a function of PGH concentration.

CONCENTRATION (PPM)	0.1	1.0	10.0	100.0	1000.0
PGH					
CONTROL-48					
GA3	57	66	63	57	65
DMT-GA3 Polymer	40	51	38	38	23

Table VI. Seedling development after 102 days. Height of seedlings (in cm) as a function of PGH concentration (ppm).

CONCENTRATION (PPM)	0.1	1.0	10.0	100.0	1000.0
SAWGRASS -CONTROL-8.4					
GA3	9.3	12.7	11.7	9.4	10.5
DMT-GA3 Polymer	15.3	14.8	23.7	18.1	16.0
CATTAIL -CONTROL-23.4					
GA3	16.3	12.9	9.3	6.4	10.3
DMT-GA3 Polymer	32.0	37.6	38.6	35.3	32.3

Downloaded by UNIV OF GUELPH LIBRARY on October 31, 2012 | http://pubs.acs.org
Publication Date: September 24, 1998 | doi: 10.1021/bk-1998-0709.ch024

Table VII. Analysis of variance for germination and seedling development.

Group	F Ratio	F Probability
Analysis of variance for germination		
Sawgrass/GA3		
Non-grouped	2.6321	0.0794
Grouped	3.7407	0.0481
Sawgrass/DMT-GA3 Polymer		
Non-grouped	1.2328	0.3527
Grouped	1.3497	0.2891
Cattail/GA3		
Non-grouped	0.6858	0.6433
Grouped	0.9121	0.4228
Cattail/DMT-GA3		
Non-grouped	0.6166	0.6899
Grouped	1.3851	0.2805
Analysis of variance for growth		
Sawgrass/GA3		
Non-grouped	0.2877	0.9108
Grouped	0.4618	0.6388
Sawgrass/DMT-GA3		
Non-grouped	4.3583	0.0171
Grouped	5.5178	0.0160
Cattail/GA3		
Non-grouped	3.3044	0.0417
Grouped	6.8194	0.0078
Cattail/DMT-GA3		
Non-grouped	0.5095	0.7641
Grouped	1.2233	0.3220

1000 ppm) concentration grouping. The second "grouping" scenario was done to increase the number of replicants within a "concentration" unit.

For sawgrass germination, statistical difference is found for both the "grouped" concentrations and for the highest (1000 ppm) and middle (1 ppm) concentrations for the GA3 treatment. Thus, germination percentages increased from a control mean of 3% to above 10% for sawgrass treated with GA3.

Cattail germination was independent of GA3 and DMT-GA3 polymer treatment for the "grouped" scenario. But, an increased germination percentage is found for seeds treated with GA3 when the results are considered for each independent concentration (non-grouped). These increases range from (control mean of 48%) about 20% (57% germination) to 50% (66% germination).

Growth of sawgrass seedlings derived from seeds treated with DMT-GA3 polymer was (statistically) increased in comparison to the control for the "grouped" concentration scenario and for all but the 1 ppm treatment. A difference was also found between seeds treated with 10 ppm DMT-GA3 polymer and those treated with other concentrations of DMT-GA3 polymer. This relationship is consistent with the presence of an optimum concentration of DMT-GA3 polymer around 10 ppm. The increased growth, based on stem length, varied from about 75% to 150%.

Cattail seedling growth from seeds treated with GA3 was significantly less for both the "grouped" concentration ranges and for all but the lowest (0.1 ppm) concentration level. The growth decreases range from about 30% to 70%. Most plant growth hormones, PGHs, either have no affect on growth or act to increase growth. This is true for GA3. A negative effect on growth has only been recently been reported for GA3. Thus Mauder reported diminished growth of rye grass and Kentucky bluegrass (28,29).

The time interval for initial sawgrass germination was shortened (to 11 days; Table III) to within the general time interval required for the initial germination of cattail seeds (control = 8 days).

In summary, the use of GA3 and DMT-GA3 polymer affects the seed germination and seedling development of both cattail and sawgrass. GA3 alone shows the most pronounced affect in germination studies. The time interval for initial sawgrass germination was effectively reduced for seeds treated with either DMT-GA3 polymer or GA3. The fraction of sawgrass germination was also increased for seeds treated with either DMT-GA3 polymer or GA3. For seedling development, both GA3 and DMT-GA3 polymer influence growth. For DMT-GA3 polymer treated seeds, seedling growth is enhanced for both cattail and sawgrass, while for GA3 treated seeds, there is increased sawgrass growth, but decreased cattail growth.

The results are also consistent with the effects of the DMT-GA3 polymer being long-lasting. This is probably the result of the retension and release of GA3 over a sustained period which may be the result of a. a controlled release mechanism, b. retention of GA3 and/or GA3-containing moieties within the soil, c. and/or retention of the GA3 and/or GA3-containing moiety within the seedling itself-either physically or chemically bound.

The results are consistent with the use of GA3 and DMT-GA3 polymer as

Downloaded by UNIV OF GUELPH LIBRARY on October 31, 2012 | http://pubs.acs.org
Publication Date: September 24, 1998 | doi: 10.1021/bk-1998-0709.ch024

viable seed treatments to produce shorter sawgrass germination times for a greater fraction of seeds and in the production of more rapidly growing seedlings.

We are pleased to acknowledge partial support of this project by the South florida Water Management District.

References

1. Davis, J. H., Geological Bulletin 25, Florida Geological Survey (1943)
2. Loveless, C. M., Ecology 1959, 40, 1-9.
3. Davis, S. M., In Everglades: The Ecosystem and Its Restoration , (S. M. Davis and J. C. Ogden, Eds.) St. Lucie Press, Delray Beach, FL, 1994, 357-378.
4. Davis, S. M.; Ogden, J. C., (Eds) Everglades : The Ecosystem and Its Restoration , St. Lucie Press, Delray Beach, FL, 1994.
5. Jensen, J. R.; Rutchey, K.; Koch, M. S.; Narumalani, S., Photogrammetric Eng. Remote Sensing, 1995, 61, 199-209.
6. Rutchey, K.; Vilchek, Photogrammetric Eng. Remote Sensing, 1994, 60, 767-775.
7. Alexander, T. R., Soil and Crop Sci Soc. Florida Proceedings, 1971, 31, 72-74.
8. Forsberg, C., Physiologia Plantarum 1966, 19, 1105-1109.
9. Miao, S. L.; Borer, R. E.; Sklar, F. H., in review.
10. Stewart, H.; Miao, S. L., Colbert, M. E.; Carraher, C. E., Wetlands, 1997, 17, 116-122.
11. McNaughton, S. J., Ecology 1968, 49, 367-369.
12. Hartman, H.; Kester, D.; Davies, F. T.; Geneve, R., Plant Propagation: Principles and Practices , 6th Ed., Prentice Hall, Upper Saddle River, NJ, 1997.
13. Thompson, W. T., Agricultural Chemicals Book III-Fumigants, Growth Regulators, Repellents and Rodenticides , Thopmson Pubs., Frensno, CA, 1988-89.
14. Carraher, C. E.; Dammeier, R. L., J. Polymer Sci. A-1, 1970, 8, 3367-3369.
15. Carraher C. E.; Butler, C. US Patient 5,043,463, 1991.
16. Carraher, C. E.; Dammeier, R. L., Die Makromolekulare Chemie, 1979, 135, 107-112.
17. Carraher, C. E., J. Chem. Ed., 1981, 58(11), 921-934.
18. Carraher, C. E.; Tisinger, L.; Solimine, G.; Williams, M.; Carraher, S.; Strother, R., Polymeric Materials: Sci. Eng., 1986, 55, 469-472.
19. Carraher, C. E., Structure-Solubility Relationships in Polymers (R. Seymour and F. Harris, Eds.), Academic Press, NY, 1977, 215-224.
20. Carraher, C. E.; Winter, D. O., Die Makromolekulare Chemie, 1971, 141, 237-244.
21. Carraher, C. E., Polymer Chemistry: An Introduction , 1997, Dekker, NY.
22. Carraher, C. E.; He, F.; Sterling, D., Polymeric Materials: Sci. Eng., 1995, 72, 114-115.
23. Carraher, C. E., Die Angew. Makromolekulare Chemie, 1973, 31, 115-122.
24. Carraher, C. E.; Li, A., Unpublished results.

Downloaded by UNIV OF GUELPH LIBRARY on October 31, 2012 | http://pubs.acs.org
Publication Date: September 24, 1998 | doi: 10.1021/bk-1998-0709.ch024

25. Carraher, C. E.; He, F.; Sterling, D.; Nounou, F.; Pennisi, R.; Louda, J. W.; Sperling, L. H., Polymer P., 1990, 31(2), 430-431.

26. Stewart, H.; Carraher, C. E.; Soldani, W.; Reckleben, L.; de la Torre, J.; Miao, S. L., Metal-Containing Polymeric Systems (C. Pitmann, C. Carraher, M. Zeldin, B. Culbertson, and J. Sheats, Eds.), Plenum Press, NY, 1996, 93-107.

27. Gebelein, C.; Carraher, C. (Eds.), Polymeric Drugs, Amer. Chem. Soc., Washington, D. C., 1982.

28. Mander, L., Science, 1995, 268, 1571-1573.

29. Mander, L., New Scientist, 1995, June, 19.

Downloaded by UNIV OF GUELPH LIBRARY on October 31, 2012 | http://pubs.acs.org
Publication Date: September 24, 1998 | doi: 10.1021/bk-1998-0709.ch024

Author Index

Akin, Hanife, 212
Bedell, Christi, 83
Bielski, Roman, 285
Burg, K. J. L., 279
Campo, Cheryl, 83
Carraher, Charles E., Jr., 295
Carraher, Shawn M., 295
Chern, Rey T., 67
Chin, Shook-Fong, 176
Cui, H., 203
Elaissari, A., 143
Erdmann, Laura, 83
Gadzinowski, M., 143
Gaonkar, Anupam, 295
Guiseppi-Elie, Anthony, 185
Harris, Frank W., 212
Heller, Jeorge, 212
Ichikawa, Masataka, 266
Ichinose, Katsuro, 266
Jiang, S. Anna, 117
Kanematsu, Takashi, 266
Kataoka, Kazunori, 105
Kim, Cherng-ju, 67
Liu, Hongbo, 117
Lowman, A. M., 156
Macdonald, P. M., 223
Mallapragada, Surya K., 176
Masaro, L., 223
Masunaga, Tatsunori, 266
Messersmith, P. B., 203
Miao, Shi Li, 295
Montenecourt, Dorsey, 285
Morishita, M., 156
Nagai, T., 156
Nagasaki, Yukio, 105
Nakashima, Mikirou, 266
Ni, Qiang, 92
Nujoma, Yvonne N., 67
Ohya, Yuichi, 266
Ouchi, Tatsuro, 266
Peppas, Nicholas A., 56, 129, 156
Petit, J.-M., 223
Pichot, C., 143
Podual, Kairali, 56
Qiu, Jin Song, 242
Roux, B., 223
Schwarte, Lisa M., 56
Scott, Robert A., 129
Shalaby, Marc, 2
Shalaby, Shalaby W., 2, 23, 125, 279
Shalaby, Waleed S. W., 23
Slomkowski, S., 143
Sosnowski, S., 143
Stewart, Herbert H., 295
Sujdak, Andrew S., 185
Thurmond, K. Bruce II, 165
Uhrich, Kathryn E., 83, 117
Wang, Nuo, 242, 254
Wilson, Anne M., 185
Wooley, Karen L., 165
Wu, Xue Shen, 242, 254
Yu, Luping, 92
Zhu, X. X., 223

Downloaded by 89.163.35.42 on October 31, 2012 | http://pubs.acs.org
Publication Date: September 24, 1998 | doi: 10.1021/bk-1998-0709.ix001

In Tailored Polymeric Materials for Controlled Delivery Systems; McCulloch, I., et al.;
ACS Symposium Series; American Chemical Society: Washington, DC, 1998.

Subject Index

A

Absorbable gel-forming injectable liquids, emerging trend for controlled release drug delivery, 18–19
Acquired immunodeficiency syndrome (AIDS)
  cumulative toxicity of zidovudine (ZDV, AZT) and ganciclovir, 3–4
  multi-drug therapy, 176
  occurrence of cytomegalovirus (CMV) retinitis, 2–3
  See also Multi-layered semicrystalline polymeric controlled release systems
Acrylate copolymer networks. *See* Ionogenic acrylate copolymer networks
AIDS. *See* Acquired immunodeficiency syndrome (AIDS)
Alginate gelation
  ability to form transparent or translucent gels in presence of Ca^{2+} ions, 204
  approach for releasing liposome-entrapped Ca^{2+} for in situ biomaterial formation, 207–208
  calcium release assay, 205–206
  composition and physical consistency of thermally gelled liposome/alginate hydrogels, 208*t*
  drug-filled liposomes by same approach as Ca-loaded liposomes, 208
  drug release experiments, 206
  experimental materials, 204
  gelation time of liposome/alginate mixtures at 33°C, 208, 209*t*
  gel time determination method, 206
  linear, water-soluble polysaccharides, 204
  liposome preparation, 205
  preparation of hydrogel precursor suspension, 206
  rapid burst-type release of drug from drug-filled liposomes, 209
  release of metronidazole from thermally crosslinked liposome/alginate hydrogels, 209, 210*f*
  schematic illustration of thermally triggered hydrogen formation, 205*f*
  strategy for in situ gelation, 204, 205*f*
  taking advantage of temperature-induced changes in lipid bilayer permeability, 206
  thermally triggered calcium release from suspended liposomes, 207*f*
Anionic hydrogels versus cationic, 57, 59*f*
Antibiotic formulations for bone infection, injectable, absorbable gel-formers, 126
Antitumor drug delivery. *See* Platinum complexes immobilized in dextran derivatives
Aromatic polyanhydrides
  alkyl chains with ester linkages to aromatic moieties, 85
  degradation studies, 87
  effect of solution pH on degradation, 91
  gel permeation chromatography method, 86–87
  infrared spectroscopy method, 86
  ortho-substitution for processibility, 85
  poly(anhydride-esters) overview, 86
  poly(anhydride-ethers) overview, 85–86
  results of poly(anhydride-esters) syntheses, 90
  results of poly(anhydride-ethers) syntheses, 90
  salicylates reaching colon intact for treatment, 85–86
  schematic of hydrolytic degradation of poly(anhydride-ester), 84
  suitable degradation and solubility for drug delivery, 83
  synthetic methods and scheme, 87–90
  thermal analysis method, 87
Aspirin delivery and stabilization. *See* Lactic/glycolic acid (LGA) oligomeric microgranules
AZT (zidovudine, ZDV), cumulative toxicity with ganciclovir, 3

B

Bioactive agents. *See* Tissue engineering
Bioactive peptides. *See* Electroconductive gels
Bioadhesive complexation networks
  crosslinked poly(methacrylic acid) microparticles with ethylene glycol grafts (P(MAA-*g*-EG)) preparation, 157–158
  dependence of mucoadhesive characteristics on pH of environmental fluid, 162, 163*f*
  drug loading procedure into P(MAA-*g*-EG) microparticles, 158
  equilibrium swelling of polymer microparticles, 159
  insulin in vitro release results, 159–161
  mucoadhesive behavior of P(MAA-*g*-EG) hydrogels, 161–162

Downloaded by 89.163.35.42 on October 31, 2012 | http://pubs.acs.org
Publication Date: September 24, 1998 | doi: 10.1021/bk-1998-0709.ix002

Downloaded by 89.163.35.42 on October 31, 2012 | http://pubs.acs.org
Publication Date: September 24, 1998 | doi: 10.1021/bk-1998-0709.ix002

- mucoadhesive studies with P(MAA-*g*-EG) films, 158–159
- problems in developing oral delivery, 156
- procedure for insulin in vitro release studies, 158
- proposed mechanism of adhesion between P(MAA-*g*-EG) hydrogels in complexed and uncomplexed states and mucosa, 163*f*
- pulsatile release of insulin from P(MAA-*g*-EG) microparticles of different concentrations and PMAA microparticles, 159, 160*f*
- ratio of diffusion coefficients for evaluating viability for oral delivery, 161
- ratio of diffusion coefficients of insulin in complexed and uncomplexed hydrogels as compared to PMAA, 161*t*
- release of insulin in vitro from P(MAA-*g*-EG) in simulated gastric fluid, 160*f*
- reversible formation of intermolecular complexes, 157
- work of adhesion for P(MAA-*g*-EG) gels containing 1:1 MAA/EG ratio and graft PEG chains of molecular weight 1000, 162*t*

Bioadhesive delivery systems, intravaginal, 38–39

Biodegradable polymers
- special type of dissolution-controlled system, 36*t*
- *See also* Lactic/glycolic acid (LGA) oligomers

Blindness, untreated cytomegalovirus (CMV) retinitis, 3

Branched polymeric micelles
- encapsulation studies using fluorescence spectroscopy, 123
- experimental materials, 118
- ^{1}H NMR spectrum of core(hex) compound, 121, 122*f*
- hydrophobic/hydrophilic ratio varying with length of alkyl and ethylene oxide chains, 121
- lidocaine evaluation with HPLC, 123
- molecular weight analysis method, 120
- nuclear magnetic resonance (NMR) methods, 118
- preparation of core molecules, 120–121
- preparation of mucic acid derivatives, 120
- side chain attachment to core for final polymer structure, 121
- synthetic scheme of polymers with topological and functional features similar to unimolecular micelles, 119
- thermal analysis method, 120
- thermodynamic instability of conventional micelles, 118

C

Cationic hydrogels
- biocompatibility with poly(ethylene glycol) (PEG) incorporation, 57
- dependence of equilibrium degree of swelling on pH, 57, 59*f*
- design aspects, 58
- dynamic swelling behavior of hydrogel with 10:1 and 50:1 methacrylate to graft ratios, 61, 64*f*, 65
- dynamic swelling behavior of hydrogel with 75:1 and 99:1 methacrylate to graft ratios between pH 4.6 and 9.3, 64*f*, 65
- equations for swelling ratios, 60
- equilibrium swelling characteristics of glucose-sensitive cationic hydrogels, 61, 63*f*
- equilibrium swelling characteristics of hydrogels with different amounts of enzymes, 61, 63*f*
- equilibrium weight ratios as function of pH, 61, 62*f*
- immobilization of glucose oxidase (GOD) in hydrogel, 60
- insulin example of stimulus-driven release properties, 57–58
- insulin imbibition, 60–61
- oscillatory swelling in response to pH, 65
- preparation of experimental terpolymer, P(DEAEM-*g*-EG), 58, 60
- release mechanism from, 59*f*
- size exclusion in, 57
- structure of experimental terpolymer, P(DEAEM-*g*-EG), 62*f*
- testing equilibrium and dynamic swelling properties, 60
- ultraviolet light absorbance to estimate GOD incorporation, 60
- versus anionic, 57, 59*f*

Chemoselective ligation (CSL). *See* Thioester end-functionalized poly(ε-caprolactone) (PCL)

Cidofovir
- dose-limiting nephrotoxicity, 5
- ease in administering, 5
- excellent anti-CMV (cytomegalovirus) activity, 4–5
- intravitreal injections for CMV retinitis, 8–10
- liposomally-encapsulated controlled drug delivery, 12–13
- safety and efficacy of intravitreal injections, 9–10

Contraception, intravaginal drug delivery, 41–42

Controlled release drug delivery
- absorbable gel-forming injectable fluids as emerging trend, 18–19
- ganciclovir-loaded polymer microspheres for CMV retinitis, 13
- ganciclovir nanoparticles for CMV retinitis, 14
- liposomally-encapsulated cidofovir for CMV retinitis, 12–13
- liposomally-encapsulated foscarnet as emerging trend, 18

Downloaded by 89.163.35.42 on October 31, 2012 | http://pubs.acs.org
Publication Date: September 24, 1998 | doi: 10.1021/bk-1998-0709.ix002

  liposomally-encapsulated ganciclovir for CMV retinitis, 10–12
  sustained-release intraocular ganciclovir implants, 14–18
  See also Alginate gelation; Drug delivery; Electroconductive gels; Injectable absorbable gel-formers; Multi-layered semicrystalline polymer controlled release systems; Tissue engineering
Controlled release of polymers containing radioactive substances. *See* Direct measurement of multi phase flow
Crystallization-induced microphase separation (CIMS), continuous-cell microporous foam preparation, 281–282
Cytomegalovirus (CMV), retinitis most common clinical consequence, 2
Cytomegalovirus retinitis
  absorbable gel-forming injectable liquids as emerging trend, 18–19
  controlled drug delivery systems, 10–18
  detrimental sequela of advanced HIV disease, 19
  drawbacks to intravenous therapy, 5
  emerging trends, 18–19
  ganciclovir-loaded polymer microspheres, 13
  ganciclovir nanoparticles, 14
  intravenous cidofovir, 4–5
  intravenous combination therapy, 4
  intravenous foscarnet, 4
  intravenous ganciclovir, 3–4
  intravitreal cidofovir injections, 8–10
  intravitreal fomivirsen injections, 10
  intravitreal foscarnet injections, 8
  intravitreal ganciclovir injections, 6–8
  liposomally-encapsulated cidofovir, 12–13
  liposomally-encapsulated foscarnet as emerging trend, 18
  liposomally-encapsulated ganciclovir, 10–12
  local therapy, 5–10
  scope and limitations of intravenous therapy, 3–5
  serious infection in AIDS patients, 2–3
  sustained-release intraocular ganciclovir implants, 14–18

D

Diffusion
  applying Fick's first law of diffusion to lattice model, 225
  effect of molecular size of diffusant in poly(vinyl alcohol) PVA-water ternary system, 233–235, 236*f*
  effect of molecular weight of PVA polymer , 229, 232
  effect of polymer concentration in PVA-water ternary system, 233
  effect of temperature of PVA-water ternary systems, 235, 237–239
  equations for drug release from slab geometry, 34–35
  experimental samples for diffusion studies, 228
  Higuchi model for drug release from slab with low drug concentration, 35
  illustration of one-dimensional diffusion through periodic energy potential, 226*f*
  influencing factors, 224
  logarithm of parameter $k\beta^2$ plotted as function of reciprocal temperature for selected diffusants, 238*f*
  model for drug absorption, 29–30
  model parameters from self-diffusion data of *t*-butanol in PVA1-water system at different temperatures, 237*t*
  molecular sizes, self-diffusion coefficients, and parameters for EG and PEG diffusants in PVA1-water systems, 233*t*
  molecular sizes, self-diffusion coefficients, and parameters for solute probes in PVA1-water systems, 232*t*
  molecular sizes, self-diffusion coefficients, and parameters from solvent diffusion at 23°C in PMMA systems, 230*t*
  needing physical models to describe self-diffusion of solvents and solute, 224
  physical model, 225–228
  polymer solution as network with diffusing molecules having to overcome periodic energy barriers, 239
  poly(methyl methacrylate) (PMMA)-organic solvent binary systems, 229
  PVA-water-solute ternary systems, 229, 232–239
  release of drugs from polymer matrices, 224
  requirements of single physical model, 224–225
  self-diffusion coefficients by pulsed-gradient spin-echo (PGSE) NMR technique, 228
  self-diffusion coefficients of solute probes in PVA1 solutions as function of PVA concentration, 234*f*
  self-diffusion coefficients of solvents in PMMA solutions as function of PMMA concentration, 231*f*
  self-diffusion coefficients of *t*-butanol in PVA1 aqueous systems as function of PVA concentration at four temperatures, 238*f*
  semi-logarithmic plot of parameter of model ($k\beta^2$) as function of hydrodynamic radius of solvent in PMMA-solvent binary system, 231*f*
  tortuosity term, 35

- total friction coefficient for diffusing molecule, 227

Direct measurement of multi phase flow
- advantage of radiation detection method from outside pipeline, 285–286
- analytical methodology advantages, 293–294
- errors in existing techniques, 285
- experimental isotopes, 287
- measurement procedures, 289
- methodology for pipeline and polymeric sample, 286–287
- mixtures with more than single phase, 285
- MPD detectors and measurement procedure, 289
- multi photon detection (MPD) technique, 286
- preparation of oil phase soluble inserts, 288–289
- preparation of polymeric samples, 288–289
- preparation of water phase soluble inserts, 288
- selection of oil phase soluble polymers, 288
- selection of water phase soluble polymers, 287–288
- sensitivity of MPD measurement technology, 294
- solubility of tested polymers in crude oil, 289–290
- summary of results for various water-soluble and oil-soluble polymers, 293*t*
- typical on-line measurements of washout of radioactive substance from polymeric insert, 290, 291*f*, 292*f*

Drug absorption
- dependence on physicochemical properties of drug, 28
- diffusion model, 29–30
- intravaginal drug delivery, 28–30
- mechanisms in vagina, 28

Drug delivery
- biocompatible, biodegradable aromatic polyanhydrides, 83
- range of systems, 117
- surfactants as promising answers, 118
- water solubility, 117
- *See also* Aromatic polyanhydrides; Bioadhesive complexation networks; Controlled release drug delivery; Injectable, absorbable gel-formers; Intravaginal drug delivery systems; Ionogenic acrylate copolymer networks; Lactic/glycolic acid (LGA) oligomeric microgranules; Multi-layered semicrystalline polymer controlled release systems; Reactive polymeric micelles; Water-soluble polyanions as oral drug carriers

Drugs, problems with introduction of free compounds into bloodstream, 117

E

Electroconductive gels
- basis of electrorelease applications, 186
- Bode plot of impedance of pristine electropolymerized polyaniline (PAn) and various PAn hydrogels in 0.1 M KCl at 20°C, 196*f*
- cathodic charge densities measured from second cyclic voltammogram (CV) scan and expressed as function of scan rate, 193, 196*f*
- CV of electropolymerized PAn and PAn hydrogels in deaerated 0.1 M KCl at 20°C, 194*f*
- electrical conductivity characterization on polymer-coated IMEs (interdigitated microsensor electrode) and free-standing hydrogels, 197
- electroactivity measurements, 188
- electrochemical characterization of prepared hydrogels, 191, 193
- electrochemical impedance spectroscopic characterization, 195, 196*f*
- electroconductive gel synthesis by two polymerization reactions, 188–191
- electrorelease of $^{45}Ca^{++}$ and corresponding CV, 199, 200*f*
- environmental stability, 197–199
- experimental materials, 186–187
- formulation of electroconductive gel dope based on polyaniline, 187*t*
- hydrogel hydration, 195, 197
- initial anodic charge density of electropolymerized PAn and PAn hydrogels, 193, 194*f*
- interpenetrating networks such as polyaniline or polypyrrole in 2-hydroxyethyl methacrylate (HEMA)-based hydrogels, 186
- photon count (cps) produced by hot Ca and corresponding CV, 200*f*
- preparation of electrodes, 187
- preparation of gels, 188
- programmable delivery of bioactive peptides, 185–186
- progress in UV/visible absorbance spectra of PAn hydrogel during exposure to 0.1 M $FeCl_3$, 199, 200*f*
- schematic illustration of two reactions in production, 192*f*
- stability of electropolymerized PAn and PAn hydrogels under laboratory conditions for 100 days, 198*f*
- structures of various monomers in network formation, 190*f*
- surface preparation and functionalization of electrodes, 188

Downloaded by 89.163.35.42 on October 31, 2012 | http://pubs.acs.org
Publication Date: September 24, 1998 | doi: 10.1021/bk-1998-0709.ix002

Downloaded by 89.163.35.42 on October 31, 2012 | http://pubs.acs.org
Publication Date: September 24, 1998 | doi: 10.1021/bk-1998-0709.ix002

Electrorelease of bioactive peptides. *See* Electroconductive gels

F

Fick's law
  applying to lattice model, 225
  diffusion model for drug absorption, 29-30
Florida Everglades
  legislative mandates for re-establishing healthy ecosystem, 295–296
  plant growth regulators (PGRs), 296
  sawgrass seed germination critical to restoration, 296
  subtropical, freshwater wetland ecosystem, 295
  See also Gibberellic acid-containing organotin polymers
Fomivirsen, intravitreal injections for cytomegalovirus (CMV) retinitis, 10
Foscarnet
  combination therapy with ganciclovir, 4
  intravitreal injections for CMV retinitis, 8
  liposomally-encapsulated system emerging trend, 18
  noncompetitive inhibitor of viral RNA and DNA polymerases, 4
Free drugs, problems with introduction into bloodstream, 117

G

Ganciclovir
  analog of acyclovir, 3
  combination therapy with foscarnet, 4
  complications of intravitreal administration, 7–8
  dose-limiting neutropenia and thrombocytopenia, 3
  intravenous therapy for cytomegalovirus (CMV) retinitis, 3–4
  intravitreal injections, 6–8
  liposomally-encapsulated controlled drug delivery, 10–12
  nanoparticles for controlled drug delivery, 14
  only anti-CMV agent as oral preparation, 4
  polymer microspheres for controlled drug delivery, 13
  sustained-release intraocular implants, 14–18
Gelation. *See* Alginate gelation
Gels. *See* Electroconductive gels; Injectable absorbable gel-formers
Gentistic acid ethanolamide (GAE). *See* Multi-layered semicrystalline polymer controlled release systems
Germination of sawgrass and cattail. *See* Gibberellic acid-containing organotin polymers
Gibberellic acid-containing organotin polymers
  advantages of controlled release polymer generating gibberellic acid (GA3), 296–297
  analysis of variance for germination, seedling development, and growth, 305*t*
  biological characterization of GA3-containing polymers, 301, 303–307
  cattail germination and seedling development, 306–307
  cyclic terpenes (gibberellins) inducing plant responses, 296
  dimethyltin-GA3 polymer chosen as least hydrophobic, 303
  germination and seedling development experiments, 297–298
  germination percentages of cattail as function of polymer concentration, 304*t*
  germination percentages of sawgrass as function of polymer concentration, 304*t*
  infrared spectral results, 299–300
  mass spectral analysis, 300–301
  most abundant ions from product of dimethyltin dichloride and GA3, 302*t*
  onset of germination for sawgrass and cattail, 304*t*
  polymer analysis methods, 297
  polymer synthesis by interfacial polycondensation, 297
  sawgrass germination and seedling development, 306–307
  seedling development after 102 days, 304*t*
  structural characterization of polymers, 298–299
  tin isotopic ratios for selected high molecular weight ion fragments of product from GA3 and dimethyltin dichloride, 302*t*
  use of "bound" tin compounds, 303
  See also Florida Everglades
Glucose oxidase, coupling with ionic hydrogels for insulin release, 57–58
Griseofulvin (gris). *See* Polyvinylpyrrolidone (PVP) dispersions
Gynecologic oncology, treatment by intravaginal drug delivery, 44–45

H

HEMA (2-hydroxyethyl methacrylate)
  basis for interpenetrating networks of inherently conductive polymers, 186, 187*t*
  See also Electroconductive gels
Higuchi model, drug release from slab with low drug concentration, 35

Downloaded by 89.163.35.42 on October 31, 2012 | http://pubs.acs.org
Publication Date: September 24, 1998 | doi: 10.1021/bk-1998-0709.ix002

Hormone replacement therapy, intravaginal delivery, 41
Human immunodeficiency virus (HIV)
  cumulative toxicity of zidovudine (ZDV, AZT) with ganciclovir, 3–4
  occurrence of cytomegalovirus (CMV) retinitis, 2–3, 19
  studying prevention of HIV transmission, 43
  See also Acquired immunodeficiency syndrome (AIDS)
Hydrogels
  anionic versus cationic, 57, 59*f*
  composition and means of crosslinking, 36–37
  drug release from, 37–38
  passive delivery of bioactive peptides, 185
  permeant classified by relative rates of diffusion and polymer relaxation, 38
  polymers for preparation, 37*t*
  See also Alginate gelation; Bioadhesive complexation networks; Cationic hydrogels; Electroconductive gels; Ionogenic acrylate copolymer networks
2-Hydroxyethyl methacrylate (HEMA)
  basis for interpenetrating networks of inherently conductive polymers, 186, 187*t*
  See also Electroconductive gels

I

Implants
  criticism of ganciclovir as sole CMV retinitis therapy, 17
  mild vitreous hemorrhage complications, 15–16
  reimplantations, 16
  sustained-release intraocular ganciclovir, 14–18
Infectious diseases, treatment by intravaginal drug delivery, 42–43
Infertility, treatment by intravaginal drug delivery, 42
Injectable absorbable gel-formers
  antibiotic formulations for bone infection, 126
  applications in controlled release systems, 126–127
  comparison to previous research, 125
  controlled release of ricin A-chain, 127
  growing interest for pharmaceutical and surgical products, 125–126
  injectable intraocular delivery, 126
  insulin controlled release systems, 126
  periodontal application, 126
  preliminary results of on-going studies, 127
  wound healing and hemostatic application, 126
Insulin
  controlled release by injectable, absorbable gel-formers, 126
  rate of permeation through poly(methacrylic acid) grafted by ethylene glycol P(MAA-*g*-EG) gels, 162
  ratio of diffusion coefficients in complexed and uncomplexed hydrogels as compared to PMAA, 161*t*
  release (in vitro) from bioadhesive complexation networks, 159–161
  release mechanism from cationic hydrogel, 59*f*
  stimulus-driven release properties of cationic hydrogel, 57–58
  See also Bioadhesive complexation networks
Interpenetrating networks in hydrogel. *See* Electroconductive gels
Intraocular delivery systems, injectable, absorbable gel-formers, 126
Intravaginal drug delivery systems
  anatomy and physiology of vagina, 24–28
  areas of interest to women of reproductive age, 23–24
  bioadhesive delivery systems, 38–39
  biodegradable systems special type of dissolution-control, 36
  considerations in drug design, 33–34
  contraception, 41–42
  current trends, 40–45
  development of flexible gels, 45
  development of reversible gels, 45–46
  diffusion-controlled systems, 34–35
  dissolution-controlled systems, 35–36
  drug absorption, 28–30
  drug disposition after vaginal administration, 30–32
  future perspectives, 46
  gynecologic oncology, 44–45
  histological features of vagina, 24–25
  hormone replacement therapy, 41
  hydrogels, 36–38
  infectious disease treatment, 42–43
  infertility treatment, 42
  ion-exchange delivery, 39–40
  for labor induction, 40–41
  mechanisms of pelvic drug distribution, 32–33
  microspheres, 39
  model of drug absorption from vagina, 30*f*
  new trends in development of drug carriers, 45–46
  osmotic delivery, 40
  polymers in diffusion-controlled drug release formulations, 34*t*
  polymers in dissolution-controlled systems, 36*t*
  polymers in hydrogel preparation, 37*t*
  polymers in semipermeable membranes, 40*t*

Downloaded by 89.163.35.42 on October 31, 2012 | http://pubs.acs.org
Publication Date: September 24, 1998 | doi: 10.1021/bk-1998-0709.ix002

  potential benefits of intravaginal administration, 24
  swelling-controlled systems, 36–38
  for topical, local, or systemic effects, 28
  vaginal anatomy, 25
  vaginal microbiology, 26–28
  vascular and lymphatic systems of pelvis, 25–26
Ion exchange
  benefits of synthetic organic resins, 68
  reversible, equilibrium process, 68
  theory for oral drug delivery design, 68–69
  See also Water-soluble polyanions as oral drug carriers
Ion-exchange delivery systems, controlled release of ionizable drugs, 39–40
Ionogenic acrylate copolymer networks
  compositions of various drug-loaded multiacrylate monomer formulations, 133*t*
  compositions of various multiacrylate systems examined, 133*t*
  diffusion coefficients for acetone and pH 2.2 and 7.4 buffers, 136, 139*t*
  dynamic mechanical analysis (DMA) method, 130
  dynamic swelling behavior of various diacrylate systems in pH 2.2 and 7.4 buffers, 137*f*, 138*f*
  early time dependence of fractional proxyphylline release on $t^{1/2}/L$ (t is time and L is polymer slab thickness), 141*f*
  measured glass transition temperatures (T_g) for poly(multiacrylate) homo- and copolymers, 132, 134*t*
  measured swelling parameters and calculated solubility parameters for diacrylate systems, 132, 135*t*
  monomer-drug mixture preparation method, 130
  monomers used in network synthesis, 130, 131*f*
  polymer design and preparation, 130, 132
  proxyphylline diffusion coefficients describing rate of release from multiacrylate polymer networks, 141*t*
  release characteristic determination method, 130
  release rates lower than typical hydrogel formulations, 129–130
  schematic representation of structural issues, 131*f*
  slowly swelling, mechanically stable hydrogels, 129
  solute release behavior, 136, 142
  solvent-free photopolymerization process, 129–130, 142
  structural characterization, 132, 136
  swelling behavior of multiacrylate copolymers by Fickian analysis, 132, 136
  time release dependence of fractional proxyphylline release for various diacrylate formulations, 139*f*, 140*f*

K

Knedels. *See* Shell crosslinked knedels (SCK)

L

Labor induction, intravaginal drug delivery, 40–41
Lactic/glycolic acid (LGA) oligomeric microgranules
  aspirin model drug, 255
  assay of effect of LGA oligomer matrix on aspirin stability, 257
  biocompatibility of LGA polymers and biodegradation products, 254
  comparison of aspirin hydrolyzing profile in buffer and LGA matrix, 263*f*
  determination of aspirin loading efficiency, 256
  drug loading efficiency of microgranules, 258*t*
  effect of drug content on in vitro drug release, 259, 261*f*, 262
  effect of LGA oligomer matrix on aspirin stability, 262
  effect of oligomer composition on in vitro drug release, 259, 260*f*
  experimental materials, 255
  high drug loading efficiency, 257, 259
  method for morphology and size of aspirin-containing microgranules, 256
  micrograph of aspirin-containing microgranules, 258*f*
  morphology and size of microgranules, 257
  preparation of aspirin-containing LGA oligomer microgranules, 255–256
  problems of delivery systems based on high molecular weight LGA polymers, 254–255
  study of in vitro aspirin release, 256
Lactic/glycolic acid (LGA) oligomers
  assay of molecular weight on biodegradation, 243–244
  change of pH of incubating medium during biodegradation of LGA oligomers of three different compositions, 248*f*
  composition effect on oligomer biodegradation, 244–246
  effect of pH of incubating medium on biodegradation, 250*f*
  experimental materials, 243

hypothetical mechanism of LGA polymer/oligomer hydrolysis at pH <7 and >7, 251*f*
investigation of composition effect on biodegradation, 243
measurement of pH change of incubating medium during biodegradation, 244
molecular weight effect on oligomer biodegradation, 246, 247*f*
pH effect on oligomer biodegradation, 246, 249
promising biomaterials in medical and pharmaceutical area, 242–243
proposed mechanism for oligomer biodegradation, 249, 251*f*
study of pH effect on biodegradation, 244
weight loss of LGA oligomers of varying compositions versus time, 245*f*

Lidocaine, encapsulation in branched polymeric micelle, 123

Liposomes
  delivery vehicles for variety of therapeutic agents, 203
  ionically crosslinked polysaccharide hydrogels like Ca-alginate, 204
  problems of intravenous injection, 203
  retention of drugs, 204
  See also Alginate gelation

M

Metronidazole
  release from thermally gelled liposome/alginate hydrogels, 209, 210*f*
  See also Multi-layered semicrystalline polymer controlled release systems

Micelles. *See* Branched polymeric micelles; Polymeric micelles; Reactive polymeric micelles; Shell crosslinked knedels (SCK)

Microparticles. *See* Bioadhesive complexation networks; Lactic/glycolic acid (LGA) oligomeric microgranules

Microspheres
  applications as polymeric carriers, 143–144
  common preparation methods, 144
  drug delivery system, 39
  natural and synthetic polymers, 39*t*
  See also Bioadhesive complexation networks; Polyester microspheres

Modeling diffusion. *See* Diffusion

Multi-drug therapy
  novel multi-layered semicrystalline poly(vinyl alcohol) devices, 176–177
  rate of release controlled by rate of phase change from crystalline to amorphous, 177, 179*f*
  zero-order release systems, 176
  See also Multi-layered semicrystalline polymeric controlled release systems

Multi-layered semicrystalline polymeric controlled release systems
  category of crystal dissolution-controlled release systems, 177
  device with single drug, 177–178
  device with two drug components, 178
  differential scanning calorimetry method (DSC), 178
  fabrication with multiple layers for same or different drugs, 177
  gentistic acid ethanolamide (GAE) and metronidazole release from single device, 184
  influence of crystallization temperature on release rate of metronidazole from two-layered double-crystallized PVA films, 178, 179*f*
  materials and methods, 177–178
  procedure for release studies, 178
  rate of release controlled by rate of phase change from crystalline to amorphous, 177, 179*f*
  rational for development, 176–177
  release kinetics of GAE from PVA devices loaded with metronidazole and GAE, 180, 182*f*
  release of GAE and metronidazole from PVA devices crystallized at 120°C, 180, 183*f*
  release of GAE and metronidazole from PVA devices crystallized at 90°C, 180, 182*f*
  release rates lower for double-crystallized than single-crystallized PVA films, 180, 181*f*
  schematic representation of multi-layered crystal dissolution-controlled systems, 179*f*
  triple-crystallized films with lower release rates, 180, 181*f*
  zero-order release of metronidazole from PVA systems, 180, 184

Multi photon detection (MPD). *See* Direct measurement of multi phase flow

Multi phase flow. *See* Direct measurement of multi phase flow

N

Networks. *See* Bioadhesive complexation networks; Electroconductive gels; Hydrogels; Ionogenic acrylate copolymer networks

Norplant system, diffusion-controlled levonorgestrel delivery, 34

O

Omeprasol
  in poly(L,L-lactide) microspheres, 146–148
  See also Polyester microspheres

Downloaded by 89.163.35.42 on October 31, 2012 | http://pubs.acs.org
Publication Date: September 24, 1998 | doi: 10.1021/bk-1998-0709.ix002

Downloaded by 89.163.35.42 on October 31, 2012 | http://pubs.acs.org
Publication Date: September 24, 1998 | doi: 10.1021/bk-1998-0709.ix002

Oncology (gynecologic), treatment by intravaginal drug delivery, 44–45
Oral drug carriers. *See* Water-soluble polyanions as oral drug carriers
Oral protein drug delivery
  problems in developing, 156
  See also Bioadhesive complexation networks
Osmotic delivery systems
  polymers for semipermeable membranes, 40*t*
  semipermeable polymeric membrane, 40

P

Periodontal applications, injectable, absorbable gel-formers, 126
Physical model of diffusion. *See* Diffusion
Plant growth regulators (PGRs). *See* Gibberellic acid-containing organotin polymers
Platinum complexes immobilized in dextran derivatives
  antitumor (in vivo) activity, 273, 277
  clinical cancer chemotherapy with *cis*-dichlorodiamineplatinum (II) (CDDP), 267, 268*f*
  cytotoxic activity of conjugates in vitro, 271, 273
  experimental materials, 269
  growth inhibitory effects of OX-Dex/Dach-Pt conjugate and free Dach-Pt against colon 26 tumor cells inoculated in CDF_1 mice, 275*f*
  higher tumor activity of *cis*-dichloro(cyclohexane-*trans-l*-1,2-diamine)platinum (II), Dach-Pt(chlorato), 267, 268*f*
  measurement of cytotoxic activity of conjugates, 270
  method for determining platinum complex release from conjugates, 270
  molecular weight measurements, 271
  photograph of tumors excised from CDF_1 mice 28 days after inoculation, 276*f*
  polymer complexes of Dach-Pt and dextran derivatives to overcome lower water-solubility of Dach-Pt, 267
  preparation of conjugates, 269–270
  procedure for in vivo antitumor activity, 270–271
  release behavior of platinum complex from conjugates, 271, 274*f*
  residual cytotoxic activity of conjugates and free platinum complexes after reincubation in medium, 274*f*
  structural data and cytotoxic activity of dextran derivatives/Dach-Pt conjugates and platinum complexes, 272*t*
  structure of dextran derivative/Dach-Pt conjugates, 268*f*
Polyanhydrides. *See* Aromatic polyanhydrides
Polyaniline. *See* Electroconductive gels
Poly(ε-caprolactone). *See* Thioester end-functionalized poly(ε-caprolactone) (PCL)
Polycarbophil, widely-studied bioadhesive, 38
Polyester microspheres
  ^{13}C MAS NMR spectrum (magic angle spinning) of poly(L,L-lactide) (poly(L,L-Lc)) microspheres, 149*f*
  crystallinity of poly(L,L-Lc) microspheres, 149–150
  dependence of diameter of poly(ε-caprolactone) (poly(CL)) on time of hydrolysis, 151*f*
  dependence of poly(CL) particle diameters on Triton X-405 concentration during partial hydrolysis, 151*f*
  diameters, diameter distributions, molecular weights, and molecular weight distributions of poly(CL) microspheres, 145–146
  GPC trace, UV spectrum, and ^1H NMR spectrum of poly(L,L-Lc/omeprasol), 148*f*
  materials and methods, 144
  methods for obtaining microspheres directly during polymerization, 144
  poly(CL) and poly(L,L-Lc) microspheres with hydroxylic and carboxylic groups in surface layers, 150–151
  poly(dodecyl acrylate)-*g*-poly(ε-caprolactone) poly(DA-CL) as surface active agent, 144
  relation between diameters, diameter distributions, molecular weight, molecular weight distributions of poly(L,L-Lc) and concentration of poly(DA-CL) in reaction, 144–145
  SEM microphotograph of poly(L,L-Lc/omeprasol) microspheres, 147*f*
  synthesis of poly(CL) microspheres, 145–146
  synthesis of poly(L,L-Lc), 144–145
  synthesis of poly(L,L-Lc) microspheres with omeprasol, 146–148
Polymeric micelles
  ability of structure to affect properties, 165
  composition and ability to change morphology, 165–166
  meeting biocompatibility requirements, 106
  preparation by three-step approach, 166, 167*f*
  properties of micelle core, 166
  release of adriamycin by cleavage from chains, 166

Downloaded by 89.163.35.42 on October 31, 2012 | http://pubs.acs.org
Publication Date: September 24, 1998 | doi: 10.1021/bk-1998-0709.ix002

See also Branched polymeric micelles; Reactive polymeric micelles; Shell crosslinked knedels (SCK)
Polymeric surfactants, promising answers for drug delivery, 118
Polymers
  biodegradable examples, 36*t*
  diffusion-controlled drug release formulations, 34*t*
  dissolution-controlled drug release formulations, 36*t*
  hydrogel preparation, 37*t*
  natural and synthetic for microspheres, 39*t*
  preparation of semipermeable membranes, 40*t*
Poly(sulfopropyl methacrylate potassium-*co*-alkyl methacrylate). *See* Water-soluble polyanions as oral drug carriers
Polyvinylpyrrolidone (PVP) dispersions
  aiding in bioavailability, 213
  comparison of griseofulvin (gris) dissolution in solid dispersions with commercial gris and physical mixtures, 215, 216, 218*f*
  effect of anionic surfactant on release of gris, 219*f*
  effect of cationic surfactant on release of gris, 220*f*
  effect of non-charged surfactant on release of gris, 221*f*
  experimental materials, 214
  experimental methods, 214
  objective for increasing dissolution rate of gris, 213
  physicochemical analysis of solid dispersion, 214
  release experiments of solid dispersion, 214–215
  release rate studies, 215–217
  surfactant effects on release of gris from solid dispersions, 217, 222
  X-ray patterns and DSC thermograms of solid dispersions, 215, 216*f*, 217*f*
Potential areas of drug delivery. *See* Tissue engineering
Potential carriers of bioactive compounds. *See* Polyester microspheres
Proxyphylline
  composition of drug-loaded polymers, 133*t*
  diffusion coefficients, 141*f*
  monomer-drug preparation, 130
  release from ionogenic acrylate copolymer networks, 136, 139*f*, 140*f*

R

Reactive polymeric micelles
  conversion of acetal to aldehyde, 112–113
  dynamic light scattering (DLS) measurements for size and shape, 111–112
  evaluating stability with sodium dodecylsulfonate (SDS) treatments, 114
  experimental materials and methods, 107
  functionalized copolymers investigation of poly(ethylene glycol) (PEG) and polylactide (PLA), 106–107
  GPC chromatograms of acetal-PEG and acetal-PEG/PLA, 109*f*
  GPC profiles of aldehyde-micelle before and after reaction with benzoic hydrazide, 113*f*
  ^{1}H NMR spectra of acetal-ended PEG-PLA and aldehyde-ended PEG-PLA, 109*f*
  micelle preparation method, 108
  polymer characterization, 108
  polymer synthesis method, 107–108
  potassium alkoxide initiator with functional group for heterotelechelic polymer, 109
  preparation of acetal-PEG/PLA micelle, 111–112
  requirements for biocompatibility, 106
  schematic illustration, 106*f*
  size distribution of acetal-PEG/PLA micelle by DLS, 112*f*
  size distribution of micelles before and after polymerizations with and without SDS treatments, 113, 114*f*
  stabilization of micelle, 113–115
  synthetic results of acetal-PEG/PLA block copolymer, 109–110
  synthetic results of acetal-PEG/PLA-methacryloyl block copolymer, 110–111
Ricin A-chain, controlled release by injectable, absorbable gel-formers, 127

S

Seedling growth of sawgrass and cattail. *See* Gibberellic acid-containing organotin polymers
Self-diffusion of solvents and solutes in polymer solutions and gels. *See* Diffusion
Sexually-transmitted diseases, treatment by intravaginal drug delivery, 42–43
Shell crosslinked knedels (SCK)
  basic procedure for formation of shell crosslinked polymer micelles from amphiphilic block copolymers, 167*f*
  α,γ-bisdiphenylene-β-phenylallyl radical (BDPA) encapsulation, 169
  block copolymers of polystyrene-*b*-poly(4-vinylpyridine) (PS-*b*-PVP) under anionic conditions, 167–168
  chemistry in synthesis of SCK, 168*f*

- coomassie blue uptake for constant mass of SCK plotted against mass of dye in solution, 171, 174*f*
- copper (II) phthalocyanine tetrasulfonic acid tetrasodium salt uptake for constant mass of SCK plotted against its mass in solution, 173, 174*f*
- core encapsulation, 169
- diversity of macromolecular structure and composition, 169*f*
- SCK synthesis, 167–169
- shell binding interactions with negatively charged small molecules, 171, 173
- uptake of hydrophobic molecules within hydrophilic system and binding of negatively charged molecules, 173
- UV-vis spectra of coomassie blue alone, with SCK, and with SCK after centrifugation, 172*f*
- UV-vis spectra of SCK and SCK plus BDPA radical, 170*f*
- *See also* Polymeric micelles

Solid dispersion
- active ingredients in inert carrier, 212
- criteria of ideal carrier, 213
- factors affecting physical form of drug and dispersion produced, 213
- *See also* Polyvinylpyrrolidone (PVP) dispersions

Surfactants (polymeric), promising answers for drug delivery, 118

Sustained solute delivery. *See* Ionogenic acrylate copolymer networks

Swelling-controlled systems. *See* Hydrogels

T

Thermally triggered gelation of alginate. *See* Alginate gelation

Thioester end-functionalized poly(ε-caprolactone) (PCL)
- application in chemoselective ligation (CSL), 100, 102
- characterization methods, 93
- CSL process, 93
- CSL representative examples, 96, 98
- experimental materials, 93
- gel permeation chromatography (GPC) profiles of polymerization resumption experiment, 96, 99*f*, 100
- general synthetic approach, 94
- GPC profiles and ^{13}C NMR spectrum of diblock copolymer, 100, 101*f*
- ^{1}H NMR spectrum and GPC profiles of coupling product of PCL and *N*-Cys-terminated mPEG, 102, 103*f*
- ^{1}H NMR spectrum of PCL-20 in $CDCl_3$, 100, 101*f*
- initiation preparation and schematic, 93, 94
- interest in thioester functionality, 93
- molecular weight and molecular weight distributions (MWDs) of synthesized PCLs, 100*t*
- plot of number-average molecular weight (M_n) versus monomer to initiator ratio, 99*f*
- ring-opening polymerization (ROP) of lactones by coordination-insertion mechanism, 92–93
- schematic of coordination-insertion mechanism of ROP of lactones, 94
- schematic of *N*-Cys-terminated mPEG synthesis, 97
- schematic of thioester end-functionalized PCL synthesis, 94
- synthesis of, 95
- synthesis of diblock copolymer, 95, 97
- synthesis of poly(ethylene glycol) methyl ether (mPEG) end terminated with *N*-Cys-, nitrophenyl-, and aminophenyl- groups, 95–96
- unique properties of PCL and its copolymers, 92

Tissue engineering
- contemporary trends in scaffold development, 281–282
- development of vasculature to support relatively thick tissue critical, 279–280
- diffusion controlled release mode, 280
- fabrication complications including thermal and chemical stability of drug, 281
- key factors influencing performance of absorbable scaffold, 281
- microporous foams for housing living cells by crystallization-induced microphase separation (CIMS) process, 281–282
- pertinent modes of controlled release of bioactive agents, 280
- potential for drug delivery systems, 282
- processing considerations, 280–281
- release of drugs from three-dimensional system, 281
- success dependent on interaction of material with tissue, 279

V

Vagina
- anatomy, 25
- influences of microbial environment, 27
- key histological features, 24–25
- microbiology, 26–28
- vascular and lymphatic systems of pelvis, 25–26

Downloaded by 89.163.35.42 on October 31, 2012 | http://pubs.acs.org
Publication Date: September 24, 1998 | doi: 10.1021/bk-1998-0709.ix002

W

Water-soluble polyanions as oral drug carriers
  chemical structure of copolymers, 69
  composition of copolymers PSPMK/MMA and PSPMK/EMA, 72
  copolymerization of 3-sulfopropyl methacrylate potassium salt (SPMK) with methyl methacrylate (MMA) and ethyl methacrylate (EMA) for PSPMK/MMA and PSPMK/EMA, 69
  dissociation/erosion rate constant and release exponent for release kinetics, 77*t*
  drug release kinetic studies, 70
  effect of buffer strength and pH on erosion rate of propranolol-PSPMK/MMA tablets, 75, 76*f*
  effect of copolymer composition on release kinetics of propranolol HCl from drug-PSPMK/MMA tablets, 78, 79*f*
  effect of drug type and solubility on release kinetics of drugs, 78, 81*f*
  effect of pH and comonomer on release kinetics, 78, 80*f*
  ion exchange resins, 68
  methods for characterization of copolymers and complexes, 70
  preparation of dosage forms, 69
  release kinetics by dissociation/erosion mechanism, 75
  release profiles of propranolol HCl from drug-PSPMK/MMA tablets, 72, 73*f*, 74*f*, 75
  theory for oral drug delivery design, 68–69
  thermograms of PSPMK/MMA, hydrochloride drugs, and their complexes, 70, 71*f*, 72
Wound healing and hemostatic applications, injectable, absorbable gel-formers, 126

Z

Zero-order drug release. *See* Multi-layered semicrystalline polymer controlled release systems
Zidovudine (ZDV, AZT), cumulative toxicity with ganciclovir, 3

Downloaded by 89.163.35.42 on October 31, 2012 | http://pubs.acs.org
Publication Date: September 24, 1998 | doi: 10.1021/bk-1998-0709.ix002